Development of Gene Therapy for the Treatment of Retinal Dystrophies caused by mutations in *AIPL1*

Mei Hong Tan

A thesis submitted for the degree of

Doctor of Philosophy

2011

Department of Genetics

Institute of Ophthalmology

University College London

Declaration

I, Mei Hong Tan confirm that the work presented in this thesis is my own. Where information has been derived from other sources, I confirm that this has been indicated in the thesis.

.....

DATE: .....

Abstract

Genetic defects in AIPL1 cause a heterogeneous set of clinical conditions depending on the severity of the mutant alleles. Diseases can range from Leber Congenital Amaurosis (LCA), the severest form of early-onset retinal degeneration, to milder forms such as retinitis pigmentosa (RP) and cone-rod dystrophy. There is currently no effective treatment for LCA and inherited retinal dystrophies, which are the commonest cause of childhood blindness. AIPL1 is expressed primarily in retinal photoreceptors and is required for the biosynthesis of photoreceptor phosphodiesterase (PDE).

This thesis describes a programme of work that examines the potential and efficacy of gene replacement therapy in the treatment of *AIPL1*- associated retinal diseases. It centres on the use of recombinant adeno-associated virus for the transfer of murine and human *AIPL1* cDNA into photoreceptor cells. AAV-mediated gene replacement was assessed in two genetically engineered mouse models carrying null and hypomorphic alleles, *Aipl1 -/-* and *Aipl1 h/h* mice, which simulate retinal degenerations similar to human LCA and RP respectively. Three different rates of photoreceptor degeneration were simulated using the mouse models. To treat the different rates of degeneration, two pseudotypes of AAV (serotype 2 and 8) exhibiting different transduction kinetics were used for gene transfer. Substantial and long term rescue of the disease phenotype was seen as a result of *Aipl1* transgene expression mediated by AAV2/2 vector in *Aipl1 h/h* mice and by AAV2/8 in rapid degenerations in light accelerated *Aipl1 h/h* mice and in *Aipl1 -/-* mice. Thus, the results presented in this thesis validates the efficacy of AIPL1 gene replacement using AAV vectors in varying rates of degeneration that reflected the clinical spectrum of disease. This is the first study to report long-term rescue of a photoreceptor-specific defect and to demonstrate effective rescue of rapid photoreceptor degeneration.

The development of an efficient therapy depends on the identification of patients and characterisation of disease phenotype. A panel of DNA samples from patients with LCA and early onset severe retinal dystrophy was

screened for mutations in the *AIPL1* gene. Patients identified with *AIPL1*-associated disease demonstrated varying severity of disease from LCA to milder form of rod cone dystrophy. Clinical characterisation and imaging of the patients highlighted distinctive features which will direct future identification and molecular screening of patients. Residual retinal integrity and function in young patients and patients with milder phenotype suggests that *AIPL1* defects may be amenable to treatment.

Publications and conference abstracts

MH Tan, AJ Smith, B Pawlyk, Xu Xiaoyun, Liu Xiaoqing, JW Bainbridge, M Basche, J McIntosh, HV Tran, A Nathwani, T Li, RR Ali. Gene therapy for retinitis pigmentosa and Leber congenital amaurosis caused by defects in *AIPL1*: effective rescue of mouse models of partial and complete Aipl1 deficiency using AAV2/2 and AAV2/8 vectors. Human Molecular Genetics. Jun 2009; Vol18(12): 2099-2114.

MH Tan, D MacKay, J Cowing, HV Tran, AJ Smith, , R Henderson, I Russell-Eggitt , AG Robson, AR Webster, GE Holder, RR Ali, AT Moore. Genetics and phenotypes of AIPL1 mutations in recessive inherited retinal degeneration. Manuscript in preparation.

Conference abstracts:

MH Tan, HV Tran, AJ Smith, , R Henderson, I Russell-Eggitt , AG Robson, AR Webster, GE Holder, RR Ali, AT Moore. Clinical spectrum of patients with *AIPL1* mutations in recessive inherited retinal dystrophies. Invest. Ophthalmol. Vis. Sci. 2010. 51: ARVO E-abstract 3087.

MH Tan, HV Tran, AJ Smith, R Henderson, P Moradi, I Russel-Eggitt, M Cheetam, AR Webster, RR Ali, AT Moore. Comparative analysis of AIPL1 mutations in recessive inherited retinal dystrophies. Invest. Ophthalmol. Vis. Sci. 2009. 50: E-abstract 4127.

MH Tan, AJ Smith, B Pawlyk, T Li, RR Ali Gene replacement therapy leads to photoreceptor survival and restores beta-phosphodiesterase localization to outer segment in AIPL1-related retinal dystrophy.. Invest. Ophthalmol. Vis. Sci. 2008. 49: E-abstract 1130.

Acknowledgement

I am truly grateful to my principal supervisor and mentor Professor Robin Ali for his unwavering support, patience, guidance and encouragement. Most of all, I am thankful for his constant positive outlook and understanding of the big picture, which has been a major motivator for the project. I would also like to thank Professor Anthony Moore, my secondary supervisor who has given me invaluable perspective and insight in the clinical discipline. I am also grateful to Alexander Smith for his technical advice and critical appraisal, which was integral to this work. It has been a pleasurable experience and I look forward to working with them again in the future.

I would like to acknowledge the generous funding that I have received from the Medical Research Council (MRC, UK) to carry out the work presented in this thesis. Many thanks also to all of the members of staff and colleagues in the Department of Genetics, Institute of Ophthalmology for their help and support. In particular, I would like to thank Emma West and Peter Munro who processed tissue specimens into the beautiful semithin and ultrathin sections respectively that are presented here and Jim Bainbridge for performing the subretinal injections.

Last but not least, I am eternally thankful to my parents, family and friends for their love, patience and their belief in me, I could not have done it without them.

"Give a man fish and he eats for a day, teach him to fish and he will have food for life"

Table of Contents

Figures

Tables

1 Introduction

Gene technology has revolutionized the 21st century and soon, it will become an important influence on many sectors of our lives. Recently, developments in gene transfer technology have opened new doors, particularly in the medical field. These advances have lead to the potential of treating genetic and acquired diseases using gene therapy, thus establishing a promising tool for the development of new and effective treatment strategies for numerous diseases which are thus far incurable. Diseases which may benefit from gene therapy include cancer, certain infectious diseases, inherited disorders of the nervous system, haematological diseases and inherited retinal degenerations. Although the use of gene therapy to treat diseases has mainly been proven in animal studies, many of these treatments have now gone to clinical trials. It may be possible, in near future, to use gene therapy to treat diseases whose genetic defects have been identified. One group of diseases which stand to benefit greatly from gene therapy is inherited eye diseases and the use of gene therapy in the treatment of ocular diseases has only recently been explored.

The human eye is regarded as the most important sense organ since 85% of the information about our environment is perceived through the eyes. Inherited retina degenerations are one of the most common causes of blindness in the western world, for which currently no efficient treatment exists. The best characterised form of inherited retinal degenerations is retinitis pigmentosa (RP) with prevalence up to 1:3500 [54]. To date, many genes responsible for inherited retinal diseases have been identified, providing a basis for the development of gene-based treatment strategies. The unique properties of the eye that makes it particularly suitable as a model system for gene therapy. The eye is a small and highly compartmentalized organ with immune-privileged properties making it possible to deliver small volumes of viral vector precisely to obtain transduction of selected retinal cell types with minimal risk of systemic dissemination or invoking vector-directed immune responses. Its transparent

nature makes it highly accessible and allows for non-invasive techniques to monitor and measure the effects of treatment such as retinal imaging, slit lamp biomicroscopy, electrophysiology and psychophysical tests [10,408]. As such, diseases of the eye are prime candidates for gene therapy approaches.

The past decade has seen an exponential increase in advances in the field of molecular genetics, particularly in genotyping and diagnostic technology. The impact on the field of ophthalmology has been tremendous; the discovery of new disease genes has lead to better understanding of disease pathogenesis. The development and discovery of animal models has culminated in successful rescue of vision in some models of hereditary retinal dystrophies using gene replacement therapy. This has occurred mainly in different studies of recessively inherited retinal dystrophies where the condition is caused by mutations resulting in the loss of function of an encoded protein. Insertion and subsequent expression of the therapeutic transgene was followed by observations of functional and morphological improvements, some of these effects were sustained over a long term. These studies have provided robust proof-of-principal for gene replacement therapy in recessively inherited retinal dystrophies which until now were untreatable, and justification to bring this research from the laboratory bench to the clinics in the form of human trials.

Previously, preclinical studies of gene replacement therapy to treat retinal degeneration have found that photoreceptor cell defects were more difficult to treat. In an early study of gene replacement therapy using a mouse model of Retinitis Pigmentosa that carried a null mutation the *Prph2* gene, subretinal delivery of an adenovirus carrying *Prph2* transgene led to structural and functional improvement but the treatment did not affect the rate of degeneration [14]. With the improvements in vector design, functional improvement and a degree of photoreceptor rescue has been reported in a few animal models with defects in photoreceptor-specific genes such as *RPGRIP, GUCY2D, ABCA4,* and *usherin* [363,496] [281,518]. These defects

cause a spectrum of retinal disorders ranging from Lebers Congenital Amaurosis, Stargardt disease, and retinitis pigmentosa respectively.

Gene replacement therapy have been more successful in conditions where the genetic defects originated in the retinal pigment epithelium such as RPE65, MERTK, and LRAT, all of which are causes of recessive hereditary retinal dystrophies [1,42,437,471]. RPE defects are generally easier to treat because the RPE forms a single layer of cells that are efficiently transduced by viral vectors, whereas many more photoreceptor cells are arranged multiple layers which makes gene transfer to these cells less efficient. Since each RPE cell is in contact with several photoreceptor cells, the transduction of a single RPE cell might protect or restore function to several photoreceptor cells, thus allowing for widespread correction of the defect. Furthermore, the photoreceptor cells in RPE-specific defects are primarily healthy and structurally intact despite the metabolic derangement. By correcting the metabolic derangement in the RPE, the function and survival of these photoreceptor cells may be restored.

Clinical trials of gene replacement therapy treating patients with early onset severe rod cone dystrophy or Lebers Congenital Amaurosis caused by *RPE65* mutations are currently in progress, one of these is being conducted by our group at the Institute of Ophthalmology. Preliminary reports that have been recently published from these trials reported good safety profile of the treatment and limited improvement in retinal function. This will pave the way for more human trials in the future and as such further experimental studies in animal models are urgently required to evaluate the potential for benefit in retinal degenerations caused by other genes. It would be particularly desirable to be able to achieve robust long term rescue in a model with photoreceptor-specific gene defect since most inherited retinal dystrophies originate from photoreceptor defects and have been more difficult to treat. This would provide proof that photoreceptor-specific defects are amenable to treatment.

1.1 Aims and objectives

1.The aim of this research project is to investigate the efficacy of gene replacement therapy for the treatment of a murine model of Type 4 Leber Congenital Amaurosis (LCA) due to a primary defect in a photoreceptor-specific gene *AIPL1*.

2. To evaluate whether AAV-mediated *AIPL1* expression leads to structural and functional rescue of photoreceptors with subsequent prolongation of their survival in this model of severe retinal degeneration.

3. To identify and characterise patients with mutations in *AIPL1* through genetic screening of a panel of patients with Leber Congenital Amaurosis and early onset severe retinal dystrophies. This will also facilitate possible future translation of this gene-based treatment by identifying suitable candidates for clinical trials and establishing baseline clinical outcome measures.

Therefore, we state that the null hypothsis is that AAV-mediated expression of *AIPL1* does not lead to structural or functional preservation of photoreceptor cells and there is no increase in photoreceptor survival following treatment.

1.2 The eye – structure and function

The primary function of the eye is to respond to visual stimuli by converting a response to light into neuronal signals that are interpreted by the brain. To perform this sensory function, the eye carries out a variety of intricate cellular and molecular processes which are dependent on maintaining a tightly regulated microenvironment within the eye through the differentiated status of various cell types, vasculogenesis and modulation of the local immune system. The vast range of cell types within the eye reflects the diversity of function that is carried out in this small organ. Consequently, the eye is highly sensitive to genetic and environmental factors. Any slight changes in

the fine balance pattern of gene expression, subtle environmental insults and infections can lead to disease. The neurosensory retina in particular is the center of many genetic diseases, many of which lead to blindness. Despite increased knowledge of the aetiology and pathology of diseases, many ocular conditions, especially inherited eye diseases currently lack effective treatments.

The differentiation of the retina during development involves the close interaction between two cell types: the photoreceptor cells and the retinal pigment epithelium (RPE) cells. Both cell types are dependent on each other during different developmental stages, by providing various survival, growth and differentiation factors. This close interaction is not only seen during development but also in the adult eye. Retinal physiology and morphology depends on the close interaction and communication of these two cell types and involves complex, cellular signaling pathways, the most important of which will be discussed in more details in the following chapters.

The mammalian eye consists of concentric layers of tissues derived from three of the primitive embryonic layers: surface ectoderm and its derivative neural crest, neural ectoderm and mesoderm. Figure 1.1 illustrates the overall layered architecture of the eye, including a magnified view of the retina which is where the capture light photons, amplification and transduction of light signals to the visual cortex take place [142].

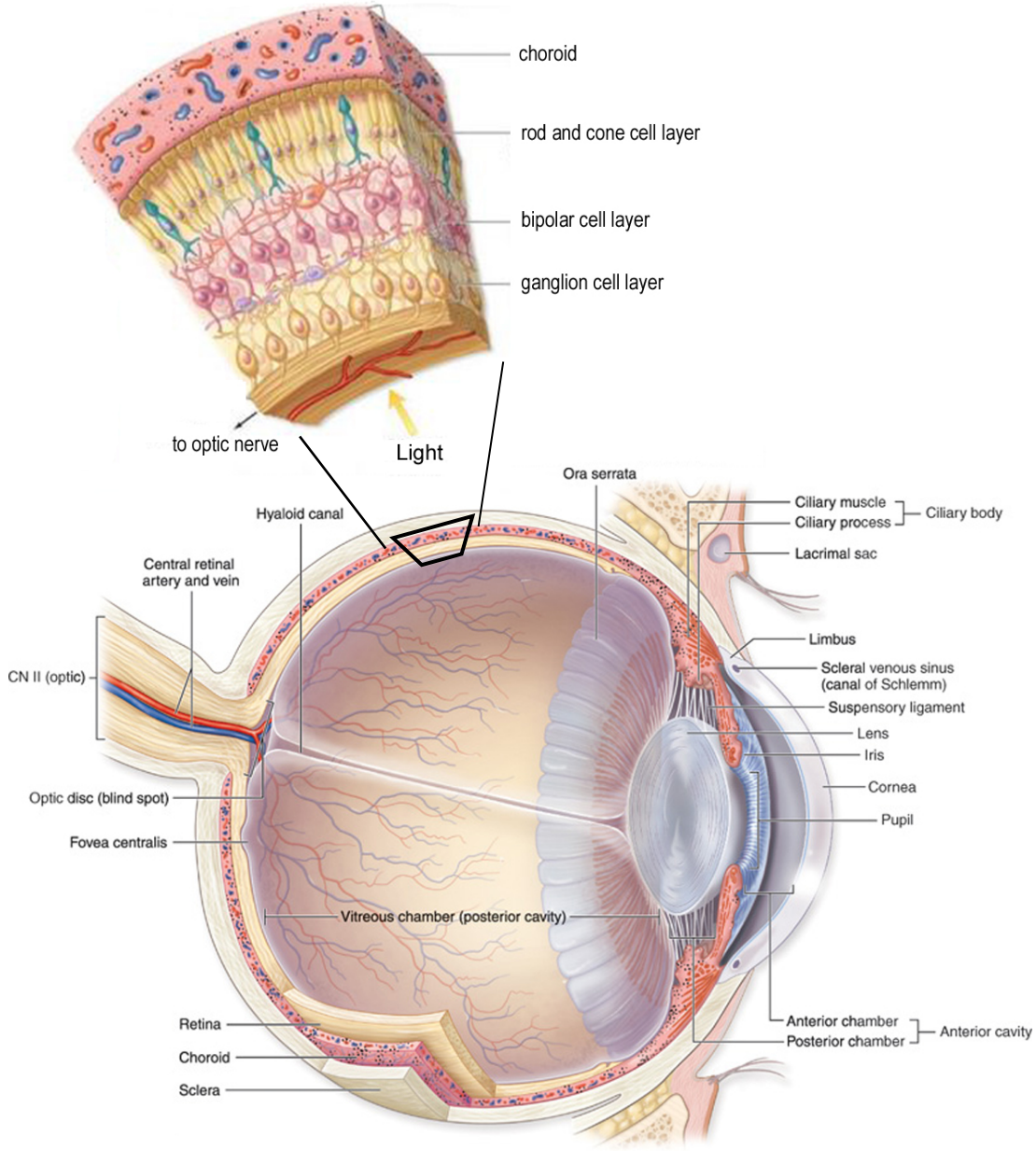

Figure 1.1 Structure of the eye

A schematic diagram showing a vertical section through the human eye.

(Adapted from McGraw-Hill)

1.2.1 The retina

The retina is primarily divided into 2 distinct tissue compartments: the inner or neurosensory retina, and the outer supporting layer of cells known as the retinal pigment epithelium (RPE). The neurosensory retina is a highly specialised laminated structure that perform the central functions in the phototransduction cascade and visual pathway. There are 10 histological layers in the retina as depicted in Figure 1.2. The outermost layer is a single layer of melanin-containing cuboidal cells known as the retinal pigment epithelium (RPE), and separates the neurosensory retina from the choroid.

There are approximately 5 million RPE cells in the human retina which regulate the movements of nutrients and metabolites required for the maintenance of the photoreceptors throughout the interphotoreceptor matrix[449]. The basal aspect of the RPE lies on the connective tissue layer known as Bruch's membrane. The apical aspect of the RPE has microvilli on its internal surface which invaginate the photoreceptor outer segments. Functionally, The RPE cells have vital roles in the maintenance of photoreceptor cells by ingesting and degrading the oldest outer segment discs of the photoreceptors [177]. They also contribute to the renewal of the retinoids in a series of reactions which are part of in the visual cycle. These RPE cells provide much of the trophic support required to maintain the photoreceptor cells in the form of various growth factors and components of the inter-photoreceptor matrix essential for the development and support of rods and cones [395]. The RPE is thus crucial for maintenance of the neurosensory retina and defects in RPE function give rise to various inherited and acquired retinal diseases; some of these diseases include important conditions such as age-related macular degeneration.

The outer and inner segments of photoreceptor cells form the photoreceptor layer which lies internal to the RPE, and distal to outer nuclear layer. There are three layers of nuclei consisting of photoreceptor cell nuclei in the outer nuclear layer, the bipolar, horizontal and amacrine cells in the inner nuclear layer, and the ganglion cells layer which lies adjacent to the vitreous.

Photoreceptor cells, the rods and the cones share the same basic structure and are one of the most highly metabolic cell types in the body. All photoreceptor cells have light-sensitive visual pigments in their outer segment membranes, which after the absorption of a photon change their structure and thereby initialise the phototransduction cascade. Rods contain the pigment rhodopsin and are sensitive to conditions of dim light, thereby are responsible for scotopic (night) vision and peripheral vision. Cones contain different cone opsins depending on which sub-type of cone cell they belong to, and thus respond to bright light of varying wavelengths allowing colour vision. Rods dominate the photoreceptor cell population in the mammalian eye; there are approximately 18 times as many rods as cones in an adult human eye. In humans, cones are responsible for central visual acuity due to their spatial distribution (see below). The human retina contains 3 types of cones, and, depending on the exact structure of the opsin molecule, are maximally sensitive to either long wavelengths of light (L-cones, red light), medium wavelengths of light (M-cones, green light) or short wavelengths of light (S-cones, blue light). Rodents and most other mammalian species are di-chromatic, meaning they only have 2 types of cone cells that respond to medium-and short-wavelength light (M- and S-cones) [5,6]. Rods and cones in the photoreceptor layer are surrounded by the processes of specialized glial cells, Műller cells which are large glial cell types found in the inner nuclear layer and provide survival factors and nutrients for the inner retinal cells. The Műller cells are linked to each other by cellular tight junctions or zonula adherens comprised of foot processes of Műller cells known as the outer limiting membrane. This barrier is essential for the intra-neuroretina homeostasis. Between the layers of nuclei, are two layers of synapses, the outer and inner plexiform layers which form connections between the interneurons, photoreceptor cells and ganglion cells. The axons of the ganglion cells and astrocytes lie in the nerve fibre layer located internal to the ganglion cell layer and through which they join to the optic nerve. The inner limiting membrane, formed by Műller cells, is the innermost layer and separates the retina from the vitreous.

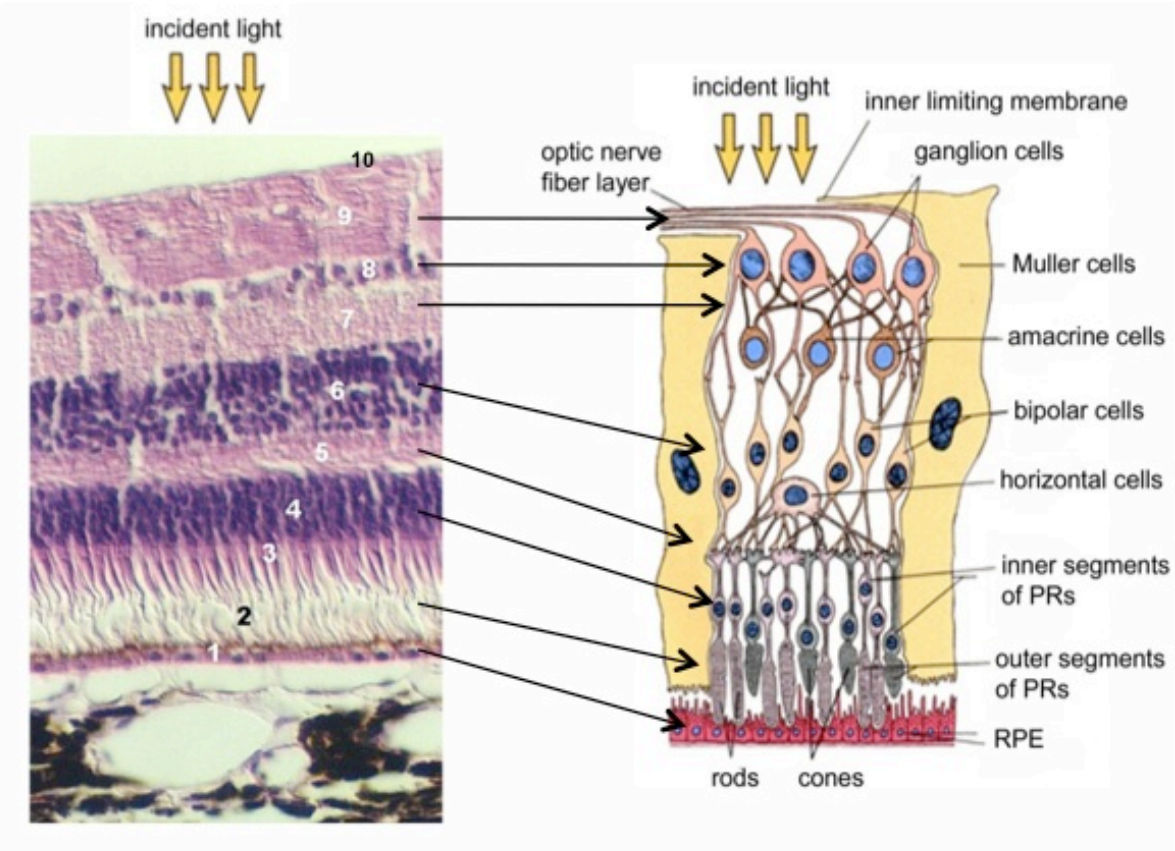

Figure 1.2. Histological and schematic cross-section of the human retina.

In all there are ten layers in the neurosensory retina and retinal pigment epithelium (RPE). The various layers as shown are, from bottom to top: 1,RPE; 2, layer of photoreceptor inner and outer segments; 3, the outer limiting membrane; 4, the outer nuclear layer; 5, the outer plexiform layer; 6, the inner nuclear layer; 7, the inner plexiform layer; 8, ganglion cell layer; 9, nerve fiber layer, and 10, the inner limiting membrane. Outside the retina lies the vascular choroid.

(histological section from http://microanatomy.net/)

The average adult human eye has 5 million cone photoreceptors and 92 million rod photoreceptors arranged in a non-uniform fashion across the scleral surface of the retina.[303] The distribution of photoreceptors varies between the central retina and the periphery. In the human retina, there is a central, pigmented portion of the retina called the macula which is enriched for cone photoreceptor cells. The macula measures approximately 5 mm in diameter and is located 3 mm lateral to the optic disc. At the center of the macula area, the central portion of retinal tissue is referred to as the fovea centralis (Figure 1.3) which subserves the central vision and contributes most to visual acuity in humans because it contains the highest concentration of cone cells. There is a lack of rod photoreceptors at the fovea, cone cells are closely packed in the centre of the retina and the inner retinal cells here are displaced away from the underlying photoreceptors, allowing a greater proportion of incident light to be absorbed by the cells in this region. This also contributes to the increase in visual acuity in this central area. Towards the periphery, the density of cones decreases while the density of rods increases and is maximal in a 5 mm ring centered in the macula. Rodents and other mammals (other than non-human primates) lack a macula, with cones and rods more evenly distributed throughout the retina. Despite lack of an anatomically defined macula in rats and mice, the murine retina remains a useful model system in which human retinal disease can be studied. Many of the hereditary retinal disorders in humans have either a naturally-occuring equivalent in rodents, or have been created using transgenic, knock-out or selective gene ablation technologies [132]. Studies based on these animal models have provided valuable insights into the pathophysiology and mechanisms of these diseases in humans. However, the differences between human and animal retinal biology must always be borne in mind when extrapolating conclusions from animal experiments and applying these to the clinical scenario.

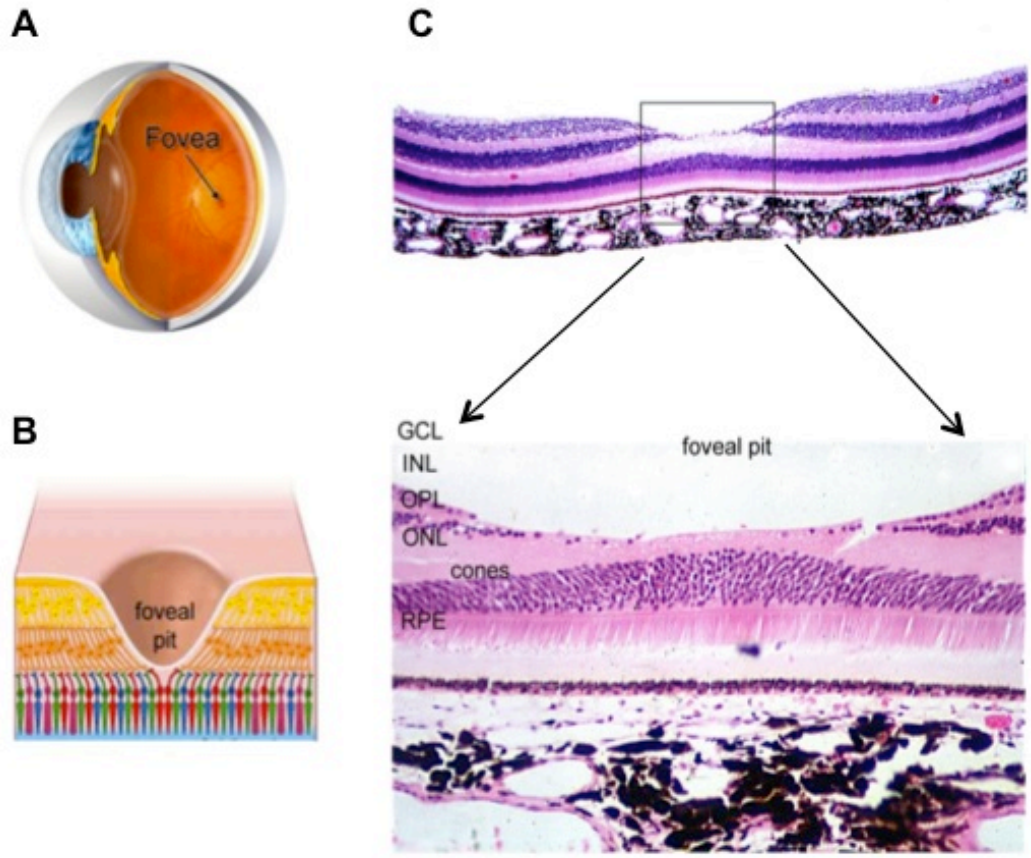

Figure 1.3. The fovea.

A. An illustration showing the location of the fovea in the eye, which is temporal to the optic disc.

B. A schematic diagram depicting the anatomy of the foveal region in the eye.

C. Histological cross-section of a primate fovea; the inner retinal cells (INL and GCL) are displaced from the foveal pit, allowing more light to reach the cone photoreceptors which are concentrated in the *fovea centralis*.

RPE, retinal pigment epithelium; ONL, outer nuclear layer; OPL, outer plexiform layer; INL, inner nuclear layer; IPL, inner plexiform layer; GCL, ganglion cell layer.

(histology figure adapted from http://www.kumc.edu/instruction/medicine/anatomy/)

Mature photoreceptors are structurally and functionally polarized neurons with four separate domains comprising of outer and inner segments, a cell body that contains the nucleus and a synaptic region (Figure1.4). The light sensitive structures of the photoreceptors are the outer segments, that lie in the inter-photoreceptor matrix (IPM) between the apical microvilli of the RPE cells. In cones, the outer segments contain lamellae which are invaginations of the plasma membrane whereas rod outer segments contain dense stacks of membranous discs which are discrete from the plasma membrane. Inserted into cone lamellae and rod discs are the structural proteins peripherin-2 and rom-1, both of which are required for the formation and maintenance of outer segments. The discs and lamellae are formed constantly and act to enlarge the sensory surface. As the discs mature, they are diplaced distally and are phagocytosed by the RPE cells when they reach the tip of the outer segment. Incorporated into the rod photoreceptors membrane discs and cone lamellae are the light sensitive pigments rhodopsin and cone opsins respectively. These are the site of light absorption and phototransduction. The cilium connects the outer segment with the inner segment and is involved in the transport of proteins between the two. The inner segment is packed with a large number of mitochondria that provides the energy required for the process of phototransduction. The synapses hold vesicles, that distribute neurotransmitters after light excitement of the photopigment, thereby passing the signal on to bipolar cells in the inner nuclear layer. The flow of visual information in the retina can follow two paths: a direct path, from light receptors to bipolar cells to ganglion cells; and an indirect path, in which horizontal cells may be interposed between the photoreceptors and bipolars, and amacrine cells between bipolars and retinal ganglion cells. Horizontal cells, amacrine cells and interplexiform cells modulate the passage of impulses on their way from the photoreceptors to the ganglion cells.

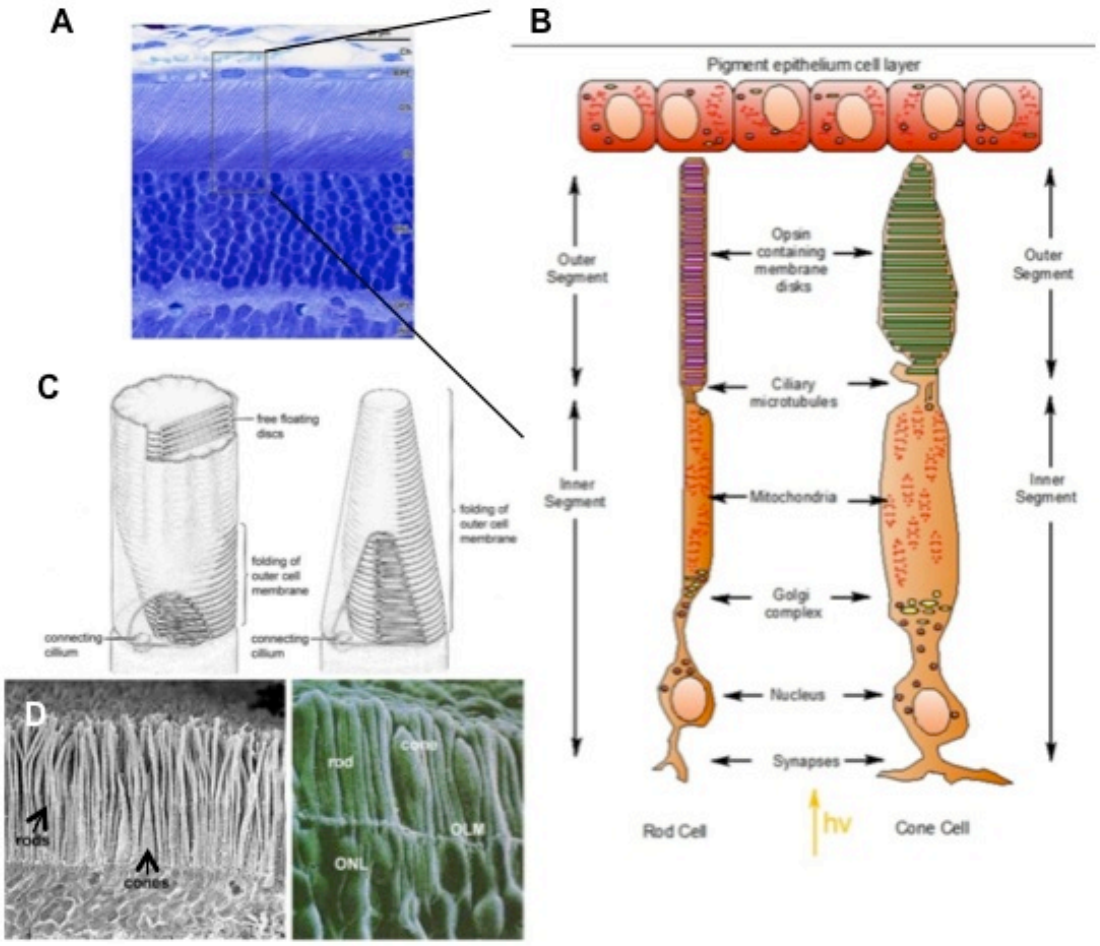

Figure 1.4. Structure of photoreceptors.

Although generally similar in structure, rods and cones differ in their size and shape, as well as in the arrangement of the membranous discs in their outer segments.

OS, outer segments; IS, inner segments; ONL, outer nuclear layer; OLM, outer limiting membrane.

A.Light microscopy of a retinal section showing photoreceptor outer segment structures.

B.Schematic of the structure of rods and cones photoreceptor cells. The basic structure of a photoreceptor cell consists of a synapse, cell body containing the nuclei, inner segment which contains numerous mitochondria and outer segment which contain membranous discs. Rods have long, cylindrical, outer segment with many discs, while cones have a short, tapering outer segment with relatively few discs.

C.The differences between the structure of rods (left) and cones (right) outer segment is shown. The rod outer segment has free-floating discs while cone outer segment consists of infolding of the outer cell membrane.

D.An electron microscope image of rods and cones is shown. The thin narrow cells are the rods and the bulbous cells are the cones.

(C , adapted from Young, R. W. (1971) The renewal of rod and cone outer segments in the rhesus monkey. J. Cell Biol. **49**, 303-318. D, first image from Peter Munro, UCL, second image adapted from www.eyedesignbook.com/ ch3/eyech3-i.html)

1.2.2 Phototransduction

The steady state for rod and cone cells is one of depolarization (Figure 1.5); unstimulated photoreceptor cells have open cation channels that allow sodium and calcium to enter and potassium ions to exit the cell. The steady influx of sodium ions maintains an electrical membrane potential of -40 mV on the inner cell membrane. At this resting membrane potential, the neurotransmitter glutamate is released into the synaptic space where it is bound by receptors on post-synaptic bipolar cells. Upon stimulation, rods and cone cells revert to a hyperpolarised state which leads to a reduction in neurotransmitter release into the postsynaptic space, and subsequently gives rise to a neural message that is sent to the brain via other neuronal cells of the retina.

The first step of translating light energy into a biological signal involves the phototransduction cascade (Figure 1.6) in photoreceptor cells.This commences with the absorption of a photon by the visual pigments in photoreceptor cells. The visual pigments are the opsins (rhodopsin in rods and cone opsins in cones) which are G-protein coupled receptors, seven-pass transmembrane proteins inserted into the membranes of outer segments discs. The opsins contain the chromophore, 11-*cis* retinal, a vitamin A-derivative which is bound at the seventh intradiscal domain of the opsin molecule (Figure 1.7). On the absorption of light, 11-*cis* retinal undergoes photoisomerization to all-*trans* retinal and releases from the opsin, triggering the conformational change in the opsin GPCR [213]. This conformation change initiates a complex intra-photoreceptor signaling pathway, the phototransduction cascade, which is finally converted and amplified into an electrical response which is passed on to retinal neurons and to the brain via the optic nerve (for reviews on phototransduction, see [66], and [26]).

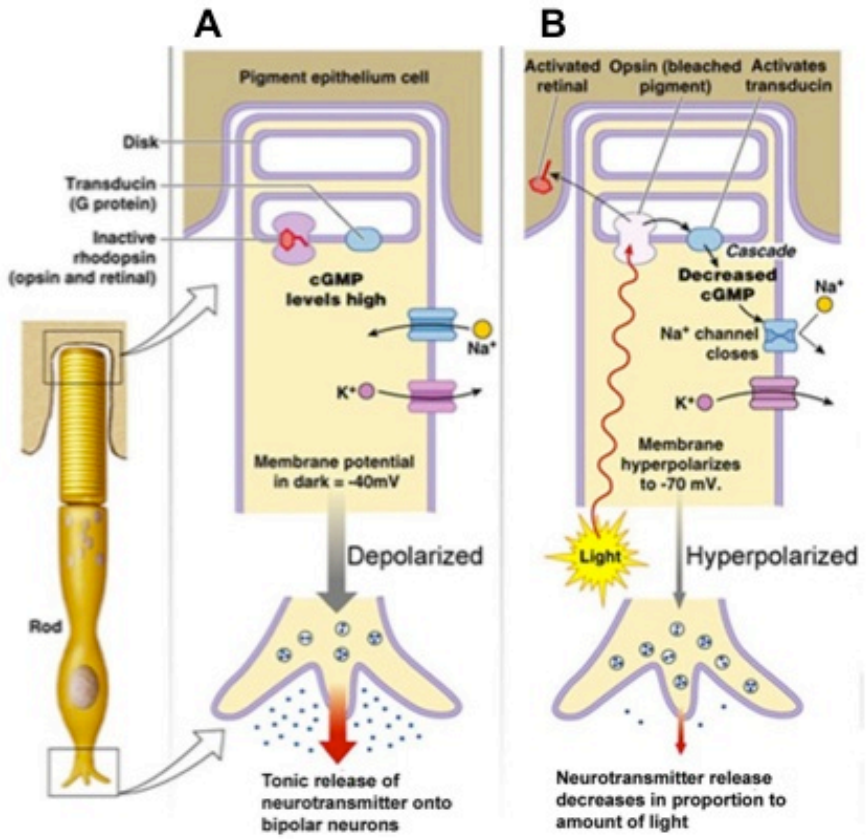

Figure 1.5. Ion transport and membrane potential in photoreceptors in dark and light conditions.

In the dark, cGMP-gated sodium channels allow an influx of Na^+ ions into the photoreceptor, maintaining a depolarised membrane potential (A). This depolarisation means that voltage-gated calcium channels remain open in the dark. Upon light excitation, reduced levels of cGMP lead to closure of Na^+ channels, and subsequent closure of voltage-gated Ca^{2+} channels, resulting in hyperpolarisation of photoreceptors (B).

(adapted from www.colorado.edu/)

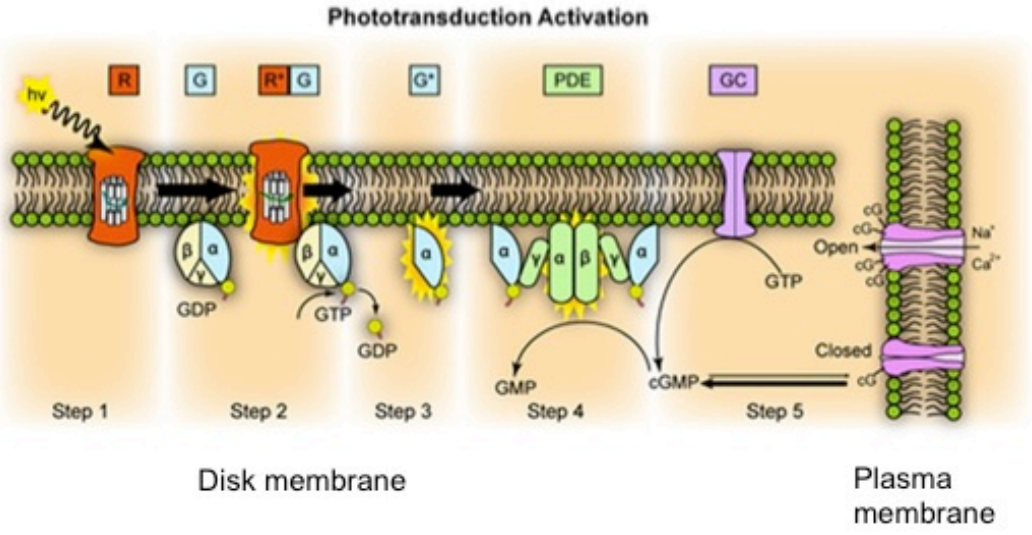

Figure 1.6 The phototransduction cascade

Representation of molecular steps in photoactivation (modified from Leskov et al., 2000). Depicted is an outer membrane disk in a rod. Step 1: Incident photon (hv) is absorbed and activates a rhodopsin by conformational change in the disk membrane to R*. Step 2: Next, R* makes repeated contacts with transducin molecules, catalyzing its activation to Gα* by the release of bound GDP in exchange for cytoplasmic GTP and dissociates from the inhibitory Gβγ dimer. Step 3: Gα* binds inhibitory γ subunits of the phosphodiesterase (PDE) activating its α and β subunits. Step 4: Activated PDE hydrolyzes cGMP. Step 5: Guanylyl cyclase (GC) synthesizes cGMP, the second messenger in the phototransduction cascade. Reduced levels of cytosolic cGMP cause cyclic nucleotide gated channels to close preventing further influx of Na^+ and Ca^{2+}.

(adapted from http://en.wikipedia.org/wiki/File:Phototransduction.png)

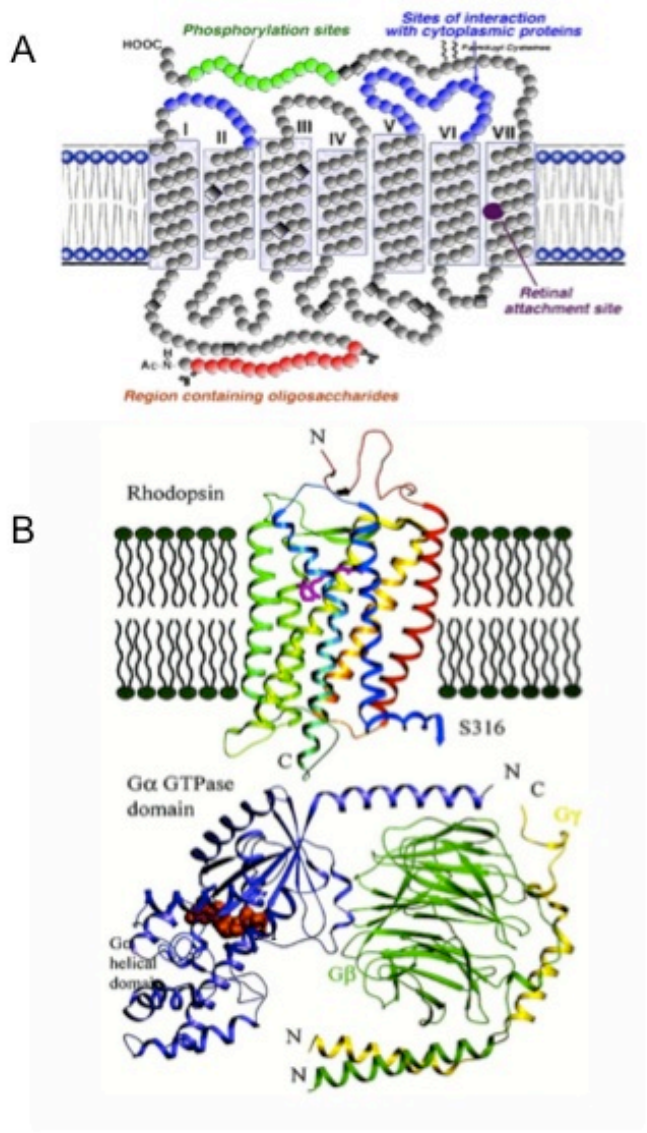

Figure 1.7. Structure of rhodopsin.

A.The secondary structure of rhodopsin is shown. Highlighted are 11-cis retinal binding site (purple), phosphorylation sites used by rhodopsin kinase (green), glycosylation sites (red), and arrestin interaction sites (blue). (From http://webvision.med.utah.edu/photo1.html.)

B.The 3-dimensional ribbon structure of rhodopsin, transducin and the lipid bilayer membrane. The protonated 11-cis retinal (structure shown in pink) is the chromophore of rhodopsin and is embedded in the pocket formed by the seven transmembrane helices that constitutes rhodopsin. Transducin (G_t) and its subunits below it. $G_t\alpha$ is colored blue, $G_t\beta$ green, and $G_t\gamma$ yellow. There is a bound GDP molecule in the $G_t\alpha$-subunit. (adapted from Hamm H.E. How activated receptors couple to G proteins. PNAS April 24, 2001 vol. 98 no. 9 4819-4821)

The conformational change in rhodopsin produces an active form of protein, metarhodopsin II [43]. Metarhodopsin II is the binding site for regulator proteins such as transducin, rhodopsin kinase and arrestin [167]. Each light-excited photopigment binds several molecules of transducin which results in a 10^2 to 10^3 amplification of the visual cascade. Transducin is a member of the guanosine-5'-triphosphate (GTP) binding protein (G protein) family that connect receptors with their second messenger pathway. On interaction with metarhodopsin II, transducin molecules exchange bound guanosine diphosphate (GDP) for guanosine triphosphate (GTP), forming an active GTP-transducin (Gα*) complex.

The newly formed Gα* molecule is an activated complex which dissociates from rhodopsin and the inhibitory Gβγ dimer. The GTP-transducin complex in turn activates phosphodiesterase (PDE) by binding to the PDE inhibitory γ-subunit. PDE enzyme is made up of three subunits, α, β and γ. The binding of the PDE γ-subunit results in the dissociation of the PDE α and β-subunits from the γ-subunit. The αβ PDE dimer hydrolyses cyclic guanosine monophosphate (cGMP) to 5'-GMP. In dark conditions, the cellular cationic channels in photoreceptor membranes are kept in an open state by bound cGMP. The decrease in intracellular cGMP following light exposure causes the cGMP-gated Na^+/Ca^+ channels to close [510]. This prevents influx of sodium ions into the rod cells, and causes hyperpolarisation of the surface membrane along the entire cell. This in turn results in the voltage-gated Ca^{2+} channels closing and a subsequent decrease in the intracellular calcium ion (Ca^{2+}) concentration. As a result, the neurotransmitter glutamate, which is continuously released in unstimulated conditions, is prevented from being released. The drop in glutamate release by the photoreceptor cells upon light exposure is sensed by bipolar cells, which respond either by depolarising or hyperpolarising their own synaptic membranes, depending whether they are ON- or OFF-bipolar cells.

To complete the phototransduction cascade, the photoreceptor must be returned to the dark state. This involves shutting down of the enzymatic cascade and restoration of intracellular cGMP levels (Figure 1.7). The low

intracellular Ca2+ concentration activates recoverin which in turn leads to the activation of rhodopsin kinase, a serine/thereonine kinase belonging to the G-protein receptor kinase family whose phosphorylation activity is limited to the active form of rhodopsin [291]. Metarhodopsin II is inactivated by the ATP-dependent phosphorylation by rhodopsin kinase which allows a second photorecovery protein, arrestin to bind. The binding of arrestin causes steric hindrance which prevents transducin to be bound to phosphorylated rhodopsin, thus halting downstream signalling in the phototransduction cascade [495]. The inactivated photopigment (phosphorylated rhodopsin) exchanges all-*trans* retinal for 11-*cis* retinal and releases arrestin.

In order for photoreceptor cells to return to their 'ground state' of depolarisation following light stimulation, the cGMP-dependent Na^{+}/Ca^{2+} channels need to reopen through the resynthesis of cGMP. The decrease in intracellular Ca^{2+} after photoexcitation causes activation of guanylate cyclase activating proteins (GCAP I and II). The GCAP proteins are part of the calmodulin-like superfamily of calcium-binding proteins [147]. At low calcium levels, the GCAP proteins bind to the intracellular domain of retinal guanylate cyclase or RetGC, thereby stimulating the resynthesis of cGMP by retinal guanylate cyclase. The increase in cGMP levels allows them to bind to the cationic channels to reopen the channels and subsequently return the photoreceptor to its initial depolarised state in the dark. The period of time following light-excitation where cells return to their ground state is known as recovery.

A key feature of phototransduction is the amplification of signal that can be achieved during the various steps in the cascade. The isomerisation of one rhodopsin molecule leads to the activation of hundreds of transducin molecules. Each activated transducin molecule then activates PDE which hydrolyses several cGMP molecules and leads to hyperpolarisation of around 1 mV. These tiers of amplification result in the sensitivity of photoreceptor cells where only a few photons are required for phtoreceptors to become hyperpolarised.

1.2.3 The visual cycle

The ability of photoreceptors to function during many hours of continuous illumination requires that the inactivated visual pigment be continuously regenerated. The inactivation of metarhodopsin II by its phophorylation and arrestin binding and subsequently by its thermal decay produces opsin apoprotein and all-trans-retinal. The conversion of all-trans-retinal back to 11-cis-retinal requires a complex sequence of biochemical reactions involving several enzymes and retinoid binding proteins. Collectively, these reactions are known as the visual cycle or retinoid cycle and take place primarily in the retinal pigment epithelium (RPE). This cycle generates a supply of new 11-cis-retinal which recombines with free opsin within the rod and cone outer segments to reform light-sensitive visual pigments (rhodopsin in rods and cone opsin in cones).The resynthesis and recovery of 11-cis retinal during the visual cycle is important to maintain sensitivity of the visual system (for reviews, see [396],[246,255].

The visual cycle (Figure 1.8) begins with the release of all-trans-retinal from metarhodopsin II and is transported out of the outer segment disc by the rim protein, ATP-binding cassette protein in the retina (ABCA4). In the photoreceptor cytoplasm, all-trans-retinal is converted to all-trans-retinol by a rod-specific dehydrogenase (t-RDH). All-trans-retinol is transferred to the RPE, bound to interphotoreceptor retinoid binding protein (IRBP). In the RPE, all-trans-retinol is then bound to the intracellular transporter protein CRBP1. The all-trans-retinol bound to CRBP1 is esterified to form all-trans-retinyl ester bylecithin retinol acyl transferase (LRAT), through the transfer of a fatty acid from phosphatidylcholine. The next reaction is the most important reaction for the whole cycle, this couples hydrolysis of the retinyl ester with all-trans to 11-cis isomerisation of retinol. The energy released by ester hydrolysis is used to power the isomerization. This reaction is mediated by the isomerohydrolase RPE65 [332,399]. Subsequent steps in the visual cycle involve the oxidation of the 11-cis-retinol to the aldehyde form, 11-cis-retinal by by 11-cis retinol dehydrogenase (c-RDH). In RPE cells, 11-cis-retinal is carried by cellular retinaldehyde-binding protein (CRALBP). To get across

the subretinal space, 11-cis retinal is bound to IRBP and transported into the photoreceptors, where it is bound to the photopigment apoprotein in the outer segment discs and forms part of the visual pigment.

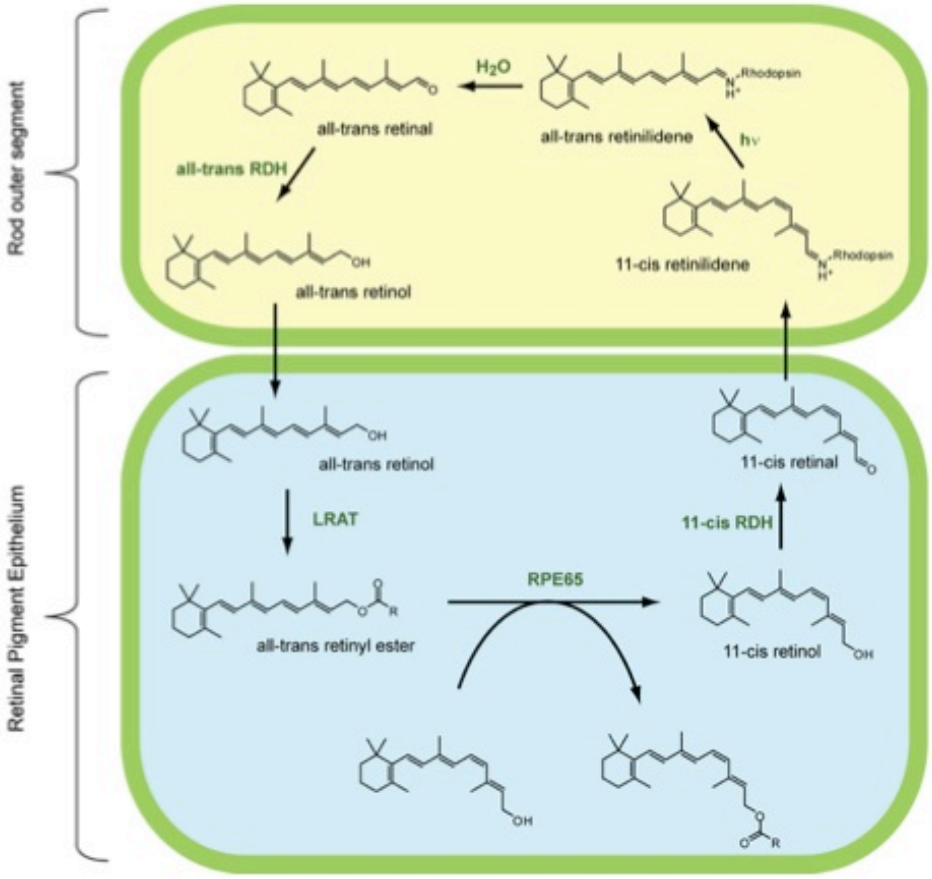

Figure 1.8 The visual cycle.

The capture of a photon causes the isomerisation of the chromophore 11-*cis*-retinal to all-*trans*-retinal of the photosensitive pigment rhodopsin in rod outer segment. Following isomerization and release from the opsin protein, all-trans retinal is reduced to all-trans retinol and travels back to the RPE to be "recharged". It is first esterified by lecithin-retinol acyltransferase (LRAT) and then converted to 11-cis retinol by the isomerohydrolase RPE65. Finally, it is oxidized to 11-cis retinal before traveling back to the rod outer segment where it can again be conjugated to an opsin to form a new, functional visual pigment (rhodopsin).

(figure from http://wiki.verkata.com/en/wiki/Visual_cycle)

The established visual or retinoid cycle described above is the only source of rod opsin regeneration. It also provides for some cone opsin regeneration as well. However, the majority of cone opsin regeneration occurs through an alternative pathway that involves interactions between cones and Muller cells (Figure 1.9)[25,304]. This alternative pathway was discovered following observations that photoisomerization rates in sunlight greatly exceeds the maximal rate of all-trans to 11-cis re-isomerization by the established retinoid cycle in RPE, and that cultured Muller cells were able to isomerize all-trans-retinol to 11-cis-retinol [98]. The cone-specific retinoid cycle is dependent on 3 unique enzymes, an all-trans-retinol isomerase, an 11-cis-retinyl synthase and an 11-cis-retinol dehydrogenase. In this cycle, all-trans-retinol leaving the photoreceptor cells is absorbed by Muller cells, where it is directly converted to 11-cis-retinol by all-trans-retinol isomerase. The isomerization of 11-trans-retinol to 11-cis-retinol is thought to be driven by mass-action through the activity of 11-cis-retinyl synthase, which uses palmitoyl-CoA as an acyl donor. The palmitoyl-CoA dependent synthesis of 11-cis-retinyl ester results in the removal of 11-cis-retinol from the reaction space so that the equilibrium between all-trans-retinol and 11-cis-retinol is shifted towards 11-cis-retinol formation. The formed 11-cis-retinyl ester is eventually hydrolysed by retinyl ester hydrolase to yield 11-cis-retinol, which is taken up by the cones. The all-trans-retinol and 11-cis-retinol within the extracellular space in transit between the cones and Muller cells are bound to IRBP. Inside cones, 11-cis-retinol is finally oxidized to 11-cis-retinal by a cone-specific 11-cis-retinol dehydrogenase. The cone-specific retinoid cycle works at 20-fold faster than the RPE-based visual cycle. The pathway can only be utilized by cones since rods are unable to oxidize 11-cis-retinol to 11-cis-retinal; this prevents isomerized retinoids from being utilized by rods under daylight conditions when rod vision is not very important. Through this cycle, rods also effectively contribute towards the regeneration of cone pigments by supplying all-trans-retinol substrate for the Muller cell isomerase. All of these features work to regenerate cone visual pigments more rapidly. This allows cone to dark adapt more rapidly than rods and also allows them to maintain an appreciable fraction of regenerated pigment even at high light intensities so that they remain responsive at almost any level of illumination[25].

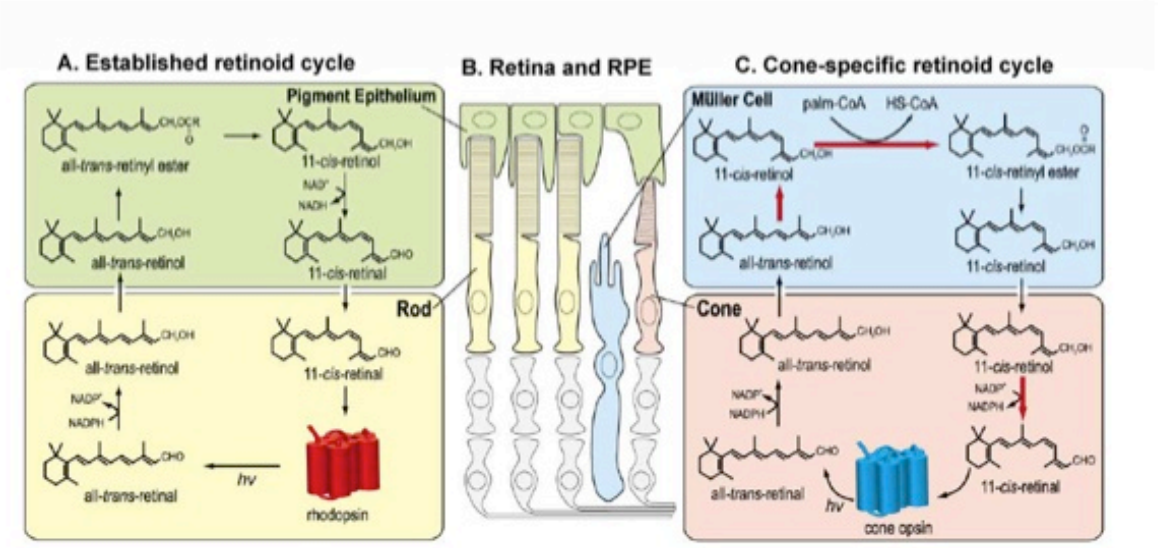

Figure 1.9. The two retinoid cycles in the retina.

The established retinoid cycle (A) provides the only source of rod opsin regeneration and some cone opsin regeneration, and takes place in the RPE(B). The cone-specific cycle (C) to regenerate exclusively cone opsin and is mediated by reactions in Muller cells and in cones.

(taken from Arshavsky V Y. 2002. Neuron 36:1-3)

The physiological processes in the phototransduction and the visual cycle depend on the close cooperation between the neuroretina and RPE. Defects in RPE-specific genes can also have deleterious effects on photoreceptor cells and vice versa. There is consequently much overlap in the clinical presentation of diseases of the photoreceptor cells and the RPE. The importance of this interaction is reflected in different retinal disorders. For example, mutations in the photoreceptor-specific gene, *ABCA4* cause a type of juvenile macular degeneration, known as Stargardt disease and presents an example where defects in photoreceptor cells leads to RPE toxicity and death which subsequently results in photoreceptor degeneration. The protein encoded by *ABCA4* is a transporter protein responsible for the ATP-dependent translocation of N-retinylidene PE, an intermediate in the visual cycle from the lumen of the outer segment discs to the photoreceptor cytoplasm. The loss of functional ABCA4 results in accumulation of these intermediates in the outer segment discs, high levels of which lead to the formation of lipofuscin. The outer segment are subsequently shed and phagocytosed by RPE cells, leading to the accumulation of toxic lipofuscin in the RPE. Patients with this type of disease present with visual loss due to loss of RPE caused by the accumulation of toxic lipofuscin in these cells [234].

Many of these defects leading to retinal degeneration are inherited. The current study is focused on one of these inherited retinal diseases that is caused by defects in a gene encoding a photoreceptor specific protein known as AIPL1.

1.3 Inherited retinal degeneration

1.3.1 Background

Inherited retinal dystrophies are a relatively common group of human diseases and include conditions such as retinitis pigmentosa (RP) and Leber Congenital Amaurosis (LCA). Approximately 1/3000 people worldwide are affected by inherited retinal degeneration. It is characterized by the progressive death of the photoreceptor cells leading to loss of vision, and there is currently no effective treatment available. Retinopathies are caused by defects in any of a number of genes and have been an area of much interest as photoreceptors are increasingly used as a model system for studying neuronal cell biology. The identification of new retinal genes has grown particularly over the last decade; to date over 197 chromosomal loci and 154 causal genes have been identified (www.sph.uth.tmc.edu/Retnet/), accounting for 50% of the genetic defects in patients (Table 1.1). Identification of these genes and elucidation of their functions have provided new insights into the understanding of disease pathogenesis and provided the impetus to develop gene-based treatment strategies. In the past decade, studies in animals have reported that some forms of inherited retinal dystrophies are amenable to gene therapy. Recently, three clinical trials treating a form of LCA using gene therapy have reported preliminary results indicating that the treatment was safe and may be beneficial [34,181,293].

The hallmark of this group of diseases is the genetic and clinical heterogeneity. Many of the mutations causing retinal dystrophies affect proteins which are specifically expressed either in photoreceptor cells or the retinal pigment epithelium. The functions of these proteins are diverse, ranging from phototransduction, visual cycle, retinal metabolism, photoreceptor structure to photoreceptor-specific transcription factors. Although the primary cell affected in retinal degeneration is often the photoreceptor cell, defects in other cell types such as the RPE or Muller cells can lead to reduced photoreceptor function and their subsequent loss (for a

review, see [467]). The mechanisms by which these disease mutations lead to death of photoreceptor cells are not completely understood. However, it is thought that in all forms of retinal degeneration, photoreceptors die via apoptosis (see [469] for a review). Mutations in the same gene can result in different diseases and different genes can share similar phenotypic features. Furthermore, allelic heterogeneity has been described where the same disease alleles can give rise to different phenotypes in patients even within the same family [432,519] (for review see[101]). The genetic and phenotypic heterogeneity of these conditions make the classification of these disorders a challenging task. Clinically, the difficulties are the overlapping signs and symptoms of the genetically distinct conditions and the intra-and inter-familial variability, in patients with the same gene defect and even in patients carrying the same mutation. Even though retinal disorders have been identified since the 19th century, the immense genetic and clinical heterogeneity present great challenges for gene identification, mutation analysis, genetic counselling and development of therapies.(for reviews see [16,54,95]).

Retinal dystrophies can be classified according to their clinical phenotype, and now increasingly according to their underlying molecular defects. Inherited retinal dystrophies can be further sub-classified according to the exact cell type affected. Rod dystrophies are caused primarily by the disruption of function and/or death of rod cells, while the cone population remains largely intact. Patients with rod dystrophies present with primarily night blindness and progressive loss of visual field. Similarly, cone dystrophies affect only cones, resulting in impairment of colour vision and visual acuity, but night vision and peripheral visual fields remain unaffected. Most of the inherited retinal dystrophies involve a degree of loss of both rods and cones, and are therefore called rod-cone or cone-rod dystrophies, depending on which photoreceptor subtype is primarily affected. Notably, in advanced stages of these retinal dystrophies, both types of photoreceptor cells are involved resulting in loss of central vision which is the primary cause of loss of quality of life in these patients. These conditions can be further classified according to whether these disorders present as stationary or

progressive conditions; stationary disorders are caused by dysfunctional photoreceptors and have a stable disease, while progressive disorders are being caused by death of photoreceptors due to their underlying mutations.

The inherited retinopathies can be classified as autosomal recessive, autosomal dominant or X-linked disorders. The main types of hereditary retinal dystrophies include RP, infantile onset LCA, achromatopsia, Stargardt's macular dystrophy and cone-rod dystrophies, and the commonest mode of inheritance in majority of these disorders is autosomal recessive. Table 1.1 summarizes the various disease genes according to sub-type of retinal degeneration they are associated with. Retinitis pigmentosa is the commonest form of hereditary retinal dystrophy affecting 1.5 million people worldwide [54]. However, it is the most severe form of inherited retinal blindness, LCA that has been the main focus of ocular gene therapy in the past decade. In treating this condition, it is hoped that this will enable further treatments to be developed for other forms of genetic eye diseases.

Disorder	Number of Loci	Number of genes identified
Retinitis pigmentosa, autosomal recessive	25	22
Retinitis pigmentosa, autosomal dominant	17	17
Retinitis pigmentosa, X-linked	6	2
Cone-rod dystrophy, autosomal recessive	7	6
Cone-rod dystrophy, autosomal dominant	7	5
Cone-rod dystrophy, X-linked	1	0
Leber congenital amaurosis, autosomal recessive	12	12
Leber congenital amaurosis, autosomal dominant	2	2
Congenital stationary night blindness, autosomal recessive	6	6
Congenital stationary night blindness, autosomal dominant	1	1
Congenital stationary night blindness, X-linked	2	2
Macular degeneration, autosomal recessive	2	2
Macular degeneration, autosomal dominant	13	7
Chorioretinal atrophy, autosomal dominant	1	1
Syndromic/systemic diseases with retinopathy, autosomal recessive	30	24
Syndromic/systemic diseases with retinopathy, autosomal dominant	8	7
Syndromic/systemic diseases with retinopathy, autosomal X-linked	3	2
Bardet-Biedl syndrome, autosomal recessive	12	12
Usher syndrome	11	9
Optic atrophy, autosomal recessive	2	1
Optic atrophy, autosomal dominant	3	1
Optic atrophy, X-linked	1	0
Other retinopathies, autosomal recessive	15	12
Other retinopathies, autosomal dominant	10	5
Other retinopathies, X-linked	8	7
Other retinopathies, mitochondrial	7	7
Ocular-retinal developmental disease, autosomal dominant	1	1
Totals **Autosomal recessive diseases: 106 genes identified** **Autosomal dominant diseases: 47 genes identified** **X-linked diseases: 13 genes identified** **Mitochondrial and other: 7 genes identified**	213	173

Table 1.1 1 Summary of the number of genes causing inherited retinopathies according to disease category. The table shows the number of loci and genes that have been found which are associated with the various types of inherited retinal disorders. (RetNet, last up-dated 8 Jan 2010)

1.3.1 Leber Congenital Amaurosis

LCA is the most severe form of retinal dystrophy, causing loss of vision before the age of 1 year and accounts for 5% of all inherited retinopathies. It is the commonest cause of congenital blindness in children accounting for 10-18% of cases[426]; with a population incidence of about 1/30000 [235], approximately 200,000 children worldwide suffer from this hereditary retinal dystrophy. It was originally described by Theodore Leber in 1869 as a congenital form of retinitis pigmentosa, presenting with blindness at birth with an essentially normal retina in appearance, nystagmus and sluggish pupils. This clinical definition was later modified to include a non-recordable or extinguished electroretinogram by Franceschetti and Dierterle in 1956[143]. Compared with other retinal dystrophies such as RP, a greater proportion of the causative genes have been identified and there are more studies demonstrating genotype-phenotype association in LCA, allowing for the prediction of the affected gene from the phenotypic characteristics. As it is well characterised, LCA has been a focus for preclinical research and the development of treatments. It is the first form of retinal dystrophy for which clinical trials of gene therapy has been developed. Success in these trials will form a stepping stone for other retinal diseases to be treated with gene therapy.

1.3.1.1 Molecular genetics of LCA

LCA is a genetically and clinically heterogenous disease. To date, more than 400 mutations have been identified in 14 genes associated with LCA (Figure 1.10A)(for a review, see[101]). A small number of dominant cases of LCA has been reported, and are associated with 2 genes, *CRX* and *IMPDH1* [59,365,406,443]. Apart from these, mutations in 12 genes, *GUCY2D, AIPL1, CRB1, RPGRIP, RPE65, RD3, RDH12, LCA5, CEP290, LRAT, TULP1* and *MERTK* have been found to be associated with the more

common type of autosomal recessive LCA. The relative disease load varies for different genes [95,235] and is shown in Figure 1.10A. Together, the currently known LCA genes account for 60-70% of the cases while the remaining 30% of cases await discovery [236]. *CEP290*(15%) *GUCY2D* (12%) and *CRB1* (10%) are the most frequently mutated genes and account for a large proportion of LCA cases.

LCA genes encode a wide variety of retinal proteins that participate in a plethora of retinal cycles and pathways (Figure 1.10B). LCA-associated proteins such as *GUCY2D* (retinal guanylate cyclase) and *AIPL1* are involved in the phototransduction pathway; GUCY2D (retinal guanylate cyclase) is an enzyme that resynthesizes cGMP required for the recovery of the dark state after phototransduction, while AIPL1 (aryl hydrocarbon receptor interacting protein-like 1) is involved in biosynthesis of phosphodiesterase. Three LCA genes encode proteins that play important roles in visual retinoid recycling; *RPE65* encodes a microsomal protein involved in the isomerization of all-trans-retinol to all-cis-retinol, *RDH12* encodes a retinol dehydrogenase that catalyzes the reduction of all-trans retinal to all-trans retinol and protects cells against the leakage of toxic all-trans retinal into the inner segments [290], and *LRAT* encodes a protein that catalyzes the synthesis of retinyl esters in the visual cycle and is a part of the process to recycle used all-trans retinal to the active chromophore 11-cis retinal [40,198]. Other genes are involved in the development of the retina such as *CRX* (cone-rod homeobox) which encodes a transcription factor that is crucial for outer segment development as it transactivates a number of key retinal proteins, while *CRB1* (Crumbs homolog protein) is critical for photoreceptor morphology and retinal architecture by ensuring correct functioning in cell-to-cell adhesion, intercellular signalling and directional transport of molecules. IMPDH1 directs the biosynthesis of guanine, a key component of DNA and cGMP which plays a vital role in phototransduction. Several LCA proteins localize to the connecting cilia of photoreceptors and are involved in protein trafficking such as RPGRIP (retinitis pigmentosa GTPase interacting protein1), CEP290 (centrosomal protein 290) and LCA5 (lebercilin), highlighting the emerging role of the ciliary processes in the

pathogenesis of LCA. CEP290 likely participates in transport of phototrasduction proteins through the ciliary apparatus of the photoreceptor. Finally *RD3* encodes a photoreceptor nuclear protein whose function is not yet known.

Recently, it has been suggested that phenotypes caused by mutations in a single gene become more severe when a mutation in an additional gene is also present and such additional gene is known as a modifier gene. Examples of modifier genes have been described in Stargardt's disease [521] and Usher's syndrome [3]. A systematic analysis of all known mutations in LCA genes revealed that a greater number of LCA patients carry a third variant or disease allele than might be expected by chance alone [519]. Family members who carried a third disease allele in another gene had a more severe phenotype than family members who did not carry this allele, suggesting that these alleles may act as genetic modifiers [432,519]. Clearly, the manifestation of the disease depends much on interplay between different genes or loci and also influences from by external factors such as the environment.

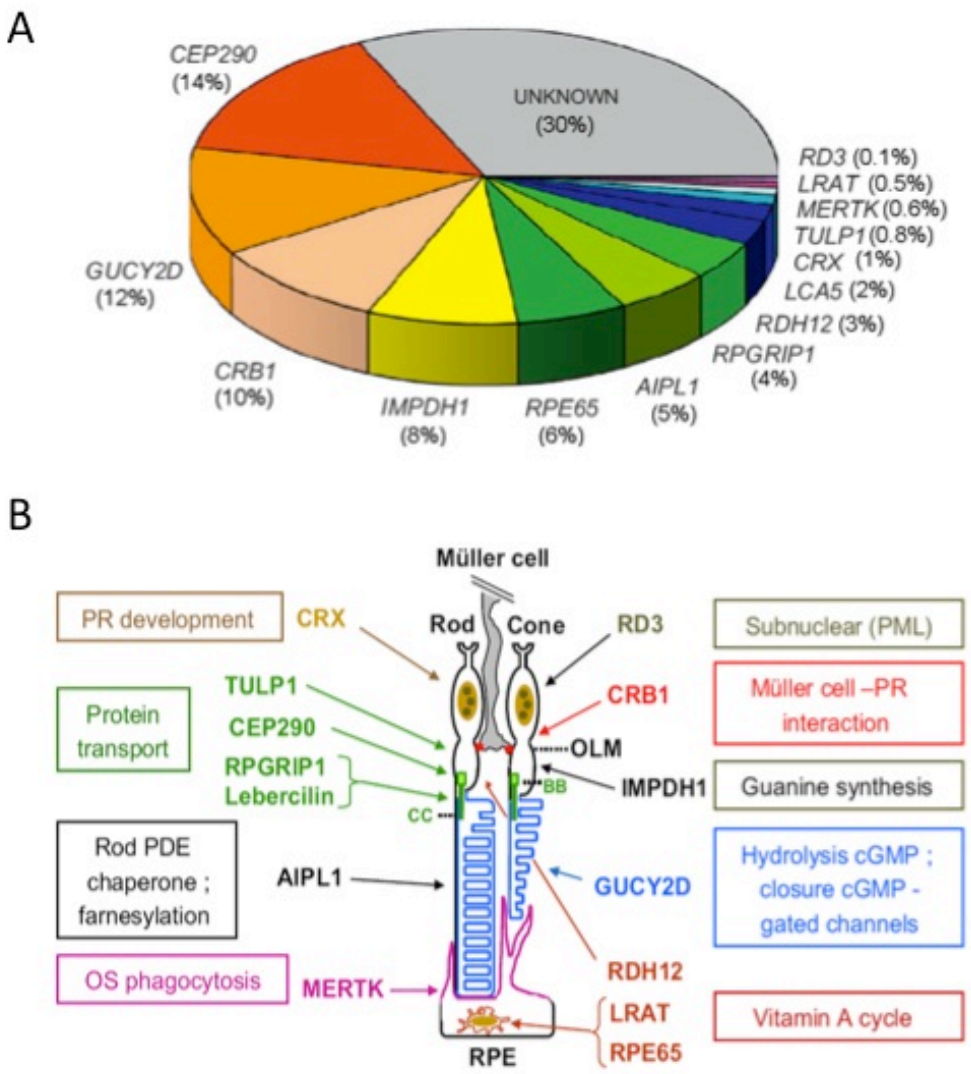

Figure 1.10. Leber congenital amaurosis (LCA) genes.

A.The prevalence of LCA-associated mutations for the 14 known genes to date is shown. Together, these 14 genes account for 70% of all LCA cases while the causative genes in 30% of cases still await discovery.

B. The localization of the proteins expressed by the LCA genes are shown. These proteins can grouped into 9 different groups according to their functions. AIPL1 and GUCY2D is predominantly located in photoreceptor outer segments, LRAT and RPE65 are located in the endoplasmic reticulum of RPE cells, CEP290 reside in the basal bodies, RPGRIP and lebercillin (LCA5) are localised to the connecting cilia (cc), IMPDH1 and RDH12 are both predominantly located in rod and cone inner segments.

PR, photorecetor; cc, connecting cilium; bb, basal bodies; OLM, outer limiting membrane; OS, outer segment; IS, inner segment.

(Taken from Hollander *et al*.2008. Prog.Retin.Eye Res.27:391-419)

1.3.2.2 Clinical features and genotype-phenotype correlation in LCA

As well as having diverse genetic causes, LCA is clinically heterogenous, making clinical diagnosis a difficult task for the practising ophthalmologist. The LCA phenotype overlaps with many other similar but separate retinal diseases, and several syndromic disease can have an “LCA-like ocular phenotype” that may initially present without the systemic features, but these develop and dominate the phenotype later on. The most important of these include Alstrom syndrome, Batten disease, Joubert syndrome, peroxisomal diseases and Senior-Loken syndrome. All of these syndromic diseases present in infancy like LCA with early central visual loss and nystagmus, but these children later develop the full syndrome with multisystem disorders. The underlying pathology, molecular defects, prognosis, inheritance and treatment of these overlapping syndromic and non-syndromic ocular diseases are entirely different from those of LCA. It is crucial to separate these overlapping eye diseases from LCA, and rapid and accurate clinical diagnosis is therefore essential.

The classical LCA patient presents early in life, at about 6 weeks with severely reduced vision, nysytagmus, poor fixation, amaroutic pupils, oculodigital behaviour and the fundal appearance is frequently unremarkable. Manifest visual function and visual acuity in LCA patients can range widely, usually from 6/60 to light perception or no perception of light. Longitudinal studies of visual function in LCA patients performed before the disease gene were identified, found that patients fell into three categories of visual prognosis. The majority (75%) of LCA patients displayed a relatively stable course, a smaller group (15%) showing visual deterioration, and the smallest group (10%) had measureable improvement in function [61,149,184]. Later, it has been found that the natural history of visual function in LCA patients could be correlated with certain genotypes (Figure 1.11). Patients with *CEP290* and *GUCY2D* mutations appear to have poor but stable visual function [235]. LCA patients with *AIPL1, RDH12* and *RPGRIP1* mutations have progressively deteriorating visual function with age

[104,236]. Patients with *CRB1* and *RPE65* mutations exhibit mild improvements in early ages, but then decline mainly during school years after a period of stability [285,517]. The reason for this transient improvement is not fully understood but a part of it may be due to postnatal physiological cone maturation. At young ages, patients with *RPE65* mutations also appear to have better visual function than is than is typically associated with other genetic forms of LCA, and a number of patients maintain some useful visual function beyond the second decade of life [468].

Fundal appearances range from essentially normal to peripheral pigmentation, vessel attenuation, and varying chorioretinal and macular atrophy. Other retinal features include pseudopapilloedema of the optic disc, maculopathy, macula coloboma, bone spicule pigmentation, nummular pigmentation, salt and pepper pigmentation, yellow confluent spots, white retinal spots, preserved para-arteriolar RPE (PPRPE) and Coats reaction. Despite the fact that hereditary retinal dystrophies and LCA gene defects converge on a limited number of apoptotic death pathways and that the highly specialized retina only has a limited number of injury responses, it appears possible to identify the causal gene based on the retinal appearance or a phenotypic parameter in certain cases. Genotype-phenotype correlations have been described in the retinal appearances and longitudinal changes in visual function [236]. These are summarised in Table 1.2. Patients with *CRB1* mutations often have a thickened immature, poorly laminated retina on optical coherence tomography (OCT) scanning and evidence of PPRPE in the fundus [205]. Improving visual function and a translucent retina suggests *RPE65* involvement [285], while a rapidly declining visual function and maculopathy suggests *RDH12* [427]. Severe visual loss and an essentially normal retinal appearance suggests defects in either *CEP290* [100] or *GUCY2D*[103], while severe visual loss with a pigmentary retinopathy suggests *RPGRIP* [103]. Figure 1.11 shows examples of the retinal appearances of LCA patients with defects in various genes, highlighting the retinal differences associated with the genotypes.

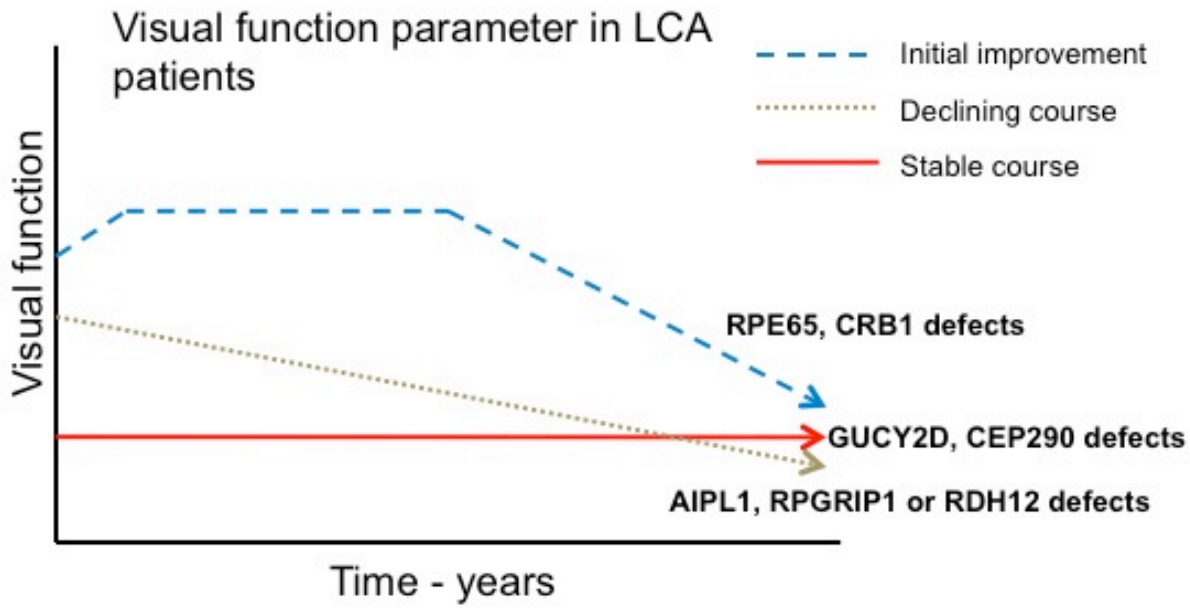

Figure 1.11 Visual evolution of three types of LCA.

Visual function in patients with mutations in GUCY2D and CEP290 exhibit a stationary course where the visual function remains relatively stable, while patients with AIPL1, RPGRIP1 and RDH1 mutations have a degenerative type of evolution with steadily declining vision . Patients with RPE65 and CRB1 mutations exhibit the improving type of visual function, which improves initially, remains stable and then declines.

(adapted from Koenekoop R K.2004. Surv.Ophthalmol.49:379-398)

Table 1.2 Summary of phenotype-genotype correlations in LCA

Phenotype characteristic	**Probable gene defect**
Preserved para-arteriolar retinal pigment epithelium (PPRE)	CRB1
Nummular retinal pigment	CRB1
Thickened retina on OCT	CRB1
Coats-like vasculopathy	CRB1
Severe early visual loss with relatively normal fundus	GUCY2D, CEP290
Severe early visual loss, progressive course and retinal pigmentation	RPGRIP1
Severe early visual loss, keratoconus, variable maculopathy, optic disc pallor	AIPL1
Moderate visual loss, maculopathy	CRX
Early moderate visual loss with progressive deterioration, maculopathy, marked retinal pigmentation	RDH12
Relatively stable vision, blond fundus	LRAT
Transient visual improvement followed by decline, translucent RPE	RPE65, LRAT
Pseudopapilloedema	LCA5

Figure 1.12. Phenotypic variability in LCA patients associated with the various genotypes.

The retinal appearances of patients with LCA due mutations in 12 causative genes vary considerably and range from near normal retinal appearances to retinal vessel attenuation, maculopathy, pseudopapilloedema of the optic disc, bone-spicule pigmentation, nummular pigmentation, salt and pepper pigmentation, yellow peripheral spots, chorioretinal atrophy, preserved para-arteriolar RPE (PPRPE) and Coats reaction.

(figures adapted from Hollander, A.I., *et al.* Prog Ret Eye Res. 2008, Dharmaraj *et al.* Arch Ophthalmol 2004, Schuster *et al.* IOVS 2007, Lorenz *et al.* IOVS 2000)

Electroretinography (ERG) is a method of recording mass retinal electrical impulses generated by photoreceptors in the retina on exposure to light stimulus and provides a measurement of the visual function in tested subjects. Indirectly, the ERG response gives an indication of the progress of photoreceptor cell loss over time (for a review, see {Holder, 2001 708 /id}) and can be used as an uninvasive means to monitor the effects of treatment over time. The electrical response generated by the retina in response to light is measured by the single flash electroretinogram which has 3 main components: The initial negative deflection is known as the a-wave and is generated by the depolarization of photoreceptors following the closure of cyclic GMP channels in the outer segments in response to photon capture. It reflects the level of phototransduction that occurs in the retina as a whole. The a-wave is followed by a large positive deflection known as the b-wave which is generated by Muller and bipolar cells in the inner nuclear layer. The b-wave amplitude depends on the degree of depolarization that has taken place in photoreceptors. Hence, the b-wave indirectly correlates with the number of functional photoreceptors in the retina. The final component of the ERG is the c-wave which is a positive signal that occurs near the end of the tracing and is largely elicited by the retinal pigment epithelium (RPE). The disappearance of the c-wave is an indication of the disturbed function of the RPE, and is often seen at an early stage a disease since RPE is integral to photoreceptor homeostasis. A series of little wavelets seen on the upslope between the a and b-waves of an ERG trace are known as oscillatory potentials. They represent postsynaptic neuronal activity in the inner retina, and reflect the health of the inner layers of the retina{Wachtmeister, 1998 707 /id}. In ERG analysis, the waveform amplitude and implicit time are normally measured. By varying the conditions of testing and adaptation, the ERG can measure rod and cone responses separately; the scotopic ERG which is performed after a period of dark adaptation measures rod responses and maximal combined response when elicited with a bright white flash, while the photopic ERG or flicker ERG isolates the cone responses. The ERG responses are classically absent or severely diminished in LCA patients. This is one of the basic features of the condition. ERG analysis of family members may also aid the identification of disease genes as cone

ERG dysfunction has been found in heterozygous carriers of GUCY2D mutations, and rod and cone ERG dysfunction has been found in heterozygous carriers of RPGRIP mutations. The advent of more detailed imaging technology has enabled further characterisation of retinal phenotype in LCA patients. Fundus autofluorescence measures lipofuscin accumulation in the RPE which is related to photoreceptor disc shedding. This allows for the visualization of disease-specific distribution of lipofuscin in the RPE which is not yet visible on ophthalmoscopy. Notably, reduced autofluoscence has been described in LCA patients with compound heterozygous or homozygous *RPE65* mutations, suggesting a lack of lipofuscin manufacture due to the loss of normal functioning of the visual cycle.

Optical coherence tomography (OCT) is a non-contact, non invasive imaging technique used to obtain cross-section images of the retinal architecture at much higher longitudinal resolution of about 10 μm in the retina. It is a useful tool in determining the extent of retinal integrity in selected retinal dystrophies and the retinal response to the genetic lesion. Work by Jacobson *et al.* using OCT imaging demonstrated that patients with *RPE65* mutations had measurable outer nuclear layer (ONL) and many had normal foveal thickness [202]. This study showed that despite advanced age and visual loss, retinal dystrophy patients with RPE65 defects have viable photoreceptors and residual cone photoreceptor structure and function persisted for decades. This finding suggested that these patients may be amenable to gene replacement therapy and visual improvement may be observed if treatment was performed at an early age. The study was instrumental in supporting clinical trials of gene replacement therapy in LCA patients with *RPE65* mutations. OCT studies of LCA patients with *CRB1* mutations on the other hand revealed a lack of normal retinal lamination, increased overall retinal thickness apart from the loss of the ONL at the foveal centre [205]. Similarly, LCA patients with *RDH12* mutations had thick retinas with the same disorganised pattern which is evidently different from *RPE65*-associated disease [207]. These findings indicate that these patients may not be particularly suitable for gene therapy as there is early derangement of the retinal structure and lack of viable photoreceptor cells

remaining in the retina. LCA patients with *RPGRIP* mutations showed normal ONL measurements at the foveal centre, although measurements rapidly declined with increasing eccentricity from the fovea [206]. LCA patients with *CEP290* mutations unexpectedly retained photoreceptors in the cone-rich fovea, despite severe visual loss [88], while patients with *GUCY2D* defects were found to contain intact cone photoreceptors up to 7 years of age [321]. LCA patients with mutations in other genes such as *AIPL1, CRX, IMPDH1, LCA5* and *RD3* have yet been analysed in the same way. These studies suggest that despite the presence of retinal modelling in LCA, viable photoreceptors appear to remain in certain forms of disease until relatively late in the disease process, providing a window of opportunity for therapeutic intervention. These types of genotype-phenotype studies must be viewed with caution, however, as the connection between gene defect and resulting phenotype is not straightforward. Environmental, genetic background, modifier alleles and overlap between gene defects affect this relationship, while different mutations in the same gene can give rise to different phenotype. The importance of genetic testing and being able to determine a molecular diagnosis in a complex and varied group of diseases such as retinal dystrophies is obvious. It allows for more specific characterisation of the disease than the clinical phenotyping can provide, facilitates information sharing, prognostication and helps to establish a genotype-phenotype correlation system. It will also aid in identifying new retinal genes and in the selection of candidates for gene-base treatments in the future.

Histopathological studies of LCA in human tissue are scarce, understandably due to the difficulty in obtaining specimens. To date, only thirteen pathological specimens from LCA patients have been described in the literature and three possible disease categories have emerged from the analysis of these studies. Seven cases appeared to represent degenerations in which the photoreceptor, inner retinal layer and RPE layer showed extensive atrophy and gliosis [138,381,453]. Three cases appeared to represent aplasias, and showed complete absence of the photoreceptor layer or the presence of very unusual looking, primitive cuboidal cells in this layer [141,157,483]. Finally, a further three cases suggested biochemical

dysfunction or dysplasia as the disease process. In these specimens, almost the entire retina was retained; the inner retinal layers, the photoreceptor layer and the RPE appeared intact despite the fact that the globes came from adults who were blind from LCA since young [141,191,235,321]. Moreover, in six of the thirteen globes, the inner retina was essentially normal in appearance and architecture based on microscopic evaluations. These observations suggest that some forms of LCA may still respond favourable to treatment based on the presence of an intact retinal structure even in advanced stages of disease. Unfortunately, most of the cases in these studies were not genotyped, thus precluding any useful histopathology-genotype correlations which may aid towards identifying the forms of LCA which may be amenable to treatment.

1.3.2.3 *AIPL1* mutations in inherited retinal dystrophies

Mutations in the aryl hydrocarbon receptor-interacting protein-like 1 gene (*AIPL1*) are thought to cause approximately 7-8% of LCA worldwide [103,174,444]. The gene was discovered during an effort to identify and map genes expressed exclusively in the retina and pineal gland as candidates for inherited retinal degeneration. *AIPL1* was mapped to chromosome 17p13.1, near the candidate region of several inherited retinal degenerations and was the fourth gene to be associated with LCA [440]. The *AIPL1* gene encompasses six exons encoding a protein of 384 amino acids in length. The AIPL1 protein is found exclusively in photoreceptors [475] and recent studies have shown that AIPL1 is expressed in both rods and cones where it is essential for the survival and function of photoreceptors [65,232].

It has been suggested that AIPL1 could fulfil a molecular chaperone function for retinal protein folding [79]. By sequence comparison, AIPL1 is related to the FK-506-binding protein (FKBP) family which comprise the immunophilin superfamily of proteins[439], many of which function as specialised chaperones. The chaperone function of this protein family does not typically act at the step of initial polypeptide folding, but rather assist client proteins in

later stages of maturation, subunit assembly, transport and degradation [511]. Many such client proteins are components of signal transduction pathways. The protein sequence of AIPL1 includes three consecutive tetratricopeptide repeat (TPR) motifs, a 34-amino acid degenerate motif comprising of a pair of anti-parellel α-helices (Figure 1.13A). TPR domains act as molecular scaffolds mediating protein interactions and are conserved in structurally related proteins that participate in diverse biological functions, including the coordination of multiprotein complex assembly and protein translocation [55]. The presence TPR motifs makes AIPL1 more closely related to the larger members of the FKBP family (Figure 1.13B) such as FKBP52 , which forms a complex with the large heat shock protein Hsp90 and functions as a specialised co-chaperone [511]. AIPL1 also shares 49% amino acid identity with aryl hydrocarbon receptor interacting protein (AIP), which is a known specialised chaperone required for bonding to aryl hydrocarbon receptor, a transcription factor that shuttles in and out of the nuclei [73,370]. These sequence similarities suggest that AIPL1 may also function as a specialised chaperone in photoreceptor cells, facilitating protein translocation and as a component of chaperone complexes. A 56-amino acid polyproline-rich sequence is present at the carboxyl-terminus of human AIPL1 protein (Figure 1.12B). This sequence forms a hinge region in the protein and is primate-specific. Sequence comparison between primate species suggest that there is a high amount of sequence conservation within this hinge region between primates (squirrel monkey, rhesus monkey, and humans). The function of this region is unknown but similar sequences are found in proteins acting in processes requiring rapid recruitment or interchange of several proteins, such as signalling cascades or initiation of transcription [223].

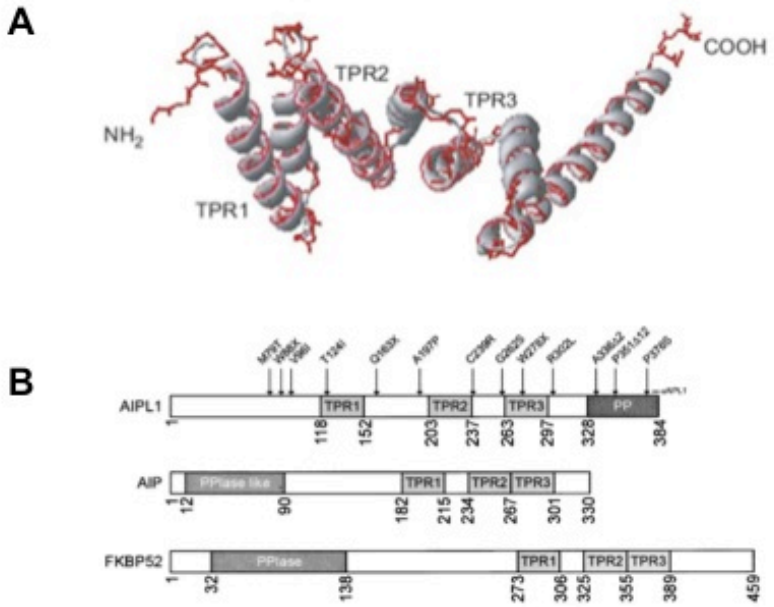

Figure 1.13.

A. Homology model of the AIP TPR domain (ribbon, grey) generated by automated comparative protein moddling server SWISS-MODEL (www.expasy.org/swissmod/SWISS-MODEL.html) from the FKBP52 TPR domain (backbone, red).

Taken from Van der Spuy. *Experimental Eye Research*, 2006

B. Schematic representation of AIPL1, AIP and FKBP52. The TPR domain is conserved in all three proteins. A primate-specific poly-proline (PP) rich region is present at the C-terminus of AIPL1. The common mutations in AIPL1 are shown.

PP, polyproline-rich sequence; PPIase,peptidyl prolyl isomerase domain.

Taken from Van der Spuy and Cheetam. *Biochemical Society Transactions*,2004.

Several possibilities have been proposed regarding the essential role of AIPL1 in the retina. Using yeast two-hybrid analysis, AIPL1 has been found to interact with Nedd8-ultimate buster protein-1 (NUB1), a ubiquitously expressed protein thought to play an important role in regulating cell cycle progression and cell signalling [7]. Through its association with NUB1, AIPL1 has been predicted to be involved in the regulation of these events. While AIPL1 is predominantly cytoplasmic, NUB1 is predominantly nuclear. Co-transfection of AIPL1 with GFP-tagged NUB1 demonstrated that AIPL1 is able to modulate the nuclear translocation of NUB1 from the nucleus to cytoplasm, and suppress the formation of inclusions by NUB1 fragments and redistribute these fragments in the cytoplasm [476]. Using site-directed mutagenesis, known pathogenic variants of *AIPL1* were generated and co-transfected into neuroblastoma cells to characterise the effect of these mutations on the ability of AIPL1 to modulate NUB1 localization and inclusion formation. This function of AIPL1 was shown to be severely compromised by the expression of some of the disease-associated mutant AIPL1 proteins such as the pathological mutation, W278X; other mutations such as R302L resulted in less efficient nuclear translocation of NUB1[476]. However, the impact of the AIPL1-specific NUB1 modulatory function on biological events downstream of NUB1 is unknown.

Yeast two-hybrid analysis also demonstrated that AIPL1 is able to interact with and aid in the processing of farnesylated proteins in the retina [393]. Farnesylation is a specific type of prenylation. In the retina, protein prenylation facilitates protein-protein and protein-membrane interactions, and is important for the maintenance of retinal and photoreceptor cytoarchitecture. Inhibition of prenylation has been shown to cause photoreceptor outer segment degeneration [378]. The ability of AIPL1 to interact with and enhance the processing of farnesylated proteins is severely compromised by certain pathogenic mutations such as M79T and the non-functional W278X. Some AIPL1 mutants such as A197P, are partially defective in their ability to facilitate the processing of farnesylated proteins, but are functional with respect to their effect on NUB1. Other mutants such as R302L on the other hand, do not show any defect in protein farnesylation

but are compromised in NUB1 function. Retinal proteins which are known to be farnesylated include cGMP PDE-α subunit, transducin and rhodopsin kinase [23,148,200,252].

Yeast two-hybrid studies however are not always reliable, and the findings from these *in vitro* studies of AIPL1 interactions do not appear to be supported by *in vivo* studies using animal models. Three mouse models of LCA have been generated with either complete or partial loss of AIPL1. Two *Aipl1 -/-* mouse strains carry targeted disruptions in the Aipl1 gene and produces no AIPL1 [119,392]. Retinal degeneration in these models is extremely rapid degeneration in this model (all photoreceptors are loss by three weeks of age). The other model, the *Aipl1 h/h* mouse contain an *Aipl1* hypomorphic mutation with reduced AIPL1 levels and has a slower rate of photoreceptor degeneration [282]. In both models, normal retinal histology and morphological photoreceptor development were observed at birth. Hence, despite evidence that seems to suggest a role for AIPL1 in cell cycle regulation and retinal development, the absence of gross abnormalities in young AIPL1-deficient mice indicate that AIPL1 is not essential for retinal proliferation or the commitment to photoreceptor cell fate. Moreover, retinal degeneration in both models did not begin until postnatal 8-10 days in the *Aipl1 -/-* mouse and 12 weeks after birth in the *Aipl1 h/h* model.

Analysis of the null and hypomorphic mouse models showed that retinal degeneration in *AIPL1* mutations is due to disturbance in the biosynthesis or stability of rod photoreceptor cGMP PDE (PDE6). Almost no PDE6 is found to accumulate in the *Aipl1* -/- mouse [392]. In the *Aipl1 h/h* mouse, there is a decline in PDE level which is proportional to the reduction in the level of AIPL1, and all three subunits α, β and γ of PDE6 are similarly affected. This observation is highly specific for PDE, as analysis of a large number of other photoreceptor proteins found no change in their expression levels in the *Aipl1 h/h* mouse [282]. Analysis by semiquantitative RT-PCR found no substantial decrease in the mRNA levels of any of the PDE6 subunits, indicating that AIPL1 acted to modulate PDE6 levels at a post-translational stage. Given the homology of AIPL1 to other members of the FKBP family, it

would seem reasonable to presume that AIPL1 functions as a specialised chaperone to assist in PDE6 biosynthesis. As a specialised chaperone, it is likely that AIPL1 plays a role in the final maturation or trafficking step of PDE6 synthesis rather than as a folding accessory protein. In all the mouse models, it was shown that apart from PDE6, levels of expression and subcellular distributions of all other retinal proteins, including rhodopsin kinase and transducin which are normally farnesylated, were unaffected [282,392]. These observations thus rule out a generalized defect in protein farnesylation in mutant photoreceptors. The link between AIPL1 and PDE6 has since been further elucidated, despite the destabilization of PDE6 in the absence of AIPL1, AIPL1 is not involved in the synthesis individual PDE6 subunits. AIPL1 has been found to interact with the α-catalytic subunit of rod PDE and is required for the proper assembly of functional PDE6 subunits[240]. In the absence of AIPL1, rod PDE6 subunits are rapidly degraded by proteosomes.

Recently, through the development of a novel transgenic mouse that expresses human *AIPL1* solely in rod photoreceptor cells (tg *hAIPL;Aipl1-/-*), it was shown that AIPL1 was also crucial to the survival and function of cone photoreceptors[232]. Although the cones lacking AIPL1 in this transgenic model developed normally, they were not functional and eventually degenerate in the absence of AIPL1. The degeneration of cones in this novel model was however significantly slower in the presence of viable rods, in contrast to the *Aipl1-/-* mouse where rods also degenerate. Further analysis by demonstrated that cone PDE6 levels was severely reduced in the retinal extracts although cone PDE mRNA was not altered despite the lack of AIPL1. This indicated that the reduction of cone PDE6 levels occurred at a post-translational level, in a similar way seen in rods lacking AIPL1[282]. Since *AIPL1*-deficiency did not cause developmental defects in cones, the lack of cone function this model was thought to be due to disruption in phototransduction consequent to the severe reduction of cone PDE6. It has been suggested that the slow degeneration of cones in this model may be analogous to the cones in the fovea of patients with *AIPL1* defects surviving

for a longer period of time[232]. This may offer an extended window for treatment that allows the preservation of cone vision.

1.3.2.4 Molecular genetics of *AIPL1* mutations

Genetic defects in *AIPL1* cause a heterogenous set of clinical conditions depending on the nature of the alleles. *AIPL1* mutations have been estimated to cause approximately 7% of recessive LCA cases [442] and have also been associated with cone-rod dystrophy and retinitis pigmentosa [103,441]. To date, at least 20 different disease-causing AIPL1 mutations have been identified (HGMD; www.hgmd.org). Often the variability in phenotype can be explained by the type of mutation. Some mutations lead to truncation of the reading frame and hence are expected to result in complete absence of a functional protein, such as nonsense mutations and splice site mutations. In these cases where there is no AIPL1 function, a severe phenotype results. On the other hand, missense mutations may not abolish protein function completely and may therefore be associated with a milder phenotype [8,393,476].

Most of the gene defects in *AIPL1* identified to date are homozygous or compound heterozygous mutations in an autosomal recessive pedigree. A homozygous mutation is present when identical sequence variants are found in both alleles, while a compound heterozygous mutation comprises of two different sequence variants found in the maternal and paternal alleles of a particular gene. The difference between a compound heterozygote and digenic disease is that in digenic inheritance, mutation in a gene causes disease only in patients who also carry mutation in a diferent gene. Two large mutation analysis studies in patients with disease-associated *AIPL1* mutations have found that the W278X mutation comprised approximately half of the total disease alleles found [103,174]. If expressed, this allele would produce a severely truncated protein that is shorter than the wild-type AIPL1 by 107 amino acids. The truncated protein includes only 20 of the 34 amino acids of the third TPR motif, a highly conserved region on the AIPL1 protein.

This mutation was originally identified in homozygous form in two consanguinous Pakistani families, a non-consanguinous family of European descent, and in compound heterozygous form in another European family [440] together with a 2-bp deletion in codon 336 (A336∆2 bp). This deletion resulted in a frameshift and a termination codon 47 amino acids later. A further study that screened *AIPL1* in a large cohort of patients with a wide range of clinical diagnosis of inherited retinal dystrophies reported homozygous and compound heterozygous W278X mutation in non-consanguinous European families; the W278X mutation was found in combination with a splice-site mutation (c.277-2A>G) and an amino acid substitution G262S [442]. Interestingly, the results from this study suggested that *AIPL1* mutations may also cause autosomal dominant cone-rod dystrophy and retinitis pigmentosa [442]. The probands of two families were heterozygous for a 12 bp deletion (P351∆12 bp) within the sequence encoding the hinge region of AIPL1. The mutant protein hinge was predicted to lack four amino acids, this included two proline residues located at positions that were conserved across the primate species. This deletion occured adjacent to a predicted casein kinase II phosphorylation site, that might be involved in protein complex regulation [327]. This deletion was not found in control individuals and in the DNA from two unaffected individuals of the family. However, the pedigrees from these families were small and DNA samples from additional family members were unavailable. It would be important for additional studies to be performed on more autosomal dominant pedigrees with these clinical diagnoses to confirm the segregation of the mutation with retinal degeneration, and further expression studies would be helpful in determining the effect of the mutation on protein structure and function. The function of the proline-rich region of AIPL1 is currently not known and the effects of mutations such as P351∆12, A336∆2 and P376S that are located within the hinge region are uncertain. Preliminary data suggests that a high amount of sequence conservation exists within the hinge region between the primate species. More importantly, this proline-rich region is only found in primates and therefore may have an important role in primate vision or in cone-rich retina.

1.3.2.5 The phenotype of LCA in patients with AIPL1 mutations

The phenotype of LCA in patients with LCA due to mutations in AIPL1 is relatively severe compared with that of most other forms of LCA [103]. Studies comprising of mutational analyses of *AIPL1* mutations in patients with retinal dystrophies are relatively few in number and most of them include only small cohorts of patients. The largest study thus far was by Dharmaraj *et.al.,* which described the phenotypic features of 26 probands with *AIPL1*-related LCA [103]. Of these subjects, 17 probands were homozygotes and 9 were compound heterozygotes, and the ages of the patients at examination ranged from 4 months to 57 years. Visual acuities were severely reduced in these patients, ranging from 6/60 to light perception. The majority of the patients achieved only light perception (LP) by the time they reached the second decade, although there was one patient in the study who maintained vision of 6/360 at the age of 27 years. The youngest patient aged 4 months, was able to fixate and follow objects. Cycloplegic refraction showed that most of these patients had moderate hypermetropia, ranging from +3.00 to +7.00 dioptres [103]. A different study by Galvin *et al.* performed a mutation screen in a cohort of LCA patients across six genes and found that LCA patients with disease-causing sequence variations in *AIPL1* had severely decreased vision at a younger age compared to other genotypes, although the number of patients identified with *AIPL1* variation in this study was small (n=7) [151]. These findings were in keeping with findings of other reports [435,440]. Longitudinal evaluations of visual acuity in *AIPL1* patients are very limited. It has been suggested that there is a progressive decline in visual acuity in many patients, usually over a 10-20 year follow up period [151]. A few patients, however, mostly those with heterozygous mutations have been noted to have relatively stable vision. One of these patients was reported to maintain visual acuity of 20/200 after 16 years [151].

Features of night blindness and photosensitivity are variable in patients with *AIPL1*-related disease. The study by Dharmaraj *et al*. reported night blindness or nyctalopia in approximately half of the patients with *AIPL1*

mutations, and photoaversion or photophobia was reported in only 15% of their patients. The study by Galvin *et al.* reported nyctalopia in almost all of the patients with *AIPL1* mutations (6 out of 7), while less than half had photophobia. These findings were in contrast to a study by Hanein *et al.* which was a comprehensive mutation analysis of 6 LCA genes (*GUCY2D, RPGRIP, AIPL1, RPE65, CRB1 and CRX)* in a cohort of 179 unrelated LCA patients. Six patients (3.4% of cases) were found to have mutations in *AIPL1* in this study. Based on clinical observations, the authors divided LCA patients into 2 groups displaying either photophobia or night blindess. Features of photophobia but not night blindess at an early age were thought to be a feature of *AIPL1* mutations. Photophobia in early stages is also seen in other LCA mutations such as *GUCY2D* and *RPGRIP.* Although the precise underlying mechanism of photophobia in retinal dystrophies is not well understood, it has been suggested that the feature is related to cone dysfunction and is a hallmark in conditions with primary derangement of cone function such as cone dystrophies and achromatopsia.

There is more consensus across various studies in terms of the fundal appearances associated with *AIPL1* mutations. At early ages, from birth to pre-school age, essentially normal retinas and maculae have been observed [103,151]. By school age, patients tend to develop diffuse hypopigmentation and RPE mottling primarily in the mid-peripheral retina (Figure 1.14A). In advanced disease, usually around the sixth and seventh decades of life, there is extensive bone-spicule pigmentary clumping, atrophy of the RPE and chorioretina, atrophic maculopathy, optic nerve pallor and attenuation of the retinal vasculature (Figure 1.14C and D) [103,151,435]. Some patients have also been described to have drusen-like deposits in the retina in the first and second decades of life (Figure 1.14B) [151]. Variable levels of maculopathy was observed in majority of patients. Early stages of maculopathy in the form of an indistinct foveal reflex may be seen in young children of school ages. Later, the maculopathy in patients can range from mild foveal atrophy to bull's eye-appearing atrophic macular lesion to gross aplasia [103,151,435]. In the study by Dhamaraj *et al*, the youngest patient with macular atrophy was 8 years old [103]. Optic nerve pallor was noted in

all patients at later ages. Compared with other genotypes, a higher proportion of *AIPL1* patients were found to have keratoconus and cataracts The types of lens opacities ranged from cortical to posterior subcapsular opacities[103,440]. The incidence of cataracts and keratoconus is increased with age; the youngest patient described with keratoconus and cataracts was 10 years patient [103]. Visual fields and electroretinogram (ERG) are generally undetectable in patients with established *AIPL*-related disease. Figure 1.15 shows ERGs from an affected proband with homozygous W88X mutation and a heterozygous carrier parent of the patient. No measureable responses are seen in the affected patient, and both scotopic and photopic responses were equally extinguished (Figure 1.15A). Although most heterozygous carriers of *AIPL1* mutations are clinically normal, some ERG abnormalities have been reported in the form of reduction of rod b-wave amplitudes below the lower limit of normal (Figure 1.15B) [103]. No abnormalities have been reported in flicker and photopic ERGs in heterozygote carriers.

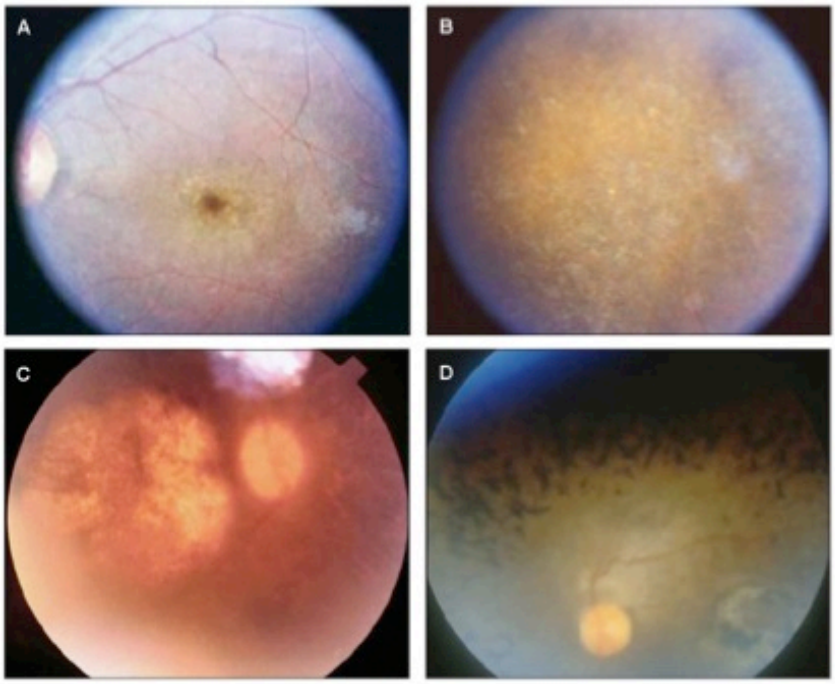

Figure 1.14 Fundal appearances of LCA patients with different stages of *AIPL1*- associated retinal dystrophy.

A. Fundal appearance of an 8-year old LCA patient carrying homozygous W278X mutation, showing early macular changes, RPE mottling and hypopigmentation.

B. Fundal appearance of a 12 year old patient with compound heterzoygous mutation T114I/P376S, showing diffuse peripheral retinal mottling and drusen-like deposits.

C. Fundus of a 25 year old LCA patient carrying homozygous W278X mutation, demonstrating atrophic maculopathy, optic nerve pallor and peripheral pigmentary changes.

D. Fundus from a 45 year old LCA patient showing advance changes due to homozygous W88X mutation in *AIPL1*. There is optid nerve pallor, extensive bone-spicule peripheral pigmentation, atrophy of the chorioretina and attenuation of the retinal vasculature.

(taken from Dharmaraj *et al*. 2004)

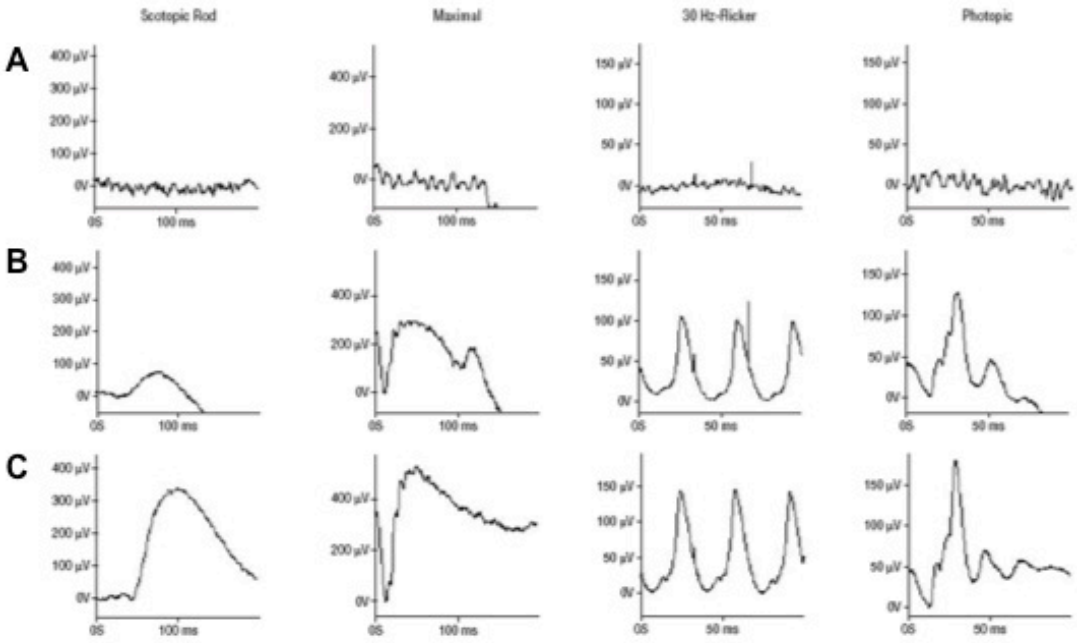

Figure 1.15 ERG of the right eyes of an LCA patient with *AIPL1* mutation and a heterozygous parent carrier.

A. The typical scotopic, photopic and combined ERG of a patient carrying homozygous AIPL1 W88X mutation shows no measureable responses.

B. The ERG of the heterozygous carrier parent of the patient shows siginificantly reduced amplitude of rod-specific scotopic ERG to one third of normal, while combined rod-cone responses , cone-specific flicker and single flash ERGs are normal.

C. Typical ERG findings in a normal control patient is shown for comparison

(Taken from Dharmaraj *et al.* 2004).

The large number of genes associated with retinal dystrophies makes genotyping a time-consuming task. However, genotyping is an essential step before any therapeutic approach can be established. One way of facilitating this is the establishment of phenotype-genotype correlations in order to direct molecular studies to the underlying gene in a new patient. With further studies and the use of more detailed imaging, it may be possible to distinguish different types of mutation within the same gene from the phenotype of patients, such as between missense mutation and null mutations which are likely to be phenotypically more severe. To date, no such correlation study has been performed. Although LCA phenotypes are variable and change with age, certain distinctive phenotypical features can be identified to suggest the underlying gene, and similarly, it may be possible to identify LCA patients who potentially have *AIPL1* mutations from their clinical presentation. However, a genetic diagnosis will always be required to confirm the gene defect.

Overall LCA patients with *AIPL1* mutations appear to have a more severe disease with a progressive course compared to patients with other LCA gene mutations. The main challenge is to be able to identify patients with *AIPL1* mutations at a young age since characteristic features of the disease such as retinal drusen deposits, peripheral bone-spicule pigmentation, chorioretinal and macular atrophy and keratoconus mainly appear at later ages, while the appearance of the fundus is relatively normal early in life. In these young patients, it is thus important is to establish an effective screening strategy that enables the identification of *AIPL1* mutations. This may require a combination of clinical and molecular strategies. Part of this study is directed at addressing these issues in addition to providing further phenotype-genotype data and the aetiology of *AIPL1*-related disease.

1.3.2 Photoreceptor cell death in inherited retinal dystrophies.

It has been shown that photoreceptor cell death in inherited retinal degenerations occurs by apoptosis [380]. However, there is little known about the mechanisms that link the genetic defects in inherited retinal dystrophies and the subsequent death of retinal cells by apoptosis. Understanding the disease mechanism by which genetic mutations lead to apoptotic cell death in inherited retinal dystrophies such as RP and LCA may provide an insight into ways to intervene to prevent or delay photoreceptor loss.

Apoptosis is one of the physiological processes required to control cell numbers in multicellular organisms and constitutes a controlled programme of cell death mediated by a signalling cascade involving the activation of caspase enzymes by proteolytic cleavage. The initial stimulus for the activation of this cascade can be intrinsic in response to damage within the cell such as in genetic retinal diseases, or extrinsic secondary to external insults or signalling from other cells (Figure 1.16). The homeostasis of intracellular Ca^{2+} levels in photoreceptor cells appear to be of central importance in the initiation of apoptosis in retinal dystrophies. In CNS diseases due to excitotoxic damage such as epilepsy and ischaemia, excessive synaptic release of glutamate leads to neuronal damage and cell death through Ca^{2+} disregulation and excessive influx of Ca^{2+} from overactivation of post synaptic receptors [27,515]. Forms of RP and inherited retinal dystrophies caused by mutations that ablate photoreceptor function completely are likely to cause cell death via calcium overload. These mutations create a metabolic state that can be equated to exposure to continuous darkness and hence the 'equivalent dark' hypothesis. An example in which elevated intracellular Ca^{2+} levels may lead to apoptosis in an inherited retinal dystrophy is the retinal degeneration (*rd)* mouse, a model of rapid retinal degeneration due to a null mutation in the *Pde6b* gene encoding β-subunit of phosphodiesterase (PDE). Loss of PDE activity results

in elevated levels of cGMP in the mutant retina and a continuous influx of calcium ions through the cGMP-and voltage-gated Ca^{2+} channels. This calcium overload eventually leads to apoptotic cell death in photoreceptor cells [123]**.** Mutations such as *AIPL1*[282]*, PDE6B [377]* and *PDE6A*[414] which result in loss or disruption of PDE activity and G*UCY1A*[356] where enhanced guanylyl cyclase sensitivity leads to increased cGMP-gated channel activity, are also thought to cause photoreceptor degeneration due to high Ca^{2+} levels triggering the apoptotic process.

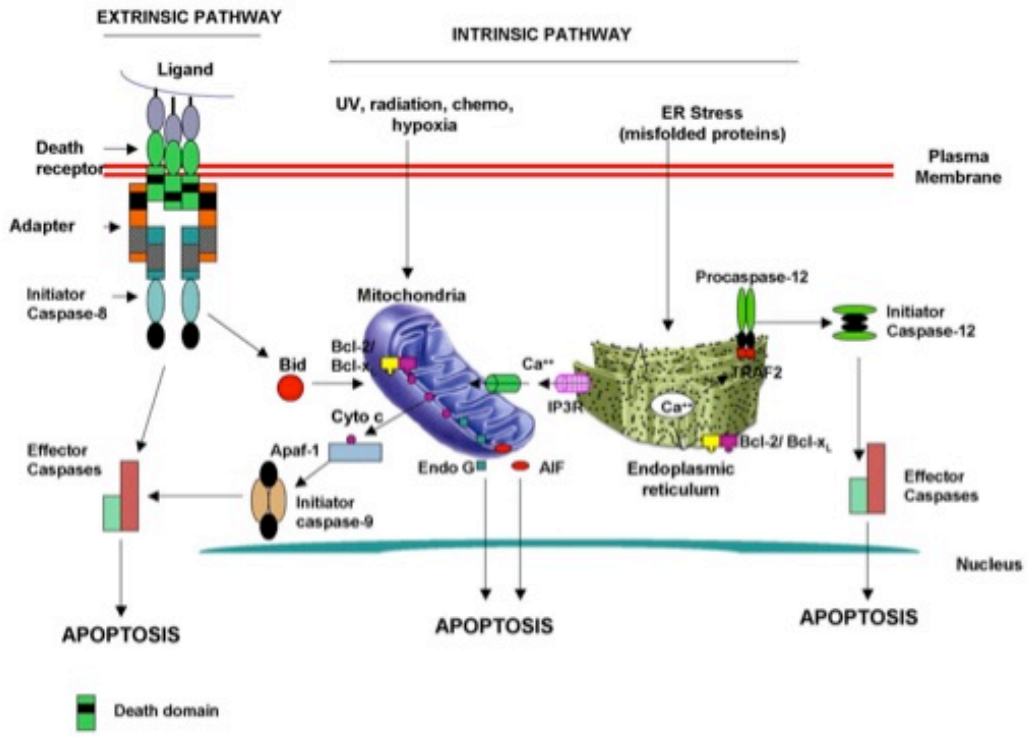

Figure 1.16. The extrinsic and intrinsic pathways of apoptosis.

Extrinsic pathway is mediated by the binding of a death ligand. This leads to recruitment of adaptor proteins to bind to the death domain, and accumulation of caspase 8 molecules. The mutual cleavage within caspase 8 aggregate subsequently initiates the caspase cascade. The intrinsic pathway is mediated by mitochondrial and the endoplasmic reticulum pathways; this leads to cytochrome C release followed by activation of pro-caspase 9 or 12 , which leads to the initiation of the caspase cascade.

(taken from Gupta *et al.* Immunity & Ageing. 2006)

Another hypothesis to explain cell death in retinal dystrophies is the 'equivalent light hypothesis' which postulates that certain mutations causing retinal dystrophies may cause constitutive overstimulation of the phototransduction cascade, resulting in signals being sent to the inner retina that are 'equivalent' to those sent in response to the detection of incident light [122,278]. The cell death in these circumstances could be similar to that seen in light damage models of RP, in which retinas exposed to either short intense intervals of light or prolonged low intensity light suffer loss of photoreceptors. Evidence has emerged from various models of RP that the equivalent light hypothesis may be the the main contributing factor to the degeneration seen in these forms of retinal dystrophies. One of the most convincing evidence to support the equivalent light hypothesis comes from the transgenic mouse model of LCA, the *Rpe65-/-* mouse. The rod photoreceptors in *Rpe65*$^{-/-}$ mice behave as if they are in the presence of a continuous background light with reduced circulating current in response to light stimulation, reduced light sensitivity and accelerated turn-off of photoresponse [500]. The lack of RPE65 protein causes photoreceptor death through accumulation of opsin that is not bound to 11-*cis* retinal in outer segments which causes the constitutive activation of the phototransduction cascade and this effectively acts like an equivalent light background. Further support for the equivalent-light hypothesis comes from studies involving the arrestin knockout (*Sag*$^{-/-}$) mouse and rhodopsin kinase knockout (*Rhok*$^{-/-}$) mouse; the photoreceptors in these animals rapidly degenerated when the animals were placed in constant light too dim to produce degeneration in normal animals, but the degeneration was spared if the animals were kept in darkness [81,82,504]. The introduction of a second mutation that blocked the transduction cascade, through the mating of these animals (*Rpe65*$^{-/-}$, *Sag*$^{-/-}$ or *Rhok*$^{-/-}$ mice) with another strain of mice that lacked the gene encoding the rod transducin α subunit, resulted in a protective effect where the double knockout animals were no longer sensitive to damage by moderate constant illumination [175,500], thus providing photoreceptor apoptosis was mediated by constitutive activation of the phototransduction cascade. Evidence from other models of retinal dystrophies also support the equivalent light hypothesis. Some mutant forms of *rhodopsin* are known to constitutively

activate transducin independent of light excitation [397,526]. Recessive mutations in the gene encoding the rod α subunit of the cGMP-gated channel [111] and retinal guanylyl cyclase (*RetGC-1*)[229,428] have been described, that would be expected to lead to a lack of functional cGMP-gated calcium gated channels and calcium not being transported into the cell. This should lead to a permanent state of hyperpolarisation in the photoreceptor inner segments and consequently a signal equivalent to light being sent to bipolar cells.

It has been hypothesized that constant hyperpolarisation may lead to cytotoxicity by two different mechanisms: an intrinsic mechanism that is a cell-autonomous intracellular pathway to cell death, and the other an extrinsic mechanism that involves other cell types. Intracellular responses from within cells that harbour mutations leading to an equivalent light signal could trigger apoptosis due to disturbances in intracellular calcium levels and oxidative stress. In the first, overstimulation of the phototransduction cascade by aberrant expression of genes result in calcium being no longer transported into the cell to maintain a depolarised 'ground state'. As a result, there is a permanent state of hyperpolarization in the photoreceptor inner segment and glutamate is never released from the photoreceptors. The exact mechanism by which low Ca^{2+} concentration lead to apoptosis is not fully understood. Evidence shows that neurons appear to tolerate a Ca^{2+} concentration only within a restricted range [277], and the same situation has been proposed for photoreceptors. Cultured neurons deprived of growth factors can be rescued in a medium containing high K^{+} which has its effects by depolarizing the cells and opening voltage-gated Ca^{2+} channels, producing an increase in the intracellular free Ca^{2+} [144,145,338]. The suggestion that prolonged decrease in Ca^{2+} levels may trigger apoptosis is supported by the existence of numerous mechanisms that photoreceptors have evolved for regulating the rate of phototransduction and maintaining Ca^{2+} concentration within certain limits; this includes the modulation of cGMP channels by calmodulin[192,193], regulation of Ca^{2+} concentration by the $Na^{+}/Ca^{2+}K^{+}$ exchanger [424] and light-dependent translocation of transducin and arrestin to decrease activation in bright light [445,520]. It has been

proposed that mutations that cause equivalent light signals and those that disrupt photoreceptor function, may also lead to cell death through an increase in oxidative stress [469]. Due to the high density of mitochondria in the inner segments, photoreceptors are particularly sensitive to mutations that alter their metabolic requirements. Mutations that cause a reduction in metabolic activity lead to an increase in mitochondrial free radical production in the form of reactive oxygen species. This is because, whist other tissues are able to modulate their blood supply by vasoconstriction, the choriocapillaris that serves the retina is largely unable to constrict, meaning the same level of oxygen is supplied to photoreceptors despite their altered metabolic state. These reactive oxygen species induce oxidative damage to the mitochondria, resulting in cytochrome–c release and subsequent activation of caspase proteins, leading to apoptosis [165,214]. The second mechanism in which cells may die in response to an equivalent light signal involves secondary messengers being released by cells in the inner retina. Bipolar cells, Müller cells and ganglion cells secrete neurotrophic factors that promote the survival of photoreceptors under normal circumstances and following retinal injury [219,491]. In retina which has been exposed to light for long periods of time, it has been observed that activated microglia invade the degenerating photoreceptor layer and alter the expression of neurotrophic factors such as nerve growth factor (NGF), ciliary neurotrophic factor (CNTF), and glial cell line-derived neurotrophic factor (GDNF)[176]. Furthermore, microglia-derived factors influence the production of secondary trophic factors in Müller cell, suggesting that microglia-Müller glia cell interactions play a critical role during photoreceptor degeneration[176]. It has been hypothesized that these microglia may either exert a cytotoxic function by releasing reactive oxygen species, nitric oxide, or inflammatory cytokines that trigger an extrinsic apoptotic pathway in the photoreceptors[201,245,346], or modulate the secretion factors that normally promote photoreceptor survival [176].

It has been observed that the microenvironment of the degenerating retina can exert a negative effect on surrounding cells, where healthy photoreceptors are known to die in the presence of mutant cells. This ‘by-

stander effect' suggests a non-cell autonomous mechanism for cell death, possibly involving secondary cells and their secreted factors [226]. Evidence for this by-stander effect comes from chimeric mice generated from albino *Prph2*$^{Rd2/Rd2}$ mice and pigmented mice that were wild-type. Photoreceptors were found to degenerate not only in the regions overlying non-pigmented RPE, but also in regions overlying pigmented RPE, indicating that the photoreceptors that are genetically normal die in the presence of photoreceptors carrying RP-causing mutations [417]. A different example of non-cell autonomous cause of photoreceptor death is seen where the loss of rods is responsible for the cone cell death. The rod-derived cone viability factor which is normally secreted by rods, was found to enhance the survival of cone-rich retinal explants from *rd1* mice in culture and *in vivo* when delivered subretinally into *rd1* mice [266,331]. Thus by understanding the different mechanisms and pathways leading to apoptotic photoreceptor cell death, therapeutic intervention to prevent the loss of cells may be made easier.

Following photoreceptor cell death in inherited retinal degeneration, it was previously thought that the neural network and cell population pattern in the inner retina was spared. It has become apparent that deafferentation of the neural retina invokes a series of changes known as remodelling, that these events commence even before there is any cell death and that neuronal remodelling is the common fate for all conditions with photoreceptor degeneration regardless of the initiating event or gene defect. Indications of altered circuitry in retinal degeneration have been documented as early as 1974[241] but the concept of retinal remodelling did not take hold until later, when different studies described sprouting from various retinal cell populations including photoreceptors, bipolar and horizontal cells in a haphazard manner during photoreceptor degeneration [128,322,375,450-452] and aberrant formation of new synapses in the degenerating retina with neuronal translocation, glial transformation and ectopic neurite complexes which were believed to be attempts by remaining neurons to find synaptic excitation [217,218,299]. Despite evidence of plasticity, this new circuitry was corruptive of retinal signal processing. The implications of retinal modelling

for therapeutic intervention would be significant as most current approaches such as cell transplantation and electronic implants are late-stage schemes and depend on the existence of an intact retinal architecture. This negative plasticity emphasizes the importance of early diagnosis and intervention to retard or prevent remodelling, and provides a compelling argument as to why gene therapy may be a more appropriate treatment for genetic retinal diseases.

More pertinent to this study are the effects of remodelling in models of fast retinal degeneration and the implications of this on therapeutic strategies to treat rapid retinal degeneration. The *rd1* mouse contains a nonsense mutation in ß subunit of phosphodiesterase (PDE) and exhibits rapid retinal degeneration, similar to that seen in *Aipl1 -/-* mice. Parallels can be drawn between the *rd1* mouse and the *Aipl1 -/-* mouse in that both conditions result in loss of PDE function, elevated cGMP which is ultimately lethal to rods. The remodelling process has been examined in the *rd1* mice and despite rapid rod degeneration, retinal modelling is slower than expected and is severely advanced at postnatal day 610 [218]. It is thought that the delay of late stage of remodelling is associated with persistence of residual cone photoreceptors [212] that provide a source of input to the neural retina and prevent complete early global remodelling. Since AIPL1 is expressed in both rods and cones, photoreceptor degeneration in the *Aipl1 -/-* mouse is much more rapid compared to the *rd1* mouse. In rapid degenerations, gliosis and aberrant sprouting occur at a slower pace compared with the loss of photoreceptors. Hence, gene therapy may be effective if the treatment is administered before there is significant loss of photoreceptor cells in rapid degenerations. In slow degenerations, there is more time for reactive changes to occur in response to the gradual loss of photoreceptor function such that by the time the condition is detected, significant remodelling has taken place. Taking these factors into consideration, it would be reasonable to expect that the *Aipl1 -/-* mouse may respond well to gene therapy. Furthermore, cone death due the the absence of AIPL1 is inherently slow; this is seen in a novel transgenic mouse model tg h*Aipl1;Aipl1 -/- ,* in which rod photoreceptors were exclusively rescued by the expression of human AIPL1 and AIPL1-deficient

cones in this novel model degenerate at a much slower rate in comparison to the complete AIPL1 knockout model [232]. It was hypothesized that the reduced rate of cone photoreceptor degeneration in tg h*Aipl1;Aipl1 -/-* mice was due to the expression of rod-derived cone viability factor from preserved rod photoreceptors and the maintainance of surrounding cell density which supported cone viability. In humans, the cone-rich fovea would be analogous to the slow-degenerating cones observed in the tg h*Aipl1;Aipl1 -/-* mouse model since this area would be immune to the influence of rod cell death on cone survival in the absence of AIPL1. This is supported by results from an adult LCA patient with a mutation in *AIPL1* who showed severe retinal degeneration and all survival cells appeared cone-like in morphology[478]. These observations suggest that the therapeutic window for gene therapy may be further extended in LCA patients, since the cone cells in the fovea may survive for a longer period of time.

1.3.4 Animal models of inherited retinal dystrophies

Much of the advances in ocular gene transfer and gene therapy would not have been possible without the availability of animal models. Animal models have been instrumental in advancing our understanding of genetic diseases processes. To develop a gene-based strategy and test the efficacy of the treatment requires an animal model with a mutation in the gene of interest. There are many naturally occurring and engineered animal models of RP and hereditary retinal dystrophies, most of which are rodents. However, some large animal models of retinal disease exist in the form of dogs, cats and pigs. Several considerations need to be taken into account when testing therapeutic strategies in animal models. The timescale of the degeneration needs to be factored in, degeneration which progresses too rapidly limits the window of opportunity for gene therapy to work while too slow a rate make assessments of efficacy difficult. The animal model chosen to investigate therapeutic strategies should reflect the human disease as closely as

possible and finally, the strategy to treat the disease should be cogniscent of the underlying disease mechanism.

Although all vertebrate eyes are similar in structure and function, there are some differences depending on the life style and survival needs of various species. Whilst animal models are valuable model systems, they should only be seen as an approximation to the morphological, physiological and pathophysiological conditions of humans. Mice and rats have been used most extensively for various reasons including their short gestation time, the existence of several readily available retinal degeneration mutants, and the possibility to create transgenic animals by genetic modification. Although rodents are frequently the animals of choice in most experiments, the differences between rodent and human eyes can make interpretation of results obtained from the animal difficult. Rodents have only 2 types of cones which detect medium and short wave-length light, and are thus unable to see long-wave light. Each neural cell in the rodent retina is connected to a larger number of photoreceptors than those of the human retina, which increases sensitivity at the expense of acuity. Humans on the other hand, have 3 types of cones and higher cone density; in humans, 5 % of the photoreceptors are cones compared to only 1-2 % in rats and mice. Another major difference is the lack of an anatomical macula or cone-rich region in rodents, while the macula is of utmost importance and subserves high acuity vision in humans and primates. Thus mutations leading to macular degeneration may be harder to study in rodents. As many animal models of disease differ in some aspects from their human counterparts, the study of therapeutic strategies need to account for these differences before conclusions from animal studies can be applied to clinical disease. Findings based on rodent models may need to be further validated in larger animal models with eyes that more closely resemble human eyes.

Larger animal models of inherited retinal dystrophies exist and are particularly useful in establishing efficacy and safety parameters prior to human trials. Large animals such as pigs and dogs have the advantages of being anatomically more similar to the human eye. Even though the pig

retina lacks a foveal-macular region, the retina has a greater proportion of cones than the rodent retina. Given the strong similarities in phenotype to that of RP patients, the transgenic pigs provide a large animal model for studying retinal degeneration (especially cone degeneration) found in RP [271,371]. The canine retina has a similar composition and distribution of cones, and contains a cone-rich area called the visual streak, which shares some of the characteristics of the macula in humans[339]. The large size of the dog eye allows intraocular surgical procedures to be carried out more easily than in rodents and it also permits fundal examination of different retinal regions of the same eye. Because the canine eye bears greater resemblance to human eye with respect to size and retinal morphology, retinal defects in dogs can provide useful animal model of disease for pre-clinical studies of gene therapy. Primate eyes are the most similar to those of humans in many ways and possess a macula that is rich in cones. It has been shown that diurnal species, such as the rhesus monkey, have a fovea that consists of all three types of cones (red, green and blue). Macular changes that are similar to that in age-related macular degeneration in humans have been reported in the rhesus monkey[369]. Because of the similarity to humans, monkeys would be the animal model of choice to investigate such disorders. However, due the long lifespan of monkeys, retinal degenerations occur over a longer period of time compared to mice and rats, making experiments long lasting. Moreover, no primate models of inherited retinal dystrophies have yet been identified and characterized.

The most widely studied naturally-occuring rodent models of RP are the *rd1* mouse and the retinal degeneration slow (*rds)* mouse. The *rd1* mouse was the first mammalian retinal degeneration model to be described [379]. Pittler *et al* identified the genetic defect causing photoreceptor degeneration in the *rd* mouse, a nonsense mutation in the phosphodiesterase beta-subunit gene (*Pde6b*) gene. This gene encodes the β-subunit of the rod cGMP phosphodiesterase (β-PDE). The phenotype in the *rd1* mouse is extremely rapid degeneration with complete loss of rod photoreceptors by postnatal week 4, although cones survive slightly longer. Mutations in the human

homolog of *Pde6b*, mostly affecting the catalytic domain, have been found in patients with autosomal recessive retinitis pigmentosa, which bears phenotypic resemblance to that in the mouse apart from one feature [312]; the disease in humans presents later in life and has a slower time course. A further discrepancy is the fact that the mutations found in humans are mostly missense substitutions affecting the catalytic domain and result in reduced protein activity as opposed to the loss of protein function from the null mutation in the mouse model [312,377]. A model that is both genetically and phenotypically more similar to *Pde6b* mutations in humans is the *rd10* mouse,a hypomorphic *Pde6b* mutant which harbours missense mutation in exon 13 [359]. The mutation causes a partial loss of PDE acitivity and a milder phenotype than the *rd1* mouse, and the rate of photoreceptor cell loss in the *rd10* mouse is more comparable to that seen in human disease.

The *rds* or *Prph2* $^{Rd2/Rd2}$ mouse is a naturally occurring mouse model that carries an insertional mutation in the *peripherin/rds* gene [288] which encodes peripherin-2, a photoreceptor-specific structural protein found in the outer segments of rods and cones. Peripherin is major structural component of the membranous discs within the outer segments. The lack of peripherin leads to the failure of disc morphogenesis and absence of outer segments from birth. As a result, phototransduction is greatly reduced and photoreceptors die although the mechanisms leading to this is not completely clear. Homozygotes show early onset retinal degeneration and an intermediate rate of photoreceptor cell loss, slower than the *rd1* mouse but faster than many other models. The outer nuclear layer in homozygotes is reduced by 50% by 2 months of age and there is complete pan-retinal loss by 12 months of age[210]. The absence of *peripherin/rds* leads to rods without outer segments that eventually undergo apoptosis[129,415,416] and therefore have negligible rod function[404], but retain functioning cones although these have atypical outer segments [130]. The heterozygous animals exhibit haploinsufficiency and a much milder phenotype; they have disorganized outer segment whorls, the mice retain normal ERG amplitude levels until adulthood and have a later onset of phenotype with a much slower progression of degeneration with 50% of outer nuclear layer lost by

18 months[182]. P*eripherin/RDS* mutations in humans are associated with a variety of retinal dystrophies depending on the causative mutation, and do not show a straightforward dependence on the position of the mutation in the primary protein sequence or the type of mutation. Moreover, a single mutation may cause a spectrum of phenotypes ranging from different macular dystrophies and cone-rod dystrophies to autosomal dominant RP[56,319,372,376,490]. This phenotypic heterogeneity along with the anatomical differences make the interpretation of animal models of the human disease more complex. Despite this, animal models have still proven valuable, particularly given the high degree of identity of peripherin/RDS sequence between human and murine orthologs (the murine *peripherin/rds* gene is 91% identical to the human orthologue) [92,470]. Studies from animal models suggest that both haploinsufficiency and dominant negative mechanisms both play a role in human retinal dystrophies caused by *peripherin/RDS* mutations; phenotypes dominated by rod photoreceptor loss may be caused by a haploinsufficiency and/or dominant negative effect, while phenotypes with predominantly cone dysfunction appear to be due to a dose-dependent dominant negative effect[129]. The *rds* mouse represents a model for *peripherin/RDS* mutations in humans that lead to haploinsufficiency or loss of function phenotype.

As well as several naturally occurring mouse models, there are several large animal models of inherited retinal dystrophies. In dogs, mutations have been identified in a number of genes including *RPGR, PDE6B* and *CNGB3* [368],[369] BEST1[170]). The *RPE65*-deficient dog, also known as the Briard dog has a homozygous 4-bp deletion within the *Rpe65* gene and is a canine model of LCA type 2[4]. Affected dogs have congenital night blindness and various degrees of visual impairment under photopic illumination. Along with the visual impairment, affected dogs have an abnormal ERG trace in keeping with severely depressed rod and cone-mediated responses. Morphologically, pathologic abnormalities were mainly confined to the RPE layer; electron microscopy studies of the retina demonstrated large, cytoplasmic lipid inclusions in the RPE, while photoreceptor outer segments appeared largely normal. No evidence of photoreceptor degeneration or cell death were seen

as indicated by the preservation of the outer nuclear layer thickness [4]. Difference however, exist between *RPE65* mutations in humans and in the dog model; although the severe visual deficit early in life is similar in human and dog, the lack of ophthalmological signs of advanced retinal degeneration in the adult dog is unlike the human condition, and the course of the disease is stationary in the dog model while in humans, the disease progresses to severe visual impairment and blindess. These issues need to be taken into consideration when evaluating therapies in the experimental treatment of the disease. Apart from canines, other large animal models of RP and retinal dystrophies exist such as the feline models of LCA caused by mutations in *CEP290*[316] and *CRX*[317].

Genetic engineering has made possible the development of transgenic animals which are created using constructs that either disrupt, imitate or over-express the candidate gene in order to mirror the human form of the disease. To date, rodents and pigs have been bioengineered to create "knockout" models representing recessive diseases or "knock-in" models that provide models of dominant forms of retinal dystrophies. Knock-out models are created by causing a specific targeted disruption of an endogenous gene which results in the loss of the protein function. Knock-out mouse models have been generated to recapitulate human LCA or RP. Table 1.5 sumarizes the available natural and man-made mouse models of LCA to date. All human LCA genes have orthologues in mouse. Four mouse LCA genes (*Cep290, Crb1, Rd3, Rpe65)* have been found to contain naturally occurring mutations, while the others have been generated mostly by targeted disruption. Most of the knock out models of LCA genes exhibit severe retinal degeneration which parallel that seen in humans, with the exception of *Crb1, Gucy2D* and *Rdh12.* Different levels of gene disruption in the *Aipl1* gene resulted in varying rates of photoreceptor cell loss. Two *Aipl1* knockout (*Aipl1-/-)* mouse models have been created, both models are fully deficient in AIPL1 activity and exhibit very rapid photoreceptor degeneration [119,391]. A relatively mild mutation was introduced in the *Aipl1* gene by the insertion of a neomycin cassette in intron 2 of the gene to create a "knock-down" model, the hypomorphic (*Aipl1h/h*) mouse. This model which has reduced levels of

Aipl1 exhibits a much slower retinal degeneration and may represent milder forms of the disease [282]. The studies presented in this thesis focus on the two models of *Aipl1*-related retinal degeneration that, by virtue of their different kinetics of photoreceptor loss and are valuable tools in assessing the efficacy of treatment strategies. Further details of these models will be discussed in the following section. Knockout models have also been generated that mimic mutations found in RP and other types of retinal dystrophies. Rhodopsin knock-out (*rhodopsin-/-)* mice exhibit a morphological absence of rod outer segments and a fast degeneration. Rod photoreceptor cell loss occurs first, followed by cone degeneration which begins at about postnatal week 6. By 3 months of age, there is almost a complete loss of photorecetors with only single row of nuclei left in the outer nuclear layer which are thought to be residual cones[194]. Heterozygous rhodopsin knockout mice carrying one functional allele on the other hand, retain majority of their photoreceptors, although the inner and outer segments of photoreceptors were shorter and the level of rhodopsin in individual rod photoreceptor cell is reduced }[194][264]. *Tulp1* knock-out (*Tulp-/-*) mice are another model of recessive RP, and exhibit mislocalisation of rod- and cone-opsins, accumulation of vesicles in the inter-photoreceptor matrix, and a relatively fast photorecetor degeneration that reaches end-stage by 5 months of age [171]. Knockout mice lacking RPGR and RPGRIP, which encode proteins found in the photoreceptor connecting cilia, serve as models of X-linked and LCA respectively [189,524]. It has been subsequently shown that RPGR is a client protein of RPGRIP, which functions to anchor RPGR in the connecting cilium [190,524]. Consistent with the notion that RPGRIP subserves the function of RPGR in regulating protein trafficking across the connecting cilia, *Rpgrip-/-* mice exhibit a more severe disease than *Rpgr-/-* mice. This difference in phenotype in the mouse models analogous to clinical findings, where *RPGR* mutations in patients manifest as X-linked RP while the loss of *RPGRIP* leads to LCA in patients.

Many transgenic models have been made that incorporate mutations in *peripherin/rds* and *rhodopsin* genes that are associated with dominant RP. *Peripherin/rds (Prph2)* transgenic mice have been generated which carry the

amino acid substitution P216L. The mutant P216L mutant protein does not preclude peripherin-2 tetramer formation but these tetramers are dysfunctional, probably due to hyperglycosylation of the protein [283,501]. Consequently, the phenotype caused by the P216L mutation is due to a dominant negative effect on rod outer segment structure.These animals exhibit a slow retinal degeneration and a phenotype similar to that of dominant RP caused by P216L mutation in patients [227]. Other transgenic mouse models with mutations in *peripherin/rds* include models that carry the C214S and R172W substitutions which cause late-onset autosomal dominant RP[412] and cone or cone-rod dystrophy in humans respectively[91,105]. Another transgenic mouse model carrying the L185P mutation in *peripherin/rds* exhibits haploinsufficientcy and is a model for digenic RP. In these mice, no photoreceptor degeneration is seen in *Rom1(+/-)/peripherin/Rds(+/+)* mice, but *Rom1(-/-)/peripherin/Rds(+/+)* mice show a mild photoreceptor degeneration[112]}[89,228]. Rhodopsin is both a key component of phototransduction and a structural protein for the outer segments. The underlying pathogenic process thus varies with the type of mutation. Most of the mutations produce a protein that is defective in folding or trafficking and has an inability to maintain outer segments[458]. The expression levels of wild-type rhodopsin need to be taken into consideration in rhodopsin disease models as overexpression of normal rhodopsin can also lead to photoreceptor degeneration. Numerous rhodopsin mutant animals have been described, most were generated as transgenic mice which carry one mutant rhodopsin allele in addition to two wild type alleles. Examples of rhodopsin transgenic models include the Q344Ter mouse in that the rhodopsin gene has a stop codon leading to a truncated protein. The result is mislocalised rhodopsin and a slow retinal degeneration, similar to that seen in patients [457]. Two rhodopsin transgenic rats are extensively studied; the S334Ter rat that has a rapid degeneration over the course of weeks [279] and the P23H rat that has a much slower degeneration which takes place over months [357]. Rats heterozygous for the P23H opsin allele lose around 50% of their photoreceptors at three months of age [357]. More recently, rhodopsin mutants which carry one mutant allele and one wild-type allele have been produced by crossing rhodopsin-transgenic with rhodopsin-

knockout mice or by targeted insertion of a mutant allele into a specific locus (knock-in models). These animals have gene dosage and mutant to wild type ratios approximating those of human patients and are better representation of the human disease.

A good animal model requires that it is representative of human disease in terms of the mutation that causes the disease and in the pathology and phenotypical features that follows. Many of the LCA mouse models such as *Aipl1-/-, Cep290 (rd16), Rd3, Rpgrip1-/-, Rpe65 (rd12)* and *Rpe65-/-* appear to mimic human LCA phenotype and demonstrate retinal degeneration at various rates (Table 1.3). Large animal models which bear greater resemblance to the human eye are excellent models for study; the *Rpe65*-deficient dog is an example which has been vital in providing proof-of-principle of gene replacement therapy. Successful restoration of vision using AAV-mediated gene therapy has been reported in these dogs [2] and provided the drive for moving into clinical trials which are ongoing [34,181,293]. Undoubtedly, a large part of this is due to the fact the disease in the dog model resembles the human version in terms of anatomy and phenotype, and it is anticipated that similar benefits from treatment should follow. For treatment efficacy studies, a model that has an intermediate rate of degeneration is ideal, so that there is a window of opportunity for intervention and yet not so slow that evaluating the efficacy of the therapy becomes difficult. Experiments in rodents have indicated that the fastest retinal dystrophies are the most difficult to treat successfully. Despite numerous attempts to treat the *Pde6b*-deficient *rd1* mouse using gene replacement therapy mediated by a variety of viral vectors [50,216,247], effective rescue of this model has proved elusive. More convincing rescue has been reported in the *rd10* mouse which has partial PDE6b deficiency and slower degeneration [359]. This difference in success may be in part due to the slower degeneration affording better timing for intervention. Since the rate of photoreceptor cell loss is in this model is more comparable to the human disease, these results indicate that patients with *PDE6B* mutations may also respond favourably. The *Crb1, Rdh12* and *Gucy2D* knock-out mice demonstrate subtle degeneration and progress at a relatively slower rate

than in humans lacking these genes. The *Rpgr -/-* mice also demonstrate very slow degeneration of photoreceptor cells compared with that in human[189]. The *Abca4-/-* mouse model of Stargardt exhibits some features of the disease such as accumulation of lipofuscin in the RPE but does not have photoreceptor degeneration that is characteristic of the human form[494]. The milder pathology in these mice thus make it difficult to assess the effects of therapeutic intervention and also to extrapolate findings to humans. In the absence of larger animal models generated by genetic bioengineering, future clinical trials may have to proceed based on efficacy data in small animal models such as rodents. Comparison of the efficacy of treatment in mice, dog and humans from previous studies may help determine the suitability of mice as models of human retinal disease, while thorough characterization and careful selection of a model will facilitate translation of animal studies into clinical trials.

Table 1.3 Overview of all natural and man-made mouse models for LCA.

Gene	Mutated exons	Method	Degeneration of photoreceptors (age)	Similarity to human LCA	References
Aipl1	1-2	KO	+++, 7 weeks	yes	[119]
	2-5	KO	+++, 3 weeks	yes	[391]
	Intron 2	KD	+, 8 months	no	[282]
Cep290	Del35-39	Natural (rd16)	+++, 4 weeks	yes	[78]
Crb1	3841delC	Natural (rd8)	+	no	[314]
	1	KO	+, 3-9 months	no	[473]
	3(C249W)	KI	+, 24 months	no	[474]
Crx	2-4	KO(-/-)	+++, 2 weeks	yes	[150]
		KO(+/-)	ERG reduced, 2 months	no	[337,375]
Gucy2D	5	KO	+, cone degeneration only	no	[509]
Impdh1	9	KO	unknown	unknown	[168]
Lrat	1	KO	++, 6-8 weeks	yes	[41]
Rdh12	1-3	KO	+/-, 1 year	No	[290]
	1-3	KO	+/-, 7 months	No	[248]
Rd3	3(R107X)	Natural (rd3)	++, 15 weeks	yes	[146,276]
Rpe65	1-3	KO	++, 15 weeks	No	[400]
		Natural (rd12)	++, 15 weeks	Yes	[360]
Rpgrip1	Intron 14 insertion	KO	+++, 2-3 months	Yes	[524]
Tulp1	8-9	KO	+++, 4 weeks	Yes	[195]

KO, knock-out; KD, knock-down; KI, knock-in; - absent; +/- subtle; + moderate; ++ severe; +++ full degeneration.

1.3.4.1 The *Aipl1-/-* mouse model of retinal degeneration

Two study groups have created mice with targeed disruption of the *Aipl1* gene[119,391]. Dyer *et al.* generated *Aipl1*-/- mice by targeted disruption of exon 1 and 2 using a 1.6kb DNA fragment containing neomycin cassette[119]. The *Aipl1*-deficiency in these mice led to early severe retinal degeneration, beginning at postnatal day 12 (P12) in a distinct central-peripheral gradient: degeneration of the central retina was faster than degeneration in the peripheral retina. At this early stage, severe shortening of rod photoreceptor outer segments and disorganisation of the membranous discs were seen, cone photoreceptors were also morphologically abnormal and thinning of the outer nuclear layer was already noticeble compared with age-matched wild type mice. Synoptogenesis in the inner plexiform layer remained relatively intact, but the outer plexiform layer showed signs of disruption of synapse formation at this stage. Down-regulation of several rod-specific markers such as *Nrl* and *Nr2e3*, and genes encoding PDEβ and γ subunits, and cGMP channel protein was detected at P15. In addition, there was also decreased expression of genes from the Wnt-frizzled signalling pathway that is involved in the regulation of retinal proliferation and cell fate determination. The central to peripheral pattern of photoreceptor degeneration progressed rapidly until there was almost total loss of photoreceptors by the time the *Aipl1 -/-* mice were 8 weeks old. Total photoreceptor cell count in *Aipl1 -/-* mice at this age was 13% of wild type counts, the contribution of cell loss was not solely from the loss of rods. The severe cell loss in the *Aipl1*-deficient mice corresponded to complete loss of photoreceptor function, indicated by absent a- and b-waves on ERG recorded from *Aipl1 -/-* mice (Figure 1.17C). Immunostaining of *Aipl1 -/-* mice retina at this age indicated a reduction of cones in addition to loss of rods and a potential expansion of bipolar cells. Although GFAP immunostaining showed a marked increase in Müller cell reactive gliosis, markers for other neuronal cell types showed no change in horizontal cells, amacrine or gangion cells. Despite the early onset of degeneration, the authors did not find evidence of abnormal cell death exceeding that of normal retinal

development nor defects in the generation of different cell types or differences in cell type proportion during early stages of retinal development. RT-PCR for markers of retinal cell proliferation and cell fate at P2 and P8 demonstrated normal expression of markers of commitment to cell fate and retinal progenitor cell genes. The abscence of gross abnormalities in early stage retinas of the *Aipl1 -/-* mouse suggests that normal retinal development occurs in the background of *Aipl1*-deficiency, and that Aipl1 is not required for retinal proliferation or the commitment to photoreceptor cell fate despite its reported interaction with NUB1, a cell cycle regulatory protein[7,8]. A possible explanation could be the presence of protein redundancy in which there may be other proteins in the pathway that are performing compensatory roles in retinal proliferation[119]. Mice that were heterozygous for *Aipl1* deficiency (*Aipl1* +/- mice) were found to demonstrate some phenotype abnormalities; ERG recordings from Aipl1 +/- mice showed increased implicit time, indicating a delayed rod response on ERG (Figure 1.17B).

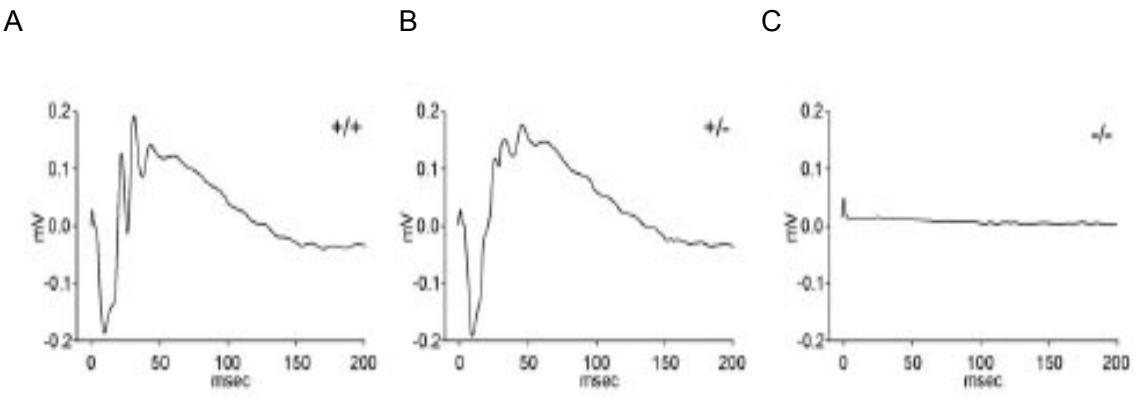

Figure 1.17 Flash ERG of normal wild-type mouse (A), heterozygous *Aipl1+/-* (B) and homozygous *Aipl1*-deficient mouse (C)[119].

This was similar to the observation that some patient carriers of AIPL1 mutations demonstrate rod function abnormalities. Additionally, 8 week old *Aipl1+/-* mice had photoreceptor cell counts that were 80% of wild type indicating some degree of cell loss had occurred.Ramamurthy *et al* engineered an *Aipl1*-/- mouse model by replacing exon 2 to 5 of *Aipl1* gene with a neomycin-resistance gene vector [391]. In these *Aipl1* null mutants, the retina was also observed to develop normally; no morphological developmental abnormalities were seen at birth and the formation of rods and cones were seen in the developing photoreceptor layer. At P8, when outer segments are being formed, electromicrograph studies of retinal ultrastructure of *Aipl1*-deficient mice did not show any difference from wild-type retina, indicating that retinal development indeed occurs normally. The earliest sign of cell death was the presence of apoptotic nuclei in the outer nuclear layer seen at P9. By P11, outer segments of *Aipl1*-/- mice appear shorter, disorganised and fragmented. Light microscopy evidence of retinal degeneration was first seen at P12, with loss of photoreceptor cell layer which progresses rapidly. By P14, only half of the photoreceptor layer was left and the degeneration was completed by 3 weeks with total loss of the outer nuclear layer in these mice. The degeneration appeared specific to the photoreceptor layer, affected both rods and cones equally and was more severe in the central retina compared to the periphery. Up-regulation of GFAP was seen in the outer nuclear and plexiform layer, while the other retinal layers, inner nuclear layer and ganglion cell layer appeared unaffected at 3 weeks of age.

To establish the relationship between AIPL1 and PDE, the authors quantified levels of PDE at P8 before any significant degeneration had occurred. Levels of all three subunits of PDE (α,β,γ) were reduced but the mRNA levels of all three PDE subunits were normal. Assay of PDE acitivity revealed no significant PDE activity in the *Aipl1*-/- mouse despite the presence of low amounts of PDE present. Additionally, levels of cGMP were elevated, a feature that precedes the retinal degeneration. The temporal and spatial course of the retinopathy in these *Aipl1*-/- mice closely resembles that of the *rd1* mouse. However distinct differences exist: in the *rd1* mouse, the loss of

the PDE-β subunit gene causes reduced levels of PDE-β mRNA and complete loss of the PDE-β subunit affecting rod photoreceptors[373], in the *Aipl1*-/- mouse, PDE mRNA are normal but all three PDE subunits are destabilized by AIPL1 deficiency resulting in loss of PDE activity which leads to photoreceptor degeneration. While the *Aipl1*-/- mouse have no detectable ERG response from birth, the *rd1* mouse produces no rod responses but has reduced responses generated by existing cones during early stages of retinal development.

To date, the most common *AIPL1* mutations in patients are premature termination mutations which are likely to be functionally null[7,103,222,440] and lead to LCA these severest phenotype. Both *Aipl1* knockout mouse models phenocopy LCA patients with *AIPL1* mutations, in whom there is lack of visual function very early in life and retinal degeneration occurs and progresses quickly. Similarly, whilst the heterozygous patient carriers of *AIPL1* mutations have some rod function abnormalities, the heterozygous *Aipl1+/-* mouse also has an increased implicit time indicating a delayed rod response on ERG.The rapid degeneration of photoreceptor cells in the AIPL1 null murine model poses logistical difficulties for a feasible gene therapy strategy. Compounded by the time lag required for AAV-mediated transgene expression, it was felt that there may not be an adequate window for effective therapeutic intervention in this model. An alternative model that may better facilitate the assessment of gene replacement therapy is the *Aipl1* hypomorphic mouse (*Aipl1h/h)*, which has a later onset and slower rate of photoreceptor degeneration, thus affording a larger time window of opportunity.

1.3.4.2 The *Aipl1 h/h* hypomorphic mouse model.

Liu *et al.* generated an *Aipl1* hypomorphic mouse (*Aipl1h/h*) in which AIPL1 function was diminished but not extinguished in an attempt to study the function of AIPL1 in the retina in more detail[282]. The AIPL1 targeting vector was generated by cloning a neomycin-resistance gene marker flanked by genomic fragments of exon 1,2 and 3 into a targeting plasmid. This construct was used to insert the neomycin resistance cassette into intron 2 of the *Aipl1* gene in the same orientation as the gene. The resultant mutant was a strong hypomorph in which the level of AIPL1 was decreased to 20-25% of that in wild-type mice. Levels of rod cGMP phosphodiesterase was reduced in parallel to 20% that of wild-type levels and all the three subunits (α,ß, and γ) of cGMP phosphodiesterase were similarly decreased.

Photoreceptors in the hypomorphic mutant develop normally but degenerate at a later age due to AIPL1 deficiency. Morphological evidence of degeneration is not seen until 12 weeks of age. However under electron microscopy, an increase in pyknotic nuclei and some outer segment disorganization can be observed in the week before this. From 3 months onwards, there is steady degeneration with a reduction in photoreceptor layer thickness and outer nuclear layer. By 8 months, more than half of the photoreceptors are lost as seen by marked thinning of the outer segments and outer nuclear layers. Cone degeneration was not detected up to 11 months of age. Full field flash ERG showed some changes in young mice (5-6 weeks old) in the form of increased latency and mean gain of phototransduction compared to wild-type mice. The a and b-wave amplitudes were normal at early ages of the *Aipl1 h/h* mice but progressively decreased due to the outer segment shortening and loss of photoreceptors with time. The single rod responses to flash stimuli showed similar characteristics to the ERG findings of the mass photoreceptor response; maximal amplitude of single rod responses to flash stimuli in young mice achieved the same levels as wild type rods, but showed delayed onset and slower initial rise of the single photon response. However, the single photon response in mutant rods

continued to rise for a longer period, taking a longer time to peak and achieved larger final amplitude compared with that in wild type rods. Mutant rods also had increased flash sensitivity and slower recovery following phototransduction. The ERG changes were thought to reflect the physiological consequences in the in PDE reduction subsequent to the AIPL1 deficiency. In darkness, cGMP hydrolysis by PDE is balanced by its synthesis by guanylate cyclases[124]. The basal activity of PDE is decreased along with a fall in PDE concentration secondary AIPL1 deficiency. Decreased PDE activity leads to a reduction in cGMP hydrolysis and accumulation of free cGMP in photoreceptors, causing more cGMP channels to open and thereby increasing intracellular Ca^{2+} levels. This would then feedback to cause a decrease in guanylate cyclase activity and bring cGMP and Ca^{2+} to an elevated steady-state. The increase in latency representing the delayed initiation of the photoresponse was consistent with the delayed diffusional encounter of activated transducin with PDE due to the lower concentration of available PDE[254]. The reduction in the gain of phototransduction and slower rise in single photon response suggested that PDE was activated at a lower rate in mutant rods. The slower recovery phase in dim flash responses and a higher sensitivity to light in mutant rods were also thought to reflect a reduction in basal PDE activity[351]. An understanding of the photoreceptor electrical response to light stimulation would provide a basis in interpretreting the ERG changes following gene replacement therapy in these animals (see later Chapter 3).

Recenly, a study described a patient with later-onset retinitis pigmentosa with caused by compound heterozygous mutation consisiting of a null mutation and a missense mutation. The clinical features and visual loss in this patient was less severe and the progression of the disease was protracted with preservation of some vision into adulthood[204]. It is thought that the *Aipl1 h/h* hypomorphic mouse is remisniscent of this subset of patients who have a milder disease due to *AIPL1* mutations.

1.4 Gene Therapy

1.4.1 The eye as a target for gene therapy

The eye has a combination of unique properties that makes it particularly suitable as a model system for gene therapy. The level of understanding of the molecular pathology of the eye is advanced compared to that of many other organ systems and a large number of inherited ocular diseases have been described at the molecular level. Furthermore, a wide range of animal models are available for the development of experimental therapies. The highly compartmentalized anatomy of the eye facilitates accurate delivery of vector suspensions to specific tissues, while the transparent nature of the cornea and lens allow direct visualization to facilitate surgery and permit non-invasive techniques to monitor and measure the effects of treatment such as using fundus photography, slit lamp biomicroscopy, electrophysiology and psychophysical tests [10,408].

It is thus possible to achieve precise targeting of vector to desired sites within the globe while minimising systemic dissemination. The globe is also easily accessible, meaning that therapeutic agents can be administered via intravitreal or subretinal injections without much disruption to other vital systems. Intraocular tissues comprise of small but stable populations of cells and may be transduced efficiently and by small volumes of vector suspension. The blood-retinal and blood-aqueous barriers maintain a degree of protection from immune responses directed against vector antigens that might otherwise invoke inflammation and limit transgene expression. Additionally, the eye has the ability to induce an immune-deviant response when exposed to new antigens and to suppress delayed-type hypersensitivity [22,49]. Finally, visual function as an outcome measure of any intervention is readily quantifiable using psychophysical and electrophysiological parameters common in standard clinical practice. As paired organs, the fellow eye can serve as a valuable internal control for experimental interventions.

1.4.2 Vectors for gene transfer to the retina

A variety of viral and non-viral vectors have been tested for their ability to transduce various cells in the retina, in particular the photoreceptor cells and RPE which are the cell types most commonly affected in retinal degeneration. The choice of vector to be used in a particular gene therapy strategy is crucial to the success of the treatment and requires several factors to be taken into consideration. Longevity of transgene expression is an important factor in the choice of gene therapy vector for retinal dystrophy because the disease requires lifelong correction. The ideal vector should have low immunogenicity as strong host immune responses result in short-term transgene expression [36,80](for a review, see also [436]. Since most cell types in the eye are non-dividing, integration of the vector DNA into the host genome is not essential for prolonged transgene expression. Moreover, integration could lead to adverse events as a result of insertional mutagenesis. Other desirable features of an gene transfer vector include cell-specificity where only targeted cells are transduced, have a large or unlimited cloning capacity, no toxicity and easy to production at high titres and purity.

1.4.2.1 Non-viral methods

Gene delivery to target tissues in the eye can be achieved without the use of a viral vector, by either injecting or electroporating cells with naked plasmid DNA (for review see [384]). The main advantages of this are safety and biocompatibility, with little risk of inducing host immune response and the possibility of delivering large size DNA or multiple constructs to target tissues. Using direct injection of plasmid DNA into corneal stroma, localised reporter gene expression has been observed although this lasted less than 2 weeks [358]. Transfection efficiency has been shown to improve substantially with adjunctive electroporation in several tissues [446]. Electroporation after intravitreal plasmid DNA injection resulted in efficient introduction of DNA into retinal ganglion cells (RGC) *in vivo* [102]. However, the value of this method

of gene delivery was limited by the transient gene expression which lasted only 21 days. Transfer of DNA into photoreceptor cells *in vivo* by electroporation is more readily achieved in immature retina. Subretinal injection of a GFP expression vector followed by electroporation into newborn mouse and rat retina resulted in highly efficient transfection of rod photoreceptors. The reporter gene expression was observed in 50% and 80% of mouse and rat retinae respectively and seen up to postnatal 50 days[305]. The gene transfer efficiency of this method of *in vivo* electroporation was sufficiently high to prove useful in functional analyses using DNA-based RNA interference (RNAi) vectors and reporter constructs carrying retinal cell-specific promoters or genes of interest. However, similar methods applied to adult mouse retina resulted in significantly fewer GFP-positive cells and immunostaining revealed these cells to be mostly Müller glial cells[305]. It has been shown that it is possible to determine the cell types that are transduced by the route of administration of plasmid DNA prior to electroporation and that the transgene expression can be further specified by using plasmids containing tissue-specific promoters [220]. These techniques may be of use for in *vivo* analysis of gene regulation or promoter analysis but are inefficient for clinical applications due to their transient effect.

Aside from electroporation, DNA can be delivered to cells in liposomes. Lipofectin or cationic liposome has been mainly used for gene transfer *in vitro*, but its ability to deliver DNA *in vivo* has been tested in tissues such as muscle [497]. Cationic lipids condense DNA and thereby protect it from degradation and facilitate endocytosis. In the eye, lipofection can lead to reporter gene expression *in vivo*; liposomal-mediated transfection has been reported in the cornea, trabecular meshwork and retina by various means of administration but the transfection efficiency remains inadequate compared to that of viral vectors and the effects are transient [31]. Novel transfection agents that incorporate ligands for specific cell-surface receptors have been developed, which allows receptor-mediated endocytosis of cationic liposome-DNA complexes to increase transfection efficiency and specificity of cell types transduced [159].

In summary, non-viral methods offer potential for gene transfer without the complications that accompany viral vectors such as immunological response, toxicity and lower the risk of insertional oncogenesis. The main disadvantage of non-viral gene transfer approaches, however, is the poor efficacy and longevity to date *in vivo*. For this reason, non-viral methods of DNA delivery may not be suitable for therapeutic uses, such as gene therapy of inherited retinal diseases.

1.4.2.2 Adenovirus

Adenoviruses are extensively exploited as gene therapy vectors because of their ability to efficiently tranduce a wide variety of cell types independent of cell cycle and to direct high-level transgene expression. In the eye, adenoviral vectors are capable of transducing a variety of cell types depending on the route of administration. Following subretinal delivery, adenoviral vectors are efficient at transducing the RPE and Muller cells [24,51,270], while intravitreal injection results in transduction of anterior segment tissues such as the iris, cornea endothelium and trabecular meshwork, and some limited transduction of retinal ganglion cells[187,215,302,334]. The transduction of photoreceptor cells by adenoviral vectors is poor. Higher levels of transduction are seen if the photoreceptors are in the process of development, such as in neonatal mice; or in the process of degeneration as in adult *rds* mice[270]. It is possible that the long densely packed outer segments and interphotoreceptor matrix in normal adult mouse retina may serve as a physical barrier virus-mediated gene transfer. As the photoreceptor outer segments in both the developing and pre-degenerate retina have shorter or absent outer segments, they may more accessible to the virus in these scenarios [270]. The former finding is of limited clinical importance though, because photoreceptor cells in humans are fully developed at birth. The transduction profile of adenoviral vectors appears to be better suited for the treatment of RPE defects. Vollrath *et al*.

were able to show a restoration of phagocytosis and consequently an improvement in photoreceptor function and numbers in areas which had subretinal injection of rAd expressing MERTK gene in the RCS rat at 1 month after treatment [482]. However, the survival of photoreceptors was not followed up for longer period, therefore it is unclear how long the improvements lasted. Adenoviral vectors may be particularly suited to deliver anti-angiogenic agents for the treatment of proliferative retinopathies because they preferentially transduced proliferative tissue following intravitreal delivery in animal models of proliferative retinopathy[334]. Additionally, adenoviral-mediated transgene expression was higher in the disease models than in wild type mice[334]. Adenoviral vectors have also been used in a Phase I clinical trial for choroidal neovascularisation associated with age-related macular degeneration (AMD) [67]. The gene transfer vector was an E1-, E3-, E4- deleted replication deficient adenovirus serotype 5 carrying the cDNA for human pigment epithelium-derived factor (PEDF), a potent anti-angiogenic protein. The trial was an open-label, dose-escalation study, using low vector titres of between $1X10^6$ and $10X10^9$ to treat patients with severe neovascular AMD [398]. No adverse effects were reported and the treatment was well tolerated overall. The authors claimed that the treatment was effective in ameliorating vision in a number of patients [67], but the efficacy data were difficult to interpret since the number of patients in the study was small and the natural history of AMD patients' visual acuity is such that some month-on-month improvement in outcome measure can be expected without intervention.

While adenoviral vectors have certain advantages over other vector systems such as the ability to carry large inserts up to 48 kb, many limitations have also become apparent with their use, particularly in humans [68]. The main difficulty with adenoviral vectors is the issue of safety and lack of longevity of expression, due to the expression of viral genes from the vector backbone in the transduced cells. This induces an immune response againset transduced cells resulting in transient transgene expression and long term toxicity [221,353]. This problem renders these vectors unsuitable for many gene therapy applications in which long term transgene expression is desired.

Much work has been carried out to develop safer and more efficient adenoviral vector, by incorporating fewer viral genes in the recombinant virion [480]. The first generation vectors are deleted in the E1 region making them replication defective, and in the E3 regions which enable these vectors to carry DNA inserts of up to 7.5kb [164,382]. Newer 'second-generation' adenovirus have been engineered with additional deletions or mutations in the viral E2 and E4 regions, preventing transcriptional control of viral gene expression and viral genome replication respectively [20,486]. Despite this, the utility of first- and second-generation adenoviral vectors for ocular gene transfer remained limited due to the aggressive immune response triggered by these vectors in the eye. Following administration to the retina, T-cell mediated responses led to the loss of transgene expression just 3 weeks after treatment. Abrogation of immune response in nude mice which lack T-cells population resulted in prolongation of transgene expression up to 3 months after treatment [402]. Immune suppression by co-injection of a adenovirus encoding CTLA4-Ig, an immunomodulatory molecule that blocks stimulatory signals for T-cell stimulation, with an adenovirus carrying a reporter gene also led to longer reporter gene expression up to 18 weeks following treatment [11].

Further improvement in the safety and efficacy of adenoviral vectors came with the development of helper-dependent adenoviral vectors (HDAds, also referred to as gutless, gutted, mini, fully-deleted, high capacity, pseudo) which are deleted of all viral coding sequences. They contain only the viral inverted terminal repeats (ITR) and packaging sequences [233,354]. They retain the advantages of first generation adenoviral vectors in terms of high-efficiency *in vivo* transduction and transgene expression, these HDAds are able to mediate high-level, longer term transgene expression in the absence of chronic toxicity [115,352,493]. Following subretinal delivery of encapsidated Ad mini-chromosomes carrying *β-PDE,* the transgene product has been found to persist in the form of mRNA for 18 weeks post-treatment and protein for up to 5 months in treated *rd1* mice [247]. Howver, there were problems associated with these techniques, such as contaminating helper

virus, vector instability and the emergence of replication-competent adenovirus [233,354,447].

1.4.2.3 Lentiviral vectors

Lentiviral vectors are being developed in ocular gene therapy because of their ability to infect non-dividing cells [481]. Lentiviruses are a subgroup of retroviruses which are RNA-based viruses that possess a reverse transcriptase, through which they are able to integrate their reverse-transribed proviral DNA into host cell chromosomes. Retroviruses have 3 transcription units - *gag, pol* and *env* and *cis*-acting RNA elements recognised by viral proteins that package the RNA into infectious particles. To generate recombinant retroviruses, the *gag, pol* and *env* are removed to give a carrying capacity of approximately 8kb; the gene of interest is cloned into a plasmid containing 3'- and 5' long terminal repeat (LTR) sequences and the 350 bp ψ sequence required to package this recombinant genome, while the *gag, pol* and *env* genes are provided in trans in helper plasmids that are ψ-negative. The general advantage of retroviruses as vectors is the ability of these viruses to integrate efficiently into host cell genome, thus confering stable longterm transgene expression. However, retroviruses are only able to infect dividing cells as they gain access to the host cell chromosomes when the nuclear membrane dissolves during cell division. This limits the target tissues for which retroviral vectors can be used, making them unsuitable for use in the eye.

While lentiviruses are similar to retroviruses in that they are both use RNA as their genomic nucleic acid, there are many distinguishing features that confer special advantages to lentiviral-based vectors. Lentiviral genomes encode additional genes such as *rev, tat, vif,* and *vip* that code for accessory proteins involved in the regulation of proviral gene expression. They mediate transgene expression in quiescent or terminally differentiated cells as well as dividing cell types because their pre-integration complex containing the reversed transcribed cDNA is able to cross the host cell nuclear membrane

by active transport via nuclear pores during interphase [64]. Vectors from various members of the lentivirus family have been developed for gene transfer, including the human immunodeficiency virus type I and II (HIV1, HIV-2), equine infectious anaemia virus (EIAV), feline immunodeficiency virus (FIV), simian immunodeficiency virus (SIV) and bovine immunodeficiency virus (BIV) [83,197,284,328,462][196]. The most commonly used lentiviral vectors are based on the HIV1 which has a natural tropism for $CD4^+$ T-lymphocytes. Tissue specificity or cellular tropism is determined by the surface glycoproteins on lentiviral envelopes. Pseudotyping results in lentiviruses expressing envelope proteins from other viruses on their surface, thus altering the expression of glycoproteins in the viral envelope and subsequently, lentiviral vectors can be modified to infect a broad range of cell types. For gene therapy applications, HIV1 is most commonly pseudotyped with vesicular stomatitis virus surface protein (VSV-G protein) because of the broad cell tropism; VSV-G envelope protein recognises a ubiquitous phospholipid in the cell membrane that enables the virus to infect different cell types. In the eye, subretinal delivery of HIV vector pseudotyped with VSV-G and driven by a ubiquitous cytomegalovirus (CMV) or spleen focus forming virus (SFFV) promoter results in reporter gene expression limited to the RPE [35]. Photoreceptor cell transduction has been reported when VSV-G pseudotyped vector is injected into neonatal mice, possibly because of better access of vector to photoreceptors whilst the retina is still developing [30,330]. However, the transduction efficiency in photoreceptors is poor compared with that achieved by AAV vectors (see section 1.4.2.4). Subretinal delivery of VSV-G pseudotyped SIV, FIV, and BIV vectors results in a similar pattern of transduction[84,117,462]. However, subretinal delivery of VSV-G pseudotyped EIAV results in some transduction of photoreceptor cells as well as efficient transduction of RPE cells [37].

The main safety concern when using HIV-based vectors in particular, is the possibility of generating wild-type viruses through recombination. The likelihood of this type of recombination depends on residual *cis*-acting sequences in the packaging plasmid, allowing some level of encapsidation, and on the extent of sequence homology between packaging and vector

constructs. This risk is minimized in newer generations of lentiviruses which have most of the viral genome deleted and the viral accessory proteins and envelope excluded from the production phase[118,528]. Third generation HIV-1 vectors are packaged by three non-overlapping expression constructs – two expressing HIV proteins and the other expressing the envelope of a different virus [225,307]. The development of self-inactivating viruses is another conceptual breakthough in which the transcriptional enhancer and promoter regions in the 3'U3 long terminal repeat (LTR) are deleted which prevents them from activating inappropriate transcription of genes downstream of the integration site. Following reverse transcription of the vector RNA, this modification is copied over into the 5' LTR, thus causing inactivation of both LTRs in the integrated proviruses [329,423,527]. The resulting vector cannot be converted into a full length vector RNA in transduced cells, thereby reducing the risk of vector genome mobilization and also reducing the likelihood of enhancement or aberrant expression of surrounding cellular genes.

Although integration into the host genome has the advantage of being able to mediate long term gene expression, it increases the risk of insertional mutagenesis. This has lead to the development of non-integrating vectors that have comparable transduction efficiencies and persist as episomal double-stranded DNA circles that are capable of transducing non-dividing cells [287,411,479]. These vectors are rendered integrase-deficient by the introduction of a point mutation in the *integrase* gene. Efficient and sustained transgene expression has been demonstrated using non-integrating lentiviral vectors *in vivo* in post-mitotic tissues such as the RPE, and at levels equivalent to that of their integration-proficient couterparts [507].

Thus the newest lentiviral vectors incorporate additional safety features that may facilitate their clinical application given the improved safety profiles; the generation of self-inactivating, pseudotyped and integrase-deficient lentiviral vectors have been found to be effective in animal gene transfer studies. Lentivirus-mediated *Mertk* expression was shown to restore RPE phagocytosis, improve rod function on ERG and maintain outer nuclear layer

thickness in the Royal College Surgeon rat, a model of retinal degeneration [471]. However so far, the use of lentiviral vectors for gene therapy in the eye appears to be limited to gene correction in the RPE as that is the only cell type transduced with high enough efficiency for therapeutic purposes. Lentiviral vectors may be of use for the treatment of photoreceptor defects by mediating the delivery of secreted factors, such as neurotrophic or anti-apoptotic factors to the RPE.

1.4.2.4 Adeno-associated viral vectors

Among all the vectors that have been used in the eye for gene transfer to the retina, vectors based on adeno-associated virus (rAAV) have emerged as the most promising in terms of efficiency and stability of gene transfer. Several main features of AAV that render them ideally suited for retinal gene therapy include the lack of pathogenicity, minimal immunogenicity, their ability to transduce non-dividing cells and their capacity to mediate long and sustained levels of therapeutic gene expression. They have been used to treat animal models of a wide range of retinal disorders from LCA and RP to autoimmune uveitis and neovascular disorder[14,29,32,34,62,250,251,280,301,311,335,363,390,403,464,525].
They have also recently been used in clinical trials for the treatment of LCA [34,181,293] (see later).

Adeno-associated viruses are one of the smallest viruses with a non-enveloped icosahedral capsid of approximately 22 nm. As they require a co-infecting helper virus for replication to occur, adeno-associated viruses are categorised as dependoviruses that is naturally replication-deficient and non-pathogenic. Wild-type AAV has a linear single-stranded DNA genome of about 4.8 kb which is composed of two open reading frames (ORFs) encoding capsid structural proteins (*cap*) and replication proteins (*rep*), flanked by two 145 bp inverted terminal repeats (ITRS). These ITRs are the minimal *cis*-acting elements necessary for viral genome integration, replication and packaging into the capsid shell. The virus does not encode a

polymerase and instead relies on cellular polymerase activities to replicate its DNA. The first ORF (*rep*) encodes four Rep proteins that are involved in replication of the viral genome, whereas the second ORF (*cap*) encodes three structural viral proteins (VP1, 2 and 3) which together assemble into near-spherical shell of 60 subunits with icosahedral symmetry. The genome of wild-type AAV is known to integrate into host chromosome DNA in a site-specific manner; this integration occurs at a locus on human chromosome 19 and is mediated by the AAV gene *rep* [244]. This property is lost in the recombinant vectors used in gene therapy due to the absence of the *rep* gene. The recombinant virus, however, retains ability to integrate with low efficiency into heterogenous sites around host genome [38,345]. The recombinant AAV genome persists mostly as high molecular weight concatemers and stable long term transgene expression with rAAV is thought to be primarily due to these extra-chromosomal vector genomes[136,318]. Most of the time AAV vector genomes persist within cells as episomes, with only fraction of the genomes integrating into host genome[345]. Vector integration events are non random and tend to favour transcriptionally active regions of chromosomes[342-344], and have been observed in various experimental studies to occur either at non-homologous sites where DNA damage may have occurred[199,323] or by homologous recombination (for a review, see [438]). Concerns were raised when a study by Donsante *et al.* suggested that insertional mutagenesis resulting from the integration of AAV vectors was associated with tumorigenesis[107]. In this study, newborn normal mice and mice with the lysosomal storage disease mucopolysaccharidoses VII that received high-dose intravenous AAV vector expressing the human β-glucuonidase gene driven by a β-actin promoter and CMV enhancer, had increased incidence of hepatocellular carcinoma.[106,107]. These findings, however, need to be considered in light of the many studies using AAV vectors which have been done in rodents, dogs and primates where no increased in the incidence of tumours have been reported. Experimental factors which were unique to the study such as the treatment of very young mice, the particular strain of mice, the route of delivery, possible effects of the transgene and promoter-related effects may have contributed to the phenomenon. Large scale studies involving adult

mice or p53-deficient mice found no evidence for AAV-induced malignancies[44,45] and thus far, the bulk of experimental evidence suggest that tumours are not routinely observed following AAV vector administration. Furthermore, the favourable safety profile, minimal risk of germline transmission[425] and long-lasting transgene expression obtained in organs of animal models of human disease have lead to the initiation of several Phase 1 and 2 clinical trials with rAAV vectors[72,93,166]. Various diseases are being targeted including Parkinson's disease, Alzheimer's, muscular dystrophy, rheumatoid arthiris, cystic fibrosis, melanoma, α1-antitrypsin deficiency, haemophilia B (factor IX deficiency) [140,224,297], Factor XIII deficiency and RPE65-associated LCA[34,181,293] (for a review see [71] and [121]). In the context of ocular gene therapy, the issue of tumorigenesis is even less likely to be a concern, given the low dose of vector that is normally being delivered, the lack of systemic dissemination (see later), and so far, there has been no reports of ocular tumours or tumours elsewhere following intraocular AAV vector delivery.

Recombinant AAV (rAAV) particles are generated by transfecting producer cells with a plasmid bearing a cloned rAAV genome flanked by the ITRs and a plasmid expressing *rep* and *cap* genes in *trans* (Figure 1.17). The ITRs contain all the *cis-acting* elements involved in genome rescue, replication and packaging. AAV is an inherently defective virus, its replication requires functions supplied by co-infection with helper viruses, such as adenovirus and herpesvirus[94,306]. In the absence of helper viruses or helper functions, the viral DNA can become integrated into host chromosomal genome to establish a latent infection[244]. AAV is capable of infecting both dividing and non-dividing cells, and has wide tropism allowing it to infect many cell types depending on the particular serotype[460,502]. To date, over 100 AAV serotypes from different animal species have been isolated[152,153,336,422]. The different serotypes differ from each other in the sequence of their capsid protein. Recombinant AAV (rAAV) vectors used for gene therapy are mainly based on the serotype 2 (AAV2); this was the first human serotype described and the best characterised AAV serotype. Since the capsid protein of AAV is responsible for its tropism and hence

efficacy, a pseudotyping strategy was developed where 'pseudotyped' or hybrid AAV vectors encode *rep* from one serotype, usually AAV2, and the *cap* gene of a different serotype. Such hybrid virions produced in this instance contain genomes usually based on AAV2 and the capsid of a different serotype such as AAV5; in this instance, the chimeric AAV vector is designated AAV2/5 where the first number indicates the ITR of origin and the second denotes the capsid. The hybrid vectors generated in this way have expanded the available repertoire and cell tropism of AAV vectors, and additionally have the combined advantage of safety and long term expression of AAV2 and the improved *in vivo* efficacy and tropism of the novel serotypes. Cell-targeting strategies determine not only the cell types with which the vector interacts with but also the efficiency of the gene transfer process since processes related to virus uptake by cells and intracellular vision trafficking depend directly or indirectly on capsid conformation[133,135,180,466]. Apart from pseudotyping, other strategies for engineering custom-made capsids have been employed to further broaden the utility of AAV vectors to either transduce tissues that are refractory to naturally occurring AAV serotypes or to limit transduction to specific tissues. These include generating mosaic capsids (composed of a mixture of capsids subunits from different serotypes), chimeric capsids (containing capsid proteins that have been modified by domain or amino acid swapping between serotypes), targeting ligand insertion into the capsid, and recently, library selection and directed evolution have emerged as promising approaches to modulate AAV tropism[58,156,179,294,340,341,364,386] (for reviews, see [320,502,516]). In the context of ocular gene therapy, pseudotyping of vectors remains the most important strategy for targeting gene delivery to specific cell types.

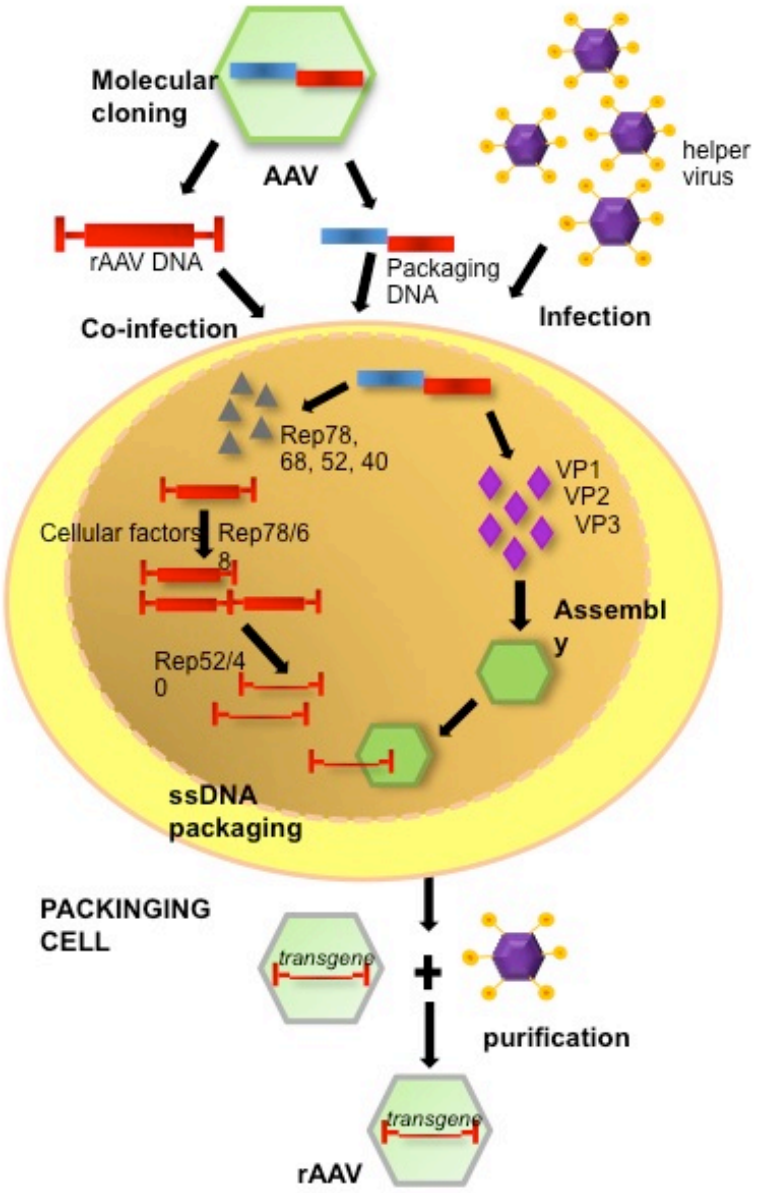

Figure 1.18 Overview of the recombinant AAV production system.

Plasmid constructs encoding rAAV genomes containing the transgene flanked by ITRs are transfected into packaging cells together with a *rep* and *cap* expression plasmid, they lead to the production of rAAV particles. Helper functions required to recapitulate the lytic phase of the AAV life cycle is provided through the infection of packaging cells with recombinant viruses based on adenovirus, HSV or baculoviruses. Following the release of infection of rAAV virion particles from producer cells, purification is undertaken using affinity column or ion-exchange chromatography.

In the eye, AAV 1 through 9 and two additional AAV capsids isolated from rhesus monkey, AAVrh8 and AAVrh10 have been evaluated in the retinas of rodents and primates[12,13,18,30,158,262,348,387,508]. Each cell type in the retina can be targeted by choosing the appropriate combination of AAV serotype, promoter and intraocular delivery route. In general, subretinal injections of AAV vectors lead to transduction of photoreceptors and RPE, while intravitreal injections transduce retinal ganglion cells. Table 1.4 displays the transduction characteristics of pseudotyped rAAV in various cell types in the eye. The first AAV serotype to be tested in the retina was AAV 2/2[13] and its transduction profile has been well established. Subretinal administration of AAV2/2 leads to transduction of photoreceptors and RPE cells, with an onset of transgene expression after 2-4 weeks and peaks at 4-6 weeks after vector administration[12,13,30,47,139,262,389,409,418,459]. Intravitreal administration of AAV2/2 leads to transduction of ganglion cells, trabecular meshwork, cells of the inner nuclear layer including Müller cells [12,30,57,116,169,273,274,300]. Amongst the other AAV serotypes tested so far in the retina, AAV 2/1, AAV 2/6 and AAV2/4 are considered ideal for RPE gene transfer[30,461,489,508]. AAV2/5, AAV2/7, AAV2/8 and AAV2/9 have been shown to be particularly promising for the delivery of transgene to photoreceptor cells, noteably the expression levels in photoreceptors mediated by AAV2/7 and AAV2/8 are six- to eightfold higher than AAV2/5, previously the favoured vector for photoreceptor gene transfer[18,286,348,508]. AAV2/9 additionally transduces Müller cells following subretinal delivery [18]. Following intravitreal injection, only AAV2/2 and AAV2/8 have been observed to transduce retinal ganglion cells, with some transduction of Müller cells[19,262,460]. Anterior segment structures such as the trabecular meshwork, iris, corneal stroma and lens epithelium are more readily transduced by AAV2/7, AAV2/8 and AAV2/9 following intravitreal delivery[262]. Previous studies have suggested that the inability of many AAV vectors to effectively transducer the inner retina from an intravitreal injection is due to the barrier created by the inner limiting membrane. However, recent studies showed that AAVrh8 and AAVrh10, novel capsids isolated from rhesus monkey, are able to transduce amacrine

cells, horizontal cells and bipolar cells effectively following intravitreal delivery[158].

As well as tropism towards given cell types, the kinetics of transgene expression are also determined to some extent by the serotype. The time of onset of transgene expression differs for the various serotypes: subretinal injection of AAV-2/1, 2/7 and 2/8 results in early onset of transgene in mice within 5 days, AAV-2/5 around 1 week and AAV2/9 at 11 days, all of which are much faster in onset compared to AAV2/2[30,262,408,418]. The transduction efficiency and intensity of expression also vary amongst the different capsids, with newer AAV serotypes such as 2/7, 2/8 and 2/9 being more efficient and mediating higher levels of transgene expression compared to AAV2/2 or AAV2/5[18,262,348]. The pseudotyping approach may also be beneficial in evading neutralizing antibodies to capsid components in individuals seropositive for AAV2 or in those patients needing vector readministration.

Table 1.4 Different cellular tropism and expression kinetics based on serotype and delivery method in the mouse retina.

Delivery method	rAAV serotype	Onset period	Cell types transduced
Subretinal	AAV2/1	Rapid, 3-4 days	RPE
Subretinal	AAV2/2	Delayed, 2-4 wks	PR, RPE, some RGCs
Subretinal	AAV2/4	2 weeks	RPE
Subretinal	AAV2/5	Rapid 3-5 days	PR, RPE
Subretinal	AAV5/5	Rapid, 3-5days	PR, RPE
Subretinal	AAV2/6	Rapid, 3-5 days	RPE
Subretinal	AAV2/7	5 days	PR, RPE
Subretinal	AAV2/8	Rapid, 1-5 days	PR, RPE, Müller cells, RGC.
Subretinal	AAV2/9	10-11 days	PR, RPE, Müller cells.
Intravitreal	AAV2/2		Inner retina, RGC, some Müller cells, optic nerve fibers trabecular meshwork, small amount of ciliary body,
Intravitreal	AAV2/7		Anterior segment (TM, corneal stroma, iris, lens epithelium), small amount of ciliary body.
Intravitreal	AAV2/8		Inner retina, RGC, some Müller cells , anterior segment (TM, corneal stroma, iris, lens epithelium), small amount of ciliary body.
Intravitreal	AAV2/9		Müller cells, anterior segment (TM, corneal stroma, iris, lens epithelium).
Intravitreal	AAVrh8		RGC, amacrine cells , horizontal cells, Müller cells
Intavitreal	AAVrh10		RGC, amacrine cells, horizontal cells, Müller cells, bipolar cells.

Compiled from various publications.[12,18,30,158,262,348,408,460,508].
PR – photoreceptor cells; RPE – retinal pigment epithelium; RGC-retinal ganglion cells.

One of the limitations of recombinant AAV is its small packaging capacity of 4.7 kb which precludes many therapeutically important coding sequences. Emerging technologies in AAV vector design employing a split gene principle (trans-splicing AAV vector system) have allowed to assembly of large cDNAs in target cells by splitting the gene and cloning the fragments in independently into the rAAV genome. The AAV encoding the 5' end of the gene is designed to possess a splice donor while the vector encoding the 3' end possesses a splice acceptor. Following co-transduction of target cells by both vectors, head-to tail heterodimerization via intermolecular recombination between the two vector DNA molecules restores the full-length expression unit and results in the desired protein synthesis [505,506][253]. Its utility for therapeutic application has thus far been limited by its lack of efficiency. The efficiency of the process depends on the number of AAV genome copies entering the nucleus, and is increased in tissue systems where transduction occur through an enclosed space, such as the muscle or subretinal space, as this favours the entry of both vectors in the same cell[401]. The use of efficient AAV serotypes which mediate high levels of transduction further increases the efficiency of transplicing since there are more genome copies of the dual vectors per cell[508]. A recent study suggests that the limited capacity of AAV2 can be exceeded by AAV5[17]. Packaging of genes up to 8.9 kb was shown to be possible using AAV2/5, and following intraocular delivery, the expression of the appropriate protein obtained and resulted in morphological and functional improvement in an animal model of retinal dystrophy[17]. Another new development in vector design is self-complementary AAV vectors (scAAV), which uses the ability of AAV to package replicons half the size of wild-type DNA in the form of single-stranded dimeric genomes with an inverted repeat configuration [308]. In the target cell, these self-complementary molecules fold back into double-stranded forms without the need for *de novo* DNA synthesis or the annealing of complementary genome that occurs in conventional rAAV replication. Self-complementary AAV has been shown to have faster initiation of gene expression in eyes that received subretinal injection of scAAV than titre- and serotype- matched single-stranded AAV [348]. Many also mediate higher

levels of expression although an expression cassette of only 2.4 kb can be used.

The tissue-specific expression patterns, non-pathogenicity, together with the replication-deficient nature of AAV make this vector a safer and attractive alternative to other available vectors. Studies evaluating biosafety of rAAV have shown minimal systemic dissemination following intraocular administration and to date, there has been no reports of tumorigenesis or toxicity in the long term[45,333]. Biodistribution of rAAV in distant organs following intraocular delivery has never been reported[408]. Biodistribution studies of different rAAV serotypes delivered to the subretinal space or intravitreally in rats and dogs failed to detect vector sequences in liver or gonad samples, indicating that the risk of germ-line transmission of vector DNA is very low [383]. Following intravitreal injection, rAAV sequences were detected in the optic nerve and along the visual pathway in the brain, indicating that anterograde and transynaptic transport of rAAV is possible. High levels of green fluorescent protein (GFP) were found in the optic nerves and brains of mice and dogs following intravitreal administration and persisted for up to 6 months[116]. However, this risk appears to be reduced with subretinal injection - in another study, vector DNA was consistently detected along the visual pathway in the brains of rats and dogs following intravitreal injection of rAAV2/2, while subretinal injection resulted in detection of vector DNA in the optic nerve only [383]. There is also evidence that the potential for transynaptic transfer is higher with AAV8; subretinal delivery of an AAV2/8 vector carrying *gfp* gene in rats and dogs resulted in the transduction of not only the RPE and photoreceptor cells, but also of the inner nuclear layer, ganglion cells and in brain tissue along the visual pathway including the lateral geniculate nucleus and beyond that in dogs. [448]. Vector sequences were also found in various parts of the brain of the contralateral hemisphere after subretinal injection of AAV8 in dogs. These findings highlight the importance of restricting expression of the transgene to the targeted tissues by using vector design which incorporate tissue-specific promoters and pseudotyping of rAAV vectors.

Compared to other viral vectors such as adenoviral vectors, rAAV is less immunogenic. However, more recent studies have shown that AAV is capable of stimulating an immune response that can inhibit the efficacy of repeated vector administration[298,488], although the route of administration and vector dose appear to be key elements in determining the degree of anti AAV immunity that is generated. A degree of humoral response to rAAV capsid proteins has been reported particularly following intravitreal delivery which was sufficient ot block vector expression upon readministration into the partner eye [269]. Subretinal delivery of rAAV is better tolerated, although there is a dose dependent effect [39]; low doses of rAAV2 did not lead to the development of neutralising antibodies in mice and transgene expression after readministration of the vector was achievable, whereas higher doses of vector lead to the induction of humoral responses which reduced the efficacy of repeated vector administration [21][39]. Immune responses to rAAV may be species-dependent; greater immune responses have been observed in large animal models such as dogs than in mice which have received the equivalent vector dose [45,46]. However attenuation of the immune responses can be achieved using transient immunosuppression, thereby permitting long-term transgene expression [33,48,286].

The potential of AAV vectors for the treatment of retinal disorders for ocular disorders has been extensively evaluated in a variety of animal models of dominant and recessive retinopathies (see section 1.4.3). The majority of retinal dustrophies are due to mutations in genes specifically expressed in photoreceptor cells. Since other vectors do not transduce photoreceptors effectively, AAV appears to be the most suitable vector for gene delivery to photoreceptors. AAV-mediated gene transfer has been evaluated a number of large animal models including dogs and primates, which better reflect the human eye in terms of anatomy, proportions and immunological responses and similar efficiency and stability of transduction have been observed [33,48,260,383]. Proof-of principle using AAV-mediated gene replacement for the treatment of LCA has been demonstrated in several animal models, including non-human primates [53,60,203,363,455,464]. Longer term studies in non-human primates and dogs have found no adverse effects on retinal

function or morphology and stable transgene expression in ocular tissues for up to 36 months following subretinal injection of rAAV [261].The pre-clinical success, long lasting transgene expression mediated by AAV vectors and their favourable safety profile has made it the vector of choice in clinical trials for LCA [34,181,293] and so far, it has shown great promise in several of the concluded phase I clinical studies (see following section below).

1.4.3 Gene therapy for inherited retinal dystrophies

Due to the tremendous genetic heterogeneity associated with inherited retinal degeneration, different gene-mediated therapy strategies have been developed for treatment of inherited retinal degenerations. These causal mutations lead to disease through the loss of function of a mutated gene for example in autosomal recessive or X-linked recessive retinal degeneration, or through a toxic gain of function such as in autosomal dominant retinal degenerations. There are two broad strategies employed to rescue retinal cells from degeneration. The first is a specific gene targeted treatment in which the aim is the correction of the underlying gene defect. “Gene correction” may be achieved by augmenting the defective gene with a functional copy in the case of monogenic recessive diseases and haploinsufficiency, or by ablating the expression of the ‘toxic’ message from a dominant mutation. The second strategy involves a more generic approach and does not depend on the underlying defect. This entails the delivery of genes that express neurotrophic factors that help prolong photoreceptor survival [63,289]. The advantage of this approach is that it is not specific to the disease and can therefore be applied to many conditions, including disorders with a multifactorial aetiology. The disadvantage is that this approach has not been very effective to date and may have a better role as a supplementary treatment to gene replacement therapy in monogenic disorders.

1.4.3.1 Gene therapy for treatment of dominant diseases

Autosomal dominant retinitis pigmentosa (AdRP) due to gain-of-function mutations in *rhodopsin (RHO)* is one of the common forms of RP and accounts for 30-40% of cases of adRP. *Rhodopsin*-based autosomal dominant RP (*RHO*-adRP) has considerable mutation heterogeneity, a situation that is mirrored in many dominantly inherited diseases. Hence, *RHO*-adRP has been frequently used as a model disorder for developing treatment for dominant diseases. In *RHO*-adRP, causal mutations can lead to the expression of mutant alleles that interfere with native wild-type alleles, hence producing a toxic gain of function[315]; studies in transgenic mice have shown that lower levels of mutant *rhodopsin* are associated with less severe disease [357]. The treatment of disorders that are associated with toxicity of a mutant allele require that the mutant gene must be repaired or silenced. Two strategies have been proposed for mRNA silencing. The first includes the use of allele-specific inhibitors that promote the degradation of only the defective mRNA and allow the expression of the normal allele that might be sufficient to maintain the function of the photoreceptor cells [275]. The second strategy is a mutation-independent approach where transcripts from both wild-type and mutant alleles are suppressed, and replaced by a non-silenced normal version [131]. Both approaches can be mediated by a variety of antisense inhibitors such as ribozymes, antisense oligonucleotides and small inhibiting RNA (siRNA). Ribozymes are catalytic RNA molecules that bind to specific mRNA sequences and catalyse the cleavage of that messages associated with the disease [108][374]. It has been established that ribozymes can limit gene expression by cleavage of targeted mRNA *in vivo* in the retina. The P23H transgenic rat is a model for adRP and carries the most frequently found mutation in *rhodopsin* [113]. AAV delivery of ribozymes specific for the P23H transgene mRNA selectively knocked down the mutant mRNA in P23H transgenic rats and led to preservation of the photoreceptors for up to 8 months [109,267][258]. However, an optimal ribozyme cleavage site had been engineered into the transgene, enhancing the efficacy of the therapy.

The considerable heterogeneity of mutations in dominant disorders renders mutation-specific gene therapies neither economically nor technically feasible because this would require the development of a large number of mutation-specific inhibitors in order to be widely applicable. The use of allele-independent RNA inhibitors is more realistic since a single reagent can be used against different mutations in the same gene. For optimal therapy, this should be accompanied by simultaneous provision of a replacement gene that encodes the wild-type protein but is resistant to suppression by utilising the degeneracy of the genetic code [355]. *In vitro* data have demonstrated that ribozymes directed against the 5' untranslated region of rhodopsin mRNA could cleave all *rhodopsin* transcripts, mutant or wild-type, and that a *rhodopsin* gene designed not to be cleaved by these ribozymes could replace the ablated gene product [324]. *In vivo* efficacy was demonstrated when AAV2/5-mediated delivery of an allele-independent mouse-specific ribozyme targeting wild-type and mutant *rhodopsin* lead to partial rescue of photoreceptor function and structural preservation in P23H transgenic rats [162]. *In vivo* mouse *rhodopsin* mRNA levels were reduced by 46% following treatment. Since the P23H mutant transgene in the rat model was derived from a mouse genomic clone, a reduction in the mutant P23H trangene was obtained while the *rhodopsin* mRNA level (which was resistant to the ribozyme) was unchanged [162].

Despite these claims of success in the application of ribozymes *in vivo*, many researchers consider RNAi a more potent and durable approach. RNA interference (RNAi) involves the use of small interfering double-stranded RNA molecules (siRNA) which are able to mediate site-specific cleavage of a target mRNA molecule [120,268] by recruiting Dicer proteins to a multi-protein complex known as RNA-induced silencing complex (RISC)[429]. A common way of using RNAi is to generate short-hairpin RNA (shRNA) molecules through transcription of DNA templates. Using a viral vector, the DNA template can be delivered to the target tissue; the shRNA is then transcribed and processed to siRNA [503]. Short-hairpin RNA have been shown to be effective in silencing more than 90% of mutant (P23H) *rhodopsin* transcript *in vitro* and in retinal explants [74,231]. *In vivo,* it has

been shown that *rhodopsin* can be effectively down-regulated with resultant decrease in retinal function and outer nuclear layer thickness by AAV2/5-delivered *rhodopsin*-specific siRNA to the retina in wild type and heterozygous *rhodopsin* knockout mice [163]

Both *in vitro* and *in vivo* validation of suppression and replacement strategy for *RHO*-adRP was demonstrated by O'Reilly *et al.* Using AAV2/5-mediated delivery of shRNA, approximately 90% *in vivo* suppression of *RHO* was obtained in mice which expressed a human transgene on *Rho-/-* background [313][355].. Using AAV2/5 vectors that express shRNA targeting *RHO* together with a codon-modified *RHO* replacement gene *in vivo* into the eyes of $P23H^{+/-}$ $Rho^{+/-}$ mice (expressing a mutant human *RHO* allele), therapeutic benefit was seen in the form of a 33% difference in outer nuclear layer thickness between treated and untreated eyes[355]. In another transgenic mouse model of adRP, the P347S mouse, AAV-mediated shRNA expression targeting *RHO* in the presence of expression of an endogenous mouse *Rho* gene that is refractory to suppression (due to divergence between mouse and human *rhodopsin*) resulted in improved retinal histology and function as assayed by ERG [76]**.** These studies thus demonstrate that RNAi-based suppression in conjunction with codon-modified gene replacement can lead to photoreceptor rescue as evidenced by structural and functional benefit following treatment in animal models of adRP.

1.4.3.2 Gene replacement therapy for treatment of recessive diseases

Early attempts at gene replacement therapy were not successful in rescuing phoptoreceptors in the *rd1* mouse, a well characterised model of autosomal recessive retinitis pigmentosa and has a homozygous nonsense mutation in the gene encoding the β-subunit of rod cGMP phosphodiesterase, *Pde6b*. These experiments were performed using a variety of viral vectors including adenovirus [50], AAVs [216], gutted adenovirus [247], and lentivirus [463].

The lack of rescue was largely due to the failure of adenovirus[51] and HIV-1[463] to efficiently transduce photoreceptors. In a study using an AAV2 vector, only faint β-PDE immunostaining and a slight shift in *in vitro* electrophysiological response was seen in the *rd1* mouse following treatment [216]. It has been very difficult to rescue the *rd1* mouse even with better AAV vectors such as AAV5 and AAV8. However, gene replacement therapy has been more effective in *rd10* mice, a hypomorphic *Pde6b* mutant with a missense mutation in exon 13. The mutation causes partial loss of PDE activity and a milder phenotype than the mutation in *rd1* mice. Loss of photoreceptor cells begins at P16 and is complete by P60. Dark rearing slows the degeneration by a further 4 weeks and allows the formation of outer segments that are not normally formed in either *rd10* or *rd1* mice. Pang et al. showed it was possible to preserve photoreceptors and retinal function following gene replacement therapy using an AAV2/5 vector. However, this was made easier by dark rearing the animals until vector administration at P14, and also for a further two weeks after treatment. They were then exposed to light for one week before the effect of treatment was assessed [359].

More convincing rescue was achieved in the *rds* mouse, another model of autosomal recessive RP, which is homozygous for a null mutation in the *peripherin2* gene encoding a membrane glycoprotein essential for the formation of photoreceptor outer segment discs. Subretinal injection of AAV-2 carrying a *peripherin2* transgene driven by a bovine rhodopsin promoter resulted in the formation of discs and restoration of photoreceptor structural integrity [14] with some long term persistence of the structures which were detectable 42 weeks post-treatment. The structural rescue was accompanied by functional improvement seen on ERG responses [420] and improved central visual function seen on recordings from visually responsive neurons in the superior colliculus [421]. These studies provided the first indication of the potential for gene replacement therapy in the treatment of photoreceptor defects. Longer term studies however, found that the functional improvements were not maintained over time; the electrophysiological improvements appeared to peak six weeks after treatment and then

assumed a downward trend following that, although treated eyes retained statistically significant improvement in b-wave amplitude over uninjected eyes [419]. Longer term improvements in function were not sustained in this model, probably due to inapropriate levels of *peripherin2* expression and the failure of the intervention to delay apoptotic photoreceptor loss.

Gene replacement therapy for inherited retinal degenerations caused by RPE defects has generally been more successful. There are several postulated reasons as to why RPE defects are more amenable to gene therapy. The photoreceptors in RPE defects are inherently healthy and structurally intact and therefore, restoring function to the underlying RPE allows these photoreceptors to resume normal function. It is also possible to influence a wider area of photoreceptors by transducing the RPE as each RPE cell communicates with numerous photoreceptors. Extensive work has been carried out on models for Lebers Congenital Amaurosis (LCA), a severe early-onset form of inherited retinal dystrophy (see Chapter 1.3). In particular, success has been reported animal models of LCA caused by defects in an RPE-specific gene, *RPE65.* The *RPE65* gene encodes a protein expressed in the RPE that is essential for the synthesis of 11-cis-retinal in the retinoid cycle. Consequently, there is an inability to generate adequate visual pigment for initiation of phototransduction. These animal models with *RPE65* defects have severely depressed dark and light ERG responses with poor vision from early life and are phenotypically similar to LCA caused by *RPE65* mutation in humans. Mice with targeted disruption of *RPE65* have a relatively slow photoreceptor degeneration, losing about 50% of photoreceptors at 4 months of age, reduced amount of opsin in photoreceptor outer segments and undetectable scotopic ERG from birth [400]. Treatment of RPE65-/- mice using AAV2/2 vector resulted in transient functional recovery of photoreceptors on but this was not accompanied by any delay in the photoreceptor degeneration[249]. Following improvements in the vector design, a different study demonstrated more substantial improvement in ERG following subretinal injection of AAV2/2 carrying chick β-actin driven human *RPE65* cDNA although the follow up period was only 3

months and there was no assessments on the effect of treatment on the rate of photoreceptor degeneration[53].

Another mouse model with a naturally occurring homozygous null mutation in the murine *Rpe65* gene is the *rd12* mouse [360]. The retinal degeneration in this mouse model is similar to the genetically engineered model, approximately one-third of the outer nuclear layer is lost by 7 months of age. Subretinal delivery of AAV2/5 vector carrying the *RPE65* transgene resulted in the normalisation of retinyl ester levels in the RPE, restoration of retinal morphology and significant delay of the photoreceptor degeneration. The improvement in morphology also correlated with dark- and light-adapted ERG responses being restored to wild-type levels and was accompanied by improvement in vision-dependent behaviour [361]. The first demonstration of long term success with the restoration of visual function was reported in a naturally-occurring canine model of Leber Congenital Amaurosis (LCA), due to RPE65 mutations[2,4]. Treatment of the Briard dogs with AAV-2 carrying normal *RPE65* gene driven by chicken βactin promoter led to the restoration of visual function in treated eyes; a 16% improvement in scotopic and cone flicker ERGs was obtained in treated compared to uninjected eyes, and higher order visual function such as pupillometry and visual evoked cortical potentials demonstrated significant improvement in function in treated eyes[2]. Evaluation of the treatment up to 3 years post-injection showed long term preservation of the treatment[1]. Another study also studied the efficacy of AAV2 containing canine *RPE65* driven by a CMV promoter delivered subretinally into the dog model [347]. Similar success in photoreceptor rescue was reported. To target transgene expression specifically to the RPE, a different study evaluated subretinal injections of AAV2/4 vector carrying a human RPE65 cDNA driven by a human RPE65 promoter in *RPE65-/-* Briard dogs and showed early restoration of rod and cone photoreceptor function which remained stable in the long term. Whereas all dogs that were treated at 8-11 months of age showed improvement, dogs that were treated at a later age of 30 months did not recover retinal function or vision, suggesting that there might be a therapeutic window for gene therapy to be successful in this model[260].

Another form of RPE-based severe early-onset retinal dystrophy is caused by mutations in the *MERTK* gene. The RCS rat, is a well characterised recessive model of RP and has a null mutation in the receptor tyrosine kinase gene, *Mertk* which is exclusively expressed in the RPE [96].The defect results in the inability to phagocytose shed photoreceptor outer segments and the accumulation of the debris which subsequently leads to photoreceptor cell degeneration. Subretinal delivery of Mertk initially using recombinant adenovirus demonstrated functional recovery of phagocytosis and a temporary delay in photoreceptor degeneration [482]. Following both AAV-mediated [437] and lentivirus-mediated [471] *Mertk* gene delivery, treated eyes showed significantly higher numbers of photoreceptors and an increased ERG b-wave amplitude when compared to contralateral uninjected eyes. However the improvement in retinal function following treatment as assessed by ERG was transient; AAV-2 mediated *Mertk* delivery resulted in significant improvement in ERG b-wave for only 9 weeks post injection [437], while lentiviral-mediated gene replacement improved ERG function for up to four months [471]. A more rapid initiation of transgene expression and better RPE targeting specificity of lentiviral vector were thought to account for the more superior therapeutic effect when using this vector.

Together, all of these studies suggest that gene replacement therapy directed to the RPE represents a promising therapeutic strategy. The reports of efficacy, particularly in the Briard dog, showed proof-of-concept of the efficacy of gene replacement in *RPE65* gene defects and provided the impetus for the start of the first human ocular gene therapy clinical trials, assessing gene replacement therapy in LCA patients with RPE65 mutations. This condition was chosen not only because of the impressive results from pre-clinical studies, but also because its characteristics enable rapid assessment of efficacy. Since photoreceptors in this condition are presumed to be healthy, gene replacement would be expected to improve vision owing to the restoration of absent photoreceptor function, whereas for many other retinal dystrophies, the aim would be to preserve vision by preventing

photoreceptor loss. In these trials, which are phase I studies, recombinant AAV 2/2 vector expressing human *RPE65* cDNA driven by either a tissue-specific [34] or constitutive promoter [181,293], was used to target retinal pigment epithelial cells in aldult patient subjects with relatively advanced disease. Differences that existed between the studies were in the type promoters used to drive transgene expression, vector titres, surgical protocols and functional assessments. Preliminary results from the trials demonstrated favorable safety profile of vector administration and lack of adverse reactions and toxicity [34,87,181,293]. Although there was no improvement detected in retinal function on electroretinography (ERG), two groups found improvements in subjective measures of vision such as visual acuity and navigational vision in dim illumination [34,293]. All three studies however detected improvements in retinal sensitivity using microperimetry, dark-adapted perimetry and pupillometry. The demonstration of improved retinal sensitivity but not by ERG suggests that the effects of treatment were relatively modest, which may be explained by the advanced stage of disease in the adult subjects[86,87][292]. Longer term evaluation showed that the functional amelioration seen in patients was stable and minimal evoked immunological responses was observed in the form of a transient rise in neutralising antibodes to the AAV capsid, which did not cause any significant loss of the treatment effect [434].

Although some forms of retinal dystrophies are caused by RPE defects, the majority of inherited retinal dystrophies originate from photoreceptor-based mutations. Gene replacement therapies have until more recently been more challenging for photoreceptor-specific defects due to the relative inefficiency of photoreceptor transduction and the fact that the defect is in the photoreceptor cell itself. Furthermore, for the treatment to be effective, highly efficient transduction over a wide area is needed as each photoreceptor cell needs to be transduced to prevent the death of photoreceptor cells. Despite this, there have been few reports of therapeutic benefit following gene replacement therapy. Recently, gene replacement studies carried out in a mouse model of LCA due to mutations in *RPGRIP* reported improvement in the phenotype following treatment [363]. The RPGRIP gene encodes a

protein which localizes to the connecting cilium linking the inner to the outer segment and has a role in tethering RPGR to the cilium and also in outer segment disc morphogenesis. RPGR is required in the regulation of protein trafficking across the cilium. The *RPGRIP* mouse model has a rapid retinal degeneration which starts at postnatal day 15 and is almost complete by 3 months of age. Subretinal injections of an AAV2/2 vector carrying an *RPGRIP* expression cassette that is driven by a photoreceptor-specific murine opsin promoter resulted in a restoration of RPGR and opsin protein localisation to the outer segments of photoreceptors. A significant slowing of photoreceptor loss in treated eyes was accompanied by electrophysiological improvements in scotopic ERG b-wave amplitudes at 5 months post injection [363]. Two animal models carrying null mutations in the *Gucy2d* gene have been used to evaluate gene replacement therapy, the naturally occurring *GUCY1B* chicken and the guanylate cyclase-1 (*GC1*) knockout mouse[172,496]. This gene is expressed in both rods and cones photoreceptors and encodes guanylate cyclase, an enzyme in the recovery phase of phototransduction whose role is to replenish cGMP stores after light exposure. Prehatch lentiviral-mediated transfer of bovine *Gucy2d* cDNA to the retina of these chicks restored visual function to these animal as evidenced by behavioural testing and ERG analysis, but did not preserve retinal structure in the long term[496]. The GC1 knockout mouse exhibits cone photoreceptor degeneration; the loss of cone function in this model precedes cone degeneration but the rod photoreceptors do not degenerate and continue to give rise to ERG responses to light due to the presense of GC2, a close relative of GC1 in the rod cells[90,509]. AAV2/2-mediated transfer of the *Gucy2d* to the post natal retinal of GC1 knockout mice restored light-driven translocation of cone arrestin but failed to restore cone ERG responses or prevent cone degeneration[172]. It was thought that the heterologous nature of the gene transfer using a bovine *Gucy2d* cDNA may be the reason for the incomplete success. A later study using AAV2/5 vector to mediate targeted delivery a murine version of *Gucy2d* to rod and cone photoreceptors of the postnatal GC1 knockout mouse demonstrated restoration of visual function and visually evoked behaviour[60]. Although the follow up period was short (3 months), evidence of restoration of cone-

mediated function was seen following treatment in the form of improved ERG amplitudes, visual acuity and contrast sensitivity, while preservation of cone photoreceptors was seen with the restoration of normal cone arrestin distribution and increased cone cell density in treated areas[60].

Mutations in *ABCA4* gene cause Stargardt disease, a form of autosomal recessive juvenile macular degeneration. The ABCA4 protein belongs to the ABC transporter family of proteins involved in the ATP-dependent transport of substrates across cellular membranes; the *ABCA4* protein is responsible for the translocation of N-retinylidene-PE, an intermediate in the visual cycle, from the lumen of the disc to photoreceptor cytoplasm. Although the ABCA4 is expressed in the disc rims of photoreceptors outer segments, the disease phenotype originates from the loss of RPE due to the accumulation of lipofuscin in these cells [234]. Until recently, the *ABCA4* cDNA was considered too large to be packaged into AAV vectors, which are the only vectors capable of efficiently transducing photoreceptors. However, recently it was found that vectors based on AAV5 can package large recombinant genomes up to 9 kb. This enabled gene replacement studies in an Abca4-/- mouse model of Stargardt disease; subretinal injection of an AAV2/5 vector carrying Abca4 lead to reduced lipofuscin content and improvement in retinal morphology and function for up to 5 months [17].

So far, most gene therapy strategies developed in rodent studies have focussed on conditions primarily affecting rod photoreceptors. This is likely due to the rod-rich nature of the rodent retina. However, recent advances in rodent ERG, a better understanding of the molecular processes in cone dystrophies and increasing use of large animal models have facilitated the study of gene therapy for inherited cone dystrophies. One such condition that is most likely to be amenable to gene therapy is achromatopsia, which is caused by mutations in any of the four causative genes known to date, *GNAT2* which encodes the alpha subunit of cone transducin[238][15,410], *PDE6C* which encodes the catalytic alpha subunit of cone phosphodiesterase[77,465], *CNGA3* [239][499] and *CNGB3* [237][456,498][325] which encodes the alpha and beta subunits of the cone

cyclic nucleotide-gated (CNG)channel located in the plasma membrane of the cone outer segment. AAV-mediated gene replacement has been shown to restore cone-mediated ERG responses to a mouse model of achromatopsia, the *Gnat2*^{cpfl2} mouse, which is homozygous for a nonsense mutation in *Gnat2* [9]. Improvement in visual acuity was also observed using an optokinetic behavioural assay. More recently, cone-directed gene therapy using AAV2/5 vector was evaluated in two independent canine models of achromatopsia[242,243]. These naturally occurring dog models of achromatopsia result from either a missense mutation in exon 6 of *CNGB3* or a genomic deletion of the entire *CNGB3* gene[430]. Single subretinal injection of AAV2/5 containing the human *CNGB3* driven by different versions of human red opsin promoter led to restoration of cone function in both *CNGB2*-mutant dog models as measured by flicker ERGs and recovery of day vision in treated animals[243]. The robustness and stability of the treatment effect was promoter and age dependent however, sustained rescue of cone function was only obtained using vectors that contained the long version of the red cone opsin promoter and in younger animals[243]. This study provided evidence that cone-specific disorders could be ameliorated using targeted AAV-mediated gene replacement and may hold promise for future therapy in humans. One step closer toward this direction has made in the form of AAV-mediated gene therapy to restore trichromacy in colour-blind primates [296]. Subretinal injection of AAV2/5 vector containing the human L-opsin gene under the control of the L/M opsin enhancer and promoter elements was delivered to adult primates with red-green colour vision deficiency, thus co-expressing the L-opsin transgene within a subset of endogenous M-cones. At about 20 weeks following subretinal injection, treated primates showed a shift in spectral sensitivity measured on colour multifocal ERG towards long wavelength light which was accompanied by evidence of trichromatic colour vision behaviour. The improvement in colour vision appeared stable for over 2 years of follow up, and demonstrates the restoration of colour vision may be possible even in adulthood as the acquisition of new colour vision capacity did not appear to require a developmental process unlike that in monocular deprivation [296]

The experiments described above demonstrate that in many models of diseases caused by loss-of-function mutations, gene therapy is able to delay apoptotic cell loss. The best results in treating hereditary retinopahies to date are obtained using gene replacement strategies. In other conditions where gene replacement may not be not possible or where there is no other available alternative, neuroprotection therapy may be used but the effects of this is often partial and transient.

1.4.3.3 Neuroprotection and anti-apoptotic therapy for treatment of retinal dystrophies

Although gene replacement and gene silencing strategies offer good prospects for the treatement of specific inherited retinal dystrophies, many other disorder, particularly inherited dystrophies that is advanced at birth, acquired and multifactorial conditions such as age-related macular degeneration (AMD) are less amenable to these corrective approaches. With the vast genetic heterogeneity of these conditions, the prospect of developing individualized corrective gene therapy strategies for patients with disorders due to rare mutations would be technically and economically unfeasible. Generic strategies do not correct the gene defect and hence do not cure the disease, but are aimed at secondary targets such as those involved in apoptosis or in modulating the microenvironment of photoreceptors in a manner that promotes cell survival in order to ameliorate condtion. Such approaches include the localized, targeted delivery of neurotrophic factors and antiapoptotic proteins with the aim of enhancing photoreceptor cell survival.

Irrespective of the gene defect, the death of photoreceptors in inherited retinal dystrophies occurs through apoptosis. Since apoptosis is a final common pathway in all genetic diseases, this form of generic therapy would be applicable across the spectrum of retinal degenerations and does not require gene-specific treatments. Gene transfer of *bcl-2*, an antiapoptotic

gene has been shown to delay retinal degeneration in the *rd* mouse, an animal model of retinitis pigmentosa [52]. However,the rescue was only detectable histologically and lasted only 6 weeks after birth, indicating that the limited benefit conferred by the treatment was not sufficient to prevent further loss of photoreceptor cells. The X-linked inhibitor of apoptosis protein (XIAP) is a potent inhibitor of apoptosis and acts by inhibiting caspase 3, 7 and 9 [265]. AAV-mediated delivery of *XIAP* to P23H and S334X rhodopsin transgenic rat models of retinitis pigmentosa was shown to inhibit caspase activity and delay photoreceptor cell loss. Six months post injection, the outer nuclear layer in treated eyes was almost twice the thickness of untreated eyes in both models. However, ERG functional improvements were observed in the P23H rat treated eyes but not in the S334X rats, indicating that increased survival of photoreceptor cells which were non-functional in the latter did not lead to restoration of function. Although anti-apoptotic gene therapy approach would theoretically provide a more comprehensive treatment applicable to a wide range genetic of inherited retinal dystrophies, this study shows that not all forms of retinal dystrophies would respond to this form of treatment. Further evaluation is needed as to which disorders are better suited and whether there are other external factors that need to be taken into account that could determine the success of the treatment.

Neurotrophic factors such as fibroblast-growth factor (FGF), glial-derived neurotrophic factor (GDNF) and ciliary neurotrophic factor (CNTF) have been found to retard photoreceptor degeneration in several animal models of retinal degeneration [125,126,259,472]. To achieve longer term effect without the need for readministration, AAV-mediated expression of genes encoding neurotrophic factors has been widely studied. AAV2-delivered bovine *FGF-2* has been found to increase photoreceptor survival for up to 4 months post injection in the S334X transgenic rat model of dominant RP which expresses a mutant *Rhodopsin* allele. Thicker outer nuclear layer seen in treated eyes although this was not reflected in improved retinal function as assayed by ERG [256]. ERG amplitudes in treated eyes were better than non-injected eyes but showed no significant difference from eyes injected with a reporter gene. It has been suggested that some degree of

photoreceptor rescue could be injection-related in keeping with the theory that retinal injury also induces the release of survival factors [126]. Subretinal delivery of GDNF using AAV2 vector in the same animal model resulted in increased photoreceptor survival with corresponding in ERG improvement in treated eyes [154]. It has been further shown that AAV-mediate expression of the gene encoding GDNF can enhance photoreceptor survival in two rodent models of retinitis pigmentosa, the *Prph2*$^{rd2/rd2}$ mouse and the RCS rat, and affords additive improvement of retinal function when combined with gene replacement [63]. In this study, animals treated with the combination of gene replacement and GDNF had up to 50% higher ERG amplitudes than those give gene replacement alone. More importantly, no deleterious effect on retinal function was seen on ERG, unlike the paradoxical effects that have been reported with AAV-mediated expression of CNTF.

Ciliary neurotrophic factor or CNTF has been shown to be a therapeutic neurotrophic agent, particularly as the delivery of the recombinant protein results in transient improvement of photoreceptor survival in rodent models of retinal degeneration [257,259]. AAV-mediated CNTF expression also resulted in slowing of photoreceptor cell death for up to 4 months in rodent models of RP such as *Prph2*$^{rd2/rd2}$ mouse, P23H and S33ter *rhodopsin* transgenic rats [272]. However, despite the morphological protection seen following treatment, significant dose-dependent deleterious effects on retinal function were seen on ERG and behavioural tests [63] [309]**.** When administered in combination with AAV-mediated gene replacement therapy in *Prph2*$^{rd2/rd2}$ mice, AAV2.*CNTF* delivery negated any improvement of retinal function by gene replacement therapy and furthermore, a marked decrease of 50% in ERG b-wave amplitude was seen following intraocular injection of AAV expressing *CNTF* into wild-type mice[420]. These data regarding vector-mediated *CNTF* delivery suggests that although CNTF exerts a potent effect on the survival of photoreceptors in retinal degeneration, there is a certain harmful effect exerted by this neurotrophic molecule that reduces overall retinal function. It has been suggested that the negative functional effects may be due to molecular changes and downregulation of photopigment expression as a consequence of long term activation of

signalling molecules downstream of CNTF [492]. Despite this, a recent phase I clinical trial of patients with end-stage retinitis pigmentosa demonstrated that a device that is implanted intraocularly and using encapsulated cell technology to deliver CNTF to the retina, is well tolerated for several months (the implants were removed after 6 months) [431]. This small scale clinical study showed that short-term CNTF delivery at low doses were well tolerated without any reports of negative effects on visual function. However, assessments of the impact on visual function were difficult to interpret due to the small number of patients involved and the study was not designed to test the efficacy of CNTF in preserving vision. As a result of the study, phase II/III trials have recently been initiated to investigate whether CNTF has any effects in prolonging visual function or improving photoreceptor function.

Pigment epithelium-derived factor (PEDF) is a growth factor that has been shown to have neuroprotective properties using the recombinant protein in models of retinal degeneration [75] although such studies are relatively few. To circumvent the transient effects of PDEF due to its short half-live, viral-mediated delivery of the protein has been used to study treatment effects. Benefit was observed when a lentivirus-mediated delivery of *PEDF* (using SIV.*PEDF*) into eyes of RCS rats showed significant preservation of photoreceptors lasting up to 24 weeks post injection [328]. Histological analysis showed twice as many photoreceptor cells in the treated areas of the retina compared with untreated areas at 4 weeks post injection, while ERG assessment demonstrated a modest improvement with higher b-wave amplitudes in SIV.PEDF-treated eyes compared with SIV.lacZ-treated control eyes [328].

Despite the encouraging aspects of these results in animal models, the clinical use of neurotrophic factors is thus far limited because the rescue effects appear to be partial and transient, and the mechanisms underlying the benefits afforded by these molecules are not yet fully understood. Ultimately, for long lasting improvement of a phenotype, it is necessary to prevent the death of the cells involved. Hence, using neuroprotection in

conjunction with gene replacement therapy could have a synergistic effect, as already shown in some studies above. Co-delivery of therapeutic genes and neurotrophic factors may result in a more effective treatment for retinal dystrophies in which gene replacement corrects the underlying pathological defect while neuroprotective agents protect against photoreceptor cell death. However, further studies using GDNF, PEDF, BDNF, CTNF and other neurotrophic factors are required before they can considered for clinical use alongside gene replacement in retinal dystrophies.

1.5 Summary

There has been major progress in the development of gene replacement therapy for inherited retinal dystrophies, made possible by technical advances in vector technology and better understanding of the underlying disease mechanisms and knowledge of potential difficulties surrounding gene transfer to specific retinal cells. This has led to successful rescue of retinal degeneration in various animal models, particularly of the forms of retinal dystrophies caused by RPE-specific defects. The recent positive preliminary results from the ongoing clinical trials of gene replacement therapy for *RPE65* defects will undoubtedly pave the way and call for more gene therapy strategies for other retinal dystrophies to be developed and translated to clinical trials. As majority of inherited retinal dystrophies are caused by defects in photoreceptor-specific genes, it would be logical and crucial to focus the development of new gene therapy strategies for these disorders. These disorders have generally been more difficult to treat and have a variety of kinetics of photoreceptor degeneration. In such disorders, improved and very efficient viral vectors would be required and are most likely to be based on AAV vectors, which are the only vectors shown to transduce photoreceptor cells well. In line with these points, this study focuses on developing gene replacement strategy and assessing its efficacy to treat a form LCA and retinal dystrophies caused by mutations in a photoreceptor-specific gene *AIPL1.* Bearing in mind the difficulty in treating

photoreceptor defects, we will investigate the efficacy using mouse models which have either reduced or no *Aipl1* expression and thus different rates of degeneration. In order to treat the different rates of degeneration, different serotypes of AAV vectors will be required. The experiments described in this study will form a comprehensive preclinical assessment of gene replacement therapy for *AIPL1*-associated retinal dystrophies and may also provide proof-of-principle for clinical trials to treat these disorders.

2 Materials and methods

2.1 Amplification of plasmid DNA in bacteria

2.1.1 Transformation of competent cells

For transformation DH5α™ competent cells (Invitrogen Ltd., Paisley, UK) were thawed on ice. A 100 µl aliquot was incubated with the plasmid DNA (30minutes on ice) before heat shock at 42^{o}C in a pre-warmed water bath for 90 seconds followed by 120 seconds on ice. LB (Luria-Bertani) medium 750µl was added at room temperature to the mix and incubated for 1 hour at 37^{o}C before spreading onto an LB agar plate containing 100 µg/ml ampicillin or kanamycin. Plates were incubated overnight at 37^{o}C to allow growth of antibiotic-resistant colonies. LB agar plates were prepared using 14 g of Bacteriological agar (Oxoid Ltd.) per litre of water, 5 g/L yeast extract, 10 g/L tryptone (Oxoid Ltd), 10 g/L sodium chloride, and 100 µg/ml ampicillin or kanamycin.

2.1.2 Amplification and recovery of recombinant plasmid DNA

Bacterial colonies from agar plates were inoculated into 2.0 ml of LB medium containing 100 µg/ml ampicillin (1000X; Sigma Aldrich Company Ltd.) the following day and incubated at 37^{o}C with gentle shaking at 1200 rpm overnight to allow growth. For small scale preparations, plasmids were recovered using QIAprep® Spin Miniprep Kit (Qiagen Ltd., Sussex, UK). For large scale preparations 200 µl of the 2 ml culture was used to inoculate a further 1000 ml LB medium and was incubated as described above. Plasmid DNA was recovered using QIAGEN® Plasmid Mega Kit (QIAGEN Ltd.).

2.1.3 Quantification of nucleic acid

Nucleic acids produced with the QIAGEN Mega Kits were quantified using a Unicam UV 500 Spectrometer and the Nanodrop™ spectrophotometer. An absorption of 1 at OD_{260nm} equals a concentration of 50 µg/ml double stranded DNA. Nucleic acids produced with QIAGEN Mini Kits were quantified on a 1% agarose gel.

2.2 DNA analysis

2.2.1 Restriction enzyme digestion

Digestion of DNA was carried out in accordance to the manufacturer's specifications (New England Biolabs Ltd., Herts, UK), in a 1X buffer with an excess of enzyme (5-10 U/µg DNA).

2.2.2. DNA electrophoresis

DNA fragments were separated on a 1-1.5% (w/v) agarose gel using 1 X TBE buffer. Ethidium bromide 1 µl of 10 mg/ml concentration per 50 ml of gel) was added to enable visualization of DNA bands. A 1 kb DNA ladder (Bioline Ltd., UK) was simultaneously run to provide size markers. Samples were loaded using gel-loading dye (6 X; 0.25% (w/v) bromophenol blue and 30% (v/v) glycerol in water). Gels were run using the voltage and duration required for the separation of the required DNA bands. Gels were photographed on an ultraviolet transilluminator.

2.3 Cloning and plasmid construction

To create a recombinant virus for the purpose of gene transfer, most of the viral genome must be replaced with a recombinant genome carrying the therapeutic gene under the control of an appropriate promoter, which drives its expression in the right cell type and at an efficient level. The genes which encode viral capsid and are required for *in-vivo* replication need to be deleted to ensure that the recombinant virus does not invoke the an immune response which would lead to removal of transduced cells and short-lived transgene expression. Recombinant viruses are produced *in-vitro* and hence consideration needs to be given towards safety and purification issues. Risks of toxicity are minimized by ensuring through purification of the viral particles. Efficiency of gene transfer is optimized by ensuring that the recombinant viruses that is administered is of sufficiently high titres.

2.3.1 Isolation of murine-AIPL1 cDNA

The murine AIPL1 cDNA (see appendix for cDNA sequence) was PCR amplified from murine cDNA. Primers used for PCR were :

Maipl5 (5–GCCTGAACAAACCTCTCCCCTA)
Maipl3 (5'-CCACCCAACCTAACCCAGTCTAAC)

The PCR fragment obtained of 1016 bp in size was checked using restriction enzyme digests and sequenced after cloning into pGem-T easy (Promega, Madison, WI).

2.3.2 Creating appropriate DNA fragments

DNA fragments that were required for cloning were made using the appropriate restriction enzyme digests as indicated by respective plasmid

maps. Where possible, non-complemetary ends were created to enhance the efficiency and ensure the correct orientation of the transgene insertion. Where necessary, the vector molecule was pre-treated with calf intestinal alkaline phosphatase (New England Biolabs (UK) Ltd.) to remove 5'-phosphate groups to prevent intra-molecular ligation. One microlitre of alkaline phosphatase was added after the restriction enzyme digest and the mixture incubated at 37^{o}C for 1 hour. Where a blunt ligation was necessary, the 5' overhang was filled with 1µl Klenow fragment DNA-polymerase I (New England Biolabs (UK) Ltd.) in the presence of excess (0.5 mM) deoxynucletide triphosphates (dNTPs- Promega UK, Southampton, UK), both added after the restriction enzyme digest and incubated at room temperature for 15 minutes. These reactions were terminated by the adding of gel loading dye or where required, heating for 20 minutes at 65^{o}C. Samples were run on agarose gel and the required bands excised with a scapel under ultraviolet light.

2.3.3 Isolation of DNA fragments from agarose gels

DNA fragments excised from agarose gels were extracted from agarose using QIAquick™ Gel Extraction Kits (QIAGEN Ltd.) according to manufacturer's specifications. DNA was eluted from the column using 50 µl of TE buffer (supplied by manufacturer). The concentration of the eluted sample was determined using the Nanodrop spectrophotometer.

2.3.4 DNA ligation

The ligation of gel purified DNA fragments was carried out at 16^{o}C for 12-16 hours, using T4 DNA ligase (New England Biolabs (UK) Ltd.) with supplied buffer at recommended concentrations and at insert to vector backbone molar ratio of 3 to 5. Where PCR fragments were ligated into pGEM®-T Easy

plasmids (Promega UK) ligations were performed according to manufacturer's instructions.

2.3.5 Checking cloned plasmids

A 20 µl sample of the ligation mixture was transformed into and amplified in bacteria. Successful ligation was determined by obtaining the appropriate DNA bands following restriction enzyme digestion of the purified plasmid DNA.

2.3.6 PCR and sequencing

To ensure that the isolated fragments have the correct sequence they were amplified using appropriate primers and cycling conditions. PCR reactions were performed in a total volume of 20 µl. 0.2 mM dNTPs (Promega UK), 25 pM of each primer and 1 U of Taq polymerase (Promega UK), and 8 µl of buffer were mixed and DNA was added to a final DNA concentration of less than 10 ng/µl. The amplified fragments were then sequenced (MWG-Biotech).

2.4 Polymerase chain reaction (PCR)

PCR reactions were performed in a volume of 30 µl using 0.33 mM dNTP (Promega UK), 0.5 µM of each primer and 1 U of *Taq* DNA polymerase (Promega UK), 0.5 mM MgI_2 and 8 µl of buffer supplied by the manufacturer. DNA was added to a final concentration of less than10 ng/µl. In each PCR run, an additional control reaction was made, to which no template DNA had been added. Reactions were cycled using a Techne Touchgene Thermal Cycler. The optimal annealing temperature for each primer set was calculated using the program PrimerSelect™ (DNASTAR Inc.)

Cycling conditions were based around the following:

Initial denaturation	5 minutes at 95°C	
Denaturation	1 minute at 94 °C	X 35 cycles
Annealing	30 seconds at T_a	
Extension	120 seconds at 72 °C	
Final extension	10 minutes at 72 °C	

During the extension step, 1 minute was allowed for every kb of amplicon (minimum extension time 1 minute). Five microlitres of each PCR reaction was analysed on an agarose gel.

2.5 Tissue culture

2.5.1 Cell lines and culture of cell lines

The baby hamster kidney (BHK) cell line was obtained from European Collection of Animal Cell Cultures (ECACC, Porton Down, UK). BHK cells were grown in BHK-21 medium (Invitrogen Ltd) supplemented with 10% heat inactivated fetal calf serum (FCS), 5% tryptose phosphate broth (Invitrogen Ltd.), 5ml of 0.1 mg/ml streptomycin and 100 U/ml penicillin (Invitrogen Ltd.), 5ml of 200 mM L-glutamine (Invitrogen Ltd.) and 4ml of 50 mg/ml geneticin G418 (Invitrogen Ltd.) were added to 500 ml of medium. 293T cells were cultured in Dulbecco's Modified Eagle's Medium (DMEM) supplemented with 5 ml/500 ml of 0.1 mg/ml streptomycin and 100 U/ml penicillin and 10% FCS. Cells were grown in a Sanyo CO^2 incubator at 37°C with 5% CO^2.

2.5.2 Passaging of cell cultures

To ensure that cells were kept at an optimal density and to avoid overgrowth of cells, they were split every 2-3 days. Prior to splitting, the old medium was removed and plates were washed twice with sterile PBS (10 X phosphate

buffered saline tablets (Oxio Ltd.) dissolved in 1L sterile ddH ^{2}O). Trypsin-EDTA (Invitrogen Ltd.) approximately 1.0 ml for each 15 cm dish was added until all the cells were thinly covered. The plates were incubated at 37^{o}C for 15 minutes. The trypsinisation was stopped with the addition of FCS-containing growth medium and the cells were split in the ratio of one in four.

2.5.3 Long term storage of cell line

Following trypsinization, the cells were pelleted by centrifugation and 5X10^{6} cells/ml were resuspended in 1 ml growth media with 20% FCS and 10% dimethylsulfoxide (DMSO, Invitrogen Ltd.) and aliquoted to storage tubes. The tubes were cooled slowly to -70^{o}C overnight in a box containing pre-cooled isopropranolol. The next day, the cells were transferred to liquid nitrogen for long term storage. Frozen cells can be re-cultured by thawing the cryovials in a water bath at 37^{o}C. Cells were then pelleted by centrifugation and the DMSO containing medium was removed. The process was repeated washing the cells with 1X PBS before resuspending them in the appropriate medium.

2.6 Adeno-associated viral vectors

2.6.1 Constructs

The murine *Aipl1* cDNA was PCR amplified from murine retinal cDNA using primers which have been designed to encompass the whole of the coding region. The PCR fragment obtained (1016 bases) was sequenced after cloning into pGem-T (Promega, Madison, WI) . The m*AIPL1* cDNA was cloned between the CMV promoter and the SV40 polyadenylation site of the construct AAV-CMV-*gfp* [523] to form the construct AAV-CMV-*Aipl1* (total length 5733 bases). The construct was then checked using a series of restriction enzyme digests StuI, KpnI AccI, PstI and StuI and sequencing.

Refer to section 3.2 for details of cloning strategy and plasmid map. Recombinant AAV2 vector was generated from the murine construct , AAV2-CMV-*Aipl1*.[523]. The human *AIPL1* cDNA was also PCR amplified from human retinal DNA using primers which covered the whole coding region and included part of the untranslated regions at the 5' and 3' ends. The PCR fragment of 1215 bases was cloned into pGem-T (Promega Madison, WI) and checked by sequencing and restriction digests. The *AIPL1* cDNA was inserted into the parental plasmid AAV-CMV-*gfp*, replacing the *gfp* gene to generate the human construct AAV-CMV-*AIPL1.* For details of the cloning and plasmid map, please refer to section 3.8. The plasmid containing human AIPL1 cDNA was packaged into AAV2 and AAV8 to generated two pseudotyped AAV viral vectors, AAV2-CMV-*AIPL1* and AAV8-CMV-*AIPL1,* as described below. Recombinant AAV2 and AAV8 vectors were also made from the parental plasmid AAV-CMV-*gfp* for control experiments.

2.6.2 Production of rAAV2

Production of recombinant rAAV2/2 (AAV2/2) was carried out by co-transfection of two plasmids in the presence of a helper virus in BHK cells as previously described [523]. Prior to the day of transfection, BHK cells were split and plated at concentration of 10^6 cells/150 mm dish and incubated overnight so that there was approximately 70% confluency on the day of transfection. Fourty dishes were used for large-scale preparation of rAAV particles. Recombinant AAV particles were produced using ITR-bearing plasmid containing AIPL1 transgene (described in section 2.6.1), the helper plasmid containing the *rep* and *cap* genes, pHAV 7.3, and the PS1 HSV helper virus. The construct plasmid containing AIPL1 and pHAV 7.3 helper plasmid were used to co-transfect BHK cells in a 1:1 ratio. Each 150 mm plate contained 30 µg of construct plasmid and 30 µg of pHAV7.3 (60 µg total/plate) in 10 ml Opti-MEM/plate. In a separate tube, 240 µg of a β-integrin-targeting peptide use to improve the binding of DNA [(K16)GACRRETAWACG)], was mixed with 45 µl of Lipofectin reagent (Invitrogen Ltd., UK). The two tubes were mixed and incubated at room

temperature for 1 hour in order for the DNA to bind the Lipofectin-peptide complex. Old medium was removed from the plates and the plates were washed twice with Opti-MEM prior to the addition of the transfection solution. Then 12.5 ml of the transfection mix was added to each plate and the cells were incubated at 37^{o}C for 4 hours. After that, the transfection solution was removed and replaced by normal growth medium containing PS1 HSV helper virus at MOI (multiplicity of infection= the ratio between the number of virus particles and the number of cells infected) of 10-20 infectious units. Cells were incubated at 37^{o}C for 24 to 36 hours. At the completion of a lytic cycle, cells were collected and pelleted by centrifugation at 3000 g for 10 minutes.

2.6.3 Purification of rAAV2

Cells were harvested in batches of 10 plates, pelleted and resuspended in 5 ml of DMEM. They were lysed by three cycles of freeze thawing between -70^{o}C and 37^{o}C. Genomic DNA was removed by digestion with 50 U of endonuclease benzonase per millilitre of lysate at 37C for 30 min. The lysate was clarified by centrifugation at 3000 g for 15 min. The supernatant which contained the virus was retained and treated with 0.5% deoxycholic acid for 30 min at 37^{o}C and filtered through 5.0 and 0.8 µm syringe filters (Millipore, USA; SLSV R25 LS and SLAA 025 LS). After filtration, the supernatant was transferred onto a heparin-agarose column (Sigma, USA) which was first prewashed with PBS-MK (1 X PBS, 2.5 mM KCL, 1 mM $MgCl_2$). After the virus solution had run through, the column was washed with 10 ml PBS-MK + 0.1 M NaCl. Viral particles were eluted with 6 ml of PBS-MK + 0.4 M NaCl. The first 2 ml were discarded and the remaining suspension containing the purified virus was collected. The eluate was concentrated using Centricon 100 columns (Millipore, USA) by centrifugation at 5000 xg for 25 minutes followed by a wash with PBS-MK. The Centricon columns were then turned upside down and the concentrated rAAV was spun into a collection tube. The average yield of the rAAV2/2 production protocol is approximately 100 µl of concentrated virus (10^{12} viral particles/ml) per 10 plates fo transfected BHK cells. The virus was then aliquoted and frozen at -80°C.

2.6.4 Production of rAAV8

Production of recombinant AAV2/8 (rAAV2/8) was carried out by co-transfection of three plasmids in 293T cells. In addition ot the pD10-based plasmids, pAAV (that carries *rep* and *cap* genes) and pHGTI (that carries helper accessory genes) plasmids were used in a $CaCl^2$-based transfection. 293T cells were seeded into 150 mm plates at a concentration of 10^6 cells/plate. The plates were incubated overnight so that they reached 70% confluency the following day. The transfection medium was prepared using the following amounts:

For 10 plates:

pAAV8 - 100 µg
pHGTI - 30 µg
pD10-RNAi - 100 µg
$CaCl^2$ 2.5M - 1.25 ml
dH_2O - up to 12.5 ml

The same amount in volume (i.e. 12.5 ml) of 2x HBS buffer was added dropwise to the plasmid solution followed by 25 ml of full DMEM medium. Five ml of the transfection solution was then added to the 293T plates without removing the old medium and the cells were incubated for 36 hours before scraping and harvesting in TD buffer.

2.6.5 Purification of rAAV8

The freeze-thaw cycles, benzonase and deoxycholic acid treatments were carried out in the same way as performed in the rAAV2/2 production. The lysate was then filtered through a 0.45 µm syringe filter before proceeding with the exchange chromatography purification using an ÄKTA™ prime FPLC apparatus (Amersham, UK) to bind the rAAB2/8 particles on an anionic sephacryl S300 and a POROS 50HQ column. The FPLC purification was carried out in Dr Amit Nathwani's laboratory (UCL) with the assistance of Dr Jenny McIntosh. FPLC purification is carried out by binding the viral lysate first to the anionic column followed by the POROS 50HQ column and eluted

using an increasing salt gradient (Buffer A and B; see Buffers and solutions). Approximately 15 ml of eluate are produced by 100 plates which are subsequently concentrated in Centricon 100 columns to a final volume of approximately 200 µl. The virus was then aliquoted and frozen at -80°C.

2.7 Titration of AAV particles

2.7.1 Isolation of viral DNA from AAV particles

Two aliquots of 1 µl and 5 µl were taken from the concentrated virus suspension produced in section 2.6. These samples were digested with 10 µg (1 µl) of proteinase K (Promega UK) in 100 µl of 2 X Protein K buffer (100 mM Tris (pH7.4), 50 mM EDTA and 0.5% SDS) and 99 µl or 95 µl ddH_20 respectively. The proteinase K digest was incubated at 56^oC for 30 minutes. The DNA was subsequently precipitated by adding the following reagents in the order specified : 20 µg (1 µl of 20 mg/ml) glycogen (Sigma Aldrich Company Ltd), 1/10 volume (20 µl) of 3 M sodium acetate and 260 µl of pure ethanol. The mixture was incubated for 30 minutes at -20^oC. DNA was pelleted by centrifugation at maximal speed 14000 rpm for 10 minutes. The supernatant was removed and the pellet was washed with 200 µl 70% ethanol and spun at maximal speed for 2 minutes and dissolved in 200 µl of 0.4 M sodium hydroxide and 10 mM EDTA solution.

2.7.2 Preparation of dot-blot

A standard curve was prepared by making a dilution series of a plasmid containing the section of DNA that was to be used as a probe. Seven samples were usually prepared which ranged from 10^6 molecules to 10^{12} molecules of plasmid in 10- fold serial dilutions. The samples were prepared with 0.4 M NaOH and 10 mM EDTA to a total volume of 200 µl. The samples from the dilution series and those from section 2.7.1 containing recombinant viral genomes were denatured at 95^oC for 2 minutes and then immediately

cooled for 2 minutes on ice to prevent re-annealing. Dot-blots were prepared on pre-wetted 0.45 µm Hybond™- N+ membrane (Amersham Pharmacia Biotech, UK, Bucks,UK) – positively charged nucleic acid binding membrane - in a dot blot manigold (Bio-Rad Laboratories Ltd., Herts, UK). Each well of the manifold was pre-washed with 200µl of ddH_20 and vacuum dried. The denatured DNA samples were loaded and the vacuum reapplied until wells were empty. Then 200 µl of 0.4 M NaOH and 10 mM EDTA was added to each well. Excess solution was removed by applying vacuum and the membrane was dried between sheets of Whatman paper at 80^oC for 120 minutes.

2.7.3 Preparation of probe

The section of DNA to be used as the probe was excised from the plasmid with a restriction enzyme digest , separated on a gel and extracted from a gel fragment and resuspended in 50 µl of water. 35 µl of the resuspended DNA fragment was placed in a fresh eppendorf tube and denatured at 95^oC for 2 minutes. Immediately after, this was placed on ice for 2 minutes, subsequently spun down to collect the evaporated fluid from the lid. A Neoblot biotinylated probe kit (Biolab) was used to label the probe according to manufacturer's instructions. According to this, the components were added to the denatured DNA fragment in the following order: 10 µl of 5 X labelling mix supplied in the kit (contains random octamers), 5 µl dNTP mix (containing biotin-dATP), and 1 µl Klenow.i The mixture was incubated at 37^oC for 1 hour to overnight. The biotynylation reaction was terminated by adding 5 µl 0.2 EDTA pH8. The probe was subsequently precipitated by adding 5 µl 3 M NaOAc, 150 µl 100% ethanol and incubated at -20^oC for 20 minutes. After centrifuging at 14000 rpm for 10 minutes, this was washed with 70% ethanol, spun down and finally resuspended in approximately 20 µl of water or TE. Five microlitres of the probe was used for each dotblot and the remainder of the probe was stored at -20^oC.

2.7.4 Hybridization of the probe to membrane

The hybridization oven and hybridization bottles were preheated to 65^{o}C for 30 minutes before use. The membrane was wetted with ddH_2O by allowing it to float on the surface of the ddH_20 before submerging. The wetted membrane was placed in the pre-warmed hybridization bottle folded between hybridization mesh. The Church mix (pre-warmed to 65^{o}C, 0.5 M sodium phosphate buffer, 7% w/v SDS, 0.01 M EDTA) was added to the hybridization bottle and the membrane pre-hybridised for 30 minutes in the hybridization oven. The biotinylated probe (section 2.7.3) was added to the Church mix and left to hybridise overnight at 65^{o}C. The membrane was then washed thrice with 50 ml of 33 mM NaPi buffer at 65^{o}C. The third wash was left for 5 minutes at 65^{o}C. The membrane was placed in a plastic container filled with 20-30 ml of block solution (5% SDS, 125 mM NaCl, 25 mM $NaPo_4$ pH7.2) and incubated at room temperature on a shaking platform for 5-10 minutes. The membrane was subsequently processed using the CDP Star kit (Biolab), according to the instruction of the manufacturer as follows. The block solution was replaced with 20-30 ml of streptavidin diluted 1:1000 in block solution and incubated again at room temperature on a shaking platform. Two 5 minute washes were then performed, each with wash solution I (which is 1 in 10 dilution of block solution) at room temperature on a shaking platform. The membrane was incubated with biotin-conjugated alkaline phosphatase that was available in a kit, Phototope-Star detection kit for nucleic acid (Biolab). The biotin-conjugated alkaline phosphatase was diluted 1:1000 in block solution and 15-20 ml of this dilution was used for the incubation for 5 minutes at room temperature with shaking. The membrane was washed once with block solution for 5 minutes at room temperature with shaking. Two further washes were performed with 20 ml of wash solution II (10mM Tris-HCL, 10mM NaCl, 1mM $MgCl_2$ pH 9.5), each for 5 minutes at room temperature on a shaking platform. During the second and final wash, CDP-Star reagent (available in the Photope-Star Detection Kit for nucleic acids) was diluted 1:100 in 1 X assay buffer (comes in 25 X concentration) to make up a total of 2.5 ml. After the final wash, the membrane was placed facing upwards on a clear plastic sheet. The diluted CDP-Star reagent was

placed over the membrane, ensuring that all areas with dots were well covered. The blot was read on a chemi-luminescence reader at settings of 470 nm, temperature -25^{o}C and approximately 1-5 minute exposure time.

2.8 Quantification of expression

2.8.1 Total RNA isolation

Whole retinas dissected from eye cups (quick frozen in liguid N_2) were resuspended in 500 ml TRI-BD® reagent (Sigma, UK). Vigorous resuspension with a pipette (or a homogeniser) is essential to ensure breaking down of the cell wall. When the solution was homogenous, 200 µl chloroform was added and the samples were mixed by inversion. Straight after, the samples were centrifuged at 5000 xg for 15 minutes at 4°C. The clear top phase (containts RNA) was removed to another tube and the organic phases were kept for protein isolation (see 2.8.3). Equal amount of isopropanol was added to the clear phase and the samples were frozen for a minimum of 2 hours at -80°C. Overnight incubation at -20°C is favourable, however, because it increases the amount of RNA precipitation. Then, the samples were spun at 5000 xg for 10 minutes at 4°C. The supernatant was carefully decanted without disturbing the pellet. One ml of ethanol was added and the RNA pellets were spun at 5000 xg for 5 minutes at 4°C. The ethanol was removed and the samples were left to air dry for 5 minutes at room temperature. Each pellet was resuspended in 20 µl dH_2O. Alternatively, the RNeasy Mini Kit (QIAGEN Ltd., UK) was used for RNA extraction of cell pellets according to manufacturer's instructions. The RNA concentration was measured using a NanoDrop® ND-1000 spectrophotometer (LabTech Int., UK). Total RNA was stored at -80°C.

2.8.2 Generation of cDNA and relative quantification

For cDNA generation the QuantiTect® Reverse Transcription Kit (QIAGEN Ltd., UK) was used according to manufacturer's instructions. Briefly, the RNA samples were thawed on ice and up to 12 µl (or up to 1 µg) were added to 2 µl of gDNA Wipeout Buffer. The reaction was made upto 14 µl with water and incubated at 42°C for 2 minutes. In a separate tube, 1 µl of Quantiscript Reverse Transcriptase, Ct4 µl of Quantiscript RT buffer and 1 µl of RT primer mix (containing random octamers and dT nucleotide mix) were mixed before adding them to the template RNA. The reaction tube (20µl final volume) was incubated at 42°C for 1 hour to enable reverse transcription, followed by a 3 minute incubation at 95°C to inactivate the Quantiscript Reverse Transcriptase. The efficiency of the reaction provides a 1:1 conversion ratio of RNA:cDNA, hence up to 1 µg of cDNA was made per sample. Total cDNA was stored in -20°C.

Fifty ng (or approximately 1 µl) of total cDNA from each sample was loaded onto a 96-well plate with 2X FastStart TaqMan® Probe Mastermix (ROX) (Roche, UK), forward and reverse primers for amplification of gene of interest (final concentration of 900 nM each), appropriate hydrolysis probe that binds the amplified area (final concentration of 250 nM; Roche, UK), ROX reference dye (final concentration of 400 nM; Roche, UK) and dH_2O to make the final reaction volume up to 50 µl. The amount of cDNA template used in each reaction ranged from 5-500 ng with 50 ng being the usual loading amount. Quantitative real-time PCR was run on an ABI Prism 7900HT Fast Real-time Sequence Detection System (Applied Biosystems, UK) and the manufacturer's software (SDS 2.2.2) was used to obtain Ct values for the reactions. The relative expression between comparable samples in relation to the expression of the gene of interest was calculated through the formula: $2^{-\Delta\Delta Ct}$

2.8.3 Protein isolation and evaluation of sample protein content

Retinal tissue was dissected from whole eye cups and lysed using a commercial buffer (RIPA, Sigma Aldrich, Gillinghan, UK) with added protease inhibitor cocktail (Sigma Aldrich, Gillingham, UK). Cell membranes were disrupted using a sonicator with a micro-tip (Soniprep 150, MSE London UK). Lysates were stored at -80°C. The concentration of protein in each sample was measured using a Lowry-based calorimetric protein assay done in triplicate (DC protein assay kit, Bio-Rad, Hemel Hempstead UK) compared to a bovine serum albumin standard curve. Samples were diluted in assay buffer to bring concentration to within linear portion of the standard curve (0.2-0.9 mg/ml). Measurement of optical density was performed using an ELISA reader (Emax, Molecular Devices Ltd, Berkshire UK) reading the absorbance at 650 nm. Equal amounts of protein were loaded in subsequent assays.

2.8.4 Western Blot

Polyacrylamide gels were made as two discontinuous gells, a 12% separating and a 4% stacking gel. Eight µg of each sample was made up to 15 µl with 1X Laemni bugger and bromophenol blue was added to 0.05% concentration. The samples were boiled for 5 minutes and loaded on the gel together with a prestained molecular weight marker (Bio-rad,UK). The gel was run in Running buffer until bromophenol blue run out of the gel (200V for 50 min). The glass plates were separated and the stacking gel removed. The separating gel was marked (cut at corner) and equilibrated in Transfer buffer for 20 minutes. Immobilon P membrane (Amersham, UK) was cut at the size of the gel and put in methanol for 15 sec. Then it was rinsed in water for 2 min, and equilibrated in Transfer buffer for 5 minutes. The transfer formation was set up on the appropriate apparatus in the order: anode-Immobilon P-Gel-Cathode with 4 pieces of Whatman 3 MM paper in between. It was run for 30 minutes at 10 V. Immediately after transfer, the membrane was washed with PBS and immersed in methanol for 10 seconds. Then it was

dried on filter paper and blocked with Blocking solution for 2 hours at 4°C. The membrane was washed 3 times with PBS-T, and the 1° antibody/antibodies (rabbit anti-Aipl1 antibody, rabbit β-PDE antibody and mouse mononclonal anti β-actin antibody [Sigma] for loading controls) were incubated in Hybridisation solution at appropriate concentration overnight at 4°C (see section 2.10.4 and 2.10 .5 for concentrations). The following day, the membrane was washed 3 times with PBS-T, then the horseradish peroxidise (HRP)- conjugated 2° antibodies (goat anti-rabbit IgG and goat anti-mouse IgG) were incubated in Hybridisation solution for 50 minutes at room temperature. The membrane was washed 3 final times with PBS-T and put on a plate. ECL reagents (ECL Plus Western Blotting Detection System, GE Healthcare) were mixed and added onto the membrane for 1 minute. The western blot was imaged using a UVIchemi Chemiluminometer (UVItec Ltd., UK).

2.9 In vivo experiments

2.9.1 Animals

Aipl1 h/h knockdown mice that expressed lower than normal levels of AIPL1 and *Aipl1 -/-* mice that were deficient in AIPL1 were used for this study. For control experiments, wild type C57B/6 mice were used. Treatment was performed only in one eye in each animal while the other eye served as an internal control in all experiments. This was to account for inter-animal variability in the rate of degeneration so that data were comparable. Each eye received two subretinal injections of viral suspensions or PBS, one in the superior hemisphere and one in the inferior hemisphere, as described in section 2.9.3. Subretinal injections were performed in 4-5 weeks old mice. Animals were sacrificed by exposure to carbon dioxide or cervical dislocation. All animals were cared for in accordance with the Animal Scientific Procedures Act 1986 and procedures were in accordance with the ARVO statement for the Use of Animals in Ophthalmic and Vision Research.

2.9.2 Animal anaesthesia

For Intraocular procedures, animals were anaesthetised by intraperitoneal injections of Dormitor (1 mg/ml, Pfizer Pharmaceuticals, UK) and ketamine (100 mg/ml, Fort Dodge Animal Health, UK) mixed with sterile water in the ratio 5:3:42. Young mice weighing 200 g received 0.2 ml of the anaesthetic solution. After treatment, 1 % Chloramphenicol (FDC International Ltd., UK) was applied topically to the cornea. To reverse the anaesthesia, 0.2 ml of Antisedan (0.10 mg/ml), Pfizer Pharmaceuticals, UK) was injected intraperitoneally and the mice were placed into an oxygenated chamber on a heat mat until they regained consciousness. All animal anaesthesia and recovery were performed by the author.

2.9.3 Subretinal injections

In the *Aipl1 h/h* mice, subretinal injections were performed at postnatal age of 4 weeks, when animals were older and their eyes less susceptible to surgical trauma and significant photoreceptor cell loss has not yet occurred at this age. In the Aipl1 -/- mice, subretinal injections were performed at postnatal day 12 due to the early onset of photoreceptor degeneration; at this age, the mouse retina is fully developed and the mice have opened their eyes thus facilitating subretinal injections and photoreceptor degeneration is not yet established at this stage. Animals were anaesthetised as described in in section 2.8.2 and pupils dilated with tropicamide 1% and phenylephrine 2.5%. Subretinal injections were performed under the guidance of an operating microscope. The fundus was visualized by means of a contact lens system consisting of a drop of coupling medium solution (Viscotears, Novartis Pharmaceuticals, UK) on the cornea and a glass coverslip placed against the cornea. A 10 mm, 34 gauge needle, mounted on a 5 µl Hamiton syringe (Hamilton, Bonaduz, Switzerland) was used to inject the vector suspensions intraocularly. The tip of the needle was guided underneath the coverslip, tangentially through the sclera at the equator of the globe to create a self-sealing tunnel into the subretinal space. Using direct visualization via

the microscope, it was possible to ascertain that the needle tip was in the correct space by bringing the needle tip into focus between the retina and the RPE. A volume of 1.5 µl of virus suspension containing around 10^8-10^9 particles of rAAV was injected to produce a transient bullous retinal detachment which involved about 30% of the fundus in the superior hemisphere. A second injection was performed subsequently to produce a similar detachment in the inferior hemisphere. All animal subretinal injections were performed by James Bainbridge with the assistance of the author.

2.9.4 Electroretinography method and analysis

Electroretinography (ERG) from mice was recorded in a standardised fashion at various pre-determined time points. All animal ERGs were performed by the author. All animals were dark-adapted overnight (16 hours) prior to ERG recording. Animals were anaesthetized for ERG and pupils were dilated using tropicamide 1% (Chauvin Pharmaceuticals Ltd.)applied topically prior to recording. A water-based coupling medium (Viscotears, Novartis Pharmaceuticals Ltd., UK) was used to improve electrical contact with the electrode and keep the eyes moist during the recording procedure. All manipulations before ERG were performed under dim red light illumination. ERGs were obtained using commercially available systems, Toennies Multiliner Vision, (Jaeger/Tonnies, Wurzburg, Germany) and Espion ERG Diagnosys system (Diagnosys LLC, Cambridge UK).

Ganzfeld ERGs were obtained from both eyes simultaneously using contact platinum corneal electrodes on each eye and one reference electrode placed sublingually. Midline reference and ground electrodes were placed subdermally in the center of the forehead and caudally. Electrode impedances were kept symmetrical and low between 5 and 10 kOhm. Scotopic flash intensity series was performed. Recordings were filtered from 0-1 kHz with a sampling frequency of 5 kHz. In all measurements, 400 ms of response was recorded. The first 10 ms of each recording was automatically used to zero the trace.

For scotopic flash recordings using the Tonnies Mulitliner Vision, single flash intensities were obtained at light intensities increasing from 0.1 mcds/m^2 to 3000 mcds/m^2. Ten responses per intensity level were averaged with an inter-stimulus interval of 5 s (0.1, 1, 10, 100 mcds/m^2) or 5 responses per intensity with 17 second interval (1000 and 3000 mcds/m^2). Readings obtained were analysed with software provided from Tonnies Multiliner Vision. For scotopic flash examination using Espion ERG Diagnosys system, a multiple flash intensity series was performed, with light intensity increasing from 0.001 cd.s/m^2 to 5 cd.s/m^2 (-3 to 0.5 log cd.s/m^2). Ten (intensities < 1 cd.s/m^2) or 5 (intensities ≥ 1 cd.s/m^2) responses per intensity were collected and averaged for use in subsequent analysis.

2.10 Histological methods

For histological and immunohistochemistry analysis, mice were sacrificed at various pre-determined time points to examine for evidence of a therapeutic effect, which took into account the transduction kinetics of the vector being used, timing of the subretinal injections and the rate of retinal degeneration in the animals. More specific details regarding exact time points used in the different experiments are described in Chapters 3 and 4.

2.10.1 Paraffin wax sectioning

Animals were sacrificed by exposure to CO_2. Eyes were immersion-fixed in 4% (w/v) paraformaldehyde overnight. Eyes were dehydrated overnight in a Leica Histokinette Processing machine and embedded in paraffin wax. Sections 7µm were cut using a microtome and stored at room temperature.

2.10.2 Cryosections

Animals were sacrificed by exposure to CO_2. Eyes that were designated for AIPL1 immunostaining were embedded directly in Optimal Cutting Temperature (O.C.T) medium (RA Lamb, E. Sussex, UK) and frozen in isopentane that had been pre-cooled in liquid nitrogen. Eyes which were designated for beta-PDE immunostaining were immersion-fixed in 4% (w/v) paraformaldehyde for 2 hours at room temperature. They were then cryoprotected by immersion in 20% (w/v) sucrose solution at 4C overnight..The eyes were then embedded in O.C.T. medium and frozen in isopentane which had been pre-cooled in liquid nitrogen. Specimens were stored at -80C and cut using a cryostat (Bright, UK) at thickness of 10-12µm. Sections were kept frozen at -20C until use.

2.10.3 Staining of sections by haemoatoxylin and eosin

Paraffin wax-embedded and cryosection specimens embedded in O.C.T were washed in xylene and alcohols to water. Sections were stained using haematoxylin for 5 minutes and washed in distilled water. Sections were then stained using eosin for 5 minutes and washed in distilled water. Slides were then passed through increasing concentrations of alcohols to xylene and mounted in DPX.

2.10.4 Immunohistochemistry of AIPL1

Unfixed cryosection slides were air dried for 10 minutes. Slides were post-fixed for 1-2 minutes with 2% (w/v) paraformaldehyde and then washed with PBS. The slides were then incubated for 1 hour in blocking buffer (5% (v/v) normal goat serum (Dako Ltd) in 1%BSA/TBS (w/v) and 0.1% Triton-X100 at room temperature. Following this,the slides were incubated overnight with the primary antibody (anti-rabbit AIPL1 – gift from Tiansen Li) at a dilution of

1:2000 in blocking buffer at 4C. After 3 washes (10 minutes with TBS), the slides were then incubated with the secondary antibody, goat anti-rabbit Alexa-471 or Alexa-546 at a dilution of 1:500 in blocking buffer and left at room temperature for 2 hours. The slides were washed again three time (10 minutes with TBS). Counterstaining of the nuclei was performed using Hoerst dye at dilution of 1:1000. Excess solution was removed and slides were mounted in fluorescent mounting medium (Fluormount, Dako), Sections were examined by fluorescent microscopy and images captured on Leica 500 (Zeiss, Germany) digital camera and viewed on Adobe Photoshop software. Sections were also analysed by confocal microscopy.

2.10.5 Immunohistochemistry of β-PDE in rod inner segments

Cryosections which were designated for beta-PDE immunochemistry (section 2.9.1) were air dried for 10 minutes. The slides were then rehydrated for 5 minutes with water and incubated with blocking buffer consisting of 4% (v/v) normal goat serum and 1% BSA (w/v) for 1 hour at room temperature. The primary anti-rabbit β-PDE antibody (Affinity BioReagents, Neshanic Station, NJ), was applied at a dilution of 1:500 in blocking buffer and left to incubate overnight at 4C. On the next day, following 3 washes using the blocking buffer (3x 10 minutes), the slides were incubated with the secondary goat anti-rabbit antibody Alexa 594-conjugated streptavidin (Molecular Probes Europe, Leiden, The Netherlands) at a dilution of 1:500 in TBS for 2 hours. The slides were then washed twice with TBS (2X 10 minutes) and Hoerst dye 1:1000 dilution in blocking buffer was applied. Following a final wash with PBS, slides were mounted with fluorescent mounting medium (Fluormount, Dako) and examined using fluorescent microscopy and images were captured on Leica 500 (Zeiss, Germany) digital camera and viewed using Adobe Photoshop software. Sections were also analysed by confocal microscopy

2.10.6 Confocal Imaging

Cryosections were analysed using the 3-laser ZEISS LSM 510UV Confocal Imager and its software was used to capture images at X40 and X60 objective, at various thickness layers (Z-stack) of the section. The images of the Z-stack were either used individually or as projected composite of each other.

2.10.7 Fixation of eyes for semithin and ultrathin sections

At various time points mice were sacrificed and their eyes were immediately removed and orientated with a nasal stitch. Then eyes were immersion fixed in 3 % glutaraldehyde and 1 % paraformaldehyde buffered to pH 7.4 with 0.07 M sodium cacodylate-HCl buffer (Karnovsky's; 0.2 M $(CH_3)_2AsO_2Na.3H_2O$ with 0.2 N HCl). After 12 hr the anterior part of the eye was removed by microdissection. The posterior segments were then osmicated for 2.5 hr in a 1% aqueous solution of osmium tetroxide, followed by a dehydration series through ascending alcohols (50 – 100%, 10 min per step). After 3 changes of 100% ethanol, specimens were passed through propylene oxide (3x 10 min) and left overnight in a 50:50 mixture of propylene oxide and araldite. Following a single change to fresh araldite (5 hr with rotation) the specimens were embedded in resin and cured for 48 hr at 60ºC.

2.10.8 Semithin sections

Semithin sections were cut and stained by Dr. Emma West. Semithin sections (0.7 µm) were cut using a Leica ultracut S microtome fitted with a diamond knife (Diatome histoknife). Sections were stained with toluidine blue stain (25 ml 2 % hydrated sodium borate, 25 ml 100 % ethanol, 0.5 g

toluidine blue, SPI-Chem^{TM}) and slides were mounted with DPX after the sections had dried. Sections were analysed using a Leitz Diaplan microscope for observation and imaged with a Leica DC 500 digital camera.

2.10.9 Ultrathin sections

The ultrathin sections were cut, stained and prepared for electron microscopy by Dr Peter Munro. Ultrathin sections (50 nm) were cut using a Leica ultracut S fitted with a diamond knife for ultrathin sections (Diatome histoknife for ultrathin sections). Sections were taken of treated areas of retinae and collected onto grids. Sections were stained with uranyl acetate for 10 min and lead citrate for 7 min and then washed with dH_2O. After the sections had dried they were analysed by electron microscopy (JEOL 1010 TEM).

2.11 Statistical Analysis

The choice of an appropriate statistical method is important to draw conclusions from data that are subject to experimental error. Generally, statistics yield the probability value for a particular result. In science, a probability (p) of 0.05 or less is usually accepted as convincing evidence that a particular outcome is significant and not due to chance.

A “Student's t-test” can be performed knowing only the mean and standard deviation of two data sets. The Student's t-test determines a probability that two populations are the same with respect to the variable tested. The populations are assumed to follow a normal distribution (Gauss distribiution). For independent samples, as it was the case for most of the histological data presented in this thesis, an unpaired Student’s t-test was used (unless stated differently). This test compares two small, independent sets of data that do not have to have the same number of data points in each group and are

collected randomly. In order to evaluate the significance of the difference in number of surviving photoreceptor cells and retinal layer thickness between either non-dystrohic or dystrophic, treated or untreated animals, cell counts and thickness meassurements were carried out and on 10 sections per eye, in the middle of the superior injection site. Since the number of animals for each condition varied, the sets of data should to be regarded as randomly collected and independent. Therefore an unpaired Student's t-test was applied.

For functional ERG results presented in this thesis, a paired Student's t-test was performed. A paired t-test can only be applied if the numbers of points in each data set are the same, and if they are organised in pairs. Generally, it is used when measurements are taken from the same subject before and after manipulation, in this case the viral mediated expression of a transgene. Since ERG records electrical responses of both eyes simultanously, and recordings can be obtained at different time points over a period of time from the same animal, a paired Student's t-test was used. For each animal, the height of b-wave amplitude of the ERG recording obtained at a flash intensity of 100 mcds/m^2 was used for statistical analysis. The b-wave values (a-wave through to b-wave peak) of the treated (right) eye were paired with the untreated contralateral (left) eye to provide an internal control. A paired Student's t-test was used to evaluate significance ($p<0.05$). This method controls for interanimal variance and test-retest variance present in rodent ERGs.

2.12 Patient Screen

2.12.1 Patients and controls

The patient panel consisted of 309 probands with simplex and autosomal recessive retinal dystrophy who were ascertained from the medical retinal clinics at Moorfields Eye Hospital. The study was conducted in accordance

with the tenets of the Declaration of Helsinki and was approved by Moorfields Hospital Ethics Committee. All patients gave written informed consent to be included in the study and provided a blood sample for subsequent DNA extraction and DNA analysis.

The control panel consisted of 96 control DNA samples originating from a normal population of randomly selected, non-related UK Caucasian blood donors. The panel (Human Random Control-1 DNA panel) was obtained from European Collection of Cell Cultures (ECACC).

2.12.2 DNA isolation

Blood samples were collected in EDTA tubes. DNA was extracted using a Nucleon Genomic DNA Extraction Kit (BACC2, Tepnel Life Sciences plc) following manufacturer's instructions. Solution A provided by thew supplier was added to each sample and samples were shaken for 5 min. After centrifugation for 7 min at 5000xg the supernatant was carefully removed. Each pellet was then resuspended in 2 ml solution B, samples were transferred to a new tub and mixed with 450 µl of sodium perchlorate. Tubes were inverted several times in order to mix the samples and 1.5 ml chloroform was added. After mixing thoroughly 300 µl of Nucleon resin was added and samples were centrifuged for 5 min at 4000xg. The aqueous phase containing the DNA was transferred into a new tube and mixed with 6 ml 100 % ethanol. After a 5 min spin the supernatant was removed and DNA pellets were washed with 500 µl 70 % ethanol. Samples were centrifuged again at 4000xg for 5 min, the ethanol was removed and pellets were air dried. The DNA was resuspended in 400 µl dH_2O, rotated over night at 4°C to dissolve DNA, and stored at -20°C.

2.12.3 PCR

Primers were designed corresponding to intronic sequences for PCR amplification of all 6 exons of *AIPL1*. Sequences of primers used are listed below. All PCR reactions were performed in a total volume of 30 µl using 200 µM dNTPs (Promega UK), 0.5 µM of each primer, 2 µM DNA, magnesium containing Optimase reaction buffer (Transgenomic UK) and 2.5 U TaqGold (Transgenomic UK). Reactions were cycled using a Techne Touchgene Thermal Cycler. The optimal annealing temperature for each primer set was calculated by using the program PrimerSelect™ (DNASTAR Inc.).

Cycling conditions were as followed:

Initial denaturation	5 min at 95°C	
Denaturation	1 min at 95°C	35 cycles
Annealing	15 sec at Ta	
Extension	1 min at 72°C	
Final extension	10 min at 72°	

AIPL1	Forward primer 5'-3'	Reverse primer 5'-3'	Ta [°C]
Exon 1	ACTGGAAGCAAAGGTGGATG	GCCCATGCTAAAGTTGAATCT	54
Exon 2	TGAACTGAGTGAGCTGACCC	GAATAAGTTTGCAGGACTGGCTTTG	58
Exon 3	CATAGTGAGGGAGCAGGATTC	CATGGCTTATGAACCCTCTCG	56
Exon 4	CTTGTCTGTATGCACTTGACCAG	CAGGGAGAAGGTCAGCCATG	60
Exon 5	GAAGTGGCGCTGACTCTGG	CGGCTGGGTGGAGACAAG	56
Exon 6	TTGAGGAAACCGAGGGATGG	CAATCGAACCAGAAGTGACCAGG	60

Table 1.1 Amplification of the human *AIPL1* gene. Primer pairs were designed to cover the entire coding sequence and important intronic sequences of the human *AIPL1* gene (see also Appendix). Primer sequences and annealing temparatures for PCR are summarised in the table.

2.12.4 Gel electrophoresis

Fragment size and purity of PCR reactions were controlled by gel electrophoresis. Samles were loaded onto a 2 % agarose gel made with 1% TBE buffer and 8 µl ethidiumbromide/200 µl total volume. The fragments were characterised under UV-light.

2.12.5 ExoSapIT treatment

Samples were processed for direct sequencing for characterisation. For each sample two reaction – one for the forward primer and one for the reverse primer – were set up. DNA fragments were purified by ExoSAP-IT® (Usb Corporation) treatment in a total volume of 18 µl using 2 µl (approximately 10 ng) of the amplified DNA fragment and 0.5 µl ExoSAP-IT enzyme with sterile dH_2O. The purification mix was incubated for 15 min at 37°C and then the enzyme was inactivated for 15 min at 80°C.

2.12.6 Big Dye

Samples were sequenced using a BigDye® Terminator v1.1 Cycle Sequencing Kit (Applied Biosystems). The Big Dye was diluted in 2.5 x Big Dye Buffer containing 200 mM Tris pH 8, 5 mM $MgCl_2$ with sterile dH_2O. To each ExoSAP IT treated sample 1 µl Big Dye v1.1 and either 1 µl (0.8 µM) forward or 1 µl reverse primer were added.
Cycling conditions were as followed:

30 cycles: 95°C for 30 sec
50°C for 30 sec
60°C for 4 min

2.12.7 Purification and sequencing

Samples were then purified using Millipore Montage™ Cleanup Kit (Millipore Corporation). The total volume of samples was transferred to a Millipore 96 plate and a vacuum (15 to 20 psi) was applied for 10 min. Each well was washed twice with 25 µl injection solution supplied by manufacturer. Between and after the washing steps a vacuum was applied. Another 25 µl of injection solution was added to each well, the plate was sealed and shaken for 5 min to recover the purified PCR samples. Samples were then transferred onto an ABI® 96 plate (Perkin Elmer, Warrington, UK) for sequencing. Samples were run over night on an ABI Applied Biosystems 373A DNA Sequencer. Sequences were analysed using the DNASTAR software package (DNASTAR Inc.).

2.13 Buffers and solutions

Ampicillin (1000 x): 50 mg/ml ampicillin (Sigma-Aldrich Company Ltd.) in dH_2O, sterile filtered, stored at -20°C

Blocking solution (for Western Blot): 1X PBS, 3% BSA or non-fat dried milk solution, 0.5% Tween

Big Dye Buffer (2.5 x): 200 mM Tris pH 8, 5 mM $MgCl_2$ with sterile dH_2O

Buffer A (for AAV2/8 purification): 5.65 g Bis-Tris propane, 2.42 g Tris up to 1 l with dH_2O, pH 9; filtered through 0.2 µm.

Buffer B (for AAV2/8 purification): Buffer A + 175.32 g NaCl; filtered through 0.2 µm.

Church Buffer: 21 g of NaH_2PO_4, 48.55 g Na_2HPO_4, 70 g of SDS, 0.5 M EDTA and dH_2O to 1 litre.

DNA loading buffer (6 x): 0.25 % (w/v) bromophenol blue and 30 % (v/v) glycerol in water

HBS (2x): 16 g NaCl, 0.74 g KCl, 0.2 g $NaH_2PO_4H_2O$, 2 g Dextrose, 10 g HEPES, up to 1 l with dH_2O, pH 7; filtered through 0.2 µm

LB growth medium: 14 g Bacteriological agar (oxoid Ltd.) per litre of water, 5 g/l yeast extract, 10 g/l tryptone (Oxoid Ltd.), 10 g/l sodium chloride, and 50 µg/ml ampicillin

PBS (1 x): 85 g NaCl, 4.3 g KH_2PO_4, dH_2O to 10 litres, pH 7.2

PBS (tissue culture): 10 phosphate buffered saline tablets (Oxio Ltd.) dissolved in 1 l sterile ddH2O

PBS-MK: 1 x PBS, 2.5 mM KCl, 1 mM $MgCl_2$

PBS-T: PBS 1x with 0.05 % (v/v) Tween-20.

Periodate lysine paraformaldehyde: 2% paraformaldehyde and 0.05% glutaraldehyde

Proteinase K buffer: 100 mM Tris (ph 7.4), 50 mM EDTA and 0.5 % SDS

Sodium cacodylate buffer (0.07 M): 0.2 M $(CH_3)_2AsO_2Na.3H_2O$ with 0.2 N HCl

Sodium phosphate buffer: 97.1 g Na_2HPO_4, 43.6 g NaH_2PO_4, pH 7.2

TBE (50x): 242 g Tris, 57.1 ml Boric acid, 18.6 g EDTA, up to 1 l with H_2O

Toluidine blue stain: 25 ml 2 % hydrated sodium borate, 25 ml 100 % ethanol, 0.5 g toluidine blue (SPI-Chem^{TM})

Western blot sample buffer: 50%(v/v) 0.5 M Tris-Cl, pH6.8, 50% (v/v) glycerol, 10% (w/v) SDS, 0.5 M dithiothereitol, 40 mM bromophenol blue.

Western blot gel buffers: Stacking gel- 0.5 M Tris-Cl, pH 6.8, 0.4% (w/v) SDS; Running gel- 1.5 M Tris-Cl, pH 8.8, 0.4% (w/v) SDS).

Western blot running buffer: 25 mM Tris base, 0.2 glycine, 0.1% SDS.

Western blot transfer buffer: 192 mM glycine, 25 mM Tris base, 20% (v/v) Methanol, 0.2% (w/v) SDS.

3 AAV2/2 - mediated gene replacement therapy in the *AIPL1* hypomorphic mouse

3.1 Introduction

The aim of the work described in this chapter was to determine the potential value of AAV2 vectors in alleviating a primarily photoreceptor-based retinal degeneration caused by defects in the *AIPL1* gene. Inherited retinal diseases such as retinitis pigmentosa and LCA are characterised by progressive visual impairment due to photoreceptor cell loss. Most forms of inherited retinal dystrophies are caused by mutations in genes expressed in rod and cone photoreceptors or in the retinal pigment epithelium (RPE).[95][407] There is currently no cure for inherited retinal dystrophies. With the advances in gene transfer systems, gene therapy holds great potential for the treatment of inherited retinal diseases[2,9,12,326,363,455,464,471,496].The goal of a gene-based strategy to treat a genetic disease such as retinal dystrophy is to achieve efficient, long-term expression of the transgene using only a single administration of vector. Many vectors based on different viruses such as adenovirus, herpes simplex virus and human immunodeficiency virus have been shown to mediate efficient gene transfer to the RPE [99]. However so far, the adeno-associated viral vectors has been particularly effective for retinal gene transfer and are the only viral vector to efficiently transduce both RPE and photoreceptor cells. [13][418].[13,388,408]

In this study, the goal is to treat a severe photoreceptor-specific degeneration and the efficient transduction of photoreceptor cells is of particular importance. Various serotypes of AAV have been isolated from non-human primate and human tissues and have different ability to transduce different retinal cell types *in vivo*.[30] [387][508]. Among these, AAV2/2 is the serotype most commonly used for the development of ocular gene therapy in the eye. Following subretinal administration, rAAV2/2

mediate gene expression in both photoreceptor and RPE cells while intravitreal delivery results in transduction of retinal ganglion cells. [178][300] Photoreceptor transduction by AAV2/2 is aided by the presence of heparan sulphate proteoglycan and other coreceptors such as human fibroblast growth receptor 1 (FGFR1) and integrins $\alpha_v ß_5$ on the cell membrane. [385][454] While there are some serotypes that transduce only the RPE, those that tranduce photoreceptor cells also tranduce the RPE.

Despite this the availability of relatively efficient vector systems, rescue of retinal degeneration has achieved mixed success. Better outcomes have been generally seen in models of retinal degeneration in which there is an RPE defect caused for example by mutations in *RPE65* and *MERTK*[1,437,471]. This is partly because even with currently available vectors, gene delivery to RPE cells is more efficient and widespread than to photoreceptors. In addition, the photoreceptor cells in these conditions are inherently healthy despite the metabolic defect in the RPE and may respond very well to partial correction of RPE function. Gene transfer approaches for photoreceptor-specific retinal degenerations have previously been more difficult, although there are now increasing number of studies reporting successful restoration of photoreceptor function and prolongation of photoreceptor survival [518][326] [363][9,243]. Another factor that might affect how amenable a mouse model may be to gene therapy is the speed of disease progression. The window of opportunity in a disease model is created by the balance between time for vector-mediated expression and rate of photoreceptor degeneration. This is particularly relevant to when sing AAV2/2 vectors. Transgene expression is detectable only at 2-3 weeks after subretinal injection, peaking after 6-8 weeks. [418] In slower retinal degenerations such as the *Mertk* and *RPE65* mutations, there is a longer time window for the onset of transgene expression before a critical mass of photoreceptors have been lost. As a result, these diseases are generally easier to treat using AAV2/2 vectors. In models of rapid degeneration, the onset and speed of disease precludes effective rescue by AAV2/2. An example is the *rd1* mouse which is characterized by rod photoreceptor degeneration from P8 onwards and total loss of rod photoreceptors by 4

weeks of age, By the time maximal transgene expression is achieved in the target tissue at 6 weeks, most photoreceptor cells would have already been lost. On the other hand, it may be difficult to detect any improvement and demonstrate effective rescue in retinal degenerations that are too slow. Following treatment with a therapeutic vector, any benefit would only become apparent once substantial cell loss has occurred in control eyes in comparison with treated eyes. An example is the *RPGR* murine model in which noticeable retinal degeneration is seen at 6 months of age and progresses slowly after[189]. As a result, any therapeutic effect would only be detected after more than 6 months following treatment.

As described in previous chapters, there are currently 2 mouse models of AIPL1-related retinal degeneration, the *Aipl1* knockout mouse model (*Aipl1 -/-)* and the hypomorphic AIPL1 mouse model (*Aipl1* h/h) in which there is reduced expression of AIPL1. Both models exhibit normal retinal histology and photoreceptor morphology at birth, and is followed by photoreceptor degeneration thereafter which occurs at different rates in each case. In the *Aipl1 -/-* mouse*,* photoreceptor degeneration is very rapid and completed by 4-6 weeks (depending on the background strain) [391][119]. As a result, the treatment of this mutant may not straightforward due to the rapid nature of the retinal degeneration which is similar to the *rd* mouse in time course. Retinal degeneration in the *Aipl1*h/h mouse occurs over months rather than weeks and approximately half of photoreceptor cell loss is seen at 6-8 months. The *Aipl1* h/h mouse is a strong hypomorph in which the level of AIPL1 is decreased to 25% of wild-type and the level of cGMP PDE, a purported client protein is similarly reduced[282]. In this slower model, normal retinal development is also noted toprior to the onset of photoreceptor degeneration. Thus there is a rationale that replacing AIPL1 would prevent the catastrophic events that commit normal photoreceptors to the fate of cell death. With a slower rate of degeneration, the hypomorphic *Aipl1* mouse model might provide a better model to assess gene-based strategies since there is a much greater window of opportunity for therapeutic intervention exists. Thus, the hypomorphic model was chosen as the initial animal model

in which to assess the efficacy of gene replacement therapy for AIPL1 deficiency.

3.2 Cloning of AIPL1 construct

To produce an rAAV2 vector expressing *Aipl1* transgene, a construct was created by cloning the mouse *Aipl1*cDNA between the ITRs of the AAV2 genome. The normal copy of murine *Aipl1* cDNA was amplified from murine cDNA using primers which have been designed to encompass the whole of the coding region. A PCR fragment of 1016 bp which was consistent with the size of murine *Aipl1* cDNA was isolated on gel electrophoresis. The *Aipl1* cDNA was cloned into the pGemT.Easy vector which contained the ampicillin resistance gene as a selection marker. The plasmid also contains a polylinker sequence that facilitates cloning since the PCR product is then flanked by a variety of different restriction enzyme sites. Following amplification of pGemT-*Aipl1,* the sequence of *Aipl1* was checked using digestion with a series of restriction enzymes and sequenced to ensure that no mutations had occurred during amplification and isolation of the fragment.

The rAAV backbone containing by the CMV promoter was obtained from another construct AAV-CMV-*gfp*. The restriction enzymes *SacII* and *NotI* were used to excise the *gfp* gene. The AAV backbone containing CMV promoter was extracted from gel as a 4642 bp fragment (Figure 3.1A). Similarly, the murine *Aipl1* cDNA was excised from the plasmid PGemT-*Aipl1* using the same enzymes *SacII* and *Not I* and following separation by gel electrophoresis, a fragment of 1091 bp was obtained (Figure 3.1B). The murine *Aipl1* fragment was then ligated into pD10 backbone between the CMV promoter and SV40 polyadenylation site to form a construct of 5733 bp termed AAV-CMV-*Aipl1* (Figure 3.2). The ligation mix was transformed into DH5α cells and DNA was prepared from the colonies. A total of 7 colonies were obtained and prepared to give 7 miniprep DNA samples. These DNA samples were checked using restriction digests with *StuI* and *KpnI*. Correct

fragments were found in 3 samples. These samples were checked with further restriction digests with *AccI, StuI, PstI* and *StuI* and correct fragments were obtained in all of them**.** Finally, a DNA megaprep prepared from sample no.2. This was rechecked using restriction digests with *AccI, StuI, KpnI* and *PstI* (Figure 3.3) and also sequencedS. This construct would later be used to generate the recombinant AAV vector expressing *Aipl1* for therapeutic assessment.

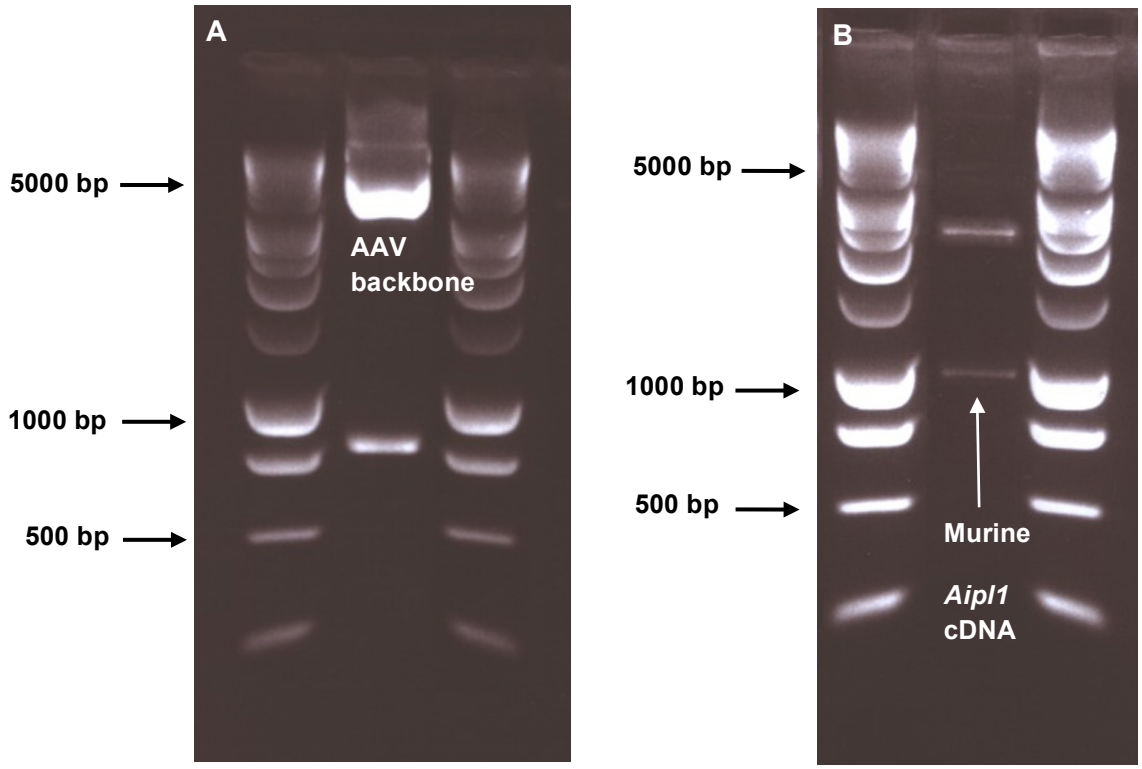

Figure 3.1. Restriction enzyme digest.

A) The ~ 4.6 kb AAV vector backbone was isolated from the parental plasmid AAV-CMV-*Egfp.*

B) The ~1.0 kb murine *Aipl1* cDNA was isolated from PgemT-*Aipl1* plasmid and cloned into the AAV backbone to form the therapeutic construct AAV-CMV-*Aipl1.* Both restriction digests are flanked by1 kb DNA ladder (Bioline Ltd., UK)

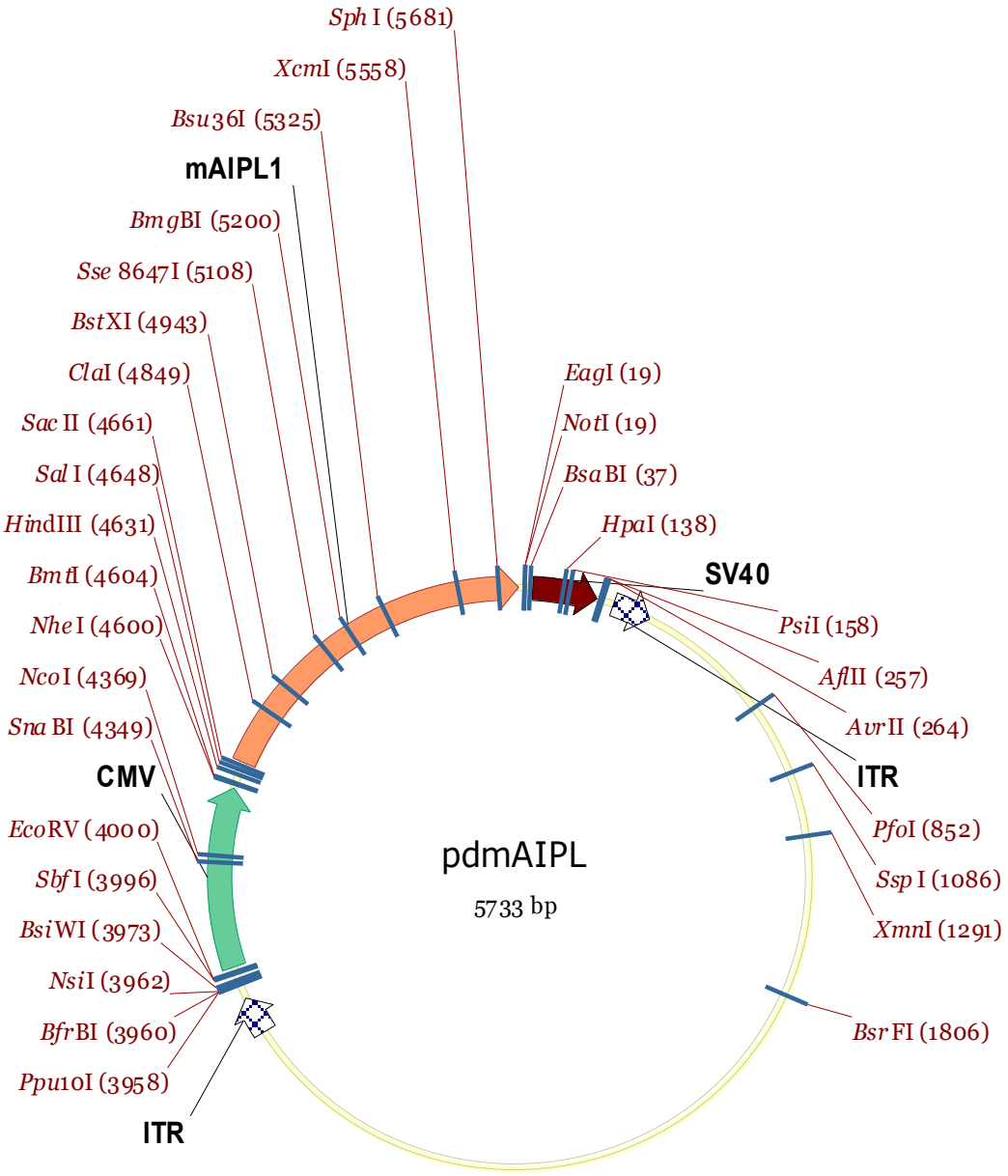

Figure 3.2. Map of the construct AAV-CMV-*Aipl1*.

The transgene AIPL1 was cloned downstream of the CMV promoter fragment , followed by SV40 polyA signal and is flanked by viral ITRs . The total size of the construct was 5733 bp.

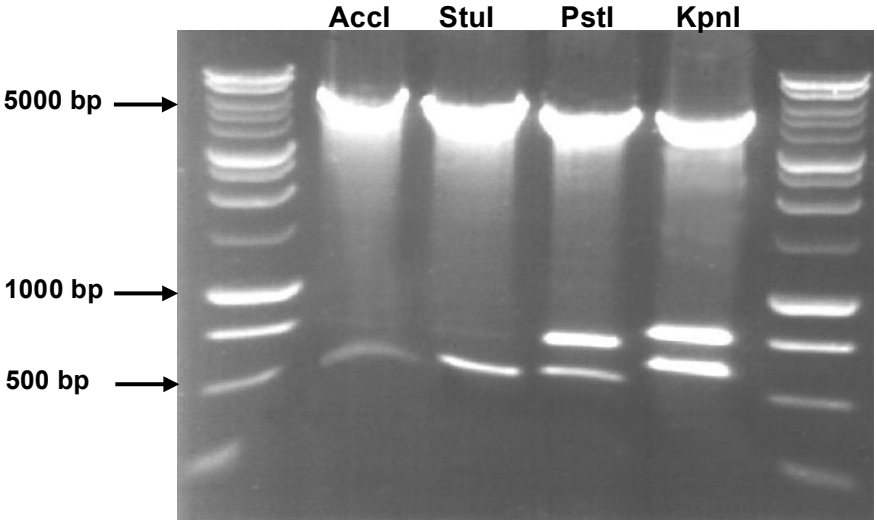

Figure 3.3. Restriction digest with AccI, StuI, PstI, KpnI of DNA megaprep from the colony 2 of ampicillin-resistant colonies of pD10-CMV-AIPL1. Correct fragments expected with AccI restriction digest were 341 bp and 5392 bp and expected fragments with StuI digest were 497 bp and 5236 bp. With PstI digest, fragments expected were 424 bp,639 bp and 4604 bp while with KpnI

Recombinant AAV serotype 2(rAAV2) carrying the *Aipl1* transgene was produced using a triple transfection method. Briefly, the method which is described in detail in section 2.6.2 uses four main components for the production of the rAAV vector. These are the rAAV plasmid, a replicating amplicon pHAV7.3 that contains the *rep* and *cap* genes and the PS1 HSV helper virus, and a packaging cell line. The rAAV constructs and pHAV7.3 were used to co-transfect BHK cells in a 1:1 ratio. The cells were then incubated for 24 to36 hours with PS1 HSV helper virus at 37^{o}C. Before the completion of the lytic cycle, the infected BHK cells were harvested and centrifuged to isolate the cell pellet. Following resuspension of the cell pellet, the suspension underwent repeated freeze-thawing and enzymatic treatment to release the virus from cells. The lysate was purified using a heparin column to isolate rAAV2 particles. The molecular titre was determined using dot-blot analysis. Concentration of the virus suspension was estimated by comparing to a dilution series, typical titres in this study were about 5 x 10^{11}. (Figure 3.4) Two constructs were used to generate rAAV2 for this

experiment, AAV-CMV-*Aipl1* and AAV-CMV-*egfp.* The AAV-CMV-*egfp* construct was a “parental” plasmid which had been previously generated. It was used in this study to serve as a negative control virus to verify treatment effects and to determine ether there was any toxicity or inflammation resulting from administration of the recombinant virus into the eye.

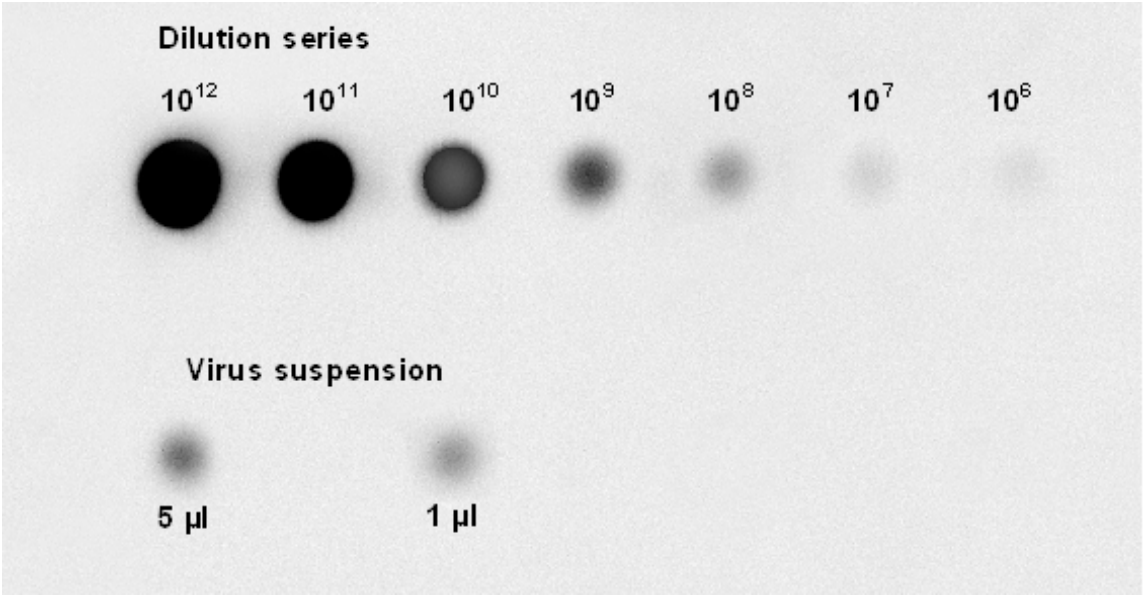

Figure 3.4. A chemiluminescence capture image of a dot blot for AAV2-CMV-*Aipl1* virus suspension.

The serial dilution of a DNA probe of known concentration serves as a standard ladder. 1 µl and 5 µl of the virus suspension were loaded and the concentration estimated by comparing the chemilumincence intensity of the sample to the dilution series. In this case it was estimated that the virus suspension had a concentration of 1×10^{11} particles /ml

3.3 Aipl1 transgene expression

3.3.1 *In vitro* assessment of gene expression from AAV-CMV-*Aipl1* and AAV-CMV-e*GFP*

In order to verify that the viral vectors AAV-CMV-*Aipl1* and AAV-CMV-*eGFP* were expressing the genes of interest, both plasmid constructs and viral vectors were used to transfect and transduce 293T cells. In a 24-well plate, 50 000 293T cells were seeded per well. 1µg of each plasmid construct was used to transfect each well along with Lipofectin and peptide 6 in the ratio described in methods section. The transfection mix containing the plasmid of interest, lipofectin and peptide 6 in Optimem was incubated at 37^{o}C for 4 hours. After this, the transfection mix was replaced with cell culture medium and incubated overnight at 37^{o}C. For infection, 1 µl of each viral suspension (10^{11} vp/ml) was added to each well of 293T cells. Replicates of twelve were made for plasmid transfection and virus transduction respectively. The next day, the cells were assessed for evidence of GFP expression. Bright green fluorescence was seen in wells where 293T cells were transfected with the plasmid AAV-CMV-*eGFP* and cells infected with the virus suspension of the same vector (Figure 3.5). No fluorescence was observed in the negative control wells or wells which were transfected with AAV-CMV-*Aipl1* plasmid construct. Since the AAV-CMV-*Aipl1* construct does not contain the *GFP* transgene, expression of the transgene could not be verified by fluorescence microscopy. Instead, the cells which had been transfected with AAV-CMV-*Aipl1* were collected 24 hours later and cells transduced with the vector suspension were harvested at 48 hours. These cells were lysed and sonicated, and the cell lysates were pooled together in their respective groups. A standard Western Blot analysis using an anti-*Aipl1* antibody was performed on the cell lysates. This included negative control samples consisting of 293T cells that had not been treated. A specific band of approximately 38 kDA corresponding to the size of murine AIPL1 was detected in transfection and infection cell lysates confirming the presence of

the protein. This observation validated the functionality of the plasmid construct and transgene expression from the viral vector (Figure 3.6).

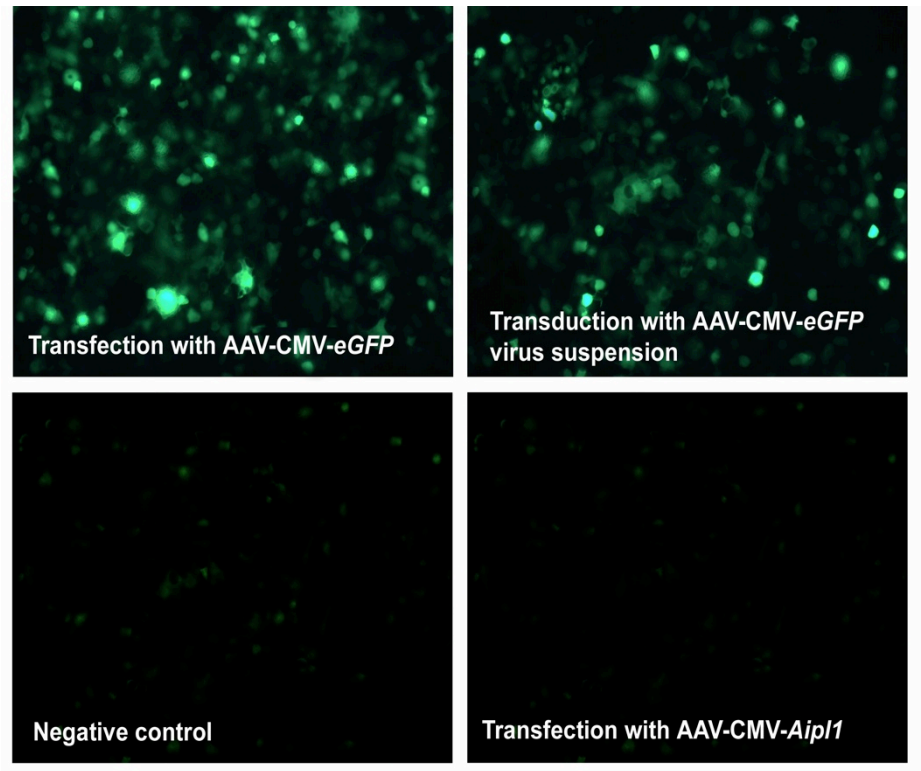

Figure 3.5. *In vitro* study of gfp expression in 293T cells.

A) Transfection of 293T cells with AAV-CMV-*eGFP* plasmid construct show green fluorescence 24 hours later.

B) 293T cells show green fluorescence following infection with AAV-CMV-*eGFP* virus suspension indicating transduction and expression in cells.

C) No green fluorescence was seen in the negative control well which was not transfected.

D) 293T cells which were transfected with AAV-CMV-*Aipl1* plasmid construct did not show any green fluorescence.

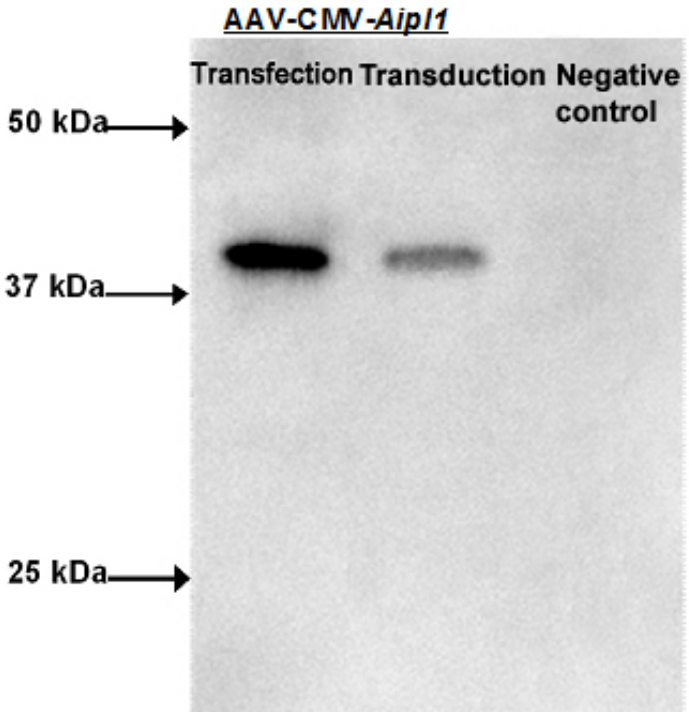

Figure 3.6. Western blot analysis of AAV2/2-CMV-*Aipl1* expression.

Lysates of 293T cells which were transfected with the plasmid construct AAV2/2-CMV-*Aipl1* and transduced with AAV2/2-CMV-*Aipl1* were subjected to western blot analysis. Band corresponding to the size of murine AIPL1 protein (≈38kD) is seen in both transfected and transduced cell lysates.

3.3.2 Expression and subcellular localization of AIPL1 in the retina following injection with AAV2-CMV-*Aipl1*

The viral vectors were injected subretinally as described in the methods section into 4- week old *Aipl1 h/h* mice. Each injected eye received 2 subretinal injections of virus suspension, one in the superior hemisphere of the retina and another in the inferior hemisphere. The volume of virus suspension per injection was 1.5 µl of virus suspension at a concentration of 1 x 10^{12} vp/µl. Each *Aipl1 h/h* mouse was received injections in one eye only, leaving the contralateral eye as an internal control. A total of 3 mice received subretinal injections for this purpose. Twenty-eight weeks after injections, these mice were culled and the eyes were taken and analysed for evidence of *Aipl1* expression.

At 28 weeks after subretinal injection of AAV2-CMV-*Aipl1*, the treated and untreated eyes of *Aipl1* h/h mice taken for immunohistochemistry. The eyes were embedded unfixed in optimal cutting temperature (OCT) medium and frozen, and then cryosectioned. Immunofluorescence analysis using an anti-AIPL1 antibody was performed on cryosections of matched injected and uninjected *Aipl1* h/h retinas and wild type retinas (Figure 3.7). To ensure that comparisons were made at the same levels in each of these eyes, the optic nerve was used as a reference point and sections which passed through the optic nerve were used for analysis. Analysis of retinas of *Aipl1 h/h* mice following injection of the therapeutic vector revealed an increased immunofluorescence with AIPL1 antibody in the layer located at the distal border of the outer nuclear layer corresponding to photoreceptor inner segments. This was consistent with the description of AIPL1 immunostaining in the retina from a previous study[282], and is similar to that seen in the wild type retinas albeit at a lower level. In contrast, uninjected control *Aipl1 h/h* retinas showed marked thinning of outer and inner nuclear layer and weak immunofluorescence for AIPL1. These data showed that subretinal injection of the AAV2-CMV-*Aipl1* vector resulted in efficient gene transfer and correct expression and localization of AIPL1 in the retina. AIPL1

immunofluorescence was also seen in the RPE layer of *Aipl1* h/h retinas injected with the therapeutic vector, while this was absent in untreated *Aipl1 h/h* and wild type retinas. This ectopic expression in the RPE layer is further verification of vector-driven *Aipl1* expression in the retina. Under the control of a ubiquitous promoter such as CMV, subretinal delivery of AAV2 results in transduction of both photoreceptor cells and the RPE.

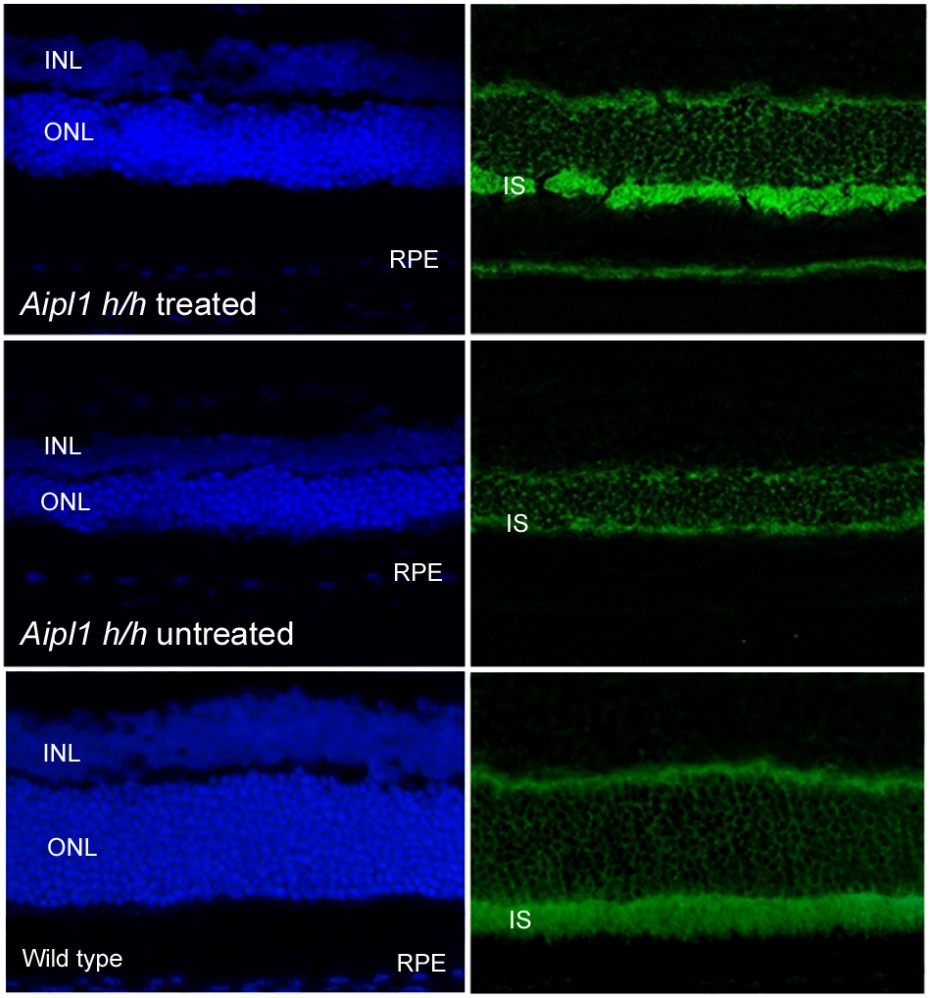

Figure 3.7. Expression and subcellular localization of AIPL1 in *Aipl1 h/h* retina following injection with AAV2-CMV-*Aipl1*

Treated *Aipl1 h/h* retina shows strong AIPL1 immunofluorescence (green) localized mainly to the inner segments (IS) in keeping with AIPL1 expression *in vivo*. The pattern of staining is similar to that seen in wild type retina. In contrast, uninjected AIPL1 h/h retina showed not only lower levels of AIPL1 immunofluorescence, but also reduced outer nuclear layer thickness.. Sections are counterstained with Hoechst nuclear dye in blue.

3.3.3 Quantification of *Aipl1* transgene expression *in vivo*

The levels of *Aipl1* transgene expression following subretinal injection of AAV-CMV-*Aipl1* into *Aipl1 h/h* mouse retina was assessed by comparing levels of transcript between vector-treated eyes and untreated eyes using quantitative PCR.

At 28 weeks post injection, eyes were taken from *Aipl1 h/h* mice that received unilateral subretinal injections of vector and from wild type mice. The neuroretina was dissected out from each of these eyes. Total RNA was isolated from the three pairs of treated and untreated *Aipl1 h/h* neuroretinas and from wild type neuroretinas, and reversed transcribed to obtain cDNA. Quantitative PCR was performed on the cDNA from these samples as described in the methods section. Since the *Aipl1* h/h mouse model is a knockdown model in which the level of *Aipl1* expression in the retina is reduced rather than extinguished, untreated eyes would not be expected to show an absence of *Aipl1* expression. Hence, in order to verify the functionality of the therapeutic vector, it was necessary to quantify the levels of *Aipl1* expression in eyes that received subretinal delivery of the vector and compare these relative to the levels in untreated eyes.

Levels of *Aipl1* expression in treated *Aipl1 h/h* eyes were found to be consistently higher compared with paired untreated eyes(Figure 3.8a). The mean relative levels of *Aipl1* expression in treated *Aipl1 h/h* eyes were more than 9 times of the mean relative levels in untreated eyes (Figure 3.8b). Compared with wild type eyes, the mean relative levels of expression in treated eyes were approximately 50% of wild type levels at 28 weeks following subretinal injection of AAV-CMV-*Aipl1* vector (Figure 3.8b), while in untreated eyes the level of *Aipl1* expression was 5% of wild type. Treatment with the viral vector therefore resulted in an increase in *Aipl1* expression of about 45% of wild type levels. The double subretinal injections of vector performed in each eye would expose approximately 60% of total area of the retina to the vector. Taking into consideration that the transduction efficiency

of AAV2/2 vector is known to be about 40-50%, it would seem that the levels of expression of *Aipl1* might be close to wild type levels in photoreceptor cells that were transduced successfully following subretinal injection of rAAV2/2 vector.

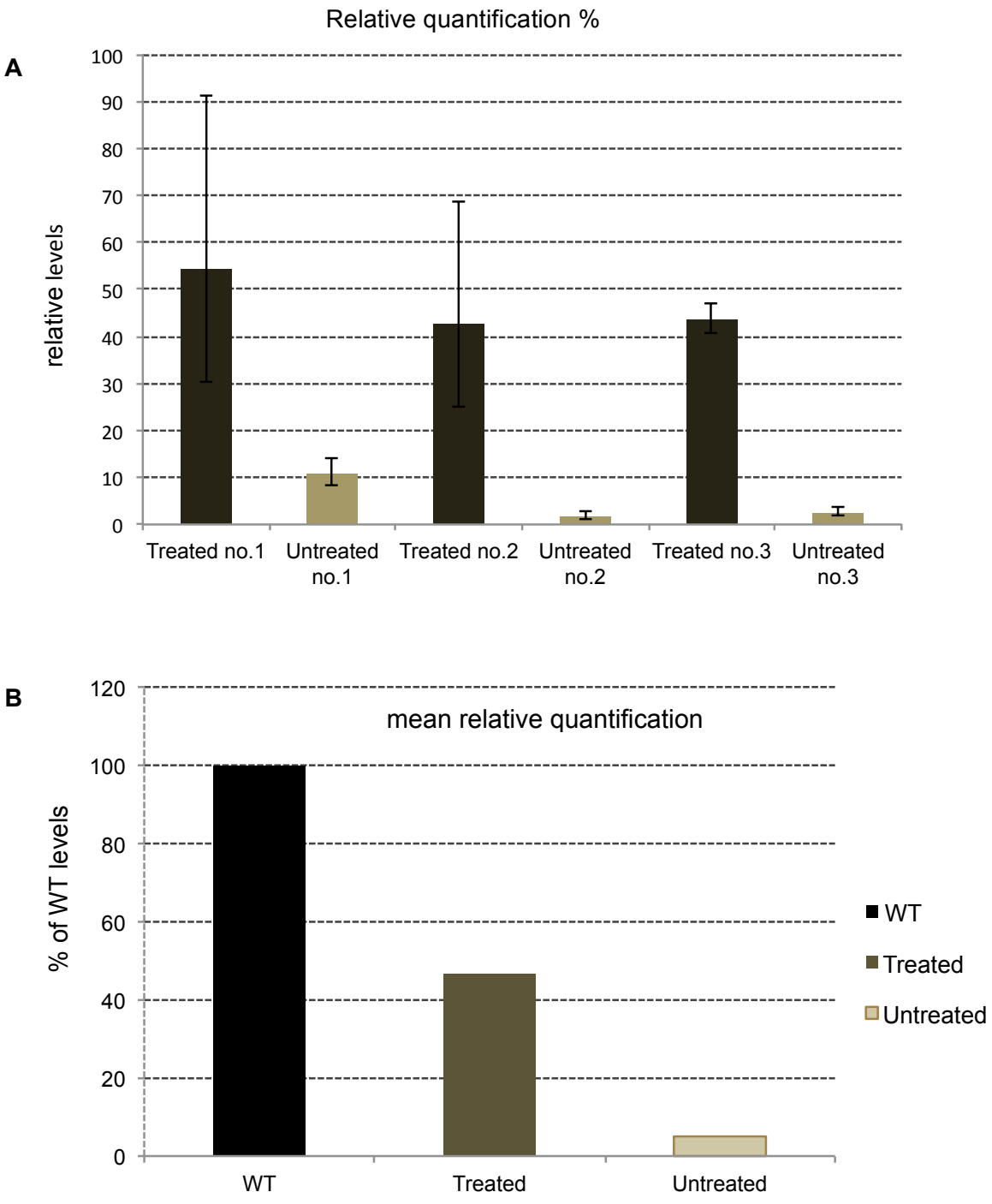

Figure 3.8. Quantitative PCR for *Aipl1* in treated and untreated retinal samples at 28 weeks following subretinal injection with AAV2/2-CMV-*Aipl1*.

A) The relative levels of *Aipl1* expression in treated and untreated retinas from 3 procedured aminals are shown. Error bars indicate standard deviation.

B) Mean relative expression of *Aipl1* in treated retinas were approximately 50% of wild type levels while in untreated retina this was approximately 5% of wild type.

3.4 Effect of AIPL1 expression on rod phosphodiesterase (PDE), a client protein.

3.4.1 Immunohistochemical analysis of AIPL1 and β-PDE in wild type mouse retina.

In the *Aipl1* h/h mouse, there is a decline in phosphodiesterase (PDE) level proportional to the reduced level of AIPL1[282]. This effect is highly specific for PDE, as analysis of a large number of photoreceptor proteins found no change in their expression levels in the hypomorphic mutant [282]. Hence, it has been hypothesized that AIPL1 is a specialized chaperone evolved to assist in photoreceptor PDE biosynthesis at a post-translational level. Phosphodiesterase is a key phototransduction enzyme in the retina and any effective therapy should aim to restore PDE biosynthesis, through reconstituting AIPL1 function, to a level sufficient to sustain photoreceptor function and survival. In view of this, we wanted to investigate the effect of rAAV-mediated *AIPL1* trangene expression on PDE expression and localization in transduced photoreceptors. In order to determine changes in PDE levels following subretinal injection of the vector, we evaluated the levels of β-PDE and AIPL1 using confocal microscopy. As shown in section 3.3.3, AIPL1 is normally localized mainly to in the inner segments of the rod photoreceptors, although some weak immunostaining for AIPL1 can be seen in the photoreceptor cell body and spherules [475]. In healthy photoreceptors, PDE is localized to the photoreceptor outer segments.

Immunostaining of β-PDE was first optimized in wild type mice retina so that a standard protocol could be established and a baseline pattern of double immunofluorescence for AIPL1 and PDE can be obtained. Since the protocol for AIPL1 immunostaining required that retinal sections were fixed as lightly as possible, the β-PDE immunostaining was optimized using unfixed retinal cryosections so that co-staining for the two proteins could be undertaken later. Eyes from wild-type mouse were extracted and immediately frozen in

OCT and then cryosectioned. The slides were divided into 3 groups: Group A – wild type retina immunostained with anti-AIPL1 antibody followed by a green secondary antibody, no second primary antibody followed by a red secondary antibody; Group B- wild type retina in which anti-AIPL1 antibody was not applied, then followed by a green secondary antibody, then anti β-PDE antibody followed by a red secondary antibody; Group C immunostained with anti-AIPL1 antibody, followed by green secondary antibody and then with anti β-PDE antibody followed by a red secondary antibody (protocols are described in section 2.9).

In group A, following immunostaining of wild type retina with anti- AIPL1 antibody, green immunofluorescence is seen mostly at the inner segments of photoreceptors with some staining detected in the cell bodies and the synaptic spherules in the outer plexiform layer (Figure 3.9 A). There was no red immunofluorescence detected as the anti β-PDE antibody was not applied in these samples. In group B, immunostaining with β-PDE antibody was present in the outer segments of photoreceptors as indicated by red immuofluorescence (Figure 3.9 B). Concurrent immunostaining for AIPL1 and β-PDE displays the correct localization of each protein with respect to each other (Figure 3.9 C), where there is a distinct layer of green and red immunofluorescence next to the outer nuclear layer representing the presence of AIPL1 and β-PDE respectively . The yellow fluorescence seen between the outer and inner segments is a result of an small degree of overlap of the AIPL1 green immunofluorescence and PDE red immunofluorescence. More importantly, this also showed that there was no non-specific binding of the red secondary antibody to the anti-AIPL1 antibody and vice versa since both of the primary antibodies were raised in rabbit.

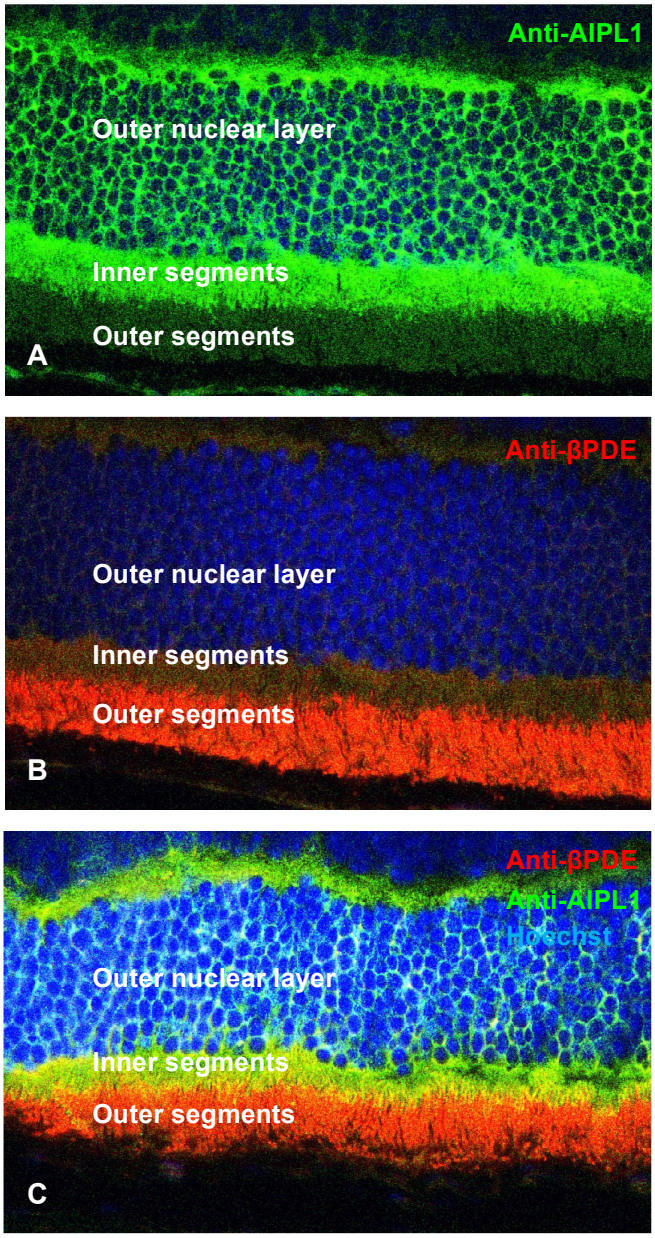

Figure 3.9. Anti-AIPL1 and anti-PDE immunofluorescence in wild-type retina.

Confocal microscopy of wild type mouse cryosections immunostained with anti-AIPL1 antibody only (Group A),; anti-βPDE only (Group B), and sequentially with anti-AIPL1 antibody and anti-PDE antibody (Group C).

A) Wild type retina immunostained with rabbit anti- AIPL1 antibody and Alexa- 488 goat anti-rabbit secondary (green); then TBS followed by Alexa-546 goat anti-rabbit secondary antibody (red).

B) Wild type retina immunostained with initially with TBS followed by Alexa-488 goat anti-rabbit secondary antibody (green); then with anti-βPDE antibody followed by Alexa-546 goat anti-rabbit secondary (red)

C) Wild type retina immunostained sequentially with anti- AIPL1 antibody followed by Alexa-488 goat anti-rabbit secondary antibody (green); then with anti- βPDE antibody and Alexa-546 goat anti-rabbit secondary antibody (red).

3.4.2 Immunohistochemical analysis of AIPL1 and β-PDE in *Aipl1 h/h* following gene transfer.

Retinas of *Aipl1* h/h mice received subretinal injection of AAV2-CMV-*Aipl1* were co-immunostained for AIPL1 and β-PDE at 28 weeks to assess if there were any differences in the levels and localization of these proteins. Representative paired retinal sections of treated and untreated eyes following treatment were co-immunostained for AIPL1 and β-PDE (Figure. 3.10).

Without treatment, retinas of *Aipl1 h/h* mice showed only weak green immunofluorescence for AIPL1 in the inner segments. Red immunofluorescence for β-PDE was reduced and mislocalized to the inner segment in untreated eyes resulting in overlapping of red and green immunofluorescence (Figure 3.10). Following treatment with AAV2-CMV-*Aipl1*, substantially increased AIPL1 immunofluorescence (green) was seen and accompanied by increased immunofluorescence for ß-PDE (red). More interestingly, a shift in the subcellular localization of β-PDE was seen in treated retinas: it appeared to be restored to the outer segments of photoreceptors (Fig. 3.10 B). The relative amount and localization of AIPL1 and β-PDE in treated eyes appeared similar to that seen in wild type sections (Fig. 3.10 C). These results indicate that not only the amount of β-PDE but also its subcellular localization is dependent on AIPL1. This association between the correct localization of β-PDE and AIPL1 has not been reported before. It is thus likely that the stability of PDE is dependent on AIPL1 and it suggests that AIPL1 functions in the final maturation step of PDE biosynthesis, as a molecular chaperone for the folding and/or cellular translocation of cGMP PDE.

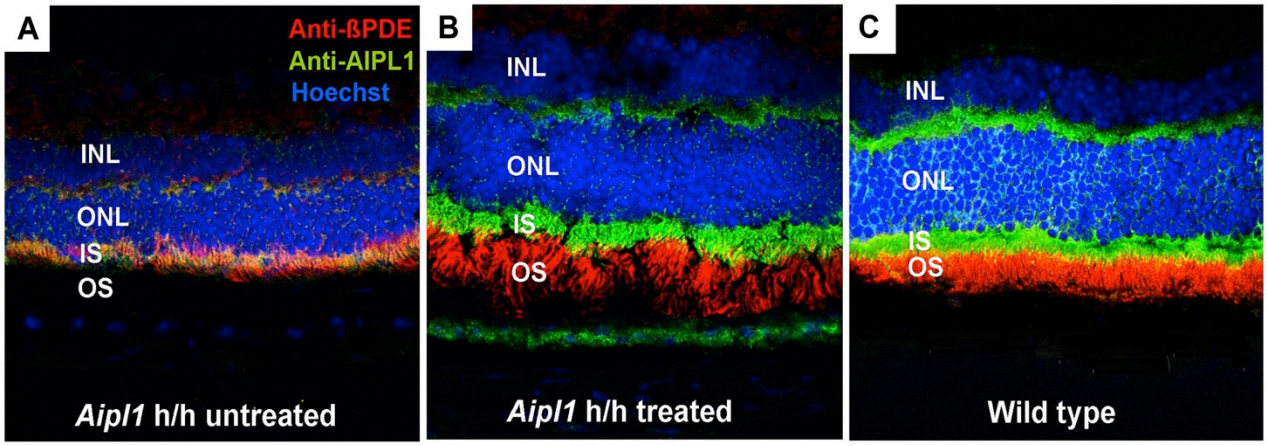

Figure 3.10. Confocal images of double immunofluorescence microscopy for AIPL1 and β-PDE in AAV2-CMV-*Aipl1* treated and untreated retinas of *Aipl1 h/h* mice at 28 weeks post injection.

Representative paired treated and untreated retinal cryosections from Aipl1 h/h mice were co-immunostained for AIPL1 and β-PDE, and imaged using confocal microscopy. Comparison of untreated and treated eyes of *Aipl1* h/h mice showed restoration of the normal localization of ß-PDE in the outer segments.

- **(A)** In untreated retina, ß-PDE immunofluorescence (red) colocalizes with AIPL1 immunofluorescence (green) in the photoreceptor inner segments (IS).
- **(B)** Following subretinal injection of AAV2-CMV-*Aipl1*, ß-PDE immunofluorescence is translocated to the outer segments (OS) in the treated retina. Hence in treated retina, AIPL1 immunofluorescence in the inner segment is separate from ß-PDE immunofluorescence in the OS, which is similar to that found in wild type retina.
- **(C)** Co-immunostaining of AIPL1 and β-PDE in wild type retina shown for comparison.

Cell nuclei were counterstained with Hoechst dye 33342 (blue).
INL- inner nuclar layer; ONL – outer nuclear layer; IS –inner segments; OS –outer segments.

3.5 Effects of AAV-mediated Aipl1 transgene expression on retinal morphology

3.5.1 Analysis of retinal histology in *Aipl1 h/h* retina following treatment with AAV2-CMV-*Aipl1* and in untreated retina

Following the verification of the vector and that the *Aipl1* transgene was expressed in treated murine retina, the next step was to evaluate the effect of the treatment on retinal morphology and whether retinal degeneration was being prevented or delayed. Sixteen *Aipl1* h/h mice received subretinal injections of AAV2-CMV-*Aipl1* viral vector. To achieve the maximal total area of treatment, the virus suspension was injected into the superior and also in the inferior hemisphere of the retina, using an injection volume of 1.5 µl viral suspension to create an area of bullous retinal detachment. Each injection created temporary bullae which covered 30-40% of the fundus. By injecting in 2 hemispheres, approximately 70% of the retina is exposed to the virus. In each animal, only the right eyes received subretinal injections and the left eye was left untreated to serve as an internal control, to eliminate external confounding factors which could influence the rate of photoreceptor cell loss and the considerable variation in the rate of retinal degeneration that exist even between animals from the same litter due to an inherent biological variability. The mice were injected at 4 weeks of age and this time point was selected based on the observation that the *Aipl1 h/h* mouse has a relatively slow degeneration in comparison to the null mutant and injecting very young mice would cause relatively more damage to the retina. Since the first signs of degeneration are only seen at 12 weeks and AAV2/2 vectors are known to give rise to transgene expression approximately 3-4 weeks following injection, we assumed that the delivery of the viral vector at 4 weeks of age should allow enough time for transgene expression to occur before there was significant photoreceptor degeneration; in this case we would expect to see *Aipl1* expression by 8-9 weeks of age. Maximal expression would be

expected to occur at about 3 months after injection, when the mice are 16 weeks old.

Two of the procedured animals were sacrificed at 8, 16 and 28 weeks respectively following subretinal injection. The eyes of these mice were orientated and fixed in paraffin before being sectioned and stained with haematoxylin and eosin. Adult wild type mice were sacrificed and eyes similarly processed for histological comparison. Using light microscopy, we examined these eyes for evidence of retinal degeneration at the various time points (Figure 3.11). At the age of 12 weeks (8 weeks following subretinal injection), no differences were seen in treated and untreated eyes and there was no evidence of any disorganization of the retinal architecture. At 20 weeks of age (16 weeks following subretinal injection), untreated eyes had noticeable thinning of the ONL and disruption of layered structure of the retina. Treated eyes at 20 weeks of age had relatively well preserved ONL and INL thickness, although there were some early signs of disorganization of the retinal architecture. At 32 weeks of age (28 weeks following subretinal injection), clear retinal degeneration was observed in untreated eyes, as indicated by the collapse of the retinal layers and substantial loss of ONL. Treated eyes at this time point had relatively well preserved retinal architecture and although some thinning of the ONL was seen, ONL loss in treated eyes was noticeably less compared with untreated eyes.

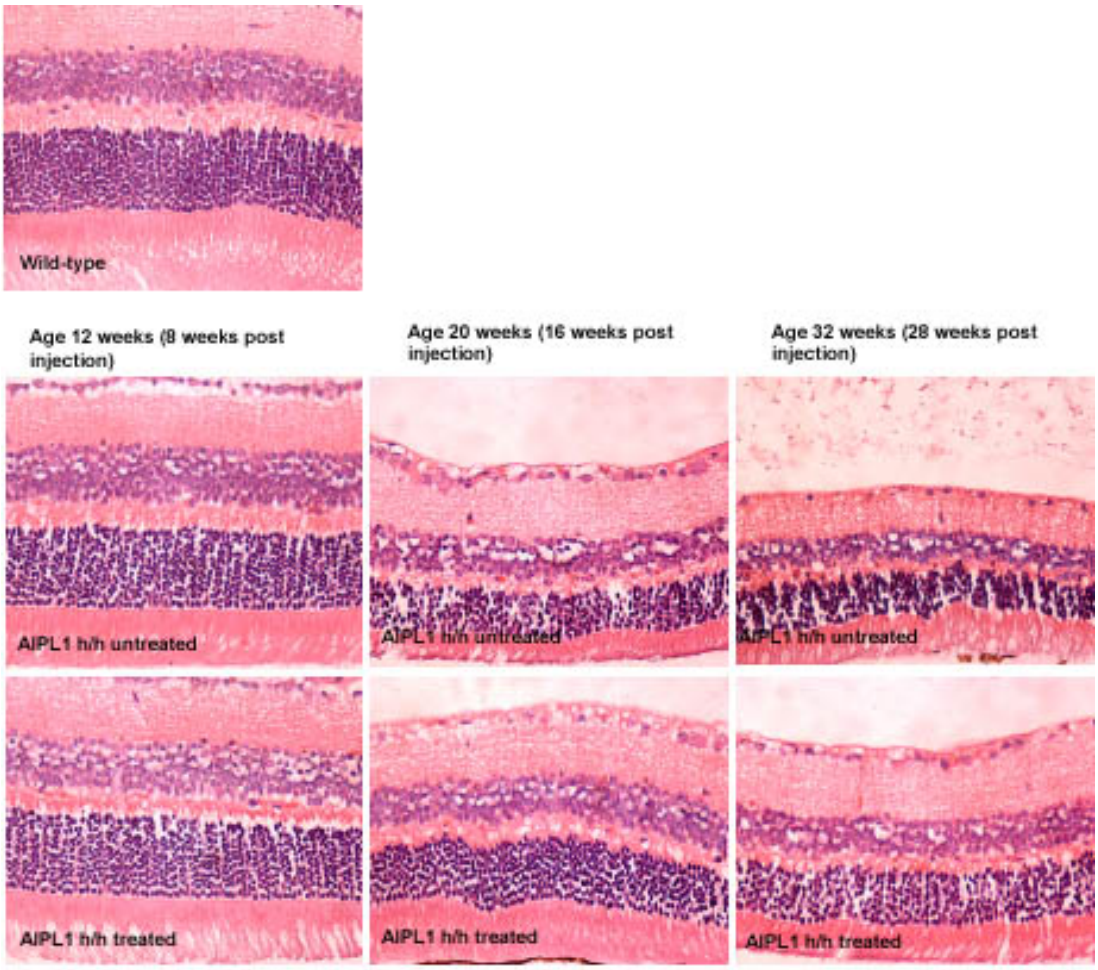

Figure 3.11. H&E comparison of representative matched pairs of treated and untreated *Aipl1h/h* eyes at 8,16 and 28 weeks following subretinal injection of AAV2/2-CMV-AIPL1.

Treated and untreated Aipl1 h/h retina at 12 weeks of age (8 weeks post injection) had no obvious signs of retinal degeneration. At 20 weeks of age (16 weeks post injection), the signs of degeneration become more evident in the untreated eye with progressive thinning of the outer and inner nuclear layers. By 32 weeks of age (28 weeks post injection), a substantial difference is seen between the treated and untreated eye in terms of disorganization of the retinal architecture and thinning of the ONL and INL that is more marked in the untreated retina. For comparison a wild-type retina at 9 weeks of age is shown. The retina in AIPL1 h/h animals appears to develop normally.

3.5.2 Morphometric analysis of the rate of retinal degeneration following gene transfer.

To quantify the extent of photoreceptor cell rescue in treated eyes compared with untreated eyes, morphometric analysis was performed on retinal sections by counting the number of photoreceptor cell nuclei in the ONL (Figure 3.12). Retinas were taken at 28 weeks post-injection for sectioning. Cryosections were taken at various depths and each eye had been orientated during embedding in such a way that when cryosectioned, each section spanned over the superior and inferior retina which were the sites of injection. The cryosections were immunostained for photoreceptor nuclei with propidium iodide (PI) and imaged using the confocal microscope. To standardise measurements and eliminate any bias, only sagitally orientated central retina sections that passed through the optic nerve head were selected for this analysis.

Eyes from a total of seven animals were analysed. For each eye, three3 central retinal sections were selected that appeared to pass through the optic nerve head. In each retinal section, images were captured from each side of the optic nerve head so that a total of two images were obtained from each section. Hence, a total of six confocal images of the retina were obtained for each eye. Standardized confocal images of photoreceptor nuclei under the same magnification were captured in the area between the ora serrata and optic nerve head approximating to the middle of the injection site. The nuclei in the outer nuclear layer in this area were counted by a single masked observer. Figure 3.12 illustrates the method of assessment and representative retinal sections from treated and untreated eyes. Photoreceptor nuclei which appeared less than 25% complete were not counted. The photoreceptor cell count for each eye was determined by averaging the cell counts from each confocal image of the particular eye. Mean number of photoreceptor nuclei was obtained for each of the 6 treated eyes and 6 matched untreated eyes. To control for inter-animal variation in

the rate of degeneration, a paired t-test was performed between the photoreceptor cell counts in the treated and untreated eyes of each animal.

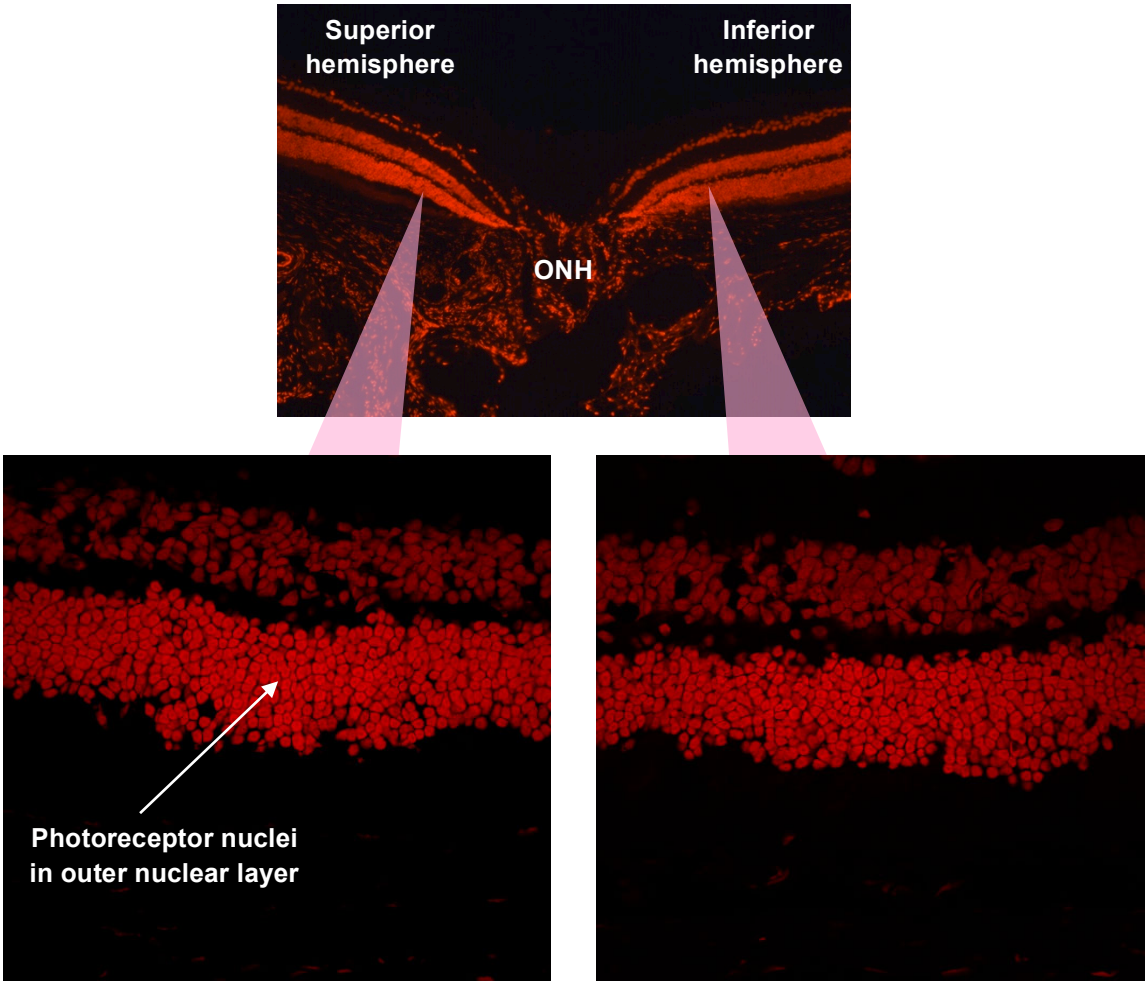

Figure 3.12. Method for assessing number of photoreceptors in outer nucler layer (ONL) in treated and untreated retina.

Sagittally orientated central sections that passed through the optic nerve head (ONH) were used. At about midway between the ONH and ora serrata, high power images of the ONL were captured on each side of the ONH using the same magnification (X40). The photoreceptor nuclei in these images were counted by a single observer.

Confocal images of representative retinal sections of treated and untreated eyes are shown in Figure 3.13. Treated retinas had substantially thicker ONL compared with untreated retinas. Statistical analysis showed that the mean number of photoreceptor cell nuclei in treated eyes of *Aipl1* h/h mice (n=7) was found to be 41 % higher than in the untreated eyes (mean photoreceptor cell count in treated eyes = 479.3 ± 16.6 versus untreated eyes = 339.3 ± 8.2 ; p=0.0003) (Figure 3.14A). Preservation of photoreceptors in treated eyes was observed in all of the seven animals that were assessed as each animal had significantly greater number of photoreceptors in treated compared with untreated contralateral control eyes ($p \leq 0.05$) (Figure 3.14B). However, the ONL cell count following treatment with the therapeutic vector was lower compared with age-matched wild type eyes (p=0.02), indicating that although retinal degeneration was slowed, it was not halted and there was still ongoing photoreceptor cell loss (Figure 3.14B).

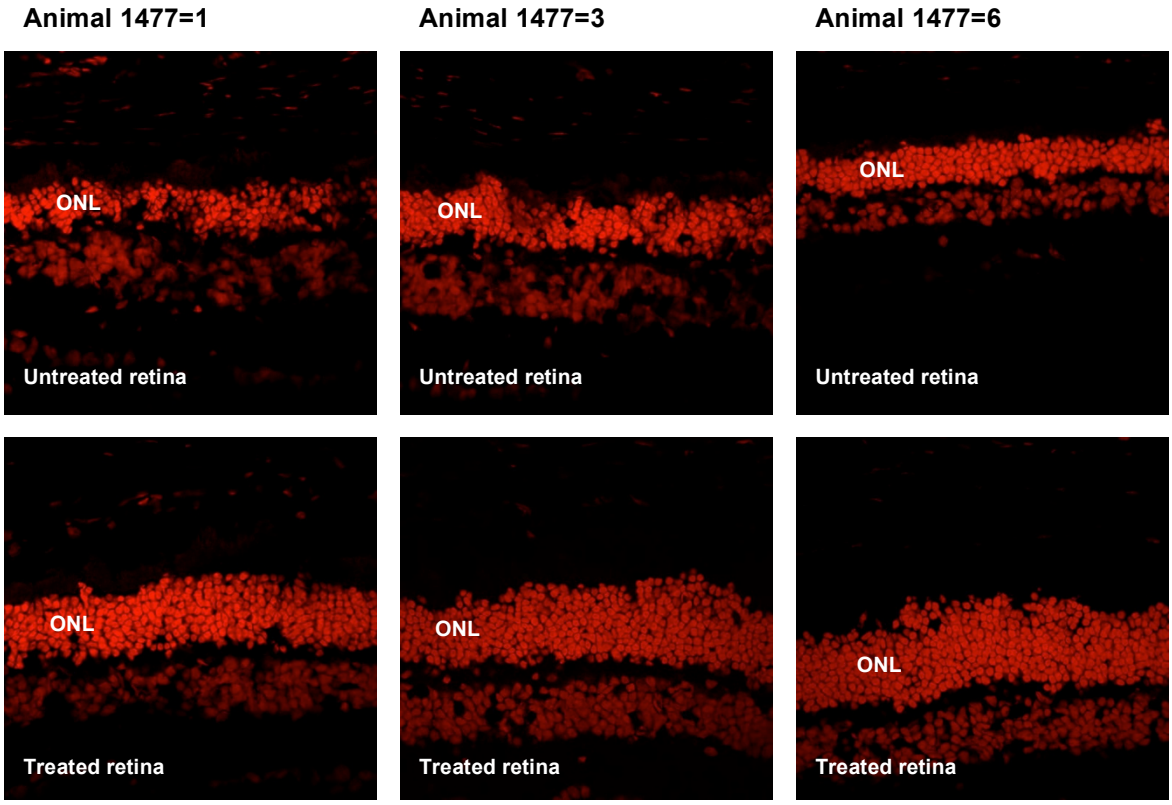

Figure 3.13. Confocal images of paired retinal sections of treated and untreated eyes from 3 representative animals that were assessed for morphometric analysis.

The number of nuclei in the outer nuclear layer were counted in each of these images by a masked observer. The paired statistical analysis of the mean number of outer nuclear layer nuclei showed significant differences between treated and untreated retinas.

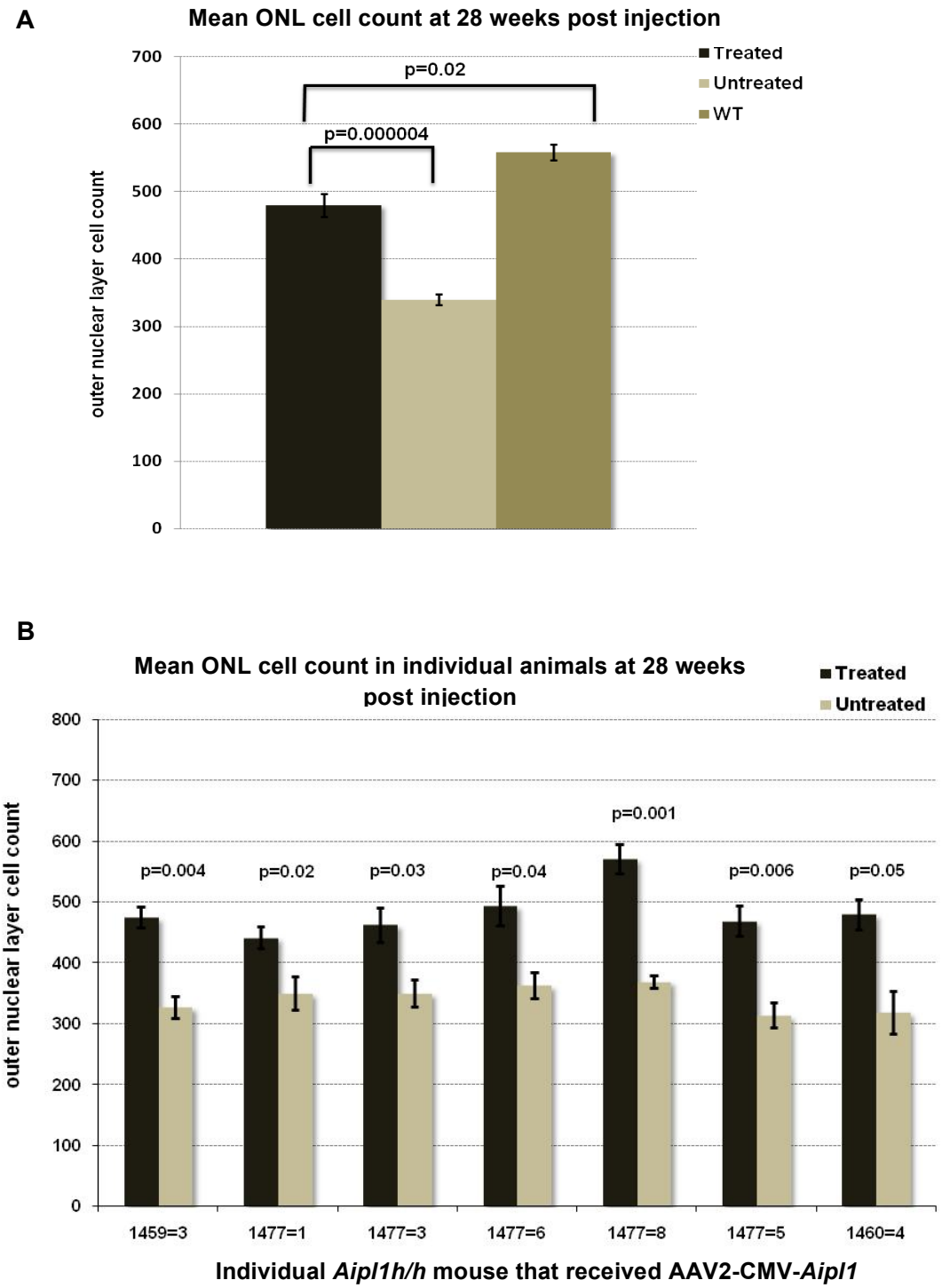

Figure 3.14 Graphs of mean ONL cell counts .

(A) Graph comparing mean ONL cell counts of 7 animals. Treated eyes have significantly higher mean ONL cell counts compared with untreated eyes indicating preservation of photoreceptor cells following subretinal injection of AAV2-CMV-*Aipl1.* However, treated eyes have lower ONL count compared with age-matched wild type eyes.

(B) ONL cell counts at 32 weeks of age (28 weeks post injection) for the right and left eyes of each individual animal is shown. There is a consistently higher cell count seen in the right treated eyes of each animal which is statistically significant ($p<0.005$).

3.6 Effects of AAV2-mediated Aipl1 expression on retinal function in Aipl1 h/h retina.

Histological analysis and quantification of the outer nuclear layer suggested that photoreceptor cell loss was significantly delayed following treatment with AAV2-CMV-*Aipl1*. AAV2-mediated *Aipl1* expression led to the correction of β-PDE mislocalization in *Aipl1* h/h retina. Consequently, the cellular biology of individual photoreceptor cells was restored, and the survival of photoreceptor cells was prolonged. It was thus important to ascertain whether this preservation of photoreceptor cells following treatment would have an effect on retinal function which could translate into visual stabilization or improvement.

Current established literature has defined a role for AIPL1 in rod and cone photoreceptor cells and therefore the retinal disease due to *AIPL1* gene mutations is attributed to an insufficiency of rod and cone PDE biosynthesis[282][232][240]. An effective therapy for this condition should aim to restore rod and cone PDE biosynthesis by reconstituting AIPL1 function. Since rods represent the majority of the population of photoreceptors in the murine retina[211][514], we looked for improvement in retinal function following AAV-mediated gene delivery by assessing rod photoreceptor function. Measurements that usually are recorded for a selected ERG signal are the amplitude and implicit time. In this study, the responses from rod photoreceptors were evaluated by analyzing the amplitudes of a and b-waves of dark-adapted ERGs that have been recorded from *Aipl1* h/h mice. The a and b-wave amplitudes were chosen as the outcome measure of retinal function. The a-wave is generated by photoreceptors and thus is a direct reflection of photoreceptor response. However, it is very much smaller in size and is more difficult to record accurately especially with a machine with limited sensitivity. The b-wave is much larger in amplitude and easier to record and measure. Although the b-wave is generated by the inner retina, the amplitude of the response relies

on the extent of the a-wave response and provides an indirect reflection of photoreceptor cell activity.

3.6.1 ERG intensity series following treatment with AAV2-CMV-*Aipl1*

To evaluate the effect of AAV-mediated *Aipl1* expression on retinal function, dark-adapted, scotopic ERG recordings were obtained from 16 *Aipl1* h/h mice that received unilateral subretinal injection of AAV2-CMV-*Aipl1* (titre of 1 x 10^{11} viral particles /ml) at 4 weeks of age. Only right eyes were injected, leaving the left eye as an internal control. The internal control is provides a means for paired analysis that would eliminate any bias caused by inter-animal variation that may occur within an ERG recording session. Scotopic ERG responses were recorded using a series of flash intensities consisting of 0.1, 1, 10, 100, 1000 and 3000 mcds/m^2 flashes via a stimulating Ganzfeld bowl. Control injections with PBS were carried out in 5 *Aipl1* h/h mice, and similarly subretinal injections of a control virus AAV2-CMV-*gfp* were performed on 6 *Aipl1* h/h mice under the same circumstances.

Simultaneous bilateral recordings were performed to optimize comparison of treated and untreated eyes, and ERG recordings were performed after a period of dark adaptation at regular intervals of 4 weeks, 8 weeks, 12 weeks, 16 weeks, 20 weeks, 24 weeks and 28 weeks post injection. Statistical analysis was performed on data obtained at flash intensities of 100 and 1000 mcds/m^2. The responses to flashes of intensities of 100 and 1000 mcds/m^2 from the eyes of treated and control animals were chosen for several reasons. At flash intensity of 100 mcds/m^2, a purely rod response is obtained. At intensity of 1000 mcds/m^2, responses from both rods and cones are recorded and provides an indication of the overall retinal function.

Representative ERG recordings from a single *Aipl1* h/h mouse at 20 weeks post-injection (Figure 3.15A) and ERG waveforms at 28 weeks post-injection are shown in Figure 3.15B. Compared with untreated eyes, the ERG

amplitudes in treated eyes were substantially higher. Oscillatory potentials, representing post-synaptic neuronal activity in the inner retina, were more obvious in the treated eye but reduced in the untreated eye. There was a general improvement in the shape of the ERG trace following treatment in that the ERG tracing resembled that of a wild type mouse ERG while the tracing from the untreated eye was flattened, indicating diminished responses. The ERG intensity series recorded from eyes that received subretinal injections of the control virus AAV-CMV-*gfp* or PBS similarly showed diminished responses (Figure 3.15C).The improvement in ERG recordings hence was a result of AAV-mediated *Aipl1* expression since injections of GFP control vector or PBS did not alter the size of the ERG response or shape of the trace.

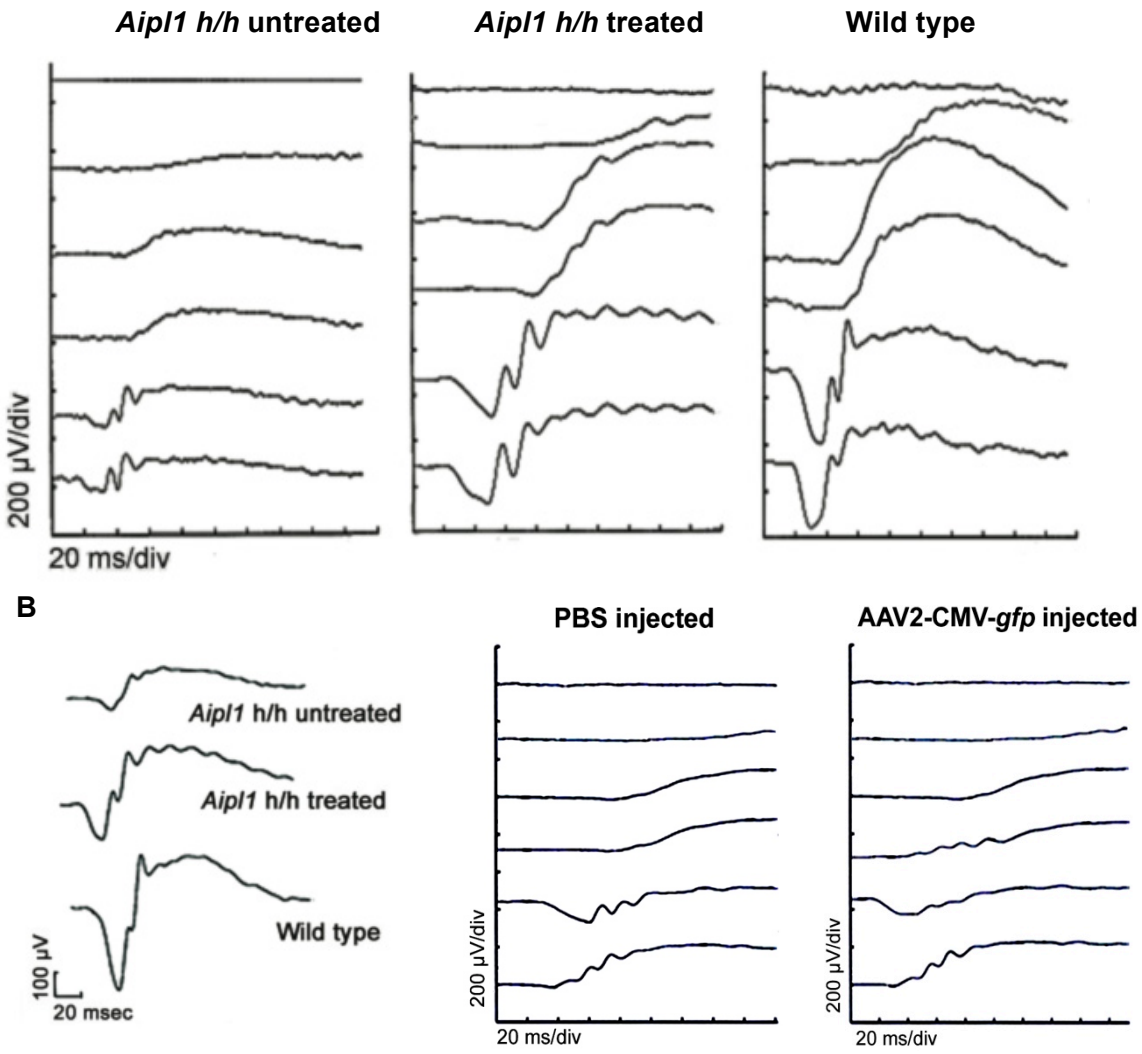

Figure 3.15. Functional rescue assessed by ERG analysis following subretinal injection of AAV2-CMV-*Aipl1*.

(A) ERG intensity series of the treated and untreated eye of a 24-week old *Aipl1 h/h* mouse at 20 weeks following treatment. ERG traces shown in each chart were recorded at intensities of 0.1, 1, 10, 100, 1000, and 3000 mcds/m^2. The treated eye maintains substantially larger amplitudes and oscillatory potentials, while in the untreated eye, there is loss of amplitude even at higher flash intensities. The ERG intensity series from a wild type animal is shown for comparison.

(B) Representative ERG waveforms at 28 weeks post-injection from the treated and untreated eyes of an *Aipl1 h/h* mouse. A wild type waveform is shown for comparison. The treated eye shows a discernible a-wave and a higher b-wave compared to the untreated eye.

(C) Injection of PBS and control vector AAV2-CMV-*gfp* did not lead to any improvement in the ERG recordings suggesting that the improvement in treated eyes was due to the AAV-mediated expression of the *Aipl1*.

3.6.2 ERG timecourse and statistical analysis ERG amplitudes.

A series of ERG recordings were obtained from the treated and untreated eyes of an *Aipl1* h/h animal at various follow up time points following subretinal injection of AAV2-CMV-*Aipl1* (Figure 3.16). This flash intensity was chosen because the electrical response of both rods and cones are obtained and this allows the analysis of the overall rescue of photoreceptor cells. Over the 28 week period, the untreated eye showed a steady decline in a-wave and b-wave amplitude, whereas the treated eye showed stabilization of amplitude and waveform. Differences in improvement between the treated and untreated eyes are more apparent from 12 weeks post injection onwards (Figure 3.16). The treated eye consistently maintained higher amplitudes throughout the follow-up period. At the final time point of 28 weeks post injection when the animal was 32 weeks of age, the ERG response from the untreated eye was markedly reduced or almost flat, while the treated eye still had good ERG responses, indicating rescue of photoreceptor function by the AAV-mediated transgene expression. This suggested that not only there were more photoreceptor cells present in the treated eyes compared to untreated eyes but that the surviving photoreceptor cells also retained normal function. The degeneration of photoreceptors appeared to be slowed by the treatment.

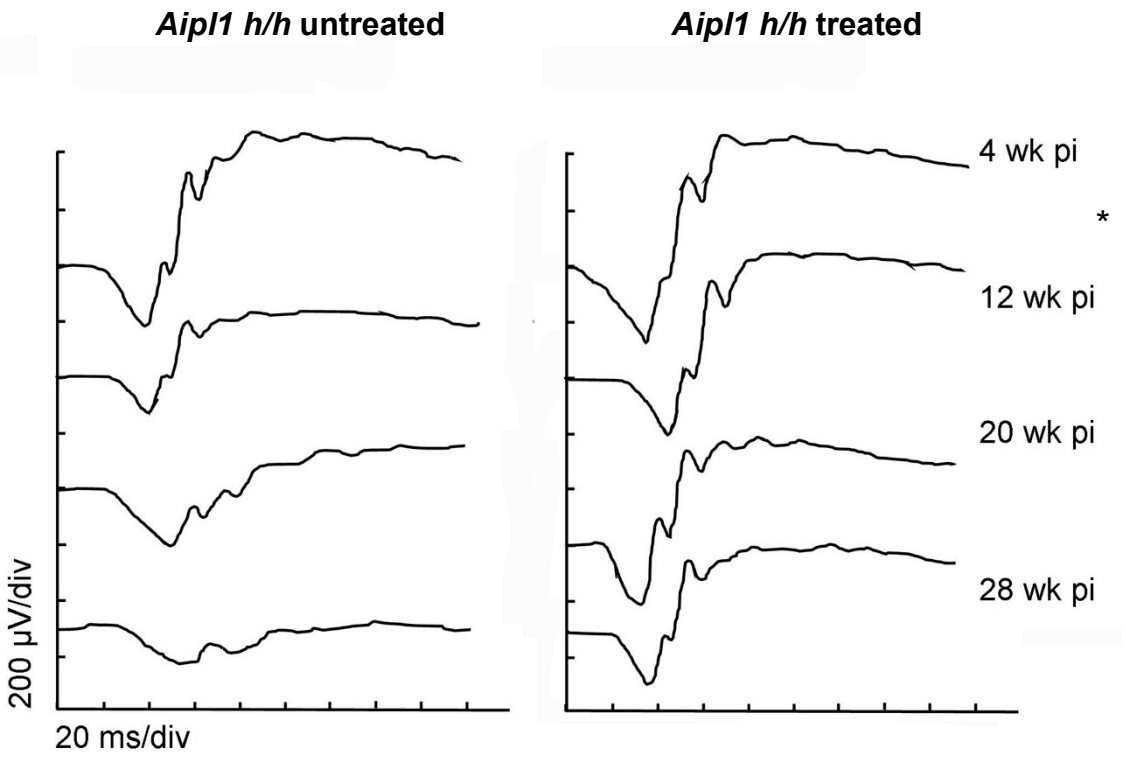

Figure 3.16 ERG time course.

Representative ERG traces from a single *Aipl1 h/h* mouse taken at various ages of 8 weeks (4 pi),16 weeks (12 weeks pi), 24 weeks (20 weeks pi) and 32 weeks (28 weeks pi) following subretinal injection of AAV2-CMV-*Aipl1* is shown. Averaged responses at a flash intensity of 1000 mcds/m^2 were recorded simultaneously from both treated and untreated eyes of the same *Aipl1* h/h mouse following treatment. From 12 weeks post injection onwards, a noticeable difference in the amplitude and shape of the trace between the two eyes is seen. ERG amplitudes from the untreated eye diminish with time, whereas ERG responses are maintained in the treated eye.

* pi- post injection

Statistical analysis of the ERG recordings was performed to ascertain whether the differences in amplitudes between treated and untreated eyes were significant. Average ERG a-wave and b-wave amplitudes of treated and untreated eyes were calculated for the various time points at flash intensities of 100 mcds/m^2 and 1000 mcds/m^2. At each time point assessed, there was considerable inter-animal variation in the ERG amplitudes in the untreated eyes of individual *Aipl1* h/h mice, indicating an element of variability in the rate of photoreceptor degeneration in this model. Furthermore, the ERG results of the same cohorts of animals varied substantially between recording sessions, suggesting inter-session variability. In view of this variation, paired *t*-tests were used to analyse the mean a-wave and b-wave amplitudes between treated and untreated eyes at the various time points from 4 to 28 weeks (Figure 3.17 and Figure 3.18). Analysis of mean a-wave amplitudes showed that treated eyes maintained higher amplitudes compared with untreated eyes, this difference was statistically significant ($p \leq 0.05$) from 20 weeks post injection onwards up to the final time point of 28 weeks post injection (Figure 3.17). At 20 weeks post injection, the mean a-wave amplitude in treated eyes (n = 15; mean = 109.6±20.4 μV) was approximately 38% higher than that in untreated eyes (n = 15; mean = 79.2+33.8 μV). Mean b-wave analysis was performed at flash intensities of 100 mcds/m^2 and 1000 mcds/m^2 representing rod response and maximal rod and cone response respectively (Figure 3.18A and B). At a flash intensity of 100 mcds/m^2, mean b-wave amplitudes in treated eyes were consistently higher compared with untreated eyes and this difference was statistically significant at 20 weeks post injection and 28 weeks post injection ($p \leq 0.05$)(Figure 3.18A). At 1000 mcds/m^2, b-wave amplitudes were significantly higher in the treated compared with the untreated eyes at 20, 24 and 28 weeks post-injection ($p \leq 0.05$) (Figure 3.18B). There was an initial increase in ERG amplitudes from birth until adulthood (8 weeks) that reflected normal development in mice. Four weeks after vector administration, there was a reduction in b-wave amplitudes in treated eyes that was probably due to injection-related trauma. However, from 20 weeks post injection onwards, b-wave amplitudes were significantly higher in treated compared with untreated eyes ($p \leq 0.05$), a difference which remained

consistent up to the final time point of 28 weeks post injection. The mean b-wave amplitude at flash intensity of 1000 mcds/m^2 in treated eyes (*n* = 15; mean = 295.3±13.6 μV) at 20 weeks post injection was approximately 20% higher than in untreated eyes (*n* = 15, mean = 243.6 ± 15.6 μV).

In the group of PBS-injected animals, no significant differences were seen in the b-wave amplitudes between injected and uninjected eyes at flash intensity of 100 mcds/m^2 and at 1000 mcds/m^2 (Figure 3.19). These results suggest that there were no detrimental effects despite the trauma of subretinal injections to the eye. In the group of *Aipl1* h/h mice that received unilateral subretinal injections of the control virus AAV2-CMV-*gfp* however, the injected eye had significantly lower b-wave amplitudes than the uninjected eye (Figure 3.20). Previous experience in our laboratory have found that that vector-mediated *gfp* expression did not result in loss of ERG amplitude nor any inflammatory or toxic effects due either to the transgene or rAAV vector. It is thus likely that this finding may have been caused by external confounding factors such as the quality of the virus purification. Impurities in the viral prep can result in toxic effects thereby decreasing the ERG response in the injected eyes. Alternative, it may suggest that *Aipl1* h/h mice are particularly sensitive to *gfp* expression. More significantly, the observations from both PBS-injected and AAV2-CMV-*gfp* injected eyes indicate that the therapeutic effect seen from AAV2-CMV-*Aipl1* injected eyes is a result of the *Aipl1* transgene expression and not due to the effects of the surgical procedure or the vector itself.

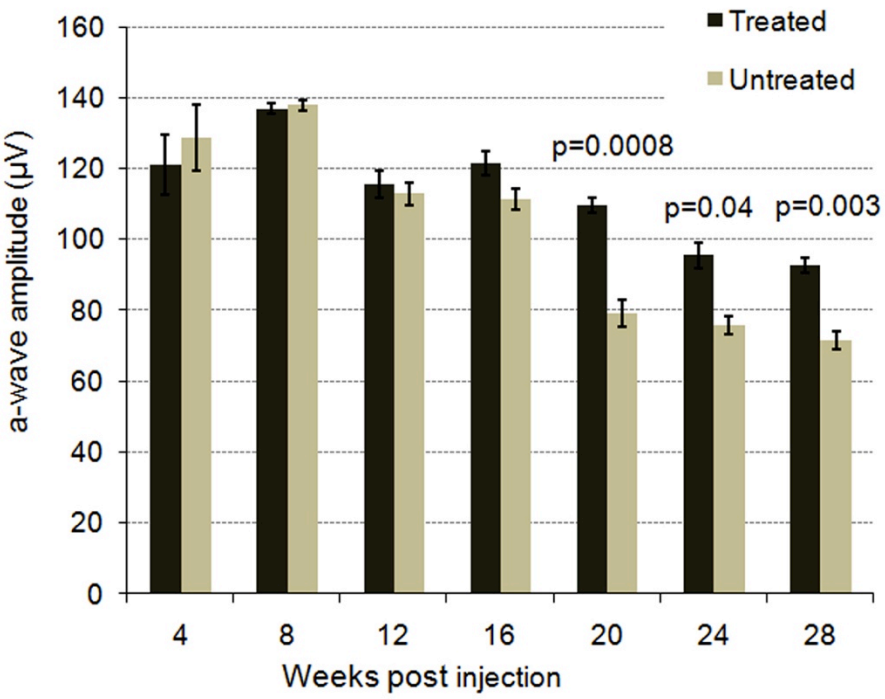

Figure 3.17. Mean ERG a-wave amplitudes at flash intensity of 1000 mcds/m^2 in *Aipl1* h/h mice that received subretinal injections of AAV2-CMV-*Aipl1.*

Treated eyes maintained higher ERG a-wave amplitudes compared with untreated eyes. Statistical differences in a-wave amplitudes were seen when the mice were 24 weeks old and upwards (at 20 weeks post-injection onwards) ($p \leq 0.05$). Error bars, ±SEM.

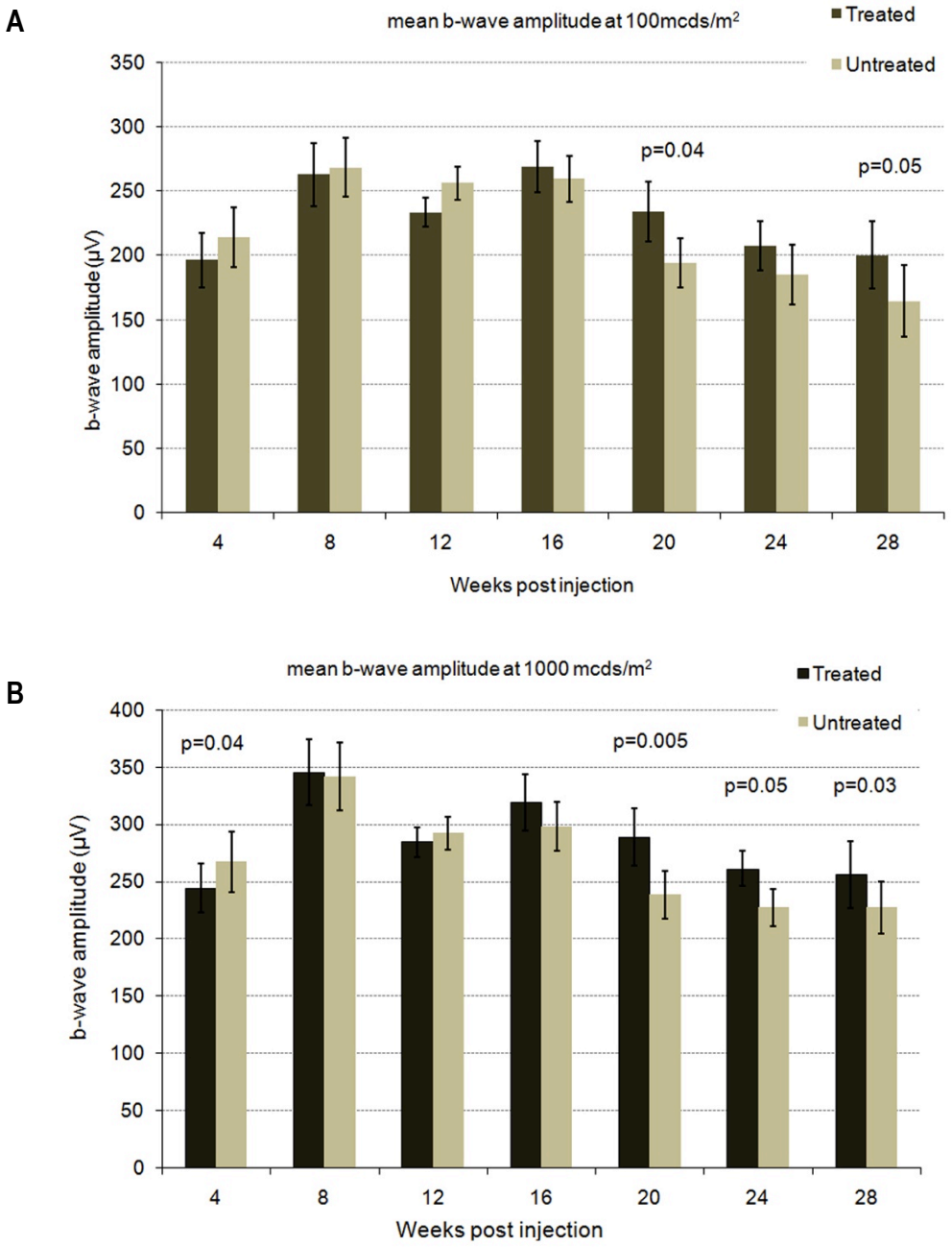

Figure 3.18 Mean ERG b-wave amplitudes in *Aipl1* h/h mice that received subretinal injections of AAV2-CMV-*Aipl1*.

The mean b-wave amplitudes and standard error of the mean (SEM) of treated and untreated eyes are shown at various time points after treatment. Statistical significance of the difference between the treated and untreated eyes was determined using a paired t-test.

(A) At a flash intensity of 100 mcds/m^2, treated eyes had consistently higher b wave amplitudes compared with untreated eyes. The difference was statistically significant when the mice were 24 weeks and 28 weeks old (at 20 weeks and 28 weeks post injection respectively) ($p<0.05$).

(B) At flash intensity of 1000 mcds/m^2, statistical significance was obtained at more time points. B-wave amplitudes of treated eyes were significantly increased from the age of 24 weeks onwards (at 20 weeks post injection onwards) ($p<0.05$).

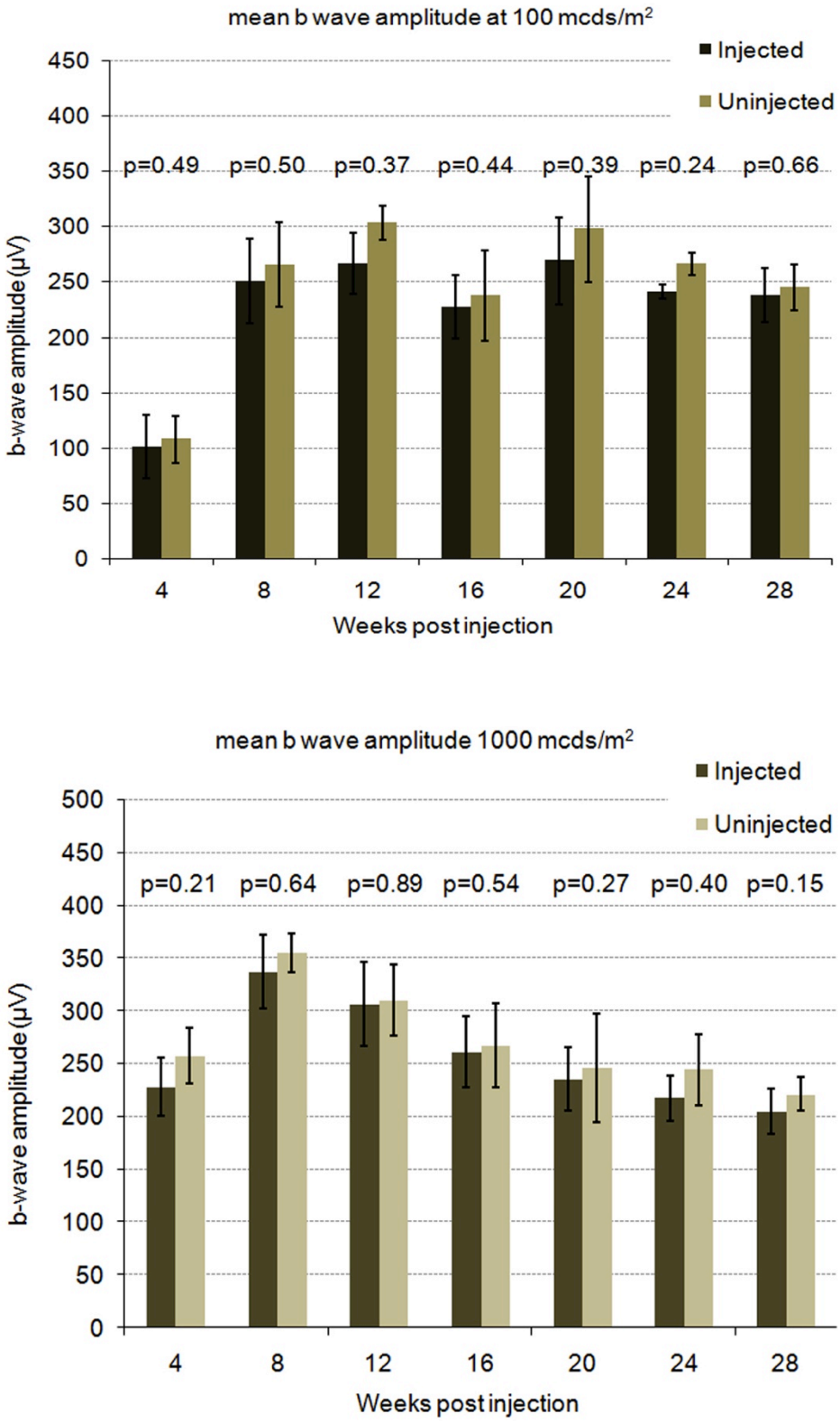

Figure 3.19 Mean ERG b-wave amplitudes in *Aipl1* h/h mice at various time points following subretinal injections of PBS.

At flash intensities of 100 mcds/m^2 and 1000 mcds/m^2, no significant differences in b-wave amplitudes were found comparing injected and uninjected eyes . Error bars, ±SEM.

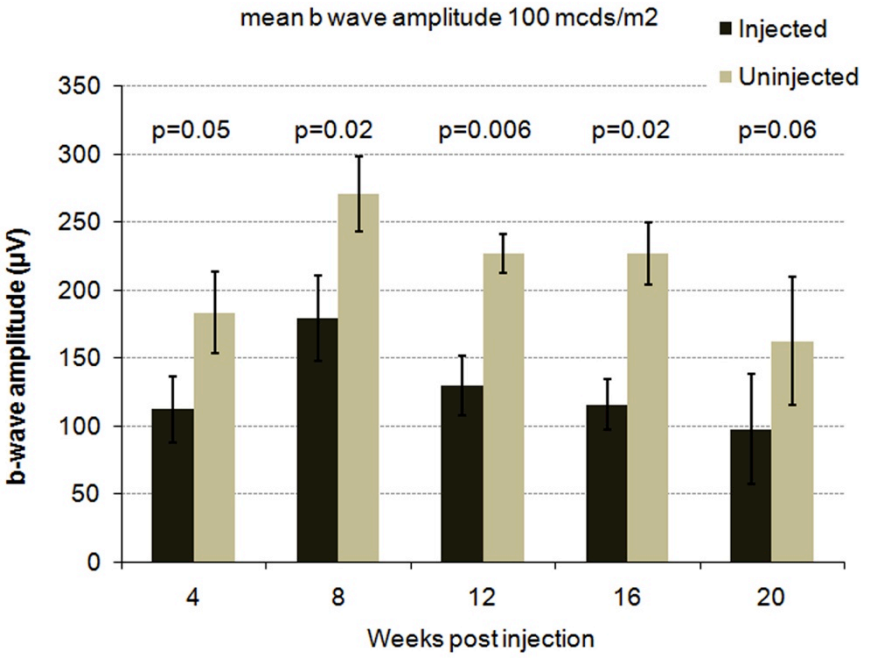

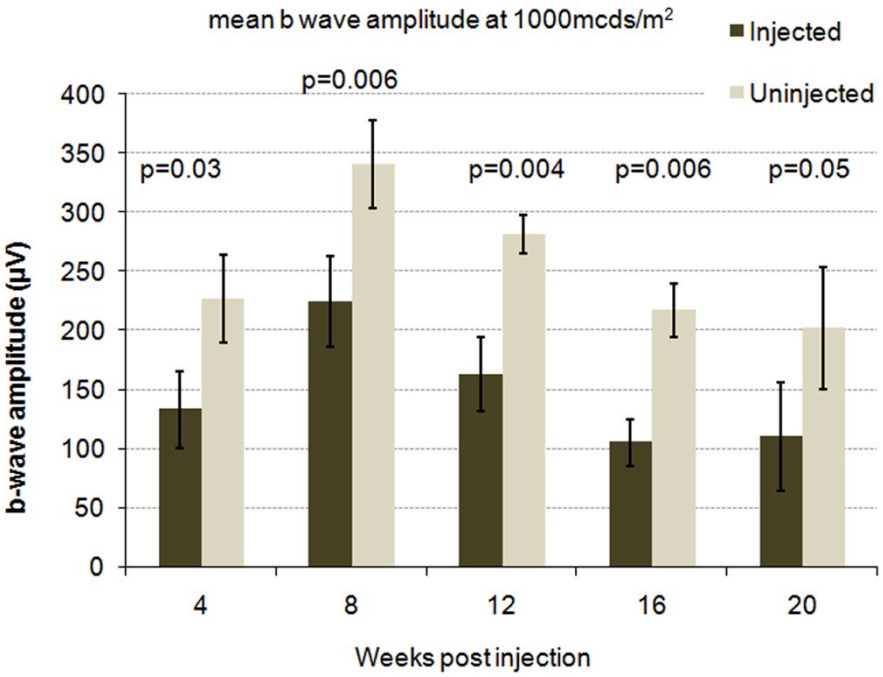

Figure 3.20 Mean ERG b-wave-amplitudes of Aipl1 h/h mice at various time points following subretinal injection of control virus AAV2-CMV-*gfp*.

At flash intensities of 100 and 1000 mcds/m^2, ERG b-wave amplitudes of injected eyes were significantly lower than b-wave amplitudes of uninjected eyes. Error bars, ±SEM.

An initial transient increase in ERG b-wave amplitude was seen up to 8 weeks post injection (or 12 weeks in age) in both treated and untreated eyes of *Aipl1 h/h* mice. This observation is most likely to be due to a manifest developmental phase that exists in mice, during which the ERG b-wave amplitude initially increases, together with a reduction in the implicit time. This physiological phenomenon has been previously described in young mice [209]. However, to exclude the possibility that this observation might have been caused by variation in recording conditions between ERG sessions, a control experiment was performed to compare the ERGs over time in *Aipl1* h/h mice and wild type mice. Two age groups of *Aipl1* h/h mice, one group aged 6 weeks (n=3) and another group aged 12 weeks (n=3) were selected along with a control group consisting of wild-type C57B/6 mice (n=4) aged 5 weeks. ERG recording was performed on the 2 groups of *Aipl1* h/h mice and the control group of wild type mice at various time points, each separated by an interval of 1 or 5 weeks. At each time point, all three groups of animals underwent ERG recording at the same session. The ERG recordings was performed under similar conditions as described for the previous experiments and by the same operator. A total of 5 sessions of ERG recording was performed and the mean b-wave amplitudes of the right and left eyes of each group is shown in Figure 3.21. A large amount of variation in b-wave amplitudes was seen between the animals during a single ERG recording session. This is indicated by the standard deviation which amounted to a substantial proportion of the mean b-wave amplitude in some sets of the data. There was also a degree of variability seen in the amplitudes obtained from the same animal during different recording sessions; although it is difficult to tell whether the variability between different recording sessions is significant, other data from our laboratory has shown that this is less substantial at higher flash intensities of 1000mcds/m^2 and above. The phenomenon of an initial transient improvement in b-wave amplitudes was observed in all 3 groups of animals, in both right and left eyes (Figure 3.21). The ERG b-wave amplitudes of the young *Aipl1 h/h* and wild-type mice increased from the age of 4 weeks up to 12-13 weeks, whereas the older *Aipl1* h/h mice showed a decrease in amplitude during the same recording sessions. These observations support the fact that this is a

physiological phenomenon seen in young animals rather than caused by external factors affecting the different recording sessions.

A

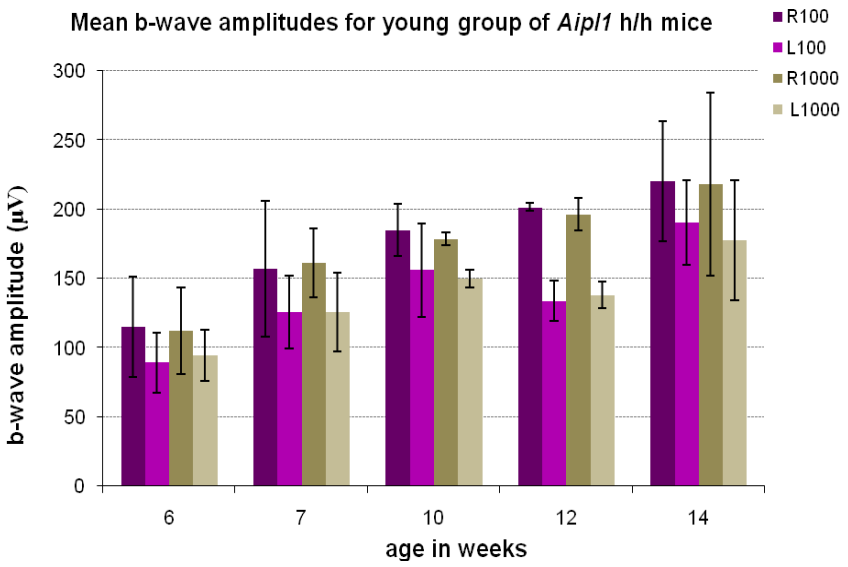
Mean b-wave amplitudes for young group of Aipl1 h/h mice
R100
L100
R1000
L1000
b-wave amplitude (µV)
300
250
200
150
100
50
0
6
7
10
12
14
age in weeks

B

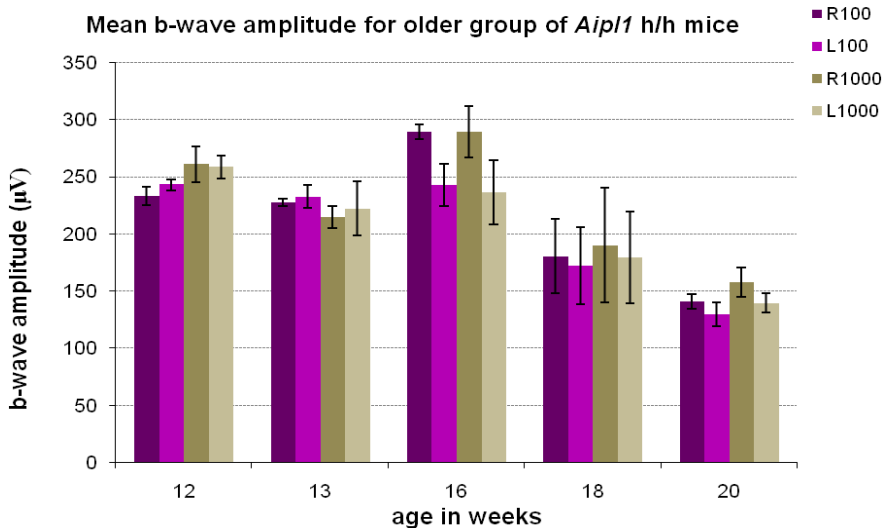
Mean b-wave amplitude for older group of Aipl1 h/h mice
R100
L100
R1000
L1000
b-wave amplitude (µV)
350
300
250
200
150
100
50
0
12
13
16
18
20
age in weeks

C

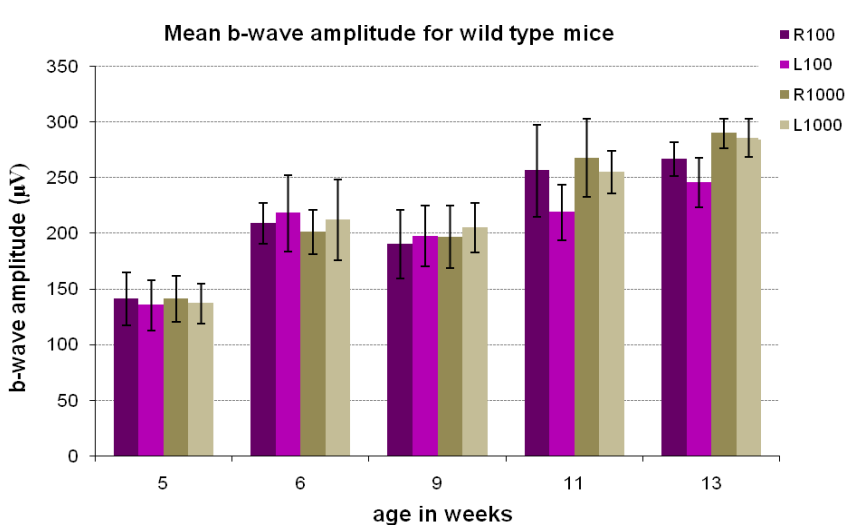
Mean b-wave amplitude for wild type mice
R100
L100
R1000
L1000
b-wave amplitude (µV)
350
300
250
200
150
100
50
0
5
6
9
11
13
age in weeks

Figure 3.21. Mean ERG b-wave amplitudes of *Aipl1* h/h mice and wild type mice of different ages.

Graphs showing the b-wave amplitudes of right and left eyes of 2 groups of AIPL1 h/h mice (young and old) and control wild-type C56B/6 mice. ERG recordings were taken at 5 different time points, indicated by 5 sets of data in each graph. Each set of data in each group of animals were recorded at a single sitting. The x-axis indicated the age of the respective animals at each ERG time point. Error bars- represent standard error of the mean.

A) In the young group of *Aipl1* h/h mice, an initial increase in b-wave amplitude with age is seen from 6 weeks up to 14 weeks of age.

B) In the older group of *Aipl1* h/h mice, b-wave amplitude is stable from 12 weeks until 16 weeks of age. From 16 weeks onward, a decrease is observed which is due to the onset of retinal degeneration.

C) In wild type mice, a similar initial increase in b-wave amplitude is seen from 5 weeks of age onwards up to 13 weeks of age.

3.7 Effects of overexpression of Aipl1 in the retina.

Vector-mediated expression is unlikely result in physiological levels of expression in target cells since this is an artificial system that is subjected to various external factors, and additionally may cause expression in other cell types that do not normally express the transgene especially if expression is driven by a strong ubiquitous promoter. Therefore, there may be overexpression or mis-expression of a transgene following gene replacement therapy. In our experiments, AAV-mediated *Aipl1* expression was driven by a CMV promoter and we observed *Aipl1* expression in the RPE in addition to photoreceptor cells. Since Aipl1 is not known to be naturally expressed in RPE cells, we sought to investigate whether the anomalous expression would have any deleterious effects, and whether higher than normal levels of *Aipl1* expression would be detrimental to photoreceptor cells.Six wild type adult C57B/6 mice received unilateral subretinal injections of the therapeutic AAV2-CMV-*Aipl1* vector into the right eyes. These animals were assessed using electroretinograms at 4 weekly intervals and were sacrificed 28 weeks later. The treated and untreated eyes of these animals were retained and processed for immunohistochemistry analysis and also for light microscopy to look for any alterations in retinal morphology.

Figure 3.22 shows representative ERG recordings from a treated and untreated eye of a wild type animal 24 weeks after treatment. The ERG traces in treated and untreated eyes have similar b-wave amplitudes and waveform. Mean b-wave amplitudes of treated and untreated eyes at various time points were obtained and analysed statistically (Figure 3.23). At both flash intensities of 100 mcds/m^2 and 1000 mcds/m^2, there were no significant differences in the b-wave amplitude between treated and untreated eyes of these wild type mice. These findings indicate that overexpression of *Aipl1* in photoreceptors and RPE did not affect retinal function adversely.

Immunostaining with an AIPL1 antibody showed AIPL1 immunofluorescence mainly in the inner segments of photoreceptors and some in the outer plexiform layer in injected and uninjected wild type eyes (Figure 3.24 A). However in the treated eyes, there was additional immunofluorescence in the RPE layer although to a lesser degree, suggesting that *Aipl1* was also being expressed in RPE cells. Light microscopy of H&E sections of treated and untreated retina from these wild type mice did not reveal any noticeable differences in terms of the overall retinal architecture and the outer nuclear layer thickness (Figure 3.24 B), suggesting that additional expression of *Aipl1* in photoreceptor cells and in the RPE did not have deleterious effects on retinal morphology or photoreceptor cell survival. The photoreceptor cell nuclei in the outer nuclear layer were counted in 5 animals using the same method as described in section 3.5.2. Representative confocal images of the retina from an injected and uninjected eye of a single animal showed no obvious differences in the quantity of photoreceptor nuclei (Figure 3.24 C). Paired t-test did not reveal any significant differences between the mean photoreceptor cell count of eyes that received subretinal injection of AAV2-CMV-*Aipl1* and uninjected eyes (Figure 3.24 D).

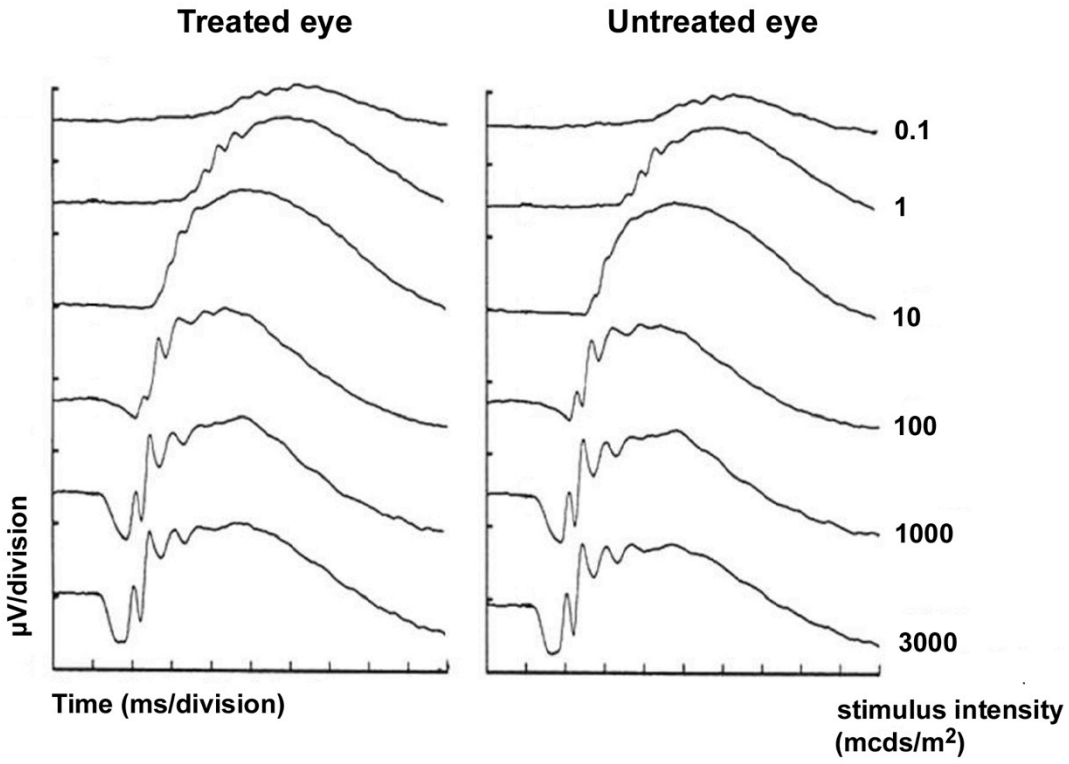

Figure 3.22. ERG intensity series of treated and untreated eyes of a wild type mouse receiving unilateral subretinal injection of AAV2-CMV-*Aipl1*.

The ERG was recorded at different light intensities at a single time point of 24 weeks. The b-wave amplitude and the shape of the trace were normal and there was no noticeable difference in amplitudes between the treated and untreated eye.

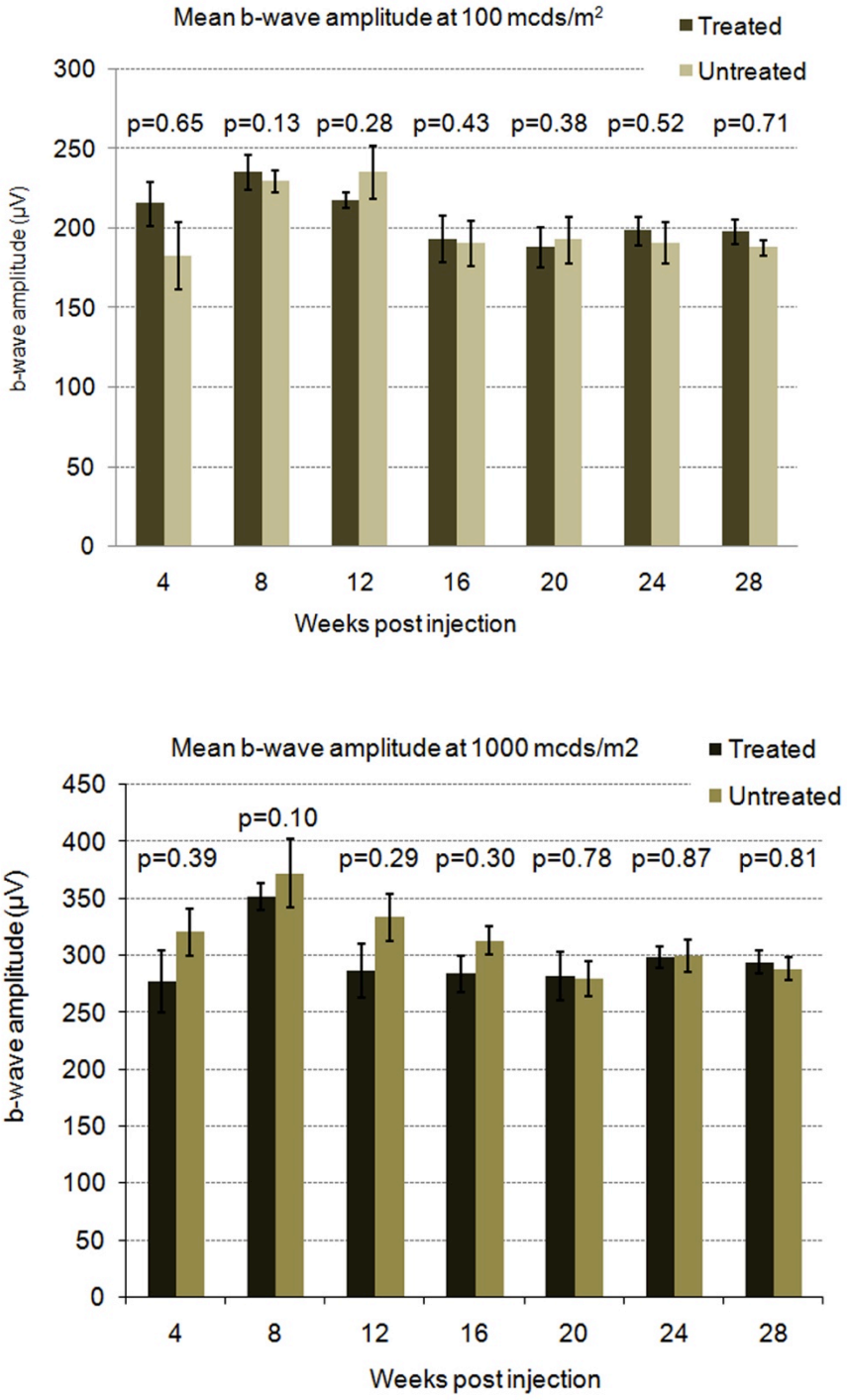

Figure 3.23 Mean b-wave amplitude for wild type mice which received unilateral subretinal injection of AAV2-CMV-*Aipl1*.

At flash intensities of 100 mcds/m^2 and 1000 mcds/m^2 , no significant difference was found between treated and untreated eyes (P>0.05) Error bars, ±standard error of the mean.

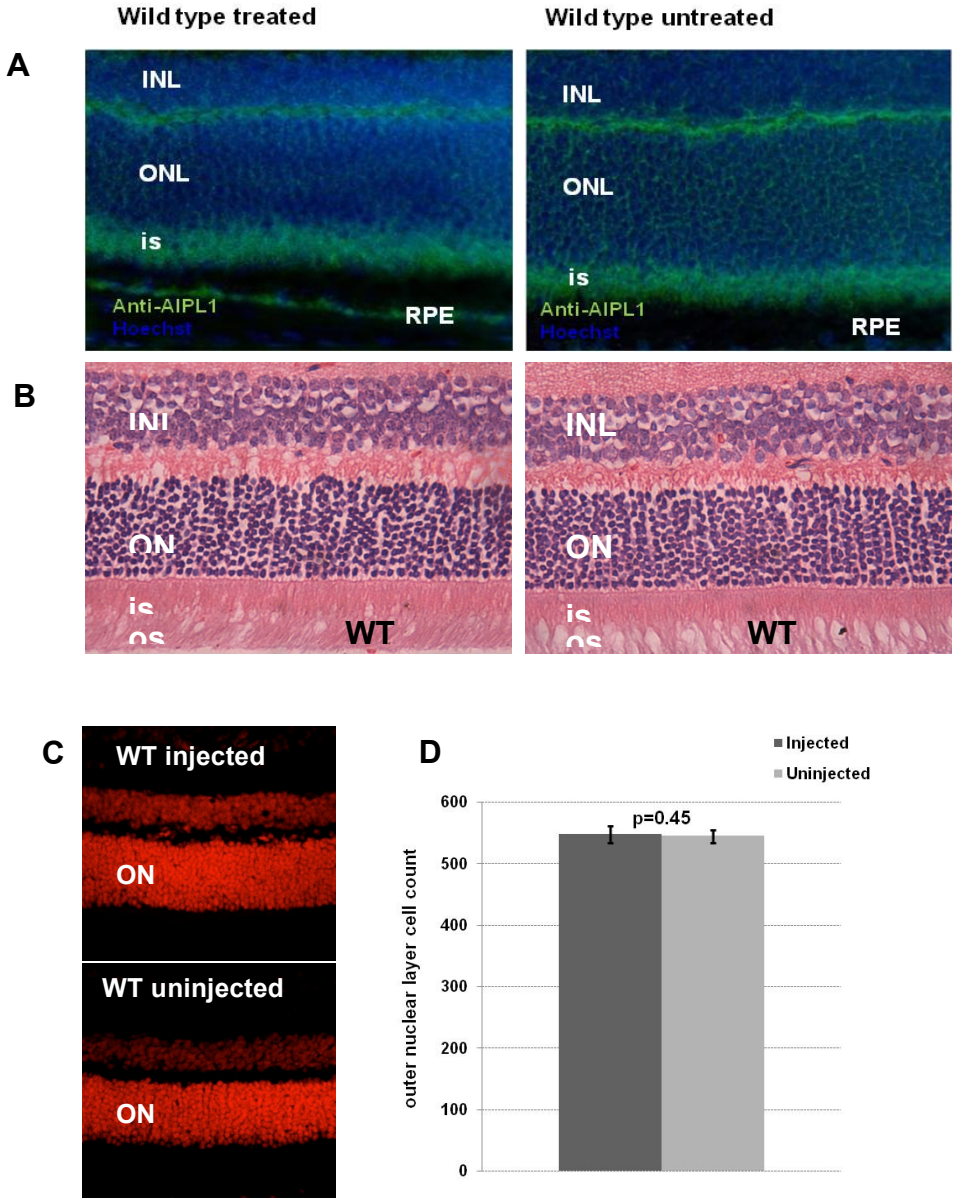

Figure 3.24. Morphological assessment and photoreceptor cell count of wild type mice receiving unilateral subretinal injection of AAV2-CMV-*Aipl1*.

(A) AIPL1 immunofluorescence is seen at the mostly at inner segment of injected and uninjected wild type eyes, but there is also AIPL1 imunofluorescence in the RPE layer of injected eyes which is not present in uninjected eyes, due to AAV2-mediated transduction. ONL, outer nuclear layer; INL, inner nuclear layer, is, inner segment.

(B) Histological analysis of H&E retinal sections showed no noticeable difference in morphology and retinal architecture between injected and uninjected WT eyes. ONL, outer nuclear layer; INL, inner nuclear layer; is, inner segment; os, outer segment

(C)&(D) Quantification of the outer nuclear layer did not reveal any statistical difference in mean photoreceptor cell count comparing injected and uninjected eyes.

is- inner stress; os- outer segment; INL-inner nuclear segment; ONL-outer segment.

3.8 Cloning of the human AIPL1 construct

In the interest of future clinical application, a therapeutic construct that might be used in clinical studies was developed by substituting the mouse *Aipl1* cDNA within the expression cassette with a human *AIPL1* cDNA. The human *AIPL1* transcript is 2970 bp with 6 exons providing a coding region of 1155 bp. The 384 amino acid human AIPL protein has 3 tetratricopeptide (TPR) repeat domains and a polyproline rich region at the C-terminus (Figure 3.25A). Mouse *Aipl1* has a smaller transcript with a size of 1076 bp consisting of 6 exons and a shorter coding region of 987 bp (Figure 3.25B). Comparing the human AIPL1 protein to the mouse protein, an 86% identity was found and 96% level of similarity between the two species, indicating that most of the AIPL1 protein is highly conserved across species (Figure 3.26). The highly conserved region includes the 3 TPR domains that are thought to be important in mediating protein-protein interactions. The human AIPL1 protein has an additional 56 amino acid proline-rich region at the C-terminus that is only found in primates, thus absent in the mouse. Its role in protein function is not yet understood.

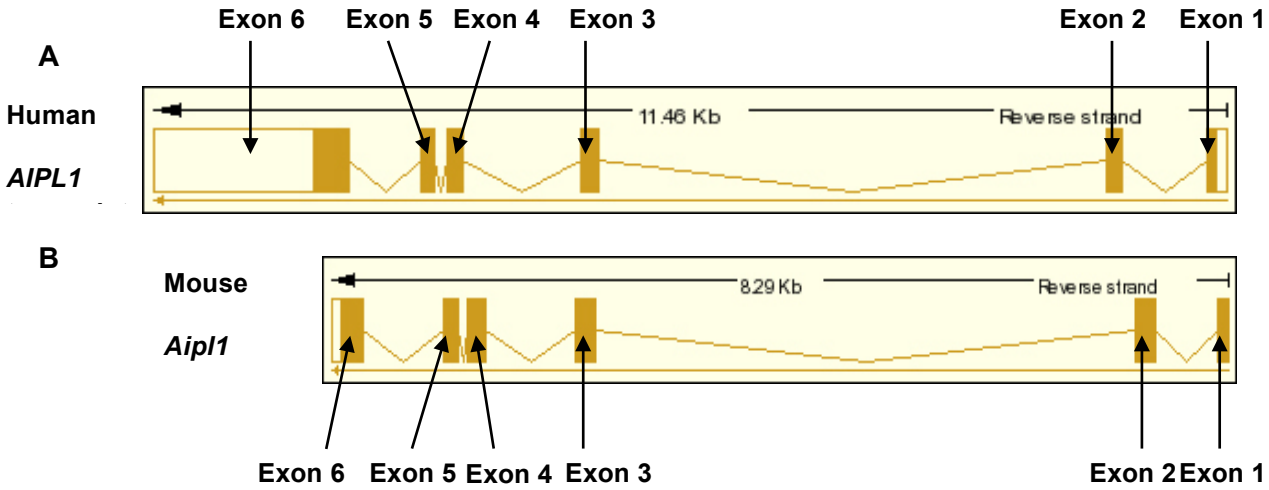

Figure 3.25 Comparison of human and mouse AIPL1 transcripts.

Both human and mouse transcripts contain 6 exons and 3 tetratricopeptide domains encoded by exons 3, 4 and 5 which are highly conserved across species. The human AIPL1 transcript is larger than the mouse. Additionally, the human transcript contains untranslated regions at the 5' and 3' ends and a 56-amino acid polyproline sequence encoded by exon 6.

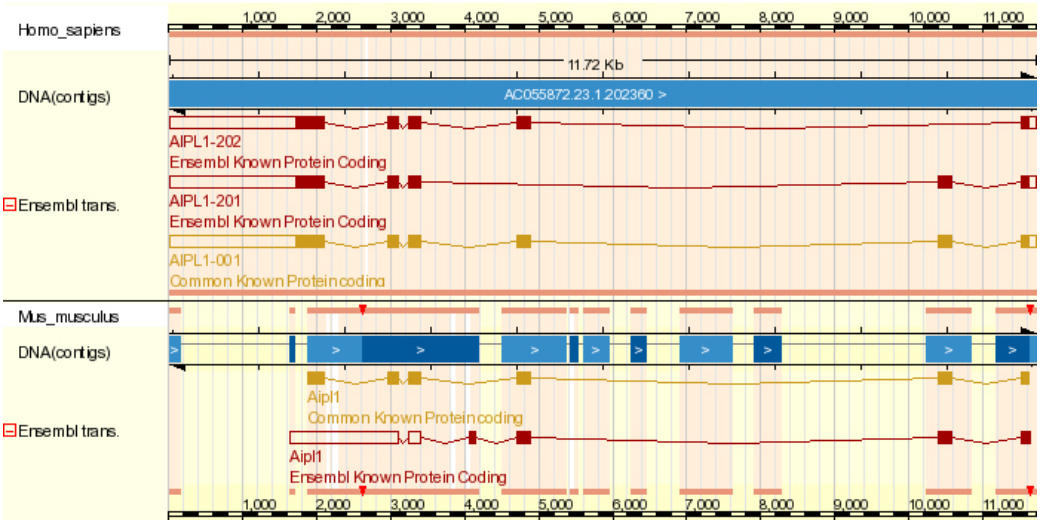


```
Score =  606 bits (1562),  Expect = 2e-171
Identities = 286/327 (87%), Positives = 316/327 (96%), Gaps = 0/327 (0%)

Human       MDAALLLNVEGVKKTILHGGTGELPNFITGSRVIFHFRTMKCDEERTVIDDSRQVGQPMH  60
            MD +LLLNVEGVKKTILHGGTGELP+FITGSRV FHFRTMKCD+ERTVIDDS+QVGQPM
Mouse       MDVSLLLNVEGVKKTILHGGTGELPSFITGSRVTFHFRTMKCDDERTVIDDSKQVGQPMS  60

Human       IIIGNMFKLEVWEILLTSMRVHEVAEFWCDTIHTGVYPILSRSLRQMAQGKDPTEWHVHT 120
            IIIGNMFKLEVWE LLTSMR+ EVAEFWCDTIHTGVYP+LSRSLRQ+A+GKDPT WHVHT
Mouse       IIIGNMFKLEVWETLLTSMRLGEVAEFWCDTIHTGVYPMLSRSLRQVAEGKDPTSWHVHT 120

Human       CGLANMFAYHTLGYEDLDELQKEPQPLVFVIELLQVDAPSDYQRETWNLSNHEKMKAVPV 180
            CGLANMFAYHTLGYEDLDELQKEPQPLVF+IELLQV+AP++YQRETWNL+N E+M+AVP+
Mouse       CGLANMFAYHTLGYEDLDELQKEPQPLVFLIELLQVEAPNEYQRETWNLNNEERMQAVPL 180

Human       LHGEGNRLFKLGRYEEASSKYQEAIICLRNLQTKEKPWEVQWLKLEKMINTLILNYCQCL 240
            LHGEGNRL+KLGRY++A++KYQEAI+CLRNLQTKEKPWEV+WLKLEKMINTLILNYCQCL
Mouse       LHGEGNRLYKLGRYDQAATKYQEAIVCLRNLQTKEKPWEVEWLKLEKMINTLILNYCQCL 240

Human       LKKEEYYEVLEHTSDILRHHPGIVKAYYVRARAHAEVWNEAEAKADLQKVLELEPSMQKA 300
            LKKEEYYEVLEHTSDILRHHPGIVKAYY+RARAHAEVWN  EAKADL+KVLELEPSM+KA
Mouse       LKKEEYYEVLEHTSDILRHHPGIVKAYYMRARAHAEVWNAEEAKADLEKVLELEPSMRKA 300

Human       VRRELRLLENRMAEKQEEERLRCRNML  327
            V RELRLLE+R+A+KQEEER RCR+ML
Mouse       VLRELRLLESRLADKQEEERQRCRSML  327
```

Figure 3.26. Comparative analysis of human *AIPL1* to mouse *Aipl1*.

Protein sequence of the human AIPL1 is compared to mouse AIPL1 which shows that the two proteins are 87% identical and share a 96% homology.

The human *AIPL1* cDNA was cloned from commercially available retinal cDNA using primers which amplified the entire coding region of *AIPL1.* The sequence of the 5'primer was GGTGAGATTATCTCCGCCTGTGCTG and 3' primer was CCTCAGGGGGCTCAGTGC. A PCR product of 1215 bp was obtained, which contained the coding region of *AIPL1* and included a part of the untranslated regions at the 5' and 3' ends. The PCR product was gel purified and ligated into pGemT-easy vector to produce a construct of 4232 bp that was named pGemT-hu*AIPL1*. The resulting plasmid was used to sequence the human *AIPL1* cDNA to ensure that no sequence changes had occurred during amplification and isolation of the fragment, and also to ascertain the orientation of the gene in the plasmid. After the sequence was confirmed, we used restriction enzymes *SpeI* and *NotI* to excise *AIPL1* from pGemT-hu*AIPL1* in which a fragment of 1238 bps was obtained (Figure 3.27). We digested the parental plasmid pd10-CMV-e*gfp* with *NheI* and *NotI* to extract a fragment of 6115 bp containing the AAV backbone (Figure 3.27). The AAV backbone was ligated with the human *AIPL1* fragment to produce the therapeutic construct AAV-CMV-*AIPL1* carrying the human cDNA (Figure 3.28). This construct was checked by restriction digests and direct sequencing to ensure that the transgene within it was correct (Figure 3.29). Recombinant AAV2 was produced from the therapeutic construct containing the human transgene using the same method as described previously and the titre of the resultant virus suspension obtained was determined to be 5 x 10^{11} vp/ml.

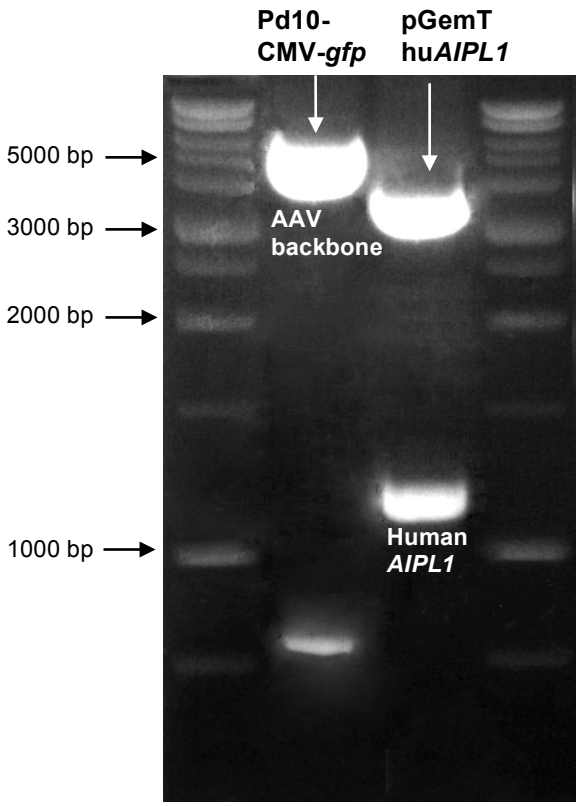

Figure 3.27. Cloning of human therapeutic construct.

The pGemT-*huAIPL1* plasmid was digested with SpeI and NotI to isolate the ~1.2 kb *AIPL1* fragment. The parental plasmid pd10-CMV-*egfp* was similarly digested with NheI and NotI to excise the ~4.5 kb AAV backbone containing the ITRs. The two fragments were subsequently ligated together to form the therapeutic construct AAV-CMV-*AIPL1.*

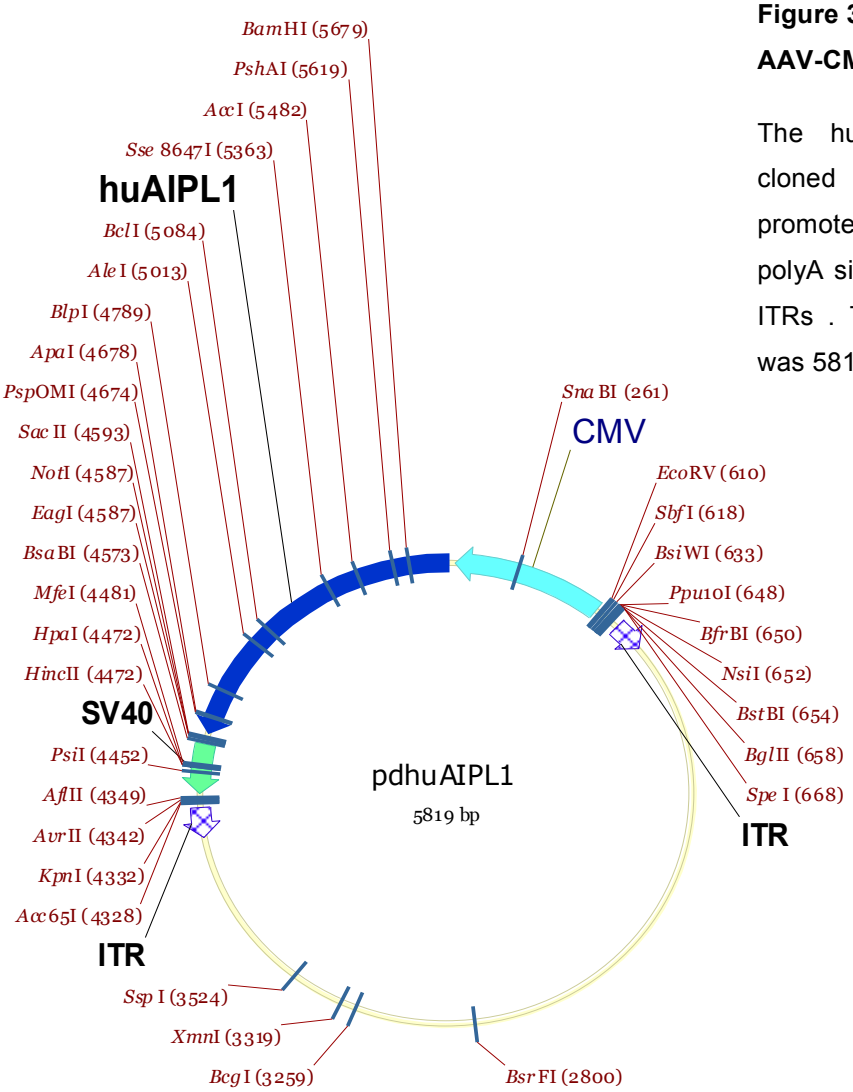

Figure 3.28. Map of the construct AAV-CMV-*AIPL1*.

The human transgene AIPL1 was cloned downstream of the CMV promoter fragment, followed by SV40 polyA signal and is flanked by two viral ITRs . The total size of the construct was 5819 bp.

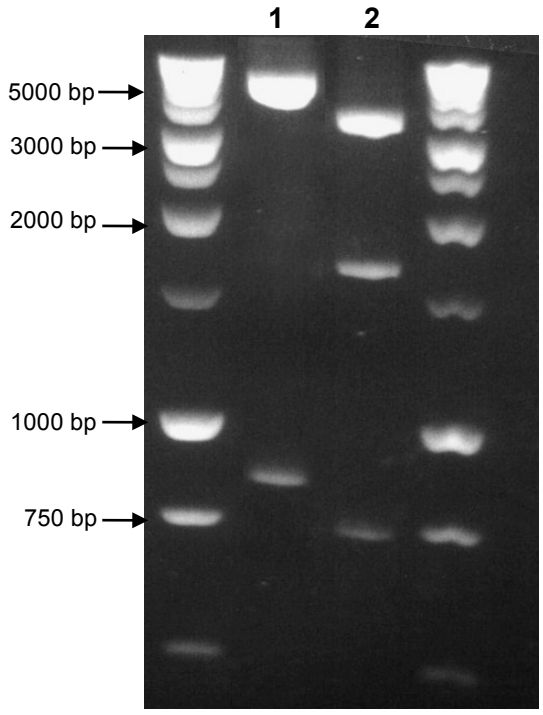

Figure 3.29. Check restriction digests of AAV-CMV-*AIPL1*.

The therapeutic construct AAV-CMV-*AIPL1* was digested with restriction enzymes to check that appropriate fragment sizes were obtained. In lane **1**, the construct was digested with XhoI and the expected fragments of ~ 4.9 kb and 850 bp were obtained. In lane **2**, the construct was digested with SmaI and the expected fragments of ~ 3.4 kb, 1.6 kb and 720 bp were obtained.

3.9 Assessment of function following AAV2/2-mediated expression of human AIPL1 in the Aipl1 h/h mouse retina.

To test whether any beneficial effects might be obtained by the expression of a human *AIPL1* transgene, a group of *Aipl1 h/h* mice (n=10) received a subretinal injection of AAV2-CMV-*AIPL1* in one eye, leaving the other eye to serve as an internal control using the same injection method as described before. All injections were performed by the same individual as for previous experiments. The animals were subjected to regular electrophysiological assessments in the form of scotopic ERG recording at various time points, starting from 4 weeks post injection onwards. The follow up period in these animals included long term time points up to a year to see whether any beneficial effects were sustained.ERG recordings were obtained simultaneously from both eyes using the similar method described previously. Analysis of functional outcome was performed on scotopic ERG b-wave amplitudes at flash intensities of 100 mcds/m^2 and 1000 mcds/m^2 .

Figure 3.30 shows the mean scotopic ERG a-wave and b-wave amplitudes of *Aipl1*h/h mice injected with AAV-CMV-*AIPL1*. Treated eyes consistently maintained higher mean ERG b-wave amplitudes compared with untreated eyes throughout the follow up period at flash intensities of 10 mcds/m^2 amd 1000 mcds/m^2 (Figure 3.30 A and B). There was statistically significant difference between treated and untreated eyes from 16 weeks post injection onwards up to 50 weeks (paired Student's t-test $p \leq 0.05$). At the final time point of 50 weeks post injection, the mean b-wave amplitude in treated eyes (n=10, mean = 194.6 ± 25.2 μV) was 57% higher than the mean b-wave amplitude in untreated eyes (n=10, 123.98 ± 20.42 μV) at a flash intensity of 1000 mcds/m^2. AAV-CMV-*AIPL1* treated eyes also showed significantly higher a-wave amplitudes than in untreated eyes between 16 and 50 weeks post injection ($p \leq 0.05$) (Figure 3.30 C).

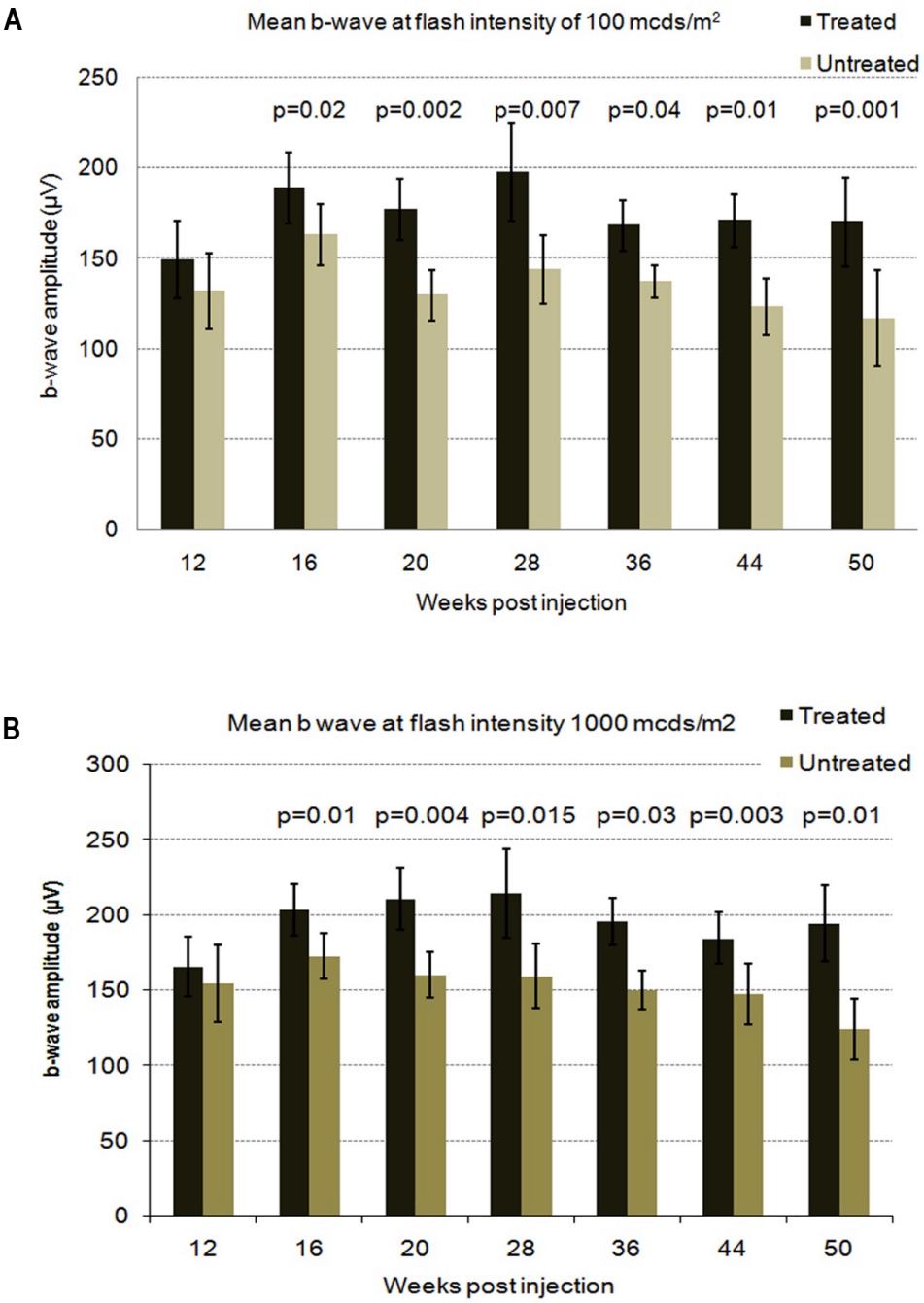

Figure 3.30 A & B. Mean ERG b-wave amplitudes for *Aipl1 h/h* mice following subretinal injection of AAV2-CMV-*AIPL1*.

At flash intensities of 100 mcds/m^2 (A) and 1000 mcds/m^2 (B), the mean b-wave amplitudes in the treated eye are significantly higher than those of the untreated eye from 16 weeks onwards. At 50 weeks post injection, there was still a significant difference ($p \leq 0.05$) between the treated and untreated eye indicating beneficial long term effect of the treatment. Statistical analysis was performed using paired t-test. Error bars , ± SEM.

C

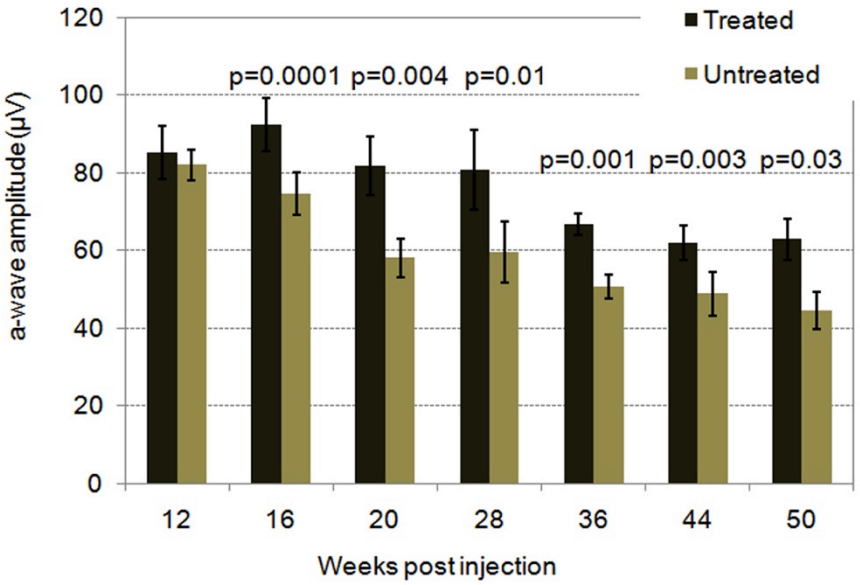

Figure 3.30 C. Mean ERG a-wave amplitudes for *Aipl1 h/h* mice following subretinal injection of AAV2-CMV-*AIPL1*.

AAV-CMV-*AIPL1* treated eyes showed significantly higher a-wave amplitudes than untreated eyes between 16 and 50 weeks post injection ($p \leq 0.05$). Error bars, ±SEM.

3.10 Morphological analysis following AAV2/2-mediated expression of human AIPL1 in the Aipl1 h/h mouse retina.

3.10.1 Light and electron microscopy of retinal sections.

To determine the effects of AAV2/2-mediated human *AIPL1* gene expression in *Aipl1 h/h* retina, the retinal morphology was assessed by light microscopy and electron microscopy. Treated eyes had received double subretinal injections of the therapeutic vector in the superior and inferior hemisphere of the eye. Animals (n=2) were sacrificed 52 weeks after treatment, the eyes were enucleated and processed for semithin and ultrathin sections (methods described in sections 2.9.6). Prior to fixation and embedding, the eyes were carefully orientated using a stitch through the conjunctiva on the nasal aspect of the eyes. The eyes were fixed in Karnovsky's fixative, and the cornea and lens were removed the next day. Using the nasal suture, the eyes were embedded sagittally so that sectioning occurred in the vertical plane and the retinal sections contained the superior and inferior retina which were the areas of treatment. Semithin sections (0.7 µm thick) were cut from treated and untreated eyes and stained with toluidine blue for light microscopy. Ultrathin sections (0.07 µm thick) were cut of the corresponding areas and following sequential contrast processing, they were analysed using a transmission electron microscope.

For histological analyses, semithin sections of treated and untreated eyes were examined with light microscopy (Figure 3.31). The untreated retina showed substantial loss of photoreceptor cell nuclei, disorganization and shortening of the outer segments (Figure 3.31 A). In contrast, the retina of treated eyes had considerably more photoreceptor cell nuclei; since there was an evidently thicker outer nuclear layer compared with untreated eyes (Figure 3.31 B). The photoreceptor outer segments were longer and more densely packed and arranged in a more organized fashion. The outer

nuclear layer was uniformly preserved throughout the whole circumference of the treated eye.

Ultrastructurally, substantial differences were seen in the morphology of photoreceptor OS. In the untreated retina, the number of photoreceptor OS were substantially reduced, markedly shortened and form disorganized rounded whorls (Figure 3.32 A). The OS disk membranes contained inside these photoreceptor OS were also disorganized, less tightly packed and there was a loss of the normal laminar arrangement (Figure 3.32 D). Vacuolar inclusions containing debris material was present in the IS region of the retina (Figure 3.32 D). The contact between the RPE and photoreceptor OS was also abnormal and reduced. Intervening vacuoles could be seen between OS tips and RPE cells. In contrast, in treated *Aipl1* h/h retina, photoreceptor OS were elongated and the membranous OS disks had a regular and densely packed laminar arrangement (Figure 3.32 B), that was similar to that seen in wild-type mice (Figure 3.32 C). The photoreceptor OS in the treated retina maintained close contact with the RPE and showed normal interdigitation with the microvilli (MV) of RPE (Figure 3.32 E). The IS also appeared more normal and contained numerous mitochondria (Figure 3.32 E).

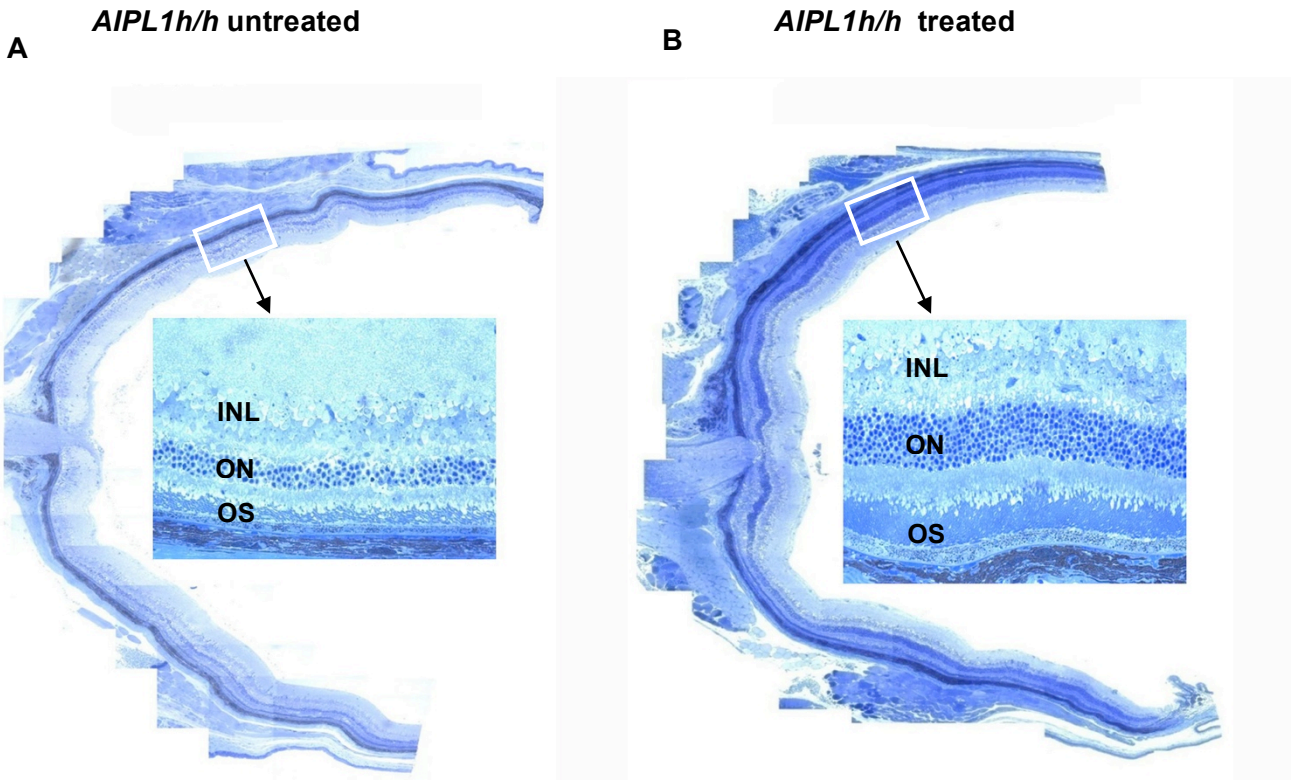

Figure 3.31. Semithin light micrographs of treated and untreated retina 52 weeks following subretinal injection of AAV2-CMV-*AIPL1.* The samples were taken from a single *Aipl1* h/h animal. Higher magnification images are shown in the centre.

(A) Semithin light micrographs of representative *Aipl1 h/h* retina treated 52 weeks after subretinal injection of AAV2-CMV- *AIPL1* shows preservation of photoreceptors. This is seen throughout the superior and inferior sections of the retina which are the treated areas. On higher magnification, it is clear that the outer nuclear layer in the treated retina is significantly thicker and the photoreceptor outer segments are longer and densely packed, indicating that *AIPL1* replacement prolongs photoreceptor survival.

(B) Semithin light micrographs of the corresponding untreated *Aipl1 h/h* retina shows loss of the outer nuclear layer thickness throughout the entire retina. Higher magnification image shows that loss of photoreceptor nuclei and also outer segment length and density

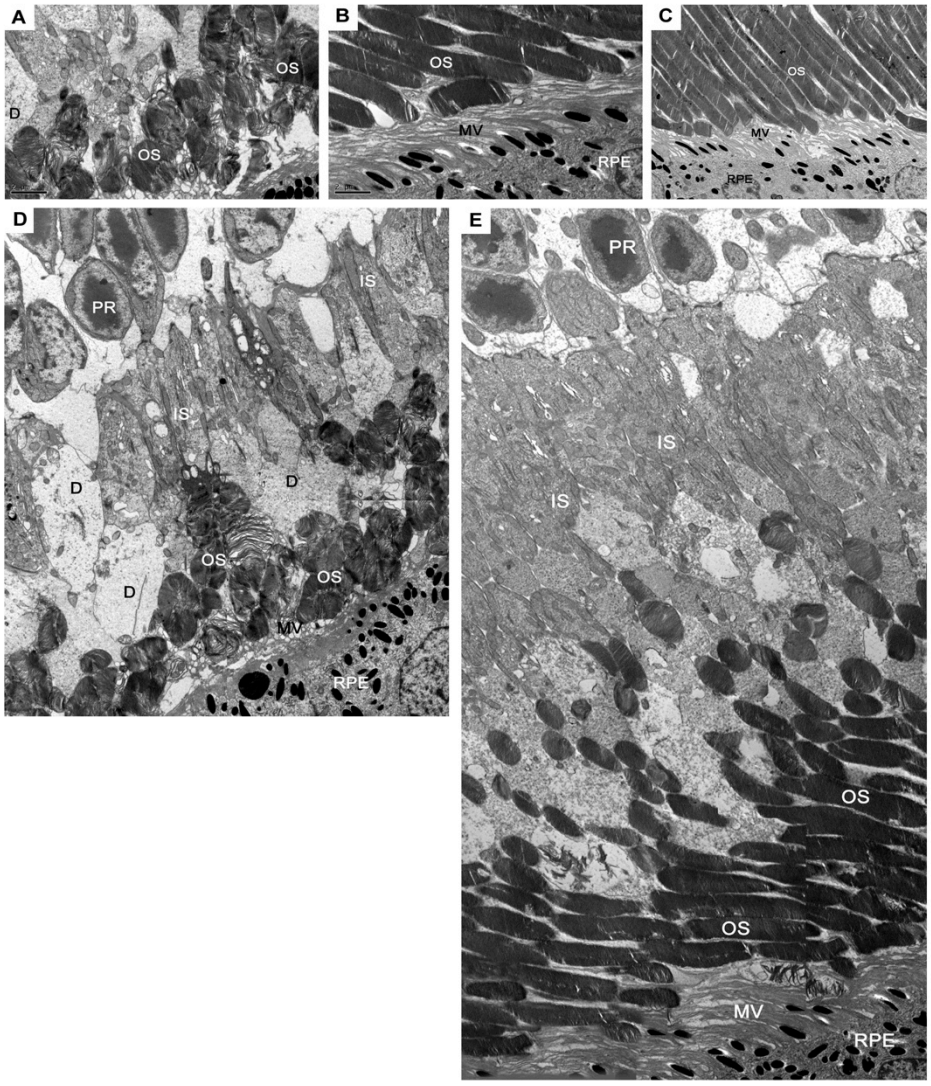

Figure 3.32. Electron microscope (EM) analysis of retinal tissue samples taken from a single *Aipl1 h/h* mouse at 52 weeks after subretinal injection of AAV2-CMV-*AIPL1* (light microscopy of retina from the same animal is shown in Figure 3.33).

(A) In untreated *Aipl1* h/h retina, the photoreceptor outer segments (OS) appear shortened, rounded and folded over. The membranous disks inside the outer segments were disorganized and formed whorls instead of stacks.

(B) Treated *Aipl1* h/h retina shows relatively well organised and densely packed outer segment membranous disks, resembling those of wild-type retina shown in **(C)**.

(C) Wild type mouse retina is shown for comparison. The outer segments in wild type retina is long containing membranous disks organized in a laminar fashion.

(D) Compared to treated retina, the untreated retina has very few outer segments and photoreceptor cell nuclei (PR). The inner segments are interrupted by multiple debris-filled vacuoles (D).

(E) Outer segments and photoreceptor cell nuclei in the treated *Aipl1 h/h* retina are numerous and show normal interdigitation with the RPE microvilli (MV), indicating that there is normal functional interactions between the outer segments and RPE. The inner segments (IS) are also densely packed and contain numerous mitochondria.

3.10.2 Quantification of the outer nuclear layer in *Aipl1* h/h mice following subretinal injection of AAV2-CMV-*AIPL1*

To assess the effect of AAV-mediated human *AIPL1* gene replacement in *Aipl1* h/h retina and also to determine whether there is sustained and long term photoreceptor cell survival, quantification of the outer nuclear layer was performed. Six of the *Aipl1 h/h* mice that received unilateral subretinal injection of AAV2-CMV-*AIPL1* were sacrificed at 50 weeks post injection and cryosectioned. Centrally located retinal sections that passed through the optic nerve and spanned the treated areas in superior and inferior hemispheres of the retina were selected for outer nuclear layer quantification. The retinal sections were stained with propidium iodide and imaged with confocal microscopy. The method of quantification was the same as described in the previous section (section 3.5.2). The photoreceptor cell count for each eye was determined by averaging the cell counts from each confocal image of the eye. To control for inter-animal variation in the rate of degeneration, a paired t-test was performed comparing the mean photoreceptor cell count in the treated and untreated eyes.

Representative confocal images of retinal sections from treated and untreated eyes of a single animal at 50 weeks post injection are shown in Figure 3.33 A. The outer nuclear layer in the treated retina is noticeably thicker than the contralateral untreated eye. Paired analysis of the mean photoreceptor cell count of all the treated and untreated eyes in the group of animals (n=6) showed that treated eyes had 73% more photoreceptor cells than untreated eyes at 50 weeks post injection (p=00006). Mean photoreceptor cell count in treated eyes was 463.5 ± 19.8, while in untreated eyes the mean photoreceptor cell count was 267.4 ±13.9 (p = 0.00006) (Figure 3.33 B). It has been reported that approximately half of the photoreceptor cells are lost by 8-9 months in the *Aipl1 h/h* mouse. This is evident in untreated *Aipl1 h/h* eyes where the outer nuclear layer cell count is approximately half of that in wild type. The mean photoreceptor cell count in treated eyes were also less than in age-matched wild type eyes (Figure 3.33

B), indicating that there was still ongoing degeneration in the treated eyes. However, this difference did not achieve a level of significance (p=0.05). Treated eyes at 50 weeks post injection had 13% fewer photoreceptor cells than wild type eyes, while untreated eyes had lost about 50% of photoreceptor cells compared with wild type. Hence, despite evidence of ongoing degeneration, AAV2-mediated expression of the human *AIPL1* have slowed down the rate of degeneration in the treated eyes. This was a consistent result in all of the animals that were assessed, as the photoreceptor cell count in the treated eye of every animal was significantly higher than in the untreated eye (Figure 3.33 C).

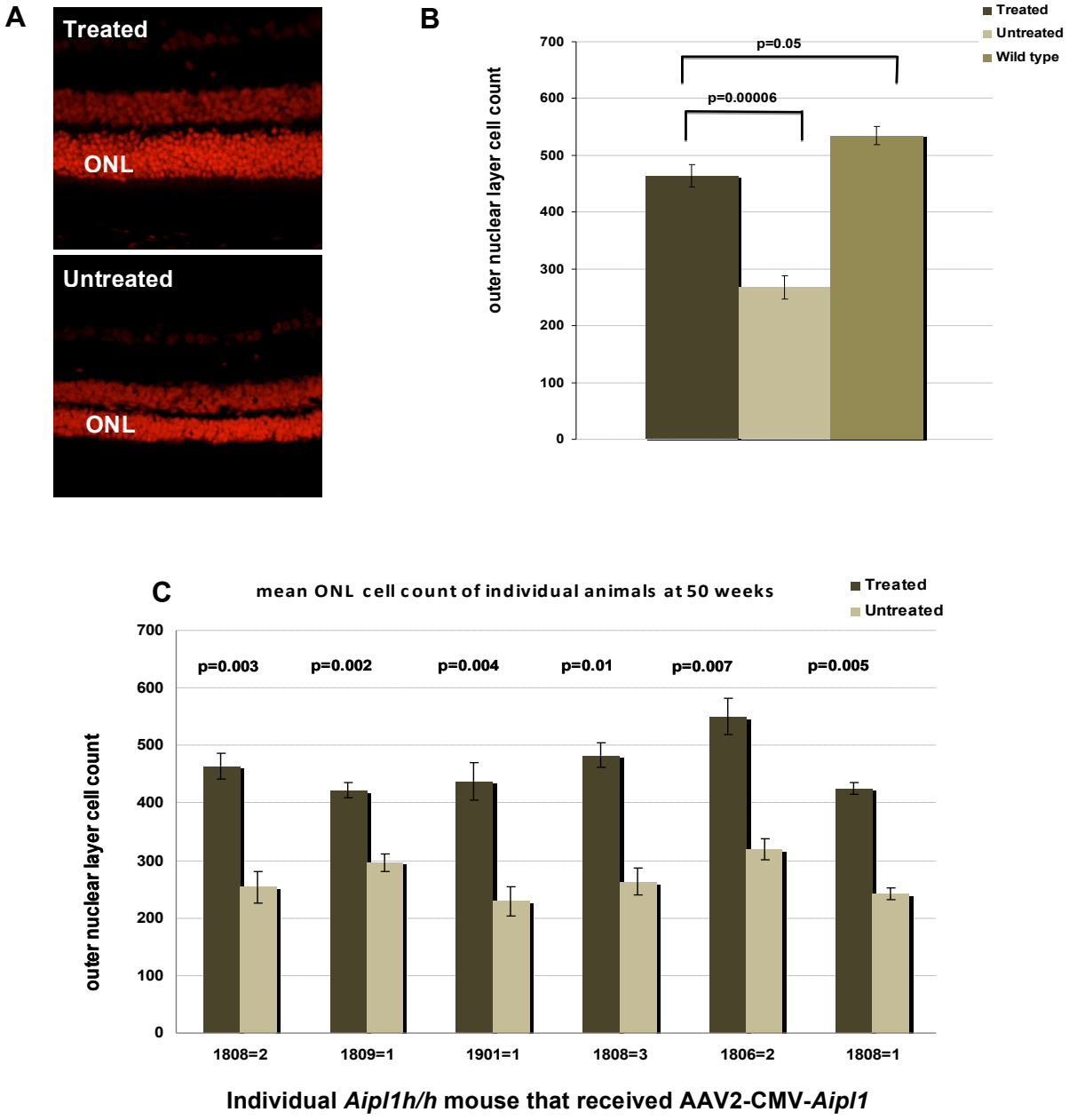

Figure 3.33. Quantification of the outer nuclear layer (ONL) in *Aipl1* h/h mice following subretinal injection of AAV2-CMV-*AIPL1.*

(A) Representative confocal images of retinal sections taken from treated and untreated eyes from a single animal at 50 weeks following injection with AAV2-CMV-*AIPL1.* The treated retina has a substantially thicker ONL compared with the untreated retina

(B) Quantification of the photoreceptor nuclei in the ONL showed that the mean photoreceptor cell count in treated eyes (n=6) were significantly higher that untreated eyes (p=0.00006). However the level of ONL count in treated eyes were lower that those of wild type eyes.

(C) There was consistency in the preservation of photoreceptor survival across all the animals that were assessed. In each mouse, the treated eye has significantly higher ONL count than the untreated eye.

3.11 Discussion

In this chapter a detailed assessment of the duration and extent of the morphological rescue and functional benefit following AAV-mediated gene replacement therapy in *Aipl1* h/h mouse was presented. The preservation of retinal function and morphology was observed up to a year. This is the most significant rescue of a retinal degeneration to date. It is also the first study to demonstrate effective long term rescue for a photoreceptor-specific defect which are generally difficult to treat. The results presented provide further evidence to support gene therapy approaches for the treatment of severe inherited retinal dystrophies.

There are three goals that gene-based treatments for autosomal recessive retinal conditions should aim to achieve; the expression of a normal copy of the defective gene leading to the production of the key protein, restoration of function to disabled cells and ultimately the prevention of progressive cell death or retinal degeneration as a result. To produce an effective long-term therapy, degeneration must be prevented. Our therapy addressed the first two goals where by subretinal delivery of AAV2-CMV-*Aipl1* and AAV2-CMV-*AIPL1* resulted in increased production of AIPL1 in photoreceptor inner segments and subsequently the restoration of normal cellular biology and function that was substantiated by the translocation of PDE from inner to the outer segments. As a result, retinal degeneration was significantly slowed. A concomitant stabilization of ERG amplitudes was also seen in treated eyes following subretinal injection of the therapeutic vector. ERG b-wave amplitudes were significantly higher in eyes treated with AAV2-CMV-*Aipl1* or AAV2-CMV-*AIPL1* compared with untreated, PBS-injected or AAV2-CMV-*gfp* injected eyes. The presence of OPs on ERG traces of treated eyes implies appropriate retinal function. After treatment with the therapeutic vectors, the pattern of the ERG response to a series of increasing stimuli resembled that of normal animals, with increasing b-wave amplitudes and decreasing b-wave latencies indicating successful functional rescue at the time point assessed. We observed improved photoreceptor cell survival, preservation of

outer segment morphology and stabilization of retinal function. Both therapeutic constructs, one containing the murine *Aipl1* cDNA and the other containing the human *AIPL1* cDNA were similarly effective. This is not surprising since *AIPL1* is highly conserved between species; there is 96% similarity and 86% identity between the murine and human cDNAs.

AAV-mediated gene replacement therapy resulted in significant preservation of photoreceptors and retinal function in *Aipl1* h/h mice one year after treatment – the latest time point examined. This is the most sustained rescue of a photoreceptor-specific gene defect reported to date. Previous gene replacement therapy studies targeting photoreceptor cell defects did not include such long term time points. [50][463][14][363][496] The most sustained rescue reported previously was following AAV-mediated gene replacement therapy in an *RPGRIP* mouse model [363]. This study demonstrated functional and histological improvement for up to 5 months.

Although significantly better than in untreated eyes, AAV-mediated gene replacement did not completely prevent loss of photoreceptor cells. The mean ERG b-wave amplitude in AAV2-CMV-*Aipl1*-treated eyes at 7 months after treatment was approximately 85% that in wild type mice at that age (data not shown). The mean b-wave amplitude in untreated *Aipl1* h/h eyes at 7 months however was about 60% of wild type, indicating that the degenerative process was very slow. Morphologically, at 28 weeks following injection, treated eyes show a 14% loss of photoreceptor cells from age-matched wild type eyes, while untreated eyes showed 40% loss from wild type eyes. In animals that were treated with the human construct, treated eyes at 50 weeks following treatment showed a 13% loss of photoreceptor cells from wild type levels while untreated eyes had approximately 50% less photoreceptor cells than wild type eyes. Although retinal degeneration was not completely prevented following treatment, photoreceptor loss was significantly delayed with the rate of degeneration substantially reduced in treated eyes to the magnitude of 3-4 fold. Furthermore, in animal which were treated with the human construct, the difference in photoreceptor cell count between treated eyes at 50 weeks post injection and wild type did not reach

statistical significance (p=0.05). Considering that transduction of the retina is usually incomplete following subretinal injections, this suggests that the expression of *AIPL1* in treated areas has a substantial effect in arresting the degeneration.

There may be several reasons why photoreceptor degeneration proceeds despite treatment. Firstly, only two-thirds of the retina, at most, is transduced following double subretinal injections into an eye and hence the transduction efficiency have not have been adequate. Considering that the transduction efficiency of AAV2/2 is not 100 %, the final area of the retina that is transduced is likely to be about 50-70 % and may have been insufficient to ultimately prevent degeneration in treated areas. Secondly, the late onset of AAV2/2-mediated expression compromises its efficacy. By the time maximal transgene expression is attained, the retinal degeneration in the *Aipl1* h/h mouse may be already significantly advanced. The animals were injected at P28 and AAV2/2-mediated transgene expression would be expected to commence 3-4 weeks later. ERG recordings from 8 week old *Aipl1* h/h mice are already lower than age-matched wild type mice[282], suggesting that damage to photoreceptors has commenced by the time the treatment takes effect. The residual one-third of the retina consisting of degenerating photoreceptor cells may further contribute to ongoing loss of photoreceptor cells by creating negative impact on photoreceptor survival in treated regions. Changes in degenerating photoreceptors are likely to generate a microenvironment that has a negative influence on the survival of healthy cells. The phenomenon of non cell- autonomous degeneration in which the loss of trophic factors normally produced from rods [185][413] or the release of toxic substances from rod cell death[226][405] has been frequently described and observed in other retinal dystrophies such as retinitis pigmentosa . In these conditions, cone loss is invariably seen even though the primary genetic defect and cell death is in rod photoreceptors. Lastly, the levels of expression in terms of gene copies per photoreceptor cell that is mediated by AAV2 may have been insufficient, despite the use of a ubiquitously expressed constitutive promoter that drives strong transgene expression. AAV2/2 vectors are known to target RPE and photoreceptor

cells, with a higher tropism for RPE cells than photoreceptors. In comparison to other AAV pseudotypes such as AAV5 and AAV8, the maximal levels of transgene expression from AAV2 vectors known to be lower as a result of fewer copies of the transgene per cell [348]. Hence, on a single cell basis, the expression levels mediated by AAV2 may not be adequate to achieve full correction of the cellular defect or restore normal cellular function and subsequently stem the retinal degeneration process.

Interestingly, the morphological rescue of *Aipl1* h/h retinas was better than might have been expected given the relatively modest functional improvement in ERG amplitudes between treated and untreated eyes. This may be due to the unusual phenotype of the *Aipl1* h/h mice. It has been previously shown that *Aipl1* h/h rods have a higher sensitivity to light compared with normal rods photoreceptor cells, and require fewer photons to elicit a response[282][295]. They manifest supra-normal ERG when young, presumable because of a larger than normal dark current due to higher free cGMP levels. The restoration of functional AIPL1 in *Aipl1* h/h rods would therefore, result in correction of this abnormality so that photoresponses become more similar to that of wild type photoreceptors with a reduction in the altered sensitivity of *Aipl1* h/h rods. Hence, it is likely that the relative modest difference in ERGs compared with difference in photoreceptor preservation seen after treatment is partly due to a reduction in ERG amplitudes as a result of a reduction in photoreceptor hypersensitivity following gene transfer.

An initial increase in ERG amplitudes was observed in treated and untreated eyes as well as in the wild type control group. This initial increase occurred from 4 weeks post injection up to about 8 weeks post injection. Similar observations of ERG amplitude rise was also seen in the control experiment which recorded ERGs from unprocedured *Aipl1* h/h mice of various ages and wild type mice. This confirmed that the phenomenon was unrelated to the treatment or the surgical procedure. A physiological increase in ERG responses have been described in young mice, normally occurring from birth

up to postnatal age of 12 weeks[209]. It is thought to reflect the normal development in mice. In AAV-CMV-*gfp* treated Aipl1 h/h mice, ERG b-wave amplitudes in injected eyes were lower than in uninjected eyes. This may be due to a particular batch of viral prep that contained impurities that might have attenuated the ERG responses, since the laboratory has extensive experience with intraocular administration of AAV vectors and has rarely observed toxic effects following injection of vectors expressing *gfp*.

A number of studies have suggested various roles for AIPL1 in the retina. It was originally suggested that AIPL1 may have a role in development as a result of its putative interactions with NUB1 [7], but this is unlikely since both *Aipl1 -/-* and *Aipl1* h/h have normal architecture prior to the onset of degeneration [282,391]. Biochemical studies using a yeast two-hybrid screen suggested AIPL1 may have a general role in enhancing the protein farnesylation in the retina. Among the retinal proteins known to be farnesylated are PDE α-subunit, γ-transducin, and rhodopsin kinase. However, this hypothesis did not appear to be supported by the findings that levels of rhodopsin kinase and transducin were unaffected in *Aipl1* -/- mice [391]. Further assessment of candidate retinal proteins in the *Aipl1* -/- and *Aipl1* h/h mouse found that cGMP-PDE was the only protein in which all three α,ß and γ subunts were absent or reduced in levels, suggesting that cGMP-PDE is a specific client protein of AIPL1[282][391]. This study confirms that that AIPL1 and cGMP-PDE are intricately linked. We found that cGMP-PDE, in particular the β-subunit of PDE was mislocalized to photoreceptor inner segments in untreated AIPL1 h/h eyes when the animals were examined at 28 weeks following subretinal injection in the other eye. In the contralateral treated eyes of these animals, the β-PDE signal was present in the photoreceptor outer segments suggesting that AIPL1 could indeed be a molecular chaperone ensuring PDE translocation to the outer segments. The fact that photoreceptor cell loss in the *Aipl1* h/h mouse proceeds slowly and outer segments are present for most of the degeneration makes it possible to compare and localize β-PDE expression in the outer segments of treated and untreated eyes. In the *Aipl1 -/-* mouse, retinal degeneration is too rapid for this analysis since most of the

photoreceptor cells and outer segments have been lost in the untreated eye by the time vector-mediated expression of *AIPL1* commences in the treated eye. Hence AIPL1 may protect PDE subunits from proteosomal degradation or assist in the assembly or folding of the PDE holoenzyme whereby only properly protein is transported to the outer segments. The exact molecular mechanism and relationship between AIPL1 and cGMP PDE remains to be elucidated. Precise regulation of cGMP synthesis and cGMP PDE degradation is critical to the health of photoreceptors and mutations which disrupt the balance between the two, result in dysregulation and degeneration of these cell [127]. Mutations in the *PDE6B* gene encoding the ß-subunit of cGMP PDE lead to abnormal increases in cGMP and subsequent photoreceptor death. Mutations in retGC1 impair synthesis of cGMP, leading to a state equivalent to sustained photo-excitation and photoreceptor cell death [127][428][366]. Similarly, one of the most important consequences of mutation in AIPL1 is likely to be the effect on cGMP PDE levels, leading to photoreceptor dysfunction and rapid retinal degeneration. This however, may not be the only function of AIPL1 in the retina or the only mechanism of cell death due to loss of AIPL1. Further studies are required to fully elucidate the exact role or AIPL1 in the retina.

In patients, *AIPL1* defects present as a clinical spectrum and present with LCA as well as cone-rod dystrophy and juvenile retinitis pigmentosa [103][442]. This variability in phenotype may be explained by the nature of the mutations. To date, 20 disease-causing mutations in *AIPL1* have been reported (HGMD; www.hgmd.org). Out of these, five of them are likely to lead to complete loss of AIPL1 function; four are nonsense mutations resulting in a severely truncated protein and one affects the splice site in intron 2 leading to a frame shift. The other mutations comprise of missense mutations in the N-terminal or the tetratricopeptide domains and deletions in the C-terminal region. *In vitro* assays have shown that many of these mutations did not lead to loss of *AIPL1* expression or abolished protein function completely [7,393,476]. It is also likely that there are other variants that give rise to an altered protein with reduced function. Hence, it is possible that *AIPL1* mutations results in a partial as well as complete loss of function

of the protein. Efficient rescue of the *Aipl1 h/h* mouse suggests that patients with mutations that do not lead to complete loss of AIPL1 function might respond particularly well to gene replacement therapy.

4. Gene replacement therapy in rapid retinal degenerations due to AIPL1 deficiency

4.1 Treatment of retinal degeneration in *Aipl1 h/h* murine model under light acceleration

Following evidence of significant rescue in the *Aipl1* h/h mouse using AAV2/2 vector encoding both the murine and human *AIPL1* gene, we proceeded to determine whether we can rescue photoreceptor cells in a faster degeneration using AAV-mediated gene replacement and by accelerating the photoreceptor cell loss in *Aipl1* h/h mice. The rate of retinal degeneration in the *Aipl1* h/h mice has been observed to increase by 2-3 fold by keeping the animals in constant white light illumination (personal communication from Tiansen Li, Massachussetts Eye and Ear Infirmary). The mechanism of the acceleration of retinal degeneration under light in these mice is not known but is thought that this could be related to the light-induced increase in mitochondria free radical production and oxidative stress. To ensure that a more rapid onset of gene expression from the AAV vector was obtained, we produced AAV2/8 pseudotyped vector containing the murine *Aipl1* cDNA under the control of the ubiquitously active cytomegalovirus (CMV) promoter. The therapeutic construct was developed in Chapter 3 (section 3.8) by cloning the murine *Aipl1* cDNA between the ITRs of the AAV2 vector genome, and we packaged this therapeutic construct using AAV8 capsid to produce AAV2/8-CMV-*Aipl1.* The murine cDNA was chosen to give the best possible chance of a rescue and to reduce the risks of rejection and protein incompatibility.

As is the case with all viral vector systems, the choice of an appropriate promoter is important to achieve efficient expression of a transgene. The

CMV promoter is a strong viral promoter that is ubiquitously active. AAV2/8-CMV-*Aipl1* was produced using a triple plasmid transfection method in 293T cells (described in Chapter 2) and purified using ion exchange chromatography. The resulting virus preparation was concentrated with Centricon 10 columns (Millipore, Bedford, MA), washed in PBS, and concentrated again to a volume of approximately 100-150 µl. Control AAV2/8 virus was also produced from the AAV-CMV-*egfp* construct (described in Chapter 3) to generate AAV2/8-CMV-*egfp* vector. This control vector will serve to verify AAV2/8 expression in photoreceptor cells and to control that any beneficial effect is due to the expression of the transgene rather than the administration of an AAV vector. Viral particle titres were determined by comparative dot-blot DNA prepared from purified viral stocks and defined plasmid controls. Purified vector concentrations used for all experiments were of 1-2 X 10^{12} viral particles/ml (Figure 4.1).

A total of 23 *Aipl1 h/h* mice received subretinal injections of AAV2/8-CMV-*Aipl1* at postnatal week 4. As in previous experiments, subretinal injections of the vector were administered to each treated eye in the superior and inferior hemisphere; each subretinal injection amounted to a volume of 1.5 µl. Only one eye in each *Aipl1 h/h* mouse was treated, leaving the contralateral eye to serve as an internal control. At 1 week after subretinal injection, the procedured mice were moved to a room with constant ambient white lighting. Care was taken to ensure all cages received equivalent amounts of light exposure, by placing them on racks of equal height and at the same level to each other. All cages consisted of transparent perspex plastic material to allow maximal light penetration into the cages and any large housing material was removed from the cages. Another group of *Aipl1 h/h* mice (n=9) received subretinal injections of the control vector AAV2/8-CMV-*egfp* while a group of C57BL/6 mice (n=10) received subretinal injections of the therapeutic vector. These control groups of animals were also subjected to the same conditions as the procedured *Aipl1 h/h* mice and were placed into constant white ambient light conditions at 1 week following subretinal injections. All animals were examined histologically to investigate the effects of treatment on retinal morphology after period of 5 months. To follow the course of degeneration

and the effects of gene replacement, retinal function was assessed using ERG recording at regular intervals over the same period of time.

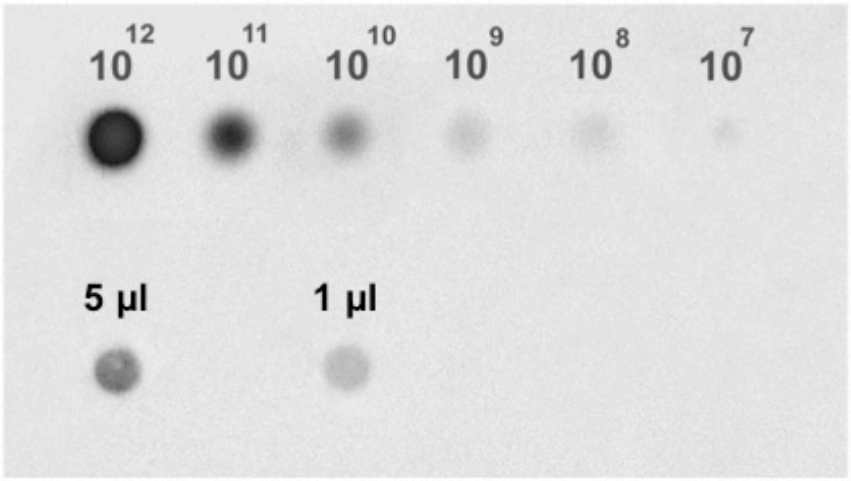

Figure 4.1. A chemiluminescence capture image of a dot blot for AAV2/8-CMV-*Aipl1* vector suspension.

A serial dilution of a DNA probe is made to a series of known concentration to serve as a standard ladder. 1 µl and 5 µl of the AAV2/8-CMV-*Aipl1* vector suspension were loaded and the concentration was estimated by comparing the chemilumincence intensity of the sample to the dilution series. In this case it was estimated that the vector suspension had a concentration of 2 x 10^{12} particles / ml.

4.2 Effects of AAV2/8-mediated Aipl1 expression on retinal function in light accelerated Aipl1 h/h retina.

The effects of AAV2/8-mediated gene replacement was evaluated in *Aipl1 h/h* mice (n=23) that received subretinal injection of AAV2/8-CMV-*Aipl1* in one eye at 4 weeks postnatally. These mice were place in continuous white light illumination at 1 week following subretinal injection, to accelerate the retinal degeneration. Retinal function was assessed through scotopic ERG analysis recorded simultaneously from the treated and untreated eyes of treated *Aipl1 h/h* mouse. To determine whether preservation of retinal function was achieved as a result of treatment with the therapeutic AAV2/8-CMV-*Aipl1* vector, ERG intensity series were performed on each treated *Aipl1 h/h* mouse at regular intervals of 4-6 weeks following subretinal injection until the final time point of 21 weeks. Before recording the ERGs, the animals were dark adapted for at least 16 hours.

After 3 months of constant light, ERG amplitudes in untreated eyes decreased to half that in wild type mice (Figure 4.2). Although the retinal degeneration progressed at a faster rate, photoreceptor rescue was still obtained. When the group of AAV2/8-treated *Aipl1 h/h* mice that underwent light acceleration was compared with the AAV2/2-CMV-*AIPL1* treated mice *Aipl1 h/h* mice that did not undergo constant light exposure, larger differences between treated and untreated eyes in terms of functional and morphological (described in Section 4.4) outcome measures were obtained in the light exposed animals. Figure 4.3 shows an ERG intensity series of a procedured animal recorded simultaneously from the treated and untreated eye at 2 different time points. At 5 weeks post-injection, differences between the ERG amplitudes in treated eyes and untreated eyes were already seen; treated eyes had higher amplitudes than untreated eyes. By 21 weeks, the ERG responses were lost in the untreated eye, while the treated eye maintained substantial ERG amplitudes and showed increasing responses

elicited by the increasing light stimuli. Normally shaped waveforms, similar to that of wild type mice, were recorded from treated eyes while from untreated eyes, the ERG was virtually undetectable. Oscillatory potentials on the ascending limb of the ERG b-wave and increasing in size with brighter stimuli were seen in treated eyes but not in untreated eyes, indicating an overall improvement of retinal activity.

Maximal rod/cone responses were measured at flash intensity of 1000 mcds/m^2 at 4-6 weekly intervals following treatment in the light accelerated *Aipl1* h/h mice over a period of 5 months**.** Figure 4.4 shows ERGs at a single flash intensity of 1000 mcds/m^2 obtained at different time points from a single animal treated with AAV2/8-CMV-*Aipl1* and subjected to constant light exposure. The traces were recorded simultaneously from the injected (right) and uninjected (left) eye. Over time, the ERG amplitudes in the untreated eye decreased rapidly and disappeared completely by 21 weeks. The ERG amplitudes in the treated eye was maintained throughout the follow-up period and remained substantially higher than in untreated eye at the final time point of 21 weeks after treatment, suggesting that photoreceptor survival was prolonged following treatment with AAV2/8-CMV-*Aipl1.*

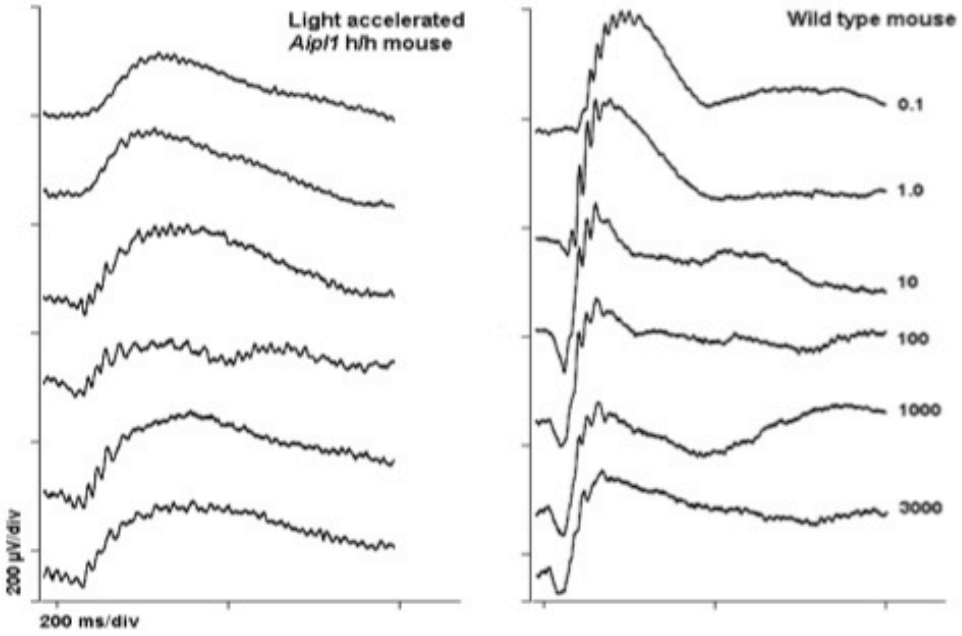

Figure 4.2 Comparison of ERG recordings from an *Aipl1 h/h* mouse and a wild type mouse following constant light exposure.

ERG was recorded at flash intensities of 0.1, 1, 10, 100, 1000 and 3000 mcd/m^2. Scotopic ERG recordings were obtained from the eye of an *Aipl1 h/h* mouse and a wild type mouse, both of which have been reared in constant white ambient light. After three three months of being in continuous light, ERG ampllitudes from the *Aipl1 h/h* mouse were decreased to approximately half of that in the wild type mouse under same conditions.

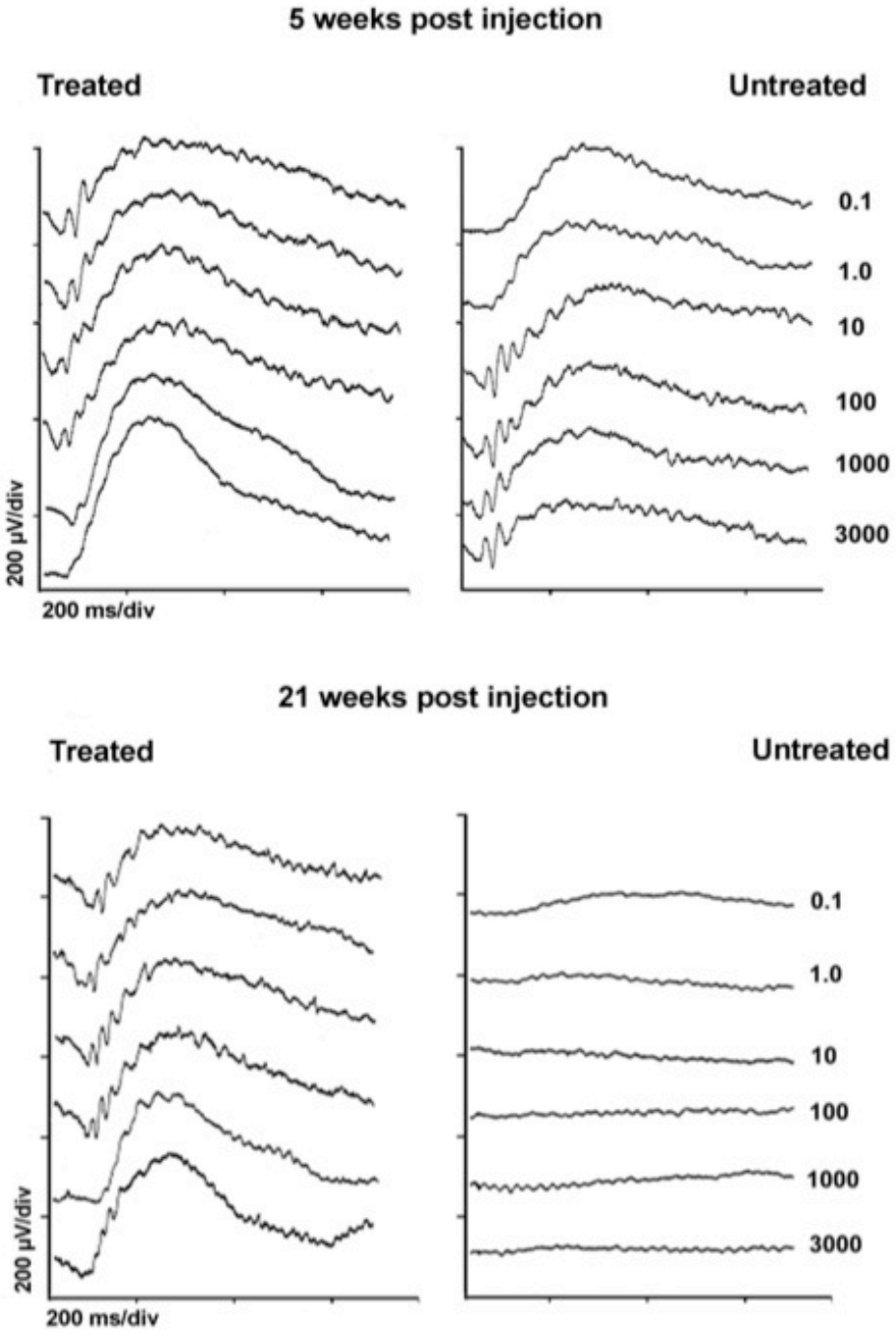

Figure 4.3 ERG intensity series recorded from a light accelerated *Aipl1 h/h* mouse which received subretinal injection of AAV2/8-CMV-*Aipl1* in one eye.

ERG was recorded at flash intensities of 0.1, 1, 10, 100, 1000 and 3000 mcd/m^2. The figure shows simultaneous recordings obtained from treated and untreated eyes of the same mouse at 5 weeks and 21 weeks following subretinal injection of AAV2/8-CMV-*Aipl1*. At 5 weeks after treatment, the b-wave amplitudes in treated eyes were higher than those of untreated eyes. By 21 weeks post treatment, the treated eye maintained good ERG responses while the untreated eye shows no discernible ERG response.

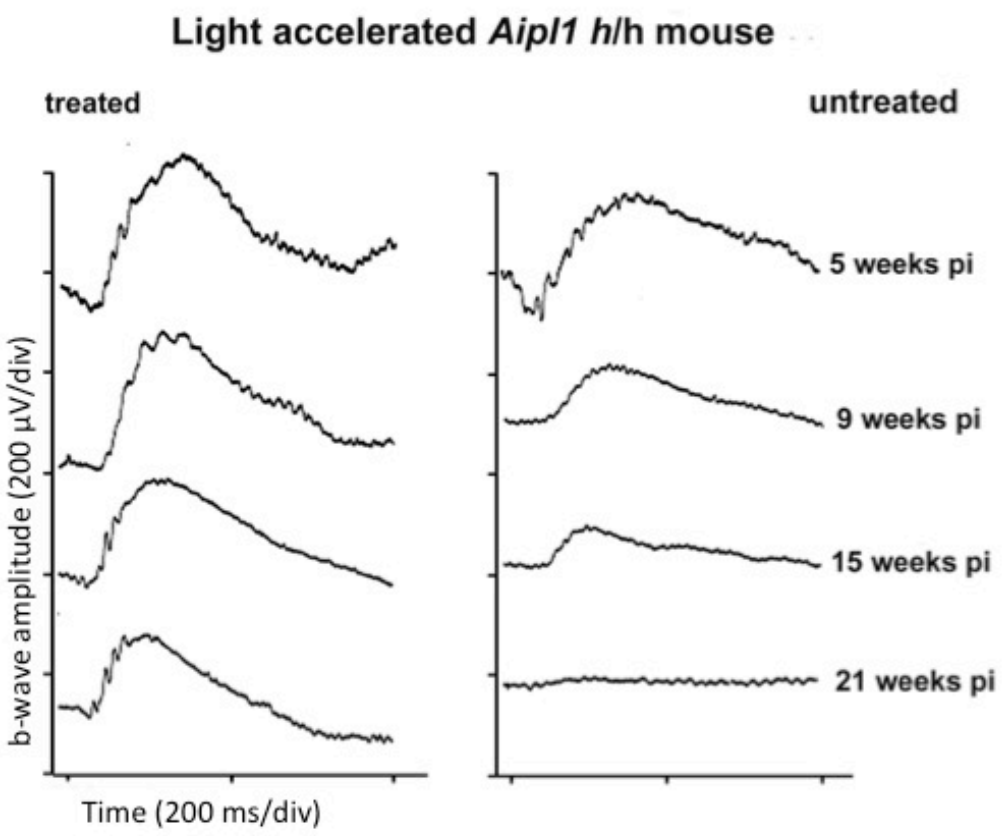

Figure 4.4 ERG time course of an *Aipl1 h/h* mouse which received unilateral subretinal injection of AAV2/8-CMV-*AIPL1*, with constant light acceleration.

ERGs at a single flash intensity of 1000 mcd s/m^2 were recorded from a single animal at various time points following subretinal AAV2/8-CMV-*Aipl1* treatment. The representative ERG recordings form a single animal showed that the treated eye had substantially higher amplitudes compared with untreated eye . Additionally, the ERG amplitudes in the treated eye was maintained over time while the ERG in the untreated eye progressively decreases with time.

The average b-wave amplitudes of the ERG recordings were evaluated statistically by using a paired Student's t-test (Figure 4.5). At 2 weeks post injection, ERG b-wave amplitudes in untreated eyes appeared higher than in treated eyes, although this difference was not statistically significant. This observation may be due to a temporary negative effect from the subretinal detachment induced by the procedure and is a well described phenomenon. Between 2 weeks and 5 weeks post injection, there was a large decrease in ERG amplitudes, indicating an acceleration of the retinal degeneration as a consequence of continuous light exposure. The apparent improvement in the ERG amplitudes between weeks 5 and 14 was thought to be due to variation occurring between recording sessions.

The AAV2/8-CMV-*Aipl1* treated eyes showed significantly higher b-wave amplitudes than the contralateral untreated eyes at time points up to 21 weeks after injection (Figure 4.5). Compared with the *Aipl1 h/h* mice treated with AAV2/2 vector in the previous chapter, the difference in mean b-wave amplitude between treated and untreated eyes was greater in mice that received AAV2/8 therapeutic vector. Statistical significance was also observed at much earlier time points (9 weeks onwards) in this group. At both flash intensities of 100 mcds/m^2 and 1000 mcds/m^2, mean b-wave amplitudes in treated eyes were significantly higher than in untreated eyes from 9 weeks following injection onwards (p<0.05). At 21 weeks post-injection, mean b-wave amplitude at flash intensity of 1000 mcds/m^2 in treated eyes (n=20; mean = 87.3 ± 5.4 μV) was 130% higher than in untreated eyes, p=0.0006 (n=20, mean = 41.5 ± 4.2 μV). Analysis of the mean ERG a-waves showed that treated eyes also had significantly higher a-wave amplitudes compared with untreated eyes (Figure 4.6). Statistically significant differences were seen at earlier time points from 5 weeks post injection onwards up to the last time point of 21 weeks post injection. At 21 weeks post injection, mean ERG a-wave in treated eyes was 16.8 ± 2.3 μV (n=20) while in untreated eyes it was 8.9 ± 2.8 μV (n=20).

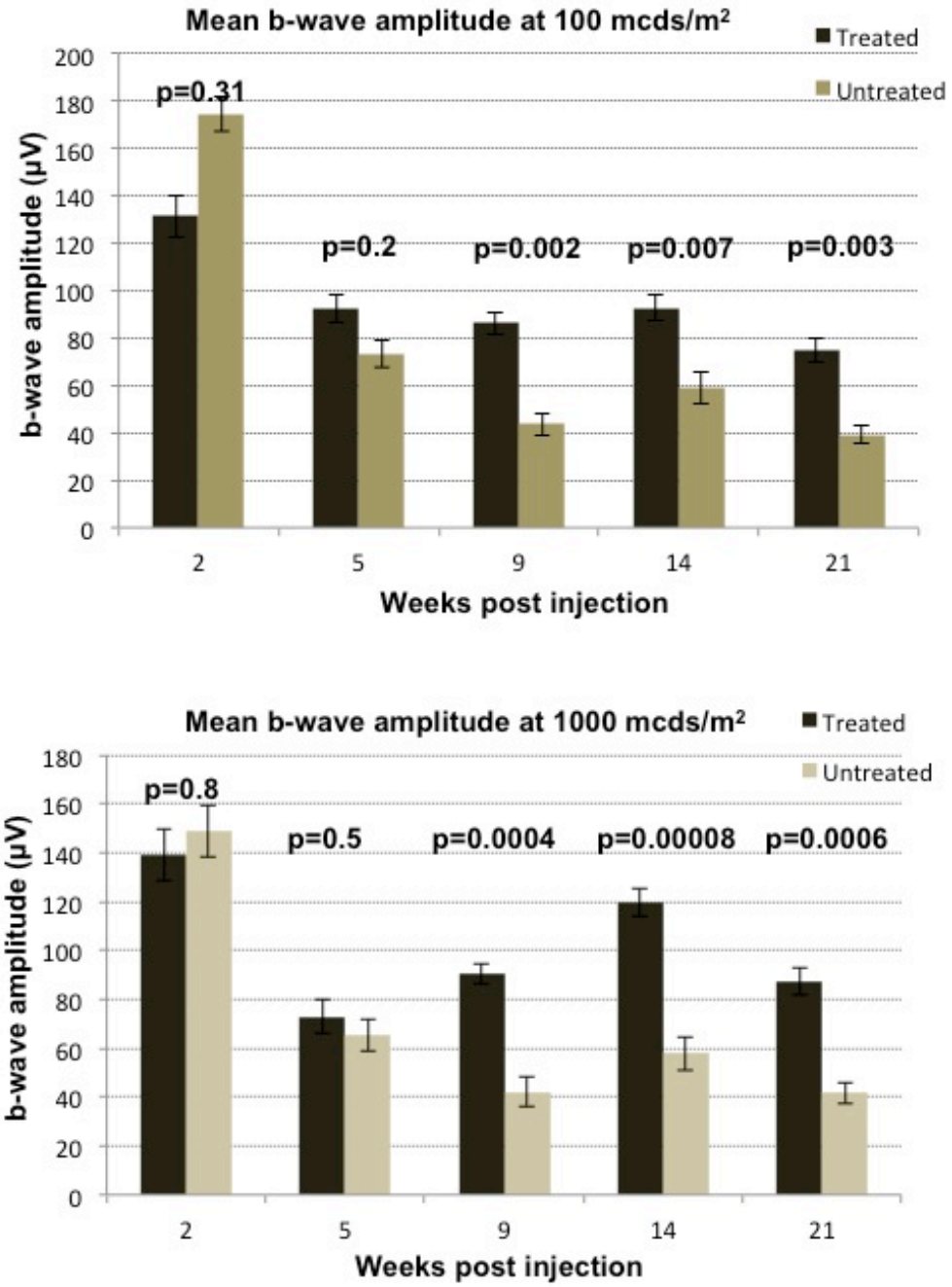

Figure 4.5 Mean ERG b-wave amplitudes in light accelerated *Aipl1 h/h* mice that received subretinal injection of AAV2/8-CMV-*Aipl1*.

The mean b-wave amplitudes and standard error of the mean (SEM) of treated and untreated eyes are shown at various time points after treatment. Statistical significance of the difference between the treated and untreated eyes was determined using a paired t-test. Mean ERG b-wave amplitudes at flash intensities of 100 and 1000 mcds/ m^2 were higher in treated compared to untreated eyes at 5 weeks post injection onwards. Statistical significance ($p<0.05$) was obtained at 9 weeks onwards up to the final time point of 21 weeks, at both 100 and 1000 mcds/m^2 flash intensities. Error bars, +/-SEM.

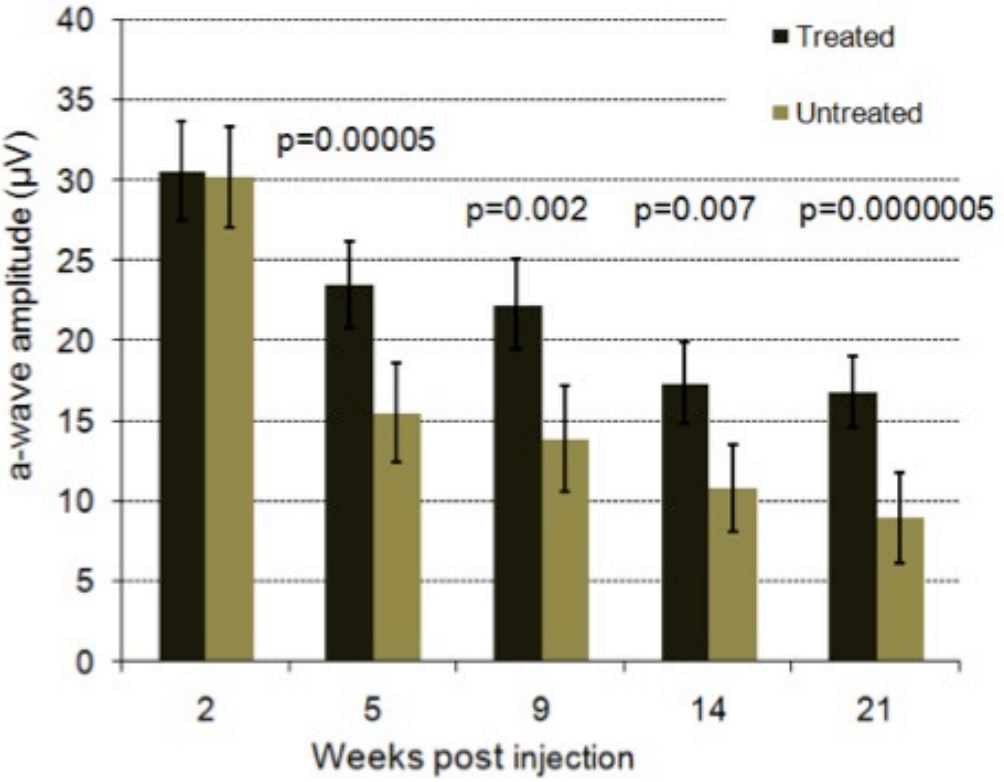

Figure 4.6 Mean ERG a-wave amplitudes in light accelerated *Aipl1 h/h* mice taht received subretinal injection of AAV2/8-CMV-*Aipl1*.

Mean ERG a-wave amplitudes at flash intensity of 1000 mcds/m^2 from treated eyes were significantly higher compared with untreated eyes from 5 weeks post injection onwards (p<0.05) .Error bars, +/-SEM.

4.3 Effects of AAV2/8-mediated Aipl1 expression on retinal morphology in light accelerated Aipl1 h/h retina.

Morphological analysis was performed to investigate the effects of treatment on photoreceptor cell loss over time. Specifically, the effects on retinal structure and photoreceptor ultrastructure following treatment was examined using light microscopy of semithin sections and electron microscopy respectively. Light accelerated *Aipl1 h/h* mice that received subretinal injection of AAV2/8-CMV-*Aipl1* were sacrificed at 10 weeks and 21 weeks post injection (n=2) and semithin sections were taken throughout the each treated and untreated eye. To assess whether the rescue effect was localized to areas adjacent to the injection sites, sagitally orientated cross sections of the eye were taken to encompass the superior and inferior hemispheres of the retina, which were the sites of subretinal injections. Eyes were taken, carefully orientated with a stitch through the conjunctiva and fixed in Karnovski fixative. Cornea and lens were removed the following day and the eyecups were processed for electron microscopy (EM). Semithin sections (0.7 μm thick) were taken and stained with toluidine blue. For electron microscopy analysis, treated areas were identified by orientating eyes so that superior and inferior sections of the retina were examined and 70 nm thick ultrathin sections were then taken of these areas. Eyes were also taken from age-matched wild type mice for semithin and ultrathin sections as positive controls.

Comparison of treated and control eyes showed a reduction in the loss of photoreceptor cells in treated eyes at different time points (Figure 4.7). At 10 weeks following treatment with AAV2/8-CMV-*Aipl1,* a substantial difference can already be seen between treated and untreated eyes. Comparing the midzone area between the ora serrata and optic nerve ie. approximate equivalent areas in treated and untreated eyes, the number of photoreceptor cells in treated eyes was substantially greater than in untreated eyes at 10

weeks post injection. This difference became more marked with time. At 21 weeks, untreated eyes showed an absence of the outer nuclear layer, no photoreceptor cells or outer segments could be found and the inner nuclear layer was seen lying adjacent to the RPE layer (Figure 4.7). In contrast, treated eyes showed preservation of the outer nuclear layer; photoreceptor cells were found in treated eyes along with numerous outer segments as seen on light micrographs (Figure 4.7). To assess the overall effect of treatment on the rate of degeneration, we examined the morphology of the whole retina in the vertical meridian from the ciliary body in the superior hemisphere to the equivalent in the inferior hemisphere of treated and untreated eyes (Figure 4.8). Untreated eyes showed complete loss of the ONL by 21 weeks and this finding was uniform throughout the eye (Figure 4.8). On the other hand, the preservation of ONL in treated eyes appeared to be present throughout the whole of the eye as depicted in the sagittally orientated cross sections of the eye, indicating that the effect was not a localized or patchy phenomenon (Figure 4.8).

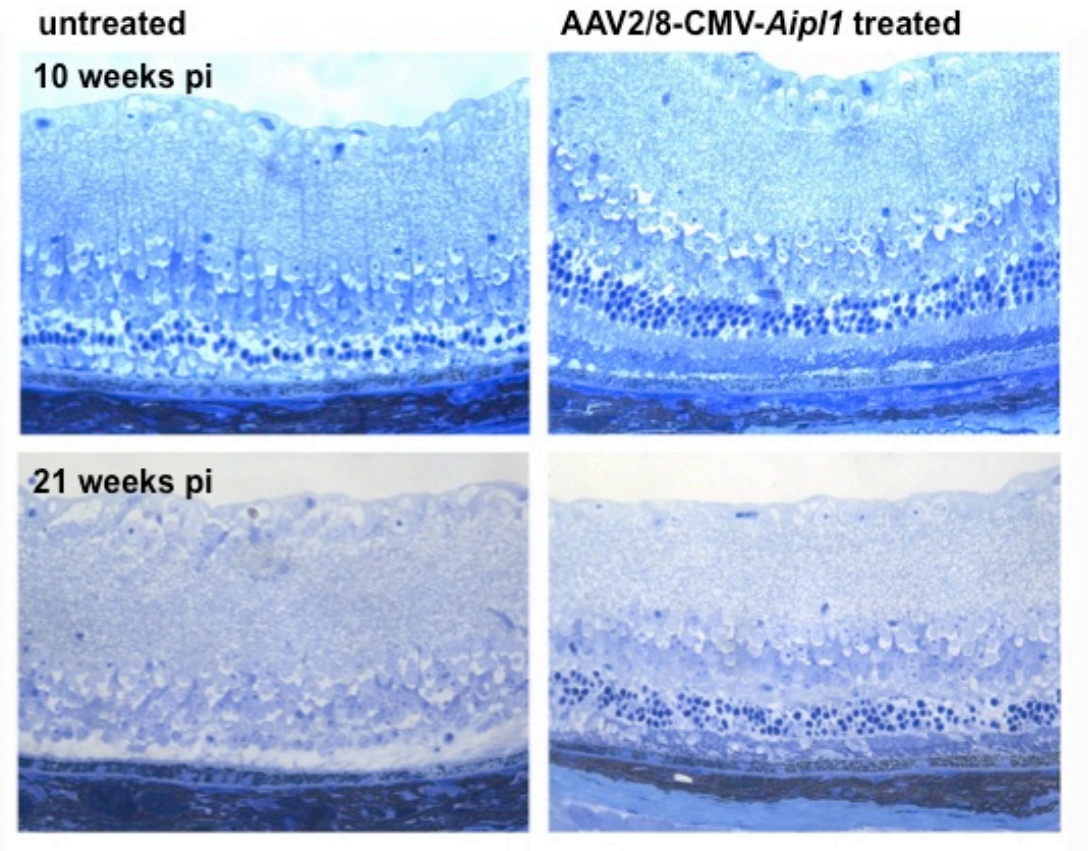

Figure 4.7 Semithin sections retinal sections of *Aipl1 h/h* mice under light acceleration taken at 10 weeks and 21 weeks following injection of AAV2/8-CMV-A*ipl1*.

Semithin retinal sections were taken of areas approximately midway between the ora serrata and the optic nerve of the superior hemisphere in treated and untreated eyes. A noticeable difference in outer nuclear layer thickness is present at 10 weeks post injection, with the treated eye showing preservation of photoreceptor cells and outer segments compared with the marked outer nuclear layer loss in untreated eye. By 21 weeks post injection, there is complete absence of the outer nuclear layer in the untreated eye, while the treated eye still maintains photoreceptors cells and outer segments.

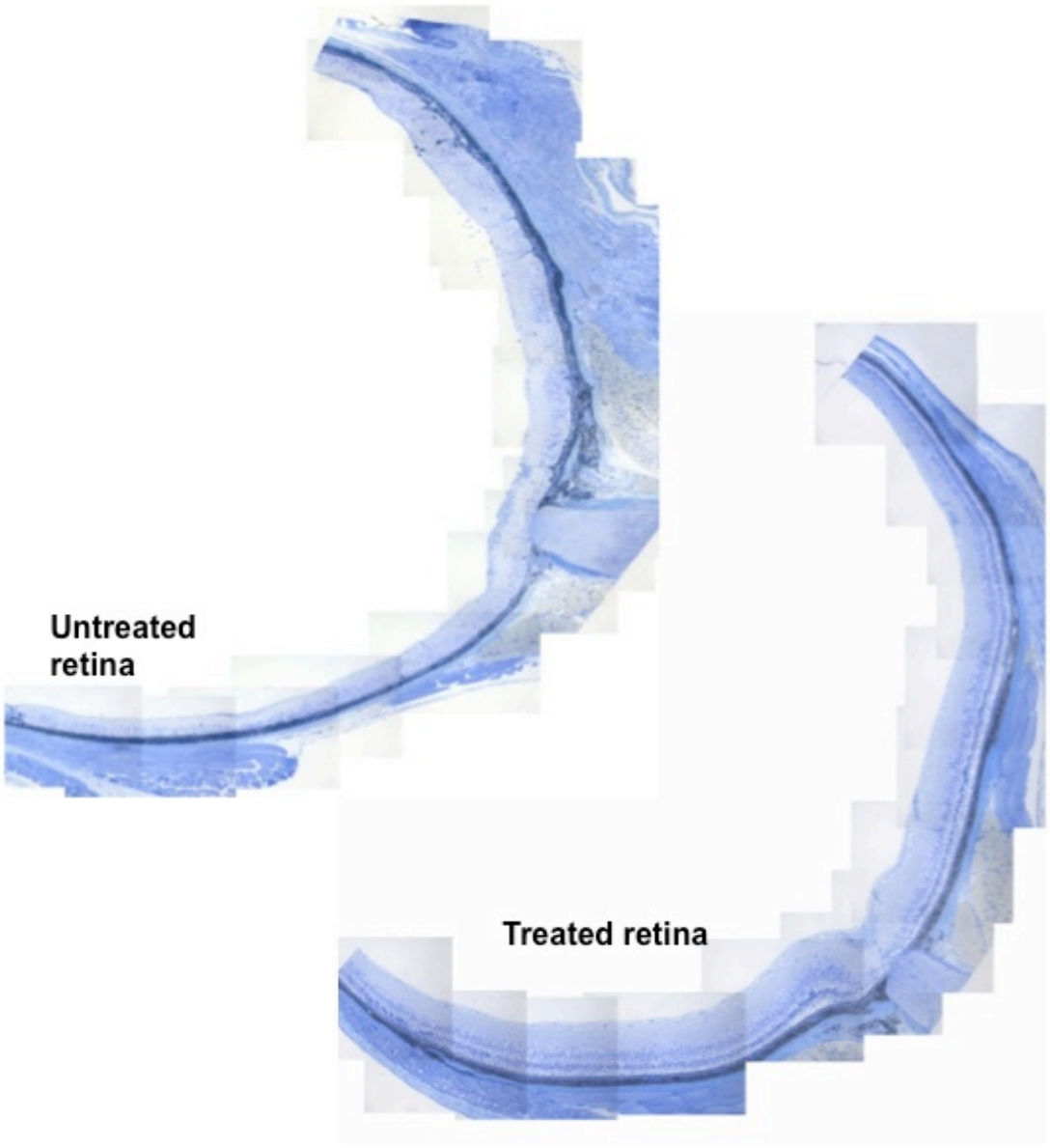

Figure 4.8. Cross sectional semithin sections taken in the vertical meridian of treated and untreated eyes of an light accelerated *Aipl1 h/h* mouse at 21 weeks following subretinal injection of AAV2/8-CMV-*Aipl1*.

Cross section of the treat eye shows preservation of the outer nuclear layer which is present throughout the whole retina, indicating that the rescue effect was not patchy or localised. The untreated eye on the other hand shows complete loss of the outer nuclear layer.

Ultrastructural features of treated and untreated eyes were examined on electron microscopy. AAV2/8-treated eyes in Figure 4.9A showed presence of numerous OS, although these were substantially shorter compared with those of animals that did not undergo light exposure in Chapter 3 (section 3.10). The membranous disks in these OS were dense but less well-organized. The close relationship between OS tips and the RPE was maintained and the OS tips were seen invaginating the microvilli (MV) (Figure 4.9A). Photoreceptor cells and IS in treated eyes had normal morphology. Numerous mitochondria could be seen in the metabolically active IS (Figure 4.9B). In contrast, no photoreceptor cells or OS could be seen in untreated eyes (Figure 4.9C and D). The INL and bipolar cells were seen to lie adjacent to the RPE. There was loss of RPE microvilli and many intervening debris-containing vacuoles (D) could be seen in the untreated retina (Figure 4.9D).

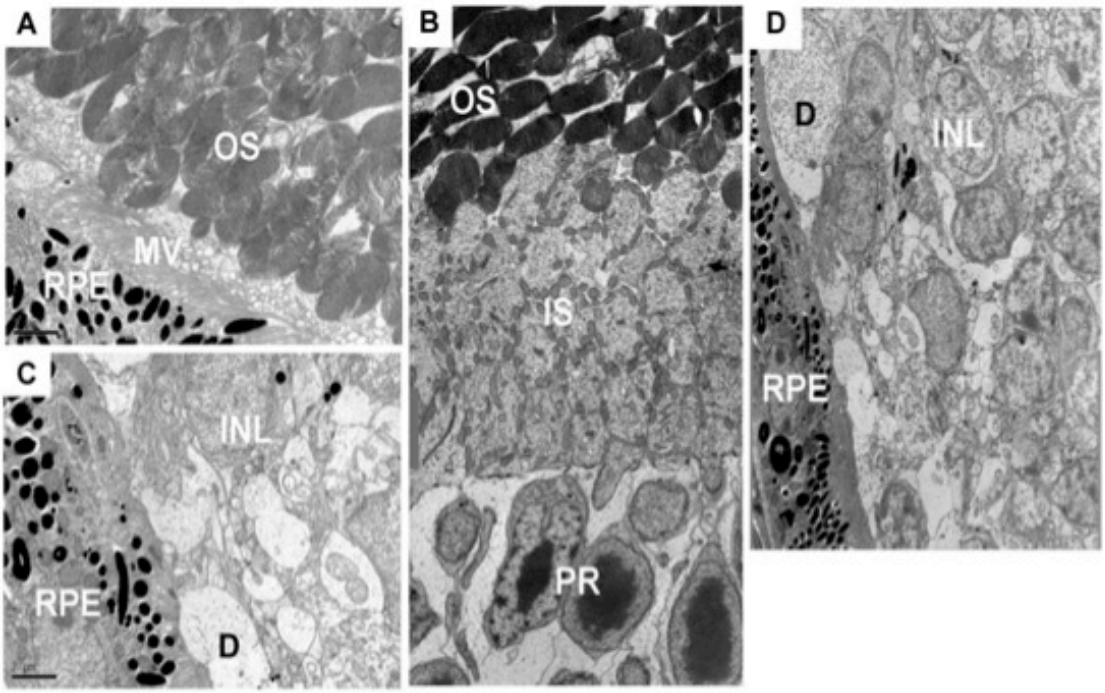

Figure 4.9 (A-D). Electron microscopy of the tissue samples taken from the treated and untreated eyes of a light accelerated *Aipl1 h/h* mouse at 21 weeks following subretinal injection of AAV2/8-CMV-*Aipl1*.

Photoreceptor outer segments (OS) are present in the treated retina although shortened with some disorganization of the membranous disks **(A)**. The OS tips appear to invaginate the microvilli (MV) of the RPE. Photoreceptor cells (PR) and OS are numerous with metabolically active inner segments (IS) containing numerous mitochondria **(B).** The untreated retina shows complete absence of outer segments with debris-filled vacuolar inclusions (D) **(C)**. There is complete loss of photoreceptor cells, only the inner nuclear layer (INL) remains lying adjacent to the RPE **(D)**.

4.4 Morphometric analysis of light accelerated degeneration in Aipl1 h/h retina following AAV2/8-mediated gene expression.

To assess the extent of photoreceptor cell survival after AAV2/8-mediated *Aipl1* gene replacement, quantification of the outer nuclear layer was performed. Whole eyes were taken from *Aipl1 h/h* mice (n=7), that had been exposed to constant white light, for 21 weeks following subretinal injection of AAV2/8-CMV-*Aipl1.* This time point corresponds to the final time point of ERG analysis that was described in earlier sections. The method used for the preparation for retinal sections for outer nuclear layer quantification has been described in section 3.5.2. Centrally located retinal sections that passed through the optic nerve and covered the superior and inferior retina were selected for outer nuclear layer quantification. These were stained with propidium iodide and images of the photoreceptor layer between the ora serrata and optic nerve head was taken using the confocal microscope. For each treated or untreated eye, 3 centrally located retinal sections were selected for imaging; 2 confocal images were taken from each side of the optic nerve in each retinal section. The photoreceptor cell count for each eye was determined by taking the average of the cell counts from each confocal image of that eye. To control for inter-animal variation in the rate of degeneration, a paired t-test was performed when comparing the mean photoreceptor cell count in the treated and untreated eyes in this group.

Figure 4.10A shows confocal images of the outer nuclear layer from a single light accelerated *Aipl1 h/h* mouse at 21 weeks after treatment with AAV2/8 vector. The treated eye has preservation of the outer nuclear layer with many more photoreceptor nuclei compared with the contralateral untreated eye in which the outer nuclear layer is largely absent or reduced to a single cell layer. Statistical analysis showed a significant difference between the mean outer nuclear layer cell count in treated eyes compared with untreated eyes (p=0.0007) (Figure 4.10B). The mean number of photoreceptor nuclei in

treated eyes was 120% higher than in untreated eyes. The mean photoreceptor cell count in treated eyes was 202.1 ± 20.2 (n=7) while in photoreceptor count in untreated eyes was 90.64 ± 23.0 (n=7) at 21 weeks post injection. There was consistent protection in all of the animals that were assessed: in each individual animal that was examined, significant photoreceptor cell preservation (p<0.05) was seen in the treated eye compared with the contralateral untreated eye (Figure 4.10C). We compared the outer nuclear layer cell count between untreated eyes in light accelerated *Aipl1 h/h* mice with age-matched untreated eyes of *Aipl1 h/h* mice that did not undergo light exposure and found that the rate of retinal degeneration in light-exposed eyes was substantially accelerated by 3-4 times. At 21 weeks post injection, the mean outer nuclear layer in untreated light accelerated *Aipl1 h/h* retina was 90.64 ±23.0, while the mean outer nuclear layer cell count in untreated eyes without light exposure at 22-24 weeks was 342.7 ± 11.3, (n=7). Treatment with AAV2/8 vector resulted in significant prolongation of photoreceptor survival, but it did not halt the degenerative process altogether. Compared to age-matched wild type eyes which had also been subjected to constant light exposure, the mean photoreceptor cell count in treated eyes was significantly lower (p=0.00008). Treated eyes at 21 weeks post injection had 54% less photoreceptor cells than age-matched and light exposed wild type eyes. Untreated eyes had lost about 80% of photoreceptor cells compared to wild type by this time point.

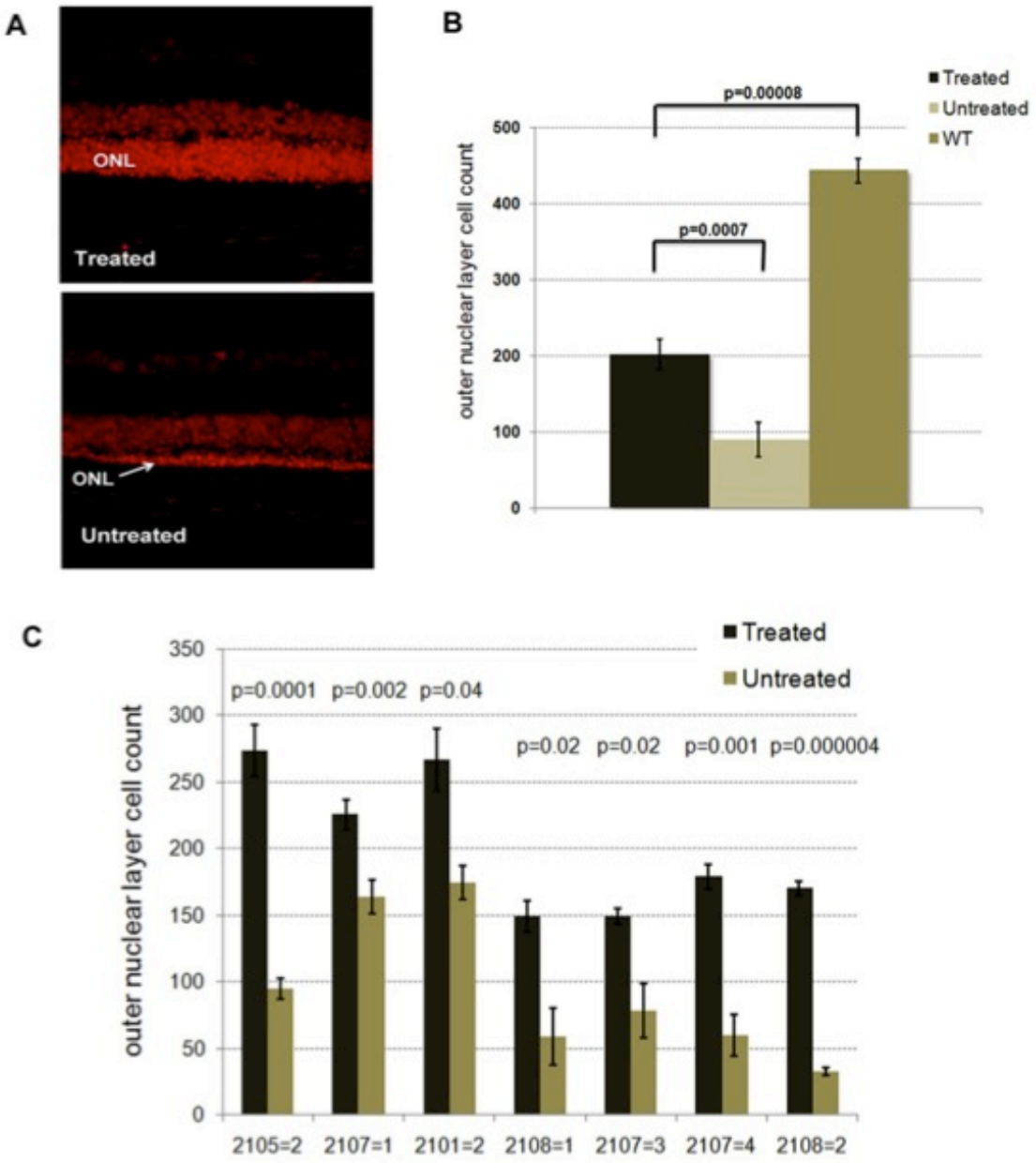

Figure 4.10. Photoreceptor preservation following AAV2/8-mediated *Aipl1* expression.

(A) Confocal images of the treated and untreated retina from a single *Aipl1 h/h* mouse at 21 weeks following subretinal injection of AAV2/8-CMV-*AIPL1*.
(B) Comparison of the mean ONL cell count (n = 7) shows a 123% increase of photoreceptor nuclei in treated eyes compared with untreated eyes (p = 0.0007).
(C) A statistically significant higher ONL count was obtained in the treated eye compared with the untreated eye ($p \leq 0.05$) in each animal that was assessed.

4.5 Effect on AAV2/8-mediated Aipl1 expression on the levels of cGMP phosphodiesterase

In view of the link between *AIPL1* and cGMP phosphodiesterase (PDE), we proceeded to investigate whether AAV2/8-mediated gene expression had any effects on the levels of cGMP PDE on treated retina. In animal models of *Aipl1* deficiency such as the *Alpl1* -/- and *Aipl1 h/h* mouse, cGMP PDE is the only known retinal protein that lost or reduced respectively[391][282], suggesting that AIPL1 is a specialized chaperone for rod PDE. While mRNA levels of *PDE6B* are not affected in these animal models of Aipl1deficiency, the level of PDE protein is absent in the *Aipl1* -/- mouse and severely reduced in the *Aipl1 h/h* mouse, indicating that Aipl1 has post-transcriptional effects on cGMP PDE.

To investigate the effect of AAV2/8-mediated *Aipl1* expression on β-PDE levels, eyes were taken from 3 procedured *Aipl1 h/h* mice that received unilateral subretinal injections of AAV2/8-CMV-*Aipl1* and reared in constant light exposure. The mice were sacrificed at 21 weeks post injection and the treated and untreated eyes from each animal was enucleated and eye cup dissection was performed. The retina was dissected out from the choroid and sclera and manually homogenised and sonicated. A total of 6 retinal homogenates consisting of treated and untreated retina from 3 procedured *Aipl1 h/h* mice were obtained. Western blot analysis was performed on these retinal homogenates from procedured *Aipl1 h/h* mice and also on retinal homogenates from wild type controls.

Immunoblotting with a β-subunit specific PDE antibody showed that β-PDE was present in treated eyes but were severely reduced or absent in untreated eyes (Figure 4.11A). Quantification of the immunoblotting results showed that β-PDE levels in treated eyes were significantly higher than in untreated eyes ($p=0.02$). At 21 weeks post injection under constant light acceleration, the mean levels of β-PDE in treated eyes were 65% of that in wild type retina. In untreated retina, β-PDE levels were 10% of that in wild

type retina (Figure 4.11B). Since treated eyes at this time point contained approximately half the normal number of photoreceptor cells following *Aipl1* gene replacement therapy, the level of β- PDE in each cell might be similar to that in wild type photoreceptors if adjustment was made for the number of cells.

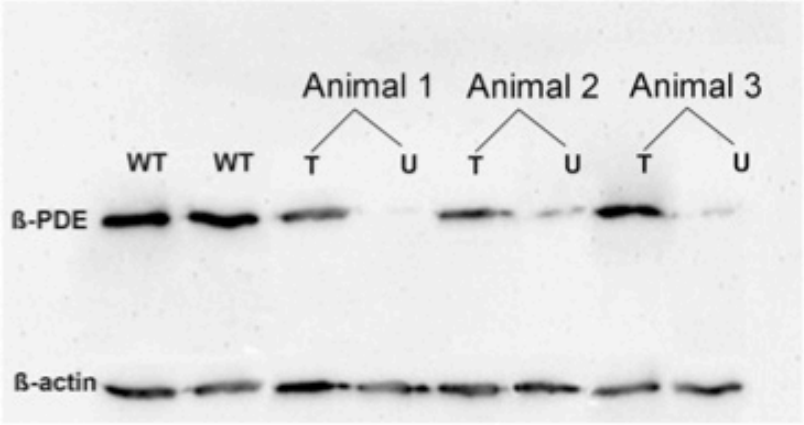

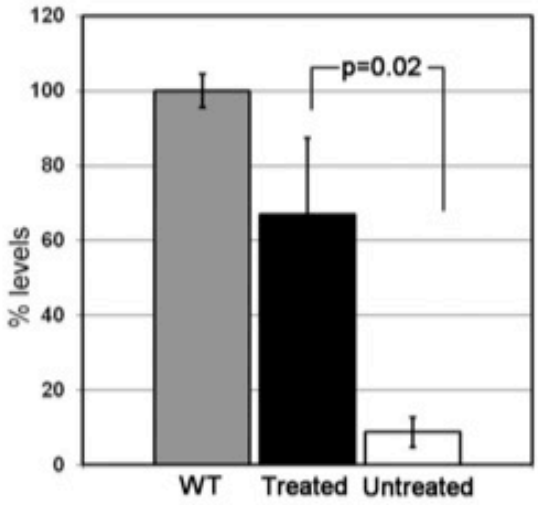

Figure 4.11. Western blot analysis of retinal homogenates from *Aipl1 h/h* mice treated with AAV2/8-CMV-*Aipl1* followed by constant light exposure for 21 weeks.

(A) At 21 weeks, western blot of retinal homogenates from 3 pairs of treated and untreated eyes showed preserved β-PDE in the treated eye while untreated eyes showed markedly reduced levels. Beta-actin was used as a loading control.

(B) Quantification of β-PDE from the 3 pairs of samples are shown as mean ± SEM and plotted as percentage of the wild type control. Levels of β-PDE in the treated eyes were approximately 65% of wild type while untreated eyes had about 10% of wild type levels (p=0.02 treated vs untreated)

4.6 Effect on subretinal injection of control vector AAV2/8-CMV-gfp in Aipl1 h/h mice with light acceleration.

There have been studies suggesting that mechanical injury can lead to expression of neurotrophic factors [69,70,491]. Consequently, surgical manipulation of the retina including subretinal surgery may result in some short term negative effects such as trauma, or positive effects such as possible trauma-induced neuroprotective effects. To determine whether any positive improvements in AAV2/8-CMV-*Aipl1* injected eyes were due induced by the surgical procedure or the AAV virus itself, rather than by *Aipl1* transgene expression, a further group of 10 *Aipl1 h/h* mice received subretinal injection of a control virus, AAV2/8-CMV-*gfp* in one eye only. The contralateral eyes were not treated to serve as negative controls. The animals were also subjected to constant light exposure from 1 week after the subretinal injections and ERG recordings were performed at various time points to monitor the effects of the procedure.

Statistical analysis of the mean b-wave amplitudes showed that there was no significant difference between treated and untreated eyes at any time point (Figure 4.12) The results obtained at flash intensities of 100 mcds/m^2 and 1000 mcds/m^2 did not differ substantially. Overall, the b-wave amplitudes for both injected and uninjected eyes continued to decrease over time. This was due to the ongoing retinal degeneration caused by the underlying genetic defect. These findings indicate that delivery of a non-therapeutic vector has no influence on photoreceptor survival over the long term.

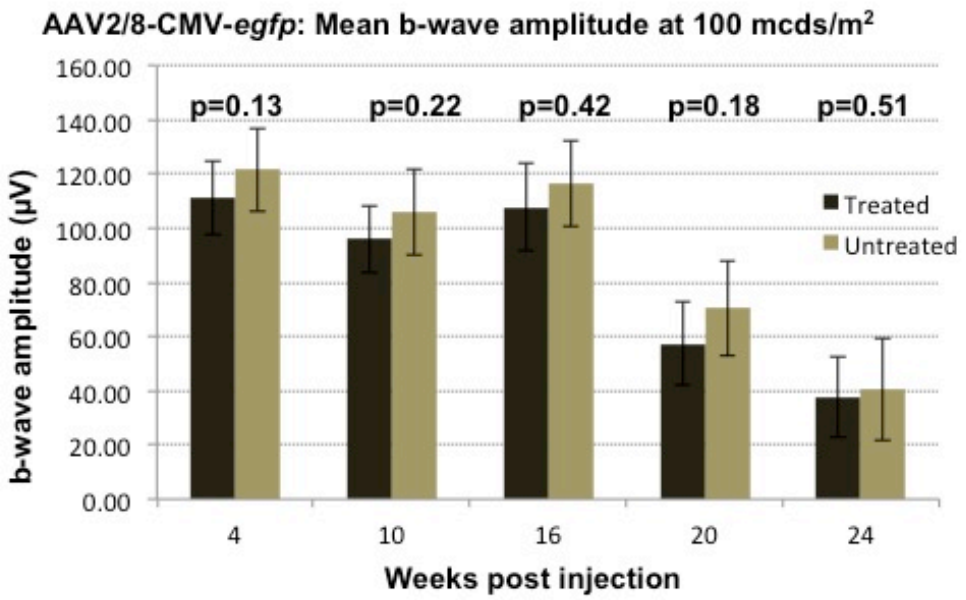

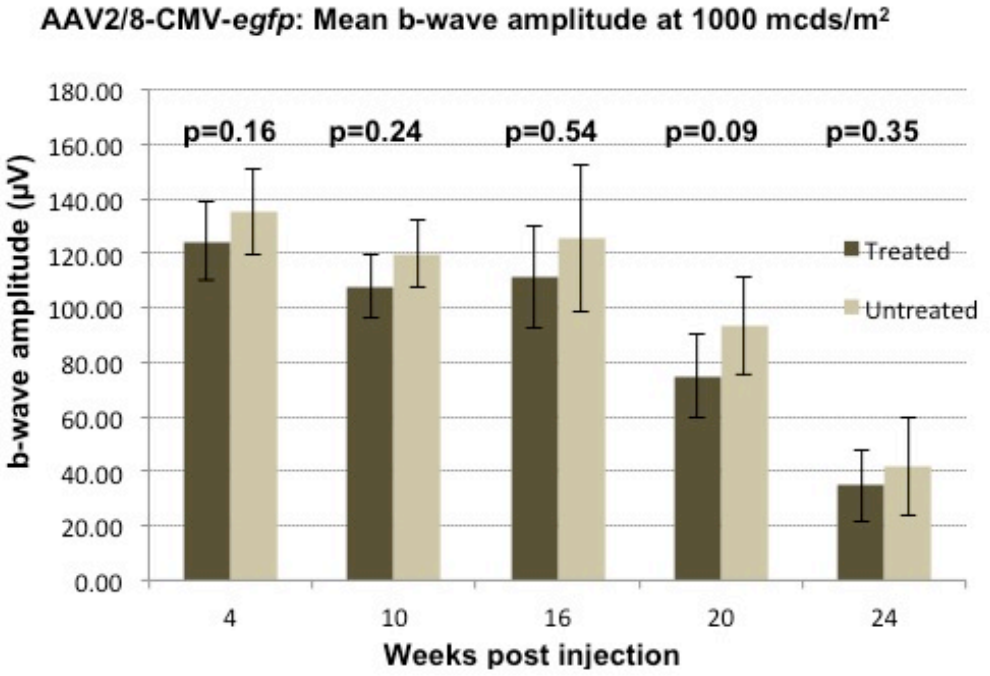

Figure 4.12 Mean ERG b-wave amplitudes in control group of light accelerated *Aipl1 h/h* mice injected with AAV2/8-CMV-*egfp*

No significant difference was seen in the mean ERG b-wave amplitudes of eyes that received subretinal injections of AAV2/8.CMV.*egfp* compared with uninjected eyes at flash intensities of 100 mcd s/m^2 and 1000 mcds/m^2 . Although the injected eyes have lower b-wave amplitudes compared with uninjected eyes throughout the follow up period, these differences were not statisticallly significant. The decrease in amplitudes with time is due to the ongoing retinal degeneration caused by the genetic defect.

4.7 Effect of AAV2/8-mediate AIPL1 overexpression.

While most other AAV serotypes preferentially transduce the RPE following subretinal delivery, a select few such as AAV serotypes 2,5,7,8 and 9 transduce both photoreceptor cells and the RPE after subretinal administration[28,508][18]. In many gene transfer studies, AAV2/5 was considered to be the most efficient vector for photoreceptor gene transfer before the discovery of novel serotypes such as AAV 7,8 and 9[18]. These novel serotypes are far more superior in terms of transduction efficiency and also mediate several fold higher levels of transgene expression. In contrast to AAV2/2 and AAV2/5 which have a higher tropism for the RPE, AAV2/8 demonstrates equal tropism for RPE and photoreceptor cells and results in 6-8 fold greater transgene expression in photoreceptor cells[18][348]. Consequently, AAV2/8 and AAV2/7 (AAV2/9 is less effective than the former two serotypes) are thought to be the most suitable vectors for treating photoreceptor gene defects[18], which cause the majority of hereditary retinal dystrophies. In this study, we elected to use AAV2/8 in combination with a CMV promoter, and we rationalized that the levels of AAV2/8 mediated *Aipl1* expression would be expected to exceed endogenous levels.

It would be important to determine whether overexpression of *Aipl1* in the retina would affect retinal function, and also whether the expression of *Aipl1* in cells such as the RPE that do not normally express *Aipl1* has any deleterious effects. To do this, 7 wild type C57B/6 mice received subretinal injections of AAV2/8-CMV-*Aipl1* in one eye only. Functional assessments were performed at regular time points using dark adapted scotopic ERG recordings obtained simultaneously from injected and uninjected eyes. A representative ERG intensity series from a wild type mouse at 24 weeks following injection of AAV2/8-CMV-*Aipl1* is shown in Figure 4.13A. The amplitudes and waveform of the ERG recordings did not differ substantially between injected and uninjected eyes. Statistical analysis of the mean b-wave amplitudes showed no significant difference between injected and

uninfected eyes (Figure 4.13B). After ERG recordings, all animals were sacrificed and their eyes processed for semithin sections. The retinal morphology and histology of eyes which received the vector injection was normal and similar to the contralateral eyes which were uninjected (Figure 4.14). These findings indicated that the high levels of *AIPL1* expression in the retina and the additional *Aipl1* expression in the RPE cells had no negative effects.

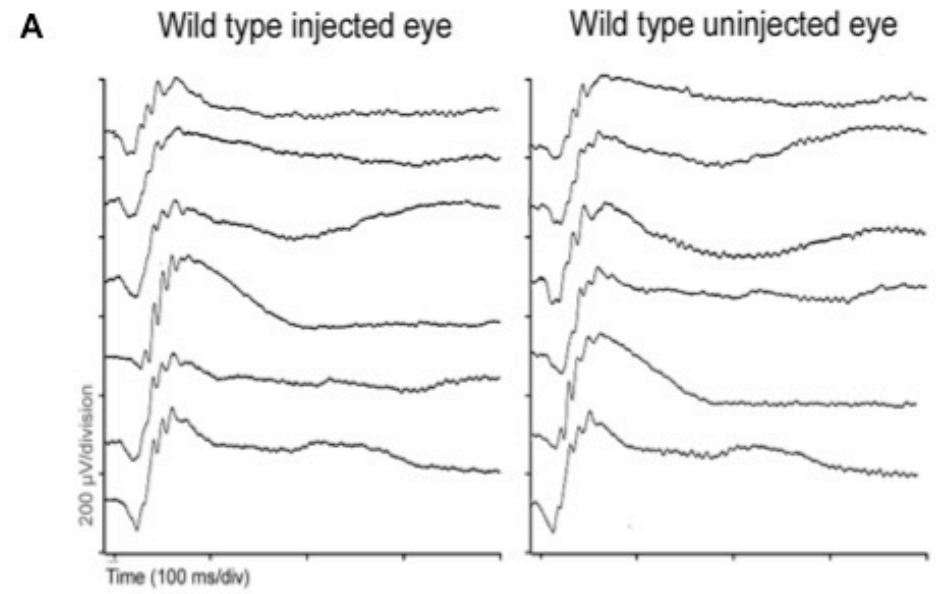

Figure 4.13A ERG intensity series and mean b-wave amplitudes of wild type mice that received a unilateral subretinal injection of AAV2/8-CMV-*Aipl1*.

ERG intensity series recorded from a single wild type mouse that received subretinal injection of AAV2/8-CMV-*Aipl1* in one eye. There is no noticeable difference in the amplitude or shape of ERG responses between the injected and uninjected eye.

B

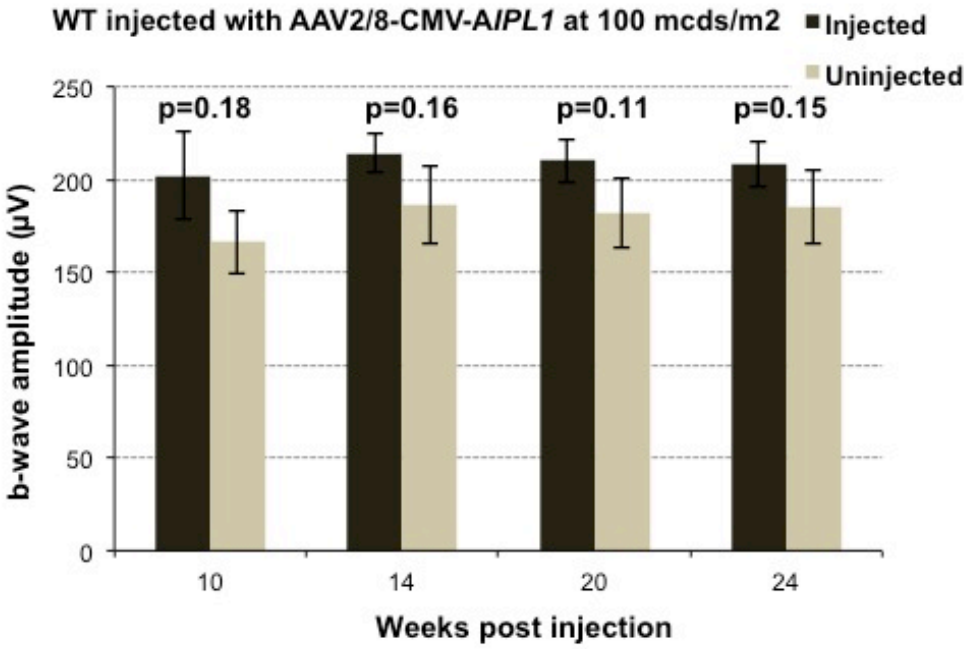

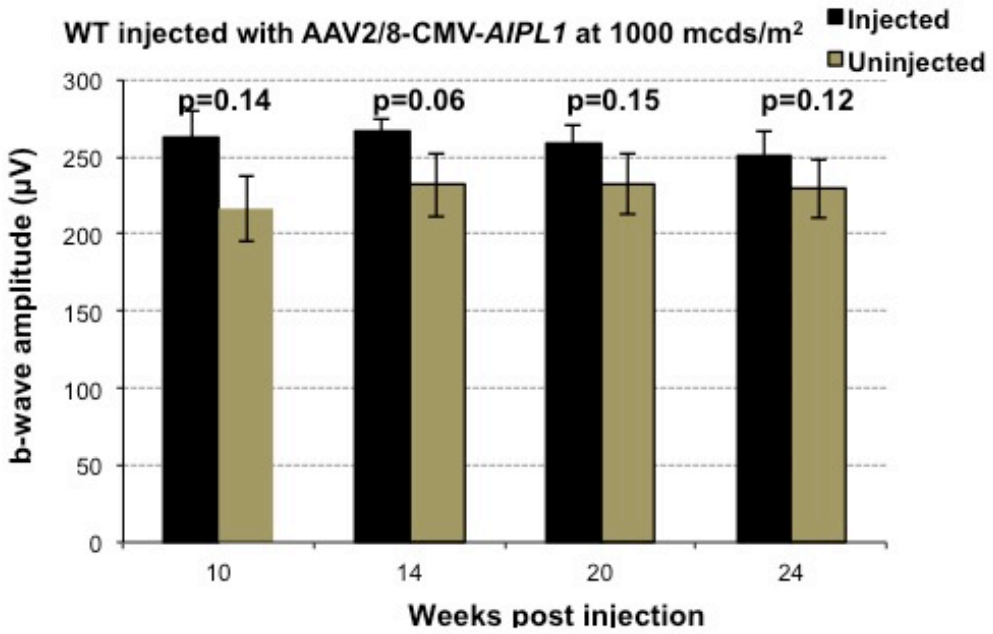

Figure 4.13B. Mean ERG b-wave amplitudes of wild type mice that received unilateral subretinal injection of AAV2/8-CMV-*Aipl1*.

Comparison of the mean ERG b –wave amplitudes from injected and uninjected eyes of wild type mice which received subretinal injection of AAV*2/8-CMV-Aipl1 is* shown. Paired t-test analysis showed that there was no significant difference in the b-wave amplitudes of injected compared with uninjected eyes at flash intensities of 100 and 1000 mcds/m^2 throughout the various time points. Error bars +/- SEM.

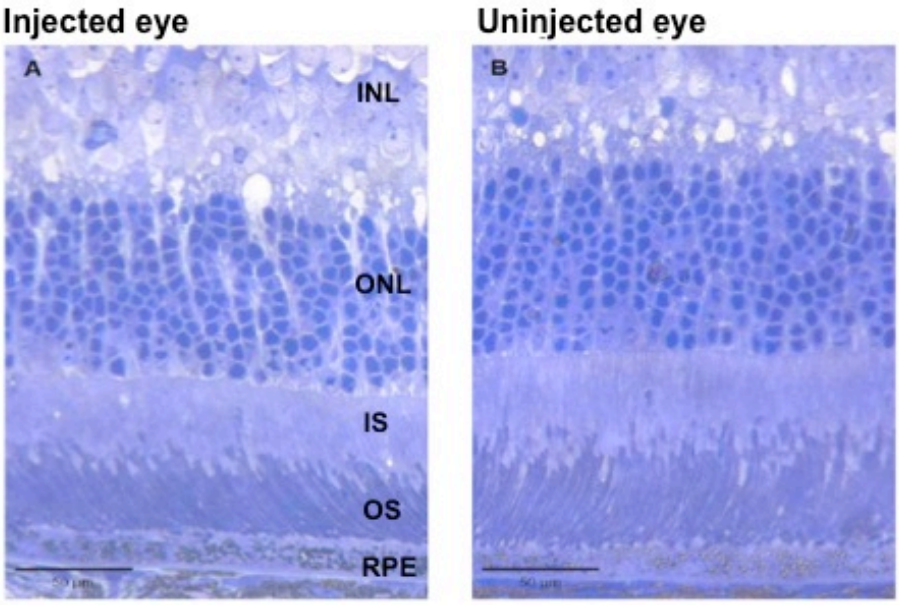

Figure 4.14 Semithin sections of retinas taken from a wild type mouse that received a unilateral subretinal injection of AAV2/8-CMV-*Aipl1*.

Twenty four weeks after subretinal injection of AAV2/8-CMV-*Aipl1* into wild type mice, the injected and uninjected eyes were taken from a single mouse and analysed histologically. The additional expression of *Aipl1* in photoreceptor and RPE cells did not alter retinal morphology in the injected eye (A). The contralateral eye served as an uninjected control (B). There was no obvious difference in the retinal morphology between the two.

INL=inner nuclear layer, ONL=outer nuclear layer, IS=inner segments, OS=outer segments, RPE=retinal pigment epithelium, size bars=50 μm.

4.9 Effects of AAV2/8-mediated gene replacement in the Aipl1 -/- mice

Since an AAV2/8 vector proved effective for mediating gene replacement therapy in the light accelerated *Aipl1 h/h* model, we proceeded to evaluate the efficacy of AAV2/8-CMV-*Aipl1* mediated gene replacement therapy in mice that are completely deficient in AIPL1. The *Aipl1 -/-* mouse is homozygous for a targeted disruption in Aipl1 and has an extremely fast degeneration, in which complete loss of photoreceptor cells is seen by 3 weeks of age (see chapter 1). Because of the early onset of photoreceptor degeneration, these animals were treated at an earlier age,at postnatal day 12 (P12). A total of 6 *Aipl1 -/-* mice received subretinal injections of AAV2/8-CMV-*Aipl1*. Each animal received double subretinal injection in the superior and inferior hemispheres of the retina in one eye only, with the contralateral eye left uninjected as an internal control. Following subretinal injections, assessments of retinal function in the form of ERG and morphological analysis of histology and immunohistochemistry were performed at earlier timepoints, given the rapid nature of the degeneration. To compare the efficacy of AAV2/2 and AAV2/8, a further group of *Aipl1 -/-* mice received with subretinal injections of AAV2/2-CMV-*Aipl1.*

Immunohistochemistry of treated and untreated *Aipl1 -/-* retina was performed at 16 days post injection, when the mice were 28 days old (Figure 4.15). In untreated *Aipl1 -/-* mice the ONL is completely absent, but in mice that had received AAV2/8-CMV-*Aip1*, we observed a thick ONL with good preservation of retinal layers. Strong immunofluorescence for AIPL1 was seen in the inner segments, accompanied by strong immunofluorescence for β-PDE in the outer segments of treated retina. In contrast, AIPL1 and β-PDE immunofluorescence were both absent in untreated eyes (Figure 4.15).

Semithin sections of retina were taken from 4 week old mice at 19 days post injection (Figure 4.16). These sections showed that treatment with the vector resulted in substantial preservation of photoreceptor cells. In untreated eyes,

no photoreceptor cells or outer segments could be seen. The inner nuclear layer was seen lying adjacent to the RPE in untreated eyes and there was marked retinal thinning. In contrast, treated retina exhibited the presence of long, densely packed outer segments and showed good preservation of the outer nuclear layer of about 6-7 rows of photoreceptor nuclei.

ERG recordings are normally extinguished by P18 in the *Aipl1* -/- mouse. ERG analysis was performed on the procedured mice at 16 days following subretinal injection with AV2/8-CMV-*Aipl1* when the animals were postnatal 28 days. Single flash scotopic and photopic responses were recorded simultaneously from treated and untreated eyes of each animal (Figure 4.17A). Scotopic and photopic ERG responses from untreated eyes showed flat ERG tracings. In contrast, treated *Aipl1* -/- eyes exhibited good scotopic and photopic ERG amplitudes approximately 2 weeks after treatment (Figure 4.17). The difference in mean scotopic ERG b-wave amplitudes between treated and untreated eyes was statistically significant (p=0.03; mean b-wave treated = 243.5 ± 67.2 μV, mean b-wave untreated = 6.25 ± 3.9 μV, n=4). Further ERG analysis was performed at later timepoint of 6 weeks post injection when the animals were approximately 8 weeks old. At this timepoint, treated eyes continued to maintain significantly higher ERG b-wave amplitude compared to untreated eyes (p=0.006; mean b-wave treated = 234.7 ± 51.1 μV, mean b-wave untreated = 28.8 ± 5.6 μV, n=6). At 3 months post injection when the animals were 14 weeks old, untreated eyes had no ERG response (mean b-wave untreated = 0 μV, n=3), while treated eyes showed a substantial ERG response (mean b-wave treated = 181.7 ± 39.4 μV, n=3).These findings indicate that early treatment using AAV2/8-CMV-*Aipl1* is able to significantly improve photoreceptor function and delay retinal degeneration in the *Aipl1* -/- mouse. ERG analysis of *Aipl1 -/-* mice injected with AAV2/2-CMV-*Aipl1* did not show any evidence of photoreceptor rescue (Figure 4.17B). These mice were also injected at the same time point of P12 and neither the treated nor untreated eyes showed any ERG responses at P28 (16 days post injection).

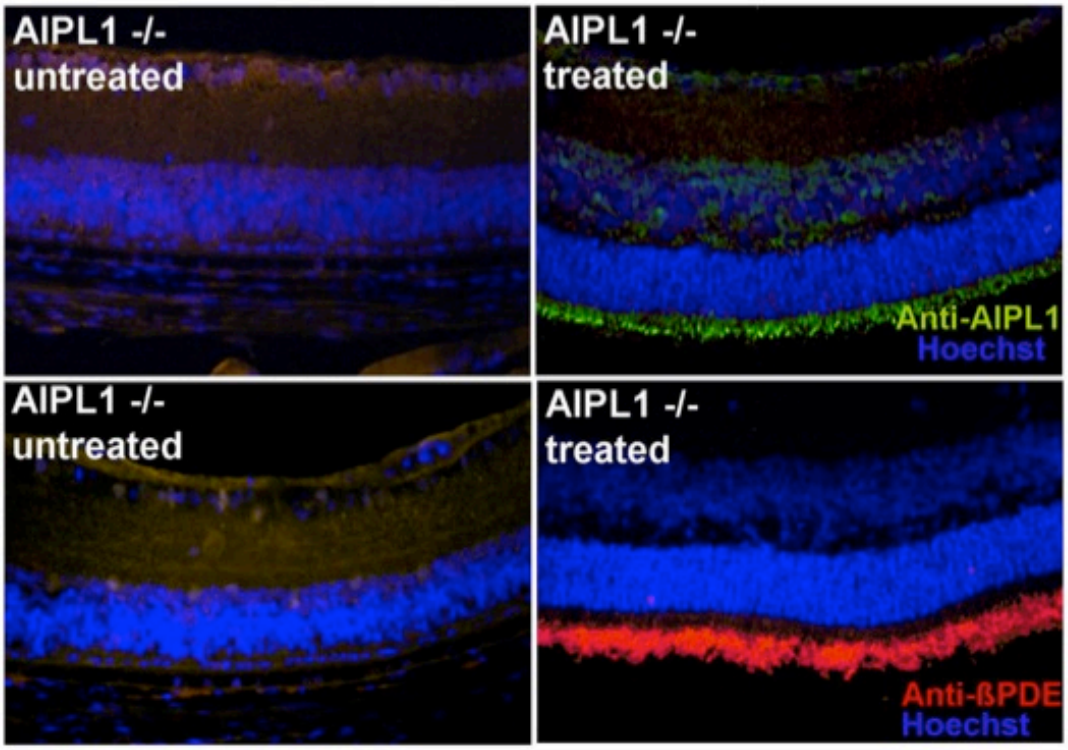

Figure 4.15. Immunohistochemistry of *Aipl1* -/- retina following subretinal injection of AAV2/8-CMV-*Aipl1*.

The untreated eye at 16 days post-injection show no AIPL1 or β-PDE on immunostaining. The treated eye shows strong AIPL1 immunofluorescence (green) in the inner segments and β-PDE immunofluorescence (red) in the outer segments. The outer nuclear layer is absent in the untreated eye while there is clear preservation of the outer nuclear layer in treated eyes.

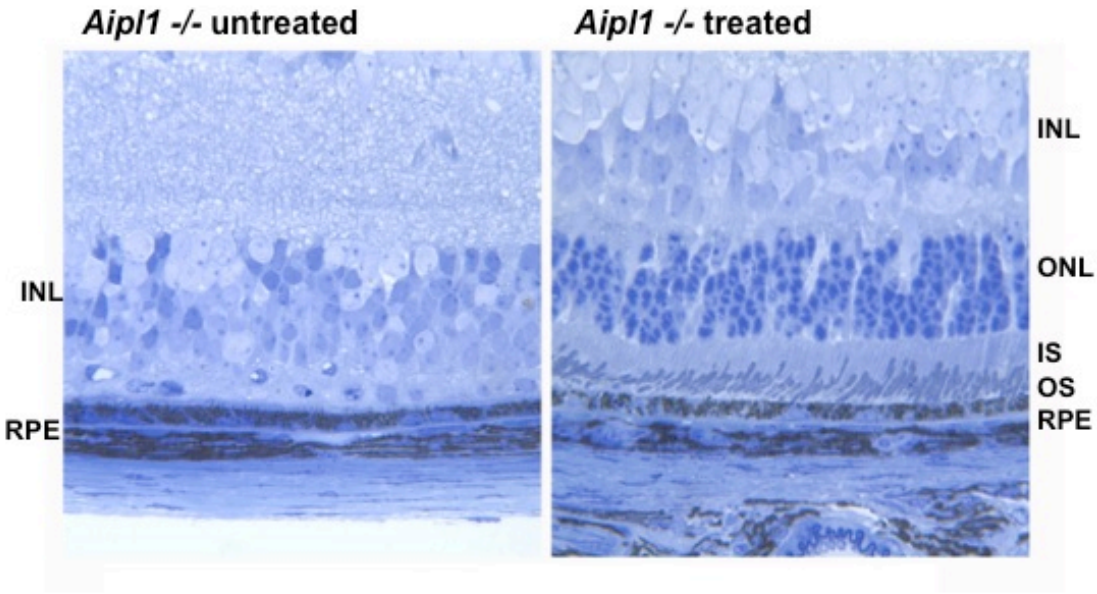

Figure 4.16 Morphological analysis of *Aipl1* -/- retina following subretinal injection of AAV2/8-CMV-*Aipl1*.

Semithin sections were taken at 19 days following subretinal injection from a procedured *Aipl1* -/- mouse. The outer nuclear layer (ONL) is absent in the untreated retina. The treated retina shows presence of photoreceptor outer segments (OS) and six to seven rows of photoreceptor cell nuclei in the outer nuclear layer (ONL).

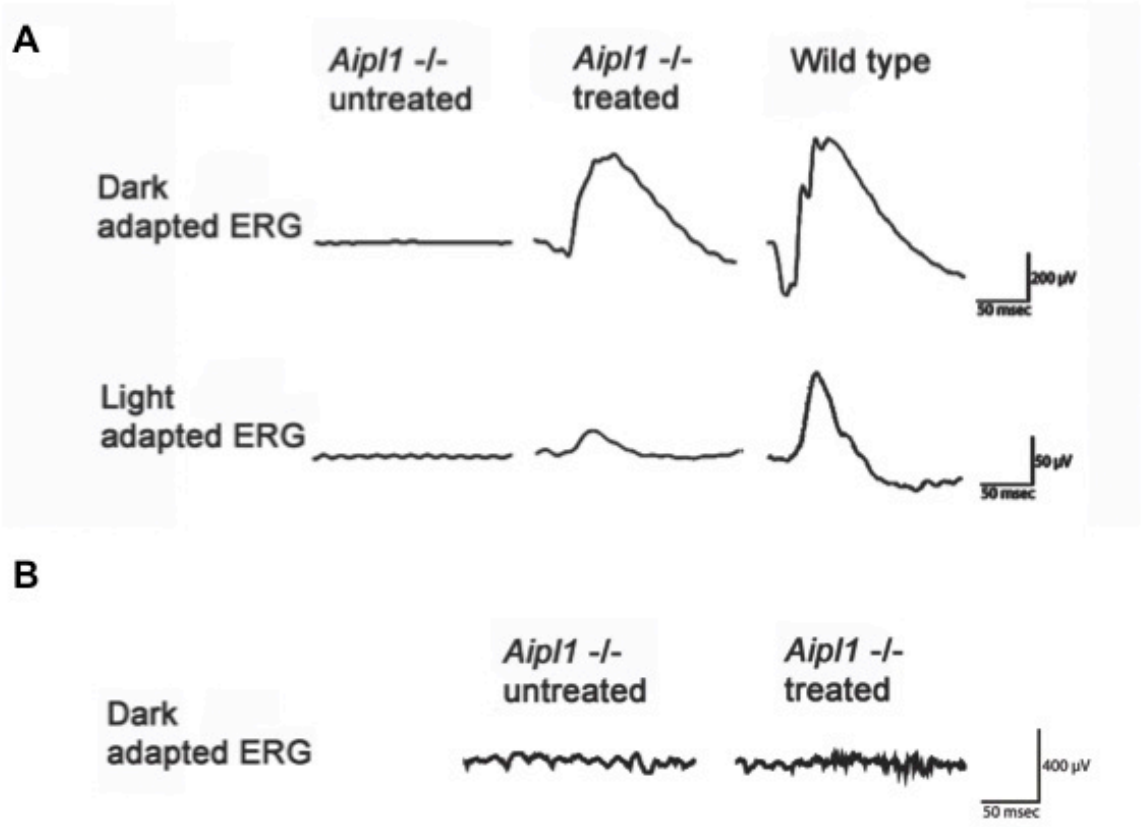

Figure 4.17 Representative dark and light adapted ERG waveforms from the untreated and treated eyes of a single *Aipl1* -/- mouse at 16 days post injection.

A. Single flash scotopic and photopic responses were obtained simultaneously from the treated and untreated eyes of an *Aipl1* -/- mouse at 16 days after subretinal injection with AAV2/8-CMV-*Aipl1*. The ERG is extinguished in the untreated eye while there is good b-wave amplitude from the treated eye. An ERG tracing from a wild type mouse is shown for comparison.
B. ERG recordings from an *Aipl1* -/- mouse injected with AAV2/2-CMV-*Aipl1* at 16 days post treatment. Both treated and untreated eyes did not show any ERG responses.

4.10 Discussion

The window of opportunity in a disease model is created by the balance between time required for vector-mediated expression and the rate of photoreceptor degeneration. In models of rapid degeneration, gene replacement therapy using AAV2/2 vectors is unlikely to be successful since most of the photoreceptors are lost before sufficient transgene expression can take place. By choosing a more suitable, faster vector to treat a rapid degeneration, the window of opportunity for intervention can be increased. This study describes the first use of an AAV2/8 vector to treat a murine model of retinal degeneration. Compared with AAV2/2 (described in Chapter 3), AAV2/8 is much more efficient at transducing the retina. We evaluated gene replacement therapy using AAV2/2 and AAV2/8 vectors and found that the most effective rescue was achieved using AAV2/8 vector.

Under constant light exposure, the *Aipl1 h/h* mice exhibited a more severe and accelerated form of retinal degeneration; a 2-3 fold increase in rate of degeneration is seen with loss of 85% of photoreceptor cells by 5 months. This suggests the photoreceptor cells in *Aipl1 h/h* mice could be more sensitive to light damage, as wild type mice kept under identical conditions showed no increased loss of photoreceptor cells. For effective treatment of this animal model, a vector with faster transduction kinetics was required. Normally, all photoreceptor cells are lost by the time *Aipl1 -/-* mice are 3 weeks old. Following AAV2/8-mediated gene replacement in *Aipl1 -/-* mice, there was significant preservation of photoreceptor cells and retinal function for over 3 months. This represents the most effective rescue of a rapid retinal degeneration to date. To ensure adequate transgene expression before a critical mass of photoreceptor cells were lost, the *Aipl1 -/-* mice were treated at a much younger age, at postnatal day 12. In doing so, the potential benefit of gene transfer had to be weighed against the risks of retinal damage from surgical manipulation in younger mice. At P12, mice have a fully developed retina and have opened their eyes, thus facilitating subretinal injections. AAV2/8-mediated gene expression should occur by P15-P16, at this time there would still be surviving photoreceptor cells in *Aipl1 -/-* mice. Superior

results using AAV2/8 may have resulted from its higher transduction efficiency and higher levels of maximal transgene expression which have been previously described [18,348]. More importantly, the rapid onset of gene expression may have been vital in preserving photoreceptor cell survival in the *Aipl1 -/-* mouse. We observed photoreceptor rescue with AAV2/8 but not with titre-matched AAV2/2 in the *Aipl1 -/-* mouse, this is most likely because photoreceptor degeneration would have been completed by the time maximal transgene expression was achieved with AAV2/2.

In the experiments described in this study, we injected a single eye of each animal with a therapeutic vector, leaving the contralateral uninjected eye to serve as an internal control during follow up assessments. Similar studies by other groups have used control injections (subretinal injections of a control vector) into the contralateral eye to detect trauma-induced neuroprotective effect. Since the statistical significance in differences between treated and untreated eyes were of such large magnitude and seen at long term time points, it is unlikely that hypothetical surgically-induced neuroprotection has any major contribution to differences observed. Whilst injection of a control vector into the contralateral eye will allow assessment of the therapeutic transgene in isolation, it is important to leave the contralateral eye as an untreated control as the aim of this study is to provide a tangible improvement in retinal function and morphology after treatment, which also includes the delivery of the treatment. Moreover, injecting the contralateral eye may increase the risk of creating false positive results, where injection of therapeutic vector results in better function than control injections, and also in an undetected worsening because of trauma-related decrease in retinal activity. Therefore, we injected one eye only in each animal with the therapeutic or control vector. In the control group of animals consisting of *Aipl1 h/h* mice that received unilateral subretinal injection of AAV2/8-CMV-*gfp* or AAV2/2-CMV-*gfp*, there was no significant differences seen in ERG amplitudes or cell count when comparing the injected eye with the contralateral uninjected eye. Further groups of animals comparing injections of PBS with untreated eyes (section 3.6.2), showed that injection-related trauma had no significant positive effect on retinal function.

Because AIPL1 is required for the biosynthesis/stability of PDE, no PDE accumulates in the photoreceptors of *Aipl1 -/-* mice and the decline in PDE levels is proportional to the reduced level of AIPL1 in *Aipl1 h/h* mice. Elevated PDE levels would be ameliorative to the downstream effects of disease at the molecular level in this disease model, and therefore would be expected to alleviate the disease phenotype. Hence, in preclinical animal studies, a useful and quantifiable outcome measure which is predictive of successful treatment would be an increase in PDE levels in rod photoreceptors of treated animals. Treatment with AAV2/8-CMV-*Aipl1* in light accelerated *Aipl1 h/h* mice led to increased production of AIPL1 in photoreceptor cells and subsequently increased levels of cGMP-PDE in photoreceptor cells as demonstrated on Western blotting (Section 4.6), and localised correctly to photoreceptor outer segments. In contrast, untreated eyes had almost undetectable PDE levels. The difference in PDE levels between treated and untreated eyes may partly be due to the loss of photoreceptor cells in untreated eyes. At 21 weeks post injection, the mean level of PDE in treated eyes was 65% of wild type while untreated eyes had 10% of wild type levels. In order to compare the levels of PDE expression in single photoreceptor cells with and without treatment, the data was corrected for the average number of cells in the treated and untreated eyes at that time point. The PDE expression levels in the samples were normalized to total protein content in the eye (β-actin was used as normalization standard) and hence, is proportional to the number of photoreceptor cells present. Using a photoreceptor-specific protein such as alpha-transducin as normalization standard, it would have been possible to directly compare the levels of PDE expression in photoreceptor cells.

In the studies presented here and the preceding chapters, ubiquitously active CMV promoter was used to drive transgene expression. The advantage of a ubiquitous viral promoter such as CMV is its high expression levels, the ability to drive expression in both rods and cones and its wide use in animal studies. For clinical application, a tissue-specific promoter would be more appropriate because patients may have deleterious effects secondary to

ectopic expression of the transgene. Particularly in situations where photoreceptors are the targets for gene delivery, a non-specific promoter would also result in the ectopic expression of the transgene in the RPE. This could have unknown long term effects, and is therefore undesirable for clinical gene therapy in humans. It has been recently shown that AIPL1 is essential for the viability and function of cone photoreceptors as well as rods, and that photoreceptor disease due to *AIPL1* gene mutations is caused by an insufficiency of rod and cone PDEs [232]. Thus an effective therapy for this condition should aim to restore rod and cone PDE biosynthesis, through reconstituting AIPL1 function to a level sufficient to sustain photoreceptor function and survival. The ideal vector design for AIPL1 gene therapy should be one with well-defined promoter/enhancer elements with uniform, photoreceptor-specific transcriptional activity and target both rods and cones in order to fully restore retinal function. AAV vectors have a relatively small carrying capacity for foreign DNA that typically does not exceed 4.5 kb. The limited carrying capacity of AAV vectors dictates that such promoters ideally be short, no more than several kilobases in length, to allow for packaging of the transgene. A number of promoters such as the derivatives of rod and cone opsin promoters have been validated as efficient and specific for driving expression in rods and cones respectively[160,161,263,487]. More recently, a human rhodopsin kinase promoter fragment was characterised and shown to be relatively small in size [512,513]. Packaged into an AAV2/5 vector, the rhodopsin kinase promoter was shown to be specifically active in both rods and cones but not in the RPE or the inner retina, driving expression at a relatively high level [230]. For human gene therapy purposes, constructs incorporating promoters such as these may be more suitable for AAV-mediated gene delivery. A further issue of importance in the context of human gene therapy is the level of expression that is produced from the therapeutic vector. Ideally, the level of vector-mediated expression should closely match that of endogenous levels. This can be addressed by choosing a suitable promoter and one that is human-derived (see Chapter 5 Final discussion).

Combining the results from this chapter with those in the previous one, we demonstrated that mouse models of AIPL1 deficiency with very different rates of disease progression respond favourably to *AIPL1* gene replacement therapy. AAV-mediated transene expression in the *Aipl1* murine models appears stable and the efficacy of rescue long-lasting. In the hypomorphic mutant, AAV2/2 and AAV2/8 mediated gene expression remained in the retina at 50 weeks and 21 weeks post injection respectively and the photoreceptor cells were well maintained at that age. Similarly, in the *Aipl1 -/-* model, AAV2/8 mediated delivery of the *AIPL1* gene appears to be stable for at least 3 months, which is the latest time point examined. The results together provide further evidence to support gene replacement therapy for the treatment severe inherited retinal dystrophies caused by defects in *AIPL1.*

5 Screening of patients with early-onset severe retinal dystrophy for mutations in AIPL1 and characterization of the phenotype

5.1 Introduction

Mutations in *AIPL1* have been estimated to account for approximately 7% of LCA cases [442]. The phenotype of *AIPL1* mutations is variable as it has also been associated with autosomal dominant cone-rod dystrophy and juvenile retinitis pigmentosa [103,440,442]. The development of potential targeted therapies for the treatment of degenerative retinal diseases has heightened the necessity for accurate molecular diagnoses. There is a need for a comprehensive molecular screen not only to establish the causative gene for the possibility of treatment in the future and further the understanding of the molecular pathways involved in the pathogenesis of the retinal disease, but also to distinguish between the types of degenerative retinal diseases. Ultimately, the vector system and gene therapy strategies developed in preceding chapters to target photoreceptors and prevent photoreceptor degeneration in the animal models of AIPL1–deficiency are aimed at treating RP and LCA due to mutations in *AIPL1*. The results presented in chapters 3 and 4 suggest that defects within this gene are suitable targets for the development of gene therapy approaches in patients. Any therapeutic intervention is more justified in a severe disease where the potential benefits far outweigh the risks; patients with *AIPL1*- related retinal degeneration generally have a severe phenotype with peripheral field loss and frequently also involvement of central vision causing marked visual loss early in life. In order to move AAV-mediated photoreceptor gene transfer from bench to bedside, identification of patients and characterization the disease caused by mutations in *AIPL1* is required. The identification of the

molecular basis of LCA is challenging, given the high genetic heterogeneity of LCA and the absence of clinical landmarks in most cases that may help distinguish one form of LCA from another. The molecular diagnosis and systematic clinical characterization of patients is instrumental for the selection of appropriate patients for gene therapy clinical trials and will enable the natural history and phenotype of the disease to be better established, especially since this is still not well ascertained. Additionally, this will contribute towards determining clinical baselines and assessment targets to guide treatment and facilitate genetic counseling of candidate patients.

5.1.1 Mutations of AIPL1

To date, there are 22 known disease-causing mutations in *AIPL1* but it is anticipated that there may be more mutations to be discovered by screening a wider population that includes patients with LCA and early onset retinal dystrophies. Table 5.1 summarizes the currently known disease-causing mutations and polymorphisms in *AIPL1* (http://www.retina-international.com/sci-news/aipl1mut.htm).

Table 5.1. AIPL1 mutation database. Current known mutations and benign variants of AIPL1 updated from March 2009. (extracted from HGMD)

Phenotype	Exon	Base change	Protein	Description	Accession number
ADCRD	6	del 1053-1064	Pro350Δ12	12 base pair deletion within hinge region.	CD003288
LCA4	1	c.40A>G	Lys14Glu	Missense mutation.	CM034773
LCA4	2	c.116C>A	Thr39Asn	Missense mutation	CM034201
LCA4	2	c.126T>A	Cys42X	Nonsense mutation.	CM042287
LCA4	2	c.211G>T	Val71Phe	Missense mutation.	CM040669
LCA4	2	c.236T>C	Met79Thr	Uncommon missense mutation.	CM003225
LCA4	2	c.244C>T	His82Tyr	Misssense mutation.	CM034202
LCA4	2	c.264G>A	Trp88 X	Nonsense mutation.	CM003226
LCA4	Intron 2	c.277-2A>G	IVS2-2A>G	Splice site mutation.	CS003285
LCA4	3	c.286G>A	Val 96 Ile	Uncommon missense mutation.	CM003227
LCA4	3	c.341C>T	Thr114 Ile	Missense mutation.	CM003228
LCA4	3	c.401A>T	Tyr134Phe	Missense mutation.	CM042288
LCA4	4	c.487C>T	Gln163 X	Nonsense mutation.	CM003229
LCA4	4	c. 589G>C	Ala197Pro	Missense mutation.	CM003230
LCA4	5	c.715T>C	Cys 239 Arg	Missense mutation.	CM000002
LCA4	5	c. 784G>A	Gly262Ser	Missense mutation.	CM003231
LCA4	6	c.809G>A	Arg270His	Missense mutation	CM074007
LCA4	6	c.834G>A	Trp 278 X	Nonsense mutation.	CM000003
LCA4	6	c.905G>T	Arg 302 Leu	Missense mutation.	CM003232
LCA4	6	del1010-1011	Ala336Δ2	2 base pair deletion.	CD001471
LCA4	6	ins12bp1122-1123	Pro374ins12 bp	12 base pair insertion	CI056866
LCA4	6	c.1126C>T	Pro376Ser	Missense mutation.	CM003233
Polymorphism	1	c.111T>C	Phe 376Phe		

Polymorphism	**2**	**c.234C>T**	**Ser 78 Ser**
Polymorphism	**2**	**c.267C>T**	**Cys 89 Cys**
Polymorphism	**3**	**c.300G>A**	**Leu 100 leu**
Polymorphism	**4**	**c.516T>C**	**His 172 His**
Polymorphism	**4**	**c.651G>A**	**Pro 217 Pro**
Polymorphism	**4**	**c.765T>C**	**Asp 255 Asp**

To date there have been three large studies of *AIPL1* mutation analysis in LCA patients. In the first study, *AIPL1* mutations were found in 11 families following screening of 118 probands [442] In another study, a comprehensive mutational analysis of all LCA-associated genes in 179 unrelated LCA patients identified *AIPL1* mutations in 6 (3.4%) patients [174]. Finally, the largest study described 26 probands with *AIPL1* mutations from a cohort of 303 unrelated patients (8.6%)[103]. The majority of the *AIPL1* alleles which have been identified so far represent null (nonsense, frameshift, or severe splice site) mutations. Most of the current reported disease-causing *AIPL1* mutations appear to lie within the sequences encoding the 3 tetratricopeptide repeat (TPR) motifs which are regions of high sequence conservation across different species. A nonsense mutation in the TPR III domain (W278X) is the most frequently reported mutation in LCA patients. It was originally found in consanguineous Pakistani families and may represent a founder mutation[97,440,442]. Despite the lesser degree of conservation in the proline-rich region, a 4 amino acid deletion in this hinge region P351^12bp has been reported in 2 unrelated patients with autosomal dominant cone-rod dystrophy and juvenile retinitis pigmentosa [442] suggesting that *AIPL1* mutations may also account for other types of inherited dystrophies.

Patients with *AIPL1*-related LCA have been described in current literature to have a particularly severe phenotype, characterized by marked early visual impairment, non-detectable fields and ERGs, optic disc pallor, maculopathy

in most patients, peripheral bone-spicule-like pigmentation. There is also a significant prevalence of keratoconus and cataracts [103]. Some of the mutations lead to a truncation of the reading frame and are not expected to produce a functional protein. Other reported mutations such as missense mutations may not abolish protein function completely and may produce a milder phenotype. A small number of patients with milder disease than LCA associated with *AIPL1* mutations have been reported. In a previous study, screening of a large cohort of retinal degeneration patients led to the observation that three probands from two families had a heterozygous 12 bp deletion in *AIPL1.* They were diagnosed with cone-rod dystrophy and juvenile RP but their phenotypic details were not provided[441]. Another recent study identified an individual with compound heterozygous mutaton in *AIPL1* who had a later-onset protracted course of disease and was diagnosed with retinitis pigmentosa[204]. Thus further screening of a large cohort of patients with RP or cone-rod dystrophy may identify more such patients with residual AIPL1 function.

Patients who are homozygous or compound heterozygous for a null mutation are reported to have more severe disease than patients who are homozygous for missense mutations. In a study of 26 probands with *AIPL1* mutations, 2 patients who were compound heterozygotes for missense mutations T114I and P376S retained visions of 20/400 and had moderate retinopathy while 9 patients who were homozygous for W278X had vision of hand motion or light perception and severe retinopathy[103]. In another study which identified 7 *AIPL1* patients from a cohort of 110 LCA patients, patients with heterozygous missense mutations were found to have better visual acuity[151]. Compared to the other LCA genotypes, there is a high prevalence of maculopathy in patients with AIPL1 mutations[103]. This may not be surprising as AIPL1 is also expressed in cones and is necessary for the continued survival of cone photoreceptors[232] . More interestingly, the majority (11 out of 16) of patients noted to have macular atrophy harboured a premature stop codon mutation in either homozygous or heterozygous states. The authors of the study noted there was a high incidence of keratoconus noted in patients with a homozygous sequence change and

suggested that this observation may be significant. The presence of significant keratoconus may be associated with severe mutations as most of these patients the study also had severe macular involvement and pigmentary retinopathy. There have also been individual reports describing unusual notable phenotype found in patients with *AIPL1* mutations such as abnormal retinal vascular morphology [183].

Aside from the phenotypic variability seen in *AIPL1* patients with different mutations, variability has been reported even when there is a common molecular genetic aetiology in a family. In a study of 4 consanguineous Pakistani families with a severe form of LCA due to a homozygous nonsense mutation in *AIPL1*, W278X, a spectrum of clinical findings were observed among the affected family members; vision ranged from hand motions to no perception light, variable fundal findings with different severity of retinopathy and maculopathy, and variable findings of keratoconus, even amongst members of similar ages [97]. The basis of this phenotypic variability within a mutation has not been completely understood, but environmental influences and possibly other modifier alleles may contribute to these observations.

5.2 Aims

This chapter aims to investigate the prevalence of sequence variants in *AIPL1* in a large cohort of DNA from patients with LCA or autosomal recessive severe childhood-onset retinal dystrophy, and to compare this with that seen in the normal population. By screening these patients for mutations in *AIPL1*, we hope to identify more patients, report any novel mutations and characterize the clinical features associated with the mutations. This project would aims to identify the subset of patients that would be candidates for gene therapy. For this purpose, a panel of 309 probands diagnosed with LCA or early-onset retinal dystrophy (EORD) was screened for mutations in *AIPL1* using a combination of microarray LCA chip analysis (Asper-Ophthalmics) and direct sequencing. Patients with early-onset retinal dystrophy or EORD

are defined as those patients with severe visual loss in early childhood before the age of 5. Sequencing of the total patient panel and half of the control panel was performed by the author. Help was obtained with segregation analysis and sequencing of part of the control panel from Dr Jill Cowing, Dr H Tran and Dr D MacKay.

5.3 Patient panel and demographics

In order to identify patients and families with mutations in *AIPL1*, mutation screening was performed on patients enrolled in a genetic database at Moorfields Eye Hospital. The genetic database used in this study consisted of patients who have been diagnosed with LCA or with EORD and were identified through the genetic ophthalmology clinics and medical retina clinics at Moorfields Eye Hospital. This database included a clinical spectrum of patients with classical LCA whose severe visual impairment was present from infancy, to patients who presented later in childhood and may have overlapping features with retinitis pigmentosa clinically classified as EORD (severe retinal dystrophy symptomatic before the age of 5 years old with an abnormal electroretinogram at the time of diagnosis). The inclusion criteria were: clinical diagnosis of LCA or a severe retinal dystrophy that was symptomatic in childhood, severely reduced or absent ERG at diagnosis and autosomal recessive inheritance. Patients with other known ophthalmological or systemic diseases that share features with LCA or a family history suggestive of autosomal dominant or X-linked recessive disease were excluded. Research procedures were in accordance with institutional guidelines and the Declaration of Helsinki. Ethics committee approval was obtained. All patients and parents were provided with information sheets before informed consent was obtained from all patients or their legal guardians for the provision of clinical information and blood samples for DNA extraction and analysis. All patients also underwent detailed phenotyping which included clinical ophthalmological examination via slitlamp biomicroscopy and indirect ophthalmoscopy, diagnostic electrophysiology,

OCT, Goldmann perimetry, fundus imaging, fluorescein angiography and autofluorescence and measurements of visual acuity and color vision. Optical coherence tomography (OCT) is a non-contact imaging technique that produces high resolution cross sectional images of the retinal architecture based on the differences in optical reflectivity of the different layers. Using time delays in reflected signals, the distance or thickness between different layers of ocular tissues can be measured. The ophthalmological examinations were conducted by R.Henderson, P. Moradi and colleagues at Moorfields Eye Hospital.

The patient panel consisted of 309 probands who have a clinical diagnosis of LCA or EORD, including rod-cone dystrophy and retinitis pigmentosa. The number of DNA samples that were screened and analysed was 326, this consisted of DNA samples from 309 probands and the remaining 17 DNA samples were from relatives of probands who agreed to be part of the study. Amongst the probands, majority, 70% (217/309) of the DNA samples were from Caucasian subjects, of either British or other European backgrounds, 21% (64/309) were of Asian extraction, mostly Pakistani or Indian, 3% (10/309) were of Middle-eastern extraction, 1.6% (5/309) were African, 0.6% (2/309) were Chinese and the remainder were of mixed backgrounds (Table 5.3). The control panel consisted of 96 control DNA samples originating from a control population of randomly selected, non-related UK Caucasian blood donors (ECACC Human Random Control-1 DNA panel).

Of the 309 probands in the panel, 26% were offsprings of consanguineous marriages. One hundred and fourty-nine (149) probands have a diagnosis of LCA, 29 had a diagnosis of early onset retinal dystrophy, 67 were diagnosed as rod-cone dystrophy, 25 were diagnosed with retinitis pigmentosa and 39 with cone-rod dystrophy (Table 5.4).

Table 5.2 Table showing the demographic breakdown of the patient population.

Ethnic group	number	percentage
Caucasian (British, European, Iranian)	217	70%
Asian (Pakistani, Indian, Bangladeshi)	64	21%
Middle-eastern	10	3%
African	5	1.6%
Chinese	2	0.6%
Mixed background/unknown	11	3%
total	309	100%

Table 5.3 Details of the LCA and EORD patient cohort.

Summary of the clinical diagnosis and mean age of diagnosis and onset of disease in the panel of patients .

Diagnosis	Patients (*n*)	Mean age at diagnosis (*y*)	Mean age at onset of symptoms (*y*)
LCA	149	1.0	0.4
EORD	29	3.8	1.8
Rod-cone dystrophy	67	5.0	2.1
Retinitis pigmentosa	25	10.7	7.3
Cone-rod dystrophy	39	5.1	3.5
Total	309		

Abbreviations: LCA-Leber Congenital Amaurosis; EORD-early onset severe retinal dystrophy

5.4 Patient screen and sequencing strategy

A two-stage screening strategy was used. First pass screening for mutations in *AIPL1* was performed using the microarray LCA chip analysis (Asper-Ophthalmics, Tartu, Estonia). Following LCA chip analysis, samples that had not returned any sequence variants or samples that returned only one allelic change on the chip were further analysed by sequencing. The DNA samples were sent to Asper Ophthalmics by R Henderson and P Moradi. The LCA disease chip allows the rapid screening of 423 likely disease-associated sequence variants in the 10 out of 13 genes known to be associated with LCA or early onset retinal dystrophy. These are *AIPL1, RPGRIP1, GUCY2D, RPE65, CRX, CEP290, RDH12, LRAT, MERTK* and *TULP.* The chip currently contains 32 *AIPL1* sequence variants, although not all of these sequence variants are listed in official mutation databases. A list of the *AIPL1* sequence variants that are contained in the LCA disease chip is shown in Table 5.4. DNA samples that did not return any mutations in any of the LCA genes using the microarray disease chip or samples in which only one *AIPL1* disease allele was found were subjected to bidirectional sequencing of *AIPL1,* in order to identify any novel mutations or the possibility of a second allele in the latter. The entire AIPL1 coding sequence was assayed, including the intron/exon junctions.

Direct sequencing of *AIPL1* was performed on genomic DNA extracted from peripheral blood leukocytes of patients' blood samples according to methods previously described (Chapter 2). The DNA samples were subjected to PCR to amplify the coding exons of *AIPL1*, except for exon 6 in which only the coding part of the exon was amplified. The primers used were designed to encompass the entire coding sequence and the flanking the splice acceptor and donor sites of each coding exon. Since the promoter region for AIPL1 is currently unknown, it was not possible screen this region in the sequencing of the gene. The primer sequences are listed in Chapter 2 (see section 2.11.3). PCR conditions for each pair of forward and reverse primer were optimized prior to sequencing of patient DNA and this is listed in Section

2.11.3 along with the annealing temperatures. Figure 5.1A shows the results of the primer optimization for each exon using normal control DNA. The fragment of appropriate sizes were obtained for each individual exon and the respective annealing temperatures for each exon is shown. For each patient DNA sample, the 6 coding exons of AIPL1 were amplified and the PCR products were checked by gel electrophoresis for specificity and quality. Figure 5.1B shows an example of the gel electrophoresis of the PCR products of exon 2 from patient DNA samples. Only samples which yielded a clean, specific PCR band of the predicted size were subsequently subjected to direct sequencing. The adenine (A) of the start codon (ATG) of the AIPL1 cDNA was assigned as nucleotide 1.

Once a sequence variant is identified, it was determined whether it is disease-causing or a polymorphism using the following attributes which increase the probability that a sequence variation causes a defect in the resulting protein: 1) the predicted effect of the base pair change on the protein product; changes such as deletions, frameshifts, splice site mutations and nonsense mutations were considered definite null mutations and therefore may have more detelerious effects, while mutations such as missense mutations or in-frame deletions or insertions may still result in some residual protein function. For other sequence variants, a web-based protein prediction program was used to help distinguish the benign from deleterious effects of a new mutation. 2) The relative frequency of the sequence variant in LCA patients versus normal controls. A sequence variation was considered likely to be pathogenic when it was found exclusively in patients and not in 192 chromosomes from 96 control DNA samples (although caution has to be taken when considering an infrequent allele), whereas >1% frequency in the controls were likely to be polymorphisms. 3) The identification of two pathogenic alleles. 4) Appropriate co-segregation of the mutant allele in the affected and non-affected members of the families. 5) Conservation of the mutant codon or protein residue across other species. The reference sequence for sequence analysis was taken from the Genbank reference sequence (accession number NM_014336.3). NCBI Reference Sequence: NP_055151.3

Table 5.4 List of *AIPL1* sequence variants contained in the LCA microarray chip by Asper-Genetics. A total of 32 different sequence variants is screened for by the chip.

Gene	Exon	nucleotide change	amino acid change
AIPL1	1	41A>G	K14E
AIPL1	2	97 ins 8bp (GTGATCTT)	FS
AIPL1	2	112delC;111C>T	R38fs;F37F
AIPL1	2	116C>A	739N
AIPL1	2	126T>A	C42X
AIPL1	2	157C>T	R53W
AIPL1	2	211G>T	V71F
AIPL1	2	236T>C	M79T
AIPL1	2	244C>T	H82Y
AIPL1	2	264G>A	W88X
AIPL1	2	265T>C	C89R
AIPL1	2	268G>C	D90H
AIPL1	IVS2-2	277-2A>G	Premature stop/frameshift/deletion
AIPL1	3	286G>A	V96I
AIPL1	3	341C>T	T114I
AIPL1	3	401A>T	Y134F
AIPL1	3	423G>T/C	Q141H
AIPL1	3	461 T>C	L154P
AIPL1	IVS3+1	IVS3+1 G>A	Premature stop/frameshift/deletion
AIPL1	4	487C>T	Q163X
AIPL1	4	538G>A	V180I
AIPL1	4	589G>C	A197P
AIPL1	4	617T>A	I206N
AIPL1	5	715T>C	C239R
AIPL1	5	733_735 del	E245del
AIPL1	5	769 del 9bp (CTCCGGAC)	frameshift
AIPL1	5	784G>A	G262S
AIPL1	6	IVS5-10_786 del	Premature stop/frameshift/deletion
AIPL1	6	834G>A	W278X
AIPL1	6	905G>T	R302L
AIPL1	6	1008 del 2bp (AG)	frameshift
AIPL1	6	1126C>T	P376S

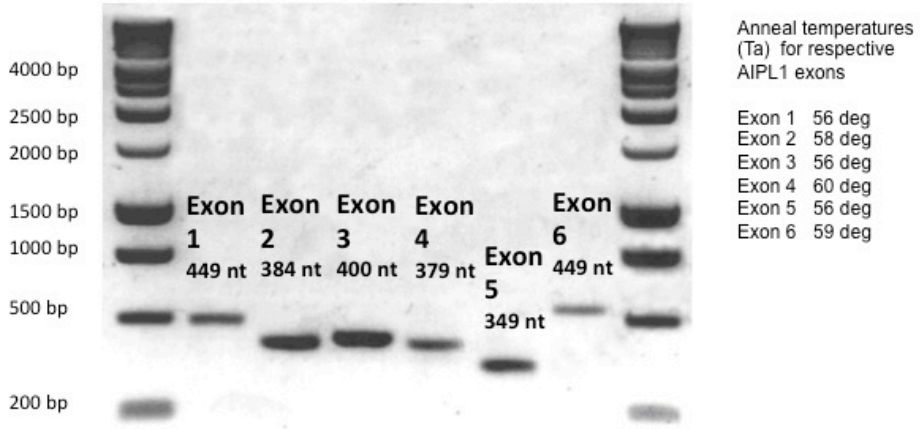

Figure 5.1A. Optimization PCR of primer pairs for each *AIPL1* exon. Single PCR band of expected size were obtained for each exon. The respective optimal annealing temperatures for each exon

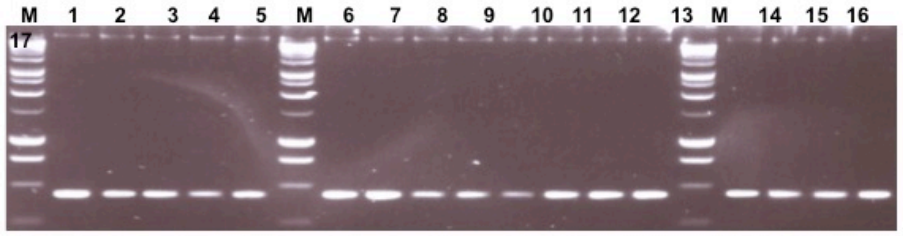

Figure 5.1B. Gel electrophoresis of PCR samples of patient DNA for exon 2. After PCR amplification of PCR samples were analysed by gel electrophoresis. An example of PCR samples of exon 2 is shown. Expected bands size was approximately 400 bp. Each lane represents PCR sample of one patient DNA. M denotes marker. Numbers 1 to 17 indicates respective PCR samples.

5.5 Results

5.5.1 Comparative analysis of *AIPL1* mutations

LCA chip analysis was performed on all of the 326 DNA samples that were obtained from the patient panel of 309 probands and 17 relatives. Bi-directional sequencing was performed on 153 proband DNA samples of all 6 exons of the *AIPL1* gene including splice-site junctions. These samples consisted of DNA from patients in whom a molecular cause had not yet been identified for their disease. Of the 153 samples that were sequenced, 129 consisted of samples that have been screened using the LCA chip prior to sequencing and did not return any mutations; 9 samples returned one allelic change on the LCA chip; and 15 samples had not been screened on the LCA chip prior to sequencing. Bi-directional sequencing of *AIPL1* was also performed on the control panel consisting of 96 control DNA samples.

The LCA chip identified *AIPL1* disease-associated variants or mutations in 17/326 of DNA samples, giving a positive hit rate of 5% for *AIPL1*. This is similar to the hit rates reported by other studies using the LCA chip and the mutation frequency in LCA [103][519]. Homozygous mutations were found in 4 (1.2%) patients and compound heterozygous mutations in 3 (0.9%) patients, and a further 10 (3.0%) patients had a single allelic change identified (Table 5.5). Of the patients with only one allelic change, a second allele was identified in another LCA gene using the same array (*RPGRIP, RDH12, CRB1*) in 5 patients. Direct sequencing identified 21/153 (14%) patients with AIPL1 mutations or missense changes (Table 5.5). Of these, 4 (2.6%) patients had homozygous mutations, 8 (5.2%) were compound heterozygotes and 8 (5.2%) had one allelic change.

Table 5.5 Comparison of mutation screening by Asper LCA chip and direct sequencing. The number of disease-associated variants and novel non-conservative variants in *AIPL1* detected by Asper LCA chip and by direct sequencing .

Method	Samples detected (*n*)	Homozygous	Compound heterozygous	Single mutation
Asper LCA chip	17/326(7%)	4(1.2%)	3(0.9%)	10(3.0%)
Direct sequencing	21/153(14%)	4(2.6%)	8(5.2%)	8(5.2%)

A total of 39 sequence variants (reported and unreported) were found on sequencing of the patient samples, of which 26 have not been reported before (Table 5.6). None of the novel variants were found on sequencing of the control DNA. Sequencing of the panel of 96 control DNA samples identified 15 sequence variants, of which 10 have not been previously reported. A comparison of the number of sequence variants identified in the patient panel and the normal control panel is presented in Table 5.6. Overall sequencing of the 153 probands revealed *AIPL1* variants (reported and unreported) in at least one allele in 109 (69%) subjects. Sequencing of normal controls identified AIPL1 sequence variants in 36/96 (39%) samples. A summary of the predicted effects of the novel variants found on sequencing of the patient and normal panel is shown in Table 5.7. Twenty-five different novel *AIPL1* variants were found. Silent mutations make up the majority (13/26), followed by missense mutations (9/26), frameshift (2/26) and splice (1/26) mutations. An overview of all the sequence variants identified by direct sequencing of *AIPL1* in the patient samples is presented in Table 5.8. The sequence variants which were found by sequencing *AIPL1* in a panel of normal DNA are presented in Table 5.9. These results suggest that *AIPL1* may be polymorphic in the general population, and sequence variants appear to be more common in the population of patients with childhood retinal dystrophies. The number of synonymous and non-synonymous single nucleotide polymorphisms observed per patient would

indicate that changes in *AIPL1* sequence are more common than expected. Furthermore, many of these changes have not been investigated at biochemical level and the functional effect of these changes is unknown.

Table 5.6 Summary of findings from sequencing of patient panel of LCA and childhood retinal dystrophies and sequencing of normal controls.

DNA panel	Total no. variants found	Reported mutations	Polymorphisms	No. of novel variants
Patient(153)	39(109)	7(19)	6(121)	26(67)
Control (96)	15(36)	0	5(92)	10(35)

Numbers in parenthesis () indicated number of samples found in the category of sequence variant

Table 5.7 Predicted effects of novel variants found through sequencing of the patient panel of LCA and childhood dystrophies and sequencing of normal controls.

DNA panel	No. of novel variants	Missense mutations	Frameshift mutations	Splice site	Silent mutation
Patient(153)	26(67)	10	2	1	13
Control (96)	10(35)	0			10

Numbers in parenthesis () indicated number of samples found in the category of sequence variant.

Table 5.8 AIPL1 sequence variants found on sequencing the patient panel of LCA and childhood-onset retinal dystrophies. A detailed analysis of the sequence variants found in AIPL1 mutation screening of the DNA from the in LCA genetic database, summarizing all the sequence changes found in the study. Novel changes are indicated in black colour, known mutations in red and known polymorphisms are in green.

Exon	*Base change*	*Codon*	*Protein*	*Effect*	*No. in patients*	*No in controls*
Ex 1	c.51G>A	CTG>CTA	Leu17Leu	Silent mutation	1 het	0
	c.1-106C >A	Intronic		May affect promoter	6 hets; 1 hom	0
Ex 2	c.268G>C	GAC>CAC	Asp90His	Rare variant	24 hets; 4 hom	24
	c.111C>T	TTC>TTT	Phe37Phe	Polymorphism	5 hets; 1 hom	4
	c.264G>A		Trp88X	Termination	2 hom	0
Ex 3	c.439C>T	CTG>TTG	Leu147Leu	Silent mutation	2 hets	0
	c.390C>A	CAC>CAA	His130Gln	Missense mutation	1 het	0
	c.277-10A>G	IVS2-10A>C		Polymorphism	15 hets; 27 hom	28
	c.277-30insG	IVS2-30insG		Silent mutation	1 het	0
	c.300A>G	CTA>CTG	Leu100Leu	Polymorphism	21 hets; 34 hom	28
	c.286G>A	GTC>ATC	Val96Ile	Missense mutation	5 hets	0
	c.341C>T	ACA>ATA	Thr114Ile	Missense mutation	1 hom	
Ex 4	c.555A>G	GGA>GGG	Gly185Gly	Silent mutation	1 het	0
	c.592T>A	TCT>ACT	Ser198Thr	Missense mutation	5 hets	0
	c.487C>T	CAG>TAG	Gln163X	Termination	1 hom	0
	c.641A>G	AAG>AGG	Lys214Arg	Missense mutation	1 het	0
	c.593C>T	TCT>TTT	Ser198Phe	Missense mutation	1 het	0
	c.466-2A>G	IVS3-2A>G		Affect splicing	2 het	0
	c.642+48G>A	IVS4+48G>A		Silent mutation	4 hets; 30 hom	0

	c.466-26T>C	IVS 3-26T>C		Silent mutation	9 hets; 5 hom	18
Ex 5	c.784+8G>C	IVS5+8G>C		Silent mutation	5 hets	0
	c.672insC			Frameshift	3 hets	0
	c.643-33C>T	IVS4-33C>T		Silent mutation	22 hets; 10 hom	7
	c.784+26G>C	IVS5+26G>C		Silent mutation	4 hets	0
	c.651A>G	CCA>CCG	Pro217Pro	Polymorphism	16 hets; 51 hom	53
	c.784+18G>A	IVS5+18G>A		Benign variant	3 hets; 1 hom	0
Ex 6	c.834G>A	TGG>TGA	Trp278X	termination	2 hets; 2 hom	0
	c.853G>A/ c.854C>A	GCG>AAG	Arg285Gln	Missense mutation	1 het	0
	c.894G>C	CAG>CAC	Gln298His	Missense mutation	1 het	0
	c.905G>T	CGC>CTC	Arg302Leu	Known mutation	6 hets; 2 hom	0
	c.971G>T	CGG>CTG	Arg324Leu	Missense mutation	1 het	2
	c.1003ins G			frameshift	1 hom	0
	c.1032A>G	GCA>GCG	Ala344Ala	Silent mutation	3 hets	0
	c.1038A>G	TCA>TCG	Ser346Ser	Silent mutation	3 hets	0
	c.1076C>T	TCT>TTT	Ser359Phe	Missense mutation	1 het	0
	c.1091C>G	GCA>GGA	Ala364Gly	Missense mutation	1 het	0
	c.1097C>G	CCC>CGC	Pro366Arg	Missense mutation	2 hets	0
	c.1126C>T	CCG>TCG	Pro376Ser	Known mutation	3 hets	0
	c.1162A>G		non coding exon	Silent mutation	1 het	0

Table 5.9 Summary of changes found in mutation screening of normal DNA samples.

Exon	*Base change*	*Protein*	*Effect*	*No. in control*
Ex 1	c.1-45 C>A		Non reported variant	2 hets
Ex 2	c.97-16C>T		Non reported variant	1 het
	c.111C>T	phe37phe	Non reported silent mutation	4 hets
	c.267C>T	cys89cys	Reported polymorphism	4 hets
	c.268G>C	Asp90His	Reported polymorphism	24 hets; 5 homo
Ex 3	c.277-10A>G		Reported polymorphism	22 hets;6 homo
	c.300A>G	Leu100Leu	Reported polymorphism	24 hets ; 4 homo
Ex 4	c.466-26T>C		Non reported variant	18 hets
	c.484G>A		Non reported variant	2 hets
Ex 5	c.651A>G	pro217pro	Reported polymorphism	15 hets ; 38 homo
	c.643-33 C>T		Non reported variant	7 hets
	c.678G>A	Glu226Glu	Non reported variant	3 hets ; 1 homo
Ex 6	c.1005C>A	Pro335Pro	Non reported variant	2 hets
	c.1110A>T	Pro370Pro	Non reported variant	1 het
	c.1023G>A	Glu341Glu	Non reported variant	3 hets ; 1 hom

5.5.2 Identification of patients with *AIPL1* mutations.

A summary of patients who are homozygous or compound heterozygous for pathogenic sequence variants in AIPL1 identified through mutation screening are shown in Table 5.10 to Table 5.12. Patients are divided into 3 groups: Patients with definite *AIPL1*-associated disease, patients with likely *AIPL1*-associated disease and patients with possible *AIPL1*-associated disease.

A total of 11 patients were identified with 2 confirmed mutations and therefore have definite AIPL1-associated disease (Table 5.10). The sequence changes were verified using bi-directional sequencing and segregation analysis. Five of these patients were found to have homozygous null mutations, and three patients were homozygous for missense mutations. One patient was compound heterozygous mutation for a missense mutation and a splice-site variant, one patient had a compound heterozygous mutation for a missense mutation and a novel nonsense variant, and a further patient was compound heterozygous for different missense mutations.

Table 5.11 summarises the patients who are likely to have *AIPL1*-associated disease. These patients were compound heterozygous for missense substitutions, some of these were novel sequence variants. Some of these patients are awaiting further confirmation on segregation analysis and verification of the pathogenicity of the novel variants.

A further 8 patients were found to have one allelic mutation in *AIPL1*, and therefore may possibly have *AIPL1*-related disease. This group is summarized in Table 5.12. Three patients in this group had another mutation found in another gene (*RDH12, RPGRIP1*).

Table 5.10. Patients with disease-causing mutations in *AIPL1*.

A summary of patients who are homozygous or compound heterozygous for pathogenic sequence variants in AIPL1 identified through mutation screening are displayed. The mutations have been confirmed with sequencing and segregation analysis.

LCA-Lebers Congenital Amaurosis; EORD- early onset retinal dystrophy.

* - denotes a novel mutation.

DNA	Mutations	Segregation	Diagnosis	ethnicity	consanguinity	Asper/sequenced
9728	W278X hom	Mother is het; no father DNA	LCA	African	no	A
07582	W278X hom	Mutation segregates	LCA	Caucasian	No	A,S
14777	Q163X hom	Mutation segregates	LCA	Middle-east	yes	A,S
14001	W88X hom	Affected sister	LCA	Pakistani	Yes	A
15000	W88X hom	Sister to 14001	LCA	Pakistani	Yes	A
14874	IVS2 277-2A>G splice G262S	Mother has splice mutation only	LCA	British	no	A,S
13484	P376S hom	Mother is het; no father DNA	LCA	African	no	A,S
13052	T114I het P376S het	Mutation segregates.	EORD	African	no	A,S
13412	R302L hom	Mutation segregates. Affected sis is hom and mother is het	LCA	Iranian	Yes	A,S
31895	V71F het W72X*	Mother has V71F; Father has W72X	LCA	Israeli	no	A,S
15618	R302L hom	Mutation segregates	EORD	Indian	No	A,S

Table 5.11. Patients with likely disease-causing mutations in *AIPL1*.

Summary of patients who have 2 or more non-conservative sequence variants in AIPL1 identified through mutation screening. The mutations are awaiting confirmation with segregation analysis and verification of the pathogenicity of the novel variants.

LCA-Lebers Congenital Amaurosis; EORD- early onset retinal dystrophy.

DNA	Mutations	Segregation	Diagnosis	ethnicity	consanguinity	Asper/sequenced
14651	T114I het T47R het* A285Q* A313S het*	One parent has T114I het	LCA	Asian	Yes	A,S
13163	S198T het * R270L het *	No DNA from family	EORD	Caucasian	no	A,S

Table 5.12. Patients with one mutation found in *AIPL1*.

Summary of patients who have been found to have one mutation or non-conservative sequence variant in AIPL1 identified through mutation screening.

LCA-Lebers Congenital Amaurosis; EORD- early onset retinal dystrophy; RP- retinitis pigmentosa.

DNA	Mutations	Segregation	Diagnosis	ethnicity	consanguinity	Asper/sequenced
13353	R302L het	Unaffected sister, brother and parent are het for this	LCA	Iranian	no	A,S
6604	P376S het	Mother is P376S het	EORD	African	no	A,S
13232	W278X het RDH12	Father has W278X het	EORD	British	yes	A,S
13278	Y134F het	Father has Y134F het	LCA	Bangladeshi	yes	A,S
14351	R302L het	Father is het for this	EORD	Pakistani	yes	A,S
14341	R302L het RPGRIP homozygous c.1107delA	Unaffected father has R302L hom	LCA	Pakistani	Yes	A,S
15324	Y134F het	Mother is Y134F het	LCA	Caucasian	No	A,S
10759	R302L het RDH12 29del3bp het	Father has R302L het	LCA	Indian	no	A,S
13026	P376S het RDH12 IVS2-12T>G	No DNA from family	RP	Carribean	no	A,S

5.5.3 Determination of significance of novel sequence variation.

A sequence variation is likely to be pathogenic when it is found exclusively in patients and not in at least 192 chromosomes from 96 control DNA samples. We screened control DNA samples by direct sequencing and were able to determine the allele frequency of any sequence variant in control subjects.

To determine whether a sequence variant is likely to be disease-causing, it is important to establish whether the sequence variants are likely to be harmful to protein function or structure. Functional analysis is not always available to investigate the effect of a missense variant on protein activity. To ascertain the likelihood whether a missense substitution was likely to be detrimental, a prediction of the functional effect of a novel missense variation was made by using information from the characteristics of the amino acid substituted, comparing interspecies amino acid conservation using ClustralW {Chenna, 2003 1010 /id} and protein structural information using Uniprot.

In-silico prediction of novel and some known missense mutations on AIPL1 protein function was performed using three protein function prediction software packages : Polyphen [394], SIFT [349] and PMut [134] . All three prediction software packages have been previously applied to various disease-gene models [350]. Table 5.13 shows the results of in-silico analysis of known missense mutations and novel variants that were found in patients with *AIPL1*-associated disease.

Figure 5.2A and B shows the amino acid alignment of AIPL1 between different species and the protein sequence comparison of AIP, another member from the FKBP protein family which shares homology with AIPL1. The positions of highly conserved residues are shown. Sequence comparison across different species and with AIP shows that there is a high degree of conservation of the protein sequence, particularly within the TPR domains which are sites of protein interaction. Figure 5.3 shows a schematic

structure of AIPL1 and the relative locations of the disease-causing mutations found in this study. The results of the in-silico analysis and conservation analysis are further discussed in the context of individual patients below.

Table 5.13. In-silico prediction of known mutations and novel sequence variants.

Change	SIFT		Polyphen		pMUT		
	Prediction	Tolerance index	Prediction	PSIC score difference	NN output	Reliability	Prediction
V96I	Tolerant	0.20	Benign	0.067	0.0794	8	Neutral
T114I	Tolerant	0.19	Benign	0.179	0.7499	5	pathological
Y134F	Tolerant	0.26	Benign	1.133	0.0715	8	Neutral
G262S	Tolerant	0.86	Benign	1.166	0.3055	3	Neutral
R302L	Tolerant	0.16	Benign	1.086	0.8448	6	Pathological
P376S	Intolerant	0.00	N/D	N/D	0.7874	4	Pathological
A285Q*	Tolerant	0.11	Benign	1.153	0.9286	8	Pathological
S198T*	Tolerant	0.44	Benign	0.025	0.2553	4	Neutral
A313S*	Tolerant	0.11	Benign	0.878	0.2607	4	Neutral
V71F*	Intolerant	0.00	Damaging	3.664	0.6540	3	Pathological
R270L*	Intolerant	0.00	Damaging	2.726	0.8584	7	Pathological
T47R*	Intolerant	0.04	Damaging	2.726	0.7359	4	Pathological

*Denotes novel sequence variant

SIFT - http://sift.jcvi.org/) – cut off is at 0.05. <0.05 predicted to have a deleterious effect. >0.05, the change is predicted to be tolerated. The higher the value, the less functional impact the substitution is likely to have.

PolyPhen algorithm http://genetics.bwh.harvard.edu/pph/ index.html). Polyphen evaluates the location of the substitution and the function of that region and whether the substitution is likely to affect the three-dimensional structure of the protein (PSIC Score). Scores greater than 2.0 indicate probably damaging to protein function, scores of 1.5–2.0 as possibly damaging, and scores of lower than 1.5 as benign.

pMUT . NN= neural network values from 0-1. >0.5 is predicted as a disease associated mutation. Reliability = values 0-9. >5 is the best prediction

N/D - Polyphen was unable to calculated for this position as it lies in the poly proline domain and this region only occurs in primates

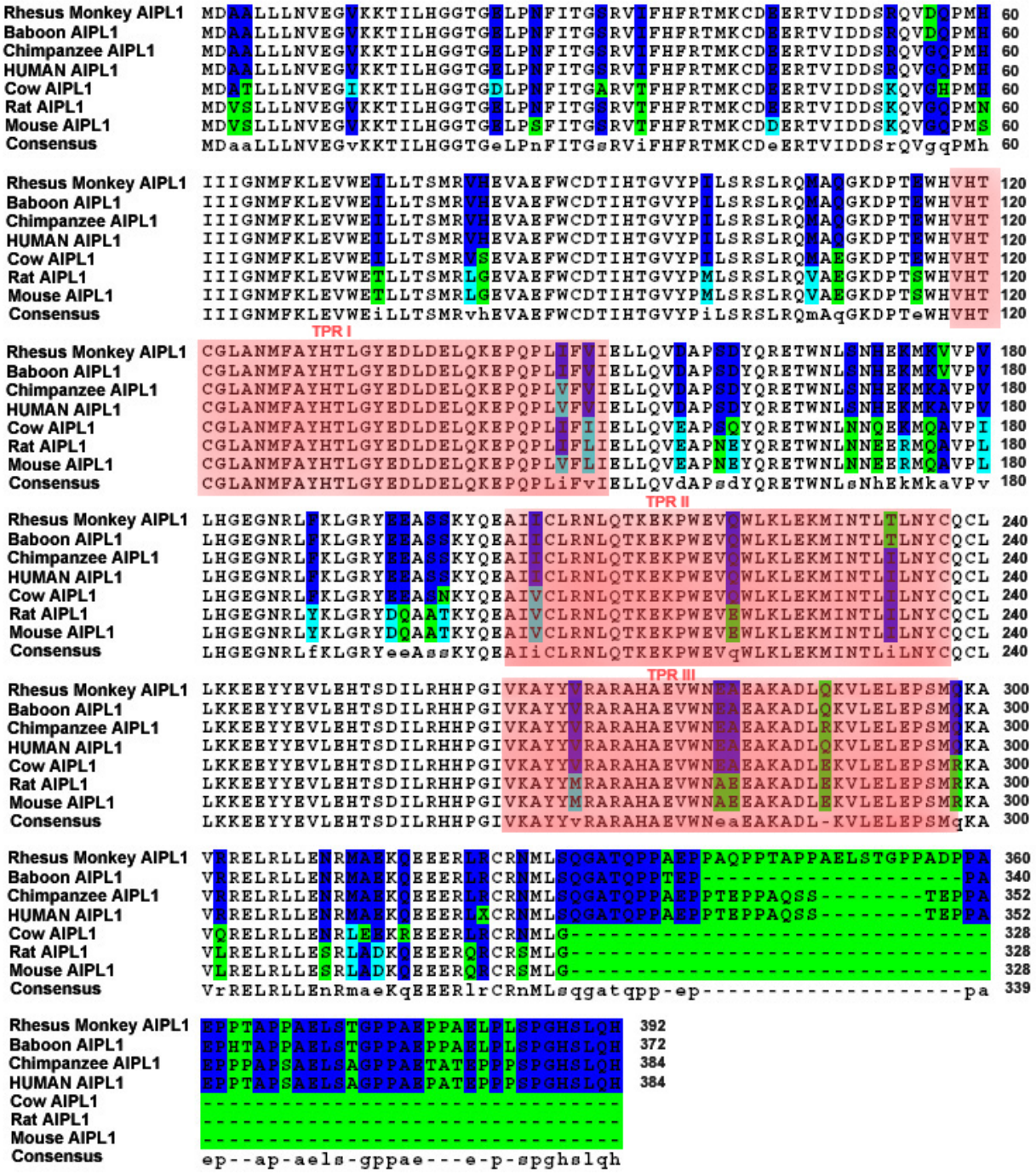

Figure 5.2 A. Comparative amino acid alignment of AIPL1 in different species.

Identical residues are in background white. Residues which are completely conserved are highlighted in blue. Residues which at which similar changes are allowed are in turquoise background. Non conserved residues are in highlighted in green. Tetratricopeptide domains (TPRs) are indicated in red background.

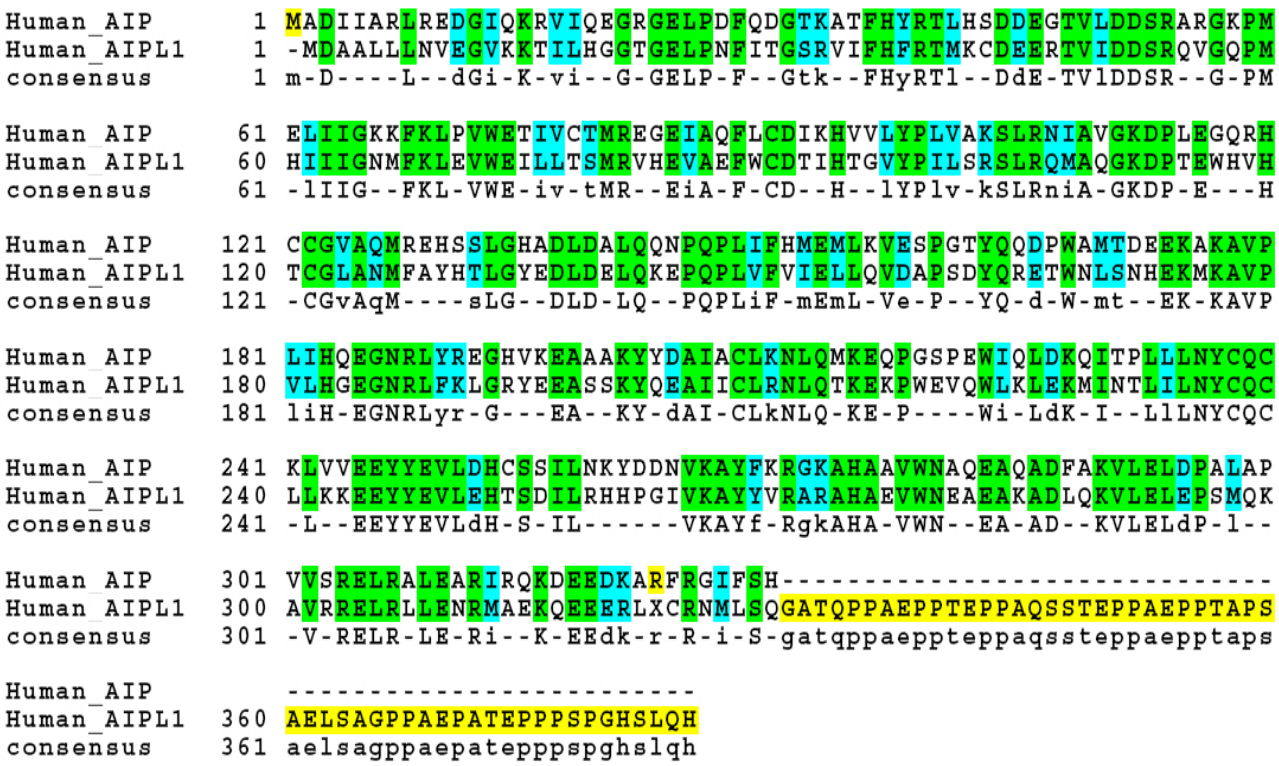

Figure 5.2B Amino acid alignment between AIPL1 and AIP from the FKBP immunophyllin family.

Completely conserved residues are highlighted in background green. Conservative amino acid changes in background blue. Positions in which there are different residues are in background white

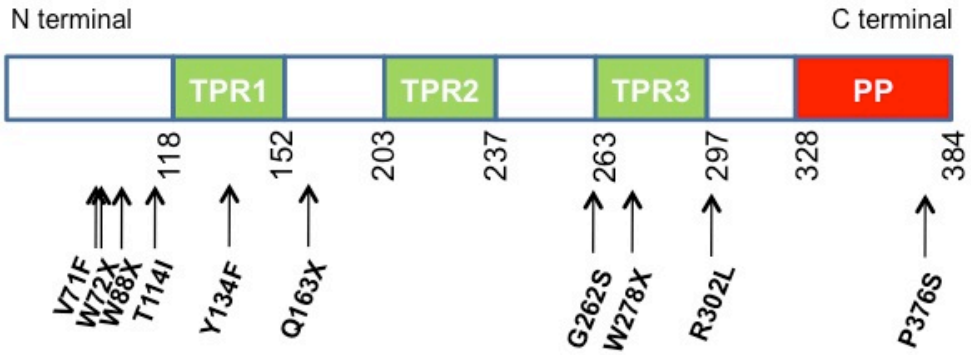

Figure 5.3. Schematic of AIPL1 and the relative locations of mutations and novel sequence variants found in patients with *AIPL1*-associated disease.

The AIPL1 motifs are labeled TPR (tetraticopeptide domain) and PP (polyproline region).

5.6 Patients with definite AIPL1-associated disease

5.6.1 Molecular analysis

Two patients (DNA no. 9728 and 07582) were found to carry homozygous nonsense mutations c.834G>A (Trp278X) in exon 6. This mutation was also present in compound heterozygous form in one proband (DNA no.13225) . This sequence variant changes the TGG codon encoding tryptophan into a premature stop codon TGA at position 278 of the amino acid chain, and effectively deletes the hinge domain on each *AIPL1* allele. When expressed, this allele is predicted to encode a severely truncated protein. It is the most frequent mutation described in *AIPL1* patients and has been reported in several families from different ethnic backgrounds around the world including Pakistani, American, French and Spanish [440].[95,103]. Two patients (No. 14001 and 15000) were homozygous for nucleotide substitution c.264G>A (Trp88X). This mutation was first described in an affected proband from a Bangladeshi family [442]. If expressed, these alleles are predicted to encode an AIPL1 protein truncated by more than two-thirds and lacking all three tetratricopeptide domains which are central to the protein function. Patient 14777 was found to have a homozygous C to T nucleotide substitution at position 487 which changes the codon for glutamine into a termination codon at position 163 of the amino acid chain (Gln163X). This is a known mutation which was first reported in homozygous form in affected individuals from a Palestinian family.[442]. If expressed, these alleles would encode an AIPL1 protein truncated by more than half, with the resulting protein lacking tetratricopeptide domains II and III. All three nonsense mutations resulted in null. This matches the phenotype that is seen in these patients and all of these patients were clinically diagnosed with LCA.

Patient 14574 is compound heterozygous for 2 known mutations; c.277-2A>G and c.784>A (G262S). The first mutation affects the canonical splice

acceptor site of intron 2 which may result in the loss or reduced specificity of the splice site. The consequences can be catastrophic, ranging from a premature stop codon, loss of an exon or insertion of an intron or loss of the reading frame and is likely to prevent functional protein biosynthesis. The second mutation is a missense substitution of glycine for serine at position 262 of the amino acid chain, and has been described as an disease-causing mutation in compound heterozygous form along with W278X in a patient with LCA [442]. This substitution is located in the main backbone of the AIPL1 protein sequence and at a position which is conserved across different species (Figure 5.2A). Both glycine and serine have different side-chain groups and this substitution could thus result in a significant change in protein function. Co-segregation studies showed that the both mutations were on separate alleles; the patient inherited the c.277-2A>G mutation from his mother and G262S from his father. Patient 14874 was diagnosed with LCA. The case histories of the patients mentioned are detailed in the appendix.

Patient 31895 was found to have a novel null mutation W72X and a missense substitution V71F. The valine at residue 71 is conserved across different species and lie in the N-terminal immunophilin domain. Mutations in this domain have been linked to LCA. Segregation analysis confirmed that the mutations were located on separate alleles, the mother was a carrier for V71F and the father was heterozygous for the null mutation W72X. The patient was diagnosed with LCA at the age of 2 years (see appendix 1 for case history). Patient 13052 was compound heterozygous for 2 mutations, c.341C>T (Thr114Ile) and c.1126C>T(Pro376Ser). The compound heterozygous amino acid substitution of both Thr114Ile and Pro376Ser has been previously described in an affected proband from an African-American family who had a clinical diagnosis of LCA.[442]. The amino acid sequence alignment of AIPL1 shows, that the threonine at position 114 is located in a region that is fully conserved between the human, chimpanzee, mouse, rat, and cow proteins (Figure 5.2a). Comparison of the sequence alignment between AIPL1 and AIP shows that only a conservative change occurs at this position (Figure 5.1b). Furthermore, the amino acids threonine and

isoleucine have different chemical properties; threonine is a polar and hydrophilic amino acid while isoleucine has an aliphatic side group and is hydrophobic and water-insoluble. The T114I is a known mutation and has been described to be associated with LCA in previous literature [442][440]. Protein prediction analysis revealed conflicting results: SIFT and Polyphen predicted that the change was benign, while pMUT revealed the mutation to be pathological. It is possible that the T114I constitutes a mild mutation. Our patient was diagnosed with less severe disease of rod-cone dystrophy (see appendix 1 for case history), and retained some vision in adulthood (see later section).

Three patients were found to carry homozygous missense mutations; patient 13484 was found to homozygous for P376S, and patients 13412 and 15618 were both found to be homozygous for R302L and were not related to each other and were from different famil and ethnic backgrounds(see appendix 1 for respective case histories). The c.1126C>T(P376S) mutation was first described in an African-American child diagnosed with LCA who was compound heterozygote for 2 amino acid substitutions, T125I and P376S [442]. Our patient 13484 who has a homozygous P376S mutation was also diagnosed with LCA. The P376S mutation represents a non-conservative substitution from proline, a non-polar hydrophobic amino acid with a rigid structure conferred by a secondary amine side group linked to the α-amino group, to serine which is a hydrophilic, polar amino acid. Due to the differences in the chemical and physical properties of the proline and serine, this missense substitution would result in major changes in the properties and function of the AIPL1 protein. This was also supported by protein prediction analysis, the substitution was found to be intolerant when applied to SIFT and pMUT software. These findings indicate that the P376S mutation is very likely to be disease-causing.

The c.905G>T (R302L) substitution in patients 13412 and 15618, was first described as a disease-causing homozygous mutation in a proband with LCA from an Indian family [442]. Similarly in this study, both patients 13412 and 15618 were diagnosed with LCA. The arginine residue at position 302 is

conserved between human, squirrel monkey, chimpanzee and rhesus monkey AIPL1 and therefore is thought to be disease-causing. Furthermore, it was not found on sequencing the normal control panel. It is interesting however to note that the arginine at this position is not conserved between human and rat and mouse AIPL1 (Figure 5.2A). The functional effect of the substitution was not unlikely to be harmful according to SIFT and polyphen protein prediction software, but is damaging according to pMUT analysis. Co-segregation study of the mutation with the phenotype in the original family described in the published study was not performed. In this study, we found a homozygous R302L change in the unaffected father (clinical state to be further confirmed) of another proband carrying a heterozygous mutation. Hence it may be possible that this sequence could represent a rare benign variant. Both missense mutations P376S and R302L are located within the hinge region of AIPL1. This C-terminal polyproline-rich region is only present in primate AIPL1 and cross-species comparative analysis of the protein sequence indicate that there is a high level of sequence conservation within the hinge region between primates (chimpanzee, baboon, rhesus monkey and humans). There is evidence to suggest that the polyproline-rich region performs an essential function in normal primate vision since reported mutations have been identified in this region which cause the severe phenotype of LCA [442][440]. Furthermore, two deletion mutations located in this region (A336Δ2 and P351Δ12) have been associated with cone-rod dystrophy and juvenile RP [442]. Further studies in determining protein function is will be necessary to establish the role of the hinge region in AIPL1 and its significance to vision.

Yeast 2-hybrid screens have demonstrated interactions between between AIPL1 and NUB1 [7], a protein implicated in regulation of proteolysis, and also between AIPL1 and farnesylated proteins[393]. AIPL1 modulates the subcellular localization of NUB1, from the nucleus towards the cytoplasm, and behaves in a chaperone-like manner to suppress the formation of inclusions arising from NUB1 fragments and redistribute these in the cytoplasm [476]. This ability requires the C-terminal region of AIPL1 to be intact. Based on these observations of interactions, studies have attempted

to characterize various sequence changes at a bio-molecular level by determining the effects AIPL1 sequence changes on AIPL1 function with respect to the NUB1 translocation or farnesylation, and protein solubility. Various mutant forms of AIPL1 were tested and these included W278X, G262S and R302L relevant to this study. Many of the mutant forms of AIPL1 were SDS-soluble (non-solubility is an indication of protein non-function) and had similar subcellular distribution compared to wild-type AIPL1, with the exception of W278X and R302L. W278X formed SDS-insoluble cytoplasmic inclusions, suggesting that the mutant protein undergoes misfolding and aggregation, and is therefore non-functional. It was also shown that W278X completely defective with respect to modulating the nuclear translocation of NUB1. R302L was shown to have reduced activity with respect to modulation of NUB1 transocation and subcellular distribution. The G262 mutation on the other hand, was found to be hyperactive in the modulation of NUB1 nuclear translocation, and it has been suggested that the basis of disease in this case may involve the interaction of AIPL1 with an alternative binding partner [476]. There is little evidence however, that NUB1 interaction with AIPL1 is physiologically relevant to the role of AIPL1 in the retina. It is therefore unclear whether the yeast 2-hybrid screen is informative with regards to the pathogenesis of LCA.

Another functional study showed that various mutations in AIPL1 lead to various degrees of abolishment of AIPL1 interaction with farnesylated proteins, with W278X having the most severe effect [393]. Interestingly, R302L substitution did not appear to affect the interaction between AIPL1 with farnsylated proteins [393], despite being less active with respect to its modulation of NUB1 translocation. The conflicting findings on biomolecular characterization indicate that AIPL1 may have complex functions involving multiple binding partners. Furthermore, strong evidence has emerged from animal models indicating that AIPL1 is critical for the biosynthesis of rod and cone PDE and that retinal degeneration seen in AIPL1 mutations is not due to any defect in farnesylation. *In vivo* expression studies using animal models would be able to provide better evidence of whether a sequence variant is pathogenic.

5.6.2 Genotype-phenotype correlation

The clinical characterisation of disease due to *AIPL1* mutations is important for assessment of any future therapies. Clinical assessment of the affected individuals included fluorescein angiography, electrophysiology, Goldmann perimetry, OCT and autofluorescent imaging. This section aims to describe the phenotypic features and clinical subtypes associated with *AIPL1* mutations and observe possible differences and similarities in the expression of fundus changes and disease severity between different mutations. The phenotype of 11 patients of different ethnic origin with confirmed mutations in *AIPL1* is described. A summary of the phenotypic characteristic of patients with AIPL1-associated disease is shown in Table 5.15

Out of the 11 probands with confirmed *AIPL1* mutations, 9 had a clinical diagnosis of LCA and 2 were diagnosed with a milder disease of early onset rod cone dystrophy (EORD). All of the patients apart from one presented with poor vision and nystagmus. Amongst those diagnosed with LCA, the age of onset of disease, or the age at which visual difficulties were noticed ranged from birth to 6 months of age, all of the probands were noted to have a visual problem before the age of 1 year. The onset of visual symptoms were considerably later in the two patients diagnosed with EORD, at ages of 2 years and 6 years. The patients were examined at various ages, depending on when they were referred to the clinic.

Visual acuities were found to vary between probands and ranged from logMAR 0.5 to light perception. Most patients had severe loss; six patients had light perception, two patient had counting fingers vision and one had hand motion vision in one eye. Three patients had measurable vision. However, comparison of the visual acuities and clinical features between the different mutations should take into consideration the fact that the probands were examined at different ages; many of them were seen as adults when the condition had progressed to advanced stages. Cycloplegic refractions performed in 5 out of 11 patients showed moderate myopia in 2 (-1.50D to -

3.00D), high myopia in one (-8.50D) and two patients had moderate hypermetropia (+3.00D to +5.00D). Astigmatism was frequently noted in these patients. Photoattraction (staring at lights) was reported in 3 patients and photoaversion in 1. Nyctalopia (night blindness) was reported in 4 patients, while about half of the patients had some form of strabismus. All except for 1 patient had nystagmus and amaurotic pupils, the exception being the patient with clinically EORD who had reasonable remaining vision.

Some form of cataract was seen in majority of patients (6 of 11 patients); lens changes included both cortical and posterior subcapsular opacities. However, cataracts appeared to be a later finding as the patients who had cataracts were in their late adolescence or adulthood. The youngest patient noted to have cataracts was 17 years old. Contrary to findings reported by Dhamaraj *et al*. [103] who found that cataracts and keratoconus were observed only in patients who were homozygous for *AIPL1* mutations, we found cataracts in patients had homozygous and compound heterozygous *AIPL1* mutations.

Retinal findings were notable for pigmentary retinopathy and retinal drusen-like deposits. Eight out of 11 patients with *AIPL1*-related disease had some form of pigmentary retinopathy that ranged from mild midperipheral bone spicule pigmentation to severe pigmentary clumping and chorioretinopathy (Figure 5.4, 5.5, 5.6, 5.7, 5.8, 5.9, 5.13). Most of these patients with pigmentary retinopathy were examined in late adolescence and adulthood. Three patients did not have any clinically evident retinal pigmentary changes **;** 2 of these patients were examined at the early ages of 2 and 7 years and were noted to have essentially normal-looking retinas (Figure 5.10 – fundal photo was taken later when patient turned 5 years old, and 5.11), one patient was aged 22 when examined and was found to have clinically unremarkable retina and macula. White drusen-like deposits at the level of the retina was observed in 2 patients around their second decades of life (Figure 5.4 and 5.8).

Some form of maculopathy of variable appearance was noted in 8 out of 11 (64%) patients. The maculopathy ranged in appearance from mild foveal atrophy with variable degrees of macular mottling to aplasia (Figure 5.4 to 5.12). The severity of maculopathy appeared to increase with age; severe macular atrophy was seen mostly in older patients aged 17 years upwards. In the young patients aged 5 and 7 years, no clinically evident maculopathy (Figure 5.10) was seen in former, while an abnormal foveal reflex which may represent an early stage of maculopathy was seen in the latter aged 7 (Figure 5.11). Exceptions to this were patients 13052 and 13412 who were aged 27 and 18 respectively in whom no obvious macular atrophy was seen at clinical examination despite their age (Figure 5.9 and 5.12). Patient 13052 had a clinical diagnosis of EORD, a milder form of disease with later onset and slower progression and retained relatively good vision into adulthood. Patient 13412 was diagnosed with LCA with onset of visual problems at the age of 2 months. However, he may have a slower course of disease progression, as he retained slightly better vision in adulthood when compared to the other adult patients. The youngest patient with macular atrophy in our study was 17 years old (patient 14874, Table 5.14, Figure 5.7). It is also interesting to note that patients with homozygous null mutations appear to have more severe macular atrophy; amongst the adult probands, patients who had severe macular atrophy carried homozygous nonsense mutations, W278X and W88X. On the other hand, patient 14874 who had moderate macular atrophy and carried compound heterozygous mutations that included a splice site mutation and a missense mutation, and patients with missense mutations exhibited milder maculopathy or none at all (patients 13052 and 13412). An exception is patient 13484 with homozygous P376S who had severe macular atrophy (Figure 5.8). This may be due to influences from other environmental factors or genetic modifiers resulting in a more severe phenotype. Varying degrees of optic nerve pallor were noted in majority of older patients who were in their second or third decades of life. In children, the optic nerve head largely appeared normal.

ID no.	ethnicity	Mutation	Age at onset	Clinical diagnosis	Presenting symptoms	Age at examination	VA logMar (OD; OS)	nystagmus	strabismus	nyctalopia	pupils	PAV /PAT	Pigmentary retinopathy	maculopathy	Disc pallor	White dots	Cataract /keratoconus	refraction
9728	african	W278X hom	0	LCA	Poor vision, nystagmus	19 y	PL;PL	y	n	n	Amaurotic	n	Moderate, bone spicule	Atrophy	n	y	none	Moderate myopia, astigmatism (-5.50)
07582	white	W278X hom	0	LCA	Poor vision, nystagmus	24 y	PL;PL	y	n	N/A	N/A	n	Moderate, bone spicule	Atrophy	n	n	NS	N/A
14777	arab	Q163X hom	2 m	LCA	Poor vision, nystagmus	2 y	PL;PL	y	ET	NA	Amaurotic	PAT	None	None	n	n	n	moderate hypermetropia (+6.50)
14001	pakistani	W88X hom	0	LCA	Poor vision, nystagmus	30 y	PL;PL	y	XT	n	Amaurotic	n	Moderate	Atrophy	y	n	PS, keratoconus	N/A
15000	pakistani	W88X hom	0	LCA	Poor vision, nystagmus	36 y	PL; PL	y	y	n	Amaurotic	n	Moderate	Atrophy	y	n	PS, keratoconus	N/A
14874	white	c.277-2A>G G262S het	6 m	LCA	Poor vision, nystagmus	17 y	PL;PL	y	n	y	Amaurotic	PAT	Moderate	Moderate atrophy	n	y	PS	Moderate myopia (-5.00)
13484	african	P376S hom	2 m	LCA	Poor vision, nystagmus	19 y	1.0;PL	y	y	y	Amaurotic	PAV	Severe, clumping	Severe atrophy	y	y	cortical	N/A
13052	african	T114I het P376S het	2 y	EORD	Poor vision	27 y	0.5;0.9	n	n	y	n	PAT	Moderate, bone spicule	Pigment changes	y	n	PS	High myopia, astigmatism (-12.00)
13412	white	R302L hom	2 m	LCA	Poor vision, nystagmus	18 y	CF;CF	y	XT	n	n	n	None	None	y	n	n	Moderate hypermetropia (+4.00)
31895	white	V71F het W72X het*	6 m	LCA	Poor vision, nystagmus	7 y	CF;CF	y	n	N/A	Amaurotic	n	None	Abnormal foveal reflex	n	n	n	N/A
15618	indian	R302L hom	6 y	EORD	Poor vision, nystagmus	21y	1.3;HM	y	XT	n	n	n	Moderate, bone spicule	Mottling	y	n	n	N/A

Table 5.14. Clinical and genetic characteristics of 11 patients with AIPL1-associated disease and confirmed mutations

A summary of patients who are homozygous or compound heterozygous for mutations in AIPL1 identified through mutation screening and segregation analysis and their clinical findings on examination. Novel sequence variants are indicated with '*'. Abbreviations: LCA-Lebers congenital amaurosis; EORD-Early onset retinal dystrophy; OD-right eye; OS-left eye; PL-perception of ligl perception of light; CF-counting fingers; XT-exotropia (divergent squint); ET-esotropia(convergent squint; PAT- photoattraction; PAV-photoaversion; NS-nuclear sclerosis; PS-posterior subcapsular; N/A-not av described.

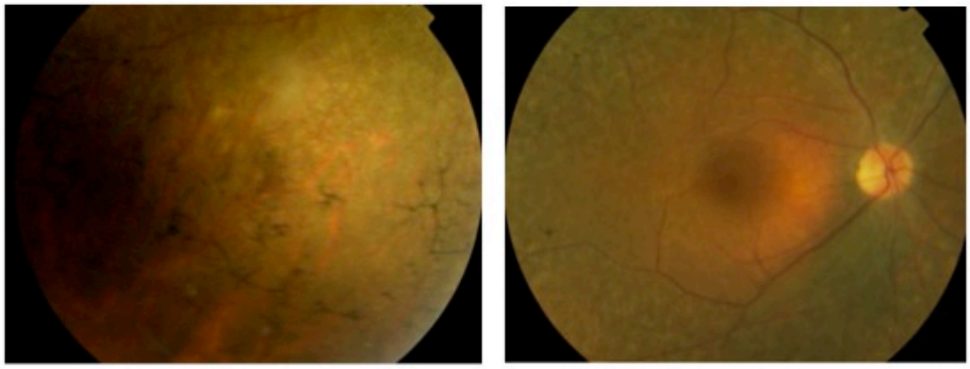

Figure 5.4. Fundus photograph of the left eye of patient 9728 with homozygous W278X mutation, at 19 years old. **A**,The posterior pole shows relatively well preserved macular and white drusen-like deposits at the level of the retina in the mid-periphery. **B**, The peripheral retina shows intra-retinal pigmentary changes and white drusen-like deposits.

Figure 5.5. Fundus photograph of the right eye of patient 07582 with homozygous W278X mutation at age 24 years of age. The macula is atrophic with pigmentary changes and there is intraretinal bone spicule-like pigment accumulation in the periphery with chorioretinal atrophy.

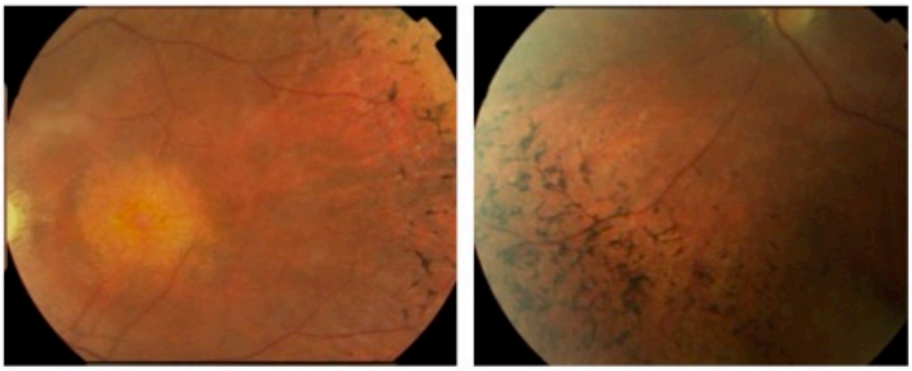

Figure 5.6. Fundus photographs of the left eye of patient 14001 with homozygous W88X mutation, taken at 30 years of age. **A,** There is established macular atrophy with RPE disruption and intraretinal pigment accumulation in the mid-periphery. **B,** Inferior mid-periphery of the same eye shows diffuse bone spicule-like pigment clumping.

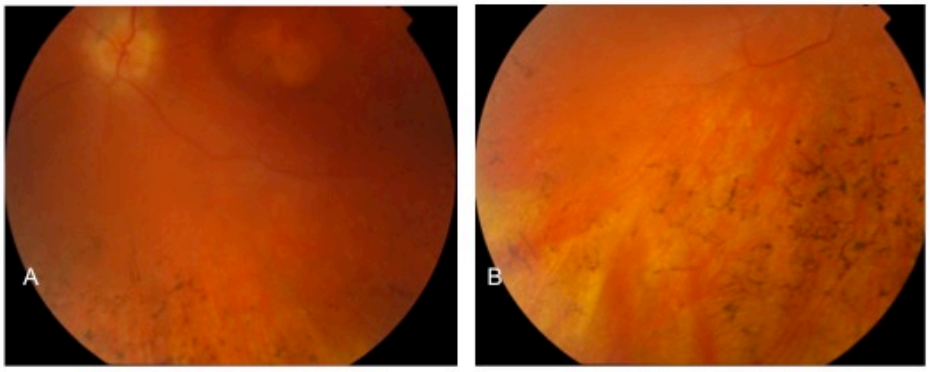

Figure 5.7. Fundus photographs of the left eye of patient 14874 who has splice site mutation c.277-2A>G and missense mutation G262S. The eye was photographed at the age of 17 years of age. **A,** There is atrophic changes and RPE loss at the macula with intraretinal pigmentary changes at the mid-periperal retina. Optic disc drusen is present. **B,** The peripheral retina has moderate pigment accumulation and early areas of chorioretinal atrophy.

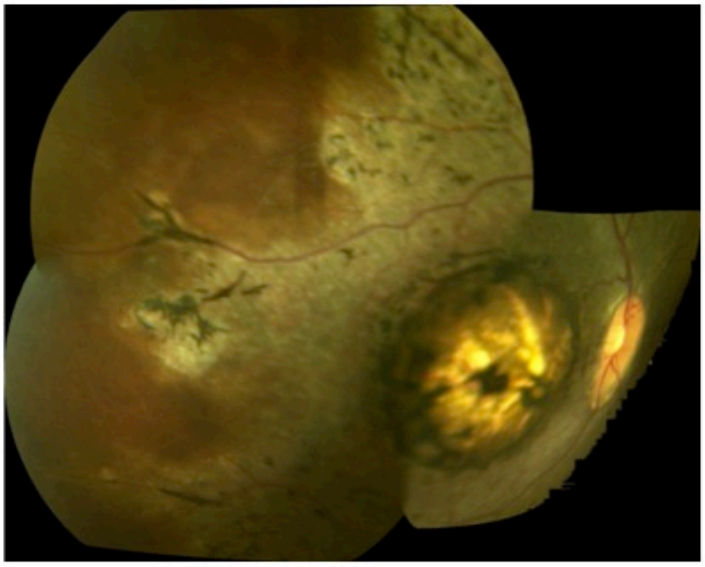

Figure 5.8. Fundus photograph of the right eye of patient 13484 with homozygous missense mutation P376S, taken at 19 years old. There is macular coloboma-like atrophy with coarse pigment clumping at the centre and edges and some intraretinal white spots. The mid-peripheral retinal shows scattered bone spicule-like pigmentation.

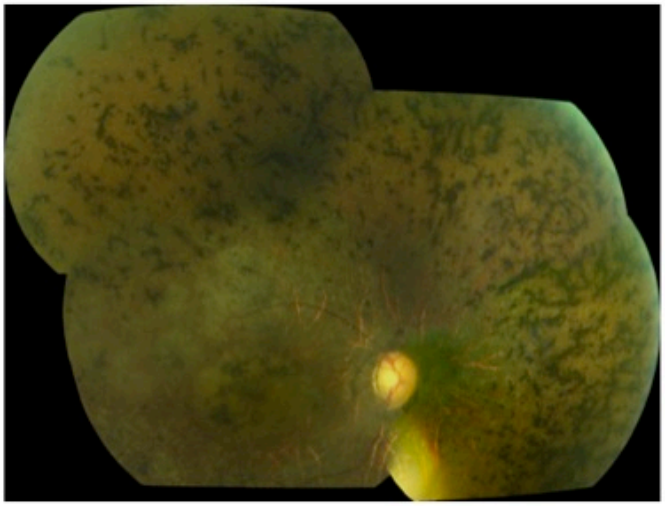

Figure 5.9. Fundus photograph of the right and left eyes of patient 13052 with compound heterozygous mutations T114I and P376S, taken at 27 years old. The patient was diagnosed with EORD. **A**,The right eye shows diffuse pigmentary clumping as well as chorioretinal atrophy in the mid-peripheral retina. There is no obvious macular atrophy but some pigmentary changes at the macula is seen. **B**, The left eye similarly shows peripheral pigmentary retinopathy and chorioretinal atrophy and RPE mottling at the macula. The blood vessels appear attenuated.

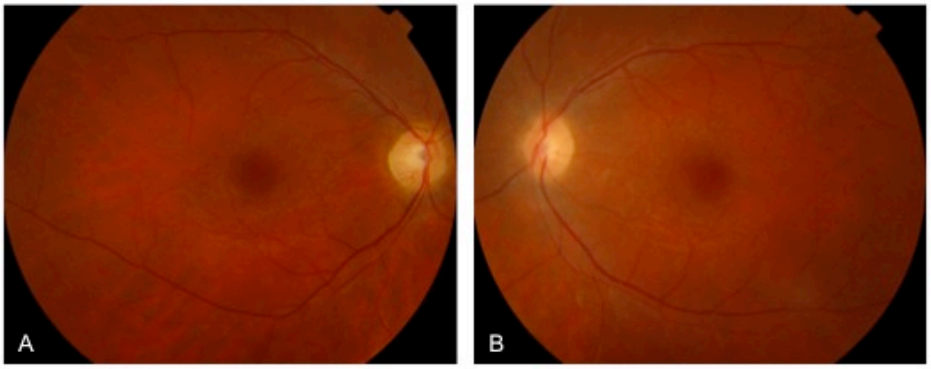

Figure 5.10. Fundus photograph of the right and left eyes of patient 14777 with homozygous Q163X mutation, taken at age of 5 years. **A**,The right eye shows relatively normal macula and surrounding retina **B**, The left eye also has a normal looking macula and the peripheral retinal is unremarkable. The optic discs in both eyes also appear normal.

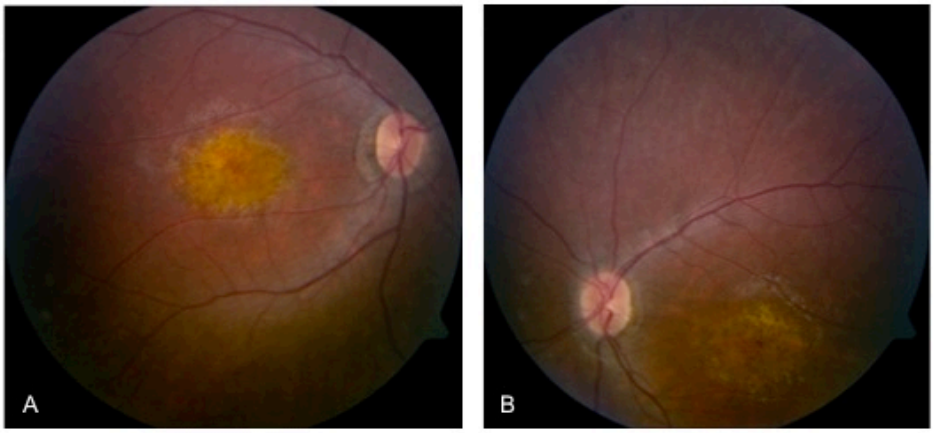

Figure 5.11. Fundus photograph of the right and left eyes of patient 31895 with compound heterozygous mutations, V71F and W72X, taken at age of 7 years. **A**,The right eye shows early macular changes and the surrounding retinal appears normal. **B**, The left eye also has an early macular lesion with normal-looking peripheral retina. The optic discs in both eyes appear normal.

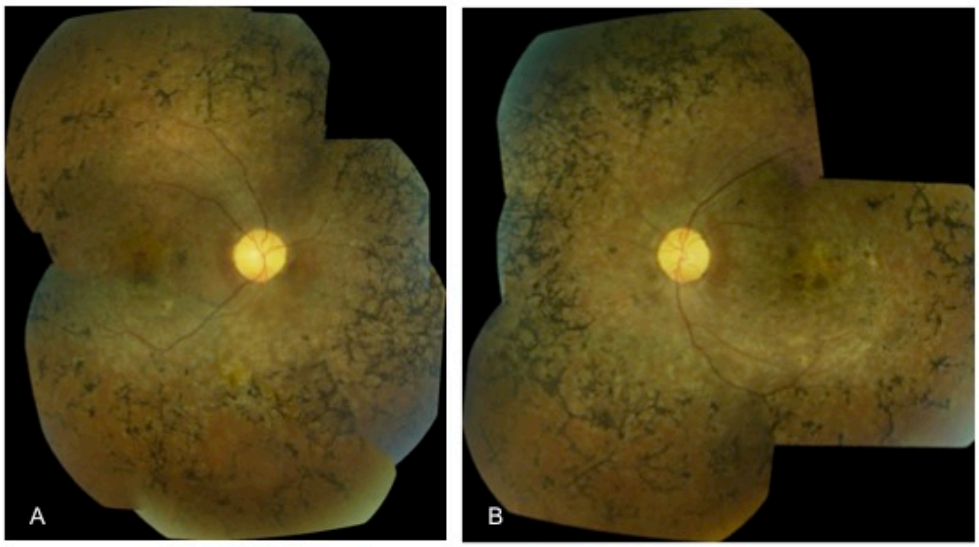

Figure 5.12. Fundus photograph of the right (A) and left (B) eyes of patient 15618 with homozygous R302L missense mutation, taken at age of 21 years. The right eye shows bone spicule pigmentation in the mid and peripheral retina and RPE mottling at the macula. There is pallor of the optic disc

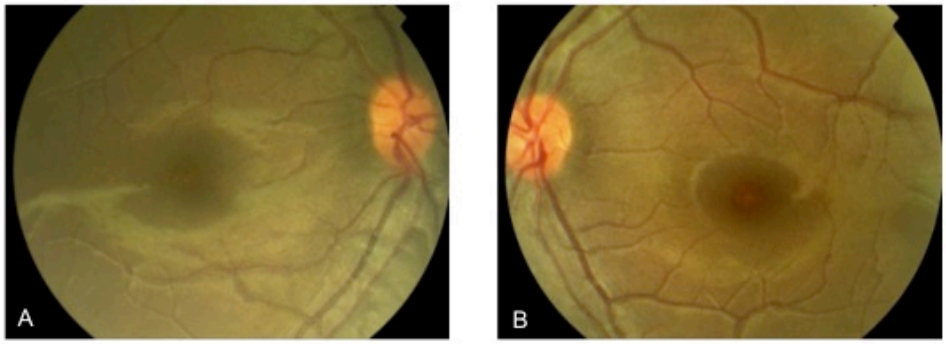

Figure 5.13. Fundus photograph of the right and left eyes of patient 13353 with heterozygous R302L missense mutation, taken at age of 11 years. The right(A) and left (B) eyes have normal looking macula and peripheral retina.

Goldman visual field (GVF) assessments were available on one patient only (Table 5.14). Most of the other patients either had visual acuities that were too poor for any visual field assessments or were too young to be able to cooperate with perimetry assessments. The Goldman visual field of patient 13052, who has a clinical diagnosis of EORD, showed severe constriction of the central visual field to a residual central field of 10 degrees, and temporal sparing of the peripheral fields in each eye (Figure 5.14). Electrodiagnostic analysis were obtained in 9 out of 11 patients. Majority of the patients showed no measurable rod or cone responses indicating severe generalized retinal dysfunction, and where recorded the visual evoked potentials (VEP) were markedly reduced (Table 5.15). Only three patients, 13484, 13052 and 15618 had residual ERG responses, although these were significantly reduced. Different ERG responses were observed between the right and left eyes of patient 13484 (Figure 5.15). In the right eye, full field ERG and rod ERG responses were subnormal with markedly reduced a and b-wave amplitudes; cone flicker ERG was markedly delayed and subnormal. In the left eye, no detectable ERG responses could be recorded. The findings in the right eye were in keeping with a generalized retinal dysfunction affecting the rods more than cone systems. The retinal dysfunction in the left eye was so severe that no definite electro-retinal activity could be detected. The pattern ERG was undetectable in either eye, indicating severe bilateral macular involvement. Patient 13052 and 15618 had residual scotopic ERG and full flash ERG responses, although the amplitudes of these were markedly attenuated. Cone flicker ERGs were subnormal and delayed . There was some preservation of macular function in patient 13052, as shown by the presence of PERGs, although they were very reduced. These findings were in keeping with a rod-cone dystrophy with some residual macular function The PERG was undetected in patient 15618.

OCT gives the possibility of in *vivo* histological examinations and can be used to generate topographical maps or cross-sections through specific areas of the retina. It is clinically useful for imaging selected retinal dystrophies and the retinal response to the genetic lesion. OCT imaging was obtained in 4 out of 11 patients. Generalised retinal thinning and decreased

foveal thickness was observed in all 4 patients, although in one patient the outer nuclear layer was clearly present at the fovea and retinal lamination was seen (patient 31895, Figure 5.16).

Fundus autofluorescence measures lipofuscin accumulation in the RPE and allows for the visualization of the accumulation and distribution of lipofuscin in the RPE, which is often not yet visible on ophthalmoscopy. It is known that loss of autofluorescence occurs in regions with chronic photoreceptor loss, due to absent outer segment turnover by the RPE. We performed fundus autofluorescence testing to determine which retinal areas had experienced severe photoreceptor degeneration. Autofluorescence imaging was performed in 4 patients with null and missense mutations (Figure 5.17); three of these patients had clinical LCA while one was diagnosed with EORD. Fundal autofluorescence imaging in patient 31895 appeared relatively normal, corresponding to their unremarkable macular findings on fundal examination. All of the other patients showed loss of autofluorescence peripherally beyond the vascular arcades, but variable preservation of autofluorescence was seen within the central macular area. A degree of loss of autofluorescence in the central foveal region was observed in patients 14874 and 9728. These areas of reduced signal corresponded to areas of macular atrophy seen on slit-lamp biomicroscopy (Figure 5.17). Patient 13052 showed patchy areas devoid of autofluorescence which was particularly marked at the fovea and perifoveal area; these areas of signal loss were consistent with areas of marked chorioretinal atrophy at the macula. There were also with scattered areas reduced signal in a bone spicule-like conformation, which were due to masking of autofluorescence by the presence of retinal pigmentation.

ID no.	ethnicity	Mutation	Age at onset	Clinical diagnosis	Presenting symptoms	Age at examination	Goldman VF	Full field ERG	Rod ERG response	Cone 30 Hz flicker ERG	PERG	VEP	OCT	Autofluorescence
9728	african	W278X hom	0	LCA	Poor vision, nystagmus	19 y	N/A	N/A	N/A	N/A	N/A	N/A	N/A	Reduction of autofluorescencesat the fovea and perifoveal region and peripheral retina
07582	white	W278X hom	0	LCA	Poor vision, nystagmus	24 y	N/A	Non detectable	Non detectable	Non detectable	Non detectable	Markedly impaired	N/A	N/A
14777	arab	Q163X hom	2 m	LCA	Poor vision, nystagmus	2 y	N/A	Non detectable	Non detectable	Non detectable	Non detectable	Non detectable	N/A	N/A
14001	pakistani	W88X hom	0	LCA	Nystagmus, strabismus	30 y	N/A	Non detectable	Non detectable	Non detectable	Non detectable	Markedly impaired	N/A	N/A
15000	pakistani	W88X hom	0	LCA	Nystagmus, strabisumus	36 y	N/A	Non detectable	Non detectable	Non detectable	Non detectable	Markedly impaired	N/A	N/A
14874	white	c. 277-2A>G G262S het	6 m	LCA	Poor vision, nystagmus	17 y	N/A	Non detectable	Non detectable	Non detectable	Non detectable	Markedly impaired	Reduced retinal and foveal thickness	Reduced foveal autofluorescence with some preserved autofluorescence in perifoveal region
13484	african	P376S hom	2 m	LCA	Poor vision, nystagmus	19 y		Reduced in OD; undetectable in OS	Subnormal in OD, undectable in OS	Subnormal and markedly delayed in OD, undectable in OS	Non detectable	Markedly impaired	N/A	N/A
13052	african	T114I het P376S het Y134F het	2 y	EORD	Poor vision	27 y	Residual central VF of 10 degrees with temporal islands	Reduced in OD and OS	Reduced in OD and OS	Subnormal and delayed in OD and OS	Present but markedly reduced	Markedly impaired	Reduced retinal and foveal thickness	Central macular region with hypoautofluorescence with preserved perifoveal autofluorescence

13412	white	R302L hom	2 m	LCA	Poor vision, nystagmus	18 y	N/A	Severely reduced in OD and OS	Severely reduced in OD and OS	Non detectable	Non detectable	Markedly impaired	Reduced retinal and foveal thickness	N/A
31895	whilte	V71F het W72X het*	6 m	LCA	Poor vision, nystagmus	7 y	N/A	Non detectable	Non detectable	Non detectable	N/A	Markedly impaired	Reduced retinal thickness	Relatively well preserved autofluorescence
15618	indian	R302L hom	6 y	EORD	Poor vision, nystagmus	21 y	N/A	Reduced in OD and OS	Reduced in OD and OS	Subnormal in OD and undetectable in OS	Non detectable	Markedly impaired	N/A	N/A

Table 5.15 Summary of Goldman perimetry, electrodiagnostic assessment, OCT and autofluorescence imaging of patients with AIPL1-associated disease and confirmed mutations.

Novel sequence variants are indicated with '*'. Abbreviations: LCA-Lebers congenital amaurosis; EORD-Early onset retinal dystrophy; OD-right eye; OS-left eye.

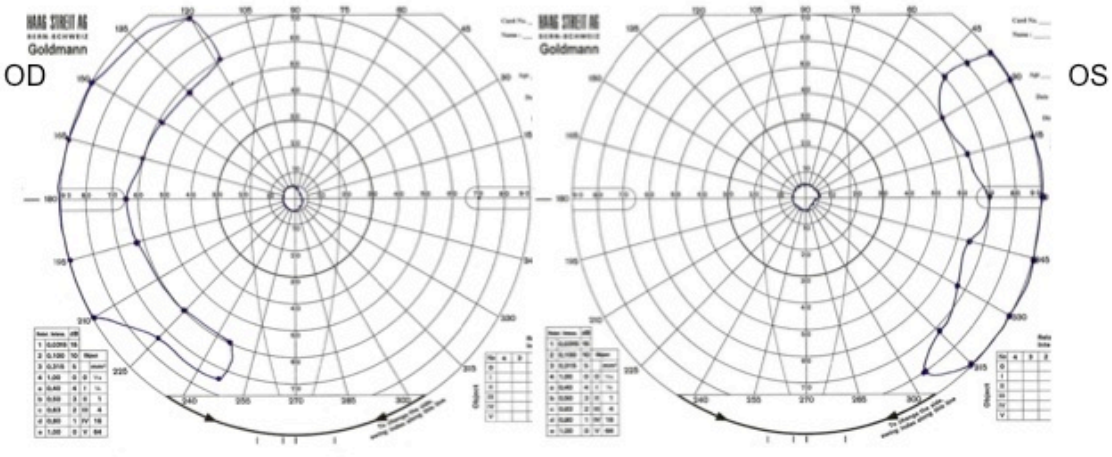

Figure 5.14. Goldman visual fields of patient 13052. There is severe loss of the peripheral visual field, leaving a residual central 10° field of vision and bilateral temporal islands of visual field.

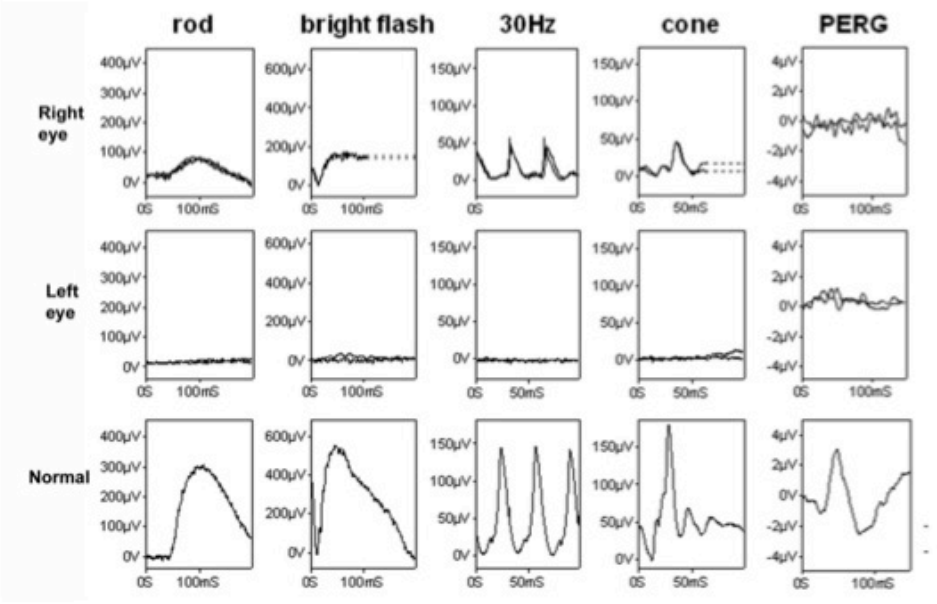

Figure 5.15. ERG traces from patient 13484. Full field ERG, scotopic and cone responses are present in the right eye but undetectable in the left. In the right eye, the rod specific ERG was subnormal. Maximal a-and b-wave amplitudes were subnormal with mild latency delay. The cone flash and flicker ERG were markedly delayed and reduced. The finding were in keeping with generalised retinal dysfunction affecting rods and cones and there is severe bilateral macular involvement.

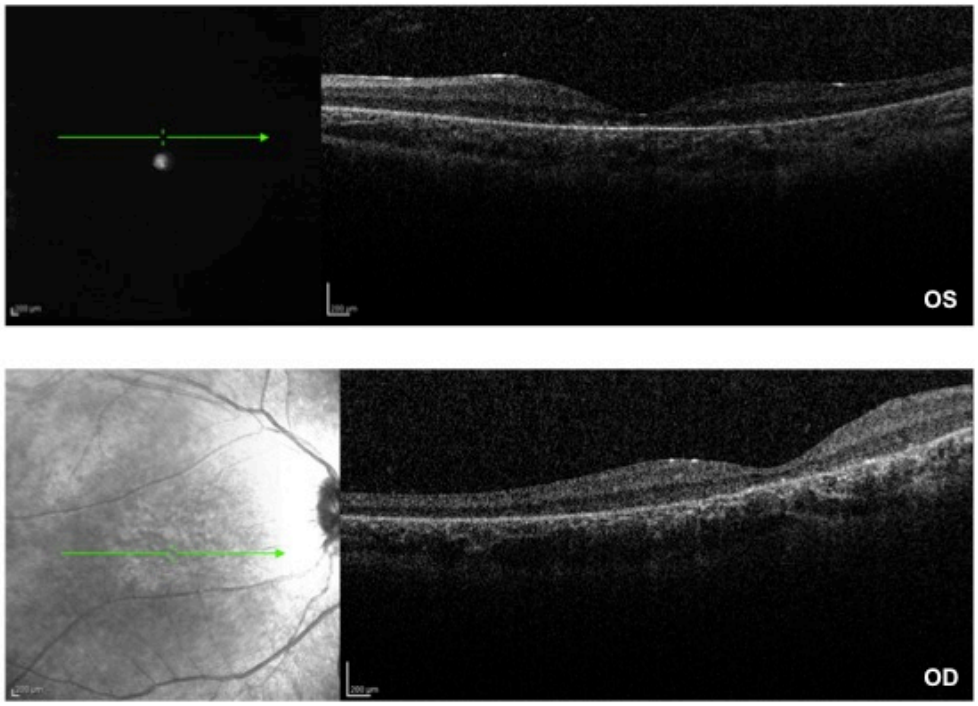

Figure 5.16. OCT scan of the right and left eyes of patient 31895 at age of 7 years. There is overall thinning of the retina although residual retinal lamination and foveal depression are present. The foveal and parafoveal ONL is seen more clearly in the right eye, OD.

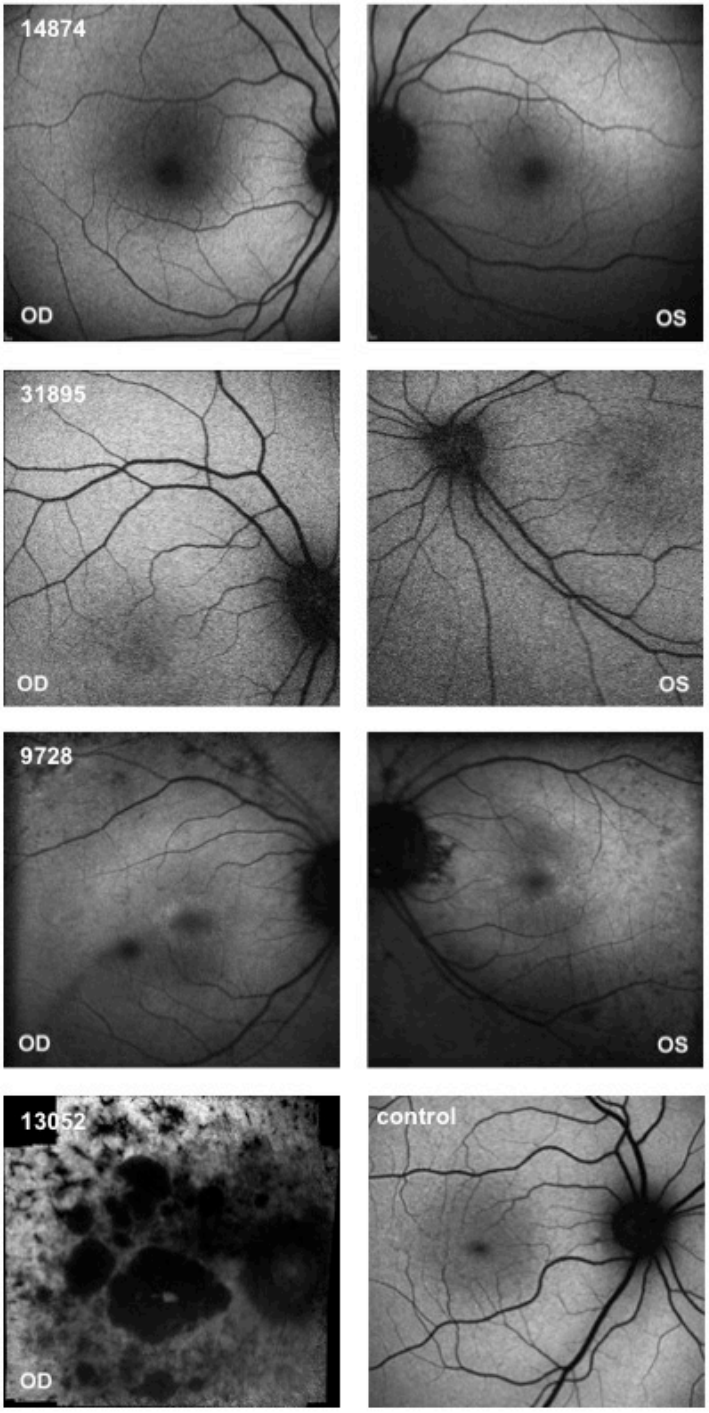

Figure 5.17. Autofluorescence (AF) of the retina of patients with AIPL1-related disease. There is loss of autofluorescence at the periphery and at the macula in patients 14874, 9728 and 13052 due to RPE loss and atrophy. Patchy masking of autofluorescence is seen in the midperipheral retina of patient 9728 and 13052 due to pigmentary accumulation. Fundal autofluorescence in patient 31895 appears relatively well preserved. An autofluorescence image from a normal control is shown for comparison.

5.7 Patients with likely AIPL1-associated disease

A summary of the phenotypic characteristic of patients with who are likely to have AIPL1-associated disease is shown in Table 5.17. These patients have been identified to have 2 or more non-conservative sequence variants, some of the variants are novel changes and the pathogenicity of these changes is therefore uncertain. At the time of writing, segregation analysis was in progress for patient 14651; DNA has been obtained from the parents and work is in progress to sequence the sample. We were unable to obtain DNA from any family members of patient 13163 for segregation analysis.

Patient 14651 is of Asian origin, specifically Indian in descent, and was from a consanguineous family. Four different mutations were identified in this patient, 3 of which have not been previously described. Segregation studies found that her mother carried one of the novel sequence variant T47R, while the mutation T114I and novel variants A313S and A285Q were inherited from her father. None of the novel variants were found in the control panel. The sequence variants T47R and A285Q are both located at highly conserved residues across different species (Figure 5.1). The change from threonine amino acid at position 47 of the AIPL1 protein to arginine represents in a change from an uncharged, hydrophobic amino acid to a charged amino acid with basic properties; the drastic differences in amino acid properties would be predicted to have significant effects on the protein function as a result. This was also supported by protein prediction analysis which found the sequence change to be damaging by three different algorithms (Table 5.13). Similarly, the change from alanine at position 285 to glutamine represents a major change in amino acid properties; alanine is small, hydrohobic amino acid, while glutamine is hydrophilic and has a large, uncharged polar amide side chain. The residue at position 285 is also located within the tetratricopeptide domain that is one of the main interacting sites. Hence any significant changes in amino acid residues are likely have a

major impact on protein function. This sequence change was predicted to be benign on SIFT and Polyphen but was found to be pathological in pMUT analysis.On the other hand, novel sequence variant A313S is located at a position where conservative substitutions are allowed (Figure 5.1). As both alanine and serine are similar in size and have uncharged side chains, the substitution would represent a conservative substitution. Protein prediction analysis (Table 5.14) further supported that the A313S sequence change was likely to be benign. Sequencing of parental DNA confirmed that the sequence variants which may have detrimental effects (T47R, A285Q and T114I) were located on different alleles. It is therefore very likely that patient 14651 has a defect in AIPL1 function that is responsible for the retinal dystrophy.

Patient 13163 was found to have 2 novel sequence variants, S198T and R270L. In-silico analysis of the S198T revealed that the substitution was unlikely to be damaging and comparison of the AIPL1 protein sequence across species showed that the residue at position 198 was not a conserved residue. It was therefore unlikely that this substitution would lead to any significant detrimental effect on AIPL1 function. The R270L change on the other hand was potentially harmful based on prediction studies, and the residue was also located in a highly conserved region within the third tetratricopeptide domain. However, as there was no DNA available from family members, it was not possible to ascertain whether the sequence variants found segregated with the disease. Given that only one of the variant could be potentially harmful and was identified in heterozygous form, it was therefore unlikely that this would result in a defect in AIPL1 function.

Phenotypically, patients 14651 and 13163 had clinically different diagnosis. Patient 14651 was diagnosed with LCA, presenting with severe visual loss at an early age. Clinical examination showed relatively normal fundal findings with no obvious signs of maculopathy (Figure). Her scotopic ERG and flash ERG responses were undetectable while her cone flicker responses showed severe delay and reduction in amplitude. Pattern ERG responses although present, were also severely reduced. Patient 14651 had a less severe

disease,early onset rod-cone dystrophy, and retained some degree of vision going into the third decade of his life. He presented to the eye clinics as an adult and despite his age, the fundal findings were unremarkable, with no intra-retinal pigmentation or macular atrophy. Electrodiagnostic testing showed reduction of the rod responses more than cone responses in keeping with a rod-cone dystrophy. Pattern ERG responses were normal.

ID no.	ethnicity	Mutation	Age at onset	Clinical diagnosis	Presenting symptoms	Age at examination	VA logMar (OD; OS)	nystagmus	strabismus	nyctalopia	pupils	PAV /PAT	Pigmentary retinopathy	maculopathy	Disc pallor	White dots	Cataract/keratoconus	refraction
14651	asian	T114I het T47R het* A285Q het* A313S het*	6 m	LCA	Not recorded	3 y	CF;CF	y	y	n	Amauros is	N/A	none	none	n	n	n	-N/A
13163	white	S198T* het R270L* het	6 m	EORD	Poor vision, nystagmus	29 y	0.96;0.96	y	y	n	Amauros is	PAV	None	None	y	n	n	-4.50/2.25 OD; -6.00/2.25 OS

Table 5.16 Clinical and genetic characteristics of 2 patients with likely AIPL1-associated disease and potentially disease-causing sequence variants.
Novel sequence variants are indicated with '*'.

Abbreviations: LCA-Leber congenital amaurosis; EORD-Early onset retinal dystrophy; OD-right eye; OS-left eye; PL-perception of light; NPL-no perception of light; CF-counting fingers; XT-exotropia (divergent squint); ET-esotropia(convergent squint; PAT- photoattraction; PAV-photoaversion; NS-nuclear sclerosis; PS-posterior subcapsular; NA-not available/not described.

5.8 Patients with possible AIPL1-associated disease

In 9 unrelated probands, only one disease allele was found (Table 5.18). First pass screening of these DNA samples using the LCA chip returned one heterozygous mutation in *AIPL1* and no other hits in the other LCA genes with the exception of patient 14341. Direct sequencing of *AIPL1* failed to identify a disease-associated mutation on the second allele. There are several possible explanations that could account for the disease in these patients. Given that all the coding regions of exons were sequenced including splice site junctions, it is unlikely that a second exonic or splice site mutation in *AIPL1* was left undetected. It remains possible that promoter or regulatory sequences of the gene contained yet unidentified mutations as the intronic regions and 3'-untranslated regions in exon 6 were not screened by our method. A large gene rearrangement or hidden mutation the unscreened region could also be complicated with these variants. A possible digenism could provide an explanation for this; digenic inheritance exists where a particular mutation in a gene causes disease only in patients who also carry a mutation in a different gene. However, digenic disease is rare and is occasionally found in proteins that function as a dimer or have a close interacting partner, such as peripherin and ROM1 or RPGRIP and RPGR. Since AIPL1 is not known to associate closely with another protein for its functions, it is unlikely that digenism is a factor in these cases. Alternatively, it is entirely possible that *AIPL1* is not responsible for the retinal dystrophies in these patients and that there is a different causative gene that is yet unidentified.

Another plausible explanation is that these alleles may act as genetic modifiers, modulating the phenotypic expression of the disease and leading to varied photoreceptor degeneration despite the same genetic background. The existence of modifier genes has been suggested by the fact that a higher amount of LCA patients carry a third allele than what would be expected by chance only [519], and further supported by the observation that

even within a single family, members who carry a third allele in a second gene presented with a more severe phenotype than members who did not carry the third allele [519][432]. Due to constraints on time and resources, it has not been possible to carry out sequencing of the other known LCA genes on these patients. One patient (patient 14341) was also included in a different mutation study and was found to have a homozygous deletion in second LCA gene, *RPGRIP.* It has been observed in many different recessive disorders, that only about 70% of the molecular defects can be identified [114].

In this group of patients, a range of clinical diagnosis was seen, ranging from LCA, EORD to RP (Table 5.18). Compared to the group of patients who had definite *AIPL1*-associated disease, over half of the patients in this category had a less severe disease such as EORD and RP. Six out of 9 patients had measureable vision at clinical examination, although it should be noted that most of them were seen at earlier ages. Fewer patients (3 out of 9) had a pigmentary retinopathy or a maculopathy, while only one patient with EORD presented with both retinal pigmentary clumping and macular atrophy. Fundal picture of the fundus of patient 13353 who has a heterozygous R302L change is showen in Figure 5.14.

ID no.	ethnicity	Mutation	Age at onset	Clinical diagnosis	Presenting symptoms	Age at examination	VA logMar (OD; OS)	nystagmus	strabismus	nyctalopia	pupils	PAV/PAT	Pigmentary retinopathy	maculopathy	Disc pallor	White dots	Cataract/keratoconus	refraction
13353	Iranian	R302L het	2 m	LCA	Poor vision, nystagmus	11 y	1,1	y	y	n	Amaurosis	PAV	n	None	n	n	n	Moderate hypermetropia
6604	african	P376S het	2 m	EORD	Poor vision, nystagmus	8 y	0.7;0.8	y	y	n	Amaurosis	PAV	Moderate, clumping	Atrophy, pigment	NA	y	n	Mild hypermetropia
13232	white	W278X het	48 m	EORD	Poor vsion	11 y	1;1	n	y	n	normal	PAV	None	Moderate atrophy	y	n	n	Mild hypermetropia
13278	pakistani	Y134F het	birth	LCA	Nystagmus	6 m	PL;PL	y	n	y	Amaurosis	n	None	Atrophy	n	y	n	N/A
14351	pakistani	R302L het	24 m	EORD	Poor vision, nystagmus, nyctalopia	5 y	1;1	y	y	y	normal	n	N/A	None	N/A	n	n	N/A
14341	white	R302L het RPGRIP homozygous c.1107delA	2 m	EORD	Poor vision, nystagmus	14 y	0.4;0.6	y	n	n	normal	PAT	Moderate	none	n	n	n	Mild myopia
15324	white	Y134F het	N/A	LCA	Poor vision, nystagmus	N/A	N/A	N/A	N/A	N/A	N/A	N/A	N/A	N/A	N/A	N/A	N/A	N/A
10759	indian	R302L het	birth	LCA	Poor vision, nystagmus	1 y	HM;HM	y	XT	n	Amaurosis	PAV	None	None	n	n	n	Moderate hypermetropia
13026	white	P376S het	2y	RP	Poor vision,	9y	3/60;3/60	n	XT	n	n	PAV	Severe	None	y	n	PS	NA

Table 5.17. Clinical and genetic characteristics of 6 patients one mutation found in AIPL1.

Abbreviations: LCA-Lebers congenital amaurosis; EORD-Early onset retinal dystrophy; OD-right eye; OS-left eye; PL-perception of light; NPL-no perception of light; CF-counting fingers; XT-exotropia (divergent squint); ET-esotropia(convergent squint; PAT- photoattraction; PAV-photoaversion; NS-nuclear sclerosis; PS-posterior subcapsular; N/A-not available/not described.

5.9 Discussion

This study presents a detailed clinical and molecular report of a series of patients affected by a severe inherited retinal dystrophy possibly due to mutations in the *AIPL1* gene and represents a comprehensive analysis of *AIPL1* in a patient cohort and a control population.

Common to the other studies in existing literature, *AIPL1* mutations have been mainly associated with LCA with a recessive inheritance pattern, although there has been one report linking the gene to juvenile RP and dominant cone-rod dystrophy[97,442]. In this study, we screened 309 unrelated probands using the LCA chip and sequenced 153 DNA samples from this panel that had not returned a molecular diagnosis following the first pass screening using the LCA chip. The patient panel consisted of patients with a range of early onset inherited retinal dystrophies to determine whether *AIPL1* mutations may cause other forms of retinal degeneration and also to determine the relative contribution of *AIPL1* mutations to severe inherited retinal dystrophies. In our study, likely disease-causing AIPL1 mutations were found in 12/309 probands, giving a prevalence of 4% in patients with various early onset retinal dystrophies, including LCA. In previous studies, *AIPL1* has been estimated to cause approximately 7% of LCA cases worldwide[440,442].

Phenotypic variability has been well established in LCA patients: heterogeneity is seen in retinal appearance, refractive errors, nyctalopia, manifest and longitudinal changes in visual function, cataracts and keratoconus. The retinal appearance can vary considerably between the different LCA genotypes, although there are gene-specific phenotypic features that have been observed in LCA (for further information, please refer to Chapter 1, section 1.3.2.2). Previous published phenotype-genotype studies of *AIPL1* mutations have been based on cohorts of patients with LCA. Compared to the other LCA genes, *AIPL1*-related LCA have been described to be particularly with severe visual loss, pronounced macular

involvement and optic nerve pallor. Our study found that *AIPL1*-associated retinal disease is clinically variable; patients identified with *AIPL1* mutations ranged from less severe early onset retinal dystrophy to LCA. This suggests that there may be a spectrum of disease associated with *AIPL1* mutations and it may be possible that screening for *AIPL1* mutations in a different patient panel of recessive RP may reveal mutations associated with other categories of inherited retinal dystrophies. Since our mutation screen was performed on a panel of patients with severe early onset retinal dystrophy, it is understandable that the phenotype seen in the patients who were identified with *AIPL1* mutations would be severe in nature. The patients in this study with LCA and *AIPL1* mutations have a severe phenotype which is in keeping with other series with *AIPL1* phenotypic data[174][103][151][310]; these patients had unmeasureable vision, significant maculopathy and some degree of optic disc pallor in adulthood. In established disease, patients with *AIPL1* mutations also develop significant pigmentary retinopathy. Features of pronounced atrophic maculopathy, optic disc pallor and significant peripheral retinal pigmentation appear to be unique to *AIPL1* mutations and distinguish this from the other genotypes; while patients with *GUCY2D* and *RPGRIP1* mutations appear similar to the *AIPL1* phenotype in terms of markedly decreased vision, visual fields and ERGs, phenotypical differences exist in terms of macular atrophy, pattern of pigmentary changes, cataract and keratoconus which are more frequent in *AIPL1* patients[367][104][110]. Macular atrophy has been reported in majority of patients with *CRX*-related LCA, but unlike in *AIPL1* mutations, pigmentary retinopathy is not a prominent feature in *CRX* mutations[208][433][443][522]. Patients with *RPE65*-related LCA are also clinically distinguishable from patients with *AIPL1* mutation; the *RPE65* phenotype is associated with measurable visual acuities, better visual fields and ERGs than the *AIPL1* phenotype. Peripheral retinal changes are subtle in *RPE65* mutations, and macular atrophy are not a feature[285][468]. Patients with LCA due to *RPE65* mutations often experience transient visual improvement in childhood followed by deterioration later in life, while the visual function in *AIPL1* patients have been described to progressively decline[285][103]. Since most of the patients in this study were examined at later ages, conclusive observations

regarding the visual evolution of patients with *AIPL1* mutations could not be made from this.

In addition to peripheral retinal pigmentation and macula atrophy, other significant posterior pole findings included various degree of RPE and choriocapillaris atrophic changes and drusen-like intraretinal white dots. Three patients (27%) with *AIPL1* mutations had drusen-like intraretinal deposits in their first and second decades of life. While extensive pigmentary changes and peripheral chorioretinal atrophy have been frequently described in other studies[440][435], intraretinal drusen-like deposits in association with *AIPL1* mutations have only been reported in one other study thus far [151]. Other genotypes which have been associated with white retinal deposits include *RPE65, RPGRIP* and *CRB1.* Neither nyctalopia nor photoaversion were frequently reported in this series and refractive findings showed moderate myopia and hypermetropia being equally common in patients. This differed from observations in other series of *AIPL1* mutations which described photoaversion and moderate hypermetropia as common findings in these patients. Anterior segment signs were significant for cataracts and keratoconus, about 55% of patients in this series had a combination of cataracts and keratoconus, which is in keeping with most other series with *AIPL1* phenotype data [174] [103][151][310]. One study has further described the association of cataracts and keratoconus with homozygous mutations only[103], but this has not been observed in this study in which cataracts were also seen in patients with compound heterozygous mutations. Many retinal and anterior segment signs were more prevalent with increasing age; peripheral retinal pigmentation, chorioretinal atrophy, macular atrophy were not seen before the first decade in this series but became increasingly prevalent after the second decade. The association of cataracts and keratoconus with other retinal dystrophies and LCA have been well documented beyond the second decade of life in patients[184][137]. In this study, cataracts and keratoconus were noted before the second decade in some patients and were more prevalent with age. Unlike other published series, assessments of perimetry, autofluorescence and OCT were included to further define the phenotype. The findings from these ancillary tests

supported the clinical phenotype, with marked peripheral visual field loss and retinal thinning due to primary photoreceptor degeneration. However, it should be noted that majority of the clinical characteristics described on clinical examination and imaging studies relate to changes seen in older patients; most fundal findings begin to appear after the first decade of life. The identification of young patients with *AIPL1* mutations remains a challenge as there are minimal clinical signs, particularly within the first year of life.

Despite the clinical heterogeneity, we found that the severity of disease and certain phenotypic features may be predicted from the underlying mutation. Patients with homozygous null mutations were found to have a more severe disease, in terms of retinal pigmentation and macular atrophy. Patients with missense mutations may have a less severe disease due to residual protein function, with better residual vision, slower progression and later onset of maculopathy and present clinically as early onset retinal dystrophy. This may be due to residual AIPL1 function from missense mutations, and may be analogous to the hypomorphic *Aipl1h/h* mouse. Variation in clinical severity has also been observed with other LCA genes; *RPGRIP1, CRB1, TULP1* and *RPE65* have been reported to cause either LCA or an acquired, later-onset rod-cone dystrophy[173][155]. It has been suggested that a more severe retinal dystrophy such as LCA may result from an excess of null alleles when compared to other less severe dystrophies such as retinitis pigmentosa.

A particular problem highlighted in this study which may render the identification of *AIPL1* patients difficult is the uncertainty surrounding the pathogenicity of the mutations and difficulty in ascertaining the true nature of sequence variants. This is compounded by the polymorphic nature of the gene, as revealed by the sequencing of both patient and control panels. Some of the published mutations have been shown not to have any deleterious effects on functional studies [476][393][7], and consequently it may be possible that some of the reported mutations in genetic databases may not be true mutations. This is particularly pertinent to the R302L

substitution which was previously described as a pathogenic mutation. Our study indicates that this may be questionable as we identified an unaffected relative who carried the homozygous mutation. Furthermore, our analysis of the predicted functional effects of the missense substitution using protein function prediction software showed that it was not deleterious. This substitution was however not found in our screening of the control panel and was found in the panel of probands with an allele frequency of 1.6% and mostly in individuals of Asian ethnic origins. It is thus possible that R302L represents a rare ethnic polymorphism.

It is difficult to be certain that the *AIPL1* mutations are disease-causing without performing biochemical and functional analysis of the mutant protein. Future work is required in this aspect, and *in vivo* functional assessment of the mutations in question is preferable to *in vitro* studies. This could be performed by creating a transgenic mouse by injecting a construct carrying the point mutation of interest into fertilized wild-type mouse oocytes and breeding the founders into mice lacking *Aipl1* (*Aipl1 -/-*) to produce mice with the transgene against an *Aipl1 -/-* background. A more elegant method that better replicates the condition in human mutations would be to create a "knock-in" mouse using a targeting construct that carries the particular point mutation as this would result in the altered gene being inserted in the specific locus and thus subjected to the normal regulatory mechanisms of expression. Histopathogical studies of the retina for signs of photoreceptor degeneration and electrophysiological assessment of these genetically engineered animals will confirm the disease-causing potential of these specific mutations. Alternatively, an easier and more readily available analysis would be to inject an AAV vector expressing the mutant *AIPL1* gene into *Aipl1 -/-* mice and examining the treated animals for signs of photoreceptor rescue. Any improvement in ERG or morphology would indicate that the mutations were probably benign. Due to constraints on time and resources, it was not possible to pursue this line of investigations in this study, and therefore certain assumptions had to be made in order to be able to draw some conclusions to the findings. As we have found disease-associated mutations, segregating among families, with no other change in

the gene sequence and are absent from ethnically matched control subjects, it was reasonable to consider these as possible disease-causing mutations.

Despite the availability of genotyping microarrays for LCA, the genetic heterogeneity of this condition continues to pose a significant challenge to clinicians. Identification of genotype-phenotype correlations in LCA and other retinal dystrophies would help to suggest the causal gene and refine the molecular screening strategy. The molecular characterization of LCA is important for genetic counseling and also with the advent of gene therapy trials, for identification of suitable candidates for potential therapy. With more correlation studies, it may become easier to use objective data such as the presence of key physical signs to implicate certain genes over others in the pathogenesis. The clinical characterization of disease in this study such as visual acuity, signs in the anterior and posterior segments are helpful in identifying patients with *AIPL1* mutations and are important to allow for the interpretation of any future therapies. The identification of patients with milder phenotype due to *AIPL1* mutations might provide a wider therapeutic window for preventative intervention. However, the prevalence of clinical signs varies with age and is subjected to environmental influences, genetic background and modifier alleles. All of these should be taken into consideration to facilitate the accurate assessment of patients.

6. Final Discussion

The last twenty years have seen enormous growth in the understanding of the molecular and histopathological basis of inherited retinal degeneration. Many of the causative genes have now been identified, providing an impetus to develop gene-based treatments to treat retinal degeneration and improve photoreceptor survival. Replacement gene therapy mediated by AAV vectors appears to be the most promising potential therapy for retinal degenerations, especially for those severe forms such as LCA which are unlikely to respond to more conservative forms of treatment. Following landmark preclinical studies demonstrating long term functional improvement as a result of gene replacement of *RPE65* in a dog model of LCA, three clinical trials of ocular gene therapy have commenced to treat early-onset severe retinal degeneration in patients with defects in the *RPE65* gene The preliminary success reported from these studies will undoubtedly pave the way for more clinical trials to treat other forms of retinal dystrophies. Hence, there is an urgent need to identify other candidate disorders suitable for translation from the laboratory to human clinical trials. These are most likely to be conditions where gene therapy has proven to be efficacious in an animal model equivalent.

The selection of a genetic disease for gene therapy clinical trials will depend on a variety of clinical and experimental criteria. The disease must be caused by loss-of-function mutations for gene replacement therapy to be applicable. Most the severe inherited retinal diseases such as LCA and early onset retinal dystrophies are caused by recessive mutations of retinal genes leading to the loss or relative lack of the encoded protein product . Replacement of these genes would restore the target protein and correct the deficiency in affected cells. Similarly, the retinal degeneration secondary to *AIPL1* mutations is caused by the loss or reduction in AIPL1 protein. Replacement of *AIPL1* in photoreceptor cells led to increased AIPL1 protein levels and correction of the downstream effects shown by increased PDE biosynthesis and the translocation of cGMP PDE to the outer segments. It

is also important that the rate of progression of the disease enables a rapid read out of the outcome of treatment. The severe nature of *AIPL1*-related retinopathies both in human and mouse would provide a clear indication of any benefit following therapeutic gene delivery in the form of either an improvement in retinal function or vision, or the delay in progression of photoreceptor cell loss. However, this could also act as a double-edged sword since experimentally, animal models of rapid retinal degeneration have previously been difficult to rescue. With advances in vector technology and the availability of faster and more efficient AAV serotypes such as AAV2/8, the prospects of treating such rapid retinal dystrophies has improved. That AAV2/8-mediated gene replacement was effective in rescuing such rapid retinal degeneration in the *Aipl1 -/-* mouse indicates that the rapid retinal degeneration in LCA patients may also respond favourably to treatment. Clinically, the prevalence of the disorder is important in determining the potential value of a therapeutic strategy. Treatment for conditions which have higher prevalence would make patient recruitment easier and have greater clinical impact compared to a rare disease. The prevalence of LCA caused by *AIPL1* mutations is approximately 7%, which is a significant portion of cases when compared to the contribution of other known LCA genes[442][103][101]. This is similar to the prevalence of LCA cases associated with *RPE65* mutations which currently being treated in clinical trials. The contribution of *AIPL1* to retinal diseases is likely to be even higher as it has also been described to cause other types of retinal dystrophies such as juvenile cone-rod dystrophy and milder forms of early onset retinal dystrophies [103,442].

The function of the transgene product may also dictate the efficacy of gene replacement therapy. High efficiency of gene transfer may not be essential for conditions where the transgene encodes for secreted protein; expression in a few target cells might be sufficient for effective treatment while useful therapy may also be achieved by transducing cell types that do not normally produce the protein. On the other hand, in conditions where the encoded protein is essential for the survival and function of photoreceptor cells such as a transcription factor or a phototransduction protein, effective therapy

would require the transgene to be delivered specifically to each targeted cell type and ideally to mediate transgene expression at physiological levels. Since AIPL1 is essential for PDE biosynthesis and photoreceptor cell survival, the treatment of *AIPL1*-related retinopathies requires specific and efficient delivery of the therapeutic gene to individual photoreceptor cells. AAV2/2 and AAV2/8 were chosen as vectors because of their capability to transduce photoreceptors following subretinal delivery. While AAV2/2 was able to slow photoreceptor degeneration in the *Aipl1 h/h* mouse, it was unsuccessful in rescuing the *Aipl1 -/-* model. Switching from AAV2/2 to AAV2/8 vector that carried the same expression construct resulted in strong therapeutic rescue in the null model. This observation indicates that in a severe disease, a faster, more efficient vector with high expression levels is needed.

The availability of an animal model that accurately reflects the disease in patients is a critical factor in the development of a treatment strategy. Success in treating an animal model that mimics the human disease provides strong justification in moving a therapeutic strategy to the clinic, as exemplified by the *RPE65* treatment trials. In humans, genetic defects in *AIPL1* give rise to a heterogeous set of clinical conditions[103,440,442] that is also reflected in the genetically engineered mouse models of *AIPL1* deficiency. The *Aipl1 -/-* and the *Aipl1 h/h* mice mirror the clinical disease spectrum, and are reminiscent of LCA and RP respectively, while the light-accelerated *Aipl1 h/h* mouse with an intermediate disease severity is similar to patients with early-onset retinal dystrophy. However, one of the requirements for the ease of translation to clinical trials is that any new therapeutical strategy must be shown to be efficacious in an eye similar to that of humans. So far, there are only a few naturally occurring large animal models of retinal dystrophies. The naturally occuring *RPE65*-deficient dog has been a critical factor in moving gene replacement therapy from preclinical studies to current ongoing clinical trials[2] [260]. Mouse models on the other hand, are not limited by the availability of naturally occurring models and many gene defects can be recreated in mice by targeted gene disruption. In the absence of larger animal models, either naturally-occurring

or artificially generated, future clinical trials may have to proceed based on efficacy data from murine studies alone.

A central issue for any human gene therapy intervention is the assessment of the risk to benefit ratio. AAV vectors are frequently used in human clinical trials, it is therefore vital to evaluate the risks of its use for personnel involved in handling the vector either in research or clinical trials as well as for the patients and their future offsprings. Thus far, AAV has shown to have an excellent safety profile; preclinical studies have consistently demonstrated the lack of toxicity, minimal inflammatory and immune responses to the vector and negligible systemic dissemination to distant organs following intraocular delivery. In the recent phase I human ocular gene therapy trials, three different groups of investigators have reported the lack of any clinically significant adverse effects from the surgical procedure and the absence of systemic dissemination, suggesting that any extraocular leakage of vector from the subretinal space was minimal [34,181,293] There was no significant intraocular inflammatory responses to vector injection and no sustained reduction in visual function despite the temporary retinal detachment in the patients one year after treatment. However, the long term ocular and systemic safety of the procedure in humans will only be known after further follow up in the later stages of the trials. Apart from the obvious risks associated with a viral vector, other hazards that need to be taken into consideration include the effects of transgene overexpression. This is less likely to cause any toxicity or adverse effects where the biological function of the protein does not require its levels to be within a narrow range. In our study, we showed that *AIPL1* overexpression did not result in deleterious effects. The ectopic expression of AIPL1 in the RPE by AAV2/2 vector driven by the ubiquitous CMV promoter did not have any negative effects on photoreceptor function or survival. As the exact function of AIPL1 is yet completely understood, it is difficult to hypothesize on the effects of *AIPL1* overexpression on the retina. AIPL1 is intricately linked to cGMP PDE, a multimeric protein composed of subunits α,β and γ and is specifically required for the proper assembly of PDE subunits[240]. The lack of toxicity

from *AIPL1* overexpression may be due the possibility that its function is limited by the availability of cGMP PDE.

The translation of a gene-based strategy into clinical trials also depends on the availability of a suitable vector. To be effective, gene therapy to the retina initially requires specific and efficient vector that can mediate widespread transduction of the target cells. It is then possible to tailor gene expression to the appropriate levels and spatial patterns through the use of specific promoter elements. It is also vital that the chosen vector for the treatment of inherited retinopathies is able to mediate long term expression of the transgene without integration into the host genome since the treatment of these disorders necessitate lifelong correction. For this purpose, AAV vectors which have considerably lower immunogenity appear to be the best suited vector for gene delivery. Together with the immunopriviliged properties of the eye, AAV vectors have been able to confer long term transgene expression lasting many years without integration into the host genome. In our study, transgene expression and therapeutic effect appeared to be long lasting and without the need for retreatment. In *Aipl1 h/h* mice that received subretinal injection with therapeutic AAV2/2 and AAV2/8 vectors, sustained transgene expression and photoreceptor rescue was noted up to over 1 year and 5 months post injection respectively. AAV2/8-mediated delivery of *AIPL1* in the null mutant, *Aipl1 -/-* mouse, appeared to be stable for at least 3 months post injection, the latest time point examined. These were the latest time point examined in the study following which the animals were culled to allow for histological examination. In order to appreciate the full durability of the therapeutic effect, further similar experiments to examine the point of decline in transgene expression with a longer period of follow up would be required. The main drawback of AAV which often limits its use for gene transfer is its small packaging capacity of 4.7 kb and its slow onset of expression after transduction. For the purpose of *AIPL1* gene replacement, the restricted carrying capacity of AAV is less of an issue since both the murine and human *AIPL1* cDNA are less than 3 kb in size. Faster onset and efficiency of *in vivo* gene transfer was obtained with the use of AAV2/8, which was subsequently used to treat faster photoreceptor degeneration.

The use of various *AIPL1* mouse models of different disease severity in this study highlights the importance of timing of gene transfer in relation to the disease course, the onset and levels of expression in determining the success rate of the treatment. As demonstrated in the difference in efficacy comparing AAV2/2 and AAV2/8 vector in the rapid models, these factors need to be tailored according to the characteristics and rate of progression of the particular condition.

Thus, *AIPL1*-related retinal dystrophy has progressed through many of the steps towards a treatment strategy, from gene identification[440][442] followed by clinical characterisation of disease[103][151][485][362] and to increased understanding of the molecular mechanism[477][282][391][240][295][186] and then now to proof-of-concept studies in animal models. The success of gene therapy in correcting the disease phenotype in *Aipl1*-deficient and hypomorphic mice described in the preceding sections suggests that human *AIPL1*-related retinopathies may be amenable to treatment and supports the further development of this preclinical work to clinical trials. This proof-of-concept study was reinforced by another recent work which targeted both rods and cones and rescued both photoreceptors following AAV-mediated *Aipl1* replacement in *Aipl1*-mutant mice[455]. In justifying a clinical trial, a key question that is posed is whether the phenotype of human disease is similar enough to that in the animal models and hence, if it is realistic to expect comparable treatment benefits in humans to that already seen in the animal models. Despite the similarities in phototransduction defect and severe phenotype in both the murine models of *Aipl1* and *PDE6β* deficiency, the human equivalents of these genetic defects reveal dramatic differences. In contrast to patient with *AIPL1*-related LCA who have severe early visual impairment, patients with autosomal recessive RP due to *PDE6β* mutations maintain good visual acuity until later in life. While the *rd1* mouse may not completely mirror the human disease, the *Aipl1*mutant models are consistent with the human condition; the *Aipl1 -/-* mouse has an early and severe degeneration which is phenotypically similar to patients with *AIPL1*-related LCA, and the *Aipl1 h/h*

hypomorphic mutant is reminiscent of the subgroup patients with autosomal recessive rod-cone dystrophy that have been described in this study and in another recently published study[204]. The main difference between human and mouse that need to be considered is anatomical distinction between the rod-dominated mouse retina and the human retina that has central cone-rich foveal region as this may impact on the treatment strategy. Since AIPL1 is essential for the maintenance and survival of both rods and cones[282][232], much of the severe visual impairment in patients with *AIPL1*-related disease is due to cone dysfunction and loss. Hence, in treating patients, it is even more vital that gene delivery vectors should target both rods and cones photoreceptors. By using a rhodopsin kinase promoter to drive transgene expression in an AAV vector, a recent study targeted and rescued both rods and cones in various *Aipl1* mutant mice[455]. Extrapolating these findings, it would be reasonable to expect that foveal cones in the human retina would benefit from such AAV-mediated gene delivery that targeted both types of photoreceptor cells. However, further verification of the rhodopsin kinase promoter may be indicated as recent studies have suggested that its ability to transduce both photoreceptor cell types may differ in between species[46].

The next important question to be answered is whether there is residual retinal architecture and viable photoreceptors in *AIPL1* patients to afford a reasonable chance of success. The current information available on the retinal phenotype of *AIPL1*-related LCA patients is limited; there are a few short clinical descriptions that accompanied the reports of molecular identification[441][440], clinical evaluations of *AIPL1* patients specifically or along with other genotypes[151][103][310][362][485][204] and rare reports bearing some histopathological descriptions of donor retinal tissue. Frequently described clinical findings included severe visual impairment even at very young ages, no visual fields, non-detectable electroretinograms, pigmentary retinopathy and atrophic maculopathy. The only two histological studies currently available described the paucity of photoreceptors and predominance of retinal gliosis with sparing of the RPE layer and Bruchs membrane in associated with *AIPL1*related disease[183][478]. However, it should be pointed out that these histological studies were performed in the

same adult patient with already advanced disease. While most patient studies relating to *AIPL1* mutations to date have mostly described clinical features seen on eye examination, the advent of new non-invasive imaging techniques and psychophysical tests provide another dimension in phenotype characterisation of patients. An single description of the OCT scan in a 22-year-old LCA patient with *AIPL1* mutation showed abnormal retinal laminar architecture[362]. A recent study of provided detailed descriptions of retinal structure and function using autofluorescence imaging, OCT, pupillometry, perimetry and electrophysiology and on *AIPL1* patients ranging from 16 to 40 years of age[204]. Findings revealed extensive loss of foveal cones and extrafoveal photoreceptors that was more severe with age, while variable thickening of the inner nuclear layer was seen that was suggestive of retinal remodeling[204]. Perimetry and pupillometry confirmed retained rod function in patients, some of whom were in the third and fourth decades of life. Some patients even had pupillary light reflexes which were within the normal range of responses. More significantly, this study also described a patient with retinitis pigmentosa associated with *AIPL1* mutations. This patient had a much later-onset protracted course of disease; the onset of symptoms was noted from the first decade of life and retained macular photoreceptors was seen up the the sixth decade of life. The authors from this novel study implied that given the severity of disease and loss of the cone-rich foveal ONL in *AIPL1* LCA patients, there may be limited response to gene replacement therapy. However, it should be pointed out that these findings are indicative of adult patients who already have established disease. Our study suggests that macular and foveal photoreceptors and RPE remain relatively well preserved in early childhood ages, this is particularly highlighted in patient 31895 who was examined at the age of 7 years; well preserved autofluorescence at the fovea and surrounding macular regions were seen and were almost normal in appearance, while OCT scanning revealed present retinal lamination and foveal and parafoveal ONL. Evidence of detectable ONL in young human retina despite early absence of rod and cone photoreceptor function by ERG would support the hypothesis that visual loss in early stages is due to rod and cone dysfunction, possibly from a phototransduction defect given the

connection with cGMP PDE. Uncorrected, this persistent derangement in phototransduction and continuing loss of PDE may later on lead to a rapid photoreceptor apoptosis and secondary retinal degeneration. Studies of the various mouse models of AIPL1 deficiency appear to support this theory, given that normal retinal architecture were observed in young mice regardless of the rate of degeneration. Hence, while adult LCA patients may not fully respond to gene replacement therapy due to advanced disease, our findings suggest that young patients might be amenable to treatment and that treatment should be administered in very early ages for maximal therapeutic benefit. A further group of patients who would stand to respond favourable to gene-base treatment are the patients who have a milder and later onset of retinal dystrophy associated with *AIPL1*-mutations. To date, there are only four patients described as having a different diagnoses other than LCA that is associated with *AIPL1* mutations; three of these had a heterozygous 12 bp deletion in *AIPL1* and were diagnosed with cone-rod dystrophy and juvenile retinitis pigmentosa[442], while one patient was recently described with later-onset retinitis pigmentosa and carried compound heterozygous null mutation and a missense mutation (W278X and G122R)[204]. Our study identified a further two patients with milder disease of rod-cone dystrophy associated with *AIPL1* mutations, and suggest that there may be a further subset of patients with diagnoses other than LCA due to *AIPL1* mutations. Screening of a large cohort of patients with the clinical diagnoses of RP or rod-cone dystrophy for *AIPL1* mutations have yet been undertaken and would be a worthwhile endeavor. Similarly, more studies in young children with *AIPL1* mutations are needed and will be crucial in characterising the retinal structure and function in this age group and also in providing further indication of the success gene-based treatment in these patients.

There are further issues to be considered in setting up a clinical trial to treat *AIPL1* patients: who would be suitable target patients to be treated first, and what would be the best strategy identify candidate patients for treatment? Given the difficulty in obtaining ethical approval for carrying out trials in young patients, the group of patients with milder *AIPL1* disease may serve

well as initial candidates in a gene therapy trial. The slower rate of disease and preservation of cones and rods well into adulthood may offer good potential of a treatment benefit, although it may take a longer period of time to demonstrate this. Ultimately, the goal would be to treat young patients with LCA who stand to benefit the most if the treatment is successful. The potential for therapeutic application in humans depend the identification of candidate patients. One of the major foreseeable obstacle is the identification of candidate patients in a timely fashion, particularly the patients with LCA. The *AIPL1-LCA* phenotype has several distinctive features such as the severity of visual impairment, retinal bone-spicule pigmentation, atrophic maculopathy and an association with keratoconus. However, many of these features are age-dependent and it can be difficult to distinguish between the different genotypes since the retina responds in similar ways to insults. Furthermore, the retina is almost always normal in appearance in very young patients with various forms of retinal dystrophies including LCA, regardless of the underlying gene mutation. While visual acuity and signs in the anterior and posterior segments may be helpful in selecting the genes or loci most likely to be implicated, molecular screening remains the mainstay of establishing definitive diagnosis, which is a pre-requisite to treatment. Specific to *AIPL1* mutations, molecular diagnosis need to be undertaken as early as possible and preferably in early childhood. In the hospital setting, it may be necessary to consider screening offsprings of patients with family history of LCA or severe inherited retinopathies and young children or infants presenting with impaired vision for *AIPL1* mutations. For cost effectiveness in a large gene therapy program involving the treatment of several different gene defects, first pass screening using the LCA chip will indicate the underlying gene involved, and should be followed by resequencing to confirm the mutations. Where there is high clinical suspicion of *AIPL1*-related disease, patients should be sequenced directly, this is now made easier with the availability of resequencing chips which will enable high volume rapid sequencing of patient DNA.

There is now robust proof of efficacy from this preclinical study and recently others to justify clinical trials to treat patients with *AIPL1* mutations. Human

gene replacement therapy offers these patients the best possibility of alleviating a disease that is currently incurable and that has invariably dire consequences. For these patients, the benefits of treatment clearly outweigh the risks. Following on from this, there are now efforts in progress to develop a clinical grade vector and the infrastructure for an *AIPL1* clinical trial, which could be expected to commence in the next five years.

Appendix:

Patient clinical histories and pedigree (where available)

Patient 9728

Patient 9728, of African origin, was the product of a consanguineous marriage between first cousins. Apart from visual problems, he also suffered from autism and epilepsy. He was diagnosed with LCA and was first examined at the age of 19 years old. At that time, he was only able to perceive light. His fundal appearances showed bilateral bone spicule-like peripheral pigmentation, attenuated blood vessels and macular scarring. However, due to difficulties with cooperation, electrophysiology studies were not performed. Autofluorescence imaging showed generalised reduction of autofluorescence at the fovea and peripheral retina with some residual signal in the parafoveal region inside the major vascular arcades.

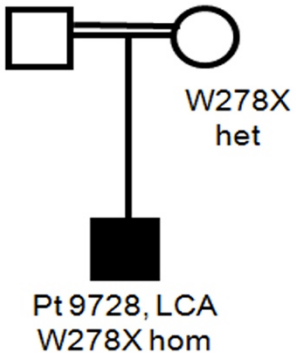

Patient 07582

Patient 07582 was a male Caucasian patient from South Africa who was first seen in 2002 at the age of 19 years old. Severe visual loss was noted since birth and a non-progressive course was described. He did not suffer from any other medical or systemic problems apart from visual symptoms. There was no history of consanguinity and no other family members were affected. At the time of examination, he was only able to perceive light in both eyes. There was bone-spicule peripheral retinal pigmentation, central foveal atrophy and attenuation of the retinal vasculature in both fundi. Both optic discs appeared normal. Electrophysiology performed at the time of assessment showed severe loss of rod and cone ERG responses. The ERG results of patient 07582 are in keeping with the clinical diagnosis of Lebers Congenital Amaurosis, with severe macular involvement. The rod-specific ERG and pattern ERG (PERG) were not detectable and the bright flash "mixed" ERG was severely reduced. Single flash cone ERGs (photopic) and 30 Hz flicker ERG showed severely reduced and delayed amplitudes.

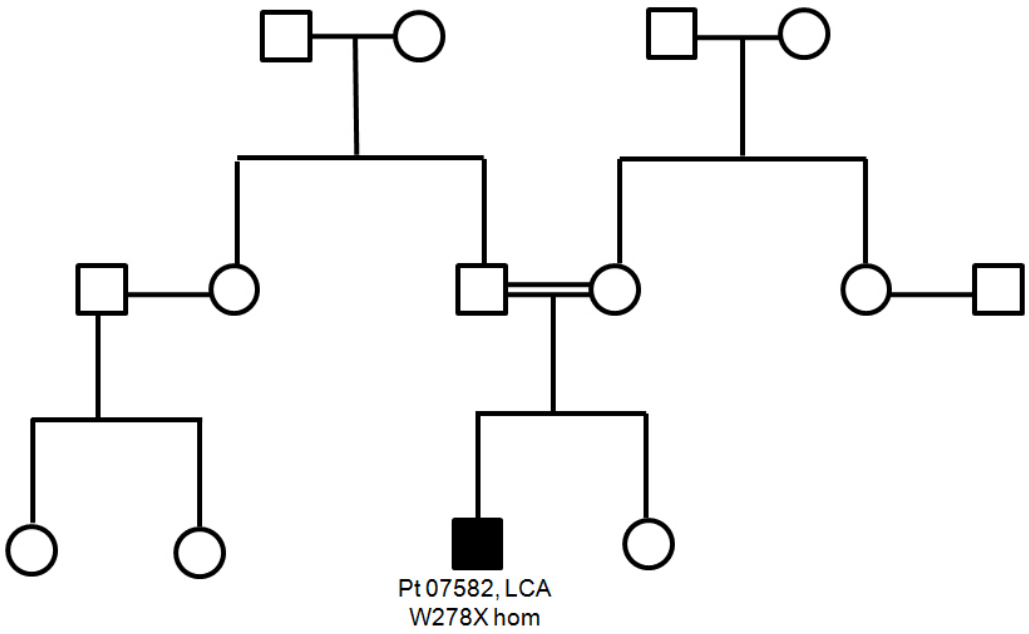

Patient 14777

Patient 14777 was from a consanguineous middle-eastern family in Dubai whose parents were first cousins. He was diagnosed with LCA at the age of 18 months. At 3 months of age, he was noted to have nystagmus, a convergent squint and poor vision, and later night blindess and peripheral field loss. He presented to the eye clinics at the age of 2 years old. Clinical examination at that time showed relatively normal-looking fundus and optic disc bilaterally. Electrophysiology tests revealed no detectable scotopic or photopic ERG amplitudes. He was too young to cooperate with Goldman perimetry assessment, while OCT and autofluorescence imaging did not reveal anything specific changes.

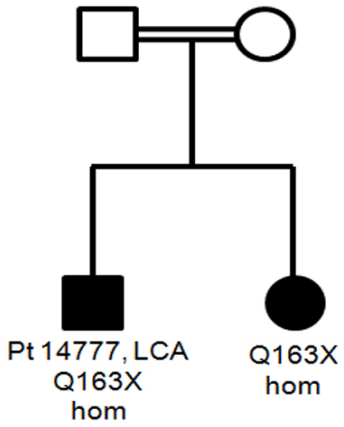

Patient 14000

Patient 14000 was first seen at the age of 30 years, and presented with a history of nystagmus, nyctalopia and strabismus which was noted from birth. Her parents were first cousins and she also had an affected sister. Her visual acuities at presentation were only perception of light in the right and left eyes. Clinical examination showed intra-retinal pigmentation, attenuated

blood vessels and macular atrophy. Both optic discs appeared pale indicating optic atrophy. There were also signs of posterior subcapsular cataract and keratoconus affecting the right eye. She was diagnosed with LCA. Electrodiagnostic tests showed no recordable activity for maximum flash ERG, pattern ERG, photopic ERG and 30 Hz flicker ERG. Goldman perimetry, OCT and autofluorescence imaging were not performed on this patient.

Patient 15000

Patient 15000, an affected sister of patient 14000, is 2 years older. She was also noted to have poor vision and nystagmus shortly after birth and later on was diagnosed with LCA. At the time of examination, she was 36 years old and was unable to perceive light. Clinical examination showed findings in keeping with end-stage retinal degeneration, with widespread intraretinal pigmentation, bilateral pale discs, severely attenuatied vessels and bilateral macula coloboma. There was also posterior subcapsular cataract and keratoconus in one eye. Electrodiagnostic tests detected no rod or cone responses.

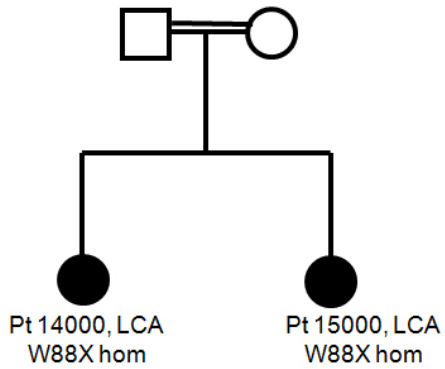

Patient 14874

Patient 14874 came from a non-consanguinous white family and diagnosed with LCA. He first presented with poor vision and nystagmus at 6 months of age. His parents noticed that he was attracted to bright lights as a child and later found that he had poor night vision and sluggish pupils. When he was seen in the eye clinic at the age of 17, he was only able to perceive light in both eyes. He had posterior subcapsular cataracts and moderate myopia. Fundal examination showed retinal pigmentary changes and RPE atrophy in the periphery. Although his optic discs appeared healthy, there was bilateral early macular atrophy and attenuation of retinal vessels. OCT scan showed reduction of foveal thickness and thinning of the macular area in both eyes. Autofluorescence imaging showed reduced autofluorescence at the fovea. Electrodiagnostic studies showed that both scotopic and photopic ERG responses were non detectable.

Patient 13484

Patient 13484 was of African-Carribean descent and has an affected sister (patient 6604). Both of them were diagnosed with rod-cone dystrophy. There was no history of consanguinity. At 2 months of age, patient 13484 was noted to have poor vision, nystagmus and nightblindness. As a child, she noted to have a habit of eye-rubbing (oculodigital sign), a divergent squint and photoaversion (dislike of light). When she presented to the eye clinic at 19 years of age, she had heavy pigment clumping in the mid-peripheral retina with RPE atrophy, attenuation of retinal vessels and macular atrophy. Her visual acuity was logMar 1.6 in the right eye and no perception of light in the left eye. Scotopic and photopic ERGs was present although severely reduced in the right eye, while the left eye had no detectable ERG response. There was no detectable pattern ERG.

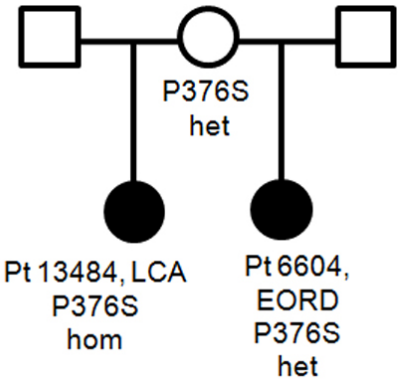

Patient 13052

Patient 13052 is of black African origin and her family came Sudan. There was no history of inter-related marriages in the family. She was diagnosed with rod-cone dystrophy, and was noted to have poor vision and night blindness since birth. As a child, she was always attracted to light (photoattraction). She first presented to the eye clinic at the age of 27 years; she was only able to perceive light in her right eye but had a visual acuity of logMar 0.9 in the left eye. Her pupillary reaction was normal and she did not have any nystagmus. Clinical examination showed that her fundal appearances were similar to that of advanced retinitis pigmentosa with peripheral bone spiccule-like pigmentation, pale optic discs, attenuated blood vessels and an epiretinal membrane at both macula. Over the follow up period of 10 years, she developed posterior subcapsular cataracts, progressive RPE atrophy, white retinal dots and macula pigmentation and atrophy. Goldman perimetry showed severe constriction of her visual fields to only 5 degrees of horizontal and vertical fields in each eye with preservation of the temporal islands. Optical coherence imaging (OCT) showed thinning of the retina from the nasal aspect to the fovea while fundus autofluorescence

imaging using the scanning laser ophthalmoscope (SLO) showed patchy areas of hyper and hypofluorescence throughout the fundus. ERG assessment was not available on this patient.

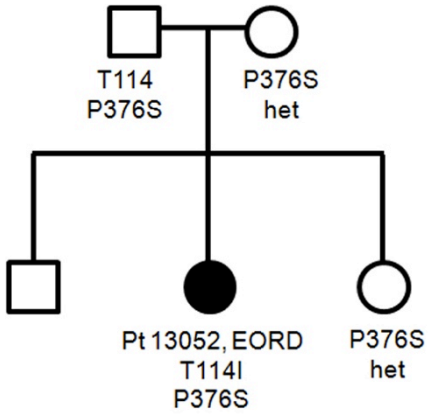

Patient 13412

Patient 13412 is from an Iranian family with a long history of consanguineous marriages in the family. He is related to another patient (No. 13353) as first cousins, who has a heterozygous Arg302Leu mutation. Patient 13412 was diagnosed with LCA when at the age of 2 months, he was noted to have poor vision and nystagmus and later developed a divergent squint. There was a history of poor vision in the family, he had an affected brother and 2 first cousins who were diagnosed with LCA (including patient 13353) and another first cousin who was diagnosed with rod-cone dystrophy. At the time of examination, he was 18 years old. His visual acuities were counting fingers bilaterally and there was a roving nystagmus. Both of his fundi appeared unremarkable on ophthalmoscopy and there was some optic disc pallors. Electrophysiology testing revealed severe reduction in scotopic and photopic responses. OCT imaging revealed thinning of the retina and fovea. Autofluorescence and goldman perimetry was not performed in this patient.

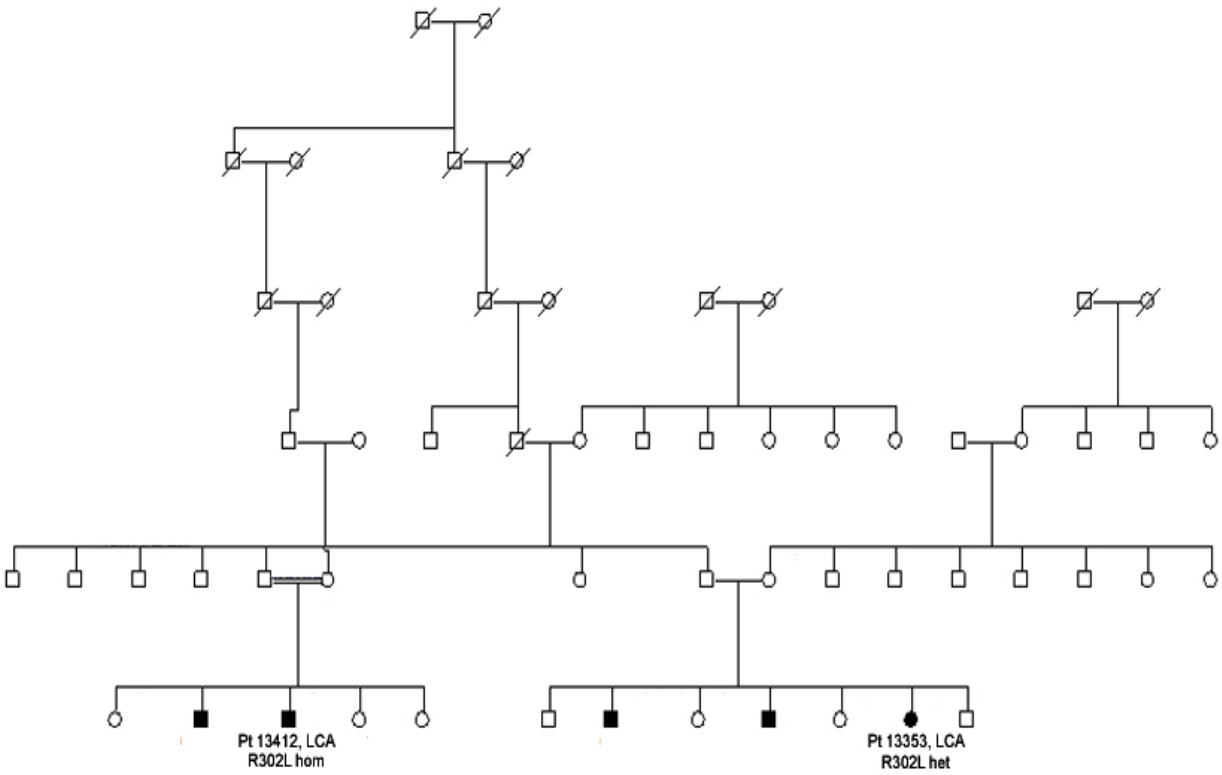

Patient 31895

Patient 31895 is from a family from Israel, whose parents are not related to each other. He was noted to have poor vision and nystagmus at the age of 6 months. There was no family history of blindness or other eye conditions. He was diagnosed with LCA at the age of 7 years. Initial ERG performed at the age of 3 years showed moderate to severely reduced rod and cone responses which was suggestive of widespread retinal degeneration. The ERG was repeated again at the age of 7 and showed non-detectable responses under all stimulus conditions. Clinical examination and details were recorded at the age of 7 years. His visual acuities then were hand movements in the right and left eye respectively. There were abnormal foveal reflexes bilaterally but no evidence of macular atrophy or pigmentation. There was no obvious peripheral retinal pigmentation or any cataract or keratoconus. Autofluorescence imaging showed relatively normal level of autofluorescence at the macula. OCT scanning revealed thinning of the retinal layers although foveal outer nuclear layer appear to be present.

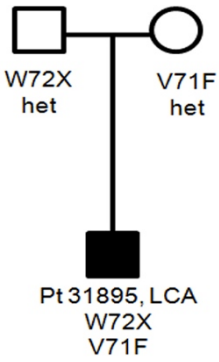

Patient 15618

Patient 15618 is of Indian descent from a non-consanguinous family. The onset of his visual symptoms were at the age of 6 years where, his parents noticed that his eyes were ‘wobbly’ and that he was having difficulties seeing objects. He also developed a divergent squint. He was examined at the age of 21 years and his visual acuities at examination was logMAR 1.3 OD and hand movements OS. Fundal examination showed bone spicule retinal pigmentation in the mid to peripheral retina and peripheral RPE atrophy. There were signs of RPE mottling and pigmentation at the macula and the optic discs appeared pale. Electrodiagnostic testing showed marked reduction of scotopic and photopic responses, worse in the left eye which was in keeping with EORD. OCT, autofluorescence and perimetry were not performed.

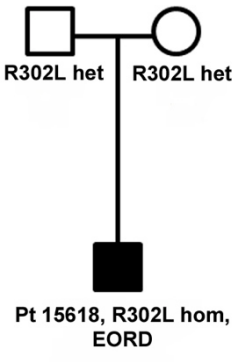

Patient 14651

Patient 14651 is from an Asian background and whose parents are first cousins. She was noted to have poor vision at the age of 6 months, accompanied by nystagmus and a squint. There was no previous family history of any eye problems or blindness. She was examined at the age of 3 and recorded visual acuities of counting fingers in both eyes. Fundal examination showed unremarkable findings in the retina and macula. ERG showed non-detectable photopic and scotopic responses in keeping with LCA.

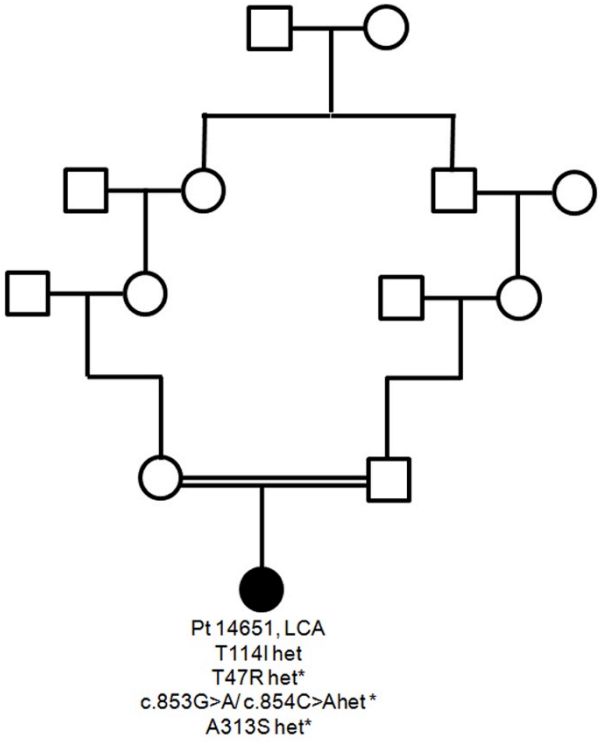

Patient 13163

Patient 13163 is from a Caucasian background and a non-consanguinous family. Poor vision and nystagus was noted at the age of 6 months. She later developed a squint. A diagnosis of EORD was made at the age of 3 year. Clinical examination was performed at the age of 29 years old. Her vision recorded then was logMAR 0.96 in the right and left eye respectively and she was moderately myopic with astigmatism but there was no signs of keratoconus. Fundal examination revealed bilateral pale discs and attenuated blood vessels but there were no obvious retinal pigmentary changes. OCT imaging showed normal retinal thickness and layered architecture. ERG responses showed absent rod responses and minimal cone responses. .

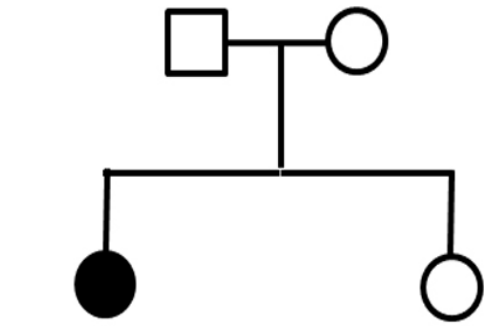

Patient 6604

Patient 6604 is the younger sister of patient 13484. They both share the same mother, but have different fathers. Patient 6604 was noted to have poor vision, eye-rubbing, nystagmus and dislike of bright lights at the age of 2 months. She presented for clinical examination at an earlier age of 8 years old, during which she was found to have pigment clumping in the peripheral retina, RPE atrophy, white dots and macular pigmentation and atrophy. She was diagnosed with rod-cone dystrophy. Her visual acuity was better compared with her sister's, achieving logMar 0.7 (*oculus dexter,* right) and logMar 0.8 (*oculus sinister,* left). Electrophysiology assessment showed absent rod and cone ERG responses and significantly delayed 30 Hz flicker ERG with low amplitude.

Patient 14351

Patient 14351 was diagnosed at the age of 2 years with early onset retinal dystrophy. He presented with visual loss, nystagmus, field loss and nyctalopia when he was 2 years old, and came from a consanguineous family where his parents were first cousins. There were no other affected family members. At the time of clinical examination, he was 5 years old; his visual acuities were 1.0 OD and OS and ophthalmoscopy showed a relatively unremarkable fundus. Unfortunately, electrophysiology testing, OCT and visual fields information were unavailable on this patient.

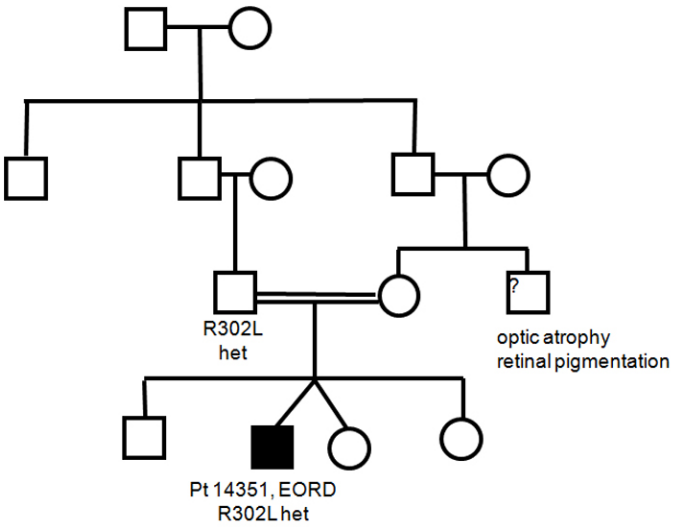

Patient 10759

Patient 10759 was noted to have poor vision and nystagmus from birth. Her parents are from Indian descent and there is no history of consanguinity. She has a non-affected older brother. She was diagnosed with LCA at the age of 6 months, after electrodiagnostic testing showed non-detectable scotopic or photopic responses. She demonstrated a dislike for light and later developed a left divergent squint. She was examined at the age of 1 year. On examination,her vision was hand movements in the right and left eye respectively. There were no pigmentary changes in the retina or any macular abnormality found. Her anterior segments were unremarkable and there were no signs of cataracts or keratoconus.

Patient 13026

Patient 13026 was from a white Caucasian background and there was no family history of consanguinity. Clinically, she was diagnosed with early onset retinal dystrophy after she was found to have poor vision and nystagmus shortly after birth and showed an aversion to light (photoaversion). When she was examined at the age of 9 years, she had visual acuities of 3/60 bilaterally with posterior subcapsular cataracts. Her fundi had moderate peripheral pigmentation accompanied by pale optic discs. There was involvement of the macular. No data was available on electrodiagnostic studies or perimetry.

List of Abbreviations

aa	amino acid
AAV	adeno-associated virus
ABCR	ATP-binding cassette transporter
Ad	adenovirus
AdRP	autosomal dominant retinitis pigmentosa
AIPL1 (human)	aryl hydrocarbon receptor-interacting protein-like 1
Aipl1 (mouse)	aryl hydrocarbon receptor-interacting protein-like 1
AMD	age-related macular degeneration
ArRP	autosomal recessive retinitis pigmentosa
ATP	adenosine-5'-triphosphate
BDNF	brain-derived neurotrophic factor
bFGF	basic fibroblast growth factor
β-PDE	β subunit of the rod cGMP phosphodiesterase
BHK	baby hamster kidney cells
bp	base pair
BRB	blood retina barrier
BSA	bovine serum albumin
cAMP	cyclic AMP
cc	connecting cilium
cDNA	coding deoxyribonucleic acid
CEP290	centrosomal protein 290
cGMP	cyclic GMP
CMV	cytomegalovirus promoter
CNTF	ciliary neurotrophic factor
CNS	central nervous system

CNV	choroidal neovascularisation
CRB	Crumbs homolog protein
CRBP	cellular retinol-binding protein
CRX	cone-rod homeobox
DMEM	Dulbecco's Modified Eagle Medium
DMSO	dimethylsulfoxide
DNA	deoxyribonucleic acid
ds	double stranded
EAM	encapsidated adenoviral mini-chromosome
EAU	experimental autoimmune uveoretinitis
EIAV	equine infections anaemia virus
gDNA	genomic deoxyribonucleic acid
eGFP	enhanced green fluorescent protein
ELISA	enzyme-linked immunosorben assay
ERG	electroretinogram
FCS	fetal calf serum
FGF	fibroblast growth factor
FIV	feline immunodeficiency virus
GCAP	guanylate cyclase activating protein
GCL	ganglion cell layer
GDNF	glial-derived neurotrophic factor
GDP	guanosine-5'diphosphate
GFAP	glial fibrillary acidic protein
GFP	green fluorescent protein
GMP	guanosine 5'-monophosphate
GTP	guanosine 5'-triphosphate
GUCY2D	guanylate cyclase-1

HIV	human immunodeficiency virus
HSV	herpes simplex virus
IL	interleukin
ILM	internal limiting memebrane
IMPDH1	inosine monophosphate dehydrogenase 1
INL	inner nuclear layer
IPL	inner plexiform layer
IPM	inter photoreceptor matrix
IRBP	interphotoreceptor retinoid-binding protein
IS	inner segments
ITR	inverted terminal repeats
kb	kilobase
kDA	kilodalton
l	litre
LCA	Leber Congenital Amaurosis
LRAT	lecithin-retinol acyltransferase
LTR	long tandem repeats
m	meter
m-	milli
µ	micro
MERTK	mer-receptor tyrosine kinase
MOI	multiplicity of infection
mRNA	messenger RNA
miRNA	microRNA
MV	microvilli
NAD^+, NADH	oxidized and reduced nicotinamide–adenine dinucleotide

$NADP^+$, NADPH	oxidized and reduced nicotinamide–adenine dinucleotide phosphate
NFL	nerve fiber layer
NO	nitric oxide
NOS	nitric oxide synthase
OCT	optical coherence tomography
O.C.T	optimal cutting temperature
ORF	open reading frame
ONL	outer nuclear layer
OP	oscillatory potential
OPL	outer plexiform layer
PBS	phosphate buffered saline
PCR	polymerase chain reaction
PDGF	platelet derived growth factor
PDE	phosphodiesterase
PEDF	pigment epithelium derived factor
PFA	paraformaldehyde
PR	photoreceptors
Prph2	peripherin”
R*	metarhodopsin
rAAV	recombinant AAV
RCS	Royal College of Surgeons
rd	retinal degeneration
RDH	retinol dehydrogenase
rds	retinal degeneration slow
retGC	retinal guanylate cyclase
RGC	retinal ganglion cells

RHO	rhodopsin
RISC	RNA induced silencing complex
RK	rhodopsin kinase
RNA	ribonucleic acid
RNAi	RNA intereference
ROM-1	retinal outer segment membrane protein-1
ROS	reactive oxygen species
RP	retinitis pigmentosa
RPE	retinal pigment epithelium
RPGR	retinitis pigmentosa GTPase regulator
RPGRIP	RPGR-interacting protein
RT	reverse transcriptase
scAAV	self complementary AAV
SCID	severe combined immunodeficiency
shRNA	short hairpin RNA
siRNA	short interfering RNA
SIV	simian immunodeficiency virus
ss	single stranded
TNF	tumor necrosis factor
TULP1	tubby-like protein
UTR	untranslated region
VEGF	vascular endothelial growth factor
vp	viral particles
VSV-G	vesicular stomatitis virus G-protein
WPRE	Woodchuck hepatitis virus post-transcriptional element
w/v	weight/volume percent or mass/volume percent
XIAP	X-linked inhibitor of apoptosis protein

Reference List

1. Acland, G. M., G. D. Aguirre, J. Bennett, T. S. Aleman, A. V. Cideciyan, J. Bennicelli, N. S. Dejneka, S. E. Pearce-Kelling, A. M. Maguire, K. Palczewski, W. W. Hauswirth, and S. G. Jacobson. 2005. Long-term restoration of rod and cone vision by single dose rAAV-mediated gene transfer to the retina in a canine model of childhood blindness. Mol. Ther. 12:1072-1082.

2. Acland, G. M., G. D. Aguirre, J. Ray, Q. Zhang, T. S. Aleman, A. V. Cideciyan, S. E. Pearce-Kelling, V. Anand, Y. Zeng, A. M. Maguire, S. G. Jacobson, W. W. Hauswirth, and J. Bennett. 2001. Gene therapy restores vision in a canine model of childhood blindness. Nat. Genet. 28:92-95.

3. Adato, A., H. Kalinski, D. Weil, H. Chaib, M. Korostishevsky, and B. Bonne-Tamir. 1999. Possible interaction between USH1B and USH3 gene products as implied by apparent digenic deafness inheritance. Am. J. Hum. Genet. 65:261-265.

4. Aguirre, G. D., V. Baldwin, S. Pearce-Kelling, K. Narfstrom, K. Ray, and G. M. Acland. 1998. Congenital stationary night blindness in the dog: common mutation in the RPE65 gene indicates founder effect. Mol. Vis. 4:23.

5. Ahnelt, P. K. 1998. The photoreceptor mosaic. Eye 12 (Pt 3b):531-540.

6. Ahnelt, P. K. and H. Kolb. 2000. The mammalian photoreceptor mosaic-adaptive design. Prog. Retin. Eye Res. 19:711-777.

7. Akey, D. T., X. Zhu, M. Dyer, A. Li, A. Sorensen, S. Blackshaw, T. Fukuda-Kamitani, S. P. Daiger, C. M. Craft, T. Kamitani, and M. M. Sohocki. 2002. The inherited blindness associated protein AIPL1 interacts with the cell cycle regulator protein NUB1. Hum. Mol. Genet. 11:2723-2733.

8. Akey, D. T., X. Zhu, M. Dyer, A. Li, A. Sorensen, T. Fukada-Kamitani, S. P. Daiger, C. Craft, T. Kamitani, and M. M. Sohocki. 2003. Functional studies of AIPL1: potential role of AIPL1 in cell cycle exit and/or differentiation of photoreceptors. Adv. Exp. Med. Biol. 533:287-295.

9. Alexander, J. J., Y. Umino, D. Everhart, B. Chang, S. H. Min, Q. Li, A. M. Timmers, N. L. Hawes, J. J. Pang, R. B. Barlow, and W. W. Hauswirth. 2007. Restoration of cone vision in a mouse model of achromatopsia. Nat. Med. 13:685-687.

10. Ali, R. R. 2004. Prospects for gene therapy. Novartis. Found. Symp. 255:165-172.

11. Ali, R. R., M. B. Reichel, A. P. Byrnes, C. J. Stephens, A. J. Thrasher, D. Baker, D. M. Hunt, and S. S. Bhattacharya. 1998. Co-injection of adenovirus

expressing CTLA4-Ig prolongs adenovirally mediated lacZ reporter gene expression in the mouse retina. Gene Ther. 5:1561-1565.

12. Ali, R. R., M. B. Reichel, A. M. De, N. Kanuga, C. Kinnon, R. J. Levinsky, D. M. Hunt, S. S. Bhattacharya, and A. J. Thrasher. 1998. Adeno-associated virus gene transfer to mouse retina. Hum. Gene Ther. 9:81-86.

13. Ali, R. R., M. B. Reichel, A. J. Thrasher, R. J. Levinsky, C. Kinnon, N. Kanuga, D. M. Hunt, and S. S. Bhattacharya. 1996. Gene transfer into the mouse retina mediated by an adeno-associated viral vector. Hum. Mol. Genet. 5:591-594.

14. Ali, R. R., G. M. Sarra, C. Stephens, M. D. Alwis, J. W. Bainbridge, P. M. Munro, S. Fauser, M. B. Reichel, C. Kinnon, D. M. Hunt, S. S. Bhattacharya, and A. J. Thrasher. 2000. Restoration of photoreceptor ultrastructure and function in retinal degeneration slow mice by gene therapy. Nat. Genet. 25:306-310.

15. Aligianis, I. A., T. Forshew, S. Johnson, M. Michaelides, C. A. Johnson, R. C. Trembath, D. M. Hunt, A. T. Moore, and E. R. Maher. 2002. Mapping of a novel locus for achromatopsia (ACHM4) to 1p and identification of a germline mutation in the alpha subunit of cone transducin (GNAT2). J. Med. Genet. 39:656-660.

16. Allikmets, R. 2004. Leber congenital amaurosis: a genetic paradigm. Ophthalmic Genet. 25:67-79.

17. Allocca, M., M. Doria, M. Petrillo, P. Colella, M. Garcia-Hoyos, D. Gibbs, S. R. Kim, A. Maguire, T. S. Rex, V. U. Di, L. Cutillo, J. R. Sparrow, D. S. Williams, J. Bennett, and A. Auricchio. 2008. Serotype-dependent packaging of large genes in adeno-associated viral vectors results in effective gene delivery in mice. J. Clin. Invest 118:1955-1964.

18. Allocca, M., C. Mussolino, M. Garcia-Hoyos, D. Sanges, C. Iodice, M. Petrillo, L. H. Vandenberghe, J. M. Wilson, V. Marigo, E. M. Surace, and A. Auricchio. 2007. Novel adeno-associated virus serotypes efficiently transduce murine photoreceptors. J. Virol. 81:11372-11380.

19. Allocca, M., A. Tessitore, G. Cotugno, and A. Auricchio. 2006. AAV-mediated gene transfer for retinal diseases. Expert. Opin. Biol. Ther. 6:1279-1294.

20. Amalfitano, A., C. R. Begy, and J. S. Chamberlain. 1996. Improved adenovirus packaging cell lines to support the growth of replication-defective gene-delivery vectors. Proc. Natl. Acad. Sci. U. S. A 93:3352-3356.

21. Anand, V., N. Chirmule, M. Fersh, A. M. Maguire, and J. Bennett. 2000. Additional transduction events after subretinal readministration of recombinant adeno-associated virus. Hum. Gene Ther. 11:449-457.

22. Anand, V., B. Duffy, Z. Yang, N. S. Dejneka, A. M. Maguire, and J. Bennett. 2002. A deviant immune response to viral proteins and transgene product is generated on subretinal administration of adenovirus and adeno-associated virus. Mol. Ther. 5:125-132.

23. Anant, J. S., O. C. Ong, H. Y. Xie, S. Clarke, P. J. O'Brien, and B. K. Fung. 1992. In vivo differential prenylation of retinal cyclic GMP phosphodiesterase catalytic subunits. J. Biol. Chem. 267:687-690.

24. Anglade, E. and K. G. Csaky. 1998. Recombinant adenovirus-mediated gene transfer into the adult rat retina. Curr. Eye Res. 17:316-321.

25. Arshavsky, V. 2002. Like night and day: rods and cones have different pigment regeneration pathways. Neuron 36:1-3.

26. Arshavsky, V. Y., T. D. Lamb, and E. N. Pugh, Jr. 2002. G proteins and phototransduction. Annu. Rev. Physiol 64:153-187.

27. Arundine, M. and M. Tymianski. 2003. Molecular mechanisms of calcium-dependent neurodegeneration in excitotoxicity. Cell Calcium 34:325-337.

28. Auricchio, A. 2003. Pseudotyped AAV vectors for constitutive and regulated gene expression in the eye. Vision Res. 43:913-918.

29. Auricchio, A., K. C. Behling, A. M. Maguire, E. M. O'Connor, J. Bennett, J. M. Wilson, and M. J. Tolentino. 2002. Inhibition of retinal neovascularization by intraocular viral-mediated delivery of anti-angiogenic agents. Mol. Ther. 6:490-494.

30. Auricchio, A., G. Kobinger, V. Anand, M. Hildinger, E. O'Connor, A. M. Maguire, J. M. Wilson, and J. Bennett. 2001. Exchange of surface proteins impacts on viral vector cellular specificity and transduction characteristics: the retina as a model. Hum. Mol. Genet. 10:3075-3081.

31. Azzam, T. and A. J. Domb. 2004. Current developments in gene transfection agents. Curr. Drug Deliv. 1:165-193.

32. Bainbridge, J. W., A. Mistry, A. M. De, E. Paleolog, A. Baker, A. J. Thrasher, and R. R. Ali. 2002. Inhibition of retinal neovascularisation by gene transfer of soluble VEGF receptor sFlt-1. Gene Ther. 9:320-326.

33. Bainbridge, J. W., A. Mistry, F. C. Schlichtenbrede, A. Smith, C. Broderick, A. M. De, A. Georgiadis, P. M. Taylor, M. Squires, C. Sethi, D. Charteris, A. J. Thrasher, D. Sargan, and R. R. Ali. 2003. Stable rAAV-mediated transduction of rod and cone photoreceptors in the canine retina. Gene Ther. 10:1336-1344.

34. Bainbridge, J. W., A. J. Smith, S. S. Barker, S. Robbie, R. Henderson, K. Balaggan, A. Viswanathan, G. E. Holder, A. Stockman, N. Tyler, S. Petersen-Jones, S. S. Bhattacharya, A. J. Thrasher, F. W. Fitzke, B. J.

Carter, G. S. Rubin, A. T. Moore, and R. R. Ali. 2008. Effect of gene therapy on visual function in Leber's congenital amaurosis. N. Engl. J. Med. 358:2231-2239.

35. Bainbridge, J. W., C. Stephens, K. Parsley, C. Demaison, A. Halfyard, A. J. Thrasher, and R. R. Ali. 2001. In vivo gene transfer to the mouse eye using an HIV-based lentiviral vector; efficient long-term transduction of corneal endothelium and retinal pigment epithelium. Gene Ther. 8:1665-1668.

36. Bainbridge, J. W., M. H. Tan, and R. R. Ali. 2006. Gene therapy progress and prospects: the eye. Gene Ther. 13:1191-1197.

37. Balaggan, K. S., K. Binley, M. Esapa, S. Iqball, Z. Askham, O. Kan, M. Tschernutter, J. W. Bainbridge, S. Naylor, and R. R. Ali. 2006. Stable and efficient intraocular gene transfer using pseudotyped EIAV lentiviral vectors. J. Gene Med. 8:275-285.

38. Balague, C., M. Kalla, and W. W. Zhang. 1997. Adeno-associated virus Rep78 protein and terminal repeats enhance integration of DNA sequences into the cellular genome. J. Virol. 71:3299-3306.

39. Barker, S. E., C. A. Broderick, S. J. Robbie, Y. Duran, M. Natkunarajah, P. Buch, K. S. Balaggan, R. E. MacLaren, J. W. Bainbridge, A. J. Smith, and R. R. Ali. 2009. Subretinal delivery of adeno-associated virus serotype 2 results in minimal immune responses that allow repeat vector administration in immunocompetent mice. J. Gene Med. 11:486-497.

40. Batten, M. L., Y. Imanishi, T. Maeda, D. C. Tu, A. R. Moise, D. Bronson, D. Possin, R. N. Van Gelder, W. Baehr, and K. Palczewski. 2004. Lecithin-retinol acyltransferase is essential for accumulation of all-trans-retinyl esters in the eye and in the liver. J. Biol. Chem. 279:10422-10432.

41. Batten, M. L., Y. Imanishi, T. Maeda, D. C. Tu, A. R. Moise, D. Bronson, D. Possin, R. N. Van Gelder, W. Baehr, and K. Palczewski. 2004. Lecithin-retinol acyltransferase is essential for accumulation of all-trans-retinyl esters in the eye and in the liver. J. Biol. Chem. 279:10422-10432.

42. Batten, M. L., Y. Imanishi, D. C. Tu, T. Doan, L. Zhu, J. Pang, L. Glushakova, A. R. Moise, W. Baehr, R. N. Van Gelder, W. W. Hauswirth, F. Rieke, and K. Palczewski. 2005. Pharmacological and rAAV gene therapy rescue of visual functions in a blind mouse model of Leber congenital amaurosis. PLoS. Med. 2:e333.

43. Baylor, D. 1996. How photons start vision. Proc. Natl. Acad. Sci. U. S. A 93:560-565.

44. Bell, P., A. D. Moscioni, R. J. McCarter, D. Wu, G. Gao, A. Hoang, J. C. Sanmiguel, X. Sun, N. A. Wivel, S. E. Raper, E. E. Furth, M. L. Batshaw, and

J. M. Wilson. 2006. Analysis of tumors arising in male B6C3F1 mice with and without AAV vector delivery to liver. Mol. Ther. 14:34-44.

45. Bell, P., L. Wang, C. Lebherz, D. B. Flieder, M. S. Bove, D. Wu, G. P. Gao, J. M. Wilson, and N. A. Wivel. 2005. No evidence for tumorigenesis of AAV vectors in a large-scale study in mice. Mol. Ther. 12:299-306.

46. Beltran, W. A., S. L. Boye, S. E. Boye, V. A. Chiodo, A. S. Lewin, W. W. Hauswirth, and G. D. Aguirre. 2010. rAAV2/5 gene-targeting to rods:dose-dependent efficiency and complications associated with different promoters. Gene Ther. 17:1162-1174.

47. Bennett, J., A. M. Maguire, A. V. Cideciyan, M. Schnell, E. Glover, V. Anand, T. S. Aleman, N. Chirmule, A. R. Gupta, Y. Huang, G. P. Gao, W. C. Nyberg, J. Tazelaar, J. Hughes, J. M. Wilson, and S. G. Jacobson. 1999. Stable transgene expression in rod photoreceptors after recombinant adeno-associated virus-mediated gene transfer to monkey retina. Proc. Natl. Acad. Sci. U. S. A 96:9920-9925.

48. Bennett, J., A. M. Maguire, A. V. Cideciyan, M. Schnell, E. Glover, V. Anand, T. S. Aleman, N. Chirmule, A. R. Gupta, Y. Huang, G. P. Gao, W. C. Nyberg, J. Tazelaar, J. Hughes, J. M. Wilson, and S. G. Jacobson. 1999. Stable transgene expression in rod photoreceptors after recombinant adeno-associated virus-mediated gene transfer to monkey retina. Proc. Natl. Acad. Sci. U. S. A 96:9920-9925.

49. Bennett, J., S. Pakola, Y. Zeng, and A. Maguire. 1996. Humoral response after administration of E1-deleted adenoviruses: immune privilege of the subretinal space. Hum. Gene Ther. 7:1763-1769.

50. Bennett, J., T. Tanabe, D. Sun, Y. Zeng, H. Kjeldbye, P. Gouras, and A. M. Maguire. 1996. Photoreceptor cell rescue in retinal degeneration (rd) mice by in vivo gene therapy. Nat. Med. 2:649-654.

51. Bennett, J., J. Wilson, D. Sun, B. Forbes, and A. Maguire. 1994. Adenovirus vector-mediated in vivo gene transfer into adult murine retina. Invest Ophthalmol. Vis. Sci. 35:2535-2542.

52. Bennett, J., Y. Zeng, R. Bajwa, L. Klatt, Y. Li, and A. M. Maguire. 1998. Adenovirus-mediated delivery of rhodopsin-promoted bcl-2 results in a delay in photoreceptor cell death in the rd/rd mouse. Gene Ther. 5:1156-1164.

53. Bennicelli, J., J. F. Wright, A. Komaromy, J. B. Jacobs, B. Hauck, O. Zelenaia, F. Mingozzi, D. Hui, D. Chung, T. S. Rex, Z. Wei, G. Qu, S. Zhou, C. Zeiss, V. R. Arruda, G. M. Acland, L. F. Dell'Osso, K. A. High, A. M. Maguire, and J. Bennett. 2008. Reversal of blindness in animal models of leber congenital amaurosis using optimized AAV2-mediated gene transfer. Mol. Ther. 16:458-465.

54. Bessant, D. A., R. R. Ali, and S. S. Bhattacharya. 2001. Molecular genetics and prospects for therapy of the inherited retinal dystrophies. Curr. Opin. Genet. Dev. 11:307-316.

55. Blatch, G. L. and M. Lassle. 1999. The tetratricopeptide repeat: a structural motif mediating protein-protein interactions. Bioessays 21:932-939.

56. Boon, C. J., M. J. van Schooneveld, A. I. den Hollander, J. J. van Lith-Verhoeven, M. N. Zonneveld-Vrieling, T. Theelen, F. P. Cremers, C. B. Hoyng, and B. J. Klevering. 2007. Mutations in the peripherin/RDS gene are an important cause of multifocal pattern dystrophy simulating STGD1/fundus flavimaculatus. Br. J. Ophthalmol 91:1504-1511.

57. Borras, T., W. Xue, V. W. Choi, J. S. Bartlett, G. Li, R. J. Samulski, and S. S. Chisolm. 2006. Mechanisms of AAV transduction in glaucoma-associated human trabecular meshwork cells. J. Gene Med. 8:589-602.

58. Bowles, D. E., J. E. Rabinowitz, and R. J. Samulski. 2003. Marker rescue of adeno-associated virus (AAV) capsid mutants: a novel approach for chimeric AAV production. J. Virol. 77:423-432.

59. Bowne, S. J., L. S. Sullivan, S. E. Mortimer, L. Hedstrom, J. Zhu, C. J. Spellicy, A. I. Gire, D. Hughbanks-Wheaton, D. G. Birch, R. A. Lewis, J. R. Heckenlively, and S. P. Daiger. 2006. Spectrum and frequency of mutations in IMPDH1 associated with autosomal dominant retinitis pigmentosa and leber congenital amaurosis. Invest Ophthalmol. Vis. Sci. 47:34-42.

60. Boye, S. E., S. L. Boye, J. Pang, R. Ryals, D. Everhart, Y. Umino, A. W. Neeley, J. Besharse, R. Barlow, and W. W. Hauswirth. 2010. Functional and behavioral restoration of vision by gene therapy in the guanylate cyclase-1 (GC1) knockout mouse. PLoS. ONE. 5:e11306.

61. Brecelj, J. and B. Stirn-Kranjc. 1999. ERG and VEP follow-up study in children with Leber's congenital amaurosis. Eye 13 (Pt 1):47-54.

62. Broderick, C. A., A. J. Smith, K. S. Balaggan, A. Georgiadis, P. K. Buch, P. C. Trittibach, S. E. Barker, G. M. Sarra, A. J. Thrasher, A. D. Dick, and R. R. Ali. 2005. Local administration of an adeno-associated viral vector expressing IL-10 reduces monocyte infiltration and subsequent photoreceptor damage during experimental autoimmune uveitis. Mol. Ther. 12:369-373.

63. Buch, P. K., R. E. MacLaren, Y. Duran, K. S. Balaggan, A. MacNeil, F. C. Schlichtenbrede, A. J. Smith, and R. R. Ali. 2006. In contrast to AAV-mediated Cntf expression, AAV-mediated Gdnf expression enhances gene replacement therapy in rodent models of retinal degeneration. Mol. Ther. 14:700-709.

64. Bukrinsky, M. I., S. Haggerty, M. P. Dempsey, N. Sharova, A. Adzhubel, L. Spitz, P. Lewis, D. Goldfarb, M. Emerman, and M. Stevenson. 1993. A nuclear localization signal within HIV-1 matrix protein that governs infection of non-dividing cells. Nature 365:666-669.

65. Bulgakov, O. V., X. Liu, and Y. Y. Li. 2005. The biosynthesis/transport of cone photoreceptor cGMP phosphodiesterases requires AIPL1, a putative chaperone protein that is defective in one form of Leber congenital amaurosis., abstr. Invest Ophthalmol.Vis.Sci. 46: 1728.

66. Burns, M. E. and D. A. Baylor. 2001. Activation, deactivation, and adaptation in vertebrate photoreceptor cells. Annu. Rev. Neurosci. 24:779-805.

67. Campochiaro, P. A., Q. D. Nguyen, S. M. Shah, M. L. Klein, E. Holz, R. N. Frank, D. A. Saperstein, A. Gupta, J. T. Stout, J. Macko, R. DiBartolomeo, and L. L. Wei. 2006. Adenoviral vector-delivered pigment epithelium-derived factor for neovascular age-related macular degeneration: results of a phase I clinical trial. Hum. Gene Ther. 17:167-176.

68. Cao, H., D. R. Koehler, and J. Hu. 2004. Adenoviral vectors for gene replacement therapy. Viral Immunol. 17:327-333.

69. Cao, W., F. Li, R. H. Steinberg, and M. M. Lavail. 2001. Development of normal and injury-induced gene expression of aFGF, bFGF, CNTF, BDNF, GFAP and IGF-I in the rat retina. Exp. Eye Res. 72:591-604.

70. Cao, W., R. Wen, F. Li, M. M. Lavail, and R. H. Steinberg. 1997. Mechanical injury increases bFGF and CNTF mRNA expression in the mouse retina. Exp. Eye Res. 65:241-248.

71. Carter, B. J. 2005. Adeno-associated virus vectors in clinical trials. Hum. Gene Ther. 16:541-550.

72. Carter, B. J. and T. R. Flotte. 1996. Development of adeno-associated virus vectors for gene therapy of cystic fibrosis. Curr. Top. Microbiol. Immunol. 218:119-144.

73. Carver, L. A. and C. A. Bradfield. 1997. Ligand-dependent interaction of the aryl hydrocarbon receptor with a novel immunophilin homolog in vivo. J. Biol. Chem. 272:11452-11456.

74. Cashman, S. M., E. A. Binkley, and R. Kumar-Singh. 2005. Towards mutation-independent silencing of genes involved in retinal degeneration by RNA interference. Gene Ther. 12:1223-1228.

75. Cayouette, M., S. B. Smith, S. P. Becerra, and C. Gravel. 1999. Pigment epithelium-derived factor delays the death of photoreceptors in mouse models of inherited retinal degenerations. Neurobiol. Dis. 6:523-532.

76. Chadderton, N., S. Millington-Ward, A. Palfi, M. O'reilly, G. Tuohy, M. M. Humphries, T. Li, P. Humphries, P. F. Kenna, and G. J. Farrar. 2009. Improved retinal function in a mouse model of dominant retinitis pigmentosa following AAV-delivered gene therapy. Mol. Ther. 17:593-599.

77. Chang, B., T. Grau, S. Dangel, R. Hurd, B. Jurklies, E. C. Sener, S. Andreasson, H. Dollfus, B. Baumann, S. Bolz, N. Artemyev, S. Kohl, J. Heckenlively, and B. Wissinger. 2009. A homologous genetic basis of the murine cpfl1 mutant and human achromatopsia linked to mutations in the PDE6C gene. Proc Natl. Acad. Sci. U. S. A 106:19581-19586.

78. Chang, B., H. Khanna, N. Hawes, D. Jimeno, S. He, C. Lillo, S. K. Parapuram, H. Cheng, A. Scott, R. E. Hurd, J. A. Sayer, E. A. Otto, M. Attanasio, J. F. O'Toole, G. Jin, C. Shou, F. Hildebrandt, D. S. Williams, J. R. Heckenlively, and A. Swaroop. 2006. In-frame deletion in a novel centrosomal/ciliary protein CEP290/NPHP6 perturbs its interaction with RPGR and results in early-onset retinal degeneration in the rd16 mouse. Hum. Mol. Genet. 15:1847-1857.

79. Chapple, J. P., C. Grayson, A. J. Hardcastle, R. S. Saliba, S. J. Van der, and M. E. Cheetham. 2001. Unfolding retinal dystrophies: a role for molecular chaperones? Trends Mol. Med. 7:414-421.

80. Chaum, E. and M. P. Hatton. 2002. Gene therapy for genetic and acquired retinal diseases. Surv. Ophthalmol. 47:449-469.

81. Chen, C. K., M. E. Burns, M. Spencer, G. A. Niemi, J. Chen, J. B. Hurley, D. A. Baylor, and M. I. Simon. 1999. Abnormal photoresponses and light-induced apoptosis in rods lacking rhodopsin kinase. Proc. Natl. Acad. Sci. U. S. A 96:3718-3722.

82. Chen, J., M. I. Simon, M. T. Matthes, D. Yasumura, and M. M. Lavail. 1999. Increased susceptibility to light damage in an arrestin knockout mouse model of Oguchi disease (stationary night blindness). Invest Ophthalmol. Vis. Sci. 40:2978-2982.

83. Cheng, L., S. Chaidhawangul, F. Wong-Staal, J. Gilbert, E. Poeschla, M. Toyoguchi, M. El-Bradey, G. Bergeron-Lynn, K. A. Soules, and W. R. Freeman. 2002. Human immunodeficiency virus type 2 (HIV-2) vector-mediated in vivo gene transfer into adult rabbit retina. Curr. Eye Res. 24:196-201.

84. Cheng, L., M. Toyoguchi, D. J. Looney, J. Lee, M. C. Davidson, and W. R. Freeman. 2005. Efficient gene transfer to retinal pigment epithelium cells with long-term expression. Retina 25:193-201.

85. Chenna, R., H. Sugawara, T. Koike, R. Lopez, T. J. Gibson, D. G. Higgins, and J. D. Thompson. 2003. Multiple sequence alignment with the Clustal series of programs. Nucleic Acids Res. 31:3497-3500.

86. Cideciyan, A. V. 2010. Leber congenital amaurosis due to RPE65 mutations and its treatment with gene therapy. Prog. Retin. Eye Res. 29:398-427.

87. Cideciyan, A. V., T. S. Aleman, S. L. Boye, S. B. Schwartz, S. Kaushal, A. J. Roman, J. J. Pang, A. Sumaroka, E. A. Windsor, J. M. Wilson, T. R. Flotte, G. A. Fishman, E. Heon, E. M. Stone, B. J. Byrne, S. G. Jacobson, and W. W. Hauswirth. 2008. Human gene therapy for RPE65 isomerase deficiency activates the retinoid cycle of vision but with slow rod kinetics. Proc. Natl. Acad. Sci. U. S. A 105:15112-15117.

88. Cideciyan, A. V., T. S. Aleman, S. G. Jacobson, H. Khanna, A. Sumaroka, G. K. Aguirre, S. B. Schwartz, E. A. Windsor, S. He, B. Chang, E. M. Stone, and A. Swaroop. 2007. Centrosomal-ciliary gene CEP290/NPHP6 mutations result in blindness with unexpected sparing of photoreceptors and visual brain: Implications for therapy of Leber congenital amaurosis. Hum. Mutat.

89. Clarke, G., A. F. Goldberg, D. Vidgen, L. Collins, L. Ploder, L. Schwarz, L. L. Molday, J. Rossant, A. Szel, R. S. Molday, D. G. Birch, and R. R. McInnes. 2000. Rom-1 is required for rod photoreceptor viability and the regulation of disk morphogenesis. Nat. Genet. 25:67-73.

90. Coleman, J. E., Y. Zhang, G. A. Brown, and S. L. Semple-Rowland. 2004. Cone cell survival and downregulation of GCAP1 protein in the retinas of GC1 knockout mice. Invest Ophthalmol Vis. Sci. 45:3397-3403.

91. Conley, S., M. Nour, S. J. Fliesler, and M. I. Naash. 2007. Late-onset cone photoreceptor degeneration induced by R172W mutation in Rds and partial rescue by gene supplementation. Invest Ophthalmol Vis. Sci. 48:5397-5407.

92. Connell, G. J. and R. S. Molday. 1990. Molecular cloning, primary structure, and orientation of the vertebrate photoreceptor cell protein peripherin in the rod outer segment disk membrane. Biochemistry 29:4691-4698.

93. Conrad, C. K., S. S. Allen, S. A. Afione, T. C. Reynolds, S. E. Beck, M. Fee-Maki, X. Barrazza-Ortiz, R. Adams, F. B. Askin, B. J. Carter, W. B. Guggino, and T. R. Flotte. 1996. Safety of single-dose administration of an adeno-associated virus (AAV)-CFTR vector in the primate lung. Gene Ther. 3:658-668.

94. Conway, J. E., S. Zolotukhin, N. Muzyczka, G. S. Hayward, and B. J. Byrne. 1997. Recombinant adeno-associated virus type 2 replication and packaging is entirely supported by a herpes simplex virus type 1 amplicon expressing Rep and Cap. J. Virol. 71:8780-8789.

95. Cremers, F. P., J. A. van den Hurk, and A. I. den Hollander. 2002. Molecular genetics of Leber congenital amaurosis. Hum. Mol. Genet. 11:1169-1176.

96. D'Cruz, P. M., D. Yasumura, J. Weir, M. T. Matthes, H. Abderrahim, M. M. Lavail, and D. Vollrath. 2000. Mutation of the receptor tyrosine kinase gene Mertk in the retinal dystrophic RCS rat. Hum. Mol. Genet. 9:645-651.

97. Damji, K. F., M. M. Sohocki, R. Khan, S. K. Gupta, M. Rahim, M. Loyer, N. Hussein, N. Karim, S. S. Ladak, A. Jamal, D. Bulman, and R. K. Koenekoop. 2001. Leber's congenital amaurosis with anterior keratoconus in Pakistani families is caused by the Trp278X mutation in the AIPL1 gene on 17p. Can. J. Ophthalmol. 36:252-259.

98. Das, S. R., N. Bhardwaj, H. Kjeldbye, and P. Gouras. 1992. Muller cells of chicken retina synthesize 11-cis-retinol. Biochem. J. 285 (Pt 3):907-913.

99. Dejneka, N. S. and J. Bennett. 2001. Gene therapy and retinitis pigmentosa: advances and future challenges. Bioessays 23:662-668.

100. den Hollander, A. I., R. K. Koenekoop, S. Yzer, I. Lopez, M. L. Arends, K. E. Voesenek, M. N. Zonneveld, T. M. Strom, T. Meitinger, H. G. Brunner, C. B. Hoyng, L. I. van den Born, K. Rohrschneider, and F. P. Cremers. 2006. Mutations in the CEP290 (NPHP6) gene are a frequent cause of Leber congenital amaurosis. Am. J. Hum. Genet. 79:556-561.

101. den Hollander, A. I., R. Roepman, R. K. Koenekoop, and F. P. Cremers. 2008. Leber congenital amaurosis: genes, proteins and disease mechanisms. Prog. Retin. Eye Res. 27:391-419.

102. Dezawa, M., M. Takano, H. Negishi, X. Mo, T. Oshitari, and H. Sawada. 2002. Gene transfer into retinal ganglion cells by in vivo electroporation: a new approach. Micron. 33:1-6.

103. Dharmaraj, S., B. P. Leroy, M. M. Sohocki, R. K. Koenekoop, I. Perrault, K. Anwar, S. Khaliq, R. S. Devi, D. G. Birch, P. E. De, N. Izquierdo, M. L. Van, M. Ismail, A. M. Payne, G. E. Holder, S. S. Bhattacharya, A. C. Bird, J. Kaplan, and I. H. Maumenee. 2004. The phenotype of Leber congenital amaurosis in patients with AIPL1 mutations. Arch. Ophthalmol. 122:1029-1037.

104. Dharmaraj, S. R., E. R. Silva, A. L. Pina, Y. Y. Li, J. M. Yang, C. R. Carter, M. K. Loyer, H. K. El-Hilali, E. K. Traboulsi, O. K. Sundin, D. K. Zhu, R. K. Koenekoop, and I. H. Maumenee. 2000. Mutational analysis and clinical correlation in Leber congenital amaurosis. Ophthalmic Genet. 21:135-150.

105. Ding, X. Q., M. Nour, L. M. Ritter, A. F. Goldberg, S. J. Fliesler, and M. I. Naash. 2004. The R172W mutation in peripherin/rds causes a cone-rod dystrophy in transgenic mice. Hum. Mol. Genet. 13:2075-2087.

106. Donsante, A., D. G. Miller, Y. Li, C. Vogler, E. M. Brunt, D. W. Russell, and M. S. Sands. 2007. AAV vector integration sites in mouse hepatocellular carcinoma. Science 317:477.

107. Donsante, A., C. Vogler, N. Muzyczka, J. M. Crawford, J. Barker, T. Flotte, M. Campbell-Thompson, T. Daly, and M. S. Sands. 2001. Observed incidence of tumorigenesis in long-term rodent studies of rAAV vectors. Gene Ther. 8:1343-1346.

108. Doudna, J. A. and V. L. Rath. 2002. Structure and function of the eukaryotic ribosome: the next frontier. Cell 109:153-156.

109. Drenser, K. A., A. M. Timmers, W. W. Hauswirth, and A. S. Lewin. 1998. Ribozyme-targeted destruction of RNA associated with autosomal-dominant retinitis pigmentosa. Invest Ophthalmol. Vis. Sci. 39:681-689.

110. Dryja, T. P., S. M. Adams, J. L. Grimsby, T. L. McGee, D. H. Hong, T. Li, S. Andreasson, and E. L. Berson. 2001. Null RPGRIP1 alleles in patients with Leber congenital amaurosis. Am. J. Hum. Genet. 68:1295-1298.

111. Dryja, T. P., J. T. Finn, Y. W. Peng, T. L. McGee, E. L. Berson, and K. W. Yau. 1995. Mutations in the gene encoding the alpha subunit of the rod cGMP-gated channel in autosomal recessive retinitis pigmentosa. Proc. Natl. Acad. Sci. U. S. A 92:10177-10181.

112. Dryja, T. P., L. B. Hahn, K. Kajiwara, and E. L. Berson. 1997. Dominant and digenic mutations in the peripherin/RDS and ROM1 genes in retinitis pigmentosa. Invest Ophthalmol. Vis. Sci. 38:1972-1982.

113. Dryja, T. P., T. L. McGee, E. Reichel, L. B. Hahn, G. S. Cowley, D. W. Yandell, M. A. Sandberg, and E. L. Berson. 1990. A point mutation of the rhodopsin gene in one form of retinitis pigmentosa. Nature 343:364-366.

114. Ducroq, D., J. M. Rozet, S. Gerber, I. Perrault, D. Barbet, S. Hanein, S. Hakiki, J. L. Dufier, A. Munnich, C. Hamel, and J. Kaplan. 2002. The ABCA4 gene in autosomal recessive cone-rod dystrophies. Am. J. Hum. Genet. 71:1480-1482.

115. Dudley, R. W., Y. Lu, R. Gilbert, S. Matecki, J. Nalbantoglu, B. J. Petrof, and G. Karpati. 2004. Sustained improvement of muscle function one year after full-length dystrophin gene transfer into mdx mice by a gutted helper-dependent adenoviral vector. Hum. Gene Ther. 15:145-156.

116. Dudus, L., V. Anand, G. M. Acland, S. J. Chen, J. M. Wilson, K. J. Fisher, A. M. Maguire, and J. Bennett. 1999. Persistent transgene product in retina, optic nerve and brain after intraocular injection of rAAV. Vision Res. 39:2545-2553.

117. Duisit, G., H. Conrath, S. Saleun, S. Folliot, N. Provost, F. L. Cosset, V. Sandrin, P. Moullier, and F. Rolling. 2002. Five recombinant simian immunodeficiency virus pseudotypes lead to exclusive transduction of retinal pigmented epithelium in rat. Mol. Ther. 6:446-454.

118. Dull, T., R. Zufferey, M. Kelly, R. J. Mandel, M. Nguyen, D. Trono, and L. Naldini. 1998. A third-generation lentivirus vector with a conditional packaging system. J. Virol. 72:8463-8471.

119. Dyer, M. A., S. L. Donovan, J. Zhang, J. Gray, A. Ortiz, R. Tenney, J. Kong, R. Allikmets, and M. M. Sohocki. 2004. Retinal degeneration in Aipl1-deficient mice: a new genetic model of Leber congenital amaurosis. Brain Res. Mol. Brain Res. 132:208-220.

120. Dykxhoorn, D. M., C. D. Novina, and P. A. Sharp. 2003. Killing the messenger: short RNAs that silence gene expression. Nat. Rev. Mol. Cell Biol. 4:457-467.

121. Edelstein, M. L., M. R. Abedi, and J. Wixon. 2007. Gene therapy clinical trials worldwide to 2007--an update. J. Gene Med. 9:833-842.

122. Fain, G. L. and J. E. Lisman. 1993. Photoreceptor degeneration in vitamin A deprivation and retinitis pigmentosa: the equivalent light hypothesis. Exp. Eye Res. 57:335-340.

123. Fain, G. L. and J. E. Lisman. 1999. Light, Ca2+, and photoreceptor death: new evidence for the equivalent-light hypothesis from arrestin knockout mice. Invest Ophthalmol. Vis. Sci. 40:2770-2772.

124. Fain, G. L., H. R. Matthews, M. C. Cornwall, and Y. Koutalos. 2001. Adaptation in vertebrate photoreceptors. Physiol Rev. 81:117-151.

125. Faktorovich, E. G., R. H. Steinberg, D. Yasumura, M. T. Matthes, and M. M. Lavail. 1990. Photoreceptor degeneration in inherited retinal dystrophy delayed by basic fibroblast growth factor. Nature 347:83-86.

126. Faktorovich, E. G., R. H. Steinberg, D. Yasumura, M. T. Matthes, and M. M. Lavail. 1992. Basic fibroblast growth factor and local injury protect photoreceptors from light damage in the rat. J. Neurosci. 12:3554-3567.

127. Farber, D. B. 1995. From mice to men: the cyclic GMP phosphodiesterase gene in vision and disease. The Proctor Lecture. Invest Ophthalmol. Vis. Sci. 36:263-275.

128. Fariss, R. N., Z. Y. Li, and A. H. Milam. 2000. Abnormalities in rod photoreceptors, amacrine cells, and horizontal cells in human retinas with retinitis pigmentosa. Am. J. Ophthalmol. 129:215-223.

129. Farjo, R. and M. I. Naash. 2006. The role of Rds in outer segment morphogenesis and human retinal disease. Ophthalmic Genet. 27:117-122.

130. Farjo, R., J. S. Skaggs, B. A. Nagel, A. B. Quiambao, Z. A. Nash, S. J. Fliesler, and M. I. Naash. 2006. Retention of function without normal disc morphogenesis occurs in cone but not rod photoreceptors. J. Cell Biol. 173:59-68.

131. Farrar, G. J., P. F. Kenna, and P. Humphries. 2002. On the genetics of retinitis pigmentosa and on mutation-independent approaches to therapeutic intervention. EMBO J. 21:857-864.

132. Fauser, S., J. Luberichs, and F. Schuttauf. 2002. Genetic animal models for retinal degeneration. Surv. Ophthalmol. 47:357-367.

133. Ferrari, F. K., T. Samulski, T. Shenk, and R. J. Samulski. 1996. Second-strand synthesis is a rate-limiting step for efficient transduction by recombinant adeno-associated virus vectors. J. Virol. 70:3227-3234.

134. Ferrer-Costa, C., M. Orozco, and I. C. de, X. 2004. Sequence-based prediction of pathological mutations. Proteins 57:811-819.

135. Fisher, K. J., G. P. Gao, M. D. Weitzman, R. DeMatteo, J. F. Burda, and J. M. Wilson. 1996. Transduction with recombinant adeno-associated virus for gene therapy is limited by leading-strand synthesis. J. Virol. 70:520-532.

136. Fisher, K. J., K. Jooss, J. Alston, Y. Yang, S. E. Haecker, K. High, R. Pathak, S. E. Raper, and J. M. Wilson. 1997. Recombinant adeno-associated virus for muscle directed gene therapy. Nat. Med. 3:306-312.

137. Fishman, G. A., R. J. Anderson, and P. Lourenco. 1985. Prevalence of posterior subcapsular lens opacities in patients with retinitis pigmentosa. Br. J. Ophthalmol 69:263-266.

138. Flanders, M., M. L. Lapointe, S. Brownstein, and J. M. Little. 1984. Keratoconus and Leber's congenital amaurosis: a clinicopathological correlation. Can. J. Ophthalmol. 19:310-314.

139. Flannery, J. G., S. Zolotukhin, M. I. Vaquero, M. M. Lavail, N. Muzyczka, and W. W. Hauswirth. 1997. Efficient photoreceptor-targeted gene expression in vivo by recombinant adeno-associated virus. Proc. Natl. Acad. Sci. U. S. A 94:6916-6921.

140. Flotte, T., B. Carter, C. Conrad, W. Guggino, T. Reynolds, B. Rosenstein, G. Taylor, S. Walden, and R. Wetzel. 1996. A phase I study of an adeno-associated virus-CFTR gene vector in adult CF patients with mild lung disease. Hum. Gene Ther. 7:1145-1159.

141. FORNI, S. and J. BABEL. 1962. [Clinical and histological study of the disease of Leventina. Disease belonging to the group of hyaline degenerescences of the posterior pole.]. Ophthalmologica 143:313-322.

142. Forrester, J. V., A. D. Dick, McMenamin P.G., and W. R. Lee. 2002. The eye.

143. FRANCESCHETTI, A. and P. DIETERLE. 1954. [Diagnostic and prognostic importance of the electroretinogram in tapetoretinal degeneration with reduction of the visual field and hemeralopia.]. Confin. Neurol. 14:184-186.

144. Franklin, J. L. and E. M. Johnson, Jr. 1994. Block of neuronal apoptosis by a sustained increase of steady-state free Ca2+ concentration. Philos. Trans. R. Soc. Lond B Biol. Sci. 345:251-256.

145. Franklin, J. L. and E. M. Johnson, Jr. 1994. Elevated intracellular calcium blocks programmed neuronal death. Ann. N. Y. Acad. Sci. 747:195-204.

146. Friedman, J. S., B. Chang, C. Kannabiran, C. Chakarova, H. P. Singh, S. Jalali, N. L. Hawes, K. Branham, M. Othman, E. Filippova, D. A. Thompson, A. R. Webster, S. Andreasson, S. G. Jacobson, S. S. Bhattacharya, J. R. Heckenlively, and A. Swaroop. 2006. Premature truncation of a novel protein, RD3, exhibiting subnuclear localization is associated with retinal degeneration. Am. J. Hum. Genet. 79:1059-1070.

147. Frins, S., W. Bonigk, F. Muller, R. Kellner, and K. W. Koch. 1996. Functional characterization of a guanylyl cyclase-activating protein from vertebrate rods. Cloning, heterologous expression, and localization. J. Biol. Chem. 271:8022-8027.

148. Fukada, Y., T. Takao, H. Ohguro, T. Yoshizawa, T. Akino, and Y. Shimonishi. 1990. Farnesylated gamma-subunit of photoreceptor G protein indispensable for GTP-binding. Nature 346:658-660.

149. Fulton, A. B., R. M. Hansen, and D. L. Mayer. 1996. Vision in Leber congenital amaurosis. Arch. Ophthalmol. 114:698-703.

150. Furukawa, T., E. M. Morrow, T. Li, F. C. Davis, and C. L. Cepko. 1999. Retinopathy and attenuated circadian entrainment in Crx-deficient mice. Nat. Genet. 23:466-470.

151. Galvin, J. A., G. A. Fishman, E. M. Stone, and R. K. Koenekoop. 2005. Evaluation of genotype-phenotype associations in leber congenital amaurosis. Retina 25:919-929.

152. Gao, G., L. H. Vandenberghe, M. R. Alvira, Y. Lu, R. Calcedo, X. Zhou, and J. M. Wilson. 2004. Clades of Adeno-associated viruses are widely disseminated in human tissues. J. Virol. 78:6381-6388.

153. Gao, G. P., M. R. Alvira, L. Wang, R. Calcedo, J. Johnston, and J. M. Wilson. 2002. Novel adeno-associated viruses from rhesus monkeys as vectors for human gene therapy. Proc Natl. Acad. Sci. U. S. A 99:11854-11859.

154. Gee Sanftner, L. H., H. Abel, W. W. Hauswirth, and J. G. Flannery. 2001. Glial cell line derived neurotrophic factor delays photoreceptor degeneration in a transgenic rat model of retinitis pigmentosa. Mol. Ther. 4:622-629.

155. Gerber, S., S. Hanein, I. Perrault, N. Delphin, N. Aboussair, C. Leowski, J. L. Dufier, O. Roche, A. Munnich, J. Kaplan, and J. M. Rozet. 2007. Mutations

in LCA5 are an uncommon cause of Leber congenital amaurosis (LCA) type II. Hum. Mutat. 28:1245.

156. Gigout, L., P. Rebollo, N. Clement, K. H. Warrington, Jr., N. Muzyczka, R. M. Linden, and T. Weber. 2005. Altering AAV tropism with mosaic viral capsids. Mol. Ther. 11:856-865.

157. Gillespie, F. D. 1966. Congenital amaurosis of Leber. Am. J. Ophthalmol. 61:874-880.

158. Giove, T. J., M. Sena-Esteves, and W. D. Eldred. 2010. Transduction of the inner mouse retina using AAVrh8 and AAVrh10 via intravitreal injection. Exp. Eye Res.

159. Glover, D. J., H. J. Lipps, and D. A. Jans. 2005. Towards safe, non-viral therapeutic gene expression in humans. Nat. Rev. Genet. 6:299-310.

160. Glushakova, L. G., A. M. Timmers, T. M. Issa, N. G. Cortez, J. Pang, J. T. Teusner, and W. W. Hauswirth. 2006. Does recombinant adeno-associated virus-vectored proximal region of mouse rhodopsin promoter support only rod-type specific expression in vivo? Mol. Vis. 12:298-309.

161. Glushakova, L. G., A. M. Timmers, J. Pang, J. T. Teusner, and W. W. Hauswirth. 2006. Human blue-opsin promoter preferentially targets reporter gene expression to rat s-cone photoreceptors. Invest Ophthalmol. Vis. Sci. 47:3505-3513.

162. Gorbatyuk, M., V. Justilien, J. Liu, W. W. Hauswirth, and A. S. Lewin. 2007. Preservation of photoreceptor morphology and function in P23H rats using an allele independent ribozyme. Exp. Eye Res. 84:44-52.

163. Gorbatyuk, M., V. Justilien, J. Liu, W. W. Hauswirth, and A. S. Lewin. 2007. Suppression of mouse rhodopsin expression in vivo by AAV mediated siRNA delivery. Vision Res. 47:1202-1208.

164. Graham, F. L. and L. Prevec. 1992. Adenovirus-based expression vectors and recombinant vaccines. Biotechnology 20:363-390.

165. Greenlund, L. J., T. L. Deckwerth, and E. M. Johnson, Jr. 1995. Superoxide dismutase delays neuronal apoptosis: a role for reactive oxygen species in programmed neuronal death. Neuron 14:303-315.

166. Grimm, D., S. Zhou, H. Nakai, C. E. Thomas, T. A. Storm, S. Fuess, T. Matsushita, J. Allen, R. Surosky, M. Lochrie, L. Meuse, A. McClelland, P. Colosi, and M. A. Kay. 2003. Preclinical in vivo evaluation of pseudotyped adeno-associated virus vectors for liver gene therapy. Blood 102:2412-2419.

167. Grunwald, G. B., P. Gierschik, M. Nirenberg, and A. Spiegel. 1986. Detection of alpha-transducin in retinal rods but not cones. Science 231:856-859.

168. Gu, J. J., A. K. Tolin, J. Jain, H. Huang, L. Santiago, and B. S. Mitchell. 2003. Targeted disruption of the inosine 5'-monophosphate dehydrogenase type I gene in mice. Mol. Cell Biol. 23:6702-6712.

169. Guy, J., X. Qi, N. Muzyczka, and W. W. Hauswirth. 1999. Reporter expression persists 1 year after adeno-associated virus-mediated gene transfer to the optic nerve. Arch. Ophthalmol. 117:929-937.

170. Guziewicz, K. E., B. Zangerl, S. J. Lindauer, R. F. Mullins, L. S. Sandmeyer, B. H. Grahn, E. M. Stone, G. M. Acland, and G. D. Aguirre. 2007. Bestrophin gene mutations cause canine multifocal retinopathy: a novel animal model for best disease. Invest Ophthalmol Vis. Sci. 48:1959-1967.

171. Hagstrom, S. A., M. Duyao, M. A. North, and T. Li. 1999. Retinal degeneration in tulp1-/- mice: vesicular accumulation in the interphotoreceptor matrix. Invest Ophthalmol. Vis. Sci. 40:2795-2802.

172. Haire, S. E., J. Pang, S. L. Boye, I. Sokal, C. M. Craft, K. Palczewski, W. W. Hauswirth, and S. L. Semple-Rowland. 2006. Light-driven cone arrestin translocation in cones of postnatal guanylate cyclase-1 knockout mouse retina treated with AAV-GC1. Invest Ophthalmol Vis. Sci. 47:3745-3753.

173. Hameed, A., A. Abid, A. Aziz, M. Ismail, S. Q. Mehdi, and S. Khaliq. 2003. Evidence of RPGRIP1 gene mutations associated with recessive cone-rod dystrophy. J. Med. Genet. 40:616-619.

174. Hanein, S., I. Perrault, S. Gerber, G. Tanguy, F. Barbet, D. Ducroq, P. Calvas, H. Dollfus, C. Hamel, T. Lopponen, F. Munier, L. Santos, S. Shalev, D. Zafeiriou, J. L. Dufier, A. Munnich, J. M. Rozet, and J. Kaplan. 2004. Leber congenital amaurosis: comprehensive survey of the genetic heterogeneity, refinement of the clinical definition, and genotype-phenotype correlations as a strategy for molecular diagnosis. Hum. Mutat. 23:306-317.

175. Hao, W., A. Wenzel, M. S. Obin, C. K. Chen, E. Brill, N. V. Krasnoperova, P. Eversole-Cire, Y. Kleyner, A. Taylor, M. I. Simon, C. Grimm, C. E. Reme, and J. Lem. 2002. Evidence for two apoptotic pathways in light-induced retinal degeneration. Nat. Genet. 32:254-260.

176. Harada, T., C. Harada, S. Kohsaka, E. Wada, K. Yoshida, S. Ohno, H. Mamada, K. Tanaka, L. F. Parada, and K. Wada. 2002. Microglia-Muller glia cell interactions control neurotrophic factor production during light-induced retinal degeneration. J. Neurosci. 22:9228-9236.

177. Hart W Jr. 2007. adlers physiology of the eye. Mosby, St Louis.

178. Harvey, A. R., Y. Hu, S. G. Leaver, C. B. Mellough, K. Park, J. Verhaagen, G. W. Plant, and Q. Cui. 2006. Gene therapy and transplantation in CNS repair: the visual system. Prog. Retin. Eye Res. 25:449-489.

179. Hauck, B., L. Chen, and W. Xiao. 2003. Generation and characterization of chimeric recombinant AAV vectors. Mol. Ther. 7:419-425.

180. Hauck, B., W. Zhao, K. High, and W. Xiao. 2004. Intracellular viral processing, not single-stranded DNA accumulation, is crucial for recombinant adeno-associated virus transduction. J. Virol. 78:13678-13686.

181. Hauswirth, W. W., T. S. Aleman, S. Kaushal, A. V. Cideciyan, S. B. Schwartz, L. Wang, T. J. Conlon, S. L. Boye, T. R. Flotte, B. J. Byrne, and S. G. Jacobson. 2008. Treatment of leber congenital amaurosis due to RPE65 mutations by ocular subretinal injection of adeno-associated virus gene vector: short-term results of a phase I trial. Hum. Gene Ther. 19:979-990.

182. Hawkins, R. K., H. G. Jansen, and S. Sanyal. 1985. Development and degeneration of retina in rds mutant mice: photoreceptor abnormalities in the heterozygotes. Exp. Eye Res. 41:701-720.

183. Heegaard, S., T. Rosenberg, M. Preising, J. U. Prause, and T. Bek. 2003. An unusual retinal vascular morphology in connection with a novel AIPL1 mutation in Leber's congenital amaurosis. Br. J. Ophthalmol. 87:980-983.

184. Heher, K. L., E. I. Traboulsi, and I. H. Maumenee. 1992. The natural history of Leber's congenital amaurosis. Age-related findings in 35 patients. Ophthalmology 99:241-245.

185. Hicks, D. and J. Sahel. 1999. The implications of rod-dependent cone survival for basic and clinical research. Invest Ophthalmol. Vis. Sci. 40:3071-3074.

186. Hidalgo-de-Quintana, J., R. J. Evans, M. E. Cheetham, and S. J. Van der. 2008. The Leber congenital amaurosis protein AIPL1 functions as part of a chaperone heterocomplex. Invest Ophthalmol Vis. Sci. 49:2878-2887.

187. Hoffman, L. M., A. M. Maguire, and J. Bennett. 1997. Cell-mediated immune response and stability of intraocular transgene expression after adenovirus-mediated delivery. Invest Ophthalmol Vis. Sci. 38:2224-2233.

188. Holder, G. E. 2001. Pattern electroretinography (PERG) and an integrated approach to visual pathway diagnosis. Prog. Retin. Eye Res. 20:531-561.

189. Hong, D. H., B. S. Pawlyk, J. Shang, M. A. Sandberg, E. L. Berson, and T. Li. 2000. A retinitis pigmentosa GTPase regulator (RPGR)-deficient mouse model for X-linked retinitis pigmentosa (RP3). Proc. Natl. Acad. Sci. U. S. A 97:3649-3654.

190. Hong, D. H., G. Yue, M. Adamian, and T. Li. 2001. Retinitis pigmentosa GTPase regulator (RPGRr)-interacting protein is stably associated with the photoreceptor ciliary axoneme and anchors RPGR to the connecting cilium. J. Biol. Chem. 276:12091-12099.

191. HORSTEN, G. P. and J. E. WINKELMAN. 1960. Development of the ERG in relation to histological differentiation of the retina in man and animals. Arch. Ophthalmol. 63:232-242.

192. Hsu, Y. T. and R. S. Molday. 1993. Modulation of the cGMP-gated channel of rod photoreceptor cells by calmodulin. Nature 361:76-79.

193. Hsu, Y. T. and R. S. Molday. 1994. Interaction of calmodulin with the cyclic GMP-gated channel of rod photoreceptor cells. Modulation of activity, affinity purification, and localization. J. Biol. Chem. 269:29765-29770.

194. Humphries, M. M., D. Rancourt, G. J. Farrar, P. Kenna, M. Hazel, R. A. Bush, P. A. Sieving, D. M. Sheils, N. McNally, P. Creighton, A. Erven, A. Boros, K. Gulya, M. R. Capecchi, and P. Humphries. 1997. Retinopathy induced in mice by targeted disruption of the rhodopsin gene. Nat. Genet. 15:216-219.

195. Ikeda, S., N. Shiva, A. Ikeda, R. S. Smith, S. Nusinowitz, G. Yan, T. R. Lin, S. Chu, J. R. Heckenlively, M. A. North, J. K. Naggert, P. M. Nishina, and M. P. Duyao. 2000. Retinal degeneration but not obesity is observed in null mutants of the tubby-like protein 1 gene. Hum. Mol. Genet. 9:155-163.

196. Ikeda, Y., M. K. Collins, P. A. Radcliffe, K. A. Mitrophanous, and Y. Takeuchi. 2002. Gene transduction efficiency in cells of different species by HIV and EIAV vectors. Gene Ther. 9:932-938.

197. Ikeda, Y., Y. Goto, Y. Yonemitsu, M. Miyazaki, T. Sakamoto, T. Ishibashi, T. Tabata, Y. Ueda, M. Hasegawa, S. Tobimatsu, and K. Sueishi. 2003. Simian immunodeficiency virus-based lentivirus vector for retinal gene transfer: a preclinical safety study in adult rats. Gene Ther. 10:1161-1169.

198. Imanishi, Y., M. L. Batten, D. W. Piston, W. Baehr, and K. Palczewski. 2004. Noninvasive two-photon imaging reveals retinyl ester storage structures in the eye. J. Cell Biol. 164:373-383.

199. Inagaki, K., S. M. Lewis, X. Wu, C. Ma, D. J. Munroe, S. Fuess, T. A. Storm, M. A. Kay, and H. Nakai. 2007. DNA palindromes with a modest arm length of greater, similar 20 base pairs are a significant target for recombinant adeno-associated virus vector integration in the liver, muscles, and heart in mice. J. Virol. 81:11290-11303.

200. Inglese, J., J. F. Glickman, W. Lorenz, M. G. Caron, and R. J. Lefkowitz. 1992. Isoprenylation of a protein kinase. Requirement of farnesylation/alpha-carboxyl methylation for full enzymatic activity of rhodopsin kinase. J. Biol. Chem. 267:1422-1425.

201. Ito, D., Y. Imai, K. Ohsawa, K. Nakajima, Y. Fukuuchi, and S. Kohsaka. 1998. Microglia-specific localisation of a novel calcium binding protein, Iba1. Brain Res. Mol. Brain Res. 57:1-9.

202. Jacobson, S. G., T. S. Aleman, A. V. Cideciyan, E. Heon, M. Golczak, W. A. Beltran, A. Sumaroka, S. B. Schwartz, A. J. Roman, E. A. Windsor, J. M. Wilson, G. D. Aguirre, E. M. Stone, and K. Palczewski. 2007. Human cone photoreceptor dependence on RPE65 isomerase. Proc. Natl. Acad. Sci. U. S. A 104:15123-15128.

203. Jacobson, S. G., S. L. Boye, T. S. Aleman, T. J. Conlon, C. J. Zeiss, A. J. Roman, A. V. Cideciyan, S. B. Schwartz, A. M. Komaromy, M. Doobrajh, A. Y. Cheung, A. Sumaroka, S. E. Pearce-Kelling, G. D. Aguirre, S. Kaushal, A. M. Maguire, T. R. Flotte, and W. W. Hauswirth. 2006. Safety in nonhuman primates of ocular AAV2-RPE65, a candidate treatment for blindness in Leber congenital amaurosis. Hum. Gene Ther. 17:845-858.

204. Jacobson, S. G., A. V. Cideciyan, T. Aleman, A. Sumaroka, A. J. Roman, M. Swider, S. B. Schwartz, E. Banin, and E. M. Stone. 2010. Human Retinal Disease from AIPL1 Gene Mutations: Foveal Cone Loss with Minimal Macular Photoreceptors and Rod Function Remaining. Invest Ophthalmol Vis. Sci.

205. Jacobson, S. G., A. V. Cideciyan, T. S. Aleman, M. J. Pianta, A. Sumaroka, S. B. Schwartz, E. E. Smilko, A. H. Milam, V. C. Sheffield, and E. M. Stone. 2003. Crumbs homolog 1 (CRB1) mutations result in a thick human retina with abnormal lamination. Hum. Mol. Genet. 12:1073-1078.

206. Jacobson, S. G., A. V. Cideciyan, T. S. Aleman, A. Sumaroka, S. B. Schwartz, A. J. Roman, and E. M. Stone. 2007. Leber congenital amaurosis caused by an RPGRIP1 mutation shows treatment potential. Ophthalmology 114:895-898.

207. Jacobson, S. G., A. V. Cideciyan, T. S. Aleman, A. Sumaroka, S. B. Schwartz, E. A. Windsor, A. J. Roman, E. Heon, E. M. Stone, and D. A. Thompson. 2007. RDH12 and RPE65, visual cycle genes causing leber congenital amaurosis, differ in disease expression. Invest Ophthalmol. Vis. Sci. 48:332-338.

208. Jacobson, S. G., A. V. Cideciyan, Y. Huang, D. B. Hanna, C. L. Freund, L. M. Affatigato, R. E. Carr, D. J. Zack, E. M. Stone, and R. R. McInnes. 1998. Retinal degenerations with truncation mutations in the cone-rod homeobox (CRX) gene. Invest Ophthalmol. Vis. Sci. 39:2417-2426.

209. Jaissle, G. B., C. A. May, J. Reinhard, K. Kohler, S. Fauser, E. Lutjen-Drecoll, E. Zrenner, and M. W. Seeliger. 2001. Evaluation of the rhodopsin knockout mouse as a model of pure cone function. Invest Ophthalmol Vis. Sci. 42:506-513.

210. Jansen, H. G. and S. Sanyal. 1984. Development and degeneration of retina in rds mutant mice: electron microscopy. J. Comp Neurol. 224:71-84.

211. Jeon, C. J., E. Strettoi, and R. H. Masland. 1998. The major cell populations of the mouse retina. J. Neurosci. 18:8936-8946.

212. Jimenez, A. J., J. M. Garcia-Fernandez, B. Gonzalez, and R. G. Foster. 1996. The spatio-temporal pattern of photoreceptor degeneration in the aged rd/rd mouse retina. Cell Tissue Res. 284:193-202.

213. Jindrova, H. 1998. Vertebrate phototransduction: activation, recovery, and adaptation. Physiol Res. 47:155-168.

214. Johnson, E. M., Jr., L. J. Greenlund, P. T. Akins, and C. Y. Hsu. 1995. Neuronal apoptosis: current understanding of molecular mechanisms and potential role in ischemic brain injury. J. Neurotrauma 12:843-852.

215. Jomary, C., T. A. Piper, G. Dickson, L. A. Couture, A. E. Smith, M. J. Neal, and S. E. Jones. 1994. Adenovirus-mediated gene transfer to murine retinal cells in vitro and in vivo. FEBS Lett. 347:117-122.

216. Jomary, C., K. A. Vincent, J. Grist, M. J. Neal, and S. E. Jones. 1997. Rescue of photoreceptor function by AAV-mediated gene transfer in a mouse model of inherited retinal degeneration. Gene Ther. 4:683-690.

217. Jones, B. W., C. B. Watt, J. M. Frederick, W. Baehr, C. K. Chen, E. M. Levine, A. H. Milam, M. M. Lavail, and R. E. Marc. 2003. Retinal remodeling triggered by photoreceptor degenerations. J. Comp Neurol. 464:1-16.

218. Jones, B. W., C. B. Watt, and R. E. Marc. 2005. Retinal remodelling. Clin. Exp. Optom. 88:282-291.

219. Ju, W. K., M. Y. Lee, H. D. Hofmann, M. Kirsch, and M. H. Chun. 1999. Expression of CNTF in Muller cells of the rat retina after pressure-induced ischemia. Neuroreport 10:419-422.

220. Kachi, S., Y. Oshima, N. Esumi, M. Kachi, B. Rogers, D. J. Zack, and P. A. Campochiaro. 2005. Nonviral ocular gene transfer. Gene Ther. 12:843-851.

221. Kafri, T., D. Morgan, T. Krahl, N. Sarvetnick, L. Sherman, and I. Verma. 1998. Cellular immune response to adenoviral vector infected cells does not require de novo viral gene expression: implications for gene therapy. Proc. Natl. Acad. Sci. U. S. A 95:11377-11382.

222. Kanaya, K., M. M. Sohocki, and T. Kamitani. 2004. Abolished interaction of NUB1 with mutant AIPL1 involved in Leber congenital amaurosis. Biochem. Biophys. Res. Commun. 317:768-773.

223. Kay, B. K., M. P. Williamson, and M. Sudol. 2000. The importance of being proline: the interaction of proline-rich motifs in signaling proteins with their cognate domains. FASEB J. 14:231-241.

224. Kay, M. A., C. S. Manno, M. V. Ragni, P. J. Larson, L. B. Couto, A. McClelland, B. Glader, A. J. Chew, S. J. Tai, R. W. Herzog, V. Arruda, F. Johnson, C. Scallan, E. Skarsgard, A. W. Flake, and K. A. High. 2000. Evidence for gene transfer and expression of factor IX in haemophilia B patients treated with an AAV vector. Nat. Genet. 24:257-261.

225. Kaye, J. F., J. H. Richardson, and A. M. Lever. 1995. cis-acting sequences involved in human immunodeficiency virus type 1 RNA packaging. J. Virol. 69:6588-6592.

226. Kedzierski, W., D. Bok, and G. H. Travis. 1998. Non-cell-autonomous photoreceptor degeneration in rds mutant mice mosaic for expression of a rescue transgene. J. Neurosci. 18:4076-4082.

227. Kedzierski, W., M. Lloyd, D. G. Birch, D. Bok, and G. H. Travis. 1997. Generation and analysis of transgenic mice expressing P216L-substituted rds/peripherin in rod photoreceptors. Invest Ophthalmol. Vis. Sci. 38:498-509.

228. Kedzierski, W., S. Nusinowitz, D. Birch, G. Clarke, R. R. McInnes, D. Bok, and G. H. Travis. 2001. Deficiency of rds/peripherin causes photoreceptor death in mouse models of digenic and dominant retinitis pigmentosa. Proc Natl. Acad. Sci. U. S. A 98:7718-7723.

229. Kelsell, R. E., K. Gregory-Evans, A. M. Payne, I. Perrault, J. Kaplan, R. B. Yang, D. L. Garbers, A. C. Bird, A. T. Moore, and D. M. Hunt. 1998. Mutations in the retinal guanylate cyclase (RETGC-1) gene in dominant cone-rod dystrophy. Hum. Mol. Genet. 7:1179-1184.

230. Khani, S. C., B. S. Pawlyk, O. V. Bulgakov, E. Kasperek, J. E. Young, M. Adamian, X. Sun, A. J. Smith, R. R. Ali, and T. Li. 2007. AAV-mediated expression targeting of rod and cone photoreceptors with a human rhodopsin kinase promoter. Invest Ophthalmol. Vis. Sci. 48:3954-3961.

231. Kiang, A. S., A. Palfi, M. Ader, P. F. Kenna, S. Millington-Ward, G. Clark, A. Kennan, M. O'reilly, L. C. Tam, A. Aherne, N. McNally, P. Humphries, and G. J. Farrar. 2005. Toward a gene therapy for dominant disease: validation of an RNA interference-based mutation-independent approach. Mol. Ther. 12:555-561.

232. Kirschman, L. T., S. Kolandaivelu, J. M. Frederick, L. Dang, A. F. Goldberg, W. Baehr, and V. Ramamurthy. 2010. The Leber congenital amaurosis protein, AIPL1, is needed for the viability and functioning of cone photoreceptor cells. Hum. Mol. Genet.

233. Kochanek, S., G. Schiedner, and C. Volpers. 2001. High-capacity 'gutless' adenoviral vectors. Curr. Opin. Mol. Ther. 3:454-463.

234. Koenekoop, R. K. 2003. The gene for Stargardt disease, ABCA4, is a major retinal gene: a mini-review. Ophthalmic Genet. 24:75-80.

235. Koenekoop, R. K. 2004. An overview of Leber congenital amaurosis: a model to understand human retinal development. Surv. Ophthalmol. 49:379-398.

236. Koenekoop, R. K., I. Lopez, A. I. den Hollander, R. Allikmets, and F. P. Cremers. 2007. Genetic testing for retinal dystrophies and dysfunctions: benefits, dilemmas and solutions. Clin. Experiment. Ophthalmol. 35:473-485.

237. Kohl, S., B. Baumann, M. Broghammer, H. Jagle, P. Sieving, U. Kellner, R. Spegal, M. Anastasi, E. Zrenner, L. T. Sharpe, and B. Wissinger. 2000. Mutations in the CNGB3 gene encoding the beta-subunit of the cone photoreceptor cGMP-gated channel are responsible for achromatopsia (ACHM3) linked to chromosome 8q21. Hum. Mol. Genet. 9:2107-2116.

238. Kohl, S., B. Baumann, T. Rosenberg, U. Kellner, B. Lorenz, M. Vadala, S. G. Jacobson, and B. Wissinger. 2002. Mutations in the cone photoreceptor G-protein alpha-subunit gene GNAT2 in patients with achromatopsia. Am. J. Hum. Genet. 71:422-425.

239. Kohl, S., T. Marx, I. Giddings, H. Jagle, S. G. Jacobson, E. pfelstedt-Sylla, E. Zrenner, L. T. Sharpe, and B. Wissinger. 1998. Total colourblindness is caused by mutations in the gene encoding the alpha-subunit of the cone photoreceptor cGMP-gated cation channel. Nat. Genet. 19:257-259.

240. Kolandaivelu, S., J. Huang, J. B. Hurley, and V. Ramamurthy. 2009. AIPL1, a protein associated with childhood blindness, interacts with alpha-subunit of rod phosphodiesterase (PDE6) and is essential for its proper assembly. J. Biol. Chem. 284:30853-30861.

241. Kolb, H. and P. Gouras. 1974. Electron microscopic observations of human retinitis pigmentosa, dominantly inherited. Invest Ophthalmol. 13:487-498.

242. Komaromy, A. M., J. J. Alexander, A. E. Cooper, V. A. Chiodo, L. G. Glushakova, G. M. Acland, W. W. Hauswirth, and G. D. Aguirre. 2008. Targeting gene expression to cones with human cone opsin promoters in recombinant AAV. Gene Ther. 15:1049-1055.

243. Komaromy, A. M., J. J. Alexander, J. S. Rowlan, M. M. Garcia, V. A. Chiodo, A. Kaya, J. C. Tanaka, G. M. Acland, W. W. Hauswirth, and G. D. Aguirre. 2010. Gene therapy rescues cone function in congenital achromatopsia. Hum. Mol. Genet. 19:2581-2593.

244. Kotin, R. M., M. Siniscalco, R. J. Samulski, X. D. Zhu, L. Hunter, C. A. Laughlin, S. McLaughlin, N. Muzyczka, M. Rocchi, and K. I. Berns. 1990. Site-specific integration by adeno-associated virus. Proc. Natl. Acad. Sci. U. S. A 87:2211-2215.

245. Kreutzberg, G. W. 1996. Microglia: a sensor for pathological events in the CNS. Trends Neurosci. 19:312-318.

246. Kuksa, V., Y. Imanishi, M. Batten, K. Palczewski, and A. R. Moise. 2003. Retinoid cycle in the vertebrate retina: experimental approaches and mechanisms of isomerization. Vision Res. 43:2959-2981.

247. Kumar-Singh, R. and D. B. Farber. 1998. Encapsidated adenovirus mini-chromosome-mediated delivery of genes to the retina: application to the rescue of photoreceptor degeneration. Hum. Mol. Genet. 7:1893-1900.

248. Kurth, I., D. A. Thompson, K. Ruther, K. L. Feathers, J. D. Chrispell, J. Schroth, C. L. McHenry, M. Schweizer, S. Skosyrski, A. Gal, and C. A. Hubner. 2007. Targeted disruption of the murine retinal dehydrogenase gene Rdh12 does not limit visual cycle function. Mol. Cell Biol. 27:1370-1379.

249. Lai, C. M., M. J. Yu, M. Brankov, N. L. Barnett, X. Zhou, T. M. Redmond, K. Narfstrom, and P. E. Rakoczy. 2004. Recombinant adeno-associated virus type 2-mediated gene delivery into the Rpe65-/- knockout mouse eye results in limited rescue. Genet. Vaccines. Ther. 2:3.

250. Lai, L., K. Lin, G. Foulks, L. Ma, X. Xiao, and K. Chen. 2005. Highly efficient ex vivo gene delivery into human corneal endothelial cells by recombinant adeno-associated virus. Curr. Eye Res. 30:213-219.

251. Lai, L. J., X. Xiao, and J. H. Wu. 2007. Inhibition of corneal neovascularization with endostatin delivered by adeno-associated viral (AAV) vector in a mouse corneal injury model. J. Biomed. Sci. 14:313-322.

252. Lai, R. K., D. Perez-Sala, F. J. Canada, and R. R. Rando. 1990. The gamma subunit of transducin is farnesylated. Proc. Natl. Acad. Sci. U. S. A 87:7673-7677.

253. Lai, Y., Y. Yue, M. Liu, A. Ghosh, J. F. Engelhardt, J. S. Chamberlain, and D. Duan. 2005. Efficient in vivo gene expression by trans-splicing adeno-associated viral vectors. Nat. Biotechnol. 23:1435-1439.

254. Lamb, T. D. and E. N. Pugh, Jr. 1992. A quantitative account of the activation steps involved in phototransduction in amphibian photoreceptors. J. Physiol 449:719-758.

255. Lamb, T. D. and E. N. Pugh, Jr. 2004. Dark adaptation and the retinoid cycle of vision. Prog. Retin. Eye Res. 23:307-380.

256. Lau, D., L. H. McGee, S. Zhou, K. G. Rendahl, W. C. Manning, J. A. Escobedo, and J. G. Flannery. 2000. Retinal degeneration is slowed in transgenic rats by AAV-mediated delivery of FGF-2. Invest Ophthalmol. Vis. Sci. 41:3622-3633.

257. Lavail, M. M., K. Unoki, D. Yasumura, M. T. Matthes, G. D. Yancopoulos, and R. H. Steinberg. 1992. Multiple growth factors, cytokines, and neurotrophins rescue photoreceptors from the damaging effects of constant light. Proc. Natl. Acad. Sci. U. S. A 89:11249-11253.

258. Lavail, M. M., D. Yasumura, M. T. Matthes, K. A. Drenser, J. G. Flannery, A. S. Lewin, and W. W. Hauswirth. 2000. Ribozyme rescue of photoreceptor cells in P23H transgenic rats: long-term survival and late-stage therapy. Proc. Natl. Acad. Sci. U. S. A 97:11488-11493.

259. Lavail, M. M., D. Yasumura, M. T. Matthes, C. Lau-Villacorta, K. Unoki, C. H. Sung, and R. H. Steinberg. 1998. Protection of mouse photoreceptors by survival factors in retinal degenerations. Invest Ophthalmol. Vis. Sci. 39:592-602.

260. Le, M. G., K. Stieger, A. J. Smith, M. Weber, J. Y. Deschamps, D. Nivard, A. Mendes-Madeira, N. Provost, Y. Pereon, Y. Cherel, R. R. Ali, C. Hamel, P. Moullier, and F. Rolling. 2007. Restoration of vision in RPE65-deficient Briard dogs using an AAV serotype 4 vector that specifically targets the retinal pigmented epithelium. Gene Ther. 14:292-303.

261. Le, M. G., M. Weber, Y. Pereon, A. Mendes-Madeira, D. Nivard, J. Y. Deschamps, P. Moullier, and F. Rolling. 2005. Postsurgical assessment and long-term safety of recombinant adeno-associated virus-mediated gene transfer into the retinas of dogs and primates. Arch. Ophthalmol. 123:500-506.

262. Lebherz, C., A. Maguire, W. Tang, J. Bennett, and J. M. Wilson. 2008. Novel AAV serotypes for improved ocular gene transfer. J. Gene Med. 10:375-382.

263. Lem, J., M. L. Applebury, J. D. Falk, J. G. Flannery, and M. I. Simon. 1991. Tissue-specific and developmental regulation of rod opsin chimeric genes in transgenic mice. Neuron 6:201-210.

264. Lem, J., N. V. Krasnoperova, P. D. Calvert, B. Kosaras, D. A. Cameron, M. Nicolo, C. L. Makino, and R. L. SIDMAN. 1999. Morphological, physiological, and biochemical changes in rhodopsin knockout mice. Proc. Natl. Acad. Sci. U. S. A 96:736-741.

265. Leonard, K. C., D. Petrin, S. G. Coupland, A. N. Baker, B. C. Leonard, E. C. LaCasse, W. W. Hauswirth, R. G. Korneluk, and C. Tsilfidis. 2007. XIAP protection of photoreceptors in animal models of retinitis pigmentosa. PLoS. ONE. 2:e314.

266. Leveillard, T., S. Mohand-Said, O. Lorentz, D. Hicks, A. C. Fintz, E. Clerin, M. Simonutti, V. Forster, N. Cavusoglu, F. Chalmel, P. Dolle, O. Poch, G. Lambrou, and J. A. Sahel. 2004. Identification and characterization of rod-derived cone viability factor. Nat. Genet. 36:755-759.

267. Lewin, A. S., K. A. Drenser, W. W. Hauswirth, S. Nishikawa, D. Yasumura, J. G. Flannery, and M. M. Lavail. 1998. Ribozyme rescue of photoreceptor cells in a transgenic rat model of autosomal dominant retinitis pigmentosa. Nat. Med. 4:967-971.

268. Lewis, D. L., J. E. Hagstrom, A. G. Loomis, J. A. Wolff, and H. Herweijer. 2002. Efficient delivery of siRNA for inhibition of gene expression in postnatal mice. Nat. Genet. 32:107-108.

269. Li, Q., R. Miller, P. Y. Han, J. Pang, A. Dinculescu, V. Chiodo, and W. W. Hauswirth. 2008. Intraocular route of AAV2 vector administration defines humoral immune response and therapeutic potential. Mol. Vis. 14:1760-1769.

270. Li, T., M. Adamian, D. J. Roof, E. L. Berson, T. P. Dryja, B. J. Roessler, and B. L. Davidson. 1994. In vivo transfer of a reporter gene to the retina mediated by an adenoviral vector. Invest Ophthalmol. Vis. Sci. 35:2543-2549.

271. Li, Z. Y., F. Wong, J. H. Chang, D. E. Possin, Y. Hao, R. M. Petters, and A. H. Milam. 1998. Rhodopsin transgenic pigs as a model for human retinitis pigmentosa. Invest Ophthalmol. Vis. Sci. 39:808-819.

272. Liang, F. Q., T. S. Aleman, N. S. Dejneka, L. Dudus, K. J. Fisher, A. M. Maguire, S. G. Jacobson, and J. Bennett. 2001. Long-term protection of retinal structure but not function using RAAV.CNTF in animal models of retinitis pigmentosa. Mol. Ther. 4:461-472.

273. Liang, F. Q., T. S. Aleman, N. S. Dejneka, L. Dudus, K. J. Fisher, A. M. Maguire, S. G. Jacobson, and J. Bennett. 2001. Long-term protection of retinal structure but not function using RAAV.CNTF in animal models of retinitis pigmentosa. Mol. Ther. 4:461-472.

274. Liang, F. Q., E. Surace, N. S. Dejneka, A. M. Maguire, and J. Bennett. 2003. Muller cell transduction by AAV2 in normal and degenerative retinas. Adv. Exp. Med. Biol. 533:439-445.

275. Liang, Y., D. Fotiadis, T. Maeda, A. Maeda, A. Modzelewska, S. Filipek, D. A. Saperstein, A. Engel, and K. Palczewski. 2004. Rhodopsin signaling and organization in heterozygote rhodopsin knockout mice. J. Biol. Chem. 279:48189-48196.

276. Linberg, K. A., R. N. Fariss, J. R. Heckenlively, D. B. Farber, and S. K. Fisher. 2005. Morphological characterization of the retinal degeneration in three strains of mice carrying the rd-3 mutation. Vis. Neurosci. 22:721-734.

277. Lipton, S. A. and S. B. Kater. 1989. Neurotransmitter regulation of neuronal outgrowth, plasticity and survival. Trends Neurosci. 12:265-270.

278. Lisman, J. and G. Fain. 1995. Support for the equivalent light hypothesis for RP. Nat. Med. 1:1254-1255.

279. Liu, C., Y. Li, M. Peng, A. M. Laties, and R. Wen. 1999. Activation of caspase-3 in the retina of transgenic rats with the rhodopsin mutation s334ter during photoreceptor degeneration. J. Neurosci. 19:4778-4785.

280. Liu, J., M. Saghizadeh, S. S. Tuli, A. A. Kramerov, A. S. Lewin, D. C. Bloom, W. W. Hauswirth, M. G. Castro, G. S. Schultz, and A. V. Ljubimov. 2008. Different tropism of adenoviruses and adeno-associated viruses to corneal cells: implications for corneal gene therapy. Mol. Vis. 14:2087-2096.

281. Liu, X., O. V. Bulgakov, K. N. Darrow, B. Pawlyk, M. Adamian, M. C. Liberman, and T. Li. 2007. Usherin is required for maintenance of retinal photoreceptors and normal development of cochlear hair cells. Proc. Natl. Acad. Sci. U. S. A 104:4413-4418.

282. Liu, X., O. V. Bulgakov, X. H. Wen, M. L. Woodruff, B. Pawlyk, J. Yang, G. L. Fain, M. A. Sandberg, C. L. Makino, and T. Li. 2004. AIPL1, the protein that is defective in Leber congenital amaurosis, is essential for the biosynthesis of retinal rod cGMP phosphodiesterase. Proc. Natl. Acad. Sci. U. S. A 101:13903-13908.

283. Loewen, C. J., O. L. Moritz, B. M. Tam, D. S. Papermaster, and R. S. Molday. 2003. The role of subunit assembly in peripherin-2 targeting to rod photoreceptor disk membranes and retinitis pigmentosa. Mol. Biol. Cell 14:3400-3413.

284. Loewen, N., D. A. Leske, J. D. Cameron, Y. Chen, T. Whitwam, R. D. Simari, W. L. Teo, M. P. Fautsch, E. M. Poeschla, and J. M. Holmes. 2004. Long-term retinal transgene expression with FIV versus adenoviral vectors. Mol. Vis. 10:272-280.

285. Lorenz, B., P. Gyurus, M. Preising, D. Bremser, S. Gu, M. Andrassi, C. Gerth, and A. Gal. 2000. Early-onset severe rod-cone dystrophy in young children with RPE65 mutations. Invest Ophthalmol. Vis. Sci. 41:2735-2742.

286. Lotery, A. J., G. S. Yang, R. F. Mullins, S. R. Russell, M. Schmidt, E. M. Stone, J. D. Lindbloom, J. A. Chiorini, R. M. Kotin, and B. L. Davidson. 2003. Adeno-associated virus type 5: transduction efficiency and cell-type specificity in the primate retina. Hum. Gene Ther. 14:1663-1671.

287. Lu, R., N. Nakajima, W. Hofmann, M. Benkirane, K. T. Jeang, J. Sodroski, and A. Engelman. 2004. Simian virus 40-based replication of catalytically inactive human immunodeficiency virus type 1 integrase mutants in nonpermissive T cells and monocyte-derived macrophages. J. Virol. 78:658-668.

288. Ma, J., J. C. Norton, A. C. Allen, J. B. Burns, K. W. Hasel, J. L. Burns, J. G. Sutcliffe, and G. H. Travis. 1995. Retinal degeneration slow (rds) in mouse results from simple insertion of a t haplotype-specific element into protein-coding exon II. Genomics 28:212-219.

289. MacLaren, R. E., R. A. Pearson, A. MacNeil, R. H. Douglas, T. E. Salt, M. Akimoto, A. Swaroop, J. C. Sowden, and R. R. Ali. 2006. Retinal repair by transplantation of photoreceptor precursors. Nature 444:203-207.

290. Maeda, A., T. Maeda, Y. Imanishi, W. Sun, B. Jastrzebska, D. A. Hatala, H. J. Winkens, K. P. Hofmann, J. J. Janssen, W. Baehr, C. A. Driessen, and K. Palczewski. 2006. Retinol dehydrogenase (RDH12) protects photoreceptors from light-induced degeneration in mice. J. Biol. Chem. 281:37697-37704.

291. Maeda, T., Y. Imanishi, and K. Palczewski. 2003. Rhodopsin phosphorylation: 30 years later. Prog. Retin. Eye Res. 22:417-434.

292. Maguire, A. M., K. A. High, A. Auricchio, J. F. Wright, E. A. Pierce, F. Testa, F. Mingozzi, J. L. Bennicelli, G. S. Ying, S. Rossi, A. Fulton, K. A. Marshall, S. Banfi, D. C. Chung, J. I. Morgan, B. Hauck, O. Zelenaia, X. Zhu, L. Raffini, F. Coppieters, B. E. De, K. S. Shindler, N. J. Volpe, E. M. Surace, C. Acerra, A. Lyubarsky, T. M. Redmond, E. Stone, J. Sun, J. W. McDonnell, B. P. Leroy, F. Simonelli, and J. Bennett. 2009. Age-dependent effects of RPE65 gene therapy for Leber's congenital amaurosis: a phase 1 dose-escalation trial. Lancet 374:1597-1605.

293. Maguire, A. M., F. Simonelli, E. A. Pierce, E. N. Pugh, Jr., F. Mingozzi, J. Bennicelli, S. Banfi, K. A. Marshall, F. Testa, E. M. Surace, S. Rossi, A. Lyubarsky, V. R. Arruda, B. Konkle, E. Stone, J. Sun, J. Jacobs, L. Dell'Osso, R. Hertle, J. X. Ma, T. M. Redmond, X. Zhu, B. Hauck, O. Zelenaia, K. S. Shindler, M. G. Maguire, J. F. Wright, N. J. Volpe, J. W. McDonnell, A. Auricchio, K. A. High, and J. Bennett. 2008. Safety and efficacy of gene transfer for Leber's congenital amaurosis. N. Engl. J. Med. 358:2240-2248.

294. Maheshri, N., J. T. Koerber, B. K. Kaspar, and D. V. Schaffer. 2006. Directed evolution of adeno-associated virus yields enhanced gene delivery vectors. Nat. Biotechnol. 24:198-204.

295. Makino, C. L., X. H. Wen, N. Michaud, I. V. Peshenko, B. Pawlyk, R. S. Brush, M. Soloviev, X. Liu, M. L. Woodruff, P. D. Calvert, A. B. Savchenko, R. E. Anderson, G. L. Fain, T. Li, M. A. Sandberg, and A. M. Dizhoor. 2006. Effects of low AIPL1 expression on phototransduction in rods. Invest Ophthalmol. Vis. Sci. 47:2185-2194.

296. Mancuso, K., W. W. Hauswirth, Q. Li, T. B. Connor, J. A. Kuchenbecker, M. C. Mauck, J. Neitz, and M. Neitz. 2009. Gene therapy for red-green colour blindness in adult primates. Nature 461:784-787.

297. Manno, C. S., A. J. Chew, S. Hutchison, P. J. Larson, R. W. Herzog, V. R. Arruda, S. J. Tai, M. V. Ragni, A. Thompson, M. Ozelo, L. B. Couto, D. G. Leonard, F. A. Johnson, A. McClelland, C. Scallan, E. Skarsgard, A. W. Flake, M. A. Kay, K. A. High, and B. Glader. 2003. AAV-mediated factor IX gene transfer to skeletal muscle in patients with severe hemophilia B. Blood 101:2963-2972.

298. Manno, C. S., G. F. Pierce, V. R. Arruda, B. Glader, M. Ragni, J. J. Rasko, M. C. Ozelo, K. Hoots, P. Blatt, B. Konkle, M. Dake, R. Kaye, M. Razavi, A. Zajko, J. Zehnder, P. K. Rustagi, H. Nakai, A. Chew, D. Leonard, J. F. Wright, R. R. Lessard, J. M. Sommer, M. Tigges, D. Sabatino, A. Luk, H. Jiang, F. Mingozzi, L. Couto, H. C. Ertl, K. A. High, and M. A. Kay. 2006. Successful transduction of liver in hemophilia by AAV-Factor IX and limitations imposed by the host immune response. Nat. Med. 12:342-347.

299. Marc, R. E., B. W. Jones, C. B. Watt, and E. Strettoi. 2003. Neural remodeling in retinal degeneration. Prog. Retin. Eye Res. 22:607-655.

300. Martin, K. R., R. L. Klein, and H. A. Quigley. 2002. Gene delivery to the eye using adeno-associated viral vectors. Methods 28:267-275.

301. Martin, K. R., H. A. Quigley, D. J. Zack, H. Levkovitch-Verbin, J. Kielczewski, D. Valenta, L. Baumrind, M. E. Pease, R. L. Klein, and W. W. Hauswirth. 2003. Gene therapy with brain-derived neurotrophic factor as a protection: retinal ganglion cells in a rat glaucoma model. Invest Ophthalmol. Vis. Sci. 44:4357-4365.

302. Mashhour, B., D. Couton, M. Perricaudet, and P. Briand. 1994. In vivo adenovirus-mediated gene transfer into ocular tissues. Gene Ther. 1:122-126.

303. Masland, R. H. 2001. The fundamental plan of the retina. Nat. Neurosci. 4:877-886.

304. Mata, N. L., R. A. Radu, R. C. Clemmons, and G. H. Travis. 2002. Isomerization and oxidation of vitamin a in cone-dominant retinas: a novel pathway for visual-pigment regeneration in daylight. Neuron 36:69-80.

305. Matsuda, T. and C. L. Cepko. 2004. Electroporation and RNA interference in the rodent retina in vivo and in vitro. Proc. Natl. Acad. Sci. U. S. A 101:16-22.

306. Matsushita, T., S. Elliger, C. Elliger, G. Podsakoff, L. Villarreal, G. J. Kurtzman, Y. Iwaki, and P. Colosi. 1998. Adeno-associated virus vectors can be efficiently produced without helper virus. Gene Ther. 5:938-945.

307. McBride, M. S., M. D. Schwartz, and A. T. Panganiban. 1997. Efficient encapsidation of human immunodeficiency virus type 1 vectors and further

characterization of cis elements required for encapsidation. J. Virol. 71:4544-4554.

308. McCarty, D. M., P. E. Monahan, and R. J. Samulski. 2001. Self-complementary recombinant adeno-associated virus (scAAV) vectors promote efficient transduction independently of DNA synthesis. Gene Ther. 8:1248-1254.

309. McGill, T. J., G. T. Prusky, R. M. Douglas, D. Yasumura, M. T. Matthes, G. Nune, K. Donohue-Rolfe, H. Yang, D. Niculescu, W. W. Hauswirth, S. V. Girman, R. D. Lund, J. L. Duncan, and M. M. Lavail. 2007. Intraocular CNTF reduces vision in normal rats in a dose-dependent manner. Invest Ophthalmol. Vis. Sci. 48:5756-5766.

310. McKibbin, M., M. Ali, M. D. Mohamed, A. P. Booth, F. Bishop, B. Pal, K. Springell, Y. Raashid, H. Jafri, and C. F. Inglehearn. 2010. Genotype-phenotype correlation for leber congenital amaurosis in Northern Pakistan. Arch. Ophthalmol 128:107-113.

311. McKinnon, S. J., D. M. Lehman, N. G. Tahzib, N. L. Ransom, H. A. Reitsamer, P. Liston, E. LaCasse, Q. Li, R. G. Korneluk, and W. W. Hauswirth. 2002. Baculoviral IAP repeat-containing-4 protects optic nerve axons in a rat glaucoma model. Mol. Ther. 5:780-787.

312. McLaughlin, M. E., T. L. Ehrhart, E. L. Berson, and T. P. Dryja. 1995. Mutation spectrum of the gene encoding the beta subunit of rod phosphodiesterase among patients with autosomal recessive retinitis pigmentosa. Proc. Natl. Acad. Sci. U. S. A 92:3249-3253.

313. McNally, N., P. Kenna, M. M. Humphries, A. H. Hobson, N. W. Khan, R. A. Bush, P. A. Sieving, P. Humphries, and G. J. Farrar. 1999. Structural and functional rescue of murine rod photoreceptors by human rhodopsin transgene. Hum. Mol. Genet. 8:1309-1312.

314. Mehalow, A. K., S. Kameya, R. S. Smith, N. L. Hawes, J. M. Denegre, J. A. Young, L. Bechtold, N. B. Haider, U. Tepass, J. R. Heckenlively, B. Chang, J. K. Naggert, and P. M. Nishina. 2003. CRB1 is essential for external limiting membrane integrity and photoreceptor morphogenesis in the mammalian retina. Hum. Mol. Genet. 12:2179-2189.

315. Mendes, H. F. and M. E. Cheetham. 2008. Pharmacological manipulation of gain-of-function and dominant-negative mechanisms in rhodopsin retinitis pigmentosa. Hum. Mol. Genet. 17:3043-3054.

316. Menotti-Raymond, M., V. A. David, A. A. Schaffer, R. Stephens, D. Wells, R. Kumar-Singh, S. J. O'Brien, and K. Narfstrom. 2007. Mutation in CEP290 discovered for cat model of human retinal degeneration. J. Hered. 98:211-220.

317. Menotti-Raymond, M., K. H. Deckman, V. David, J. Myrkalo, S. J. O'Brien, and K. Narfstrom. 2010. Mutation discovered in a feline model of human congenital retinal blinding disease. Invest Ophthalmol Vis. Sci. 51:2852-2859.

318. Miao, C. H., R. O. Snyder, D. B. Schowalter, G. A. Patijn, B. Donahue, B. Winther, and M. A. Kay. 1998. The kinetics of rAAV integration in the liver. Nat. Genet. 19:13-15.

319. Michaelides, M., G. E. Holder, K. Bradshaw, D. M. Hunt, and A. T. Moore. 2005. Cone-rod dystrophy, intrafamilial variability, and incomplete penetrance associated with the R172W mutation in the peripherin/RDS gene. Ophthalmology 112:1592-1598.

320. Michelfelder, S. and M. Trepel. 2009. Adeno-associated viral vectors and their redirection to cell-type specific receptors. Adv. Genet. 67:29-60.

321. Milam, A. H., M. R. Barakat, N. Gupta, L. Rose, T. S. Aleman, M. J. Pianta, A. V. Cideciyan, V. C. Sheffield, E. M. Stone, and S. G. Jacobson. 2003. Clinicopathologic effects of mutant GUCY2D in Leber congenital amaurosis. Ophthalmology 110:549-558.

322. Milam, A. H., Z. Y. Li, and R. N. Fariss. 1998. Histopathology of the human retina in retinitis pigmentosa. Prog. Retin. Eye Res. 17:175-205.

323. Miller, D. G., L. M. Petek, and D. W. Russell. 2004. Adeno-associated virus vectors integrate at chromosome breakage sites. Nat. Genet. 36:767-773.

324. Millington-Ward, S., B. O'Neill, G. Tuohy, N. Al-Jandal, A. S. Kiang, P. F. Kenna, A. Palfi, P. Hayden, F. Mansergh, A. Kennan, P. Humphries, and G. J. Farrar. 1997. Strategems in vitro for gene therapies directed to dominant mutations. Hum. Mol. Genet. 6:1415-1426.

325. Milunsky, A., X. L. Huang, J. Milunsky, A. DeStefano, and C. T. Baldwin. 1999. A locus for autosomal recessive achromatopsia on human chromosome 8q. Clin. Genet. 56:82-85.

326. Min, S. H., L. L. Molday, M. W. Seeliger, A. Dinculescu, A. M. Timmers, A. Janssen, F. Tonagel, N. Tanimoto, B. H. Weber, R. S. Molday, and W. W. Hauswirth. 2005. Prolonged recovery of retinal structure/function after gene therapy in an Rs1h-deficient mouse model of x-linked juvenile retinoschisis. Mol. Ther. 12:644-651.

327. Miyata, Y., B. Chambraud, C. Radanyi, J. Leclerc, M. C. Lebeau, J. M. Renoir, R. Shirai, M. G. Catelli, I. Yahara, and E. E. Baulieu. 1997. Phosphorylation of the immunosuppressant FK506-binding protein FKBP52 by casein kinase II: regulation of HSP90-binding activity of FKBP52. Proc. Natl. Acad. Sci. U. S. A 94:14500-14505.

328. Miyazaki, M., Y. Ikeda, Y. Yonemitsu, Y. Goto, T. Sakamoto, T. Tabata, Y. Ueda, M. Hasegawa, S. Tobimatsu, T. Ishibashi, and K. Sueishi. 2003. Simian lentiviral vector-mediated retinal gene transfer of pigment epithelium-derived factor protects retinal degeneration and electrical defect in Royal College of Surgeons rats. Gene Ther. 10:1503-1511.

329. Miyoshi, H., U. Blomer, M. Takahashi, F. H. Gage, and I. M. Verma. 1998. Development of a self-inactivating lentivirus vector. J. Virol. 72:8150-8157.

330. Miyoshi, H., M. Takahashi, F. H. Gage, and I. M. Verma. 1997. Stable and efficient gene transfer into the retina using an HIV-based lentiviral vector. Proc. Natl. Acad. Sci. U. S. A 94:10319-10323.

331. Mohand-Said, S., A. udon-Combe, D. Hicks, M. Simonutti, V. Forster, A. C. Fintz, T. Leveillard, H. Dreyfus, and J. A. Sahel. 1998. Normal retina releases a diffusible factor stimulating cone survival in the retinal degeneration mouse. Proc. Natl. Acad. Sci. U. S. A 95:8357-8362.

332. Moiseyev, G., Y. Chen, Y. Takahashi, B. X. Wu, and J. X. Ma. 2005. RPE65 is the isomerohydrolase in the retinoid visual cycle. Proc. Natl. Acad. Sci. U. S. A 102:12413-12418.

333. Monahan, P. E., K. Jooss, and M. S. Sands. 2002. Safety of adeno-associated virus gene therapy vectors: a current evaluation. Expert. Opin. Drug Saf 1:79-91.

334. Mori, K., P. Gehlbach, A. Ando, K. Wahlin, V. Gunther, D. McVey, L. Wei, and P. A. Campochiaro. 2002. Intraocular adenoviral vector-mediated gene transfer in proliferative retinopathies. Invest Ophthalmol Vis. Sci. 43:1610-1615.

335. Mori, K., P. Gehlbach, S. Yamamoto, E. Duh, D. J. Zack, Q. Li, K. I. Berns, B. J. Raisler, W. W. Hauswirth, and P. A. Campochiaro. 2002. AAV-mediated gene transfer of pigment epithelium-derived factor inhibits choroidal neovascularization. Invest Ophthalmol. Vis. Sci. 43:1994-2000.

336. Mori, S., L. Wang, T. Takeuchi, and T. Kanda. 2004. Two novel adeno-associated viruses from cynomolgus monkey: pseudotyping characterization of capsid protein. Virology 330:375-383.

337. Morrow, E. M., T. Furukawa, E. Raviola, and C. L. Cepko. 2005. Synaptogenesis and outer segment formation are perturbed in the neural retina of Crx mutant mice. BMC. Neurosci. 6:5.

338. Moulder, K. L., R. J. Cormier, A. A. Shute, C. F. Zorumski, and S. Mennerick. 2003. Homeostatic effects of depolarization on Ca2+ influx, synaptic signaling, and survival. J. Neurosci. 23:1825-1831.

339. Mowat, F. M., S. M. Petersen-Jones, H. Williamson, D. L. Williams, P. J. Luthert, R. R. Ali, and J. W. Bainbridge. 2008. Topographical

characterization of cone photoreceptors and the area centralis of the canine retina. Mol. Vis. 14:2518-2527.

340. Muller, O. J., F. Kaul, M. D. Weitzman, R. Pasqualini, W. Arap, J. A. Kleinschmidt, and M. Trepel. 2003. Random peptide libraries displayed on adeno-associated virus to select for targeted gene therapy vectors. Nat. Biotechnol. 21:1040-1046.

341. Muzyczka, N. and K. H. Warrington, Jr. 2005. Custom adeno-associated virus capsids: the next generation of recombinant vectors with novel tropism. Hum. Gene Ther. 16:408-416.

342. Nakai, H., Y. Iwaki, M. A. Kay, and L. B. Couto. 1999. Isolation of recombinant adeno-associated virus vector-cellular DNA junctions from mouse liver. J. Virol. 73:5438-5447.

343. Nakai, H., E. Montini, S. Fuess, T. A. Storm, M. Grompe, and M. A. Kay. 2003. AAV serotype 2 vectors preferentially integrate into active genes in mice. Nat. Genet. 34:297-302.

344. Nakai, H., X. Wu, S. Fuess, T. A. Storm, D. Munroe, E. Montini, S. M. Burgess, M. Grompe, and M. A. Kay. 2005. Large-scale molecular characterization of adeno-associated virus vector integration in mouse liver. J. Virol. 79:3606-3614.

345. Nakai, H., S. R. Yant, T. A. Storm, S. Fuess, L. Meuse, and M. A. Kay. 2001. Extrachromosomal recombinant adeno-associated virus vector genomes are primarily responsible for stable liver transduction in vivo. J. Virol. 75:6969-6976.

346. Nakajima, K. and S. Kohsaka. 2001. Microglia: activation and their significance in the central nervous system. J. Biochem. 130:169-175.

347. Narfstrom, K., M. L. Katz, R. Bragadottir, M. Seeliger, A. Boulanger, T. M. Redmond, L. Caro, C. M. Lai, and P. E. Rakoczy. 2003. Functional and structural recovery of the retina after gene therapy in the RPE65 null mutation dog. Invest Ophthalmol. Vis. Sci. 44:1663-1672.

348. Natkunarajah, M., P. Trittibach, J. McIntosh, Y. Duran, S. E. Barker, A. J. Smith, A. C. Nathwani, and R. R. Ali. 2007. Assessment of ocular transduction using single-stranded and self-complementary recombinant adeno-associated virus serotype 2/8. Gene Ther.

349. Ng, P. C. and S. Henikoff. 2001. Predicting deleterious amino acid substitutions. Genome Res. 11:863-874.

350. Ng, P. C. and S. Henikoff. 2006. Predicting the effects of amino acid substitutions on protein function. Annu. Rev. Genomics Hum. Genet. 7:61-80.

351. Nikonov, S., T. D. Lamb, and E. N. Pugh, Jr. 2000. The role of steady phosphodiesterase activity in the kinetics and sensitivity of the light-adapted salamander rod photoresponse. J. Gen. Physiol 116:795-824.

352. Nomura, S., A. Merched, E. Nour, C. Dieker, K. Oka, and L. Chan. 2004. Low-density lipoprotein receptor gene therapy using helper-dependent adenovirus produces long-term protection against atherosclerosis in a mouse model of familial hypercholesterolemia. Gene Ther. 11:1540-1548.

353. O'Neal, W. K., H. Zhou, N. Morral, E. guilar-Cordova, J. Pestaner, C. Langston, B. Mull, Y. Wang, A. L. Beaudet, and B. Lee. 1998. Toxicological comparison of E2a-deleted and first-generation adenoviral vectors expressing alpha1-antitrypsin after systemic delivery. Hum. Gene Ther. 9:1587-1598.

354. O'Neal, W. K., H. Zhou, N. Morral, C. Langston, R. J. Parks, F. L. Graham, S. Kochanek, and A. L. Beaudet. 2000. Toxicity associated with repeated administration of first-generation adenovirus vectors does not occur with a helper-dependent vector. Mol. Med. 6:179-195.

355. O'reilly, M., A. Palfi, N. Chadderton, S. Millington-Ward, M. Ader, T. Cronin, T. Tuohy, A. Auricchio, M. Hildinger, A. Tivnan, N. McNally, M. M. Humphries, A. S. Kiang, P. Humphries, P. F. Kenna, and G. J. Farrar. 2007. RNA interference-mediated suppression and replacement of human rhodopsin in vivo. Am. J. Hum. Genet. 81:127-135.

356. Olshevskaya, E. V., P. D. Calvert, M. L. Woodruff, I. V. Peshenko, A. B. Savchenko, C. L. Makino, Y. S. Ho, G. L. Fain, and A. M. Dizhoor. 2004. The Y99C mutation in guanylyl cyclase-activating protein 1 increases intracellular Ca2+ and causes photoreceptor degeneration in transgenic mice. J. Neurosci. 24:6078-6085.

357. Olsson, J. E., J. W. Gordon, B. S. Pawlyk, D. Roof, A. Hayes, R. S. Molday, S. Mukai, G. S. Cowley, E. L. Berson, and T. P. Dryja. 1992. Transgenic mice with a rhodopsin mutation (Pro23His): a mouse model of autosomal dominant retinitis pigmentosa. Neuron 9:815-830.

358. Oshima, Y., T. Sakamoto, T. Hisatomi, C. Tsutsumi, Y. Sassa, T. Ishibashi, and H. Inomata. 2002. Targeted gene transfer to corneal stroma in vivo by electric pulses. Exp. Eye Res. 74:191-198.

359. Pang, J. J., S. L. Boye, A. Kumar, A. Dinculescu, W. Deng, J. Li, Q. Li, A. Rani, T. C. Foster, B. Chang, N. L. Hawes, J. H. Boatright, and W. W. Hauswirth. 2008. AAV-mediated gene therapy for retinal degeneration in the rd10 mouse containing a recessive PDEbeta mutation. Invest Ophthalmol. Vis. Sci. 49:4278-4283.

360. Pang, J. J., B. Chang, N. L. Hawes, R. E. Hurd, M. T. Davisson, J. Li, S. M. Noorwez, R. Malhotra, J. H. McDowell, S. Kaushal, W. W. Hauswirth, S.

Nusinowitz, D. A. Thompson, and J. R. Heckenlively. 2005. Retinal degeneration 12 (rd12): a new, spontaneously arising mouse model for human Leber congenital amaurosis (LCA). Mol. Vis. 11:152-162.

361. Pang, J. J., B. Chang, A. Kumar, S. Nusinowitz, S. M. Noorwez, J. Li, A. Rani, T. C. Foster, V. A. Chiodo, T. Doyle, H. Li, R. Malhotra, J. T. Teusner, J. H. McDowell, S. H. Min, Q. Li, S. Kaushal, and W. W. Hauswirth. 2006. Gene therapy restores vision-dependent behavior as well as retinal structure and function in a mouse model of RPE65 Leber congenital amaurosis. Mol. Ther. 13:565-572.

362. Pasadhika, S., G. A. Fishman, E. M. Stone, M. Lindeman, R. Zelkha, I. Lopez, R. K. Koenekoop, and M. Shahidi. 2010. Differential macular morphology in patients with RPE65-, CEP290-, GUCY2D-, and AIPL1-related Leber congenital amaurosis. Invest Ophthalmol Vis. Sci. 51:2608-2614.

363. Pawlyk, B. S., A. J. Smith, P. K. Buch, M. Adamian, D. H. Hong, M. A. Sandberg, R. R. Ali, and T. Li. 2005. Gene replacement therapy rescues photoreceptor degeneration in a murine model of Leber congenital amaurosis lacking RPGRIP. Invest Ophthalmol. Vis. Sci. 46:3039-3045.

364. Perabo, L., J. Endell, S. King, K. Lux, D. Goldnau, M. Hallek, and H. Buning. 2006. Combinatorial engineering of a gene therapy vector: directed evolution of adeno-associated virus. J. Gene Med. 8:155-162.

365. Perrault, I., S. Hanein, S. Gerber, F. Barbet, J. L. Dufier, A. Munnich, J. M. Rozet, and J. Kaplan. 2003. Evidence of autosomal dominant Leber congenital amaurosis (LCA) underlain by a CRX heterozygous null allele. J. Med. Genet. 40:e90.

366. Perrault, I., J. M. Rozet, P. Calvas, S. Gerber, A. Camuzat, H. Dollfus, S. Chatelin, E. Souied, I. Ghazi, C. Leowski, M. Bonnemaison, P. D. Le, J. Frezal, J. L. Dufier, S. Pittler, A. Munnich, and J. Kaplan. 1996. Retinal-specific guanylate cyclase gene mutations in Leber's congenital amaurosis. Nat. Genet. 14:461-464.

367. Perrault, I., J. M. Rozet, I. Ghazi, C. Leowski, M. Bonnemaison, S. Gerber, D. Ducroq, A. Cabot, E. Souied, J. L. Dufier, A. Munnich, and J. Kaplan. 1999. Different functional outcome of RetGC1 and RPE65 gene mutations in Leber congenital amaurosis. Am. J. Hum. Genet. 64:1225-1228.

368. Petersen-Jones, S. 2005. Advances in the molecular understanding of canine retinal diseases. J. Small Anim Pract. 46:371-380.

369. Petersen-Jones, S. M. 1998. Animal models of human retinal dystrophies. Eye (Lond) 12 (Pt 3b):566-570.

370. Petrulis, J. R. and G. H. Perdew. 2002. The role of chaperone proteins in the aryl hydrocarbon receptor core complex. Chem. Biol. Interact. 141:25-40.

371. Petters, R. M., C. A. Alexander, K. D. Wells, E. B. Collins, J. R. Sommer, M. R. Blanton, G. Rojas, Y. Hao, W. L. Flowers, E. Banin, A. V. Cideciyan, S. G. Jacobson, and F. Wong. 1997. Genetically engineered large animal model for studying cone photoreceptor survival and degeneration in retinitis pigmentosa. Nat. Biotechnol. 15:965-970.

372. pfelstedt-Sylla, E., M. Theischen, K. Ruther, H. Wedemann, A. Gal, and E. Zrenner. 1995. Extensive intrafamilial and interfamilial phenotypic variation among patients with autosomal dominant retinal dystrophy and mutations in the human RDS/peripherin gene. Br. J. Ophthalmol 79:28-34.

373. Phelan, J. K. and D. Bok. 2000. Analysis and quantitation of mRNAs encoding the alpha- and beta-subunits of rod photoreceptor cGMP phosphodiesterase in neonatal retinal degeneration (rd) mouse retinas. Exp. Eye Res. 71:119-128.

374. Phylactou, L. A., M. W. Kilpatrick, and M. J. Wood. 1998. Ribozymes as therapeutic tools for genetic disease. Hum. Mol. Genet. 7:1649-1653.

375. Pignatelli, V., C. L. Cepko, and E. Strettoi. 2004. Inner retinal abnormalities in a mouse model of Leber's congenital amaurosis. J. Comp Neurol. 469:351-359.

376. Piguet, B., E. Heon, F. L. Munier, P. A. Grounauer, G. Niemeyer, N. Butler, D. F. Schorderet, V. C. Sheffield, and E. M. Stone. 1996. Full characterization of the maculopathy associated with an Arg-172-Trp mutation in the RDS/peripherin gene. Ophthalmic Genet. 17:175-186.

377. Pittler, S. J. and W. Baehr. 1991. Identification of a nonsense mutation in the rod photoreceptor cGMP phosphodiesterase beta-subunit gene of the rd mouse. Proc. Natl. Acad. Sci. U. S. A 88:8322-8326.

378. Pittler, S. J., S. J. Fliesler, P. L. Fisher, P. K. Keller, and L. M. Rapp. 1995. In vivo requirement of protein prenylation for maintenance of retinal cytoarchitecture and photoreceptor structure. J. Cell Biol. 130:431-439.

379. Pittler, S. J., C. E. Keeler, R. L. SIDMAN, and W. Baehr. 1993. PCR analysis of DNA from 70-year-old sections of rodless retina demonstrates identity with the mouse rd defect. Proc. Natl. Acad. Sci. U. S. A 90:9616-9619.

380. Portera-Cailliau, C., C. H. Sung, J. Nathans, and R. Adler. 1994. Apoptotic photoreceptor cell death in mouse models of retinitis pigmentosa. Proc. Natl. Acad. Sci. U. S. A 91:974-978.

381. Porto, F. B., I. Perrault, D. Hicks, J. M. Rozet, N. Hanoteau, S. Hanein, J. Kaplan, and J. A. Sahel. 2002. Prenatal human ocular degeneration occurs in Leber's congenital amaurosis (LCA2). J. Gene Med. 4:390-396.

382. Prevec, L., B. S. Christie, K. E. Laurie, M. M. Bailey, F. L. Graham, and K. L. Rosenthal. 1991. Immune response to HIV-1 gag antigens induced by recombinant adenovirus vectors in mice and rhesus macaque monkeys. J. Acquir. Immune. Defic. Syndr. 4:568-576.

383. Provost, N., M. G. Le, M. Weber, A. Mendes-Madeira, G. Podevin, Y. Cherel, M. A. Colle, J. Y. Deschamps, P. Moullier, and F. Rolling. 2005. Biodistribution of rAAV vectors following intraocular administration: evidence for the presence and persistence of vector DNA in the optic nerve and in the brain. Mol. Ther. 11:275-283.

384. Prud'homme, G. J., Y. Glinka, A. S. Khan, and R. Draghia-Akli. 2006. Electroporation-enhanced nonviral gene transfer for the prevention or treatment of immunological, endocrine and neoplastic diseases. Curr. Gene Ther. 6:243-273.

385. Qing, K., C. Mah, J. Hansen, S. Zhou, V. Dwarki, and A. Srivastava. 1999. Human fibroblast growth factor receptor 1 is a co-receptor for infection by adeno-associated virus 2. Nat. Med. 5:71-77.

386. Rabinowitz, J. E., D. E. Bowles, S. M. Faust, J. G. Ledford, S. E. Cunningham, and R. J. Samulski. 2004. Cross-dressing the virion: the transcapsidation of adeno-associated virus serotypes functionally defines subgroups. J. Virol. 78:4421-4432.

387. Rabinowitz, J. E., F. Rolling, C. Li, H. Conrath, W. Xiao, X. Xiao, and R. J. Samulski. 2002. Cross-packaging of a single adeno-associated virus (AAV) type 2 vector genome into multiple AAV serotypes enables transduction with broad specificity. J. Virol. 76:791-801.

388. Rabinowitz, J. E. and R. J. Samulski. 2000. Building a better vector: the manipulation of AAV virions. Virology 278:301-308.

389. Rabinowitz, J. E. and R. J. Samulski. 2002. The adeno-associated virus crystal: impact inversely proportional to size. Mol. Ther. 6:443-445.

390. Raisler, B. J., K. I. Berns, M. B. Grant, D. Beliaev, and W. W. Hauswirth. 2002. Adeno-associated virus type-2 expression of pigmented epithelium-derived factor or Kringles 1-3 of angiostatin reduce retinal neovascularization. Proc. Natl. Acad. Sci. U. S. A 99:8909-8914.

391. Ramamurthy, V., G. A. Niemi, T. A. Reh, and J. B. Hurley. 2004. Leber congenital amaurosis linked to AIPL1: a mouse model reveals destabilization of cGMP phosphodiesterase. Proc. Natl. Acad. Sci. U. S. A 101:13897-13902.

392. Ramamurthy, V., G. A. Niemi, T. A. Reh, and J. B. Hurley. 2004. Leber congenital amaurosis linked to AIPL1: a mouse model reveals destabilization

of cGMP phosphodiesterase. Proc. Natl. Acad. Sci. U. S. A 101:13897-13902.

393. Ramamurthy, V., M. Roberts, A. F. van den, G. Niemi, T. A. Reh, and J. B. Hurley. 2003. AIPL1, a protein implicated in Leber's congenital amaurosis, interacts with and aids in processing of farnesylated proteins. Proc. Natl. Acad. Sci. U. S. A 100:12630-12635.

394. Ramensky, V., P. Bork, and S. Sunyaev. 2002. Human non-synonymous SNPs: server and survey. Nucleic Acids Res. 30:3894-3900.

395. Rando, R. R. 1992. Molecular mechanisms in visual pigment regeneration. Photochem. Photobiol. 56:1145-1156.

396. Rando, R. R. 2001. The biochemistry of the visual cycle. Chem. Rev. 101:1881-1896.

397. Rao, V. R., G. B. Cohen, and D. D. Oprian. 1994. Rhodopsin mutation G90D and a molecular mechanism for congenital night blindness. Nature 367:639-642.

398. Rasmussen, H., K. W. Chu, P. Campochiaro, P. L. Gehlbach, J. A. Haller, J. T. Handa, Q. D. Nguyen, and J. U. Sung. 2001. Clinical protocol. An open-label, phase I, single administration, dose-escalation study of ADGVPEDF.11D (ADPEDF) in neovascular age-related macular degeneration (AMD). Hum. Gene Ther. 12:2029-2032.

399. Redmond, T. M., E. Poliakov, S. Yu, J. Y. Tsai, Z. Lu, and S. Gentleman. 2005. Mutation of key residues of RPE65 abolishes its enzymatic role as isomerohydrolase in the visual cycle. Proc Natl. Acad. Sci. U. S. A 102:13658-13663.

400. Redmond, T. M., S. Yu, E. Lee, D. Bok, D. Hamasaki, N. Chen, P. Goletz, J. X. Ma, R. K. Crouch, and K. Pfeifer. 1998. Rpe65 is necessary for production of 11-cis-vitamin A in the retinal visual cycle. Nat. Genet. 20:344-351.

401. Reich, S. J., A. Auricchio, M. Hildinger, E. Glover, A. M. Maguire, J. M. Wilson, and J. Bennett. 2003. Efficient trans-splicing in the retina expands the utility of adeno-associated virus as a vector for gene therapy. Hum. Gene Ther. 14:37-44.

402. Reichel, M. B., R. R. Ali, A. J. Thrasher, D. M. Hunt, S. S. Bhattacharya, and D. Baker. 1998. Immune responses limit adenovirally mediated gene expression in the adult mouse eye. Gene Ther. 5:1038-1046.

403. Renwick, J., M. A. Narang, S. G. Coupland, J. Y. Xuan, A. N. Baker, J. Brousseau, D. Petrin, R. Munger, B. C. Leonard, W. W. Hauswirth, R. G. Korneluk, and C. Tsilfidis. 2006. XIAP-mediated neuroprotection in retinal ischemia. Gene Ther. 13:339-347.

404. Reuter, J. H. and S. Sanyal. 1984. Development and degeneration of retina in rds mutant mice: the electroretinogram. Neurosci. Lett. 48:231-237.

405. Ripps, H. 2002. Cell death in retinitis pigmentosa: gap junctions and the 'bystander' effect. Exp. Eye Res. 74:327-336.

406. Rivolta, C., E. L. Berson, and T. P. Dryja. 2001. Dominant Leber congenital amaurosis, cone-rod degeneration, and retinitis pigmentosa caused by mutant versions of the transcription factor CRX. Hum. Mutat. 18:488-498.

407. Rivolta, C., D. Sharon, M. M. DeAngelis, and T. P. Dryja. 2002. Retinitis pigmentosa and allied diseases: numerous diseases, genes, and inheritance patterns. Hum. Mol. Genet. 11:1219-1227.

408. Rolling, F. 2004. Recombinant AAV-mediated gene transfer to the retina: gene therapy perspectives. Gene Ther. 11 Suppl 1:S26-S32.

409. Rolling, F., W. Y. Shen, N. L. Barnett, H. Tabarias, Y. Kanagasingam, I. Constable, and P. E. Rakoczy. 2000. Long-term real-time monitoring of adeno-associated virus-mediated gene expression in the rat retina. Clin. Experiment. Ophthalmol. 28:382-386.

410. Rosenberg, T., B. Baumann, S. Kohl, E. Zrenner, A. L. Jorgensen, and B. Wissinger. 2004. Variant phenotypes of incomplete achromatopsia in two cousins with GNAT2 gene mutations. Invest Ophthalmol Vis. Sci. 45:4256-4262.

411. Saenz, D. T., N. Loewen, M. Peretz, T. Whitwam, R. Barraza, K. G. Howell, J. M. Holmes, M. Good, and E. M. Poeschla. 2004. Unintegrated lentivirus DNA persistence and accessibility to expression in nondividing cells: analysis with class I integrase mutants. J. Virol. 78:2906-2920.

412. Saga, M., Y. Mashima, K. Akeo, Y. Oguchi, J. Kudoh, and N. Shimizu. 1993. A novel Cys-214-Ser mutation in the peripherin/RDS gene in a Japanese family with autosomal dominant retinitis pigmentosa. Hum. Genet. 92:519-521.

413. Sahel, J. A., S. Mohand-Said, T. Leveillard, D. Hicks, S. Picaud, and H. Dreyfus. 2001. Rod-cone interdependence: implications for therapy of photoreceptor cell diseases. Prog. Brain Res. 131:649-661.

414. Sakamoto, K., M. McCluskey, T. G. Wensel, J. K. Naggert, and P. M. Nishina. 2009. New mouse models for recessive retinitis pigmentosa caused by mutations in the Pde6a gene. Hum. Mol. Genet. 18:178-192.

415. Sanyal, S., R. A. De, and R. K. Hawkins. 1980. Development and degeneration of retina in rds mutant mice: light microscopy. J. Comp Neurol. 194:193-207.

416. Sanyal, S. and H. G. Jansen. 1981. Absence of receptor outer segments in the retina of rds mutant mice. Neurosci. Lett. 21:23-26.

417. Sanyal, S. and G. H. Zeilmaker. 1984. Development and degeneration of retina in rds mutant mice: light and electron microscopic observations in experimental chimaeras. Exp. Eye Res. 39:231-246.

418. Sarra, G. M., C. Stephens, F. C. Schlichtenbrede, J. W. Bainbridge, A. J. Thrasher, P. J. Luthert, and R. R. Ali. 2002. Kinetics of transgene expression in mouse retina following sub-retinal injection of recombinant adeno-associated virus. Vision Res. 42:541-549.

419. Schlichtenbrede, F. C., C. L. da, C. Stephens, A. J. Smith, A. Georgiadis, A. J. Thrasher, J. W. Bainbridge, M. W. Seeliger, and R. R. Ali. 2003. Long-term evaluation of retinal function in Prph2Rd2/Rd2 mice following AAV-mediated gene replacement therapy. J. Gene Med. 5:757-764.

420. Schlichtenbrede, F. C., A. MacNeil, J. W. Bainbridge, M. Tschernutter, A. J. Thrasher, A. J. Smith, and R. R. Ali. 2003. Intraocular gene delivery of ciliary neurotrophic factor results in significant loss of retinal function in normal mice and in the Prph2Rd2/Rd2 model of retinal degeneration. Gene Ther. 10:523-527.

421. Schlichtenbrede, F. C., A. J. Smith, J. W. Bainbridge, A. J. Thrasher, T. E. Salt, and R. R. Ali. 2004. Improvement of neuronal visual responses in the superior colliculus in Prph2(Rd2/Rd2) mice following gene therapy. Mol. Cell Neurosci. 25:103-110.

422. Schmidt, M., E. Grot, P. Cervenka, S. Wainer, C. Buck, and J. A. Chiorini. 2006. Identification and characterization of novel adeno-associated virus isolates in ATCC virus stocks. J. Virol. 80:5082-5085.

423. Schnell, T., P. Foley, M. Wirth, J. Munch, and K. Uberla. 2000. Development of a self-inactivating, minimal lentivirus vector based on simian immunodeficiency virus. Hum. Gene Ther. 11:439-447.

424. Schnetkamp, P. P., D. K. Basu, X. B. Li, and R. T. Szerencsei. 1991. Regulation of intracellular free Ca2+ concentration in the outer segments of bovine retinal rods by Na-Ca-K exchange measured with fluo-3. II. Thermodynamic competence of transmembrane Na+ and K+ gradients and inactivation of Na(+)-dependent Ca2+ extrusion. J. Biol. Chem. 266:22983-22990.

425. Schuettrumpf, J., J. H. Liu, L. B. Couto, K. Addya, D. G. Leonard, Z. Zhen, J. Sommer, and V. R. Arruda. 2006. Inadvertent germline transmission of AAV2 vector: findings in a rabbit model correlate with those in a human clinical trial. Mol. Ther. 13:1064-1073.

426. Schuil, J., F. M. Meire, and J. W. Delleman. 1998. Mental retardation in amaurosis congenita of Leber. Neuropediatrics 29:294-297.

427. Schuster, A., A. R. Janecke, R. Wilke, E. Schmid, D. A. Thompson, G. Utermann, B. Wissinger, E. Zrenner, and A. Gal. 2007. The phenotype of early-onset retinal degeneration in persons with RDH12 mutations. Invest Ophthalmol. Vis. Sci. 48:1824-1831.

428. Semple-Rowland, S. L., N. R. Lee, J. P. Van Hooser, K. Palczewski, and W. Baehr. 1998. A null mutation in the photoreceptor guanylate cyclase gene causes the retinal degeneration chicken phenotype. Proc. Natl. Acad. Sci. U. S. A 95:1271-1276.

429. Sen, G. L. and H. M. Blau. 2006. A brief history of RNAi: the silence of the genes. FASEB J. 20:1293-1299.

430. Sidjanin, D. J., J. K. Lowe, J. L. McElwee, B. S. Milne, T. M. Phippen, D. R. Sargan, G. D. Aguirre, G. M. Acland, and E. A. Ostrander. 2002. Canine CNGB3 mutations establish cone degeneration as orthologous to the human achromatopsia locus ACHM3. Hum. Mol. Genet. 11:1823-1833.

431. Sieving, P. A., R. C. Caruso, W. Tao, H. R. Coleman, D. J. Thompson, K. R. Fullmer, and R. A. Bush. 2006. Ciliary neurotrophic factor (CNTF) for human retinal degeneration: phase I trial of CNTF delivered by encapsulated cell intraocular implants. Proc. Natl. Acad. Sci. U. S. A 103:3896-3901.

432. Silva, E., S. Dharmaraj, Y. Y. Li, A. L. Pina, R. C. Carter, M. Loyer, E. Traboulsi, G. Theodossiadis, R. Koenekoop, O. Sundin, and I. Maumenee. 2004. A missense mutation in GUCY2D acts as a genetic modifier in RPE65-related Leber Congenital Amaurosis. Ophthalmic Genet. 25:205-217.

433. Silva, E., J. M. Yang, Y. Li, S. Dharmaraj, O. H. Sundin, and I. H. Maumenee. 2000. A CRX null mutation is associated with both Leber congenital amaurosis and a normal ocular phenotype. Invest Ophthalmol. Vis. Sci. 41:2076-2079.

434. Simonelli, F., A. M. Maguire, F. Testa, E. A. Pierce, F. Mingozzi, J. L. Bennicelli, S. Rossi, K. Marshall, S. Banfi, E. M. Surace, J. Sun, T. M. Redmond, X. Zhu, K. S. Shindler, G. S. Ying, C. Ziviello, C. Acerra, J. F. Wright, J. W. McDonnell, K. A. High, J. Bennett, and A. Auricchio. 2010. Gene therapy for Leber's congenital amaurosis is safe and effective through 1.5 years after vector administration. Mol. Ther. 18:643-650.

435. Sitorus, R. S., B. Lorenz, and M. N. Preising. 2003. Analysis of three genes in Leber congenital amaurosis in Indonesian patients. Vision Res. 43:3087-3093.

436. Smith, A. J., J. W. Bainbridge, and R. R. Ali. 2009. Prospects for retinal gene replacement therapy. Trends Genet. 25:156-165.

437. Smith, A. J., F. C. Schlichtenbrede, M. Tschernutter, J. W. Bainbridge, A. J. Thrasher, and R. R. Ali. 2003. AAV-Mediated gene transfer slows photoreceptor loss in the RCS rat model of retinitis pigmentosa. Mol. Ther. 8:188-195.

438. Smith, R. H. 2008. Adeno-associated virus integration: virus versus vector. Gene Ther. 15:817-822.

439. Snyder, S. H., M. M. Lai, and P. E. Burnett. 1998. Immunophilins in the nervous system. Neuron 21:283-294.

440. Sohocki, M. M., S. J. Bowne, L. S. Sullivan, S. Blackshaw, C. L. Cepko, A. M. Payne, S. S. Bhattacharya, S. Khaliq, M. S. Qasim, D. G. Birch, W. R. Harrison, F. F. Elder, J. R. Heckenlively, and S. P. Daiger. 2000. Mutations in a new photoreceptor-pineal gene on 17p cause Leber congenital amaurosis. Nat. Genet. 24:79-83.

441. Sohocki, M. M., S. P. Daiger, S. J. Bowne, J. A. Rodriquez, H. Northrup, J. R. Heckenlively, D. G. Birch, H. Mintz-Hittner, R. S. Ruiz, R. A. Lewis, D. A. Saperstein, and L. S. Sullivan. 2001. Prevalence of mutations causing retinitis pigmentosa and other inherited retinopathies. Hum. Mutat. 17:42-51.

442. Sohocki, M. M., I. Perrault, B. P. Leroy, A. M. Payne, S. Dharmaraj, S. S. Bhattacharya, J. Kaplan, I. H. Maumenee, R. Koenekoop, F. M. Meire, D. G. Birch, J. R. Heckenlively, and S. P. Daiger. 2000. Prevalence of AIPL1 mutations in inherited retinal degenerative disease. Mol. Genet. Metab 70:142-150.

443. Sohocki, M. M., L. S. Sullivan, H. A. Mintz-Hittner, D. Birch, J. R. Heckenlively, C. L. Freund, R. R. McInnes, and S. P. Daiger. 1998. A range of clinical phenotypes associated with mutations in CRX, a photoreceptor transcription-factor gene. Am. J. Hum. Genet. 63:1307-1315.

444. Sohocki, M. M., L. S. Sullivan, D. L. Tirpak, and S. P. Daiger. 2001. Comparative analysis of aryl-hydrocarbon receptor interacting protein-like 1 (Aipl1), a gene associated with inherited retinal disease in humans. Mamm. Genome 12:566-568.

445. Sokolov, M., A. L. Lyubarsky, K. J. Strissel, A. B. Savchenko, V. I. Govardovskii, E. N. Pugh, Jr., and V. Y. Arshavsky. 2002. Massive light-driven translocation of transducin between the two major compartments of rod cells: a novel mechanism of light adaptation. Neuron 34:95-106.

446. Somiari, S., J. Glasspool-Malone, J. J. Drabick, R. A. Gilbert, R. Heller, M. J. Jaroszeski, and R. W. Malone. 2000. Theory and in vivo application of electroporative gene delivery. Mol. Ther. 2:178-187.

447. Steinwaerder, D. S., C. A. Carlson, and A. Lieber. 1999. Generation of adenovirus vectors devoid of all viral genes by recombination between inverted repeats. J. Virol. 73:9303-9313.

448. Stieger, K., M. A. Colle, L. Dubreil, A. Mendes-Madeira, M. Weber, M. G. Le, J. Y. Deschamps, N. Provost, D. Nivard, Y. Cherel, P. Moullier, and F. Rolling. 2008. Subretinal delivery of recombinant AAV serotype 8 vector in dogs results in gene transfer to neurons in the brain. Mol. Ther. 16:916-923.

449. Strauss, O. 2005. The retinal pigment epithelium in visual function. Physiol Rev. 85:845-881.

450. Strettoi, E. and V. Pignatelli. 2000. Modifications of retinal neurons in a mouse model of retinitis pigmentosa. Proc. Natl. Acad. Sci. U. S. A 97:11020-11025.

451. Strettoi, E., V. Pignatelli, C. Rossi, V. Porciatti, and B. Falsini. 2003. Remodeling of second-order neurons in the retina of rd/rd mutant mice. Vision Res. 43:867-877.

452. Strettoi, E., V. Porciatti, B. Falsini, V. Pignatelli, and C. Rossi. 2002. Morphological and functional abnormalities in the inner retina of the rd/rd mouse. J. Neurosci. 22:5492-5504.

453. Sullivan, T. J., J. G. Heathcote, S. M. Brazel, and M. A. Musarella. 1994. The ocular pathology in Leber's congenital amaurosis. Aust. N. Z. J. Ophthalmol. 22:25-31.

454. Summerford, C., J. S. Bartlett, and R. J. Samulski. 1999. AlphaVbeta5 integrin: a co-receptor for adeno-associated virus type 2 infection. Nat. Med. 5:78-82.

455. Sun, X., B. Pawlyk, X. Xu, X. Liu, O. V. Bulgakov, M. Adamian, M. A. Sandberg, S. C. Khani, M. H. Tan, A. J. Smith, R. R. Ali, and T. Li. 2010. Gene therapy with a promoter targeting both rods and cones rescues retinal degeneration caused by AIPL1 mutations. Gene Ther. 17:117-131.

456. Sundin, O. H., J. M. Yang, Y. Li, D. Zhu, J. N. Hurd, T. N. Mitchell, E. D. Silva, and I. H. Maumenee. 2000. Genetic basis of total colourblindness among the Pingelapese islanders. Nat. Genet. 25:289-293.

457. Sung, C. H., C. Makino, D. Baylor, and J. Nathans. 1994. A rhodopsin gene mutation responsible for autosomal dominant retinitis pigmentosa results in a protein that is defective in localization to the photoreceptor outer segment. J. Neurosci. 14:5818-5833.

458. Sung, C. H. and A. W. Tai. 2000. Rhodopsin trafficking and its role in retinal dystrophies. Int. Rev. Cytol. 195:215-267.

459. Surace, E. M. and A. Auricchio. 2003. Adeno-associated viral vectors for retinal gene transfer. Prog. Retin. Eye Res. 22:705-719.

460. Surace, E. M. and A. Auricchio. 2008. Versatility of AAV vectors for retinal gene transfer. Vision Res. 48:353-359.

461. Surace, E. M., A. Auricchio, S. J. Reich, T. Rex, E. Glover, S. Pineles, W. Tang, E. O'Connor, A. Lyubarsky, A. Savchenko, E. N. Pugh, Jr., A. M. Maguire, J. M. Wilson, and J. Bennett. 2003. Delivery of adeno-associated virus vectors to the fetal retina: impact of viral capsid proteins on retinal neuronal progenitor transduction. J. Virol. 77:7957-7963.

462. Takahashi, K., T. Luo, Y. Saishin, Y. Saishin, J. Sung, S. Hackett, R. K. Brazzell, M. Kaleko, and P. A. Campochiaro. 2002. Sustained transduction of ocular cells with a bovine immunodeficiency viral vector. Hum. Gene Ther. 13:1305-1316.

463. Takahashi, M., H. Miyoshi, I. M. Verma, and F. H. Gage. 1999. Rescue from photoreceptor degeneration in the rd mouse by human immunodeficiency virus vector-mediated gene transfer. J. Virol. 73:7812-7816.

464. Tan, M. H., A. J. Smith, B. Pawlyk, X. Xu, X. Liu, J. B. Bainbridge, M. Basche, J. McIntosh, H. V. Tran, A. Nathwani, T. Li, and R. R. Ali. 2009. Gene therapy for retinitis pigmentosa and Leber congenital amaurosis caused by defects in AIPL1: effective rescue of mouse models of partial and complete Aipl1 deficiency using AAV2/2 and AAV2/8 vectors. Hum. Mol. Genet. 18:2099-2114.

465. Thiadens, A. A., A. I. den Hollander, S. Roosing, S. B. Nabuurs, R. C. Zekveld-Vroon, R. W. Collin, B. E. De, R. K. Koenekoop, M. J. van Schooneveld, T. M. Strom, J. J. van Lith-Verhoeven, A. J. Lotery, N. van Moll-Ramirez, B. P. Leroy, L. I. van den Born, C. B. Hoyng, F. P. Cremers, and C. C. Klaver. 2009. Homozygosity mapping reveals PDE6C mutations in patients with early-onset cone photoreceptor disorders. Am. J. Hum. Genet. 85:240-247.

466. Thomas, C. E., T. A. Storm, Z. Huang, and M. A. Kay. 2004. Rapid uncoating of vector genomes is the key to efficient liver transduction with pseudotyped adeno-associated virus vectors. J. Virol. 78:3110-3122.

467. Thompson, D. A. and A. Gal. 2003. Genetic defects in vitamin A metabolism of the retinal pigment epithelium. Dev. Ophthalmol 37:141-154.

468. Thompson, D. A., P. Gyurus, L. L. Fleischer, E. L. Bingham, C. L. McHenry, E. pfelstedt-Sylla, E. Zrenner, B. Lorenz, J. E. Richards, S. G. Jacobson, P. A. Sieving, and A. Gal. 2000. Genetics and phenotypes of RPE65 mutations in inherited retinal degeneration. Invest Ophthalmol. Vis. Sci. 41:4293-4299.

469. Travis, G. H. 1998. Mechanisms of cell death in the inherited retinal degenerations. Am. J. Hum. Genet. 62:503-508.

470. Travis, G. H., M. B. Brennan, P. E. Danielson, C. A. Kozak, and J. G. Sutcliffe. 1989. Identification of a photoreceptor-specific mRNA encoded by the gene responsible for retinal degeneration slow (rds). Nature 338:70-73.

471. Tschernutter, M., F. C. Schlichtenbrede, S. Howe, K. S. Balaggan, P. M. Munro, J. W. Bainbridge, A. J. Thrasher, A. J. Smith, and R. R. Ali. 2005. Long-term preservation of retinal function in the RCS rat model of retinitis pigmentosa following lentivirus-mediated gene therapy. Gene Ther. 12:694-701.

472. Unoki, K. and M. M. Lavail. 1994. Protection of the rat retina from ischemic injury by brain-derived neurotrophic factor, ciliary neurotrophic factor, and basic fibroblast growth factor. Invest Ophthalmol. Vis. Sci. 35:907-915.

473. van de Pavert, S. A., A. Kantardzhieva, A. Malysheva, J. Meuleman, I. Versteeg, C. Levelt, J. Klooster, S. Geiger, M. W. Seeliger, P. Rashbass, B. A. Le, and J. Wijnholds. 2004. Crumbs homologue 1 is required for maintenance of photoreceptor cell polarization and adhesion during light exposure. J. Cell Sci. 117:4169-4177.

474. van de Pavert, S. A., J. Meuleman, A. Malysheva, W. M. Aartsen, I. Versteeg, F. Tonagel, W. Kamphuis, C. J. McCabe, M. W. Seeliger, and J. Wijnholds. 2007. A single amino acid substitution (Cys249Trp) in Crb1 causes retinal degeneration and deregulates expression of pituitary tumor transforming gene Pttg1. J. Neurosci. 27:564-573.

475. Van der, S. J., J. P. Chapple, B. J. Clark, P. J. Luthert, C. S. Sethi, and M. E. Cheetham. 2002. The Leber congenital amaurosis gene product AIPL1 is localized exclusively in rod photoreceptors of the adult human retina. Hum. Mol. Genet. 11:823-831.

476. Van der, S. J. and M. E. Cheetham. 2004. The Leber congenital amaurosis protein AIPL1 modulates the nuclear translocation of NUB1 and suppresses inclusion formation by NUB1 fragments. J. Biol. Chem. 279:48038-48047.

477. Van der, S. J., J. H. Kim, Y. S. Yu, A. Szel, P. J. Luthert, B. J. Clark, and M. E. Cheetham. 2003. The expression of the Leber congenital amaurosis protein AIPL1 coincides with rod and cone photoreceptor development. Invest Ophthalmol. Vis. Sci. 44:5396-5403.

478. Van der, S. J., P. M. Munro, P. J. Luthert, M. N. Preising, T. Bek, S. Heegaard, and M. E. Cheetham. 2005. Predominant rod photoreceptor degeneration in Leber congenital amaurosis. Mol. Vis. 11:542-553.

479. Vargas, J., Jr., G. L. Gusella, V. Najfeld, M. E. Klotman, and A. Cara. 2004. Novel integrase-defective lentiviral episomal vectors for gene transfer. Hum. Gene Ther. 15:361-372.

480. Verma, I. M. and M. D. Weitzman. 2005. Gene therapy: twenty-first century medicine. Annu. Rev. Biochem. 74:711-738.

481. Vigna, E. and L. Naldini. 2000. Lentiviral vectors: excellent tools for experimental gene transfer and promising candidates for gene therapy. J. Gene Med. 2:308-316.

482. Vollrath, D., W. Feng, J. L. Duncan, D. Yasumura, P. M. D'Cruz, A. Chappelow, M. T. Matthes, M. A. Kay, and M. M. Lavail. 2001. Correction of the retinal dystrophy phenotype of the RCS rat by viral gene transfer of Mertk. Proc. Natl. Acad. Sci. U. S. A 98:12584-12589.

483. VRABEC, F. 1951. [Histological findings in case of congenital pigmentary retinal degeneration.]. Ophthalmologica 122:65-75.

484. Wachtmeister, L. 1998. Oscillatory potentials in the retina: what do they reveal. Prog. Retin. Eye Res. 17:485-521.

485. Walia, S., G. A. Fishman, S. G. Jacobson, T. S. Aleman, R. K. Koenekoop, E. I. Traboulsi, R. G. Weleber, M. E. Pennesi, E. Heon, A. Drack, B. L. Lam, R. Allikmets, and E. M. Stone. 2010. Visual acuity in patients with Leber's congenital amaurosis and early childhood-onset retinitis pigmentosa. Ophthalmology 117:1190-1198.

486. Wang, Q. and M. H. Finer. 1996. Second-generation adenovirus vectors. Nat. Med. 2:714-716.

487. Wang, Y., J. P. Macke, S. L. Merbs, D. J. Zack, B. Klaunberg, J. Bennett, J. Gearhart, and J. Nathans. 1992. A locus control region adjacent to the human red and green visual pigment genes. Neuron 9:429-440.

488. Wang, Z., J. M. Allen, S. R. Riddell, P. Gregorevic, R. Storb, S. J. Tapscott, J. S. Chamberlain, and C. S. Kuhr. 2007. Immunity to adeno-associated virus-mediated gene transfer in a random-bred canine model of Duchenne muscular dystrophy. Hum. Gene Ther. 18:18-26.

489. Weber, M., J. Rabinowitz, N. Provost, H. Conrath, S. Folliot, D. Briot, Y. Cherel, P. Chenuaud, J. Samulski, P. Moullier, and F. Rolling. 2003. Recombinant adeno-associated virus serotype 4 mediates unique and exclusive long-term transduction of retinal pigmented epithelium in rat, dog, and nonhuman primate after subretinal delivery. Mol. Ther. 7:774-781.

490. Weleber, R. G., R. E. Carr, W. H. Murphey, V. C. Sheffield, and E. M. Stone. 1993. Phenotypic variation including retinitis pigmentosa, pattern dystrophy, and fundus flavimaculatus in a single family with a deletion of codon 153 or 154 of the peripherin/RDS gene. Arch. Ophthalmol 111:1531-1542.

491. Wen, R., Y. Song, T. Cheng, M. T. Matthes, D. Yasumura, M. M. Lavail, and R. H. Steinberg. 1995. Injury-induced upregulation of bFGF and CNTF mRNAS in the rat retina. J. Neurosci. 15:7377-7385.

492. Wen, R., Y. Song, S. Kjellstrom, A. Tanikawa, Y. Liu, Y. Li, L. Zhao, R. A. Bush, A. M. Laties, and P. A. Sieving. 2006. Regulation of rod phototransduction machinery by ciliary neurotrophic factor. J. Neurosci. 26:13523-13530.

493. Wen, S., S. Graf, P. G. Massey, and D. A. Dichek. 2004. Improved vascular gene transfer with a helper-dependent adenoviral vector. Circulation 110:1484-1491.

494. Weng, J., N. L. Mata, S. M. Azarian, R. T. Tzekov, D. G. Birch, and G. H. Travis. 1999. Insights into the function of Rim protein in photoreceptors and etiology of Stargardt's disease from the phenotype in abcr knockout mice. Cell 98:13-23.

495. Wilden, U. 1995. Duration and amplitude of the light-induced cGMP hydrolysis in vertebrate photoreceptors are regulated by multiple phosphorylation of rhodopsin and by arrestin binding. Biochemistry 34:1446-1454.

496. Williams, M. L., J. E. Coleman, S. E. Haire, T. S. Aleman, A. V. Cideciyan, I. Sokal, K. Palczewski, S. G. Jacobson, and S. L. Semple-Rowland. 2006. Lentiviral expression of retinal guanylate cyclase-1 (RetGC1) restores vision in an avian model of childhood blindness. PLoS. Med. 3:e201.

497. Wilson, M. O., K. T. Scougall, J. Ratanamart, E. A. McIntyre, and J. A. Shaw. 2005. Tetracycline-regulated secretion of human (pro)insulin following plasmid-mediated transfection of human muscle. J. Mol. Endocrinol. 34:391-403.

498. Winick, J. D., M. L. Blundell, B. L. Galke, A. A. Salam, S. M. Leal, and M. Karayiorgou. 1999. Homozygosity mapping of the Achromatopsia locus in the Pingelapese. Am. J. Hum. Genet. 64:1679-1685.

499. Wissinger, B., D. Gamer, H. Jagle, R. Giorda, T. Marx, S. Mayer, S. Tippmann, M. Broghammer, B. Jurklies, T. Rosenberg, S. G. Jacobson, E. C. Sener, S. Tatlipinar, C. B. Hoyng, C. Castellan, P. Bitoun, S. Andreasson, G. Rudolph, U. Kellner, B. Lorenz, G. Wolff, C. Verellen-Dumoulin, M. Schwartz, F. P. Cremers, E. pfelstedt-Sylla, E. Zrenner, R. Salati, L. T. Sharpe, and S. Kohl. 2001. CNGA3 mutations in hereditary cone photoreceptor disorders. Am. J. Hum. Genet. 69:722-737.

500. Woodruff, M. L., Z. Wang, H. Y. Chung, T. M. Redmond, G. L. Fain, and J. Lem. 2003. Spontaneous activity of opsin apoprotein is a cause of Leber congenital amaurosis. Nat. Genet. 35:158-164.

501. Wrigley, J. D., C. L. Nevett, and J. B. Findlay. 2002. Topological analysis of peripherin/rds and abnormal glycosylation of the pathogenic Pro216-->Leu mutation. Biochem. J. 368:649-655.

502. Wu, Z., A. Asokan, and R. J. Samulski. 2006. Adeno-associated virus serotypes: vector toolkit for human gene therapy. Mol. Ther. 14:316-327.

503. Xia, H., Q. Mao, H. L. Paulson, and B. L. Davidson. 2002. siRNA-mediated gene silencing in vitro and in vivo. Nat. Biotechnol. 20:1006-1010.

504. Xu, J., R. L. Dodd, C. L. Makino, M. I. Simon, D. A. Baylor, and J. Chen. 1997. Prolonged photoresponses in transgenic mouse rods lacking arrestin. Nature 389:505-509.

505. Yan, Z., T. C. Ritchie, D. Duan, and J. F. Engelhardt. 2002. Recombinant AAV-mediated gene delivery using dual vector heterodimerization. Methods Enzymol. 346:334-357.

506. Yan, Z., R. Zak, Y. Zhang, and J. F. Engelhardt. 2005. Inverted terminal repeat sequences are important for intermolecular recombination and circularization of adeno-associated virus genomes. J. Virol. 79:364-379.

507. Yanez-Munoz, R. J., K. S. Balaggan, A. MacNeil, S. J. Howe, M. Schmidt, A. J. Smith, P. Buch, R. E. MacLaren, P. N. Anderson, S. E. Barker, Y. Duran, C. Bartholomae, K. C. von, J. R. Heckenlively, C. Kinnon, R. R. Ali, and A. J. Thrasher. 2006. Effective gene therapy with nonintegrating lentiviral vectors. Nat. Med. 12:348-353.

508. Yang, G. S., M. Schmidt, Z. Yan, J. D. Lindbloom, T. C. Harding, B. A. Donahue, J. F. Engelhardt, R. Kotin, and B. L. Davidson. 2002. Virus-mediated transduction of murine retina with adeno-associated virus: effects of viral capsid and genome size. J. Virol. 76:7651-7660.

509. Yang, R. B., S. W. Robinson, W. H. Xiong, K. W. Yau, D. G. Birch, and D. L. Garbers. 1999. Disruption of a retinal guanylyl cyclase gene leads to cone-specific dystrophy and paradoxical rod behavior. J. Neurosci. 19:5889-5897.

510. Yau, K. W. 1994. Cyclic nucleotide-gated channels: an expanding new family of ion channels. Proc. Natl. Acad. Sci. U. S. A 91:3481-3483.

511. Young, J. C., J. M. Barral, and H. F. Ulrich. 2003. More than folding: localized functions of cytosolic chaperones. Trends Biochem. Sci. 28:541-547.

512. Young, J. E., K. W. Gross, and S. C. Khani. 2005. Conserved structure and spatiotemporal function of the compact rhodopsin kinase (GRK1) enhancer/promoter. Mol. Vis. 11:1041-1051.

513. Young, J. E., T. Vogt, K. W. Gross, and S. C. Khani. 2003. A short, highly active photoreceptor-specific enhancer/promoter region upstream of the human rhodopsin kinase gene. Invest Ophthalmol. Vis. Sci. 44:4076-4085.

514. Young, R. W. 1985. Cell proliferation during postnatal development of the retina in the mouse. Brain Res. 353:229-239.

515. Yuan, J., M. Lipinski, and A. Degterev. 2003. Diversity in the mechanisms of neuronal cell death. Neuron 40:401-413.

516. Yuan, L., I. Kurek, J. English, and R. Keenan. 2005. Laboratory-directed protein evolution. Microbiol. Mol. Biol. Rev. 69:373-392.

517. Yzer, S., L. I. van den Born, J. Schuil, H. Y. Kroes, M. M. van Genderen, F. N. Boonstra, H. B. van den, H. G. Brunner, R. K. Koenekoop, and F. P. Cremers. 2003. A Tyr368His RPE65 founder mutation is associated with variable expression and progression of early onset retinal dystrophy in 10 families of a genetically isolated population. J. Med. Genet. 40:709-713.

518. Zeng, Y., Y. Takada, S. Kjellstrom, K. Hiriyanna, A. Tanikawa, E. Wawrousek, N. Smaoui, R. Caruso, R. A. Bush, and P. A. Sieving. 2004. RS-1 Gene Delivery to an Adult Rs1h Knockout Mouse Model Restores ERG b-Wave with Reversal of the Electronegative Waveform of X-Linked Retinoschisis. Invest Ophthalmol. Vis. Sci. 45:3279-3285.

519. Zernant, J., M. Kulm, S. Dharmaraj, A. I. den Hollander, I. Perrault, M. N. Preising, B. Lorenz, J. Kaplan, F. P. Cremers, I. Maumenee, R. K. Koenekoop, and R. Allikmets. 2005. Genotyping microarray (disease chip) for Leber congenital amaurosis: detection of modifier alleles. Invest Ophthalmol. Vis. Sci. 46:3052-3059.

520. Zhang, H., W. Huang, H. Zhang, X. Zhu, C. M. Craft, W. Baehr, and C. K. Chen. 2003. Light-dependent redistribution of visual arrestins and transducin subunits in mice with defective phototransduction. Mol. Vis. 9:231-237.

521. Zhang, K., M. Kniazeva, A. Hutchinson, M. Han, M. Dean, and R. Allikmets. 1999. The ABCR gene in recessive and dominant Stargardt diseases: a genetic pathway in macular degeneration. Genomics 60:234-237.

522. Zhang, Q., S. Li, X. Guo, L. Guo, X. Xiao, X. Jia, and Z. Kuang. 2001. Screening for CRX gene mutations in Chinese patients with Leber congenital amaurosis and mutational phenotype. Ophthalmic Genet. 22:89-96.

523. Zhang, X., A. M. De, S. L. Hart, F. W. Fitzke, S. C. Inglis, M. E. Boursnell, R. J. Levinsky, C. Kinnon, R. R. Ali, and A. J. Thrasher. 1999. High-titer recombinant adeno-associated virus production from replicating amplicons and herpes vectors deleted for glycoprotein H. Hum. Gene Ther. 10:2527-2537.

524. Zhao, Y., D. H. Hong, B. Pawlyk, G. Yue, M. Adamian, M. Grynberg, A. Godzik, and T. Li. 2003. The retinitis pigmentosa GTPase regulator (RPGR)-interacting protein: subserving RPGR function and participating in disk morphogenesis. Proc. Natl. Acad. Sci. U. S. A 100:3965-3970.

525. Zhou, Y., V. Pernet, W. W. Hauswirth, and P. A. Di. 2005. Activation of the extracellular signal-regulated kinase 1/2 pathway by AAV gene transfer protects retinal ganglion cells in glaucoma. Mol. Ther. 12:402-412.

526. Zhukovsky, E. A., P. R. Robinson, and D. D. Oprian. 1991. Transducin activation by rhodopsin without a covalent bond to the 11-cis-retinal chromophore. Science 251:558-560.

527. Zufferey, R., T. Dull, R. J. Mandel, A. Bukovsky, D. Quiroz, L. Naldini, and D. Trono. 1998. Self-inactivating lentivirus vector for safe and efficient in vivo gene delivery. J. Virol. 72:9873-9880.

528. Zufferey, R., D. Nagy, R. J. Mandel, L. Naldini, and D. Trono. 1997. Multiply attenuated lentiviral vector achieves efficient gene delivery in vivo. Nat. Biotechnol. 15:871-875.